

ISSN 0021-9673

VOL. **346** OCTOBER 18, 1985
COMPLETE IN ONE ISSUE

JOURNAL OF

CHROMATOGRAPHY

NATIONAL JOURNAL ON CHROMATOGRAPHY, ELECTROPHORESIS AND RELATED METHODS

EDITOR, Michael Lederer (Switzerland)
ASSOCIATE EDITOR, K. Macek (Prague)
EDITOR, SYMPOSIUM VOLUMES, E. Heftmann (Berkeley, CA)
EDITORIAL BOARD

W. A. Aue (Halifax)
V. G. Berezkin (Moscow)
V. Betina (Bratislava)
A. Beyenue (Honolulu, HI)
P. Bocek (Brno)
P. Boulanger (Lille)
A. A. Boulton (Saskatoon)
G. P. Cartoni (Rome)
S. Dilli (Kensington, N.S.W.)
L. Fishbein (Jefferson, AR)
R. W. Frei (Amsterdam)
A. Frigerio (Milan)
C. W. Gehrke (Columbia, MO)
E. Gil-Av (Rehovot)
G. Guiochon (Palaiseau)
I. M. Hais (Hradec Králové)
J. K. Haken (Kensington, N.S.W.)
S. Hjertén (Uppsala)
E. C. Horning (Houston, TX)
Cs. Horváth (New Haven, CT)
J. F. K. Huber (Vienna)
A. T. James (Sharnbrook)
J. Janák (Brno)
E. sz. Kováts (Lausanne)
K. A. Kraus (Oak Ridge, TN)
E. Lederer (Gif-sur-Yvette)
A. Liberti (Rome)
H. M. McNair (Blacksburg, VA)
Y. Marcus (Jerusalem)
G. B. Marini-Bettolo (Rome)
A. J. P. Martin (Lausanne)
Č. Michalec (Prague)
R. Neher (Basel)
G. Nickless (Bristol)
J. Novák (Brno)
N. A. Parris (Wilmington, DE)
R. L. Patience (London)
P. G. Righetti (Milan)
O. Samuelson (Göteborg)
R. Schwarzenbach (Dübendorf)
G. Semeriza (Zürich)
L. R. Snyder (Yorktown Heights, NY)
A. Zlatkis (Houston, TX)

EDITORS, BIBLIOGRAPHY SECTION

Z. Deyl (Prague), J. Janák (Brno), K. Maček (Prague)

ELSEVIER

JOURNAL OF CHROMATOGRAPHY

Scope. The *Journal of Chromatography* publishes papers on all aspects of chromatography, electrophoresis and related methods. Contributions consist mainly of research papers dealing with chromatographic theory, instrumental development and their applications. The section *Biomedical Applications*, which is under separate editorship, deals with the following aspects: developments in and applications of chromatographic and electrophoretic techniques related to clinical diagnosis (including the publication of normal values); screening and profiling procedures with special reference to metabolic disorders; results from basic medical research with direct consequences in clinical practice; combinations of chromatographic and electrophoretic methods with other physicochemical techniques such as mass spectrometry. In *Chromatographic Reviews*, reviews on all aspects of chromatography, electrophoresis and related methods are published.

Submission of Papers. Papers in English, French and German may be submitted, in three copies. Manuscripts should be submitted to: The Editor of *Journal of Chromatography*, P.O. Box 681, 1000 AR Amsterdam, The Netherlands, or to: The Editor of *Journal of Chromatography, Biomedical Applications*, P.O. Box 681, 1000 AR Amsterdam, The Netherlands. Review articles are invited or proposed by letter to the Editors and will appear in *Chromatographic Reviews* or *Biomedical Applications*. An outline of the proposed review should first be forwarded to the Editors for preliminary discussion prior to preparation. Submission of an article is understood to imply that the article is original and unpublished and is not being considered for publication elsewhere. For copyright regulations, see below.

Subscription Orders. Subscription orders should be sent to: Elsevier Science Publishers B.V., P.O. Box 211, 1000 AE Amsterdam, The Netherlands. The *Journal of Chromatography* and the *Biomedical Applications* section can be subscribed to separately.

Publication. The *Journal of Chromatography* (incl. *Biomedical Applications, Chromatographic Reviews* and *Cumulative Author and Subject Indexes, Vols. 326-350*) has 38 volumes in 1986. The subscription prices for 1986 are:

J. Chromatogr. (incl. *Chromatogr. Rev.* and *Cum. Indexes, Vols. 326-350*) + *Biomed. Appl.* (Vols. 374-383): Dfl. 6080.00 plus Dfl. 912.00 (postage) (total ca. US\$ 2411.00)

J. Chromatogr. (incl. *Chromatogr. Rev.* and *Cum. Indexes, Vols. 326-350*) only (Vols. 346-373): Dfl. 5040.00 plus Dfl. 672.00 (postage) (total ca. US\$ 1969.75)

Biomed. Appl. only (Vols. 374-383):

Dfl. 1850.00 plus Dfl. 240.00 (postage) (total ca. US\$ 720.75).

Journals are automatically sent by airmail at no extra costs to Australia, Brasil, Canada, China, Hong Kong, India, Israel, Japan, Malaysia, New Zealand, Pakistan, Singapore, South Africa, South Korea, Taiwan and the U.S.A. Back volumes of the *Journal of Chromatography* (Vols. 1 through 345) are available at Dfl. 219.00 (plus postage). Claims for issues not received should be made within three months of publication of the issue. If not, they cannot be honoured free of charge. Customers in the U.S.A. and Canada wishing information on this and other Elsevier journals, please contact Journal Information Center, Elsevier Science Publishing Co. Inc., 52 Vanderbilt Avenue, New York, NY 10017. Tel. (212) 916-1250.

Abstracts/Contents Lists published in Analytical Abstracts, Biochemical Abstracts, Biological Abstracts, Chemical Abstracts, Chemical Titles, Current Contents/Physical, Chemical & Earth Sciences, Current Contents/Life Sciences, Deep-Sea Research/Part B: Oceanographic Literature Review, Index Medicus, Mass Spectrometry Bulletin, PASCAL-CNRS, Referativnyi Zhurnal and Science Citation Index.

See page 3 of cover for Publication Schedule, Information for Authors and information on Advertisements.

© ELSEVIER SCIENCE PUBLISHERS B.V. — 1985

0021-9673/85/\$03.30

All rights reserved. No part of this publication may be reproduced, stored in a retrieval system or transmitted in any form or by any means, electronic, mechanical, photocopying, recording or otherwise, without the prior written permission of the publisher, Elsevier Science Publishers B.V., P.O. Box 330, 1000 AH Amsterdam, The Netherlands.

Upon acceptance of an article by the journal, the author(s) will be asked to transfer copyright of the article to the publisher. The transfer will ensure the widest possible dissemination of information.

Submission of an article for publication implies the transfer of the copyright from the author(s) to the publisher and entails the authors' irrevocable and exclusive authorization of the publisher to collect any sums or considerations for copying or reproduction payable by third parties (as mentioned in article 17 paragraph 2 of the Dutch Copyright Act of 1912 and in the Royal Decree of June 20, 1974 (S. 351) pursuant to article 16 b of the Dutch Copyright Act of 1912) and/or to act in or out of Court in connection therewith.

Special regulations for readers in the U.S.A. This journal has been registered with the Copyright Clearance Center, Inc. Consent is given for copying of articles for personal or internal use, or for the personal use of specific clients. This consent is given on the condition that the copier pays through the Center the per-copy fee stated in the code on the first page of each article for copying beyond that permitted by Sections 107 or 108 of the U.S. Copyright Law. The appropriate fee should be forwarded with a copy of the first page of the article to the Copyright Clearance Center, Inc., 27 Congress Street, Salem, MA 01970, U.S.A. If no code appears in an article, the author has not given broad consent to copy and permission to copy must be obtained directly from the author. All articles published prior to 1980 may be copied for a per-copy fee of US\$ 2.25, also payable through the Center. This consent does not extend to other kinds of copying, such as for general distribution, resale, advertising and promotion purposes, or for creating new collective works.

Special written permission must be obtained from the publisher for such copying.

Printed in The Netherlands

CONTENTS

(Abstracts/Contents Lists published in *Analytical Abstracts*, *Biochemical Abstracts*, *Biological Abstracts*, *Chemical Abstracts*, *Chemical Titles*, *Current Contents/Physical, Chemical & Earth Sciences*, *Current Contents/Life Sciences*, *Deep-Sea Research/Part B: Oceanographic Literature Review*, *Index Medicus*, *Mass Spectrometry Bulletin*, *PASCAL-CNRS*, *Referativnyi Zhurnal* and *Science Citation Index*)

Theory of anion contributions to non-linear electron-capture detector response by G. Wells (Walnut Creek, CA, U.S.A.) (Received June 10th, 1985)	1
Continuous-flow nuclear magnetic resonance by K. Alber, M. Nieder and E. Bayer (Tübingen, F.R.G.) and M. Spraul (Rheinstetten, F.R.G.) (Received June 17th, 1985)	17
Chromatographic properties of oxidised OV-17 stationary phase by B. A. Colenutt and R. M. Clinch (Uxbridge, U.K.) (Received July 1st, 1985)	25
Use of equivalent chain lengths for the characterization of fatty acid methyl esters separated by linear temperature-programmed gas chromatography by J. Krupčík (Bratislava, Czechoslovakia) and P. Bohov (Malacky, Czechoslovakia) (Received June 25th, 1985)	33
Äthenmessung durch eine gaschromatographische Anreicherungstechnik mit Flammenionisationsdetektion von J. Goliáš (Lednice na Moravě, Tschechoslowakei) und J. Novák (Brno, Tschechoslowakei) (Eingegangen am 25. Juni 1985)	43
Quantum chemical parameters in correlation analysis of gas-liquid chromatographic retention indices of amines by K. Ośmiałowski, J. Halkiewicz, A. Radecki and R. Kaliszan (Gdańsk, Poland) (Received June 13th, 1985)	53
Evaluation of the suitability of selected porous polymers for preconcentration of organosulphur compounds from water by A. Przyjazny (Gdańsk, Poland) (Received June 11th, 1985)	61
Separation of oligomers with UV-absorbing side groups by supercritical fluid chromatography using eluent gradients by F. P. Schmitz, H. Hilgers, B. Lorenschat and E. Klesper (Aachen, F.R.G.) (Received June 7th, 1985)	69
Liquid chromatographic retention behavior of large, fused polycyclic aromatics. Normal bonded phases by J. C. Fetzer and W. R. Biggs (Richmond, CA, U.S.A.) (Received June 17th, 1985)	81
Noble, diatomic and aliphatic gas analysis by aqueous high-performance liquid chromatography by J. O. Baker, M. P. Tucker and M. E. Himmel (Golden, CO, U.S.A.) (Received June 28th, 1985)	93
Protein precipitation induced by a textile dye. Precipitation of human plasminogen in the presence of Procion Red HE3B by O. Bertrand, S. Cochet, Y. Kroviarski, A. Truskolaski and P. Boivin (Clichy, France) (Received June 7th, 1985)	111
The occurrence and origin of system peaks in non-suppressed ion chromatography of inorganic anions with indirect ultraviolet absorption detection by P. E. Jackson and P. R. Haddad (Kensington, Australia) (Received June 5th, 1985)	125
Performance characteristics of some commercially available low-capacity anion-exchange columns suitable for non-suppressed ion chromatography by P. R. Haddad, P. E. Jackson and A. L. Heckenberg (Kensington, Australia) (Received June 25th, 1985)	139

(Continued overleaf)

ห้องสมุดรวมวิทยาศาสตร์

๑๑ ๒๕๓๕

Contents (continued)

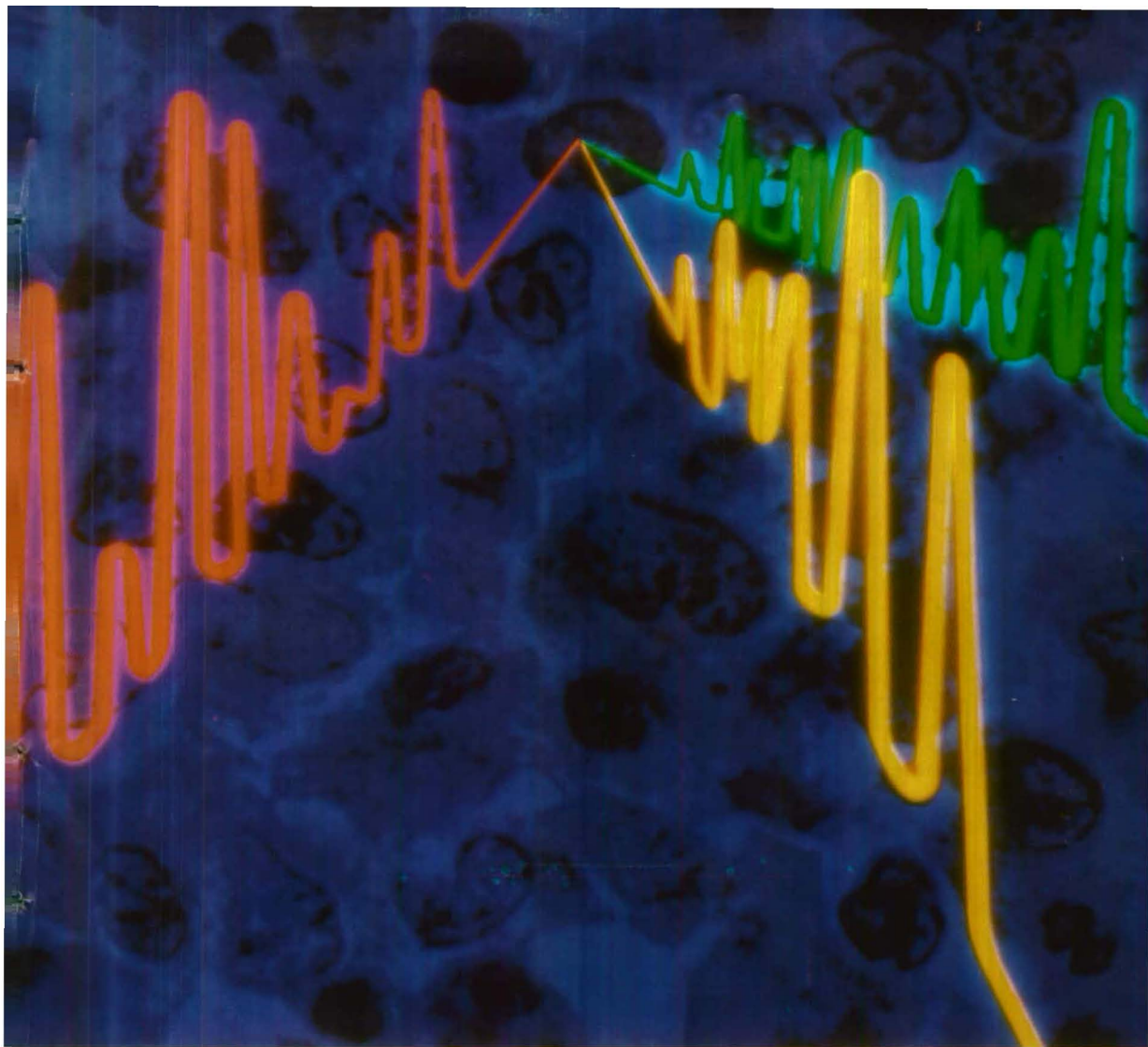
The performance of some cell designs for laser-induced fluorescence detection in open-tubular liquid chromatography by H. P. M. van Vliet and H. Poppe (Amsterdam, The Netherlands) (Received June 25th, 1985)	149
Direct coupling of micro high-performance liquid chromatography with fast atom bombardment mass spectrometry by Y. Ito, T. Takeuchi, D. Ishii and M. Goto (Nagoya-shi, Japan) (Received May 28th, 1985)	161
Multichannel spectrophotometric detector for fused-silica capillary tube isotachopheresis by M. Goto, K. Irino and D. Ishii (Nagoya-shi, Japan) (Received June 7th, 1985)	167
Quantitative analysis of hydrocarbons in gasolines by capillary gas-liquid chromatography. II. Isothermal and temperature-programmed analyses by E. Matisová, J. Krupčík, P. Čellár and A. Kočan (Bratislava, Czechoslovakia) (Received June 17th, 1985)	177
Capillary gas chromatographic method for the determination of complex mixture of isocyanates and amines by G. Skarping, L. Renman, C. Sangö, L. Mathiasson and M. Dalene (Lund, Sweden) (Received May 28th, 1985)	191
An improved solvent-extraction based procedure for the gas chromatographic analysis of resin and fatty acids in pulp mill effluents by R. H. Voss and A. Rapsomatiotis (Pointe Claire, Canada) (Received June 13th, 1985)	205
Pentafluorobenzyl <i>p</i> -toluenesulphonate as a new derivatizing reagent for gas chromatographic determination of anions by K. Funazo, M. Tanaka, K. Morita, M. Kamino and T. Shono (Osaka, Japan) and H.-L. Wu (Kaohsiung, Taiwan) (Received May 28th, 1985)	215
3-Bromomethyl-6,7-dimethoxy-1-methyl-2(1 <i>H</i>)-quinoxalinone as a new fluorescence derivatization reagent for carboxylic acids in high-performance liquid chromatography by M. Yamaguchi, S. Hara, R. Matsunaga, M. Nakamura and Y. Ohkura (Fukuoka, Japan) (Received May 20th, 1985)	227
Decapreno- β -carotene as an internal standard for the quantification of the hydrocarbon carotenoids by high-performance liquid chromatography by F. Khachik and G. R. Beecher (Beltsville, MD, U.S.A.) (Received June 20th, 1985)	237
A combined recycling affinity column-filtration technique by J. P. Charlton (Charlottesville, VA, U.S.A.) (Received June 20th, 1985)	247
Three independent methods for quantitative determination of octyl covalently coupled to Sepharose CL-4B by B.-L. Johansson and I. Drevin (Uppsala, Sweden) (Received June 7th, 1985)	255
Adaptation of the equipment for high-performance electrophoresis to isoelectric focusing by S. Hjertén and M.-D. Zhu (Uppsala, Sweden) (Received June 25th, 1985)	265
Isotachopheretic control of peptide synthesis and purification. A novel approach using ultraviolet detection at 206 nm by P. Stehle and P. Fürst (Stuttgart, F.R.G.) (Received June 3rd, 1985)	271
Quantitation of long-chain alkylbenzenes in environmental samples by silica gel column chromatography and high-resolution gas chromatography by H. Takada and R. Ishiwatari (Tokyo, Japan) (Received June 17th, 1985)	281
Isolation and quantitative analysis of phosphatidylglycerol and glycolipid molecular species using reversed-phase high-performance liquid chromatography with flame ionization detection by L. A. Smith, H. A. Norman, S. H. Cho and G. A. Thompson, Jr. (Austin, TX, U.S.A.) (Received May 30th, 1985)	291

Simultaneous determination of free and conjugated ecdysteroids by liquid chromatography by S. Scalia (Ferrara, Italy) and E. D. Morgan (Keele, U.K.) (Received June 5th, 1985)	301
Isolation of erythromycins and related substances from fermentation residues of <i>Streptomyces erythreus</i> by high-performance liquid chromatography on silica gel by I. O. Kibwage, G. Janssen, E. Roets, J. Hoogmartens and H. Vanderhaeghe (Leuven, Belgium) (Received June 13th, 1985)	309
Isolation and stereospecific determination of the enantiomers of oxindazac by direct liquid chromatographic resolution on triacetylcellulose by E. Francotte, H. Stierlin and J. W. Faigle (Basle, Switzerland) (Received June 17th, 1985)	321
Studies on the analysis of food additives by high-performance liquid chromatography. V. Simultaneous determination of preservatives and saccharin in foods by ion-pair chromatography by H. Terada and Y. Sakabe (Nagoya, Japan) (Received June 17th, 1985)	333
<i>Notes</i>	
Preparation of glass and fused-silica capillary columns coated with immobilized XE-60 by W. Blum (Basle, Switzerland) and K. Grob (Dübendorf, Switzerland) (Received June 27th, 1985)	341
A microscopic investigation of the surface of carbon-silica adsorbents. II. Relationships between the type of information obtainable about the surface and the microscopic techniques used for its examination by E. Tracz and R. Lebeda (Lublin, Poland) (Received June 13th, 1985)	346
Comparative gas chromatographic studies of bonded and physically coated PEG 20M and its derivative phases with reference to some high-boiling isomeric solutes by S. B. Bendre, A. N. Kadam and B. B. Ghatge (Pune, India) (Received May 30th, 1985)	359
Determination of furosin by gas-liquid chromatography by W. Büser (Kronshagen, F.R.G.) and H. F. Erbersdobler (Kiel, F.R.G.) (Received July 1st, 1985)	363
Determination of phenylurea herbicides by high-performance liquid chromatography with electrochemical detection by G. Chiavari and C. Bergamini (Bologna, Italy) (Received July 5th, 1985)	369
Direct determination of acrylamide in tissue culture solution by liquid chromatography using column switching by N. L. Freshour, P. W. Langvardt, S. W. Frantz and M. D. Dryzga (Midland, MI, U.S.A.) (Received June 24th, 1985)	376
Séparation et dosage des différents constituants de la troxérutine par chromatographie liquide haute performance en phase inverse. Application au contrôle pharmaceutique par M. D. Le Hoang, E. Postaire, P. Prognon et D. Pradeau (Paris, France) et A. Blondin et J. Sauziere (Buc, France) (Reçu le 24 juin 1985)	382
Reversed-phase high-performance liquid chromatography of natural and synthetic sauvagines by L. Rusconi and P. C. Montecucchi (Milan, Italy) (Received July 5th, 1985)	390
Analytical and preparative reversed-phase liquid chromatography of secoiridoid glycosides by D. Schaufelberger and K. Hostettmann (Lausanne, Switzerland) (Received June 25th, 1985)	396
Analytical isoelectric focusing of native and modified haemoglobins after treatment with 4-hydroxymercuribenzoate by T. I. Přistoupil, M. Kramlová, H. Fořtová and V. Fričová (Prague, Czechoslovakia) (Received June 25th, 1985)	401

(Continued overleaf)

Contents (continued)

Gas chromatographic and mass spectrometric identification of sulphur gases in kraft digestion plants by J. Kangas (Kuopio, Finland) (Received June 21st, 1985)	405
Simple method for concentrating volatiles in water for gas chromatographic analysis by vacuum distillation by R. P. Kozloski (New Haven, CT, U.S.A.) (Received July 23rd, 1985)	408
Separation of phenylthiocarbamyl amino acids by high-performance liquid chromatography on Spherisorb octadecylsilane columns by C.-Y. Yang and F. I. Sepulveda (Houston, TX, U.S.A.) (Received July 10th, 1985)	413
High-performance liquid chromatographic analysis of Aspartame by G. Verzella and A. Mangia (Milan, Italy) (Received June 24th, 1985)	417
High-performance liquid chromatography system for the separation of ergot alkaloids with appli- cability to the analysis of illicit lysergide (LSD) by R. Gill and J. A. Key (Reading, U.K.) (Received July 22nd, 1985)	423
Plantes médicinales africaines. XIX. Dosage de la vitexine par chromatographie liquide haute per- formance dans un extrait brut de <i>Combretum micranthum</i> G. Don par E. Bassene, A. Laurance, D. Olschwang et J. L. Pousset (Dakar, Sénégal) (Reçu le 22 juillet 1985)	428
Semi-preparative isolation of crepenynic acid, a potential inhibitor of essential fatty acid metabolism by G. L. Ford (North Ryde, Australia) (Received July 18th, 1985)	431
Rapid and convenient separation of pentachlorophenol from human fat using silica Sep-Pak™ car- tridges by G. A. S. Ansari and P. Y. Hendrix (Galveston, TX, U.S.A.) (Received July 2nd, 1985)	435
A rapid method for the separation and quantification of simple phenolic acids in plant material using high-performance liquid chromatography by M.F. Wilson (Surbiton, U.K.) (Received July 4th, 1985)	440
Reversed-phase high-performance liquid chromatography of methyl isocyanate by C. D. Raghuvveran and M. P. Kaushik (Madhya Pradesh, India) (Received June 3rd, 1985)	446
High-performance liquid chromatographic determination of melamine extracted from cups made of melamine resin by T. Inoue, H. Ishiwata, K. Yoshihira and A. Tanimura (Tokyo, Japan) (Received June 3rd, 1985)	450
Gradient separation of fatty acids (C ₁₄ -C ₃₀) by reversed-phase high-performance liquid chromato- graphy by T. Řezanka and M. Podojil (Prague, Czechoslovakia) (Received June 25th, 1985)	453
Reversed-phase high-performance liquid chromatographic separation of closely related furocou- marins by C. A. J. Erdelmeier, B. Meier and O. Sticher (Zürich, Switzerland) (Received July 1st, 1985)	456
Shelf-life of unused high-performance liquid chromatographic columns by N. G. S. Gopal and G. Sharma (Bombay, India) (Received June 7th, 1985)	461
Separation of organic quaternary salts by reversed-phase thin-layer chromatography by S. Munavalli, F.-L. Hsu, S. F. Hatem and E. J. Poziomek (Aberdeen Proving Ground, MD, U.S.A.) (Received June 18th, 1985)	463
<i>Letter to the Editor</i>	
Effect of copper(II) sulphate impregnation of Chromarods on the sensitivity of the Iatrascan detec- tion system to lipids by A. S. Ritchie (Reading, U.K.) (Received July 15th, 1985)	468
<i>Author Index</i>	469
<i>Erratum</i>	472



ZORBAX® Bio Series columns lift your biological separations to new peaks!

Du Pont's new Zorbax® Bio Series—a growing family of high-resolution HPLC columns to meet specific separation needs.

Separate proteins by size, from 4,000 to 900,000 daltons, with the Zorbax® Bio Series GF-250 and GF-450 alkali-stable (up to pH 8.5) silica gel filtration columns.

Isocratic analysis of PTH amino acids with excellent results using the Zorbax® Bio Series PTH Amino Acid column. Isocratic analysis maximizes reproducibility, simplifies separation adjustment, and provides long column life.

Separate peptides and proteins with the reversed phase Zorbax® Bio Series PEP-RP1 column. Optimized large-pore packing for higher resolution and excellent loading capacity.

Large-scale chromatography—Zorbax® Bio Series preparative columns and packings allow direct scale-up from analytical with no need for additional method development.

Du Pont manufactures Zorbax® Chromatography Packings in plant-scale facilities, thereby assuring long-term supplies of reproducible products.

For more information and free literature on the growing Bio Series family, call 1-800-237-8400, or write: DuPont, Biotechnology Systems, Leadtrack, 595 Colonial Park Drive, Room 250, Roswell, GA 30075.

Biotechnology Systems



MN enlarges HPLC programme

NUCLEOSIL® 120 **pressure stable up to** **min. 800 bar (ca. 11,600 psi)**

NUCLEOSIL® 120 (3 μ , 5 μ , 7 μ and 10 μ) offers the following advantages:

- pressure stable up to min. 800 bar (ca. 11,600 psi)
- higher packing pressure, therefore higher packing density
- longer column life
- shorter analysis times, due to higher flow rates
- lower solvent consumption, since pore volume is only 0.7 ml/g
- many different chemically bonded phases available

NUCLEOSIL® also available with

50, 100, 300, 500 and 1,000 Å pore diameters.

Please request your free copy of our HPLC Catalogue today from:
MACHEREY-NAGEL GmbH & Co. KG · P.O.Box 307
D-5160 Düren, West Germany
☎ (02421) 61071 · Telex 833893 mana d



MACHEREY-NAGEL · DÜREN

MN

513

For advertising information please contact our advertising representatives

U.S.A./CANADA

Michael Baer

50 East 42nd St,
Suite 504,
NEW YORK, NY 10017
Tel.: (212) 682-2200

GREAT BRITAIN

T.G. Scott & Son Ltd.

Mr. M.L. White
30-32 Southampton Street
LONDON WC2E 7HR
Tel.: (01) 379-7264

OR

General Advertising Department

ELSEVIER/EXCERPTA MEDICA/NORTH-HOLLAND

Ms W. van Cattenburch
P.O. Box 211
1000 AE AMSTERDAM, The Netherlands
Tel.: (020) 5803.714/715 Telex: 18582 ESPA NL

New Gilson auto-sampling injector for HPLC.

NOW THE MOST BORING PROCEDURES ARE AUTOMATIC.

Gilson introduces Model 231-401, a new robotic unit with advanced capabilities for HPLC sample preparation and injection:

Automatic sample preparation.

Speeds-up routine procedures including on-line pre-column derivatizations. Adds internal standards. Performs sequential dilutions for calibration plots.

Automatic sample injection.

Loads contamination-free with minimal loss. Handles up to 120 analytes. Injects variable volumes with unlimited replicates. Automatically dilutes samples generating over-scaled peaks.

Fast, reliable, automatic. The 231-401 takes the tedium out of HPLC.



GILSON
INTERNATIONAL

France : Gilson Medical Electronics (France) S.A., B.P. 45, F - 95400 Villiers-le-Bel, France, Tél. (1) 39.90.54.41 - Télex : 696 682.

United States : Gilson Medical Electronics, Inc., Box 27, 3000 W. Beltline, Middleton, WI 53562 U.S.A., Tel. 608/836-1551, Telex : 265478. MTWI.



Gilson chromatographers examine the results of several overnight unattended experiments with septum-sealed vials. The coefficient of variation was lower than 0.3 % for peak area repeatability.

Gilson Model 231-401 auto-sampling injector

STATISTICAL TREATMENT OF EXPERIMENTAL DATA

By J.R. GREEN, *Lecturer in Computational and Statistical Science, University of Liverpool, U.K.* and D. MARGERISON, *Senior Lecturer in Inorganic, Physical and Industrial Chemistry, University of Liverpool, U.K.*

PHYSICAL SCIENCES DATA 2

This book first appeared in 1977. In 1978 a revised reprint was published and in response to demand, further reprints appeared in 1979, 1980 and 1983. Intended for researchers wishing to analyse experimental data, this work will also be useful to students of statistics. Statistical methods and concepts are explained and the ideas and reasoning behind statistical methodology clarified. Noteworthy features of the text are numerical worked examples to illustrate formal results, and the treatment of many practical topics which are often omitted from standard texts, for example testing for outliers, stabilization of variances and polynomial regression.

What the reviewers had to say:

"The index is detailed; the format is good; the presentation is clear; and no mathematics beyond calculus is assumed".

—CHOICE

"A lot of thought has gone into this book and I like it very much. It deserves a place on every laboratory bookshelf".

—CHEMISTRY IN
BRITAIN

1977. Reprinted 1978,
1979, 1980, 1983
x + 382 pages
US \$ 50.00 / Dfl. 135.00
ISBN 0-444-41725-7



ELSEVIER

P.O. Box 211, 1000 AE Amsterdam, The Netherlands.
P.O. Box 1663, Grand Central Station, New York, NY 10163.

The Dutch guilder price is definitive.

If you have to say FPLC you are half way there ...

... because PepRPC™ and ProRPC™ from Pharmacia are the state of the art in reversed phase chromatography media for separating and recovering biological molecules.

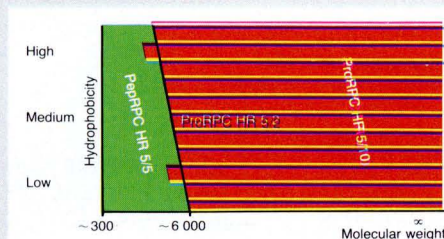
Pharmacia reversed phase chromatography columns have been specially designed for high resolution chromatography of peptides, polypeptides and proteins, forming a natural complement to ion exchange

chromatography and chromatofocusing when separating biomolecules using the Pharmacia FPLC System.

Pharmacia media PepRPC and ProRPC provide you with new and unique reversed phase selectivities (C_2/C_{18} and C_1/C_8) optimised for peptides and proteins. Excellent control over the new synthesis ensures reproducibility from batch to batch.

... so go all the way.

The Pharmacia RPC media are prepacked in borosilicate glass columns with optimised lengths to utilize a range of reversed phase separation techniques for high resolution and high recoveries of both large and small polypeptides.



- Controlled synthesis for batch to batch reproducibility
- High recoveries of peptides and polypeptides
- High resolution of hydrophobic fragments
- Optimised bonded phase composition

FPLC from Pharmacia
goes beyond HPLC with biocompatibility,

ATOMIC ABSORPTION SPECTROMETRY

edited by

J. E. CANTLE

*VG Isotopes Ltd., Winsford,
Great Britain*

Techniques and Instrumentation in Analytical Chemistry Vol. 5

Atomic absorption spectroscopy is now established as one of the most useful tools for analysing trace metals in samples which may be taken into solution. It has wide applicability, is inexpensive and can be used with confidence by a wide range of analysts. The rapid growth and advancement of electrothermal atomisation methods and their subsequent automation has consolidated the technique's position by extending the dynamic analytical range down to concentration levels that other techniques cannot reach.

The topic is treated here in a very practical manner and the book is mainly concerned with real-life analyses for practising instrument users. The book is invaluable to those working in all laboratories where the technique is used as the methods described can be interpreted to fit all suppliers' hardware.

**Of interest to those working in:
Analytical Chemistry, Spectroscopy,
Geochemistry, Agricultural and
Environmental Chemistry**

CONTENTS: 1. Basic Principles (*J. W. Robinson*). 2. Instrumental Requirements and Optimisation (*J. E. Cantle*). 3. Practical Techniques (*J. E. Cantle*). 4a. Water and Effluents (*B. J. Farey and L. A. Nelson*). 4b. Marine Analysis by AAS (*H. Haraguchi and K. Fuwa*). 4c. Analysis of Airborne Particles in the Workplace and Ambient Atmospheres (*T. J. Kneip and M. T. Kleinman*). 4d. Application of AAS to the Analysis of Foodstuffs (*M. Ihnat*). 4e. Applications of AAS in Ferrous Metallurgy (*K. Ohls and D. Sommer*). 4f. The Analysis of Non-ferrous Metals by AAS (*F. J. Bano*). 4g. Atomic Absorption Methods in Applied Geochemistry (*M. Thompson and S. J. Wood*). 4h. Applications of AAS in the Petroleum Industry (*W. C. Campbell*). 4i. Methods for the Analysis of Glasses and Ceramics by Atomic Spectroscopy (*W. M. Wise et al.*). 4j. Clinical Applications of Flame Techniques (*B. E. Walker*). 4k. Elemental Analysis of Body Fluids and Tissues by Electrothermal Atomisation and AAS (*H. T. Delves*). 4l. Forensic Science (*U. Dale*). 4m. Fine, Industrial and Other Chemicals. **Subject Index.** (All chapters begin with an Introduction and end with References.)

1982 xvi + 448 pages
US \$ 83.25 / Dfl. 225.00
ISBN 0-444-42015-0

ELSEVIER



P.O. Box 330,
1000 AH Amsterdam,
The Netherlands.

P.O. Box 1663,
Grand Central Station,
New York, NY 10163.

The Dutch guilders price is definitive. US \$ prices are subject to exchange rate fluctuations.

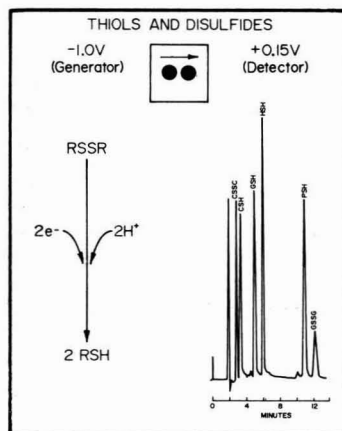
Liquid Chromatography / Electrochemistry

In 1974 BAS introduced the first commercial LCEC system. With over 5000 units installed and the largest research team to support them, it's not surprising that our nearest competitors are several generations behind us. Our thin-layer transducers lead the way with a wide selection of electrode materials in a variety of interchangeable configurations. The latest member of the family is the new LC4B/17 dual electrode amperometry package. Parallel and series amperometry can enhance selectivity, detection limits, speed and gradient compatibility. Let us show you how it's done, no one else can.

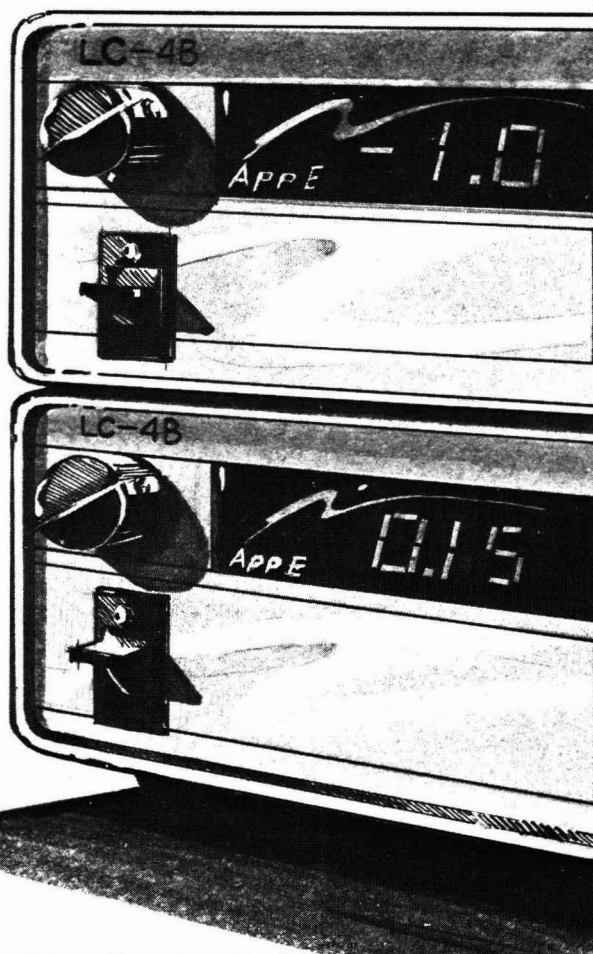
BAS

Purdue Research Park,
2701 Kent Avenue,
West Lafayette, IN. 47906
317-463-4527 TLX 276141

CANADA: Mandel Scientific
FRANCE: Biochrom s.a.r.l. (Vindelle)



Dual Electrode Detection: Standard mixture of Cystine, Cysteine, Glutathione, Homocysteine, Penicillamine, Glutathione Disulfide



When you say "why FPLC" you are half way there ...

... because FPLC™ instrumentation from Pharmacia is the state of the art in high performance chromatography equipment for the separation of biologically active molecules.

Unlike any other chromatography system, the FPLC System was designed from the beginning to meet the demands for high performance separations of complex biomolecules. Since all wetted surfaces are of glass, titanium and fluoroplastics, aqueous

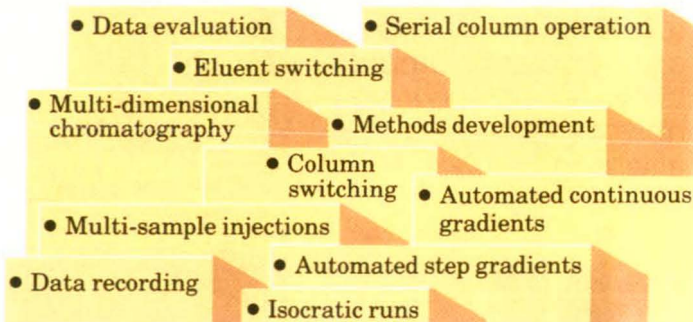


buffer solutions and organic solvents may be used for separating biological molecules while maintaining biological activity.

The Pharmacia FPLC System is modular and can be tailored to your needs and budget. Depending on the exact configuration chosen, the FPLC System will provide you with any of the following techniques using both the new high performance columns and traditional chromatographic procedures.

... so go all the way.

With the Pharmacia FPLC System separations of biomolecules are easily performed. Chromatography can be fully automated and reproducible results will be obtained while operator time is kept to a minimum.



FPLC from Pharmacia
goes beyond HPLC with biocompatibility



Laboratory Separation Division
S-751 82 Uppsala, Sweden



Use
this
coupon
(or xerox
copy) for free
information on
the advertised
products.
Just
quote
ad
no.

Reader service coupon

JOURNAL OF

CHROMATOGRAPHY

INTERNATIONAL JOURNAL ON CHROMATOGRAPHY, ELECTROPHORESIS AND RELATED METHODS

I would like to receive, without any obligation, further information on the following advertisement numbers:

I am especially interested in the fields indicated below:

- | | |
|--|--|
| <input type="checkbox"/> 6040 Analytical Chemistry | <input type="checkbox"/> 6240 Pharmaceutical Chemistry |
| <input type="checkbox"/> 6042 Laboratory Instrumentation | <input type="checkbox"/> 6241 Medicinal Chemistry |
| <input type="checkbox"/> 6050 Chromatography | <input type="checkbox"/> 6242 Clinical Chemistry |
| <input type="checkbox"/> 6140 Spectroscopy | <input type="checkbox"/> 6260 Environmental Chemistry |
| <input type="checkbox"/> 6150 Mass Spectrometry | <input type="checkbox"/> 16290 Scientific Software |

Name: _____

Position: _____

Address: _____

please use
envelope;
mail as
printed
matter

ELSEVIER SCIENCE PUBLISHERS

Advertising department

P.O. BOX 211,

1000 AE AMSTERDAM – THE NETHERLANDS



please use
envelope;
mail as
printed
matter

ELSEVIER SCIENCE PUBLISHERS

Advertising department

P.O. BOX 211,

1000 AE AMSTERDAM – THE NETHERLANDS



Reader service coupon



*Use
this
coupon
(or photo
copy) for free
information on
the advertised
products.
Just
quote
ad
no.*

I would like to receive, without any obligation, further information on the following advertisement numbers:

I am especially interested in the fields indicated below:

- | | |
|--|--|
| <input type="checkbox"/> 6040 Analytical Chemistry | <input type="checkbox"/> 6240 Pharmaceutical Chemistry |
| <input type="checkbox"/> 6042 Laboratory Instrumentation | <input type="checkbox"/> 6241 Medicinal Chemistry |
| <input type="checkbox"/> 6050 Chromatography | <input type="checkbox"/> 6242 Clinical Chemistry |
| <input type="checkbox"/> 6140 Spectroscopy | <input type="checkbox"/> 6260 Environmental Chemistry |
| <input type="checkbox"/> 6150 Mass Spectrometry | <input type="checkbox"/> 16290 Scientific Software |

Name: _____

Position: _____

Address: _____

JOURNAL OF CHROMATOGRAPHY

VOL. 346 (1985)

JOURNAL *of* CHROMATOGRAPHY

INTERNATIONAL JOURNAL ON CHROMATOGRAPHY,
ELECTROPHORESIS AND RELATED METHODS

EDITOR

MICHAEL LEDERER (Switzerland)

ASSOCIATE EDITOR

K. MACEK (Prague)

EDITOR, SYMPOSIUM VOLUMES

E. HEFTMANN (Berkeley, CA)

EDITORIAL BOARD

W. A. Aue (Halifax), V. G. Berezkin (Moscow), V. Betina (Bratislava), A. Bevenue (Honolulu, HI), P. Boček (Brno), P. Boulanger (Lille), A. A. Boulton (Saskatoon), G. P. Cartoni (Rome), S. Dilli (Kensington, N.S.W.), L. Fishbein (Jefferson, AR), R. W. Frei (Amsterdam), A. Frigerio (Milan), C. W. Gehrke (Columbia, MO), E. Gil-Av (Rehovot), G. Guiochon (Palaiseau), I. M. Hais (Hradec Králové), J. K. Haken (Kensington, N.S.W.), S. Hjertén (Uppsala), E. C. Horning (Houston, TX), Cs. Horváth (New Haven, CT), J. F. K. Huber (Vienna), A. T. James (Sharnbrook), J. Janák (Brno), E. sz. Kováts (Lausanne), K. A. Kraus (Oak Ridge, TN), E. Lederer (Gif-sur-Yvette), A. Liberti (Rome), H. M. McNair (Blacksburg, VA), Y. Marcus (Jerusalem), G. B. Marin-Bettolo (Rome), A. J. P. Martin (Lausanne), Č. Michalec (Prague), R. Neher (Basel), G. Nickless (Bristol), J. Novák (Brno), N. A. Parris (Wilmington, DE), R. L. Patience (London), P. G. Righetti (Milan), O. Samuelson (Göteborg), R. Schwarzenbach (Dübendorf), G. Semenza (Zürich), L. R. Snyder (Yorktown Heights, NY), A. Zlatkis (Houston, TX)

EDITORS, BIBLIOGRAPHY SECTION

Z. Deyl (Prague), J. Janák (Brno), K. Macek (Prague)



ELSEVIER

AMSTERDAM — OXFORD — NEW YORK — TOKYO

J. Chromatogr., Vol. 346 (1985)

All rights reserved. No part of this publication may be reproduced, stored in a retrieval system or transmitted in any form or by any means, electronic, mechanical, photocopying, recording or otherwise, without the prior written permission of the publisher, Elsevier Science Publishers B.V., P.O. Box 330, 1000 AH Amsterdam, The Netherlands.

Upon acceptance of an article by the journal, the author(s) will be asked to transfer copyright of the article to the publisher. The transfer will ensure the widest possible dissemination of information.

Submission of an article for publication implies the transfer of the copyright from the author(s) to the publisher and entails the authors' irrevocable and exclusive authorization of the publisher to collect any sums or considerations for copying or reproduction payable by third parties (as mentioned in article 17 paragraph 2 of the Dutch Copyright Act of 1912 and in the Royal Decree of June 20, 1974 (S. 351) pursuant to article 16 b of the Dutch Copyright Act of 1912) and/or to act in or out of Court in connection therewith.

Special regulations for readers in the U.S.A. This journal has been registered with the Copyright Clearance Center, Inc. Consent is given for copying of articles for personal or internal use, or for the personal use of specific clients. This consent is given on the condition that the copier pays through the Center the per-copy fee stated in the code on the first page of each article for copying beyond that permitted by Sections 107 or 108 of the U.S. Copyright Law. The appropriate fee should be forwarded with a copy of the first page of the article to the Copyright Clearance Center, Inc., 27 Congress Street, Salem, MA 01970, U.S.A. If no code appears in an article, the author has not given broad consent to copy and permission to copy must be obtained directly from the author. All articles published prior to 1980 may be copied for a per-copy fee of US\$ 2.25, also payable through the Center. This consent does not extend to other kinds of copying, such as for general distribution, resale, advertising and promotion purposes, or for creating new collective works.

Special written permission must be obtained from the publisher for such copying.

CHROM. 17 959

THEORY OF ANION CONTRIBUTIONS TO NON-LINEAR ELECTRON-CAPTURE DETECTOR RESPONSE

GREGORY WELLS

Varian Instrument Group, Walnut Creek Division, 2700 Mitchell Drive, Walnut Creek, CA 94598 (U.S.A.)

(Received June 10th, 1985)

SUMMARY

A theoretical model is developed to investigate the effects of anion collection on the linear response of the constant-current mode of operation of an electron-capture detector. The results indicate that a non-linear response is expected at high pulse frequencies. The dependence of the linear range on reference current, base frequency, electron concentration and attachment rate constant is examined. A means of extending the linear range by preventing the collection of anions is discussed.

INTRODUCTION

Many theories have been formulated to describe the basic operation of electron-capture detectors. The earliest kinetic model was that of Wentworth *et al.*¹ for the constant-frequency pulsed mode of operation. This mode suffers from having a limited linear range. A substantial improvement in the linear response was effected by Maggs *et al.*² who suggested that the electron-capture detector be operated in the constant-current mode. Using a simplified form of Wentworth's equation, in which the reverse of the electron attachment process was neglected, Maggs showed that the collected current I , for a given electron production rate per unit volume $k_p q$, in a cell of volume V , is given by

$$I = \frac{k_p q V}{(k_d + ck_1)T} \left[1 - e^{-(k_d + ck_1)T} \right] \quad (1)$$

where c is the sample concentration, k_1 the attachment rate constant, k_d the pseudo recombination rate constant and T is the pulse period. If the pulse frequency ($f = 1/T$) is changed as the sample concentration is varied, so as to keep the collected current I equal to a constant reference current I , then

$$(k_d + ck_1) T = K = (k_d + ck_1)/f \quad (2)$$

where K is a constant. The change in frequency is proportional to the sample concentration and is given by

$$f - f_0 = c \frac{k_1}{K} \quad (3)$$

where $f_0 = k_d/K$ ($c = 0$).

Although the constant-current mode was found to significantly increase the linear range of the electron-capture detector, the linearity was not limitless as is implied by eqns. 1–3. Some additional mechanisms must exist to account for the observed non-linear response at high sample concentrations. The inability of this model to account for this discrepancy is due to the simplifying assumptions that were made in deriving these equations. An extended analysis by Sliwka *et al.*³ included the effects of the finite pulse width and electron drift velocity in the operation of the electron-capture detector. More recently Gobby *et al.*⁴ investigated many of the assumptions of these theories and proposed a model based on space charge driven charge migration, which included the dynamical effects of the positive ions. Although many of the basic assumptions were quite different from those of the classical model, the resulting equations describing the response as a function of sample concentration were identical to those derived by Wentworth. These models were quite successful in describing most of the main features that have been experimentally observed for small sample concentrations. Lovelock^{5,6}, and Knighton and Grimsrud^{7,8} have successfully applied similar theories to the case of strongly attaching compounds, where the effective concentration of analyte in the detector cell is reduced due to destructive electron attachment. However, none of the models even qualitatively can account for the loss in detector sensitivity that is known to occur at higher sample concentrations for the constant-current electron-capture detector.

In this paper a theoretical model which includes the collection of anions is used to investigate the importance of this process in the reduction of the response. It will be shown that many of the experimentally observed features that occur at large sample concentrations can be qualitatively explained in terms of anion collection effects.

MATHEMATICAL MODEL

The analysis presented here not only includes those processes involving the electrons, but also specifically takes into account the dynamic effects of the anions formed by the electron-attachment process. The chemical processes to be considered are listed in eqns. 4a–4d and are: (4a) ^{63}Ni -induced thermal electron formation; (4b) irreversible electron attachment; (4c) loss of electrons by recombination with positive ions; and (4d) loss of anions by recombination with positive ions. In addition to the chemical processes the dynamic effect of charge removal by the applied electric field must be included. These processes are given in eqn. 5.





The rate equations to be solved that describe the processes given in eqns. 4 and 5 can be divided into two different time regions. Region A where the electric field is on ($0 \leq t \leq t_p$), where t_p is pulse width; and region B where the electric field is off ($t_p \leq t \leq T$), where T is the pulse period. The differential equations for the two regions are given in eqns. 6 and 7.

(A) $0 \leq t \leq t_p$

$$\frac{d(e^-)}{dt} = k_p - k_e(e^-) \quad (6a)$$

$$\frac{d(A^-)}{dt} = k_1(A)(e^-) - k_A(A^-) \quad (6b)$$

$$k_e = k_1(A) + (P^+)k_{2e} + k_{3e} \quad (6c)$$

$$k_A = k_{2A}(P^+) + k_{3A} \quad (6d)$$

(B) $t_p < t \leq T$

$$\frac{d(e^-)}{dt} = k_p - k'_e(e^-) \quad (7a)$$

$$\frac{d(A^-)}{dt} = k_1(A)(e^-) - k'_A(A^-) \quad (7b)$$

$$k'_e = k_1(A) + (P^+)k_{2e} \quad (7c)$$

$$k'_A = k_{2A}(P^+) \quad (7d)$$

In order to make analytical solutions to eqns. 6 and 7 more tractable, some assumptions need to be made. The first assumption is that the processes within the cell are homogeneous. Grimsrud and Connally⁹ have investigated the spacial distribution of ions and electrons within cells of cylindrical symmetry. He has found that for a cell with a diameter of 5 mm, the relative ion density at the center is only 20% less than

at the walls where the ^{63}Ni source is located. This is sufficiently homogeneous for the discussion given here. The rate at which electrons and positive ions are created per unit time and volume can thus be approximated by a constant, k_p . The second assumption is that the positive ion density remains constant, independent of pulse frequency. This would allow the quantities involving (P^+) in eqns. 6c and d, and 7c and d to be taken as constants. The results of Gobby *et al.*⁴ and the investigations of Grimsrud and co-workers^{8,10-12} indicate that this is a quite reasonable assumption for the constant current mode of operation. The last approximation is that the electric field is constant throughout the cell. This allows the rate constant for charge removal by the field to be expressed as a constant

$$k_{3e} = v_e A / V \quad (8a)$$

$$k_{3A} = v_A A / V \quad (8b)$$

$$v_{e,A} = K_{e,A} U \quad (8c)$$

where $v_{e,A}$ = electron or anion drift velocity; A = area of anode; V = volume of cell; K_e = electron mobility^{13,14}; K_A = anion mobility^{13,14}; U = cell potential.

Although these rate constants are strictly true only for constant electric fields, E (*i.e.*, parallel planar electrode geometry where $E \propto U$) this approximation should be reasonable if the average field is used and since all other kinetic processes have been assumed to be homogeneous throughout the cell. A more detailed analysis of this assumption will be made in a later section of this paper.

It can be seen from eqns. 6b and 7b that the solutions of the equations for the anions require a knowledge of the electron concentrations as a function of time for the time intervals A and B. The solution of eqn. 6a for region A for one time cycle is

$$(\text{e}^-)_t = \frac{k_p}{k_e} + \left[(\text{e}^-)_0 - \frac{k_p}{k_e} \right] e^{-k_e t} \quad (9)$$

where $(\text{e}^-)_0$ is the electron concentration at $t = 0$, which is initially unknown, but must match that at the end of the first time cycle $t = T$. The general solution of eqn. 7a for region B is

$$(\text{e}^-)_t = \frac{k_p}{k'_e} + \left[(\text{e}^-)_{t_p} - \frac{k_p}{k'_e} \right] e^{-k'_e(t - t_p)} \quad (10)$$

The solution given in eqn. 10 for $t = T$ can be used to solve for $(\text{e}^-)_t$ in region A for the next cycle of time. The electron concentration after m cycles at the beginning of the voltage pulse in region A at time mT is

$$(\text{e}^-)_{mT} = \frac{k_p}{k'_e} + \left[(\text{e}^-)_{mt_p} - \frac{k_p}{k'_e} \right] e^{-k'_e(T - t_p)} \quad (11)$$

where

$$(e^-)_{mt_p} = \frac{k_p}{k_e} + \left[(e^-)_{(m-1)T} - \frac{k_p}{k_e} \right] e^{-k_e t_p} \quad (12)$$

After several cycles

$$\lim_{m \rightarrow \infty} (e^-)_{mT} = (e^-)_{(m-1)T} \equiv (e^-)_T$$

and

$$\lim_{m \rightarrow \infty} (e^-)_{mt_p} = (e^-)_{(m-1)t_p} \equiv (e^-)_{t_p}$$

Thus

$$(e^-)_T = \frac{k_p}{k'_e} + \left\{ \frac{k_p}{k_e} + \left[(e^-)_T - \frac{k_p}{k_e} \right] e^{-k'_e t_p} - \frac{k_p}{k'_e} \right\} e^{-k'_e (T - t_p)} \quad (13)$$

Which allows the electron concentration at the beginning of the extraction pulse in region A to be found

$$(e^-)_T = \frac{\frac{k_p}{k'_e} + \left(\frac{k_p}{k_e} - \frac{k_p}{k'_e} \right) e^{-k'_e (T - t_p)} - \frac{k_p}{k'_e} e^{-k_e t_p - k'_e (T - t_p)}}{1 - e^{-k_e t_p - k'_e (T - t_p)}} \quad (14)$$

Thus the general solution of equation 6a for region A is

$$(e^-)_t = \frac{k_p}{k_e} + \left[(e^-)_T - \frac{k_p}{k_e} \right] e^{-k_e t} \quad (15)$$

The electron current collected at the anode during the extraction pulse is

$$I_e = \frac{1}{T} \int_0^{t_p} (e^-)_t q A v_e dt \quad (16)$$

where $(e^-)_t$ is given by eqn. 15. The result is

$$I_e = q A v_e \left\{ \frac{k_p}{k_e} \frac{t_p}{T} + \frac{k_p}{k_e T} [\chi] \left[1 - e^{-k_e t_p} \right] \right\} \quad (17)$$

$$\chi = \frac{1}{k'_e} + \left(\frac{1}{k_e} - \frac{1}{k'_e} \right) e^{-k'_e (T - t_p)} - \frac{1}{k_e} e^{-k_e t_p - k'_e (T - t_p)} \quad (18)$$

Now that expressions for the electron concentration as a function of time for region A have been obtained, eqn. 15; and for region B, eqn. 10; it is possible to return to eqns. 6b and 7b and solve for the anion concentrations as a function of time. Using the same approach as above and requiring:

$$\lim_{m \rightarrow \infty} (A^-)_{mT} = (A^-)_{(m-1)T} \equiv (A^-)_T$$

and

$$\lim_{m \rightarrow \infty} (A^-)_{mt_p} = (A^-)_{(m-1)t_p} \equiv (A^-)_{t_p}$$

The resulting solutions are
Region A

$$(A^-)_t = \left[(A^-)_T - \frac{A}{k_A} + \frac{B}{(k_e - k_A)} \right] e^{-k_A t} + \frac{A}{k_A} - \frac{B}{(k_e - k_A)} e^{-k_e t} \quad (19)$$

where

$$A = \frac{k_p k_1}{k_e} \text{ and } B = \left[(e^-)_T - \frac{k_p}{k_e} \right] k_1$$

Region B, $t = T$

$$(A^-)_T = \frac{\left[\frac{-A}{k_A} + \frac{B}{(k_e - k_A)} \right] e^{-k_A t_p} + \frac{A}{k_A} - \frac{B}{(k_e - k_A)} e^{-k_e t_p}}{e^{-k'_A(T - t_p)} - e^{-k_A t_p}} \cdot \frac{\frac{-\alpha}{k'_A} + \frac{\beta}{(k'_e - k'_A)} e^{-k'_e t_p} + \left[\frac{\alpha}{k'_A} - \frac{\beta}{(k'_e - k'_A)} e^{-k'_e T} \right] e^{k'_A(T - t_p)}}{e^{-k'_A(T - t_p)} - e^{-k_A t_p}} \quad (20)$$

where

$$\alpha = \frac{k_p k_1}{k'_e} \text{ and } \beta = k_1 \left\{ \frac{k_p}{k_e} + \left[(e^-)_T - \frac{k_p}{k_e} \right] e^{-k_p t_e} - \frac{k_p}{k'_e} \right\} e^{k'_e t_p}$$

The anion contribution to the collected current is thus

$$I_A = \frac{1}{T} \int_0^{t_p} (A^-)_t qAv_A dt \quad (21)$$

$$I_A = \frac{qAv_A}{T} \left\{ \frac{-I}{k_A} \left[(A^-)_T - \frac{A}{k_A} + \frac{B}{(k_e - k_A)} \right] \left[e^{-k_A t_p} - 1 \right] + \right. \\ \left. + \frac{A}{k_A} t_p + \frac{B}{k_e(k_e - k_A)} \left[e^{-k_e t_p} - 1 \right] \right\} \quad (22)$$

The total current collected at the anode is therefore

$$I_t = I_e + I_A \quad (23)$$

It is of interest to examine some of the limits of each term in eqn. 23. In particular:

$$\lim_{\substack{T \rightarrow \text{large} \\ v_A \rightarrow \text{small}}} (I_e + I_A) = I_e \quad (24)$$

$$\lim_{t_p/T \rightarrow 0} I_{\text{cd}} = \left[\frac{qAv_e k_p}{Tk_e} \right] \left[\frac{1}{k'_e} - \frac{1}{k_e} \right] \left[1 - e^{-k'_e T} \right] \quad (25)$$

Using eqns. 6c and 7c to express eqn. 25 explicitly

$$M = \left[\frac{qk_p}{T} \right] \left[\frac{Av_e}{k_1(\chi) + (P^+)k_{2e} + \frac{v_e A}{V}} \right] \cdot \left[\frac{1}{k_1(\chi) + (P^+)k_{2e}} - \right. \\ \left. \frac{1}{k_1(\chi) + (P^+)k_{2e} + \frac{v_e A}{V}} \right] \left[1 - e^{-(k_1(\chi) + (P^+)k_{2e})T} \right] \quad (26)$$

$$\lim_{EK_e \rightarrow \text{large}} M = \frac{qk_{pv}}{k'_e} \left[1 - e^{-k'_e T} \right] \quad (27)$$

This is identical to the classical equation of Wentworth, eqn. 1.

EXPERIMENTAL

A Varian Vista 6000 gas chromatograph with a 1075 split/splitless injector was used for this study. A Varian 402 chromatography data system was used to store raw data and process it. The electron-capture detector cell was a standard 0.300 ml displaced coaxial design^{15,16} and the constant-current electronics were modified to allow the reference current and pulse voltage to be variable. The detector temperature was maintained at 300°C and 30 ml/min of nitrogen was added to the cell in addition to the 1 ml/min helium column flow. The column was a 15 m \times 0.32 mm I.D. bonded methylsilicone (SGE). The calculations for the numerical model were done with a HP1000 computer.

DISCUSSION

Fig. 1 shows a plot of the solution of eqn. 23 for the constant current mode using the parameters listed in Table I, in which the value of the frequency, $f = 1/T$, was iterated until $I_t = I_{ref.}$ The line marked (W) is the solution for the classical Wentworth equation, eqn. 27. The remaining curves are for different values of anion drift velocities; 0–300 cm/sec. In the limit in which the anion drift velocity is equal to that of the electron, they both would contribute equally to the collected current.

Fig. 2 shows sensitivity plots for several compounds. Although each compound has a different sensitivity and hence a different detection limit, the concentration at which the compound sensitivity is decreased by 10% is also different. The result is that the linear range is approximately the same for all of these compounds. In addition, the pulse frequency at which this non-linearity begins is almost the same for every compound, 65 kHz (dashed line in Fig. 2). The only significant property that is different for each compound is the attachment rate constant k_1 . From eqns. 6 and 7 it can be seen that this always enters the equations as the product $k_1(A)$. Therefore,

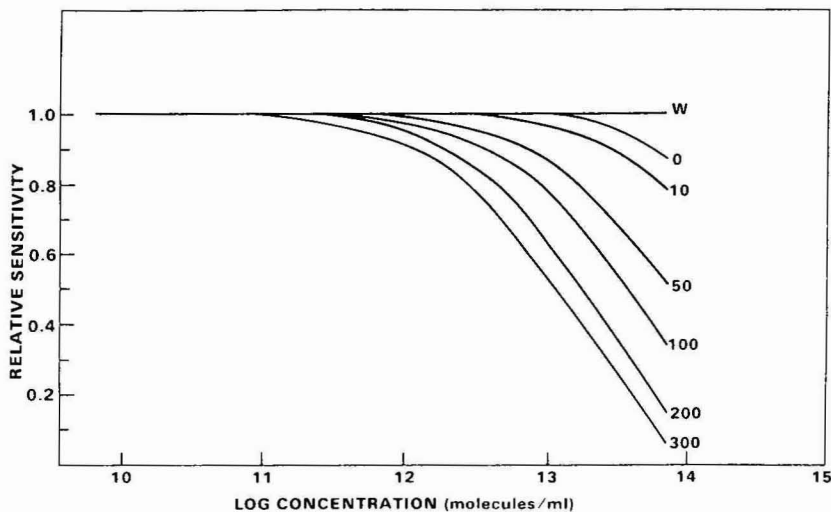


Fig. 1. Calculated sensitivities for values of anion drift velocities 0, 10, 50, 100, 200 and 300 cm/sec.

TABLE I
PARAMETERS FOR CALCULATION

Parameter	Value	Reference Nos.
k_p	$7.4 \cdot 10^{10} \text{ ml sec}^{-1}$	7-12
k_{2e}	$3 \cdot 10^{-6} \text{ ml sec}^{-1}$	7-12
k_{2A}	$3 \cdot 10^{-6} \text{ ml sec}^{-1}$	7-12
k_1 (lindane)	$8 \cdot 10^{-8} \text{ ml sec}^{-1}$	25, 26
(P^+)	$1.6 \cdot 10^8 \text{ ml sec}^{-1}$	7-12
v_e	$3 \cdot 10^5 \text{ cm sec}^{-1}$	21, 22, 24
v_A	200 cm sec^{-1}	23, 24
V	40 V	
A	0.300 ml	
t_p	0.200 cm ²	
I_{ref}	$6 \cdot 10^{-7}$	
	$2.96 \cdot 10^{-10} \text{ A}$	
Contaminant concentration (C)	$1 \cdot 10^{10} \text{ molecules ml}^{-1}$	
Rate constant (k_{1c})	$1 \cdot 10^{-7} \text{ ml sec}^{-1}$	
Recombination (k_{2Ac})	$3 \cdot 10^{-6} \text{ ml sec}^{-1}$	

if all other parameters in eqn. 23 are kept constant this implies

$$k_1(A)_{\max} = \text{constant} \quad (28)$$

Fig. 3 shows a graph of a series of sensitivity calculations using the data in Table I, and only changing the attachment rate constant k_1 . The calculation was performed by using literature values for k_p , k_{2e} , k_{2A} , (P^+) and v_e . The value of v_A was varied so as to best match the experimental roll off in sensitivity for lindane. The value of k_1 was then chosen to yield the same concentration at which the sensitivity was decreased by 10% as was experimentally observed for lindane. The resulting values for v_A and k_1 are physically reasonable, although no literature values are accurately known for these quantities. The detection limits were calculated by assuming a con-

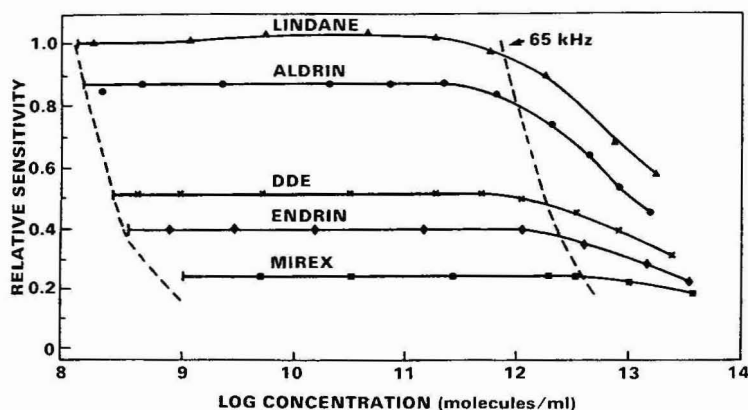


Fig. 2. Experimental sensitivities. Dashed line on right is the interpolated concentration for which the response equals 65 kHz. Reference current $2.96 \cdot 10^{-10} \text{ A}$.

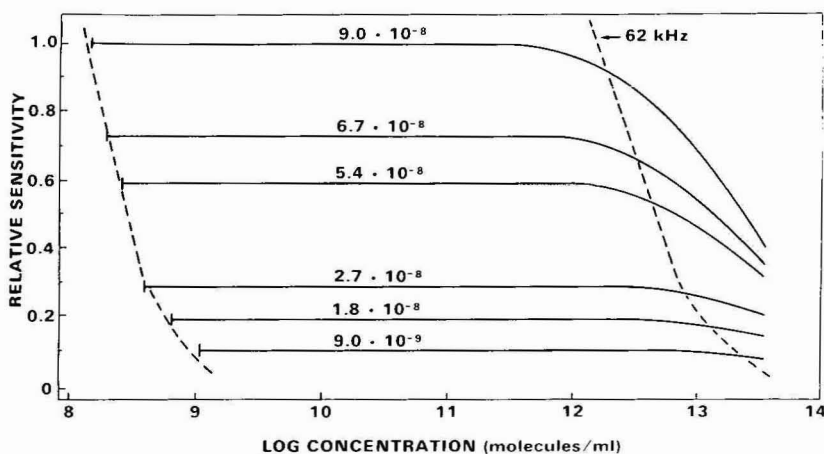


Fig. 3. Calculated sensitivities using the parameters in Table I. Reference current $2.96 \cdot 10^{-10}$ A. Attachment rate constant k_1 is varied from $9 \cdot 10^{-8}$ to $9 \cdot 10^{-9}$ ml sec $^{-1}$.

stant noise level, due to the presence of an electron-attaching contaminant. Again the calculation confirms that as long as the anions and electron drift velocities remain constant, the pulse frequency at which the sensitivity is decreased by 10%, f_{\max} , is always the same even though the concentration C_{\max} is different.

The effects of changing the reference current is shown in Fig. 4 using lindane as the test compound. As the reference current I_{ref} is changed, the average electron concentration in the cell changes and therefore the base frequency f_0 , and also the frequency at which the non-linear response occurs. However, the sample concentration C_{\max} remains the same. The calculated sensitivities shown in Fig. 5 again used the data from Table I and only the reference current was varied. At extremely high concentrations the model predicts a greater loss in sensitivity than is observed. This may be due to the build-up of enough space charge due to the anions, that a counter field has developed^{17,18}.

As discussed previously the noise level was assumed to be due to the presence

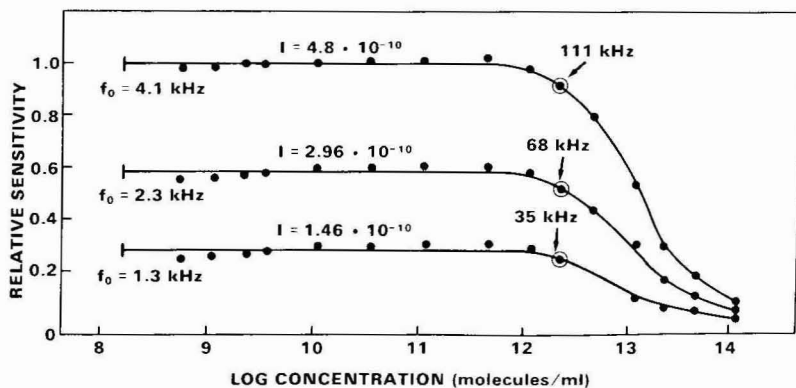


Fig. 4. Experimental sensitivities for lindane. Reference current varied: $1.46 \cdot 10^{-10}$, $2.96 \cdot 10^{-10}$, $4.8 \cdot 10^{-10}$. The circled points are the frequencies where the sensitivities are reduced by 10%.

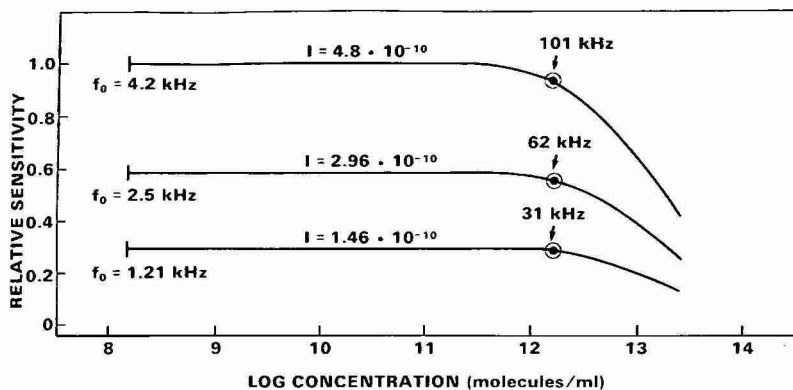


Fig. 5. Calculated sensitivities using the parameters in Table I. Reference current varied: $1.46 \cdot 10^{-10}$, $2.96 \cdot 10^{-10}$, $4.8 \cdot 10^{-10}$. The circled points are the frequencies where the sensitivities are reduced by 10%.

of a contaminant, such as oxygen which is always present at levels of a few ppm. When the reference current is changed, not only is the sensitivity for the sample changed; but also the sensitivity (and the noise level) of the contaminant. Thus the calculations predict that the signal-to-noise ratio will be unchanged. The actual measured signal and noise as a function of base frequency is shown in Fig. 6. The base

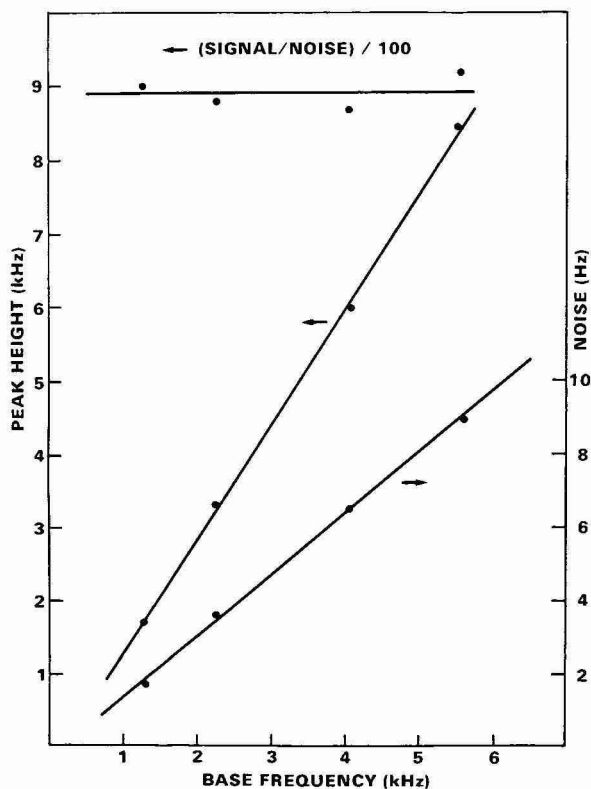


Fig. 6. Experimental response to 16 pg lindane, noise and signal-to-noise ratio.

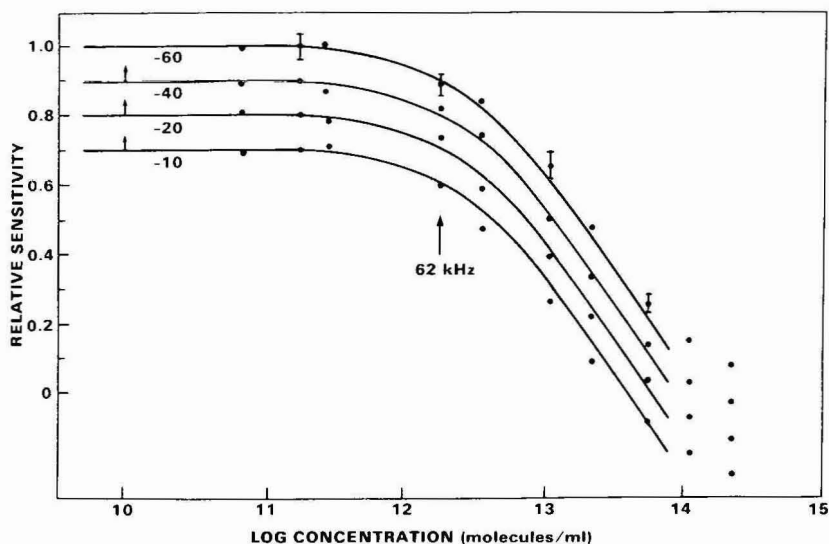


Fig. 7. Experimental sensitivities for lindane for different pulse voltage amplitude: -60 , -40 , -20 and -10 V. Solid line is calculated as described in text. Curves for -40 , -20 and -10 have been displaced down by 0.1 , 0.2 and 0.3 units, respectively.

frequency was varied by changing the reference current. It can be seen that the signal-to noise ratio is essentially a constant.

As a final test of the model, the effect of changing the pulse voltage was investigated. As the pulse voltage was changed, the reference current was adjusted so as to have the same base frequency. The experimental points are shown in Fig. 7, along with the calculated (solid) curves. The curves for -40 , -20 and -10 V are displaced downward for clarity. The model predicts, and the data confirms within the experimental error, that the response is the same. Each experimental data point is the average of three injections. The experimentally measured reference currents that were required to maintain a constant base frequency were found to vary almost as the square root of the pulse voltage, and are listed in Table II. Also listed are the drift velocities used in the calculation to maintain a constant f_0 when the experimental values of reference current were used. These drift velocities were obtained by iteratively changing them until the same experimental value of f_0 was obtained for each new value of I_{ref} . The value of the anion drift velocity was then changed assuming

TABLE II

CALCULATED DRIFT VELOCITIES

$f_0 = 2.5 \cdot 10^3$ Hz.

U (V) (exp)	I_{ref} ($\cdot 10^{10}$ A) (exp)	v_e (cm/sec) (calc.)	v_A (cm/sec) (calc.)
-60	$3.61 \cdot 10^{-10}$	$3.7 \cdot 10^5$	245
-40	$2.96 \cdot 10^{-10}$	$3.0 \cdot 10^5$	200
-20	$2.14 \cdot 10^{-10}$	$2.2 \cdot 10^5$	146
-10	$1.45 \cdot 10^{-10}$	$1.5 \cdot 10^5$	100

that it changed linearly with the average electric field. The model as presented above predicts a linear relationship between the collected current and the applied potential if all other parameters, including f_0 , are kept constant. This is due to the assumption of a uniform electric field within the cell as shown in eqn. 16, which according to eqn. 8 is linearly proportional to the applied voltage. This equation describes the volume of the cell from which electrons can be extracted by the applied field during the time t_p . This volume is given by the product of the cross sectional area of the cell, A , the drift velocity, v_e , and the time interval, t_p . If all other parameters, *i.e.*, f_0 , are kept constant, then increasing U will result in a linear increase in the collected current. However, the electric field within the displaced coaxial cell used in this work is not uniform. In a previous paper¹⁵ the electric field distributions for various cell geometries were calculated. It could be seen from the distribution of the equipotential surfaces that the field near the anode in the displaced coaxial cell was similar, although somewhat weaker, than the fields in a coaxial cell of similar dimensions. As a first approximation the coaxial field can be used to estimate the volume of the cell from which charge can be extracted by a given applied potential. The collected current is given by

$$I = \frac{q}{T} (\bar{e^-}) \cdot AR \quad (29)$$

where $\bar{e^-}$ is the time averaged electron concentration, the last term AR is the volume from which charge can be removed in time t_p , and R is the maximum axial distance from the anode from which an electron can be collected. The latter quantity can be determined from

$$\frac{dr}{dt} = k_e E_r \quad (30)$$

where k_e is the electron mobility¹⁴, r is the axial position of the charge and E_r the electric field intensity for the concentric cylinder symmetry, is given by¹⁹

$$E_r = \frac{UG}{r} \quad (31)$$

where U is the applied potential and G is a geometry factor.

Integrating eqn. 30 gives

$$\int_0^R \frac{1}{E_r} dr = \int_0^{t_p} K_e dt \quad (32a)$$

$$R = (2UGk_e t_p)^{1/2} \quad (32b)$$

Thus from eqn. 29:

$$I \propto (U)^{1/2} \quad (33)$$

TABLE III
CALCULATED COLLECTION VOLUMES

U (V)	I ($\cdot 10^{10}$ A) (exp)	I^*	V_c^{**}
-60	3.61	2.49	2.15
-40	2.91	2.01	1.80
-20	2.14	1.48	1.35
-10	1.45	1.00	1.00

* Experimental values normalized to I_{ref} at -10 V.

** V_c is the relative collection volume calculated from the electron trajectories.

Therefore the value of the drift velocity used to determine the rate constants in eqn. 8 is not directly proportional to the applied potential, but should represent an average value throughout the region of the cell from which charge can be extracted. This quantity varies more like the square root of the potential.

A more accurate determination of the relation between the applied voltage and the collected current was obtained by numerically calculating the electric field throughout the cell, as was done previously¹⁵ for the voltages listed in Table III. From a uniform distribution of initial points throughout the cell, the equations of motion were solved and the actual trajectories of the electrons were determined. Only those starting points that resulted in a trajectory striking the anode within the time period t_p , were counted in the collection volume. The relative number of points that made up the collection volume at each applied potential, should be proportional to the collected current. The values that were calculated in this manner are listed in Table III and are in reasonable agreement with the experimental values.

In order to prevent the collection of anions at high pulse frequencies a bipolar pulsed circuit has recently been employed²⁰. The first pulse was of negative voltage, followed immediately by a positive pulse of equal duration. The results were encouraging. No effect was observed with the bipolar circuit until pulse frequencies greater than 50 kHz were encountered. Beyond this value an increase in linear response was observed as the amplitude of the positive pulse approached that of the negative pulse. An improvement in the linear response by almost an order of magnitude was effected; the improvement being greatest when the base frequency was lowest.

CONCLUSIONS

The model developed in this paper has been shown to be capable of providing a semi-quantitative explanation for the decreased sensitivity of the constant-current electron-capture detector at high sample concentrations. A more accurate calculation requires a more precise determination of the parameters in Table I. In addition is shown that it is not necessary to remove all of the electrons from the cell in order to obtain a linear response. In a future paper additional experimental data will be presented for measured electron and anion contributions in the electron-capture detector, including relative drift velocities obtained under actual electron-capture detection conditions; *i.e.*, atmospheric pressure and high temperature.

It would appear that the continued development of a more accurate model of the electron-capture detector would require a finite element analysis. This approach would allow one to take into account the inhomogeneities of the different processes that are occurring within the cell. The expression given by Grimsrud and Connolly⁹ would allow the determination of the electron-ion production rate (k_p) at each nodal point within the cell. In a previous paper¹⁵ a numerical solution of Poisson's equation for an arbitrary charge distribution allowed the calculation of electron and anion drift velocities with cells of various geometries. This allows the determination of charge flux (electron, anion and cations) into and out of each nodal point within the cell, due to the applied electric field, i.e., k_{3e} and k_{3A} in eqn. 5 would be known as a function of time and space. The additional field due to the space charge at the surrounding nodal points should now be included. Knowing the charge density at each point would allow the solution of the coupled kinetic eqns. 6 and 7 at each point in space and time without the assumption $(P^+) = \text{constant}$. The integration of these equations with respect to time would determine the collected charge at the anode, for a single pulse cycle. This process would have to be iteratively repeated until a self consistent solution is obtained. The value of being able to solve such a complex model is that it would allow the design of an optimized electron-capture detector from an understanding of all processes that are occurring; not simply those that are the easiest to solve for analytically. The value of simple analytical models such as the one presented in this paper is that it provides a guide for experimental investigations, as well as a check for the more complex numerical simulations.

REFERENCES

- 1 W. E. Wentworth, E. C. Chen and J. E. Lovelock, *J. Phys. Chem.*, 70 (1966) 445.
- 2 R. J. Maggs, P. L. Joynes, A. J. Davies and J. E. Lovelock, *Anal. Chem.*, 43 (1971) 1966.
- 3 I. Śliwka, J. Lasa and J. Rosiek, *J. Chromatogr.*, 172 (1979) 1.
- 4 P. L. Gobby, E. P. Grimsrud and S. W. Warden, *Anal. Chem.*, 52 (1980) 473.
- 5 J. E. Lovelock, *J. Chromatogr.*, 99 (1974) 3.
- 6 J. E. Lovelock and A. J. Watson, *J. Chromatogr.*, 158 (1978) 123.
- 7 W. B. Knighton and E. P. Grimsrud, *Anal. Chem.*, 55 (1983) 713.
- 8 W. B. Knighton and E. P. Grimsrud, *J. Chromatogr.*, 288 (1984) 237.
- 9 E. P. Grimsrud and M. J. Connolly, *J. Chromatogr.*, 239 (1982) 397.
- 10 M. J. Connolly, W. B. Knighton and E. P. Grimsrud, *J. Chromatogr.*, 265 (1983) 145.
- 11 E. P. Grimsrud and S. E. Warden, *Anal. Chem.*, 52 (1980) 1842.
- 12 E. P. Grimsrud, S. H. Kim and P. L. Gobby, *Anal. Chem.*, 51 (1979) 223.
- 13 J. R. Acton and J. D. Swift, *Cold Cathode Discharge Tubes*, Academic Press, New York, 1963, Ch. 2.
- 14 E. W. McDaniel, *Collosion Phenomena In Ionized Gases*, Wiley, New York, 1964, Ch. 11.
- 15 G. Wells and R. Simon, *J. High Resolut. Chromatogr. Chromatogr. Commun.*, 6 (1983) 427.
- 16 G. Wells, *J. High Resolut. Chromatogr. Chromatogr. Commun.*, 6 (1983) 651.
- 17 W. A. Aue and S. Kapila, *J. Chromatogr.*, 188 (1980) 1.
- 18 W. A. Aue and K. W. M. Siu, *J. Chromatogr.*, 239 (1982) 127.
- 19 J. R. Reitz and F. J. Milford, *Foundations of Electromagnetic Theory*, Addison-Wesley, New York, 1967.
- 20 R. Simon and G. Wells, *J. Chromatogr.*, 302 (1984) 221.
- 21 T. E. Bortner, G. S. Hurst and W. G. Stone, *Rev. Sci. Instr.*, 28 (1957) 103.
- 22 G. H. Wannier, *Bell Syst. Tech. J.*, 32 (1953) 170.
- 23 T. Fujii and G. G. Meisels, *J. Chem. Phys.*, 75 (1981) 5067.
- 24 J. C. Tou, R. Ramstad and T. J. Nestrick, *Anal. Chem.*, 51 (1979) 781.
- 25 G. Wells, *J. Chromatogr.*, 285 (1984) 395.
- 26 L. G. Christophorou, *Chem. Rev.*, 76 (1976) 409.

CHROM. 17 965

CONTINUOUS-FLOW NUCLEAR MAGNETIC RESONANCE*

KLAUS ALBERT, MICHAEL NIEDER and ERNST BAYER*

Institut für Organische Chemie, Auf der Morgenstelle 18, D-7400 Tübingen (F.R.G.)

and

MANFRED SPRAUL

Bruker Analytische Messtechnik GmbH, Silberstreifen, D-7512 Rheinstetten-Fo (F.R.G.)

(Received June 17th, 1985)

SUMMARY

The effect of the volume of the detector flow cell upon peak broadening in high-performance liquid chromatography with nuclear magnetic resonance detection has been monitored using a modified fluorescence detector. The results of solvent-resonance suppression using 1331 hard pulse sequences are described. The possibility of obtaining ^{13}C distortionless enhancement by polarization transfer spectra in the flow system is demonstrated.

INTRODUCTION

Continuous-flow nuclear magnetic resonance (NMR) spectroscopy is beginning to become an accepted analytical tool¹. It allows the monitoring of kinetics and metabolic events by ^1H , ^{19}F or ^{13}C NMR spectroscopy^{1–6} and can be used as a special detector in direct on-line coupling of high-performance liquid chromatography (HPLC) and NMR spectroscopy^{4–8}.

The optimum volume of the continuous-flow cell for HPLC–NMR is still a matter of discussion. On the one hand, HPLC peak broadening should remain as small as possible, on the other hand the limited sensitivity of the NMR method necessitates a relative large volume for detection. Up to now the effect of peak broadening caused by a NMR flow cell was measured by connecting a UV detector after the NMR flow probehead^{4,7}. With this arrangement, the dead volume of the effluent also contributed to peak broadening. The true cell-volume effect may be obtained by directly observing a test separation within the NMR flow cell. In this case UV methods cannot be used because of the optical cut-off of the Pyrex glass used in the construction of the flow cell. For this reason, we resorted to fluorescence detection using a modified commercially available fluorescence detector.

* Presented at the *International Symposium on High-Performance Liquid Chromatography, Kyoto, January 28–30, 1985*. The majority of the papers presented at this symposium have been published in *J. Chromatogr.*, Vol. 332 (1985).

An additional and significant problem in HPLC- ^1H NMR is that of solvent suppression. Up to now most applications of direct HPLC-NMR have been with adsorption chromatography^{1,3-5,8}. In routine HPLC however, about 80% of separations are performed in the reversed-phase mode. When water-acetonitrile mixtures are employed as the mobile phase the resonances of both solvent components have to be suppressed. This was achieved by the use of the gated homodecoupling technique⁷. In a typical HPLC analysis, a total presaturation time of 2 sec was needed. Therefore in these cases the stop-flow technique is obligatory.

Recently, a new effective 1331 hard pulse solvent-suppression technique was described by Hore⁹. The application of this technique to reduce the delay time between acquisition scans and improve suppression factors during continuous flow ^1H NMR spectroscopy has been investigated.

It has been demonstrated that broadband-decoupled ^{13}C NMR spectra of acceptable quality can be obtained in a flowing system^{2,6}. Nowadays, in ^{13}C NMR spectroscopy, elegant signal-multiplicity assignment techniques using polarization transfer between ^1H and ^{13}C nuclei (distortionless enhancement by polarization transfer, DEPT) are employed^{10,11}. Thus, we also investigated the possibility of polarization transfer in continuous-flow systems, and of obtaining DEPT spectra.

EXPERIMENTAL

Constant and reproducible flow-rates in all experiments were obtained by use of the pump of a Bruker LC 31 system.

Fluorescence measurement

In order to obtain information about HPLC peak broadening, a Biotronik fluorescence detector was modified to allow different types of flow cell to be adjusted in the beam (Fig. 1). A halogen lamp provided the exciting radiation at a wavelength of 360 nm. Photodiode detection was performed at 470 nm. Dansyl-amino acids used for the test separation (Fig. 2) were prepared as described earlier¹².

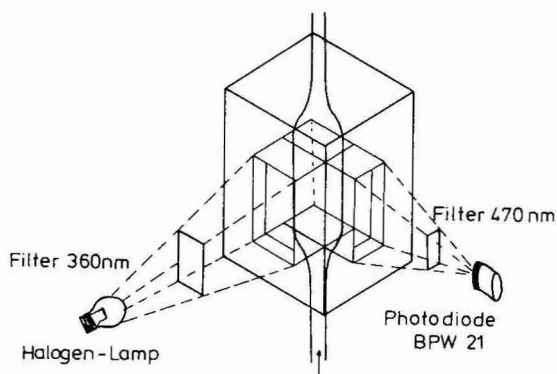


Fig. 1. Modified fluorescence detection arrangement for the determination of peak broadening in different flow cells.



Fig. 2. Separation of dansyl-amino acids: aspartic acid (retention time, $t_R = 2.73$ min), glycine ($t_R = 3.26$ min), arginine ($t_R = 3.86$ min) and alanine ($t_R = 4.84$ min). Mobile phase: methanol-water (60:40), pH 2.0, flow-rate 1 ml/min. Fluorescence detection: excitation wavelength 360 nm, emission wavelength 470 nm (Biotronik BT 6630).

NMR measurements

^1H NMR spectra were recorded on a Bruker AM 300 NMR spectrometer (7.0 T) controlled by the computer system Aspect 3000 including an array processor. A disk system (Control Data Corporation) with a transfer time of less than 2 sec per 8 K interferogram was used for data storage. ^{13}C NMR spectra were recorded on a Bruker WM 400 NMR spectrometer (9.4 T) controlled by the computer system Aspect 2000. Data were stored on a 80-Mbyte disk system (Control Data Corporation). For continuous-flow spectra, NMR flow cells^{6,7} were used. The internal diameter of the glass tube in the measuring range was 4 mm, thus resulting in a total measuring volume of 188.5 μl and a residence time of 11.3 sec at a flow-rate of 1 ml/min. In the case of the ^{13}C NMR flow probehead, an additional decoupling coil was mounted axially to the measuring coil.

Solvent suppression was carried out using the 1331 hard pulse method of Hore⁹. The timing of the sequence is: P_1 , D_2 , P_3 , D_2 , P_3 , D_2 , P_1 , Acquisition, D_1 , where P_n = excitation pulse and D_n = delay time. The $\pi/2$ pulse is divided into four hard pulses in which $P_3 = 3 P_1$. By adjusting the pulse carrier frequency to the that of the resonance of water, further nulls in the net magnetization (for instance at the acetonitrile resonance) occur at intervals of $1/D_2$. The original pulse of 5.8 μsec was attenuated to 32.0 μsec with the help of a 20-dB attenuator. According to the 1331 sequence, this value was divided into pulse lengths of 4 and 12 μsec , respectively. For data acquisition at a flow-rate of 1 ml/min, a delay, D_1 between scans of 0.1 sec was used. The delay, D_2 , between pulses was set according to the frequency difference between the resonances of water and of acetonitrile. In all experiments the total sum of transients was 16.

DEPT spectra were recorded by appropriate change of $\pi/2$ pulse of 42 μsec with a delay time between scans of 2 sec. Thirty-two scans were accumulated in all cases.

RESULTS AND DISCUSSION

Peak broadening in on-line HPLC-NMR

For maximum sensitivity of the NMR measurement, a cell volume equivalent to the chromatographic peak volume is required. On the other hand, chromatographic peak broadening becomes significant when the volume of the detector cell approaches the chromatographic peak volume. The influence of the detector volume upon peak broadening was observed for two analytical columns (4.6 mm I.D., length 125 and 250 mm, Figs. 3 and 4) and a semipreparative column (250 \times 8 mm I.D.,

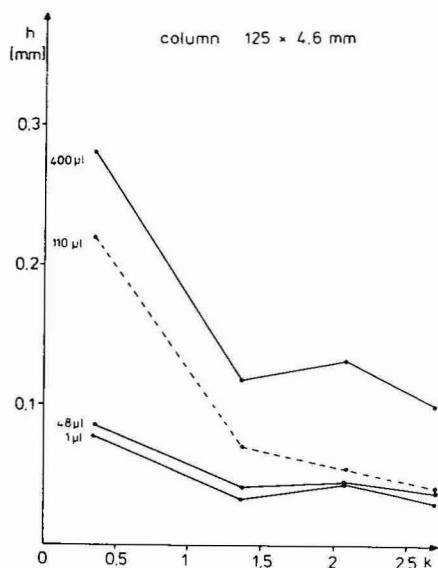


Fig. 3. Effect on plate height (h) of different flow cell volumes using an analytical column (125 x 4.6 mm).

Fig. 5) using the experimental arrangement shown in Figs. 1 and 2. In all cases LiChrosorb RP-18, 7 μ m (Merck, Darmstadt, F.R.G.) was used as column packing material. For peaks with capacity factors (k') above 2, detector volumes up to about 200 μ l can be tolerated without significant loss in resolution in all cases investigated. Shorter analytical columns and peaks with small k' values require smaller cell volumes. In these cases stop-flow measurement is advantageous.

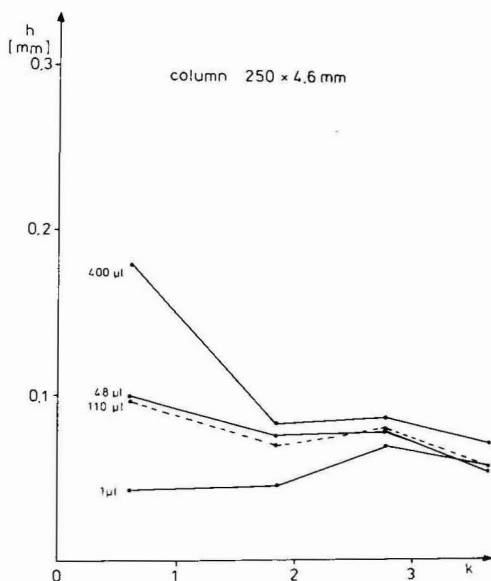


Fig. 4. Effect on plate height of different flow cell volumes using a long analytical column (250 x 4.6 mm).

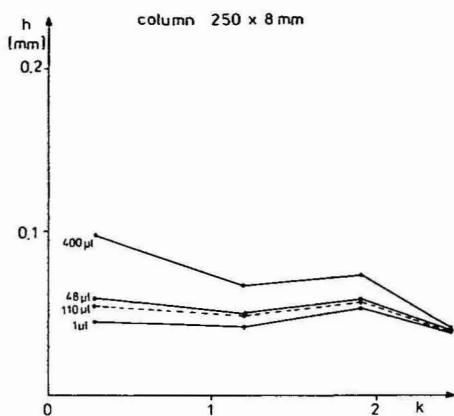


Fig. 5. Effect on plate height of different flow cell volumes using a semipreparative column (250 \times 8 mm).

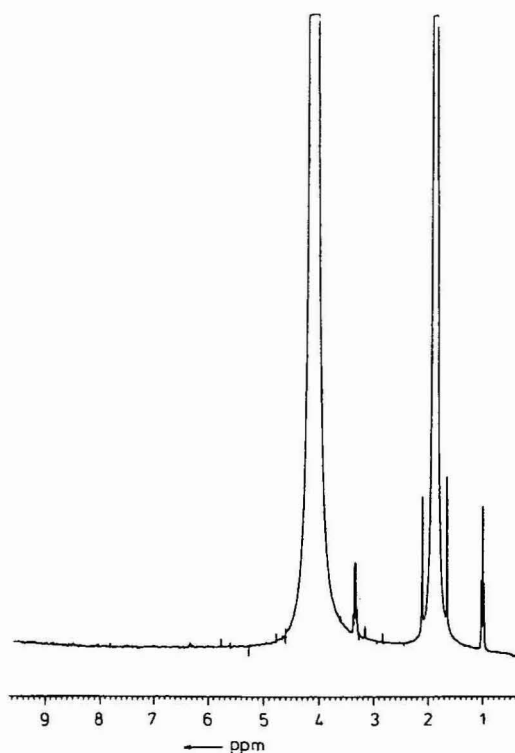


Fig. 6. Continuous-flow ^1H NMR spectrum (300 MHz) of a 1% solution of diethyl ether in acetonitrile-water (50:50). Flow-rate: 1 ml/min. Pulse repetition time: 2.05 sec. Number of data points: 16K. Number of scans: 16. Spectral width: 4000 Hz.

Solvent suppression

The continuous flow ^1H NMR spectrum of a 1% solution of diethyl ether in acetonitrile–water (50:50) is shown in Fig. 6. Using the 1331 hard pulse sequence the solvent signals are effectively reduced (Fig. 7a). By treating the raw data with weighting functions used in two-dimensional experiments, the spectrum of Fig. 7b results. Thus suppression ratios of approximately 200:1 are obtained. In principle, a further decrease in the signal hump and refinement of the hard pulse sequence is possible and can lead to even higher suppression ratios.

Continuous-flow DEPT spectra

The multiplicity of ^{13}C NMR signals may easily be recognized by using the DEPT sequence introduced by Doddrell and co-workers^{10,11}. This pulse sequence consists of two spin-echo experiments ($\pi/2, \tau, \pi$) for ^1H and for ^{13}C nuclei, together with a delay time t_1 . Polarization transfer is caused by a variable pulse, θ , after the correlated motion of ^1H and ^{13}C nuclei has occurred. The delay time, t_1 , is related to the median ^1H – ^{13}C coupling constant, J , by $t_1 = 1/2 J$. Fig. 8 shows the spectra obtained with the ^{13}C NMR flow cell (volume 188 μl). In the decoupled spectrum of cholesteryl acetate (BB) all resonances appear. In this continuous-flow spectrum even the signals of an impurity, ethylbenzene, are visible. In the DEPT CH_x spectrum ($\theta = \pi/4$) all quaternary carbon atoms are suppressed. In the CH spectrum ($\theta = \pi/2$), suppression of the CH_2 – and CH_3 – signals is imperfect because of pulse-angle irregularities at the end of the detection coil. The $\theta = 3\pi/4$ continuous-flow DEPT spectrum clearly distinguishes between primary, secondary and tertiary carbon atoms. Using this technique the signal multiplicity in flowing liquids can rapidly be obtained. This is of great interest for continuous process control.

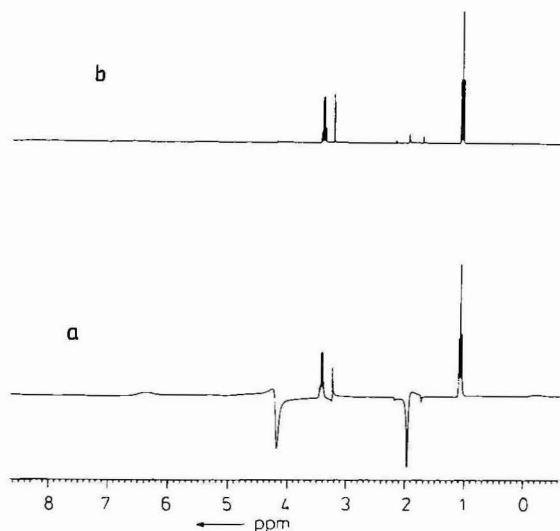


Fig. 7. Continuous-flow ^1H NMR spectrum as in Fig. 6 but using 1331 hard pulse solvent suppression. Pulse repetition time: 2.15 sec. Other details as in Fig. 6. a, Spectrum without further data manipulation; b, spectrum after multiplication of the free induction decay with a sine-square filter function.

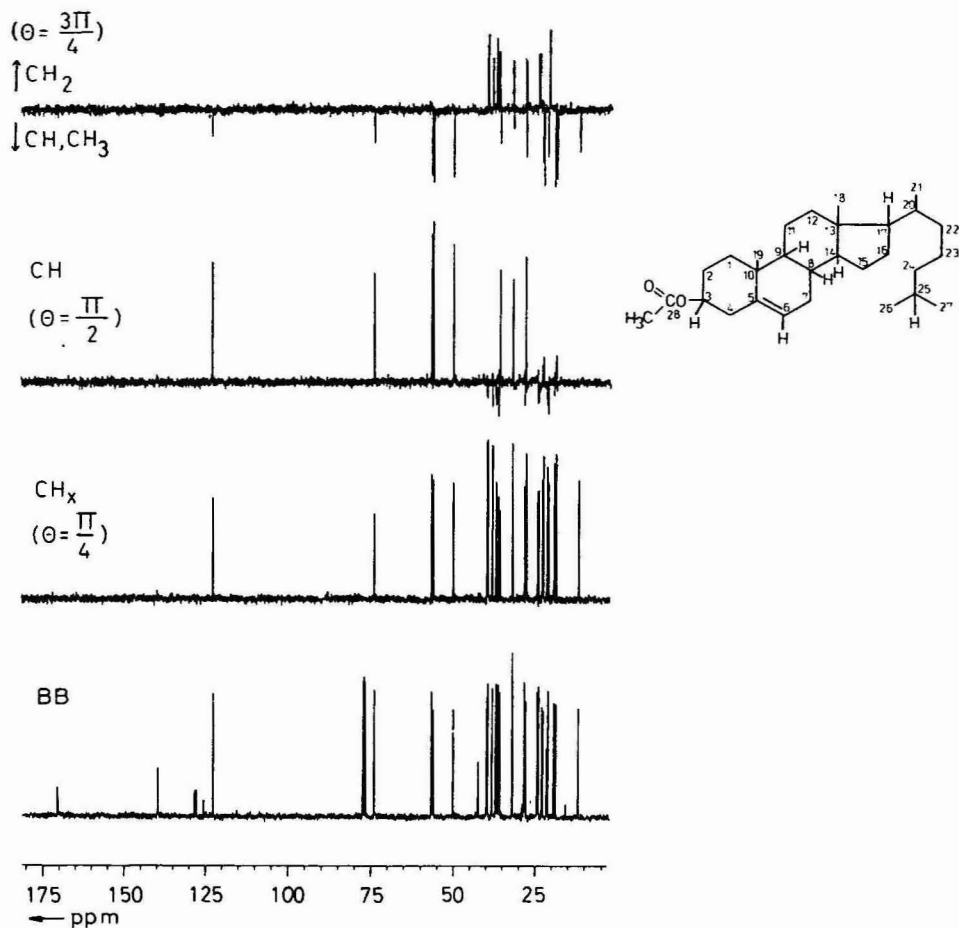


Fig. 8. Continuous-flow ^{13}C NMR spectra (100.6 MHz) of cholesteryl acetate under various conditions. Flow-rate: 1 ml/min. Number of data points: 32 K. Number of scans: 32. Spectral width: 23 800 Hz. Line broadening: 1.5 Hz. BB-spectrum: pulse repetition time, 1.7 sec; composite pulse decoupling. DEPT spectra: pulse repetition time, 2.7 sec; variable pulse angle θ ($\pi = 42 \mu\text{sec}$).

CONCLUSION

Continuous-flow NMR spectroscopy is approaching the status of static-rotation NMR. The NMR peak broadening in the flow system is compensated by an increased sensitivity obtainable at low flow-rates^{7,8} with adequate detector volumes. The peak broadening effect of these detector volumes in HPLC separation may be neglected. Newly developed one-dimensional pulse sequences are also possible in continuous-flow NMR spectroscopy, allowing many applications.

REFERENCES

- 1 H. C. Dorn, *Anal. Chem.*, 56 (1984) 747 A.
- 2 K. Albert, G. Kruppa, K.-P. Zeller, E. Bayer and F. Hartmann, *Z. Naturforsch., C: Biosci.*, 39 (1984) 859.
- 3 E. Bayer, K. Albert, M. Nieder, E. Grom and T. Keller, *J. Chromatogr.*, 186 (1979) 497.
- 4 E. Bayer, K. Albert, M. Nieder, E. Grom and Zhu An, *Fresenius' Z. Anal. Chem.*, 304 (1980) 111.
- 5 J. Buddrus and H. Herzog, *Anal. Chem.*, 55 (1983) 1611.
- 6 E. Bayer and K. Albert, *J. Chromatogr.*, 312 (1984) 91.
- 7 E. Bayer, K. Albert, M. Nieder, E. Grom, G. Wolff and M. Rindlisbacher, *Anal. Chem.*, 54 (1982) 1747.
- 8 D. A. Laude and C. L. Wilkins, *Anal. Chem.*, 56 (1984) 2471.
- 9 P. J. Hore, *J. Magn. Reson.*, 54 (1983) 539.
- 10 D. M. Doddrell and D. T. Pegg, *J. Am. Chem. Soc.*, 102 (1980) 6388.
- 11 M. R. Bendall, D. T. Pegg, D. M. Doddrell, S. R. Jones and R. I. Willing, *J. Chem. Soc., Chem. Commun.*, (1982) 1138.
- 12 E. Bayer, E. Grom, B. Kaltenegger and R. Uhmman, *Anal. Chem.*, 48 (1976) 1106.

CHROM. 17 991

CHROMATOGRAPHIC PROPERTIES OF OXIDISED OV-17 STATIONARY PHASE

B. A. COLENUTT* and R. M. CLINCH

Chemistry Department, Brunel University, Uxbridge, Middlesex, UB8 3PH (U.K.)

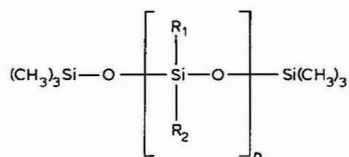
(First received May 24th, 1985; revised manuscript received July 1st, 1985)

SUMMARY

OV-17 stationary phase has been modified by heating at 340°C and 380°C in a stream of oxygen. Many polar compounds produce peaks with improved symmetry on the modified phase and there is little or no change in the symmetry of other less polar compounds. The improvements in peak symmetry are accompanied by small changes in retention index and there is a reduction in the polarity of the stationary phase as measured by the McReynolds value.

INTRODUCTION

The silicone liquid phases are widely used in the analysis of a variety of substances. They are polymers based on the siloxane skeleton



Non-polar silicones have methyl substituents on the skeleton (R_1 , R_2) and polarity may be increased by replacement of the methyl groups with phenyl groups or other more polar species. Thus, by incorporation of appropriate groups in the skeleton, stationary phases covering a wide range of polarity can be obtained.

A major virtue of the silicone stationary phases is their relative stability whereby they are capable of operating at up to 300°C. However, Gough and Baker¹ have noted that, if they are heated at high temperature in a stream of air, the resulting modified phases produce peaks with symmetry characteristics significantly different from those of the original liquid. In particular some polar compounds showed improved peak symmetry when analysed. Gough and Baker modified the silicone stationary phases by heating at 340°C for 3 h in a stream of air, followed by conditioning for 15 h at 250°C in a stream of nitrogen.

Although the preliminary study indicated some modification resulting in improved peak symmetry there was no systematic study of the oxidation or its effect. In the study reported here a single stationary phase, OV-17, has been selected and systematically examined.

OV-17 is a mildly polar stationary liquid where 50% of the methyl groups on the siloxane skeleton have been substituted by phenyl groups. The measure of polarity often used is the McReynold constant² whereby five or seven compounds are used. The Kováts retention index (I) is determined for each compound on the stationary phase and the corresponding value for the same substances on squalane is subtracted to yield ΔI

$$\Delta I = I_{\text{ph}} - I_{\text{sq}}$$

where I_{ph} is the Kováts index for compound X on the stationary phase and I_{sq} is the Kováts index for compound X on squalane.

The sum of the ΔI values is the McReynolds value, an arbitrary but useful measure of polarity.

One objective of the study was to establish how modification of the stationary phase was apparent as a change in the polarity of the phase. Another aspect of the work was to investigate how peak symmetry varied with treatment of the stationary phase.

Peak symmetry was determined by examination of each peak. The position of half peak height was established and from the perpendicular from the peak maximum measurements were made to the leading and trailing edges of the peak. Symmetry was calculated as follows:

$$S = \frac{y}{x}$$

where S is the symmetry factor, and x and y are the distances from point at half height of perpendicular from peak maximum to leading edge and trailing edge, respectively.

Thus an absolutely symmetrical peak has a value of 1.0, a trailing peak a value greater than 1, and a fronting peak a value less than 1.

The final objective of this work was to establish whether any modification which occurred was an oxidative effect or merely a physical effect due to the elevated temperature used.

EXPERIMENTAL

All the gas chromatography was carried out using a Pye Unicam GCD gas chromatograph fitted with dual flame ionisation detectors. The columns were constructed of glass, 2 m \times 4 mm I.D.

The OV-17 stationary phase was used at a loading of 5% (w/w) on 60–80 mesh diatomite. After dissolving the OV-17 in chloroform with heating and stirring the solution was added to the appropriate weight of diatomite. Subsequently the solvent was removed using a rotary evaporator and gentle heating. Sufficient of the packing material was prepared initially to enable all of the columns required to be packed

with the product. In this way the initial condition was constant. The glass columns were packed under a flow of nitrogen gas at low pressure and with gentle vibration.

After packing, primary conditioning of all of the columns was carried out to remove any volatile material remaining from the preparation and packing, followed by various treatments. A summary of the column treatments is given in Table I.

TABLE I
CONDITIONING AND TREATMENT OF THE COLUMNS

Primary conditioning was for 15 h at 270°C with a stream of nitrogen at a flow-rate of 30 ml min⁻¹.

Column number	Treatment (oxidation)	Final conditioning
1*	—	—
2	3 h at 340°C in oxygen (30 ml min ⁻¹)	15 h at 250°C in nitrogen (30 ml min ⁻¹)
3	9 h at 340°C in oxygen (30 ml min ⁻¹)	15 h at 250°C in nitrogen (30 ml min ⁻¹)
4	9 h at 380°C in oxygen (30 ml min ⁻¹)	15 h at 250°C in nitrogen (30 ml min ⁻¹)
5**	9 h at 340°C in nitrogen (30 ml min ⁻¹)	15 h at 250°C in nitrogen (30 ml min ⁻¹)

* For reference purposes.

** Control column.

Various groups of compounds were selected to evaluate the columns and their stationary phases. The *n*-alkanes from *n*-pentane to *n*-decane were required in order to calculate the Kováts indices for all the other compounds.

Benzene, *n*-butanol, pentanone, nitropropane, and pyridine were studied in order to establish the McReynold value for each column.

Since initial indications were that polar compounds were most influenced by the modification process the other substances studied were largely of this type. Several alcohols and ketones were selected together with halogenated compounds and some nitrogen-containing compounds.

The samples used were all sufficiently pure to produce a single peak in the chromatogram. All samples were analysed on each of the columns at a temperature of 70°C. Injections of 0.1 µl were made by means of a microlitre syringe. Duplicate injections were made and where these did not replicate further injections were made. The injection port was heated to a temperature of 250°C as was the detector. Nitrogen carrier gas was used at a flow-rate of 30 ml min⁻¹.

After the chromatographic analysis had been completed the packings were removed from the columns and extracted with chloroform in a Soxhlet apparatus for 6 h. Subsequently the chloroform was removed by rotary evaporation leaving a residue of the liquid stationary phases. The residues were examined by nuclear magnetic resonance (NMR) spectroscopy and infra-red (IR) spectroscopy in order to ascertain whether chemical changes had taken place during the modification and conditioning.

RESULTS AND DISCUSSION

Comparison of peak symmetry data in Table II clearly shows that there is a marked improvement in peak shape for particular compounds. Variations for the non-polar *n*-alkanes are insignificant but there are real changes in the peaks for the five compounds used in the calculation of McReynold's constant.

The *n*-alkanes show no consistent pattern across the range of columns. Since their peak symmetry is good on the OV-17 it is unlikely that much improvement could be made. More important there is no deterioration in peak symmetry with oxidation. The worst peak shapes are obtained with column 5 which has merely been heated in the absence of oxygen.

Benzene follows a trend similar to that of the *n*-alkanes. The peak on unmodified OV-17 is reasonably symmetrical and treatment, if anything, tends to worsen the shape. However, the loss of symmetry is not very marked except in the case of column 5. Clearly the extreme heating has had a deleterious effect on the stationary phase which heating in a stream of oxygen does not have.

Butanol exhibits a remarkable increase in peak symmetry with increasingly strong oxidation of the stationary phase. The original peak on the unmodified phase grossly tails but there is steady improvement in symmetry with oxidation until on column 4 the peak shape is quite acceptable. As was the case with benzene, simply heating the stationary liquid in the presence of nitrogen fails to have any beneficial effect and the peak symmetry is little better than that for the unmodified liquid.

The symmetry of the peaks for pentanone shows changes similar to those of benzene. Here, however, the improved symmetry is most marked immediately after oxidation. The peak symmetry values are similar for columns 2, 3 and 4 and there seems to be no significant improvement with continued and more drastic oxidation. Column 5, which was merely overheated, once again yields the worst peak symmetry.

Pyridine follows essentially the same pattern as *n*-butanol and pentanone although in this case the dramatic loss of performance with simple overheating is not as marked.

Nitropropane like benzene produces a relatively symmetrical peak on the unmodified OV-17 and only shows slight improvement when analysed on the oxidised phases. The most pronounced effect here was the dramatic loss of peak symmetry on the overheated column.

Thus, the initial results showed quite conclusively that there was a well defined effect on oxidising the OV-17 stationary phase and that the effect was distinctly different from continued conditioning or merely overheating of the stationary liquid in a stream of nitrogen gas. In almost every case the overheated column 5 produced worse shaped peaks than the reference column 1, and in no case was there any significant improvement in peak shape.

Of the substances originally studied the improvement in peak symmetry was most marked for those substances producing the least symmetrical peaks on the untreated OV-17. In general these were polar compounds and to test the validity of this conclusion further examples of polar compounds were analysed.

Thus the series of alcohols listed in Table II all show the same trend as *n*-butanol. All exhibit a gradual improvement in peak symmetry as the severity of the oxidation is increased. As before column 5 produced the worst peak symmetry for

TABLE II

PEAK SYMMETRY VALUES FOR VARIOUS COMPOUNDS ON MODIFIED AND UNMODIFIED OV-17

Compound	Column number				
	1	2	3	4	5
<i>n</i> -Pentane	1.2	1.2	1.2	1.3	1.6
<i>n</i> -Hexane	1.3	1.2	1.3	1.2	1.4
<i>n</i> -Heptane	1.2	1.2	1.3	1.3	1.4
<i>n</i> -Octane	1.4	1.3	1.3	1.4	1.3
<i>n</i> -Nonane	1.5	1.5	1.4	1.5	1.5
<i>n</i> -Decane	1.4	1.5	1.4	1.5	1.6
Benzene	1.9	1.7	1.8	2.4	6.2
<i>n</i> -Butanol	6.5	5.4	3.9	2.8	5.9
Pentanone	4.3	2.4	2.3	2.2	5.7
Nitropropane	1.3	1.2	1.2	1.3	2.8
Pyridine	6.3	4.9	3.5	2.5	6.8
Methanol	12.0	9.1	6.5	3.8	16.2
Ethanol	10.5	8.8	7.6	6.0	12.4
<i>n</i> -Propanol	13.2	7.2	6.5	4.8	15.4
<i>n</i> -Pentanol	8.9	6.0	4.3	3.5	10.2
<i>n</i> -Hexanol	8.3	4.9	2.3	2.4	10.5
Acetone	10.7	5.1	4.8	4.2	12.1
Methyl ethyl ketone	8.8	4.9	4.0	3.2	9.0
Methyl isopropyl ketone	6.7	4.1	2.2	2.0	6.0
Benzaldehyde	6.0	3.5	2.0	2.1	8.4
Bromoform	1.5	1.5	1.6	1.5	1.9
Trichloroethane	1.6	1.5	1.6	1.7	1.8
Trichloroethylene	1.4	1.4	1.4	1.4	2.1
Chlorobenzene	1.5	1.3	1.3	1.4	1.8

all compounds. Similarly the ketones and aldehydes analysed showed improved peak symmetry where they were eluted from the column.

A number of nitrogen containing polar compounds such as amines were also examined but in many cases they were difficult to elute reproducibly from the columns. For that reason no data are produced here, but in general there seemed to be little improvement in the symmetry of the peaks produced even on the drastically oxidised stationary phase.

Some less polar halogenated compounds were also analysed. They were eluted with reasonable symmetry from the untreated OV-17 stationary phase and there was no significant trend towards improvement or deterioration of peak shape as oxidation progressed. Nevertheless, all these substances produced markedly worse peak symmetry on the overheated stationary phase.

Kováts indices for benzene, *n*-butanol, pentanone, nitropropane and pyridine were obtained on each of the stationary phases. The data are recorded in Table III. Each substance had a lower Kováts index on the unoxidised phase (column 1) than on the variously treated oxidised phases. The smallest differences were 2.0 and 2.7 for nitropropane and benzene, respectively, while pyridine showed a decrease of 10.6.

TABLE III

KOVÁTS INDICES FOR VARIOUS COMPOUNDS ON MODIFIED AND UNMODIFIED OV-17

Compound	Column number				
	1	2	3	4	5
Benzene	742.2	739.5	740.4	739.3	744.8
<i>n</i> -Butanol	757.3	752.6	752.0	753.0	788.1
Pentanone	786.6	780.3	778.0	781.0	853.7
Nitropropane	880.0	878.0	881.0	879.2	897.4
Pyridine	879.1	868.5	869.4	866.2	853.7

There was some correlation between the substances showing the greatest improvement in peak symmetry and those showing the greatest variation in retention index. Thus benzene and nitropropane, in addition to having the smallest reduction in retention index, also produced little or no improvement in peak symmetry. Pyridine, nitropropane, and *n*-butanol all showed substantial improvement in peak symmetry and had significant reductions in retention index.

Although there were changes in retention indices between untreated OV-17 and the least oxidised stationary phase (column 2), more stringent oxidation produced no further significant variation. There were minor differences in retention index for each compound on columns 2, 3 and 4 but there was no systematic variation and no trend. The magnitude of the changes in retention index was less than those between the oxidised and the untreated stationary phases and so small as to be merely an indication of the experimental error associated with the measurements. Indeed it might be argued that, at least in some cases, the differences between retention indices on columns 1 and 2 were also within the limits of experimental error. This seems not to be the case however since, when the ΔI values for each of the five compounds are totalled for each stationary phase to produce the McReynolds values for each of the phases there is a marked difference between untreated OV-17 and the variously oxidised phases, as shown in Table IV. By this measure of polarity the oxidised stationary phases are less polar by about 25 units. The three oxidised phases, columns 2, 3 and 4, exhibit small variations but in no systematic way. Certainly the differences between these three columns are much less than those between oxidised and unoxidised phases.

In the measurement of McReynolds values the most noticeable effect is that associated with the overheated column 5. Here there are a variety of changes in ΔI compared to the other four columns, and the changes are generally of greater magnitude than those observed between the oxidised and unoxidised columns. Although the value for benzene is little different from that of untreated OV-17 there are considerable reductions in the values for *n*-butanol and pyridine and significant increases in values for pentanone and nitropropane. Overall, in the calculation of McReynolds value the increases outweigh the decreases in ΔI and the overheated stationary phase is rather more polar than untreated OV-17. This is distinctly different from the oxidised OV-17 phases which were all less polar than untreated OV-17.

Although the oxidation of the OV-17 has resulted in demonstrable changes in

TABLE IV

AI VALUES AND McREYNOLDS CONSTANTS FOR MODIFIED AND UNMODIFIED OV-17

Compound	<i>AI</i> value on column number				
	1	2	3	4	5
Benzene	103.3	100.6	101.5	100.4	105.9
<i>n</i> -Butanol	158.3	153.6	153.0	154.0	139.1
Pentanone	159.5	153.2	150.9	153.9	226.6
Nitropropane	232.3	230.3	233.3	231.5	249.7
Pyridine	185.8	175.2	176.1	172.9	160.4
McReynolds constant	839.2	812.9	814.8	812.7	881.7

peak symmetry and retention, it has proved impossible to explain them in terms of chemical changes in the stationary phase.

The stationary phases were extracted from the support and examined by NMR and IR spectroscopy. NMR analysis failed to reveal any significant structural changes in the OV-17 during modification. The IR spectra of oxidised and unoxidised OV-17 were different although the differences were not great. A peak at 1640 cm^{-1} in the untreated OV-17 spectrum was reduced in the column 2 extract and missing from the spectra of the extracts of columns 3 and 4. Additionally the oxidised stationary phases produced spectra with peaks of increasing intensity at 1460 cm^{-1} and 2925 cm^{-1} . Although these peaks were present in the spectrum of untreated OV-17 their intensity was much less and in the oxidised phases their intensity increased with increasing severity of oxidation.

These changes in the IR spectrum indicate that some reactions have occurred but are not sufficient to identify them. Coleman³ has reported that cyclisation may occur but it is not possible to deduce what has happened on the basis of these results.

In the light of the evidence produced here there seems to be a case for conditioning OV-17 stationary phases in a stream of oxygen rather than nitrogen. Indeed unless all oxygen is removed from the carrier gas stream before it is passed through the column such oxidation may occur unintentionally, at least to a limited extent. The data produced for OV-17 demonstrate that there are benefits in terms of improved peak symmetry for polar solutes without loss of symmetry for non-polar compounds.

REFERENCES

- 1 T. A. Gough and P. B. Baker, *J. Chromatogr. Sci.*, 19 (1981) 227.
- 2 W. O. McReynolds, *J. Chromatogr. Sci.*, 8 (1970) 685.
- 3 A. E. Coleman, *J. Chromatogr. Sci.*, 11 (1973) 198.

CHROM. 17 980

USE OF EQUIVALENT CHAIN LENGTHS FOR THE CHARACTERIZATION OF FATTY ACID METHYL ESTERS SEPARATED BY LINEAR TEMPERATURE-PROGRAMMED GAS CHROMATOGRAPHY

J. KRUPČÍK*

Slovak Technical University, Chemical Faculty, Department of Analytical Chemistry, 1 Jánška Str., 812 37 Bratislava (Czechoslovakia)

and

P. BOHOV

Research Institute of Gerontology, P.O.B. 25, 901 01 Malacky (Czechoslovakia)

(Received June 25th, 1985)

SUMMARY

C₁₂–C₂₆ fatty acid methyl esters (FAMES) were separated by glass capillary gas chromatography on SP 2340 as stationary phase, both isothermally in the temperature range 150–220°C and using linear temperature-programmed capillary gas chromatography (LTPCGC) with gradients of 0.5–3.5°C/min. The dependences of the equivalent chain lengths on temperature are linear. An equation as well as a graphic procedure are derived for the prediction of the retention temperatures of FAMES separated by LTPCGC on SP 2340. Good agreement between predicted and experimental retention temperatures was found.

INTRODUCTION

Since 1959 when Lipsky *et al.*^{1,2} demonstrated the use of capillary gas chromatography for the separation of fatty acid methyl esters (FAMES), many papers have dealt with the application of this technique to the field of lipid research. Both non-polar (Apiezon and methylsilicones) and polar (various types of polyesters and polar silicones) liquids have been used as stationary phases. The highly polar siloxanes allow rapid and effective separation of FAMES, including the separation of geometrical and positional isomers of unsaturated acids. Heckers *et al.*³ demonstrated the potential of the cyanopropylsiloxane type of stationary liquid (SP 2340) in the glass capillary gas chromatographic separation of long chain FAMES. Cyanoalkylpolysiloxanes (Silar 9CP, 10C, SP 2340, OV-275) have greater thermal stability than polyesters⁴. No significant variations in retention over a period of 6 months were found on Silar 5CP and 10C⁵.

For tentative identification of fatty acids in lipids, relative retentions are used. The use of esters of normal saturated carboxylic acids as standards has found general acceptance in the analysis of FAMES. The equivalent chain length (ECL) relationship

was developed by Woodford and Van Gent⁶ and Miwa *et al.*⁷

$$\text{ECL} = z + \frac{\log (t'_{R,i}/t'_{R,z})}{\log (t'_{R,z+1}/t'_{R,z})} \quad (1)$$

where z is the number of carbon atoms in the alkyl chain of the normal saturated carboxylic acid and t'_R are corrected retention times which decrease in the order

$$t'_{R,z+1} > t'_{R,i} > t'_{R,z} \quad (2)$$

where i denotes the FAMES of interest.

Golovnya *et al.*⁵ preferred ECL values for identification purposes when a mixture consisted only of FAMES, whereas Kovát's retention indices were used in the presence of other types of compounds, *e.g.*, long-chain hydrocarbons, alcohols, carbonyls and waxes. However, it should be stressed that ECL values can be used for tentative identification of FAMES separated by gas chromatography only under isothermal conditions. We have shown that the dependence of ECL values on temperature, $d(\text{ECL})/dT$, can be used for tentative identification of the geometrical isomers of monounsaturated FAMES⁸. In a narrow range of temperatures, the dependence of the ECL values can be considered linear and expressed by

$$\text{ECL} = A + BT \quad (3)$$

where A and B are constants depending on the nature of the solute and chromatographic system. However, isothermal capillary gas chromatography of FAMES is tedious in analytical practice or does not resolve all FAMES, therefore the analyses are mostly performed under temperature-programmed conditions.

At present, the tentative identification of FAMES separated by temperature-programmed gas chromatography (TPGC) cannot be performed using ECL values and therefore the available standards must be analyzed after each change in the temperature program. The aim of this paper is to describe a procedure for the tentative identification of FAMES separated by linear temperature-programmed gas chromatography (LTPGC) using ECL values.

THEORETICAL

In linear temperature-programmed capillary gas chromatography (LTPCGC), we have used the following simplifying assumptions⁹:

- (i) Linear temperature programming begins when the sample is injected. There is no isothermal period at the beginning of the analysis.
- (ii) All compounds of interest are eluted under LTPCGC conditions.
- (iii) The isothermal ECL values vary linearly with temperature [$d(\text{ECL})/dT = \text{constant}$].
- (iv) The experimental conditions, particularly the initial temperature and carrier gas flow-rate, are kept constant.

Under similar conditions, we have derived for hydrocarbons a formula for prediction of the retention temperature from isothermal Kovát's indices and elution temperatures of n -alkanes in LTPCGC⁹.

Using this procedure for FAMES chromatographed by TPCGC, we have derived the following equation for the retention temperature

$$T_{R,i} = \frac{(T_{R,z+1} - T_{R,z})[\text{ECL}(T_1) - T_1B - z] + T_{R,z}}{1 - B(T_{R,z+1} - T_{R,z})} \quad (4)$$

where T_R are the retention temperatures, i denoting the compound of interest, z is the number of carbon atoms in the alkyl chain of the normal saturated fatty acid methyl ester; $\text{ECL}(T_1)$ is the value determined isothermally at temperature T_1 and B is the coefficient from eqn. 3.

EXPERIMENTAL

A Carlo Erba high resolution gas chromatograph, Model 4160, equipped with a flame ionization detector and a Spectra Physics integrator, Model SP-4000, were used for all analyses. The chromatograph was fitted with a glass capillary column (75 m \times 0.3 mm I.D.) coated dynamically with cyanopropylsiloxane SP 2340 (Supelco, Bellefonte, PA, U.S.A.) as described elsewhere¹⁰. The analyses were performed isothermally at 150–220°C with a 10°C step, and using LTPGC from 150 to 230°C with gradients of 1–3°C/min and a step of 0.5°C. A Grob splitting system was incorporated in the instrument: the splitting ratio was 1:70. The carrier gas (hydrogen) flow-rate was 25–30 cm/s. The injector and detector temperatures were 235°C. The standards and a model mixture of fatty acid methyl esters were purchased from Supelco. The sample volumes injected were in the range of 1–5 μl of a 0.5% solution of the model mixture prepared from standards in hexane. The elution temperatures were obtained by multiplying the retention times by the temperature gradients and simultaneously read from the thermometer at the peak maxima.

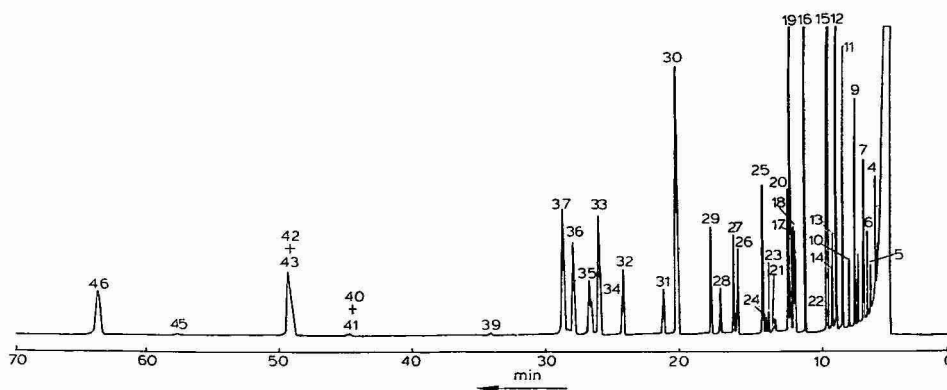


Fig. 1. Separation of FAMES on a SP 2340 glass capillary column at 170°C. For other conditions, see Experimental. Peaks: 2 = 10:0; 4 = 12:0; 5 = 13:0; 6 = iso- 14:0; 7 = 14:0; 8 = aiso- 15:0; 9 = 15:0; 10 = iso- 16:0; 11 = 16:0; 12 = 16:1 ω 7t; 13 = 16:1 ω 7c; 14 = aiso- 17:0; 15 = 17:0; 16 = 18:0; 17 = 18:1 ω 9t; 18 = 18:1 ω 7t; 19 = 18:1 ω 9c; 20 = 18:1 ω 7c; 21 = 19:0; 22 = 18:2 ω 6t,t; 23 = 18:2 ω 6c,t; 24 = 18:2 ω 6t,c; 25 = 18:2 ω 6c,c; 26 = 18:3 ω 6c-all; 27 = 20:0; 29 = 20:1 ω 9c; 30 = 21:0; 31 = 20:2 ω 6c,c; 32 = 20:3 ω 6c-all; 33 = 22:0; 34 + 35 = 20:4 ω 6c-all + 20:3 ω 3c-all; 36 = 22:1 ω 9c; 39 = 20:5 ω 3c-all; 40 = 24:0; 41 = 22:4 ω 6c-all; 42 = 24:1 ω 9c; 43 = 22:4 ω 6c-all; 45 = 22:5 ω 6c-all; 46 = 22:6 ω 3c-all.

TABLE I

COEFFICIENTS OF THE EQUATION $\log t'_R = a + b/T$ FOUND USING THE METHOD OF LEAST SQUARES FOR FAMES SEPARATED ON SP 2340 AT 150–220°C

r = Correlation coefficient.

FAME	a	b	r
9:0	−6.291	2637.8	0.9919
10:0	−5.658	2413.7	0.99986
11:0	−5.640	2460.6	0.99978
12:0	−5.797	2588.0	0.99901
13:0	−6.001	2738.2	0.99919
iso-14:0	−6.073	2794.9	0.9982
14:0	−6.150	2856.3	0.9990
aiso-15:0	−6.293	2961.2	0.9990
15:0	−6.340	298.5	0.9989
iso-16:0	−6.539	3116.2	0.9989
16:0	−6.600	3170.6	0.9992
16:1 ω 7t	−6.572	3184.6	0.9992
16:1 ω 7c	−6.496	3162.6	0.9989
aiso-17:0	−6.800	3300.3	0.9995
17:0	−6.829	3333.3	0.9993
18:0	−7.060	3490.4	0.9994
18:1 ω 9t	−6.979	3475.8	0.9994
18:1 ω 7t	−7.033	3502.6	0.9994
18:1 ω 9c	−6.936	3466.2	0.99949
18:1 ω 7c	−7.001	3498.9	0.99961
19:0	−7.302	3656.3	0.9996
18:2 ω 6tt	−7.434	3711.9	0.99968
18:2 ω 6c,t	−7.099	3572.7	0.99777
18:2 ω 6t,c	−7.035	3551.1	0.99956
18:2 ω 6c,c	−6.934	3512.1	0.99959
18:3 ω 6c-all	−6.918	3538.6	0.99961
20:0	−7.508	3805.2	0.99964
18:3 ω 3c-all	−6.998	3594.5	0.99960
20:1 ω 9c	−7.383	3776.4	0.99962
21:0	−7.802	3996.8	0.99962
20:2 ω 6c,c	−7.379	3819.7	0.99962
20:3 ω 6c-all	−7.307	3819.7	0.99970
22:0	−8.027	4154.5	0.99965
20:3 ω 3c-all	−7.429	3895.6	0.99977
20:4 ω 6c-all	−7.255	3818.2	0.99971
22:1 ω 9t	−7.919	4123.7	0.99968
22:1 ω 9c	−7.848	4098.4	0.99971
23:0	−8.208	4293.7	0.99969
20:5 ω 3c-all	−7.135	3815.3	0.99975
24:0	−8.296	4387.9	0.99977
22:4 ω 6c-all	−7.495	4033.9	0.99982
24:1 ω 9c	−8.117	4329.0	0.99981
25:0	−8.473	4522.8	0.99995
25:5 ω 3c-all	−7.555	4113.5	0.99979
22:6 ω 3c-all	−7.534	4125.4	0.99983
26:0	−8.675	4670.7	0.99996

RESULTS AND DISCUSSION

A model mixture of FAMES was chromatographed isothermally in the region of 150–220°C on a glass capillary column coated with SP 2340. A typical chromatogram obtained at 170°C is shown in Fig. 1. From the obtained retention data, a linear dependence of $\log t'_R$ upon $1/T$ was found

$$\log t'_R = a + b/T \quad (5)$$

where t'_R is the corrected retention time, a and b are constants and, T is the column temperature. The coefficients of eqn. 5 were evaluated by the method of least squares. From the correlation coefficients, r , in Table I it is seen that eqn. 5 is valid for all FAMES chromatographed at temperatures from 150 to 220°C. The slopes (coefficients b in eqn. 5) differ for all the FAMES in Table I, from which it can be concluded that the problems with the separation of some pairs of FAMES in Fig. 1 can be solved by temperature optimization in isothermal gas chromatography.

In Table II the coefficients of eqn. 3 are given, as determined using the method

TABLE II

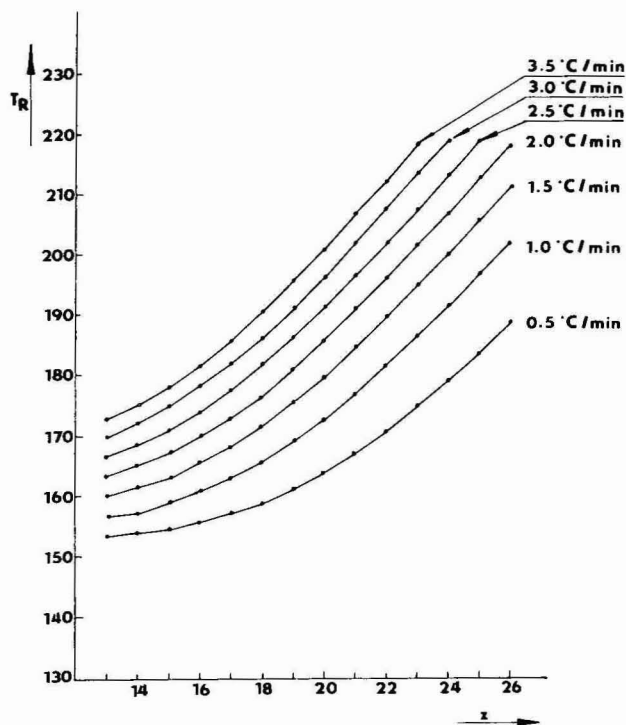
COEFFICIENTS OF THE EQUATION $ECL = A + BT$ FOUND USING THE METHOD OF LEAST SQUARES FOR FAMES SEPARATED ON SP 2340 AT 150–220°C

FAME	A	B	r
iso-14:0	13.40	0.0005861	0.2525
aiso-15:0	14.76	−0.0002664	−0.4292
iso-16:0	15.73	−0.001250	−0.7623
16:1 ω 7t	16.02	0.00260	0.9652
16:1 ω 7c	15.75	0.00532	0.9480
aiso-17:0	16.90	−0.00109	−0.6028
18:1 ω 9t	17.84	0.003114	0.9988
18:1 ω 7t	18.05	0.00220	0.9832
18:1 ω 9c	17.72	0.00470	0.9967
18:1 ω 7c	17.96	0.00376	0.9795
18:2 ω 6t,t	18.38	0.00300	—
18:2 ω 6c,t	18.01	0.00682	0.9931
18:2 ω 6t,c	18.15	0.00639	0.9930
18:2 ω 6c,c	17.85	0.00871	0.9985
18:3 ω 6c-all	17.94	0.01162	0.9983
18:3 ω 3c-all	18.26	0.01180	0.9986
20:1 ω 9c	19.55	0.00525	0.9950
20:2 ω 6c,c	19.66	0.00905	0.9970
20:3 ω 6c-all	19.60	0.01251	0.9980
20:3 ω 3c-all	20.13	0.01152	0.9974
20:4 ω 6c-all	19.63	0.01462	0.9982
22:1 ω 9t	21.78	0.00295	0.9945
22:1 ω 9c	21.60	0.00468	0.9975
22:5 ω 3c-all	19.94	0.01840	0.9779
22:4 ω 6c-all	21.04	0.01731	0.9980
24:1 ω 9c	23.44	0.00531	0.9806
22:5 ω 6c-all	21.7	0.01917	0.9964
22:5 ω 3c-all	21.60	0.01949	0.9878
22:6 ω 3c-all	21.6	0.02129	0.9877

TABLE III

COMPARISON OF EXPERIMENTALLY FOUND, ECL_F , AND PUBLISHED, ECL_P , DATA FOR FAMES SEPARATED ON SP 2340 STATIONARY PHASE

FAME	170°C		200°C	
	ECL_F	ECL_P^A	ECL_F	ECL_P^B
iso-14:0	13.52	13.43	13.47	13.52
aiso-15:0	14.70	14.56	14.71	14.74
iso-16:0	15.52	15.43	15.47	15.52
16:1 ω 7t	16.46	16.61	16.55	16.52
16:1 ω 7c	16.66	16.89	16.79	16.73
aiso-17:0	16.70	—	16.71	16.72
18:1 ω 9t	18.37	18.54	18.46	18.37
18:1 ω 7t	18.42	18.56	18.48	—
18:1 ω 9c	18.53	18.77	18.67	18.62
18:1 ω 7c	18.70	18.84	18.73	18.70
18:2 ω 6t,t	19.01	19.31	19.04	19.05
18:2 ω 6c,c	19.34	19.71	19.60	19.47
20:1	20.44	20.77	20.62	20.55
20:2 ω 6c,c	21.19	21.71	21.47	21.41
22:1 ω 9t	22.28	22.54	22.36	22.30
22:1 ω 9c	22.39	22.47	22.50	22.50

Fig. 2. Dependence of the elution temperatures, T_R , of normal saturated FAMES on the number of carbon atoms, z , in their alkyl chains.

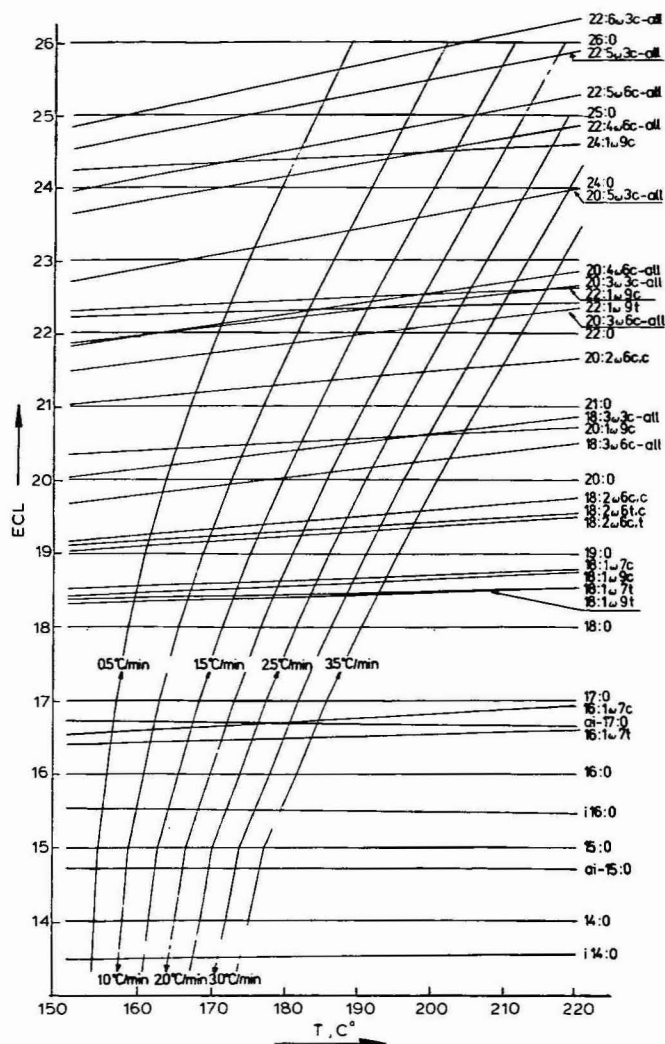


Fig. 3. Graph for prediction of elution temperatures in LTPGC, plotted using data from Table II and Fig. 2.

of least squares for FAMES separated on SP 2340 at 150–220°C. From the correlation coefficients, r , it can be concluded that eqn. 3 is not valid for branched FAMES. Also, that the values of the slopes B increase with increasing number of double bonds. The slopes for monoenoic FAMES are higher for the *cis* than for the *trans* isomers, in agreement with our previously published results on other types of liquid phases⁸.

The use of published ECL data for the tentative identification of FAMES is very difficult since the reproducibility is very poor, as can be seen from Table III. In order to improve the reproducibility, standardization of experiment conditions, e.g., stationary film thickness and polarity of the capillary walls, will be necessary.

It was reported that in LTPGC there exists a linear relationship between the

TABLE IV

COMPARISON BETWEEN PREDICTED, $T_{R,p}$, AND EXPERIMENTAL, $T_{R,t}$, ELUTION TEMPERATURES OF FAMES SEPARATED ON SP 2340 USING DIFFERENT TEMPERATURE GRADIENTS

FAME	0.5°C/min		1.0°C/min		1.5°C/min		2.0°C/min		2.5°C/min		3.0°C/min		3.5°C/min	
	$T_{R,p}$	$T_{R,t}$	$T_{R,p}$	$T_{R,t}$	$T_{R,p}$	$T_{R,t}$	$T_{R,p}$	$T_{R,t}$	$T_{R,p}$	$T_{R,t}$	$T_{R,p}$	$T_{R,t}$	$T_{R,p}$	$T_{R,t}$
aiso-15:0	154.5	154.6	158.9	158.8	162.9	162.8	166.6	166.5	170.3	170.2	174.0	173.9	177.4	177.3
iso-16:0	155.3	155.3	160.2	160.1	164.6	164.5	168.6	168.6	172.6	172.5	176.5	176.5	180.0	180.1
16:1 ω 7t	156.4	156.3	161.9	161.8	166.9	166.7	171.4	171.2	175.7	175.5	180.0	179.7	183.9	183.6
16:1 ω 7c	156.6	156.6	162.3	162.2	167.4	167.2	172.0	171.8	176.5	176.1	180.9	180.5	184.8	184.4
aiso-17:0	156.7	156.7	162.5	162.4	167.4	167.5	171.9	172.1	176.3	176.4	180.6	180.8	184.5	184.7
18:1 ω 9t	159.6	159.5	167.0	166.8	173.2	173.0	178.6	178.4	183.6	183.2	188.5	188.1	192.8	192.4
18:1 ω 7t	159.8	159.7	167.1	167.0	173.4	173.2	178.8	178.6	183.7	183.5	188.6	188.3	193.0	192.7
18:1 ω 9c	159.9	159.8	167.4	167.2	173.8	173.5	179.3	178.9	184.3	183.9	189.4	188.8	193.7	193.2
18:1 ω 7c1	160.2	160.0	167.7	167.5	174.1	173.8	179.6	179.3	184.6	184.3	189.7	189.2	194.0	193.6
18:2 ω 6t	161.0	160.9	169.0	168.9	175.6	175.4	181.2	181.2	186.3	186.2	191.5	191.3	195.8	195.7
18:2 ω 6c,t	161.4	161.3	169.6	169.4	176.4	176.1	182.4	181.8	187.6	187.0	193.0	192.2	197.4	196.6
18:2 ω 6t,c	161.4	161.5	169.6	169.6	176.4	176.4	182.4	182.4	187.6	187.4	193.0	192.6	197.4	197.0
18:2 ω 6c,c	161.8	161.6	170.3	169.9	177.4	176.7	183.2	182.5	188.6	187.8	194.1	193.0	198.7	197.5
18:3 ω 6c-all	163.4	163.1	172.6	172.0	180.2	179.3	186.4	185.4	192.2	190.8	197.8	196.1	202.7	200.9
18:3 ω 3c-all	164.4	164.1	174.5	173.5	181.5	180.9	188.4	187.2	194.2	192.7	199.9	198.2	204.7	202.9
20:1 ω 9c	165.2	164.9	174.8	174.4	182.4	181.9	188.8	188.1	194.3	193.6	199.8	199.0	204.5	203.6
20:2 ω 6c,c	167.6	167.4	178.3	177.7	186.4	185.6	193.2	192.1	198.6	197.8	204.8	203.5	209.7	208.2
20:3 ω 6c-all	169.7	169.2	181.0	180.0	189.6	188.6	196.5	195.0	202.1	200.9	208.6	206.8	213.8	211.6
20:3 ω 3c-all	171.2	170.6	182.7	181.8	191.4	190.2	198.4	197.0	204.5	202.9	210.7	208.8	215.7	213.7
20:4 ω 6c-all	171.3	170.6	183.0	181.9	191.9	190.4	199.0	197.2	205.4	203.3	211.6	209.3	217.1	214.1
22:1 ω 9t	171.8	171.7	183.2	182.9	191.4	191.1	198.2	197.8	203.4	203.6	209.8	209.3	214.6	214.1
22:1 ω 9c	172.4	172.1	183.9	183.3	192.3	191.7	199.1	198.4	204.5	203.6	210.8	209.3	215.7	214.1
20:5 ω 3c-all	175.6	174.4	188.6	186.6	198.0	195.5	205.4	202.7	212.0	208.9	218.6	215.5		
22:4 ω 6c-all	179.9	179.0	193.6	191.9	203.3	201.0	210.7	208.3	217.6	214.6				
24:1 ω 9c	181.0	180.6	194.0	193.3	203.0	202.2	210.0	209.1	216.3	215.2				
22:5 ω 6c-all	181.8	180.6	196.0	193.7	205.8	203.0	213.4	210.3	220.0	216.7				
22:5 ω 3c-all	185.0	183.2	199.4	196.7	209.4	206.2	217.1	213.6						
22:6 ω 3c-all	187.1	185.0	201.6	198.7	212.0	208.4	220.0	215.8						

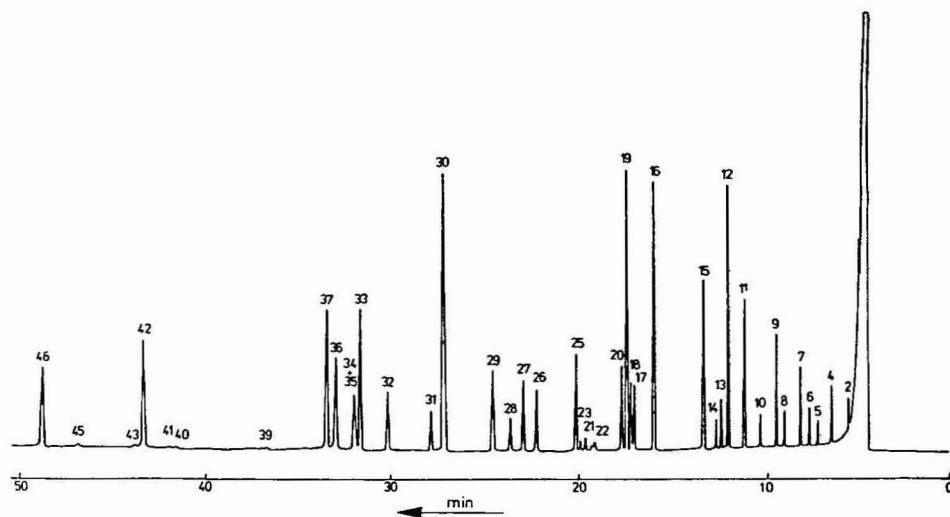


Fig. 4. Separation of FAMES on a SP 2340 glass capillary column using LTPGC from 150 to 220°C with a gradient of 1°C/min. For other conditions, see Experimental. For peak identification, see Fig. 1.

retention times and the carbon numbers of homologous series¹¹. Since the retention time, t_R , in LTPGC corresponds to the elution temperature, T_R , we could expect a linear relationship between the latter and the carbon number, z , for the alkyl chain of normal saturated FAMES. From Fig. 2 it is seen that this dependence is not linear when FAMES are separated on SP 2340 as stationary phase. The slopes of the lines change with the temperature gradient as well as with the carbon number, z . This is why we do not use "ECL values calculated in the LTPGC conditions" for the purposes of tentative identification of FAMES separated by LTPGC.

Knowing the isothermal ECL values (Table II) and the retention temperatures, T_R , of normal saturated FAMES, we were able to predict the retention temperatures of branched and unsaturated FAMES using eqn. 4. Table IV compares predicted, $T_{R,p}$, and experimental $T_{R,f}$, elution temperatures of FAMES separated on SP 2340 by LTPGC using different temperature gradients. There is good agreement between these values for branched and monoenic FAMES, the differences being less than 1.2°C. The largest difference, $T_R = T_{R,p} - T_{R,f}$, was found for 22:6 ω 3c-all, namely 4.2°C.

We have found that for the prediction of retention temperature a graphic procedure can be used as shown in Fig. 3, where the dependences of isothermal ECL values on temperature (data from Table II) as well as of retention temperatures of normal saturated FAMES on the carbon number (data from Fig. 2) are given. It can be concluded that the elution order of FAMES can be dramatically changed by changing the temperature gradient in LTPGC. For example, the separation of FAMES using LTPGC with a gradient of 1°C/min is shown on Fig. 4. A comparison of Figs. 1 and 3 demonstrated the improved separation of pairs 13,14 and 17,18, but the pair 34,35 is still not resolved. From Fig. 3 the optimum gradient for LTPGC can be found by computation¹².

REFERENCES

- 1 S. R. Lipsky, J. E. Lovelock and R. A. Landowne, *J. Am. Chem. Soc.*, 81 (1959) 1010.
- 2 S. R. Lipsky, R. A. Landowne and J. E. Lovelock, *Anal. Chem.*, 31 (1959) 852.
- 3 H. Heckers, F. W. Melcher and V. Schloeder, *J. Chromatogr.*, 136 (1977) 311.
- 4 H. Heckers, K. Dittmar, F. W. Melcher and H. D. Kalinowski, *J. Chromatogr.*, 135 (1977) 93.
- 5 R. V. Golovnya, V. P. Uralets and T. E. Kuzmenko, *J. Chromatogr.*, 121 (1976) 118.
- 6 F. P. Woodford and C. M. van Gent, *J. Lipid Res.*, 1 (1960) 188.
- 7 T. K. Miwa, K. L. Mikolajczak, F. R. Earle and I. A. Wolf, *Anal. Chem.*, 32 (1960) 1739.
- 8 J. Hrivňák, L. Soják, J. Krupčík and Y. P. Duchesne, *J. Am. Oil Chem. Soc.*, 50 (1973) 68.
- 9 J. Krupčík, P. Čellár, D. Repka, J. Garaj and G. Guiochon, *J. Chromatogr.*, in press.
- 10 P. Bohov, V. Baláž and J. Hrivňák, *J. Chromatogr.*, 286 (1984) 247.
- 11 M. van den Dool and P. Kratz, *J. Chromatogr.*, 11 (1963) 463.
- 12 J. Krupčík, P. Bohov and Š. Gergely, in preparation.

CHROM. 17 979

ÄTHENMESSUNG DURCH EINE GASCHROMATOGRAPHISCHE ANREICHERUNGSTECHNIK MIT FLAMMENIONISATIONSDETEKTION

JAN GOLIÁŠ

Institut für Obst- und Gemüse-technologie der Landwirtschaftlichen Hochschule Brno, 69144 Lednice na Moravě (Tschechoslowakei)

und

JOSEF NOVÁK*

Institut für analytische Chemie der Tschechoslowakischen Akademie der Wissenschaften, 61142 Brno (Tschechoslowakei)

(Eingegangen am 25. Juni 1985)

SUMMARY

Determination of ethylene by a gas chromatographic enrichment technique with a flame ionization detector

A method for the determination of ethylene produced by pulpy fruits is described, consisting in the equilibration trapping of ethylene in a column packed with Carbosieve G, thermal desorption of the deposit, and analysis of the concentrate by gas chromatography with a flame ionization detector. Ethylene concentrations at the nanograms per litre level in the ambient atmosphere can be determined in this way. With 0.1 g of Carbosieve in the trap, the detection limit is *ca.* 0.08 nl l^{-1} (ppb) of ethylene in the air analyzed. The detection limits attainable when using different methodical variants of gas chromatographic analysis are compared. The detection limits have been calculated from the chromatographic conditions and the parameters of the detection system. From the theoretically derived equations, it is possible to estimate the ethylene concentration quickly without it being necessary to calibrate the instrument, which is advantageous in trace analysis.

EINLEITUNG

Äthen als einfachstes Pflanzenhormon wird allgemein von pflanzlichen Geweben produziert. Bei fleischiges Obst ist es oft notwendig, Äthen in solchen niedrigen Konzentrationen zu messen, bei denen schon eine physiologische Aktivität eintreten kann. Wenn auch die Messgenauigkeit der direkten Probenanalyse durch Gaschromatographie mit Flammenionisationsdetektor bei vielen praktischen Anwendungen ausreichend ist, gibt es doch Situationen, bei denen der Einsatz von Anreicherungstechniken ratsam erscheint oder notwendig ist. Durch direkte Dosierung des analysierten Gases in den Chromatographen kann man etwa bis auf 10 ppb Äthen genau

messen. Durch die Verwendung von Anreicherungstechniken, die die Adsorption des zu analysierenden Stoffes in der Anreicherungskolonie mit einem geeigneten Sorbents¹⁻⁴, die Wärmedesorption und die Analyse des Konzentrates umfassen, kann man entweder die Empfindlichkeit der Analyse noch bedeutend erhöhen oder unter stabileren Bedingungen arbeiten, indem man eine geringere Empfindlichkeit des Elektrometers einstellt und so zu sichereren Ergebnissen kommt. Jedoch bindet sich Äthen an den herkömmlichen Sorbentien nur schwach, so dass der Konzentrierungseffekt gering ist. Um eine höhere Konzentrierung zu erreichen, benutzten Goliáš *et al.*⁵ eine zweistufige Methode. In einer Anreicherungskolonie mit einer relativ grossen Menge (etwa 1 g) Porapak Q bindet sich Äthen durch einen Gleichgewichtsprozess⁶ und nach thermischer Desorption gelangt das Konzentrat mit dem Strom des Trägergases in eine zweite, kleine Anreicherungskolonie mit etwa 0,1 g Porapak Q, die durch festes Kohlendioxyd gekühlt wird. Von hier wird dann das Konzentrat nach thermischer Desorption in den Gaschromatographen eingeleitet und analysiert. Durch diese Methode wurde die Empfindlichkeit der Analyse um etwa eine Grössenordnung erhöht. Ein im wesentlichen gleiches Verfahren benutzten später Bečka und Feltl⁷.

In der vorliegenden Arbeit verwendeten wir als Füllung für die Anreicherungskolonie Aktivkohle Carbosieve G (Supelco, Bellefonte, PA, U.S.A.), die dank ihrer hohen Sorptionsaktivität einen wesentlich höheren Konzentrierungseffekt, auch schon bei einstufiger Anordnung, ermöglicht.

THEORETISCHER TEIL

Beziehungen zwischen den Ausgangsgrössen des Chromatographen und der Äthenkonzentration im analysierten Gas

Die unmittelbare Anzeige des Flammenionisationsdetektors, R_i , auf die augenblickliche Konzentration des Analysates i im Effluent aus der Kolonne, q_i , ist⁸

$$R_i = \beta \frac{(\Sigma C_{\text{eff}})_i}{M_i} F q_i \quad (1)$$

dabei sind β die Effektivität der Ionisation (in Coulomb pro Grammatom Paraffinkohlenstoff) in der Flamme; M_i und $(\Sigma C_{\text{eff}})_i$ die Molekülmasse des Analysates und die Summe der effektiven Kohlenstoffatome im Molekül des Analysates (in Grammatomen des effektiven Paraffinkohlenstoffes in einem Mol des Analysates); und F die Volumenflussgeschwindigkeit des Effluents aus der Kolonne. F und q_i werden bei der Temperatur der Kolonne und dem Druck am Ausgang der Kolonne gemessen. Die Reaktion R_i hat die Einheiten eines Ionisationsstromes.

Die Gleichung 1 führt zu den Beziehungen⁹

$$A_i = \frac{b \beta}{a k_U k_D} \frac{(\Sigma C_{\text{eff}})_i}{M_i} v_{(i)} \rho_i \quad (2)$$

$$h_i = \frac{\beta}{a k_U k_D} \frac{(\Sigma C_{\text{eff}})_i}{M_i} \frac{\sqrt{N/2\pi}}{t_R} v_{(i)} \rho_i \quad (3)$$

Dabei sind: A_i und h_i die Fläche und die Höhe des Peaks des Analysates in der graphischen Aufzeichnung am Chromatographen; b , die Geschwindigkeit des Papiervorschubes bei der Registrierung; a , der Faktor der Empfindlichkeitsverringierung des Elektrometers; k_U , das Verhältnis des Ionisationsstromes zur entsprechenden Austrittsspannung aus dem Elektrometer bei voller Empfindlichkeit; k_D , das Verhältnis der Austrittsspannung aus dem Elektrometer zur entsprechenden Längenabweichung der Feder des Schreibers; N , die Anzahl der theoretischen Böden der Kolonne (für das Analysat i); t_R , die Retentionszeit des Analysates in der chromatographischen Kolonne unter den Versuchsbedingungen; $v_{(i)}$, das dosierte Volumen des analysierten Gases; ρ_i die Konzentration (Masse/Volumen) des Analysates im analysierten Gas.

Bei Benutzung von Anreicherungstechniken gehen die Gleichungen 2 und 3 über in

$$A_i = \frac{b\beta}{a k_U k_D} \frac{(\Sigma C_{\text{eff}})_i}{M_i} V \rho_i \quad (4)$$

bzw.

$$A_i = \frac{b\beta}{a k_U k_D} \frac{(\Sigma C_{\text{eff}})_i}{M_i} V_{R,S} \rho_i \quad (5)$$

und

$$h_i = \frac{\beta}{a k_U k_D} \frac{(\Sigma C_{\text{eff}})_i}{M_i} \frac{\sqrt{N/2\pi}}{t_R} V \rho_i \quad (6)$$

bzw.

$$h_i = \frac{\beta}{a k_U k_D} \frac{(\Sigma C_{\text{eff}})_i}{M_i} \frac{\sqrt{N/2\pi}}{t_R} V_{R,S} \rho_i \quad (7)$$

Gleichungen 4 und 6 gelten bei vollständiger Adsorption des Analysates und Gleichungen 5 und 7 bei Gleichgewichtsadsorption. V ist das Volumen des analysierten Gases, das man durch die Anreicherungskolonne durchsaugen kann, ohne die Front des Analysates zu durchbrechen. $V_{R,S}$ ist das Retentionsvolumen des Analysates in der Anreicherungskolonne mit dem Sorbens S unter den Bedingungen der Probenentnahme. Für das Maximalvolumen V_{max} bei der vollständigen Adsorption und das Minimalvolumen V_{min} bei der Gleichgewichtsadsorption gilt näherungsweise^{10,11}

$$V_{\text{max}} \leq V_{R,S} \left(1 - \frac{2}{\sqrt{n}} \right) \quad (8)$$

$$V_{\text{min}} \geq V_{R,S} \left(1 + \frac{2}{\sqrt{n}} \right) \quad (9)$$

wobei n die Zahl der theoretischen Böden in der Anreicherungskolonne ist. Das Retentionsvolumen ist gegeben durch

$$V_{R,S} = K V_S + V_G = V_g W_s \frac{T}{273} + V_G \quad (10)$$

K und V_g sind der Verteilungskoeffizient und das spezifische Retentionsvolumen^{1,2} des Analysates auf dem Sorbens unter den Bedingungen der Probenentnahme; V_S und W_s das Volumen und die Masse des Sorbens in der Anreicherungskolonne; T ist die absolute Temperatur der Anreicherungskolonne bei der Probenentnahme; und V_G ist das freie Volumen der Anreicherungskolonne. Die Gleichungen 4-7 ermöglichen es, aus der Fläche oder der Höhe des chromatographischen Peaks des Analysates die Konzentration Äthens im analysierten Gas ausreichend genau zu bestimmen, ohne eine direkte Eichung durchführen zu müssen.

Die minimal wahrnehmbare Konzentration des Analysates im analysierten Gas (die Höhe des Peaks ist gleich zweimal der Rauschbreite) ρ_i^{\min} kann man für die Variante der vollständigen bzw. Gleichgewichtsadsorption aus den folgenden Gleichungen^{1,3} schätzen:

$$\rho_i^{\min} = \frac{2 d_n}{V_{R,S} [1 - (2/\sqrt{n})]} \frac{k_U k_D}{\beta} \frac{M_i}{(\Sigma C_{\text{eff}})_i} \frac{t_R}{\sqrt{N/2\pi}} \quad (11)$$

bzw.

$$\rho_i^{\min} = \frac{2 d_n k_U k_D}{V_{R,S} \beta} \frac{M_i}{(\Sigma C_{\text{eff}})_i} \frac{t_R}{\sqrt{N/2\pi}} \quad (12)$$

Dabei ist d_n die Rauschbreite bei der graphischen Aufzeichnung des Chromatogramms. Für die Bestimmung von ρ_i^{\min} im Falle der direkten Analyse ersetzt man in

Gleichung 11 $V_{R,S} [1 - (2/\sqrt{n})]$ durch das maximale Volumen des analysierten Gases, das man noch ohne Probleme direkt in den Chromatographen dosieren kann.

EXPERIMENTELLER TEIL

Prinzip der Methode

Eine Probe des untersuchten Obstes wird in ein Gefäß gegeben, das mit Luft durchströmt wird. Das Äthen, das aus der Probe in den Luftstrom abgegeben wird, bindet sich nach dem Gleichgewichtsprinzip an das Sorbens in der Anreicherungskolonne. Die Masse der analysierten Fruchtanteile beträgt etwa 50 g. Die Zeitdauer der Analyse ist im wesentlichen durch die Zeit gegeben, die notwendig ist, damit sich zwischen der Äthenkonzentration in der durchströmenden Luft und im Gewebe der Frucht ein Gleichgewicht einstellt. Das durchströmte Volumen im System Probe-durchströmendes Gas wurde so klein wie möglich gehalten, indem der Innenraum des Gefäßes die Form einer Hohlkugel erhielt, wodurch weitgehend die Entstehung nichtdurchmischter Räume verhindert wurde. Der Luftstrom wurde durch eine Membranluftpumpe erzeugt. Die Durchströmgeschwindigkeit der Luft wurde mit einem

Kapillar-Durchflussmesser gemessen und durch ein Nadelventil gesteuert. Zum Auffangen des Wasserdampfes aus der Luft und aus der Probe wurde in das System eine Trocknungskolonnie mit Silikagel eingefügt. Die einzelnen Teile sind wie folgt nacheinander angeordnet: Probengefäß–Trockenturm–Anreicherungskolonnie–Kapillar-Durchflussmesser–Nadelventil–Saugpumpe.

Spezifisches Elutionsvolumen des Äthens auf dem Sorbens Carbosieve G

Das Sorbens Carbosieve G ist eine speziell präparierte Aktivkohle, die eine hohe spezifische innere Oberfläche von etwa $1000 \text{ m}^2/\text{g}$ Adsorbens hat und die man folglich zur wirksamen Konzentrierung von Äthen benutzen kann. Den Wert V_g ermittelt man auf herkömmliche Art und Weise¹², das heisst durch Messung der Verweilzeit des Äthens in der chromatographischen Kolonne, die mit diesem Sorbens gefüllt ist, unter definierten Bedingungen. Die Messung erfolgte bei einigen Temperaturen im Bereich zwischen 30°C und 90°C . Für die Beziehung zwischen $\log V_g$ und dem Kehrwert der absoluten Temperatur ($1/T$) wurde folgende lineare Regressionsgleichung ermittelt (Korrelationskoeffizient $r = 0,99986$):

$$\log V_g = 1720,430554/T - 2,499852 \quad (13)$$

Arbeitsmethode und Berechnung der Ergebnisse

Etwa 8 min nach dem Einlegen der Probe in das Strömungssystem erreicht die Äthenkonzentration im Luftstrom einen stationären Wert. Dann wird die vorher aktivierte Anreicherungskolonnie mit dem Sorbens mit einer Masse $W_s = 41,5 \text{ mg}$ eingeschaltet. Die Durchströmzeit, die zum Erreichen des Gleichgewichts notwendig ist, wird durch den Wert $V_{R,S}$ und durch die Volumengeschwindigkeit des Luftstromes bestimmt. Bei einer Temperatur von 20 bis 25°C und einer Sauggeschwindigkeit von 100 ml min^{-1} reichen 6 min. Das adsorbierte Äthen wird in einer Heizpatrone bei 170°C desorbiert und das so erhaltene Konzentrat gelangt mit dem Strom des Trägergases in die chromatographische Kolonne, die mit Poropak Q gefüllt ist (Länge der Kolonne $1,2 \text{ m}$). Im Chromatogramm des Konzentrats miss man die Fläche des Äthenpeaks. Einen Eichpeak für Äthen erhält man, indem man getrennt ein definiertes Volumen der Eichlösung mit bekannter Äthenkonzentration unter gleichen Bedingungen dosiert und das Chromatogramm aufnimmt. Die Äthenkonzentration im Luftstrom c_i ist gegeben durch

$$c_i = \frac{(A_i/A_s) v_{(s)} c_s}{V_g W_s T/273,16} \quad (14)$$

mit: A_i , Fläche des Peaks im Chromatogramm der untersuchten Probe (mm^2); A_s , Peakfläche des Äthens im Chromatogramm der Eichlösung (mm^2); $v_{(s)}$, Volumen der eingespritzten Eichprobe (ml); c_s , Konzentration des Standards in der Eichprobe (ml l^{-1}); V_g , spezifisches Elutionsvolumen des Äthens (ml g^{-1}); W_s Masse des Sorbens in der Anreicherungskolonnie (g); T absolute Temperatur der Anreicherungskolonnie ($^\circ\text{K}$).

Das spezifische Elutionsvolumen V_g bestimmt man aus der empirischen Gleichung 13 für die gegebene Temperatur der Anreicherungskolonnie, die vor der

Äthenadsorption immer auf gleicher Temperatur gehalten wird. Die Äthenproduktion G_i (in $\mu\text{g kg}^{-1} \text{ h}^{-1}$), die in den Abbildungen angegeben ist, erhält man aus der Beziehung

$$G_i = \frac{c_i F}{W} 1000 \quad (15)$$

mit: F , Volumenflussgeschwindigkeit des Luftstromes (l.h^{-1}); W , Masse der Obstprobe im Probengefäß (kg).

ERGEBNISSE UND DISKUSSION

Die praktische Anwendung der Gleichungen 11 und 12 kann man durch die Berechnung von ρ_i^{\min} aus den Parametern auf den rechten Seiten dieser Gleichungen darstellen. Die Parameter k_U und k_D sind durch die technischen Eigenschaften des Elektrometer- und des Registriersystems gegeben, M_i und $(\Sigma C_{\text{eff}})_i$ durch die chemische Zusammensetzung des gemessenen Stoffes, β wird durch Eichung oder Schätzung bestimmt, d_n liest man aus dem Chromatogramm ab, t_R und N berechnet man aus den Parametern des Peaks des gemessenen Stoffes im Chromatogramm, $V_{R,S}$ berechnet man nach Gleichung 10, wobei V_g aus der empirischen Gleichung 13 und n aus der Länge der Anreicherungskolonne bestimmt werden (in der Regel kann man davon ausgehen, dass $V_{R,S} [1 - (2/\sqrt{n})] = 0,5 V_{R,S}$ ist). Alle Parameter, die zur Berechnung von ρ_i^{\min} notwendig sind, lassen sich also leicht bestimmen. In Tabelle I sind einige Werte von ρ_i^{\min} angeführt, die für einige methodische Varianten unter typischen Arbeitsbedingungen berechnet wurden. Für die Rechnungen wurden folgende Werte der einzelnen Parameter verwendet: $d_n = 5 \text{ mm}$, $k_U = 10^{-12} \text{ A/mV}$, $k_D = 4 \times 10^{-3} \text{ mV/mm}$, $\beta = 0,15 \text{ Coulomb/g-Atom } C_{\text{par}}$, $M_i = 28 \text{ g/mol}$, $(\Sigma C_{\text{eff}})_i = 2 \text{ g Atom } C_{\text{par}}/\text{mol}$, $t_R = 51 \text{ s}$, $n = 20$, $N = 554$; Carbosieve G: $\log V_g = 1720,43/T - 2,4998$; Porapak Q: $\log V_g = 1282,9/T - 3,084$ (siehe Literaturhinweis 5); Temperatur der Anreicherungskolonne 20°C . Mit Ausnahme der Werte W_s (bei den Versuchen in dieser Arbeit waren $W_s = 0,0415 \text{ g}$ und die Länge der Anreicherungskolonne 20 mm) und dem geschätzten Wert $n = 20$ (für eine angenommene Länge der Anreicherungskolonne von 40 mm) stellen alle angeführten Werte reelle experimentelle Parameter dar. Die Werte $W_s = 0,1 \text{ g}$ bei den Methoden 2–5 und $W_s = 1 \text{ g}$ bei den Methoden 6 und 7 (siehe Tabelle I) wurden in Hinsicht auf einen leichteren Vergleich gewählt. Die Verwendung einer Anreicherungskolonne mit $0,1 \text{ g}$ Carbosieve G wäre durchaus real, und der Unterschied zwischen den Werten von ρ_i^{\min} mit $W_s = 0,1 \text{ g}$ und $W_s = 0,0415 \text{ g}$ ist nicht gravierend. Der berechnete Wert $\rho_i^{\min} = 0,792 \times 10^{-1} \text{ ppb}$ für Variante 3 in Tabelle I stellt also gut die minimale wahrnehmbare Äthenkonzentration unter den Bedingungen dieser Methode dar. Was die Beispiele mit zweistufigem trapping (Varianten 6 und 7 in Tabelle I) betrifft, so unterscheidet sich die gewählte Masse $W_s = 1 \text{ g}$ kaum von der Masse ($W_s = 1,139 \text{ g}$), die in unserer vorhergehenden Arbeit⁵ verwendet wurde.

Aus den Ergebnissen von Tabelle I ist ersichtlich, dass die Verwendung von Porapak Q als Anreicherungsorbens beim einstufigen trapping praktisch wirkungslos ist (vergleiche Varianten 4 und 5 mit Variante 1), während Carbosieve G unter den gleichen Bedingungen die Wahrnehmbarkeitsgrenze etwa um zwei Zehnerpoten-

TABELLE I

NACHWEISGRENZEN (DETEKTIONSLIMITEN) FÜR VERSCHIEDENE METHODISCHE VARIANTEN

No.	Methode	ρ_i^{\min}	
		g/ml	Volumen ppb
1	Direktes Einspritzen von 1 ml des zu analysierenden Gases	$2,03 \cdot 10^{-11}$	$1,74 \cdot 10^1$
2	Vollständiges trapping, Anreicherungskolonne mit Carbosieve G, $W_s = 0,1$ g	$1,67 \cdot 10^{-13}$	$1,43 \cdot 10^{-1}$
3	Gleichgewichtstrapping, Anreicherungskolonne mit Carbosieve G, $W_s = 0,1$ g	$0,923 \cdot 10^{-13}$	$0,792 \cdot 10^{-1}$
4	Vollständiges trapping, Anreicherungskolonne mit Porapak Q, $W_s = 0,1$ g	$1,63 \cdot 10^{-11}$	$1,40 \cdot 10^1$
5	Gleichgewichtstrapping, Anreicherungskolonne mit Porapak Q, $W_s = 0,1$ g	$0,902 \cdot 10^{-11}$	$0,774 \cdot 10^1$
6	Zweistufiges trapping ⁵ , Anreicherungskolonne mit Carbosieve G, $W_s = 1$ g	$0,923 \cdot 10^{-14}$	$0,792 \cdot 10^{-2}$
7	Zweistufiges trapping ⁵ , Anreicherungskolonne mit Porapak Q, $W_s = 1$ g	$0,902 \cdot 10^{-12}$	$0,774 \cdot 10^0$

zen vergrößert. Im Falle zweistufigen trappings mit Carbosieve G als Anreicherungsorbens und $W_s = 1$ g kann man Äthenkonzentrationen im analysierten Gas noch in der Größenordnung von einigen ppt ($1 \cdot 10^{-12}$ Volumenteile) nachweisen. Es besteht kein wesentlicher Unterschied in der Nachweisbarkeitsgrenze zwischen dem vollständigen und dem Gleichgewichtstrapping. Bei den Angaben in Tabelle I handelt es sich um die Wahrnehmbarkeitsgrenzen. Von einer Messung der Konzentration kann man erst dann sprechen, wenn die Konzentrationen um etwa eine Zehnerpotenz höher sind. Durch Einsetzen der oben angeführten Werte für β , k_U , k_D , $(\Sigma C_{\text{eff}})_i$, M_i , N und t_R in Gleichungen 2 und 3 erhalten wir

$$A_i = 2,678 \frac{b}{a} v_{(i)} \rho_i \cdot 10^{12}$$

$$h_i = \frac{4,933}{a} v_{(i)} \rho_i \cdot 10^{11}$$

Diese zwei Gleichungen sind eigentlich theoretisch abgeleitete Eichgeraden in den Koordinaten $A_i - v_{(i)} \rho_i$ und $h_i - v_{(i)} \rho_i$. Werden konstante Arbeitsbedingungen eingehalten, so kann man bei gegebener Anordnung der Geräte diese Gleichungen benutzen, um die Äthenkonzentration aus der Fläche oder Höhe ihres Peaks in Chromatogramm und aus dem Volumen der dosierten Probe ohne Eichung zu bestimmen.

Aus den Daten aus den Fig. 1–3 geht nach entsprechenden Berechnungen hervor, dass die niedrigste stationäre Äthenkonzentration im Luftstrom einige nl l^{-1} beträgt, was einer Konzentration entspricht, die sich durch direktes Einspritzen nur schwierig messen lässt. Die Durchsaugtemperatur kann man in einem breiten Bereich wählen ($0\text{--}30^\circ\text{C}$), so dass man die Probenentnahme unter verschiedenen Bedingungen durchführen kann. In allen Fällen müssen aus dem zu analysierendem Gas, bevor es in die Anreicherungskolonne eintritt, verschiedene Stoffe, wie Ester, Alkohole und ähnliches, entfernt werden, da diese das Sorbens inaktivieren und den V_g -Wert des Äthens herabsetzen würden. Bei den untersuchten Obstarten zeigt die Äthenproduktion zwei Grundtendenzen.

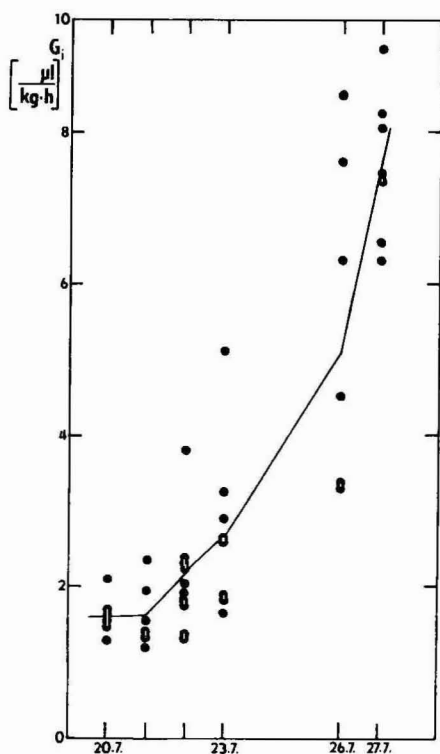


Fig. 1. Äthenproduktion bei Aprikosen während des Reifens am Baum.

(a) Grund- oder Schwellenphase der Äthenproduktion. Sie beträgt bei Aprikosen $1,5\text{--}2,0 \mu\text{l kg}^{-1} \text{h}^{-1}$, bei Pfirsichen $0,6\text{--}1,5 \mu\text{l kg}^{-1} \text{h}^{-1}$, bei Äpfeln ist sie kleiner als $0,6 \mu\text{l kg}^{-1} \text{h}^{-1}$. Diese vorklimakterische Phase wird durch wenig veränderliche Schwankungen der Äthenkonzentration gekennzeichnet.

(b) Phase des progressiven Anstiege der Äthenproduktion. Sie eröffnet den typischen Reifeprozess, bei dem viele weitere Merkmale auftreten (z.B. Bildung von Aromastoffen, Färbung der Schale). In dieser eingeleiteten klimakterischen Phase verläuft die Äthenproduktion exponentiell (Aprikosen, Pfirsichen); bei Äpfeln ist die Reaktion auf die Äthenproduktion im fortgeschrittenen Reifezustand sortenmässig

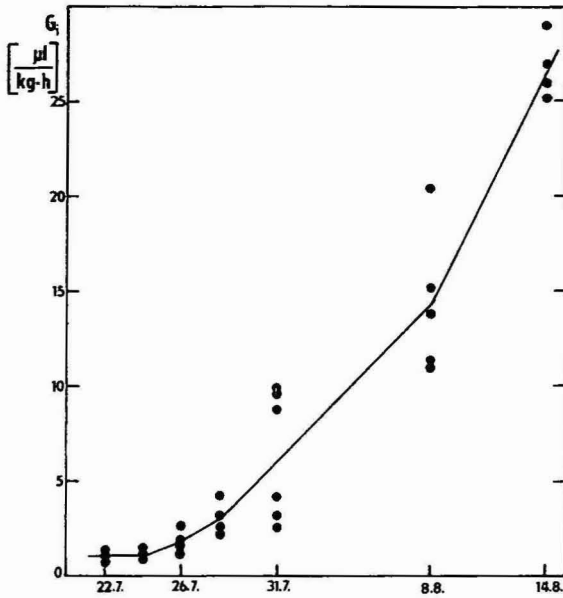


Fig. 2. Äthenproduktion bei Pfirsichen der Sorte "Red Haven" beim Reifen am Baum.

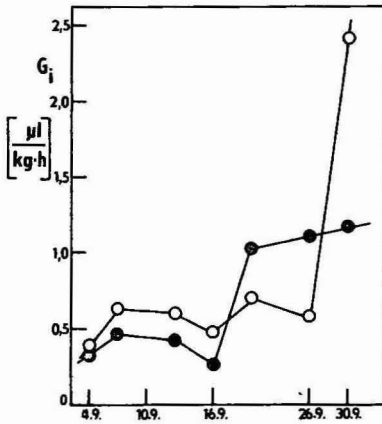


Fig. 3. Äthenproduktion bei Äpfeln der Sorten "Idared" (●) und "Starkrimson" (○) beim Reifen am Baum.

unterschiedlich und hängt, neben anderen Faktoren, besonders von der Lagertemperatur ab.

SCHLUSSFOLGERUNGEN

Auf der Grundlage chromatographischer Gleichgewichtsmethode wurde ein Verfahren der einstufigen Äthenadsorption aus dem analysierten Gas in einem Sorbens und seiner nachfolgenden gaschromatographischen Messung ausgearbeitet. Die

Methode ermöglicht die Messung von Äthenkonzentrationen in der Größenordnung von einigen nl l^{-1} . Die Geräteanordnung ist für die Messung der Äthenproduktion bei fleischigem Obst geeignet, und zwar bei intakten Früchten wie auch bei Schnitten mit einer Masse von etwa 30–50 g. Die Zeit für die Vorbereitung des Konzentrats ausser der eigentlichen gaschromatographischen Analyse überschreitet nicht 15 min. Es werden die Grenzkonzentrationen von Äthen bestimmt, die sich unter den experimentellen Bedingungen dieser Arbeit bei den verschiedenen methodischen Varianten der gaschromatographischen Analyse noch bestimmen lassen.

ZUSAMMENFASSUNG

Es wird eine Methode zur Messung des von fleischigen Früchten produzierten Äthens beschrieben. Sie besteht aus der Gleichgewichtsadsorption des Äthens in einer Kolonne mit Carbosieve G, aus der Wärmedesorption des Deposits und der gaschromatographischen Analysen des Konzentrats mit Flammenionisationsdetektor. Es können mit ihr Äthenkonzentrationen im Bereich von nl l^{-1} in der Umgebungsluft gemessen werden. Beträgt die Carbosieve-Masse 0,1 g, liegt die Wahrnehmungsgrenze etwa bei 0,08 ppb. Die Wahrnehmungsgrenzen für verschiedene Varianten der gaschromatographischen Analyse werden verglichen. Sie werden aus den chromatographischen Bedingungen und den Parametern des elektrometrischen Detektorsystems berechnet. Aus den theoretisch abgeleiteten Gleichungen kann man schnell die Äthenkonzentration im analysierten Gas abschätzen, ohne dass man eine Eichprobe benutzen muss, was bei der Spurenanalyse vorteilhaft ist.

LITERATUR

- 1 K. Widmark und G. Widmark, *Acta Chem. Scand.*, 16 (1962) 575.
- 2 A. P. Altshuller, *J. Gas Chromatogr.*, 1 (1963) 6.
- 3 E. R. Colson, *Anal. Chem.*, 35 (1963) 1111.
- 4 F. R. Crooper und S. Kaminski, *Anal. Chem.*, 35 (1963) 737.
- 5 J. Golíáš, J. Růžicková und J. Novák, *Acta Univ. Agric. Ser. C. Brno*, 23 (1975) 115.
- 6 J. Novák, V. Vašák und J. Janák, *Anal. Chem.*, 37 (1965) 660.
- 7 J. Bečka und L. Feltl, *J. Chromatogr.*, 131 (1977) 179.
- 8 J. Novák, *Quantitative Analysis by Gas Chromatography*, Marcel Dekker, New York, 1975, S. 57.
- 9 J. Novák, VI. Konferenz "Chromatographische Methoden und ihre Bedeutung für die Gesundheit des Menschen", Stará Lesná, 6.–8. November, 1984.
- 10 A. Raymond und G. Guiochon, *J. Chromatogr. Sci.*, 13 (1975) 173.
- 11 J. Novák, J. Golíáš und J. Janák, *NBS Spec. Publ. U.S.*, 519 (1979) 739.
- 12 D. H. Desty, E. Glueckauf, A. T. James, A. I. M. Keulemans, A. J. P. Martin und C. S. G. Phillips, in D. H. Desty (Herausgeber), *Nomenclature Recommendations: Vapour Phase Chromatography*, Butterworths, London, 1957, S. XI.
- 13 J. Novák, *Pokroky Chemie I, Kvantitativní analýza kolonovou chromatografií*, Academia, Prag, 1981, S. 71.

CHROM. 17 971

QUANTUM CHEMICAL PARAMETERS IN CORRELATION ANALYSIS OF GAS-LIQUID CHROMATOGRAPHIC RETENTION INDICES OF AMINES

KRZYSZTOF OŚMIAŁOWSKI, JAN HALKIEWICZ, ALEKSANDER RADECKI and ROMAN KALISZAN*

Faculty of Pharmacy, Medical Academy, K. Marksa 107, Gdańsk 80-416, (Poland)

(First received February 26th, 1985; revised manuscript received June 13th, 1985)

SUMMARY

For a structurally diverse set of primary, secondary and tertiary heterocyclic amines, correlations were found between the Kováts retention indices obtained on the methyl phenyl silicone phase OV-101 and quantum chemically calculated parameters. The total energy calculated by CNDO/2 molecular orbital method was chosen as a measure of a solute's ability to participate in dispersive interactions with the stationary phase. As a measure of the solute's ability to undergo polar interactions with the stationary phase, a parameter was proposed which reflects the highest local intermolecular dipole moment. It is defined as the largest difference in electron charges between two atoms. A two-parameter regression equation was derived which describes satisfactorily the retention of structurally different polar solutes on a relatively non-polar stationary phase. Some evidence is also provided that charge-transfer complexes are formed during the separations process.

INTRODUCTION

The distribution of a solute between a mobile and a stationary chromatographic phase is dependent on the forces existing between the solute molecules and those of each phase. Most generally, these forces are divided in two groups: (1) polar forces, arising from permanent or induced electric fields associated with both the solute and the molecules of the two phases; (2) non-polar, non-specific dispersion forces (London or Van der Waals forces). This classification of the forces has been employed in many theoretical and practical approaches to the description of retention data in molecular terms^{1–6}, although the individual authors differ as to their definition of polar interactions.

To find the structural descriptors best related to the ability of a particular solute to undergo both polar and dispersive interactions is an important step to understanding of the processes of chromatographic separations. Having established the quantitative relationships between the structural parameters and the retention data, one can get a deeper insight into the mechanism of a particular type of chromatographic separation. Conversely, some structural information may be obtained

from the retention data of solutes, which is of paramount importance for correlation analysis with other properties of solutes, *e.g.*, pharmacological activity^{7,8}.

THEORETICAL

For some time, correlation analysis has been applied in chromatography. Usually, however, liquid chromatographic retention data have been correlated with other experimental, free-energy-related parameters or substituent contributions^{9–12}. Since the successful application of topological indices^{13–15}, correlation analysis has occasionally been used for the description of gas–liquid chromatographic (GLC) retention indices of more or less congeneric groups of compounds. A number of equations have been reported for such homologous or congeneric sets of solutes, relating GLC retention indices to such constitutive-additive properties of solutes as molecular connectivity, refractivity, polarizability, etc. The best correlations found were for the less polar stationary phases and the more congeneric sets of solutes. Intuitively, in this context, the term congeneric means possessing the same or similar ability to undergo one type of interaction with the chromatographic phase, *i.e.*, dispersive or polar interactions. Usually the compounds studied were congeneric in respect of their polarities, whereas their dispersive properties could vary significantly as was the case with homologous series.

In attempts to correlate retention data with structural parameters for more diverse sets of solutes the dipole moment has been considered as a quantitative measure of solute polarity, either determined experimentally or calculated quantum chemically. The two-parameter correlation equations describing GLC retention indices in terms of molar refractivity (dispersion parameter) and dipole moment (polarity parameter) have been of limited statistical value in the case of a non-congeneric set of substituted phenols⁵.

In 1983 Buydens *et al.*¹⁶ published the results of studies on the prediction of GLC retention indices for a group of solutes consisting of aliphatic ethers, esters, alcohols, ketones and aldehydes. To get meaningful structure–retention relationships, subsets of mono- and bifunctional derivatives were considered separately. Multiple regression analysis was carried out with the following quantum chemically (CNDO/2) calculated electronic parameters: magnitude of the total dipole moment; sum of the absolute values of the charges in a given molecule; sum of the corresponding charges on the atoms constituting the functional group and on the atoms in α position to this functional group. The last parameter, which may be considered as describing a local molecular polarity, was found to be much more important for solute retention than the total dipole moment.

In 1976 Karger *et al.*² and Scott¹ observed that compounds like dioxane or 1,4-dichlorobutane have an overall dipole moment of approximately zero (two dipoles in opposite directions cancel) but behave as polar solutes.

Bearing in mind all these observations, we came to the conclusion that the overall dipole moment does not properly reflect the ability of a solute to take part in polar interactions during the chromatographic process. In a search for a suitable submolecular measure of solute polarity, we turned our attention to the largest difference in atomic charges.

To parametrize atomic charge differences in a given molecule we applied stan-

standard quantum chemical calculations, using the commercially available standard computer programs. Thus, at present one need not be a professional quantum chemist to generate structural data of interest for correlation analysis. To calculate molecular parameters from orbitals, the now classical Roothaan method is commonly applied which involves the complete neglect of differential overlap (CNDO/2 method). This semiempirical approximate molecular orbital method, in which only the valence electrons are considered explicitly, is recognized as satisfactorily reflecting the electronic properties of solutes.

First we chose for correlation analysis a relatively non-polar GLC stationary phase, OV-101. The set of solutes consisted of primary, secondary and tertiary, saturated and unsaturated alkyl and heterocyclic amines. Thus, the solutes were not congeneric in respect of their dispersive and polar properties, but on the other hand the nitrogen lone electron pair present in each compound made feasible some additional interactions with the stationary phase, *e.g.*, charge-transfer interactions.

EXPERIMENTAL

Chromatography

Gas chromatographic studies were carried out using a Pye Unicam Series 104 apparatus with a flame ionization detector. A coil-shaped Pyrex glass column (1 m \times 2 mm I.D.) was silanized with a 5% solution of dimethylchlorosilane (DMCS) in toluene. The column was next washed with pure toluene and heated in the chromatograph oven at 300°C. The stationary phase, 5% methyl phenyl silicone (OV-101, Applied Science) on Chromosorb W HP (80–100 mesh), was packed into the column. The carrier gas (argon) flow-rate was 30 cm³/min.

The solutes under study were injected into the column either as pure liquids or as solutions.

The detector temperature was fixed at 250°C. Several oven temperatures (precision $\pm 0.1^\circ\text{C}$) were applied in order to study the temperature dependence of the retention times: the respective plots were extrapolated to 130°C. The retention times were measured with an electronic timer with a mean standard deviation of 0.1 sec. For any given amine or *n*-alkane standard, the difference between the retention time of the solute and that of a non-retained gas, methane was calculated. Each measurement of retention time was done in triplicate and the results were averaged. The Kováts retention indices calculated are given in Table I.

Quantum chemical calculations

The calculations were done by the CNDO/2 molecular orbital method. The program^{17,18} was adapted for the RIAD system computer. Standard values of the bond lengths and angles were assumed¹⁹. The quantum chemical parameters used subsequently in correlation analysis are given in Table I. These are: (1) total energy, E_T , assumed by us as a bulk measure of the solute's ability to participate in non-specific interactions with a stationary phase; (2) energy of the highest occupied molecular orbital, E_{HOMO} , the parameter related to the ability of the solute to form charge-transfer complexes; (3) submolecular polarity parameter, Δ , introduced by us as a measure of the solute's ability to take part in polar solute-stationary phase interactions.

TABLE I
KOVÁTS RETENTION INDICES NORMALIZED TO 130°C AND STRUCTURAL PARAMETERS OF THE AMINES STUDIED

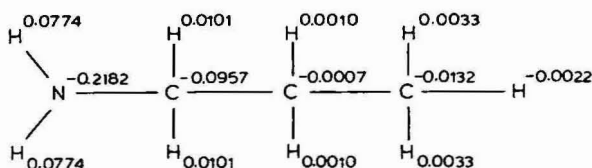
No.	Solute	Retention indices* (I_{0v-101})	Temperature of column** (°C)	Total energy, E_T (a.u.)***	Polarity parameter, Δ (electrons)	Energy of HOMO (a.u.)	Dipole moment, μ (D)	Molar refractivity (MR)
1	Allylamine	463	100-140	-38.100	0.3101	-0.4964	1.7229	18.926
2	<i>n</i> -Butylamine	553	100-150	-48.597	0.3110	-0.4843	1.8984	24.044
3	<i>sec</i> .-Butylamine	471	100-150	-48.596	0.3413	-0.4847	1.8975	24.044
4	<i>tert</i> .-Butylamine	501	100-140	-48.593	0.3600	-0.4895	1.8971	24.044
5	<i>n</i> -Pentylamine	635	110-150	-57.281	0.3113	-0.4767	1.9067	28.688
6	<i>n</i> -Propylamine	466	100-140	-39.917	0.3139	-0.4936	1.8930	19.400
7	Isopentylamine	615	110-150	-57.272	0.3145	-0.4793	1.8896	28.688
8	Isopropylamine	469	100-140	-39.921	0.3439	-0.5048	1.8317	19.400
9	Diallylamine	660	110-180	-62.519	0.2833	-0.4686	1.7733	32.572
10	Di- <i>n</i> -propylamine	694	100-150	-65.964	0.2917	-0.4655	1.8426	33.520
11	Diethylamine	527	100-140	-48.602	0.2897	-0.4767	1.8613	24.323
12	Methyl- <i>n</i> -pentylamine	706	110-180	-65.963	0.2786	-0.4626	1.8929	33.520
13	Methyl- <i>n</i> -hexylamine	871	110-190	-74.583	0.2786	-0.4590	1.9108	38.164
14	Methyl- <i>n</i> -butylamine	630	110-180	-57.279	0.2786	-0.4670	1.8793	28.876
15	Di- <i>n</i> -butylamine	943	130-210	-83.242	0.2875	-0.4595	1.8501	42.808
16	Pyrazine	696	110-180	-54.621	0.1723	-0.4564	0.0048	21.482
17	Pyridine	692	110-200	-50.866	0.2338	-0.4707	2.1019	23.890
18	β -Picoline	841	110-200	-59.554	0.2198	-0.4652	2.1261	28.508
19	3-Chloropyridine	890	110-210	-66.356	0.2570	-0.4757	2.1976	26.349
20	Chloropyrazine	895	110-210	-70.038	0.3024	-0.4658	2.1565	28.757
21	2-Chloropyridine	870	150-210	-66.245	0.3120	-0.4737	3.6424	26.349
22	4-Cyanopyridine	955	150-220	-68.643	0.2471	-0.4809	0.9618	28.205

* Retention index value extrapolated 130°C.

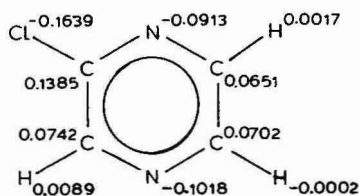
** Temperature range over which a linear dependence of retention data on temperature was found.

*** a.u. = Atomic units.

The parameter, Δ , represents the largest difference in atomic charges. To determine it, electron densities on particular atoms in the molecule are calculated and the two atoms which have the highest electron excess and deficiency respectively yield Δ (see Fig. 1 for illustration).



$$\Delta = 0.0957 - [-0.2182] = 0.3139$$



$$\Delta = 0.1385 - [-0.1639] = 0.3024$$

Fig. 1. Examples of electron excess charge densities and polarity parameter, Δ .

For the sake of comparison the overall dipole moment, μ , was calculated for each solute by the CNDO/2-MO method. The numerical data are given in Table I along with the molar refractivities, MR, calculated by summing individual bond refractivities according to Vogel *et al.*²⁰.

RESULTS AND DISCUSSION

The multiple regression analysis carried on with the data in Table I has yielded several statistically valid equations. The "best" is eqn. 1

$$I_{OV-101} = (301.88 \pm 306.70) - (11.66 \pm 2.74)E_T - (1016.80 \pm 752.66)\Delta$$

$$n = 22, s = 67.45, R = 0.93 \quad (1)$$

relating the Kováts retention index normalized to 130°C, I_{OV-101} , to the quantum chemically calculated total energy, E_T , and polarity parameter, Δ , where n is the number of compounds considered, s the standard deviation from the regression equation and R the multiple correlation coefficient; the 95% confidence limits calculated by the t-test are indicated. The equation is significant at the $p < 0.0001$ significance level.

The one-parameter equation relating I_{OV-101} to E_T is also significant at

$p < 0.0001$, but the correlation coefficient is much lower, $R = 0.89$. The equation relating $I_{\text{OV-101}}$ to Δ is of lower statistical significance: $p < 0.06$; $R = 0.51$. However, in eqn. 1 the term Δ ($p < 0.006$) and E_{T} ($p < 0.0001$) are of high statistical significance.

The statistical analysis for the whole set of compounds studied confirms the predominance of non-specific interactions in the retention of amines on the relatively non-polar stationary phase OV-101. On the other hand, polar interactions, as characterized by the submolecular polarity parameter, Δ , are also of importance. A negative sign of the coefficient for Δ in eqn. 1 indicates that, in the case of two solutes having the same E_{T} but different Δ , the more polar one would be less strongly retained on the non-polar OV-101 phase.

The polarity parameter, Δ , proposed here characterizes the ability of solutes to participate in polar interactions much better than does the overall molecular dipole moment, μ . Replacing Δ in eqn. 1 by μ is not valid statistically; the significance level for μ is $p < 0.50$. This observation supports the assumption that interactions of the dipole-dipole type between the stationary phase and the solute concern the local dipoles in the molecules. Thus, the use of the overall molecular dipole moment as a measure of solute polarity may be misleading. The same may be true in the case of other types of intermolecular interactions, *e.g.*, drug-receptor interactions.

Eqn. 1, although highly significant, describes about 87% ($R^2 \times 100\%$) of the retention index changes in structural terms; more than 10% of the changes remains unexplained. This may be the result of errors in the determination of retention indices, especially upon extrapolation of experimental data. Another cause of the deviation of eqn. 1 from the ideal is the more or less approximate nature of the quantum chemical data, especially as the actual molecular conformations, bond lengths and angles are not known precisely.

The main source of error, however, is probably the approximate nature of the polarity measure. The parameter Δ is a better measure of the polar interactions of the solutes with the stationary phase than is the overall dipole moment. On the other hand, the polar interactions considered are actually the sum of contributions from several local intramolecular dipoles in closest contact with the phase; Δ is the best approximation of these interactions for the largest of the dipoles.

One can now ask whether any improvement of eqn. 1 is possible with the data given in Table I. In fact, eqn. 2 gives better statistics than eqn. 1 but its validity may be questioned:

$$I_{\text{OV-101}} = (-3076.91 \pm 1822.57) - (16.59 \pm 3.34)E_{\text{T}} - (1988.44 \pm 766.38)\Delta - (7098.45 \pm 3798.55)E_{\text{HOMO}}$$

$$n = 22, s = 50.26, R = 0.96 \quad (2)$$

All the parameters used in eqn. 2 are significant, at least at the $p < 0.0005$ level, but there is quite a strong intercorrelation between some regression parameters: the correlation between E_{T} and E_{HOMO} is $R = 0.77$. For comparison, the intercorrelation between E_{T} and Δ is only $R = 0.30$, which means that only 10% of the information provided by one of the parameters is contained in the other one.

To examine further the significance of E_{HOMO} for retention we excluded compounds 1, 6, 8 and 15 in Table I from the regression analysis, in order to decrease

the intercorrelation between E_T and E_{HOMO} from 0.77 to 0.53. The equation derived for the remaining eighteen solutes has the form:

$$I_{OV-101} = -(3143.57 \pm 2284.40) - (17.38 \pm 4.15)E_T - (1919.95 \pm 875.68)\Delta - (7106.91 \pm 4856.36)E_{HOMO}$$

$$n = 18, s = 55.05, R = 0.95 \quad (3)$$

The term E_{HOMO} in eqn. 3 is significant at the $p < 0.004$ level.

Thus, we can say that there is some evidence that E_{HOMO} is meaningful for quantitative description of the retention of amines on the non-polar phase OV-101. This, in turn, would suggest that in the process of chromatographic separation the charge-transfer complexes are formed between a donor solute molecule and the stationary phase acting as an electron acceptor.

It seemed interesting to compare the total energy, E_T , and molar refractivity, MR, as measures of the ability of the molecules to take part in non-specific, non-polar interactions. Molar refractivity has often been used in correlation analysis of retention data. The total energy calculated by the CNDO/2 method has been found to correlate with Kováts indices for a homologous series of esters²¹. One may expect that, in the case of closely congeneric sets of solutes, the two parameters MR and E_T will be strongly intercorrelated. Thus, both of them can serve as a good quantitative measure of the abilities of the compounds to participate in dispersive interactions. In the case of a more diverse class of substances the total energy seems to be the more reliable parameter. Some evidence in support of this assumption may be gained from the data given below. If the subseries of primary, secondary and tertiary (heterocyclic) amines are analysed separately, the correlations between the retention indices and MR are similar to those between retention indices and E_T , but only for the primary and secondary amines (Table II). For heterocyclic amines differing significantly in structure, the total energy, E_T , is much better correlated with retention than molecular refractivity.

TABLE II

CORRELATION COEFFICIENTS OF LINEAR EQUATIONS RELATING KOVÁTS INDICES, I_{OV-101} , TO MOLAR REFRACTIVITY, MR, AND TOTAL ENERGY, E_T

<i>Amines</i>	<i>Correlation with molar refractivity (MR)</i>	<i>Correlation with total energy, E_T</i>
Primary, nos. 1-8 Table I	0.90	0.90
Secondary, nos. 9-15 Table I	0.98	0.98
Tertiary (heterocyclic), nos. 16-22 Table I	0.85	0.94

We would stress that the correlation analysis of Kováts indices with the CNDO/2 data provides evidence to support the importance in retention of the molecular interactions, which generally can be separated into non-specific, dispersive interactions and rather complex polar interactions. To parametrize dispersive interactions, the quantum chemically calculated total energy may be applied. E_T has little or no chemical meaning. It is likely, however, that it reflects the non-specific properties of the solutes indirectly, and that other more chemically significant parameters are contained within it.

The submolecular polarity parameter proposed here, defined as largest difference in atomic charges in the molecule, seems to be more reliable for characterizing a molecule's ability to participate in polar interactions than is the overall dipole moment. The use of both E_T and Δ as molecular descriptors allows the prediction of retention data for test solutes covering a range of polarities.

This study is a preliminary one in the sense that the primary focus has been on the elucidation of non-empirical descriptors of retention, especially as regards molecular polarity. Application of quantum chemical parameters in correlation analysis of retention data allows the prediction of chromatographic behaviour (at least semiquantitatively) for solutes of diverse structures. For polar solutes chromatographed on a phase of low polarity, such an analysis has been successfully performed. In the case of polar stationary phases, the hydrogen bonding with the solute probably affects the solute's electronic structure and has to be considered when calculating quantum chemical parameters.

REFERENCES

- 1 R. P. W. Scott, *J. Chromatogr.*, 122 (1976) 35.
- 2 B. L. Karger, L. R. Snyder and C. Eon, *J. Chromatogr.*, 125 (1976) 71.
- 3 Cs. Horváth, W. Melander and I. Molnar, *J. Chromatogr.*, 125 (1976) 129.
- 4 M. Gassiot-Matas and G. Firpo-Pamies, *J. Chromatogr.*, 187 (1980) 1.
- 5 R. Kaliszan and H. D. Höltje, *J. Chromatogr.*, 234 (1982) 303.
- 6 H. Lamparczyk and A. Radecki, *Chromatographia*, 18 (1984) 615.
- 7 R. Kaliszan, *J. Chromatogr.*, 220 (1981) 71.
- 8 R. Kaliszan, *J. Chromatogr. Sci.*, 22 (1984) 362.
- 9 E. Tomlinson, *J. Chromatogr.*, 113 (1975) 1.
- 10 B. K. Chen and Cs. Horváth, *J. Chromatogr.*, 171 (1979) 5.
- 11 G. Dahlmann, H. J. K. Köser and H. H. Oelert, *Chromatographia*, 12 (1979) 665.
- 12 K. Jinno and K. Kawasaki, *Chromatographia*, 18 (1974) 90.
- 13 R. Kaliszan, *Chromatographia*, 10 (1977) 529.
- 14 R. Kaliszan and H. Lamparczyk, *J. Chromatogr. Sci.*, 16 (1978) 246.
- 15 D. Bonchev, Ov. Mekenjan, G. Protic and N. Trinajstić, *J. Chromatogr.*, 176 (1979) 149.
- 16 L. Buydens, D. L. Massart and P. Geerlings, *Anal. Chem.*, 55 (1983) 738.
- 17 J. A. Pople and G. A. Segal, *J. Chem. Phys.*, 44 (1966) 3289.
- 18 P. A. Dobosh, *Quantum Chemistry Program Exchange*, 11 (1969) 141.
- 19 *Tables of Interatomic Distances and Configurations in Molecules and Ions, Suppl. 1956–1959*, The Chemical Society, London, 1965.
- 20 A. J. Vogel, W. T. Cresswell and J. Leicester, *J. Phys. Chem.*, 58 (1954) 174.
- 21 F. Saura-Calixto, A. Garcia-Raso and M. A. Raso, *J. Chromatogr. Sci.*, 22 (1984) 22.

CHROM. 17 964

EVALUATION OF THE SUITABILITY OF SELECTED POROUS POLYMERS FOR PRECONCENTRATION OF ORGANOSULPHUR COMPOUNDS FROM WATER

ANDRZEJ PRZYJAZNY

Institute of Inorganic Chemistry and Technology, Technical University of Gdańsk, 11/12 Majakowski St., 80-952 Gdańsk (Poland)

(Received June 11th, 1985)

SUMMARY

The breakthrough volumes (V_B) of a number of porous polymeric sorbents (Amberlite XAD-2, XAD-4, XAD-7; Chromosorb 102, 105, 106) have been determined for a variety of organosulphur compounds (thiols, sulphides, disulphides, thiophenes) in aqueous samples. The determination was based on a headspace gas chromatographic technique developed earlier. Among the investigated sorbents, Chromosorb 106 and Amberlite XAD-2 were found to be best suited for preconcentration of organic sulphur compounds from water. An attempt was undertaken to correlate the experimental V_B values with the aqueous solubility determined previously from the distribution constants in gas-liquid systems, in order to predict the capacity of sorbents for any organic solute using only the solubility of the analyte. The prediction is useful as a guide for estimating the appropriate ratio of sample to sorbent size in the preconcentration of organic solutes from water.

INTRODUCTION

Organosulphur compounds constitute a significant source of environmental pollution. They are frequently present in industrial wastes, particularly in the effluents from the paper industry. Because of the high toxicity of these pollutants, the corresponding tolerance limits are very low. For example, the maximum allowable concentrations in class I waters for the production of drinking water are 0.003 and 2 mg/l for dimethyl sulphide and thiophene, respectively¹. The odour of some sulphur-containing compounds can be detected at extremely low levels, *e.g.*, 0.00025 mg/l for diethyl sulphide, 0.81 $\mu\text{g/l}$ for di-*n*-propyl sulphide and 0.075 $\mu\text{g/l}$ for *n*-propanethiol¹, thus reducing the suitability of water for drinking purposes.

On the other hand, biologically produced sulphur compounds are thought to account for one half of the total sulphur in the atmosphere. The identity of the sulphur carriers, which must be volatile, biogenically derived compounds transferring sulphur from the sea to the atmosphere, remains to be determined. Efforts to identify these compounds have resulted in the measurement of several sulphur-containing

compounds²⁻⁶. The discovery that living organisms produce volatile, methylated sulphur compounds⁷ has led to investigations of the importance of dimethyl sulphide in the transfer of sulphur from the sea to the atmosphere.

The solution of the analytical problems presented above requires extremely sensitive methods which should permit selective determination of sulphur compounds at the ppm level or below. Numerous papers have dealt with the determination of volatile organosulphur compounds in aqueous samples using headspace gas chromatography (HSGC)^{3,8-18}. Although this method has inherent advantages resulting from the elimination of errors due to the instability and ease of oxidation of the sulphur derivatives, the detection limit of static HSGC is of the order of ppb^{11,13,19}, which may be insufficient in some cases*. For this reason, a preconcentration step was included in procedures for determination of organosulphur solutes, particularly dimethyl sulphide (DMS). One preconcentration procedure involves extraction of DMS via carbon tetrachloride and mercury(II) chloride from large volumes (15 dm³) of sea-water^{2,20}. The determination of dipropyl disulphide and DMS through a purge-and-trap method has also been reported^{21,22}. A search of the recent analytical literature indicates, however, that the most frequently employed method of preconcentration of organic compounds from water involves sorption on solid sorbents, particularly on porous polymers²³. A fundamental parameter characterizing the usefulness of a given sorbent for preconcentration purposes is the breakthrough volume, V_B . For liquid samples, this is a function of a number of variables, the most important being the type of sorbent and geometry of the sorbent bed, the type of compounds and their concentration, the properties of the liquid and its flow-rate through the sorbent bed and the presence of other inorganic and organic compounds in the sample matrix. The determination of V_B values for organic solutes is an essential step in the optimization of analytical procedures for trace impurities, enabling calculations of the safe sampling volumes and the detection limit. Breakthrough volumes can be determined by connection of the outlet of a sorbent tube through which a sample is passed to a high-performance liquid chromatographic (HPLC) detector²⁴⁻²⁶. However, some of these detectors lack sufficient sensitivity (refractive index detectors) or are not universal enough (UV detectors) for this purpose.

This paper presents the results of a determination of the V_B values on a number of porous polymeric sorbents for ten organosulphur compounds (thiols, sulphides, disulphides, thiophenes) in artificial sea-water²⁷ samples using an HSGC technique developed earlier²⁸. The method permits the determination of V_B values for volatile organic compounds at concentrations down to 50 ppb in complex inorganic or organic matrices. The design of the apparatus and the practical application of the method²⁹ are very simple.

An attempt is made to correlate the experimental V_B values with the fundamental physicochemical parameter, aqueous solubility, as determined previously from distribution constants in gas-liquid systems¹⁹, in order to predict the capacity of sorbents for any organic solute using only the solubility of the analyte³⁰. The prediction is useful as a guide for estimating the appropriate ratio of sample to sorbent size in the preconcentration of organic solutes from water.

* Throughout this article, the American billion (10⁹) is meant.

EXPERIMENTAL

Apparatus

The design of the apparatus for the determination of breakthrough volumes by means of the HSGC technique has been described elsewhere²⁸. A Carlo Erba Fractovap Model 2200 gas chromatograph equipped with a flame ionization detector was employed for GC analysis. The chromatographic conditions were as follows: stainless-steel column, 2 m \times 4 mm I.D.; packing, 10% DC-200 on Chromosorb P DMCS (80–100 mesh); carrier gas, argon at 40 cm³/min; injector temperature, 175°C; column temperature, dependent on the compound; detector temperature, 200°C; sample volume, 1 cm³.

Materials

Model solutions of sulphur compounds in artificial sea-water were prepared from stock solutions in methanol (*ca.* 3000 ppm). The concentration of the stock solution was determined daily. All reagents (E. Merck, F.R.G.) were of analytical-reagent grade.

Amberlite XAD-2, XAD-4, XAD-7 resins (20–50 mesh; Rohm & Haas, Philadelphia, PA, U.S.A.) and Chromosorb 102, 105 and 106 (60–80 mesh; Johns-Manville, Denver, CO, U.S.A.) were cleaned as described previously³¹. Sorbents were packed in glass tubes (4 cm \times 8 mm I.D.). The bed contained *ca.* 0.6 g of the sorbent. Desorption of the retained solutes from the sorbent bed was carried out by washing the tubes with five 1-cm³ portions of methanol, followed by heating for 1 h at 150°C in a stream of argon.

Procedure

The temperature of the headspace cell was 70°C, the flow-rate of the solutions was 40 cm³/h (in some experiments it was varied from 40 to 400 cm³/h), the concentration of sulphur compounds was 1 ppm (w/w) and gas samples were taken at 10- or 100-cm³ intervals. Breakthrough curves were determined on the basis of the peak heights of the investigated compounds.

RESULTS AND DISCUSSION

The breakthrough volumes of the investigated organosulphur compounds on selected porous polymers are listed in Table I. It is seen that the V_B values range from *ca.* 0.2 to 38 dm³/g, the largest values corresponding to compounds with the highest molecular weights and hence boiling points. Among the investigated sorbents, Chromosorb 106 is best suited for preconcentration of thiols and thiophenes, Amberlite XAD-2 for disulphides, whereas either Chromosorb 106 or Amberlite XAD-2 can be used for preconcentration of sulphides (Table I).

The dependence of V_B on the flow-rate was studied for dimethyl disulphide on Amberlite XAD-2 in the range 40–400 cm³/h. It was established that V_B decreased steadily from 3.17 dm³/g at 40 cm³/h to 0.6 dm³/g at 400 cm³/h. This suggests that the adsorption at flow-rates exceeding 40 cm³/h (20 bed volumes) may be a non-equilibrium process. An identical amount of Amberlite XAD-2 was then packed into a glass tube (16 cm \times 4 mm I.D.) and the V_B value of dimethyl disulphide was

TABLE I

BREAKTHROUGH VOLUMES (dm^3/g) ON VARIOUS SORBENTS FOR SELECTED ORGANOSULPHUR SOLUTES IN SEA-WATERTemperature: 20°C. Concentration: 1 ppm. Flow-rate: 40 cm^3/h .

Compound	Sorbent					
	Chromosorb 105	Chromosorb 106	Amberlite XAD-2	Amberlite XAD-4	Amberlite XAD-7	Chromosorb 102
Dimethyl sulphide	0.52	0.37	0.40	0.55	0.22	0.42
Diethyl sulphide	1.29	1.10	2.11	1.10	0.44	1.66
Di- <i>n</i> -propyl sulphide	12.1	38.0	34.0	12.0	1.78	28.3
Diisopropyl sulphide	8.8	13.5	6.1	8.7	0.67	13.3
Dimethyl disulphide	2.32	2.56	3.17	2.74	1.11	0.42
Diethyl disulphide	8.7	12.8	37.7	8.5	1.78	4.99
Thiophene	2.9	2.86	2.29	1.37	0.72	
2-Methylthiophene	7.5	11.7	2.56	1.51	0.91	
Ethanethiol	0.46	1.10	0.90	0.55	0.22	0.42
<i>n</i> -Propanethiol	0.82	1.83	1.51	1.51	0.56	0.62

determined at a flow-rate of 40 cm^3/h . The value obtained was 1.73 dm^3/g , which is consistent with the previous results, since the linear velocity of the sample in a tube of smaller diameter is four times higher than in the tube with 8 mm I.D. Consequently, a flow-rate of 20 bed volumes per hour (40 cm^3/h) was used in the investigations.

The molar aqueous solubilities, S_i , of the compounds studied were calculated from distribution coefficients in the air-water system and other relevant thermodynamic data¹⁹. These values are listed in Table II together with other physicochemical

TABLE II

ESTIMATED VALUES OF SOLUBILITY IN SEA-WATER FOR SELECTED ORGANOSULPHUR COMPOUNDS CALCULATED FROM THE DISTRIBUTION COEFFICIENTS AT 20°C AND OTHER RELEVANT THERMODYNAMIC DATA

 p_i^0 = Saturated vapour pressure.

Compound	Mol.wt. (g/mol)	B.p. (°C)	p_i at 20°C (atm)	K_i at 20°C*	S_i (mol/dm ³)
Dimethyl sulphide	62	37.3	0.523	13.81	0.301
Diethyl sulphide	90	92.1	0.060	12.80	0.032
Di- <i>n</i> -propyl sulphide	118	142.38	0.006	6.98	0.002
Diisopropyl sulphide	118	120.02	0.014	5.94	0.004
Dimethyl disulphide	94	109.7	0.029	19.73	0.024
Diethyl disulphide	122	154	0.004	13.09	0.002
Thiophene	84	84.16	0.082	11.10	0.038
2-Methylthiophene	98	112.56	0.027	9.96	0.011
Ethanethiol	62	35	0.572	6.73	0.160
<i>n</i> -Propanethiol	76	67.7	0.162	5.75	0.039

* $K_i = c_L/c_G$, where c_L and c_G are the equilibrium concentrations of the analyte in the liquid and gaseous phases, respectively.

TABLE III

PARAMETERS OF THE REGRESSION CURVE $\log V_B = a + b \cdot \log S_i$ FOR VARIOUS SORBENTS V_B is expressed in dm^3/g and S_i in mol/dm^3 .

Parameter	Sorbent					
	Chromosorb 105	Chromosorb 106	Amberlite XAD-2	Amberlite XAD-4	Amberlite XAD-7	Chromosorb 102
Number of compounds, n	10	10	10	10	10	8
Intercept, a	-0.75	-0.80	-0.67	-0.73	-0.84	-0.98
Slope, b	-0.68	-0.80	-0.72	-0.63	-0.39	-0.78
Correlation coefficient, r	0.938	0.946	0.926	0.951	0.896	0.928

constants. When the logarithms of S_i for the ten solutes were plotted vs. $\log V_B$, rather well defined linear relationships were found with a correlation coefficient greater than 0.9 (except for Amberlite XAD-7). Parameters of the regression curves $\log V_B = a + b \cdot \log S_i$ are presented in Table III. This relationship between V_B and S_i can be attributed to the hydrophobic effect as reported by Karger *et al.*³². Exemplary plots of the $\log V_B = f(\log S_i)$ dependence for Chromosorb 106 and Amberlite XAD-2 are shown in Figs. 1 and 2. It follows from the data in Table III and Figs. 1 and 2 that the aqueous solubilities can be used to predict V_B values for diverse organic solutes when preconcentrating them on non-ionic porous polymers of low or moderate polarity.

From a comparison of the solubility values in Table II with the V_B values in Table I it is seen that although the S_i values and hence the solute-solvent interactions determine the affinity of the solutes for the sorbents, two other factors associated

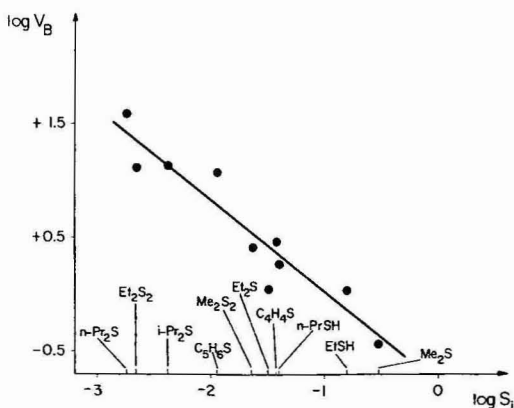


Fig. 1. The dependence of the breakthrough volume (dm^3/g) for organosulphur compounds on Chromosorb 106 on their molar solubility in artificial sea-water. Concentration: 1 ppm (w/w). Flow-rate: 40 cm^3/h . Temperature: 20°C. Compounds: $n\text{-Pr}_2\text{S}$ = di- n -propyl sulphide; Et_2S_2 = diethyl disulphide; $i\text{-Pr}_2\text{S}$ = diisopropyl sulphide; $\text{C}_5\text{H}_6\text{S}$ = 2-methylthiophene; Me_2S_2 = dimethyl disulphide; Et_2S = diethyl sulphide; $\text{C}_4\text{H}_4\text{S}$ = thiophene; $n\text{-PrSH}$ = n -propanethiol; EtSH = ethanethiol; Me_2S = dimethyl sulphide.

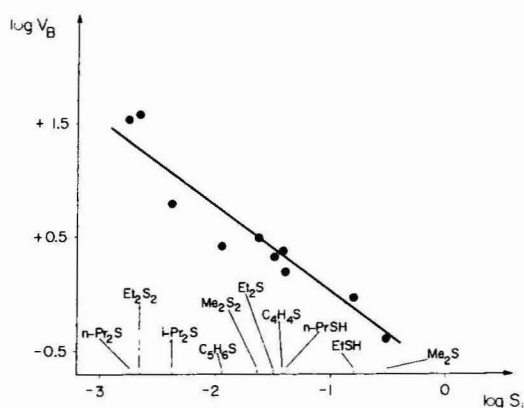


Fig. 2. The dependence of the breakthrough volume (dm^3/g) for organosulphur compounds on Amberlite XAD-2 on their molar solubility in artificial sea-water. Conditions and compounds as in Fig. 1.

with the solute-sorbent interactions should be considered. The first one is connected with the type of sorbent used for preconcentration, *i.e.*, with its monomer composition and surface area. As mentioned above, Chromosorb 106, which is a non-polar polystyrene copolymer with a specific surface area of $700\text{--}800\text{ m}^2/\text{g}^{23}$, is recommended for preconcentration of thiols and thiophenes, whereas Amberlite XAD-2 (styrene-divinylbenzene copolymer with average specific surface area $290\text{--}330\text{ m}^2/\text{g}^{23}$) is best suited for extraction of disulphides from aqueous solutions. Although in the latter case Amberlite XAD-4 should apparently give larger V_B values, since it has the same monomer composition as XAD-2 but considerably higher specific surface area ($750\text{ m}^2/\text{g}^{23}$), a decisive factor in this case might be the average pore diameter, which is equal to $8.5\text{--}9\text{ nm}$ and 5 nm for XAD-2 and XAD-4, respectively²³. The second factor concerns the type of solute retained on the sorbent. It can be seen from Table I that aromatic compounds are better retained than aliphatics of similar solubility (*cf.*, thiophene, $S_i = 0.038\text{ mol}/\text{dm}^3$ and propanethiol, $S_i = 0.039\text{ mol}/\text{dm}^3$). The same holds true for compounds of different polarity: less polar di-*n*-propyl sulphide ($S_i = 0.002\text{ mol}/\text{dm}^3$) is better sorbed than diethyl disulphide ($S_i = 0.002\text{ mol}/\text{dm}^3$). Hence, when selecting a sorbent for preconcentration of organic solutes from water, the solubilities of the solutes and the chemical composition as well as the type of sorbent should all be considered. Finally, it should be pointed out that when isolating compounds of low molecular weight, *e.g.*, dimethyl sulphide or ethanethiol, from aqueous solutions of typical volume 1 dm^3 , the sorbent bed should have a mass of several grams in order to avoid losses of the analyzed compounds.

On the basis of the above discussion the following conclusions can be drawn.

(1) The V_B values of the analytes studied range from *ca.* 0.2 to *ca.* $38\text{ dm}^3/\text{g}$, the largest values corresponding to compounds with the lowest aqueous solubility (Table I and II).

(2) Among the investigated sorbents, Chromosorb 106 is best suited for preconcentration of thiols and thiophenes, Amberlite XAD-2 for disulphides, whereas either Chromosorb 106 or Amberlite XAD-2 can be used for preconcentration of sulphides (Table I).

(3) Due to the dependence of V_B on the sample flow-rate, all determinations

should be carried out at a constant flow-rate not exceeding 20 bed volumes per hour.

(4) There is a rather well defined linear relationship between $\log S_i$ and $\log V_B$ (see Table III and Figs. 1 and 2). This dependence can be used to predict the capacity of any sorbent of low polarity for solutes, using only the solubility of the analyte.

ACKNOWLEDGEMENTS

This work was supported by grant MR. I-15 from the Institute of Oceanology (Sopot) of the Polish Academy of Sciences. The author also thanks Mrs. L. Zaslawska for her help in carrying out the experiments.

REFERENCES

- 1 K. Verschuieren, *Handbook of Environmental Data on Organic Chemicals*, Van Nostrand-Reinhold, New York, 1977.
- 2 B. C. Nguyen, A. Gaudry, B. Bonsang and G. Lambert, *Nature (London)*, 275 (1978) 637.
- 3 R. A. Rasmussen, *Tellus*, 26 (1974) 254.
- 4 J. E. Lovelock, R. J. Maggs and R. A. Rasmussen, *Nature (London)*, 237 (1972) 452.
- 5 P. J. Maroulis and A. R. Bandy, *Science (Washington, D.C.)*, 196 (1976) 647.
- 6 R. S. Braman, J. M. Ammons and J. L. Bricker, *Anal. Chem.*, 50 (1978) 992.
- 7 F. Challenger, *Adv. Enzymol.*, 12 (1951) 429.
- 8 T. G. Field and J. B. Gilbert, *Anal. Chem.*, 38 (1966) 628.
- 9 A. G. Vitenberg, B. V. Ioffe and V. N. Borisov, *Chromatographia*, 7 (1974) 610.
- 10 A. G. Vitenberg and L. M. Kuznetsova, *Anal. Chem.*, 49 (1977) 128.
- 11 I. H. Williams and F. E. Murray, *Pulp Pap. Mag. Can.*, (1966) 347.
- 12 T. T. Toan, R. Bassette and T. J. Claydon, *J. Dairy Sci.*, 48 (1965) 1174.
- 13 J. C. Miers, *J. Agric. Food Chem.*, 14 (1966) 419.
- 14 M. Kawabata, K. Ohtsuki, H. Kokura and Y. Wakahara, *Agric. Biol. Chem.*, 41 (1977) 2285.
- 15 T. Takahashi, S. Nakajima, I. Konishi, H. Miedauer and L. Narziss, *Brauwissenschaft*, 31 (1978) 1.
- 16 O. Leppanen, J. Denslow and P. Ronkainen, *J. Inst. Brew.*, 85 (1979) 350.
- 17 G. Mazza, M. Le Maguer and D. Hadziyev, *Can. Inst. Food Sci. Technol. J.*, 13 (1980) 87.
- 18 H. Murayama, I. Kifune and T. Uemura, *Niigata Rikagaku*, 6 (1980) 11.
- 19 A. Przyjazny, W. Janicki, W. Chrzanowski and R. Staszewski, *J. Chromatogr.*, 280 (1983) 249.
- 20 A. Gaudry, B. Bonsang, B. C. Nguyen and P. Nadaud, *Chemosphere*, 10 (1981) 731.
- 21 M. Gottauf, *Fresenius' Z. Anal. Chem.*, 218 (1966) 175.
- 22 M. O. Andreae and W. R. Barnard, *Anal. Chem.*, 55 (1983) 608.
- 23 M. Dressler, *J. Chromatogr.*, 165 (1979) 167.
- 24 M. Krejčí, M. Roudná and Z. Vavrouch, *J. Chromatogr.*, 91 (1974) 549.
- 25 D. Ishii, K. Hibi, K. Asai and M. Nagaya, *J. Chromatogr.*, 152 (1978) 341.
- 26 B. Zygmunt, J. Visser, U. A. Th. Brinkman and R. W. Frei, *Int. J. Environ. Anal. Chem.*, 15 (1983) 263.
- 27 J. P. Riley and G. Skirrow (Editors), *Chemical Oceanography*, Vol. 1, Academic Press, London, New York, 1965, p. 648.
- 28 A. Przyjazny, W. Janicki, W. Chrzanowski and R. Staszewski, *J. Chromatogr.*, 245 (1982) 256.
- 29 M. Biziuk and E. Kozłowski, *Fifth European Conference on Analytical Chemistry "Euroanalysis V"*, Cracow, August 26-31, 1984, Book of Abstracts, p. 248.
- 30 E. M. Thurman, R. L. Malcolm and G. R. Aiken, *Anal. Chem.*, 50 (1978) 775.
- 31 A. Przyjazny, W. Janicki, W. Chrzanowski and R. Staszewski, *J. Chromatogr.*, 262 (1983) 199.
- 32 B. L. Karger, J. R. Gant, A. Hartkopf and P. H. Weiner, *J. Chromatogr.*, 128 (1976) 65.

CHROM. 17 949

SEPARATION OF OLIGOMERS WITH UV-ABSORBING SIDE GROUPS BY SUPERCRITICAL FLUID CHROMATOGRAPHY USING ELUENT GRADIENTS

FRANZ P. SCHMITZ*, HEINZ HILGERS, BENNO LORENSCHAT and ERNST KLESER
Lehrstuhl für Makromolekulare Chemie der RWTH Aachen, Worringerweg, D-5100 Aachen (F.R.G.)
(Received June 7th, 1985)

SUMMARY

The chromatographic separation of oligomers prepared from vinyl arene compounds was achieved using eluent gradients with the eluent pair *n*-pentane–1,4-dioxane, which had previously been applied to oligostyrene separations. Separations were found to occur not only with respect to degree of oligomerization, but also between sub-series of oligomeric species. Transition from the supercritical to the liquid state, which may occur during an eluent gradient run if the selected column temperature is relatively little above T_c at the beginning of the gradient, does not seem to reduce the resolution considerably. The combination of two gradient techniques, a pressure gradient and a gradient of eluent composition, was applied for the separation of the difficult to elute N-vinylcarbazole oligomers. Supercritical fluid chromatograms showed considerably superior separation compared with high-performance liquid chromatograms obtained at ambient temperature using the same eluent gradient.

INTRODUCTION

The use of adsorption chromatographic techniques for the separation of oligomers has been increasing for some years. In addition to chromatography with liquid eluents, [high-performance liquid chromatography (HPLC)], chromatography with supercritical mobile phases [supercritical fluid chromatography (SFC)] has been shown to be applicable. The viscosity of supercritical fluids is lower than that of liquids and diffusion coefficients in supercritical gaseous phases are considerably higher than those in liquids^{1–3}. This favours equilibrium processes in the distribution of substrates between mobile and stationary phases and thus chromatographic separations can be improved and accelerated.

For the separation of substrate mixtures with greatly differing solubilities, gradient techniques have to be applied that enhance the solvating power of the eluent during the chromatographic run and thus lead to reasonable analysis times. With homologous systems such as oligomer mixtures, solubility decreases with increasing molecular weight. In SFC, the solvating power of an eluent can be enhanced by lowering the temperature, thereby increasing the density, increasing the pressure or changing the chemical composition of the mobile phase.

While changes in temperature are of lesser importance for gradient separations⁴, changes in pressure or density and in mobile phase composition are of considerable importance in SFC. Oligomer separations by means of pressure gradients have frequently been reported⁵⁻¹⁰; for improving the resolution still further, simultaneous pressure and temperature gradients have been applied¹¹.

It has also been shown that gradients of eluent composition, which are common in HPLC, are also applicable to SFC^{4,12,13}. With eluent gradients, using an increasing content of a component with higher viscosity there may simultaneously occur a pressure increase, depending on the instrumentation used, *i.e.*, with an unchanged setting of the pressure-reducing valve at the outlet of the apparatus. Hence the effect of the applied gradient is enhanced¹³. For the separation of oligostyrenes, the eluent system *n*-pentane-1,4-dioxane has been found suitable^{12,13}, the stationary phase being normal-phase silica. In this paper it is shown that this eluent system can also be used for the separation of related oligomers.

EXPERIMENTAL

The SFC apparatus consists of a modified HPLC instrument¹³ (1084B, Hewlett-Packard); the modifications consist mainly of an additional oven, which is capable of operating at higher temperatures, valves for setting the pressure levels at the outlet of the separation column and of the detector, and an additional loop injector.

1,4-Dioxane and *n*-pentane were distilled from sodium and degassed. Dioxane was stored in dark bottles in order to prevent the formation of peroxides.

The stainless-steel separation columns (25 cm × 4.6 mm I.D.) were packed with LiChrosorb Si 60, 10 µm (Merck, Darmstadt, F.R.G.) using a slurry method. The slurry consisted of a suspension of the stationary phase (2.5 g) in a mixture of

TABLE I
DATA FOR THE CHROMATOGRAMS SHOWN IN FIGS. 2-6

Chromatogram	Substrate*	λ (nm)**	T (°C)	p_i (bar)***	Dioxane programme§	Type
Fig. 2a	OVBP	254	250	49	5; 60; 220	SFC
Fig. 2b	OVBP	254	270	45	5; 60; 220	SFC
Fig. 3a	O1VN	278	250	46	5; 55; 180	SFC
Fig. 3b	O1VN	278	270	50	5; 55; 180	SFC
Fig. 4a	O2VN	278	240	52	5; 40; 160	SFC
Fig. 4b	O2VN	278	270	51	5; 50; 160	SFC
Fig. 5a	O1VN	278	Ambient	49	5; 55; 180	HPLC
Fig. 5b	OVBP	254	Ambient	50	5; 60; 220	HPLC
Fig. 6a	ONVC	295	270	40	See Fig. 7a	SFC
Fig. 6b	ONVC	295	270	41	See Fig. 7b	SFC

* Abbreviations: OVBP = oligo(4-vinylbiphenyl); O1VN = oligo(1-vinylnaphthalene); O2VN = oligo(2-vinylnaphthalene); ONVC = oligo(N-vinylcarbazole).

** Detection wavelength.

*** Column inlet pressure at the start of the chromatogram.

§ Initial dioxane content (% v/v); final dioxane content (% v/v); programme time (min). For programme type, see text and Fig. 1.

TABLE II
OLIGOMERIZATION REACTIONS

Monomer	Solvent	Monomer concentration (g/ml)	Monomer/initiator ratio	Initiation	Reaction temperature (°C)	Reaction time (min)
1	Tetrahydrofuran	0.025	1:1.33	Anionic	-20	3
2	Tetrahydrofuran	0.0175	1:1	Anionic	-20	3
3	Tetrahydrofuran	0.050	1:2	Anionic	-20	3
4	Toluene	0.025	5:1	Radical	90	60

toluene (20 ml) and cyclohexanol (30 ml), which was packed by pumping heptane on to the slurry in a reservoir at the top of the column.

After each chromatographic run, the column had to be flushed with high concentrations of dioxane to elute high-molecular-weight compounds present in the oligomer mixtures. Owing to their broad molecular weight distribution, this is especially necessary for oligomer samples prepared by radical initiation.

The flow-rate was 1 ml/min for the chromatograms shown in Figs. 2-5, measured at the pumps in the liquid state at ambient temperature. Further chromatographic conditions are summarized in Table I.

Anionic oligomerizations (Table II) took place in tetrahydrofuran at -20°C, using *n*-butyllithium as initiator. Reaction times were 3 min, the reactions being stopped by addition of methyl iodide. Radical oligomerization was performed in toluene, using azobisisobutyronitrile as initiator (Table II).

RESULTS AND DISCUSSION

Members of homologous series such as oligomers become less soluble with increasing molecular weight, requiring gradient techniques for chromatographic separations. However, with increasing molecular weight, the solubility differences decrease on going from a degree of oligomerization n to $n + 1$. Consequently, the slope of the gradient should decrease during a chromatographic run in order to obtain equally spaced peaks. It was found experimentally that on linear variation of the ratio Q_B the resulting gradients were suitable for oligomer separation:

$$Q_B = \frac{P_B}{1 - P_B}$$

where P_B is the volume fraction of eluent B, measured at the pumps in the liquid state. The resulting gradients of %B vs. time have the general shape shown in Fig. 1.

The oligomers obtained from the monomers 4-vinylbiphenyl (I), 1-vinylnaphthalene (II), 2-vinylnaphthalene (III) and N-vinylcarbazole (IV) were soluble in 1,4-dioxane, analogous to oligostyrenes. It was expected that for the chromatographic separation of these oligomers the eluent pair *n*-pentane-1,4-dioxane, which had previously been found suitable for oligostyrenes, could be applied.

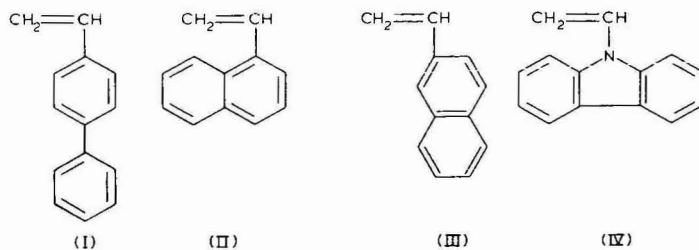


Fig. 2a shows the separation of oligomers prepared by anionic oligomerization of 4-vinylbiphenyl (OVBP). About 45 peaks or peak groups can be observed in this chromatogram; using higher detector sensitivities up to 55 oligomers could be detected. The chromatographic conditions were chosen such that the early eluting peaks of the oligomer series were eluted with large spacing in order to separate the broad peaks (indicated by arrows), which do not seem to belong to the oligomeric series. At least two different sub-series can be observed, which differ in their elution behaviour. In the course of the separation, a smaller side peak separates from the main peak, having a degree of oligomerization n , and finally merges into the peak corresponding to a degree of oligomerization $n + 1$. As the structural assignments of the different oligomeric sub-series are not known at present, it is possible that the differences between these sub-series are due to variations in the repeating units of the oligomer chains or to different end groups.

In Figs. 3 and 4, separations of oligomers from anionic oligomerization of 1-vinylnaphthalene (O1VN) (Fig. 3a) and 2-vinylnaphthalene (O2VN) (Fig. 4a) are shown. As with the separation of vinylbiphenyl oligomers, separation into sub-series was achieved. Particularly for the 2VN oligomers, the "wandering" of a peak from one peak group to the next can be observed during the separation. Up to three oligomeric sub-series were separated; however, the irregular peak shapes that can be observed for the lower oligomers suggest that further sub-series or by-products may

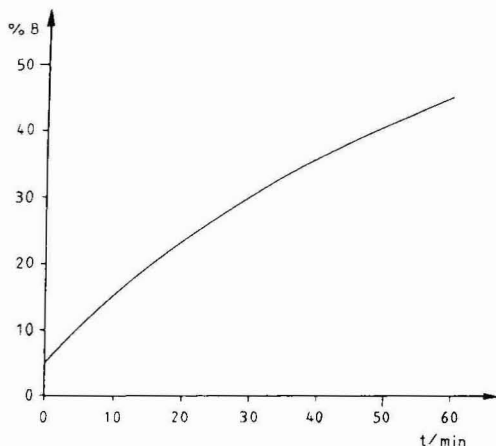


Fig. 1. General shape of gradients in eluent composition applied for the separations shown in Figs. 2–5. Programme data for this example: initial dioxane content, 5%; final dioxane content, 45%; programme time, 60 min.

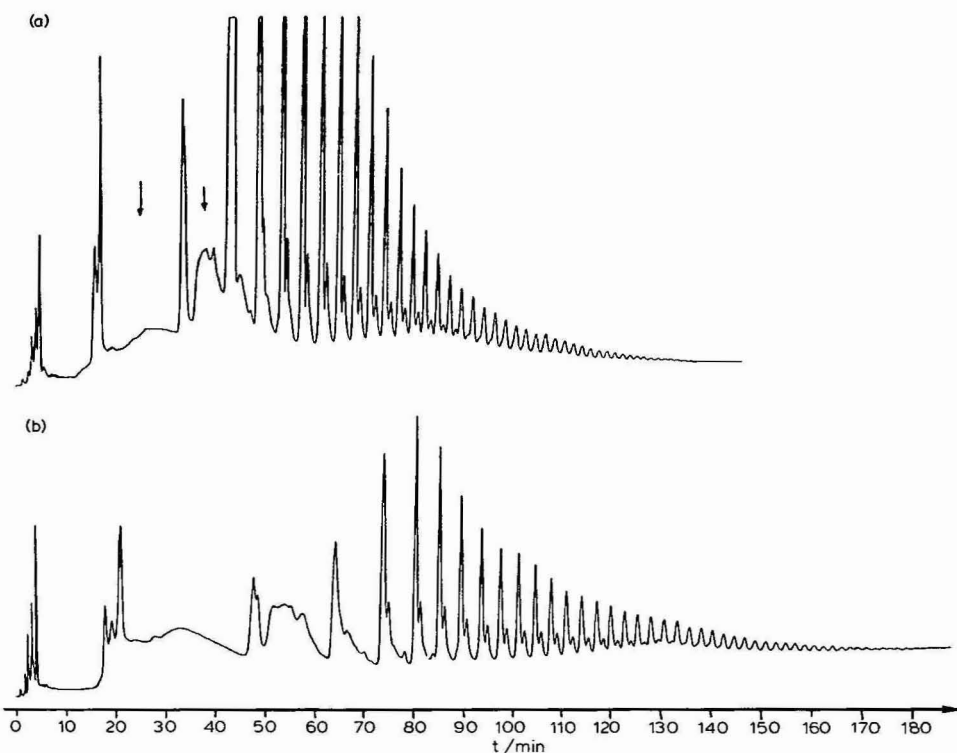


Fig. 2. SFC separations of 4-vinylbiphenyl oligomers. Column temperatures: (a) 250°C; (b) 270°C. See Table I and Experimental.

be present in the samples. For higher degrees of oligomerization, n , the different homologous sub-series merge into one peak per n .

Increasing the dioxane content leads to increasing critical values for temperature and pressure for the resulting eluent mixtures (Table III). Thus, during the separations shown in Figs. 2a, 3a and 4a, a transition from the supercritical to the liquid state occurs during the chromatographic run owing to the increasing dioxane content. To determine whether such a phase transition has a detrimental effect on the separation, the same chromatograms were run at 270°C, but with slightly different pressures. At this temperature, the mobile phase remains in the supercritical state until a dioxane content of about 55% is reached. Figs. 2b and 3b show that the separations were similar to those obtained at 250°C. However, the analysis times were longer and the separations, especially those into sub-series, were enhanced. The latter effect is not surprising, because resolution has been reported to show maxima at slightly supercritical temperatures¹⁵⁻¹⁸.

Elution can be accelerated to yield analysis times comparable to those obtained at lower temperatures in two ways. First, the column pressure at the start of the chromatogram can be increased, which leads to higher eluent densities, thereby compensating for the effect of the decreasing density at increasing temperature. Increasing the column pressure by about 20 bar leads to analysis times being even shorter than those at 250°C, but a loss in information is observed only for the early eluting peaks.

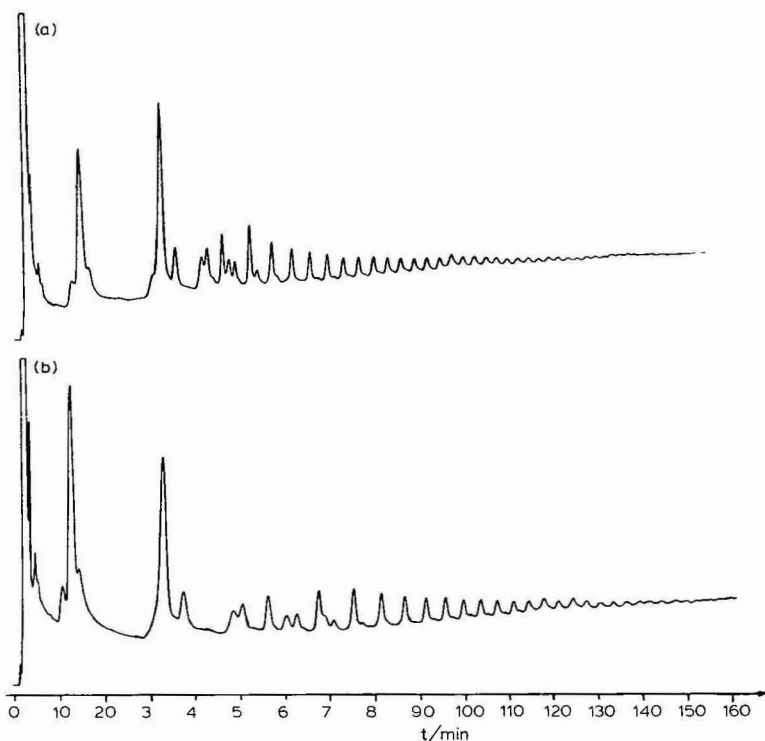


Fig. 3. SFC separations of 1-vinylnaphthalene oligomers. Column temperatures: (a) 250°C; (b) 270°C. See Table I and Experimental.

The second means of reducing analysis times at higher temperatures is to increase the slope of the gradient. Fig. 4b shows a separation of the O2VN sample at 270°C, where the slope of the gradient has been increased compared with the chromatogram at 240°C (Fig. 4a). Again, the analysis times become comparable, but the chromatograms show some differences. First, at the higher temperature the resolution of the sub-series is lower. This may be attributed to temperature-dependent changes in selectivity¹⁹. Second, more oligomer species are eluted under the conditions applied for the chromatogram in Fig. 4b. It seems that for the elution of the higher oligomers the chemical composition of the mobile phase is more effective than the density.

TABLE III

CRITICAL DATA FOR MIXTURES OF *n*-PENTANE AND 1,4-DIOXANE

The data were calculated according to procedures described by Chueh and Prausnitz (*cf.*, ref. 14).

Parameter	Value											
B (%) [*]	0	5	10	20	30	40	50	60	70	80	90	100
<i>T_c</i> (°C)	196.5	203.9	211.2	225.2	238.4	250.9	262.8	274.1	284.8	295.0	304.7	313.9
<i>p_c</i> (bar)	33.7	37.4	40.8	46.7	51.4	54.9	57.1	58.2	58.1	56.9	54.9	52.1

* Content of 1,4-dioxane in *n*-pentane (% v/v).

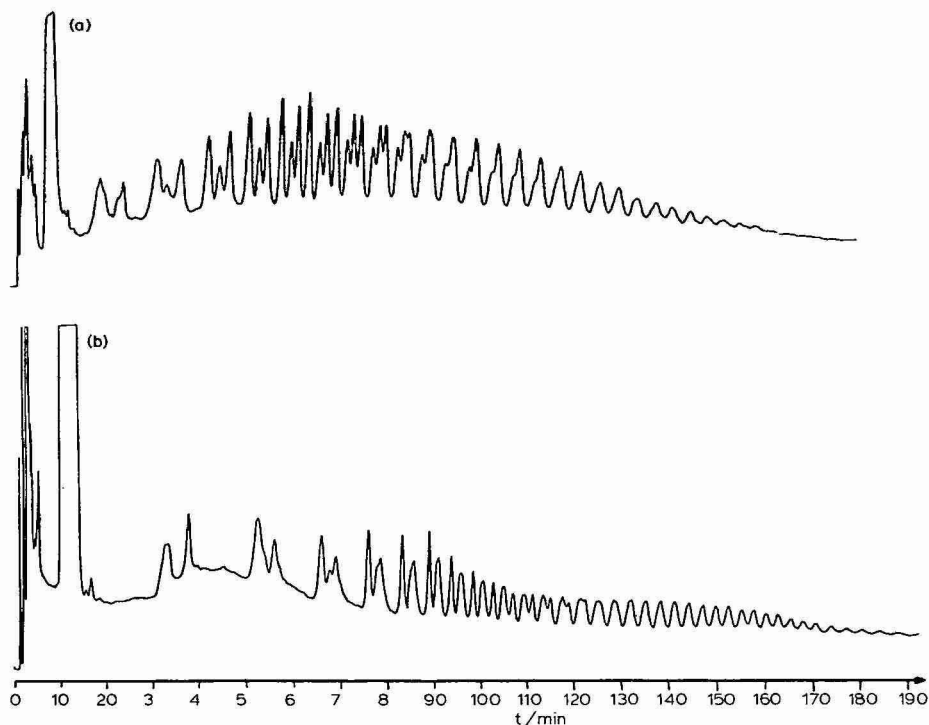


Fig. 4. SFC separations of 2-vinylnaphthalene oligomers. Column temperatures: (a) 240°C; (b) 270°C. Gradients: (a) 5–40% dioxane within 160 min; (b) 5–50% dioxane within 160 min. See Table I and Experimental.

The eluent system *n*-pentane–1,4-dioxane is not only suitable for the separation of vinylarene oligomers under supercritical conditions but also, in principle, at ambient temperature, *i.e.*, under HPLC conditions. However, as can be seen from Fig. 5, the resolution obtained is smaller than that in the SFC chromatograms. Fig. 5a shows an HPLC separation of the O1VN sample where the gradient and the column pressure were similar to those applied for the chromatograms shown in Fig. 3. The oligomer peaks are broad but no separation into the sub-series can be observed. Comparison of the OVBP separations in Figs. 5b (HPLC) and 2 (SFC) demonstrates that the separation under HPLC conditions is considerably poorer than that under SFC conditions. Decreasing the pressure for the HPLC separation does not yield a substantial enhancement of resolution.

For the separation of N-vinylcarbazole oligomers (ONVC), the application of a gradient of eluent composition was not sufficient for obtaining good separations. It was found that an eluent gradient had to be combined with a pressure gradient; this pressure gradient was generated by increasing the flow-rate at a given setting of the outlet valve. The applied flow-rates ranged from 0.75 to 1.9 ml/min. With such flow-rates good to at least usable resolutions can be obtained, as has already been found with *n*-pentane as the eluent¹⁸. Fig. 6a shows a separation obtained by application of a pressure gradient with a slightly decreasing slope (*cf.*, Fig. 7a). The pro-

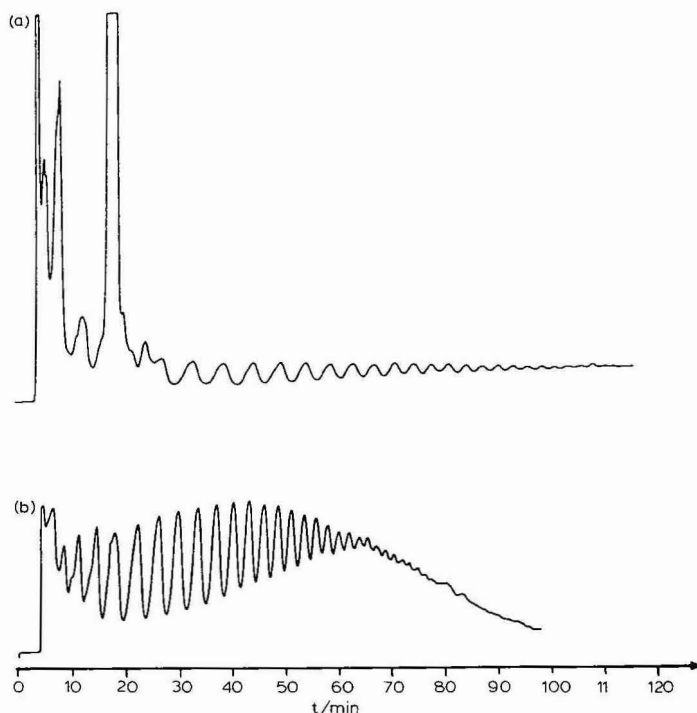


Fig. 5. HPLC separation of (a) 1-vinylnaphthalene oligomers and (b) 4-vinylbiphenyl oligomers. See Table I and Experimental.

grammes were started 10 min after the start of the chromatogram in order to separate low-molecular-weight compounds, which appear at the beginning of the chromatogram, from the homologous oligomer series. About 25 oligomers can be recognized in the chromatogram, which also shows a separation into some sub-series for the lower members of the oligomer series. At the beginning of the chromatogram the mobile phase is under slightly supercritical or even at subcritical conditions with respect to pressure; elution of the homologous series takes place with the transition to supercritical pressures. This elution behaviour is even more pronounced in the chromatogram shown in Fig. 6b, where a sharp rise in pressure (*cf.*, Fig. 7b) causes immediate start of elution of the NVC oligomers.

In conclusion, it can be stated that the combination of an alkane with 1,4-dioxane as the eluent system is not only applicable to SFC separations of oligostyrenes but also to separations of chemically related oligomers. Although these eluent pairs can also be used in the liquid state, *i.e.*, under HPLC conditions, the resolution of the HPLC separations was found to be distinctly inferior to that obtained under supercritical conditions using the same eluent gradient. In contrast, a transition from the supercritical to the liquid state, while still near T_c , which may occur owing to an increasing content of the higher boiling component in the eluent, does not seem to reduce the resolution greatly.

Changes in the chromatographic conditions (temperature, pressure, shape and slope of the gradient) may affect the selectivity α of a separation and thus lead to

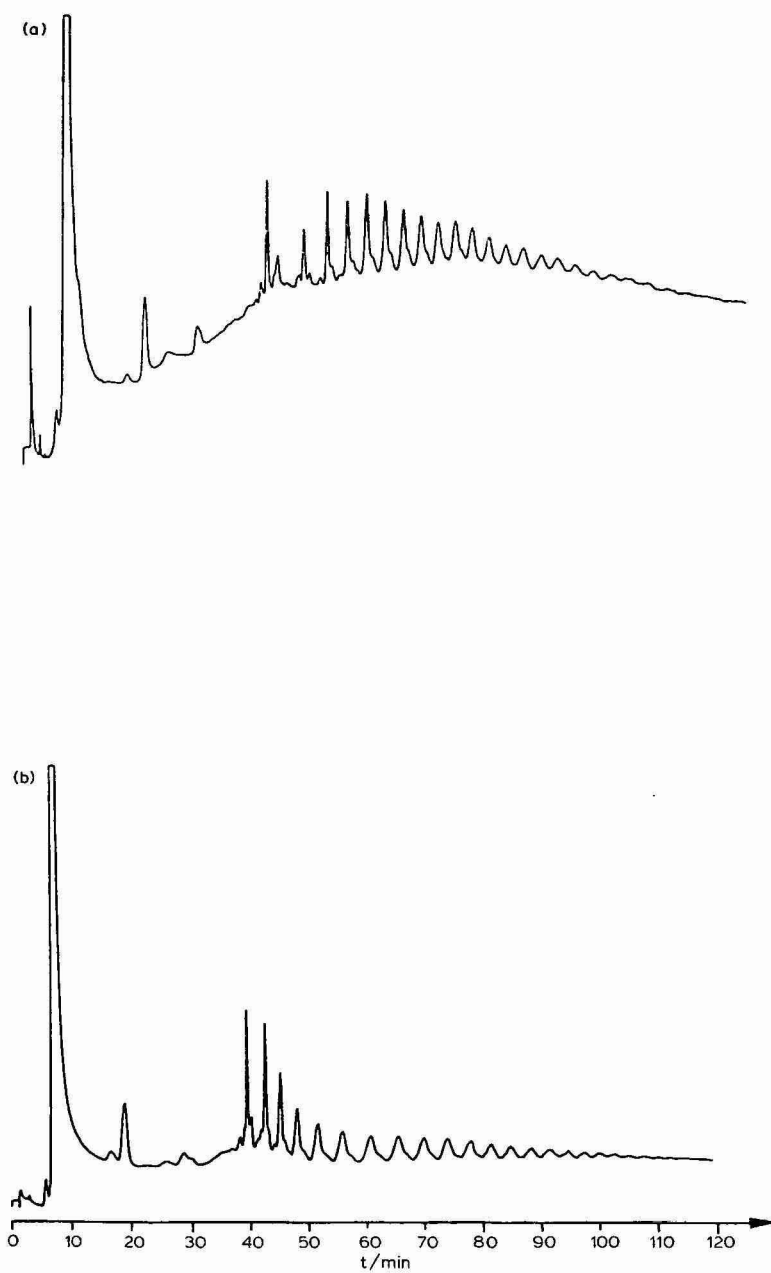


Fig. 6. SFC separations of N-vinylcarbazole oligomers. (a) Column temperature, 270°C. Flow-rate kept constant at 0.75 ml/min for 10 min and then increased to 1.65 ml/min at 130 min. For eluent and pressure gradients, see Fig. 7a; for further chromatographic conditions, see Table I and Experimental. (b) Column temperature, 270°C. Flow-rate, increased from 0.75 ml/min at the start of the chromatogram to 1.9 ml/min at 120 min. For eluent and pressure gradients see Fig. 7b; for further chromatographic conditions, see Table I and Experimental.

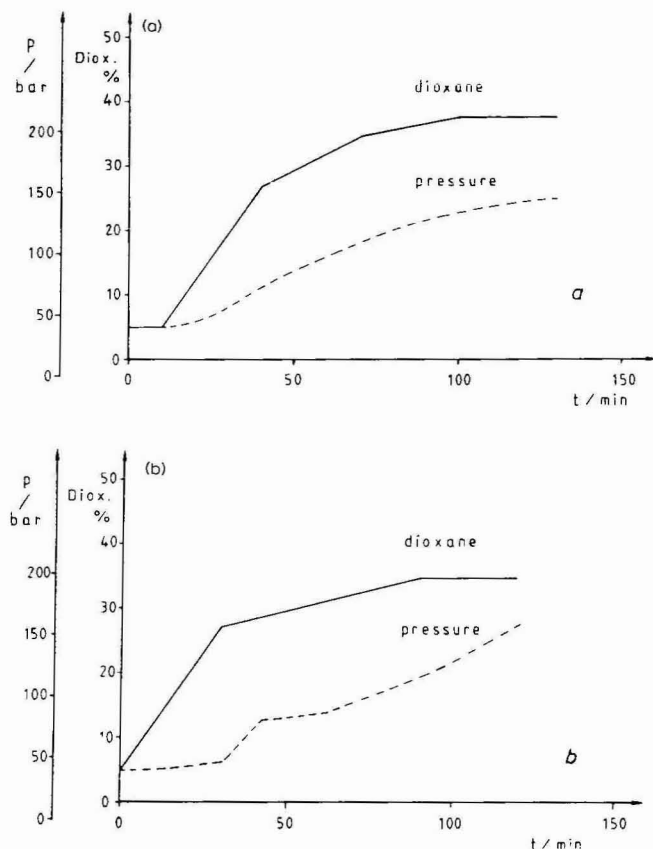


Fig. 7. Eluent and pressure gradients for the chromatograms in Figs. 6a (a) and 6b (b). Solid line, dioxane content (% v/v) in the eluent mixture; broken line, pressure at column inlet.

changes in the order of elution of sub-series within the homologous oligomer series. This opens up the possibility of optimizing separations, either with respect to the separation of such sub-series or with respect to a separation according to the degree of oligomerization.

Finally, for substrates that are difficult to elute, combined programmes of eluent composition and pressure may be applied in order to effect a particular separation.

ACKNOWLEDGEMENT

Thanks are expressed to the Arbeitsgemeinschaft Industrieller Forschungsvereinigungen (AIF) for financial support.

REFERENCES

- 1 E. Klesper, *Angew. Chem.*, 90 (1978) 785; *Angew. Chem., Int. Ed. Engl.*, 17 (1978) 738.
- 2 L. G. Randall, *Separ. Sci. Technol.*, 17 (1982) 1.
- 3 G. M. Schneider, *Ber. Bunsenges. Phys. Chem.*, 88 (1984) 841.
- 4 F. P. Schmitz and E. Klesper, *Polym. Bull.*, 5 (1981) 603.
- 5 R. E. Jentoft and T. H. Gouw, *J. Chromatogr. Sci.*, 8 (1970) 138.
- 6 J. A. Nieman and L. B. Rogers, *Separ. Sci.*, 10 (1975) 517.
- 7 E. Klesper and W. Hartmann, *J. Polym. Sci., Polym. Lett. Ed.*, 15 (1977) 9.
- 8 J. E. Conaway, J. A. Graham and L. B. Rogers, *J. Chromatogr. Sci.*, 16 (1978) 102.
- 9 J. C. Fjeldsted, W. P. Jackson, P. A. Peaden and M. L. Lee, *J. Chromatogr. Sci.*, 21 (1983) 222.
- 10 Y. Hirata, *J. Chromatogr.*, 315 (1984) 39.
- 11 E. Klesper and W. Hartmann, *Eur. Polym. J.*, 14 (1978) 77.
- 12 F. P. Schmitz and E. Klesper, *Makromol. Chem., Rapid Commun.*, 2 (1981) 735.
- 13 F. P. Schmitz, H. Hilgers and E. Klesper, *J. Chromatogr.*, 267 (1983) 267.
- 14 P. L. Chueh and J. M. Prausnitz, *AIChE J.*, 13 (1967) 1099; cited in R. C. Reid, J. M. Prausnitz and T. K. Sherwood, *The Properties of Gases and Liquids*, McGraw-Hill, New York, 3rd ed., 1977, p. 140.
- 15 F. P. Schmitz, D. Leyendecker and E. Klesper, *Ber. Bunsenges. Phys. Chem.*, 88 (1984) 912.
- 16 F. P. Schmitz, H. Hilgers, D. Leyendecker, B. Lorenschat, U. Setzer and E. Klesper, *J. High Resolut. Chromatogr. Chromatogr. Commun.*, 7 (1984) 590.
- 17 D. Leyendecker, F. P. Schmitz and E. Klesper, *J. Chromatogr.*, 315 (1984) 19.
- 18 D. Leyendecker, F. P. Schmitz, D. Leyendecker and E. Klesper, *J. Chromatogr.*, 321 (1985) 273.
- 19 F. P. Schmitz, in preparation.

CHROM. 17 974

LIQUID CHROMATOGRAPHIC RETENTION BEHAVIOR OF LARGE, FUSED POLYCYCLIC AROMATICS

NORMAL BONDED PHASES

J. C. FETZER* and W. R. BIGGS

Chevron Research Company, P.O. Box 1627, Richmond, CA 94802 (U.S.A.)

(Received June 17th, 1985)

SUMMARY

The normal bonded-phase retention behavior of 26 large polycyclic aromatic hydrocarbons (PAHs) was investigated. The retention on aminopropyl-, nitropropyl-, and tetranitrofluorenoimidopropyl-derivatized columns were compared using *n*-hexane-methylene chloride mobile phases. The PAHs studied showed three distinct types of retention behavior. Changes in elution order are dependent on the degree of non-planarity of the compounds in the solvent systems used, as evidenced by the UV-VIS spectra.

INTRODUCTION

The analysis of crude oils or residua and their resulting products is a complex task. Complimentary methods are necessary for accurate characterization of a feed and the products of any process because many types of hydrocarbon- and heteroatom-containing molecules are present. One important class is the polycyclic aromatic hydrocarbons (PAHs). The separation of mixtures of PAHs by high-performance liquid chromatography (HPLC) has become a routine technique for identifying these components in many types of samples. Both normal- and reversed-phase separations have been used. A lack of standard compounds, for use in comparison of detector responses and retention times, has been one major limitation in development of PAH analyses. Another has been the complexity of most samples, making unequivocal identification of the chromatographic peaks difficult or impossible. These problems have been partially overcome by the synthesis and isolation of large PAHs, the production of columns with greater separating power, and the development of more selective detectors. The "full-spectrum" photodiode array detector is an ideal detector of PAHs. This detector collects the UV spectrum of an eluting peak by monitoring the UV intensity at all wavelengths in a spectral range. The UV spectra of the PAHs are very characteristic, containing several absorbance maxima and the corresponding minima. The location of these spectral features is determined by the size and shape of the PAH¹. Thus, very similar PAHs can be easily identified and quantified. These developments, however, do not totally solve the problems of separation and identification.

Other characteristics of the PAHs must be used to differentiate them. For example, the use of the retention times could be another identifying characteristic for those PAHs that cannot be unambiguously identified by their UV spectra. Retention time relationships have been proposed for both normal- and reversed-phase HPLC as a useful parameter for identification of the PAH²⁻⁵. These studies found correlations between the number of π electrons or rings and the expected retention times. Other parameters, such as the partition coefficients between aqueous and organic phases, solubilities in various solvents, and molecular shape, have all been used for predicting retention behavior (see ref. 6 and references contained therein, and ref. 7). All of these studies were of PAHs of six or less rings (the only ones readily available commercially). Recent work in our laboratory on the reversed-phase separation of several seven-, eight-, and nine-ring PAHs of the peropyrene class showed a much more complex behavior^{8,9}. The retention of these PAHs was based on solute-solvent interactions that were a function of the intramolecular steric strain of the PAHs. This strain would not be present in the smaller PAHs used in most studies, but would be more prevalent with an increase in the number of rings in the molecule¹⁰. Intramolecular steric strain produces anomalous retention behavior in the peropyrene-type PAHs because the effective surface area of the PAHs becomes smaller in certain solvents. The sterically strained PAHs could become non-planar in those solvents, reducing the strain but at the same time reducing the area of the PAH that interacted with the chromatographic stationary phase.

Since many PAHs appear to have structural features similar to those with anomalous retention behavior and also possess UV spectral features suggesting steric strain^{8,9}, a series of experiments was undertaken. While anomalous retention behavior had only been seen in reversed-phase separations, the proposed mechanism of a solvent-induced non-planarity should also occur in other types of chromatography, producing similar behavior for many PAHs besides those studied previously. The same "strong" solvents (ethyl acetate, tetrahydrofuran, chloroform, and methylene chloride) are used in both reversed- and normal-phase chromatography, so the solvent interactions with the PAHs should be similar in both types of chromatography. These were also the solvents which caused anomalous elution behavior and spectroscopic changes for the peropyrene-type PAHs. A number of 26 fused-ring PAHs (Fig. 1 and Table I) were chosen as standard compounds because of size and shape differences. These included various isomeric sets that differed in their UV spectral characteristics and possibilities for intramolecular strain. Three types of bonded normal-phase columns were studied: an aminopropyl-bonded phase, a nitropropyl-bonded phase and a tetranitrofluorenoimidopropyl (TENF)-bonded phase. These columns have greatly differing affinities and selectivities for PAHs, thereby allowing study of a wide range of mobile phases.

EXPERIMENTAL

All chromatograms were run on a DuPont Model 8800 liquid chromatograph in the isocratic mode at ambient temperature. A Valco C6U injection valve with a 25- μ l loop was used for sample introduction. A Hewlett-Packard 1040A photodiode array detector was used, and all data were evaluated with that unit's HP 85 computer. The software used was the original HP package expanded with Infometrix MCR 2

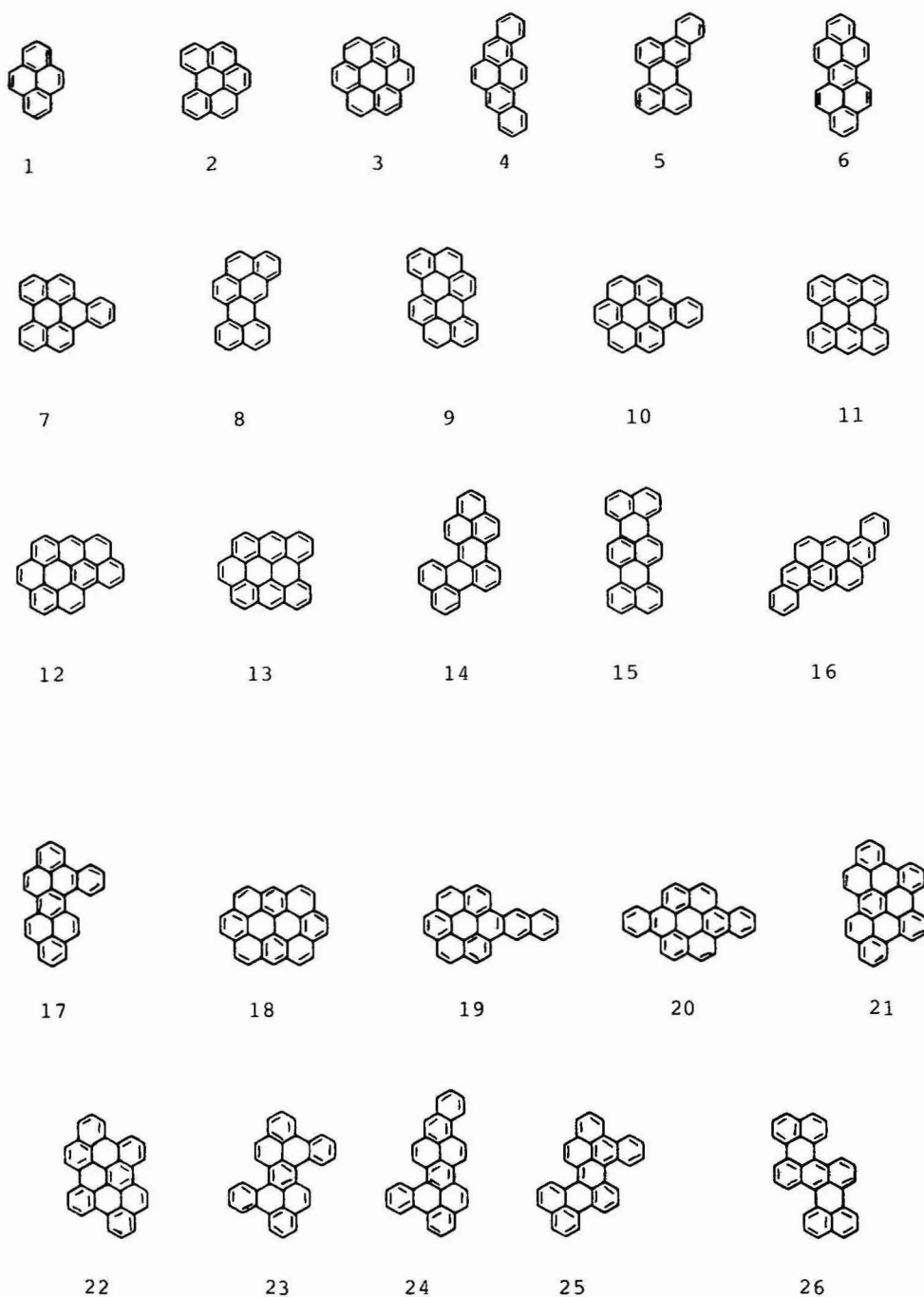


Fig. 1. PAHs studied (see Table I for names).

TABLE I
MODEL COMPOUNDS USED IN THIS STUDY

<i>Compound number</i>	<i>Name</i>
1	Pyrene
2	Benzo[ghi]perylene
3	Coronene
4	Benzo[rst]pentaphene
5	Benzo[b]perylene
6	Dibenzo[cd,lm]perylene
7	Naphtho[1,2,3,4ghi]perylene
8	Naphtho[8,1,2bcd]perylene
9	Benzo[pqr]naphtho[8,1,2bcd]perylene
10	Benzo[a]coronene
11	Phenanthro[1,9,10,8fghi]perylene
12	Naphtho[8,1,2abc]coronene
13	Dibenzo[bc,ef]coronene
14	Phenaleno[1,9ab]perylene
15	Tribenzo[de,kl,rst]pentaphene
16	Pyranthrene
17	Tribenzo[a,cd,lm]perylene
18	Ovalene
19	Naphtho[2,3a]coronene
20	Dibenzo[a,j]coronene
21	Dibenzo[fg,ij]phenanthro[2,1,10,9,8,7pqrstuv]pentaphene
22	Benzo[cd]chryseno[4,5,6,7fghijk]perylene
23	Tetrabenzo[a,cd,j,lm]perylene
24	Benzo[rst]phenanthro[1,10,9,cde]pentaphene
25	Benzo[cd]naphtho[1,8jk]perylene
26	Tetrabenzo[de,hi,op,st]pentacene

(Infometrix, Seattle, WA, U.S.A.). The solvent-effect comparison UV spectra were run on a Perkin-Elmer Lambda 3 spectrophotometer as in the previous work⁹.

The bonded-phase columns were a 25 × 0.46 cm I.D. DuPont aminopropyl-bonded phase, a 20 × 0.46 cm I.D. Macherey-Nagel nitropropyl-bonded phase, and a 30 × 0.46 cm I.D. ES Industries TENF-bonded phase. All packages were derivatized 5-μm spherical silicas. All mobile phases were premixed using Burdick & Jackson solvents. The PAHs were either synthesized in our laboratory^{8,9} or purchased from various commercial sources. Three mixtures of eight or nine PAHs were dissolved in a minimum amount of methylene chloride and diluted with *n*-hexane, to ensure solubilization of the PAHs and to minimize adverse chromatographic effects. Relative retention times were measured as the average of the values found for each PAH at each set of chromatographic conditions, two or three replicate values being the norm. In the spectral comparisons, the PAHs were dissolved in methylene chloride and either diluted with nine parts *n*-hexane or methylene chloride.

RESULTS AND DISCUSSION

The use of plots of the logarithm of relative retention times *versus* percentage of strong solvent in the mobile phase can indicate changes in the various factors that

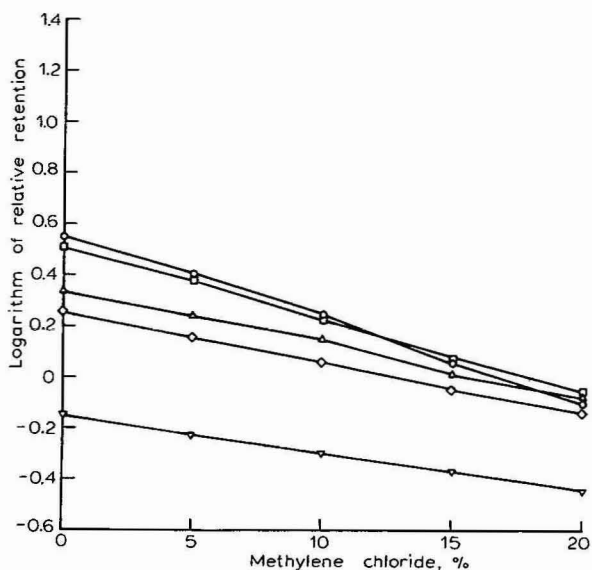


Fig. 2. Relative retention plots of the PAHs of molecular weights 202-302. ▽ = Pyrene; ◇ = benzo[ghi]perylene; △ = coronene; □ = benzo[rs]pentaphene; ○ = benzo[b]perylene.

control retention^{11,12}. If the various factors that effect retention had the same mechanisms in each solvent mixture, then a linear plot would result. If there was a drastic change in the controlling mechanisms or in the relative influence of the mechanism, the plot would curve. The logarithm of the relative retention values found with *n*-hexane-methylene chloride mixtures on the aminopropyl-bonded phase column are

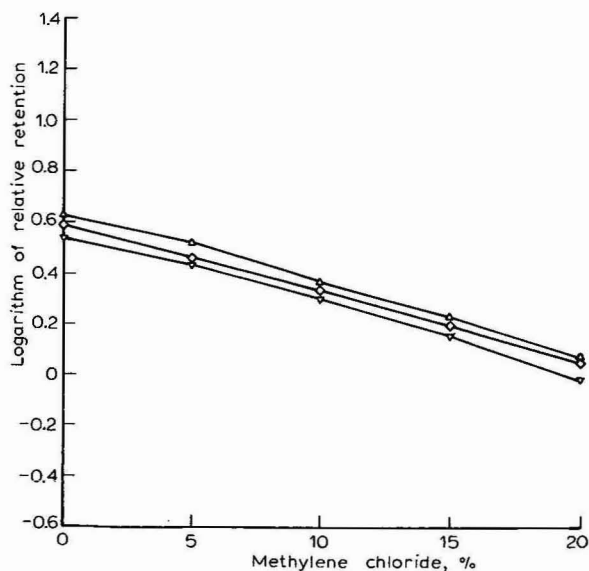


Fig. 3. Relative retention plots of the PAHs of molecular weight 326. ▽ = Dibenzo[cd,lm]perylene; ◇ = naphtho[1,2,3,4ghi]perylene; △ = naphtho[8,1,2bcd]perylene.

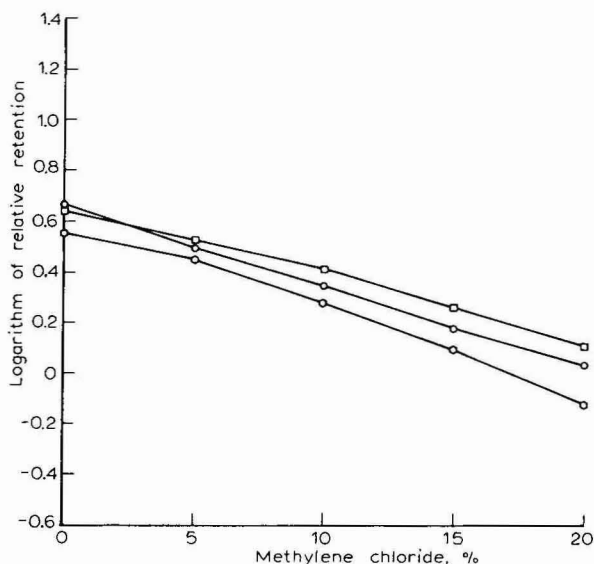


Fig. 4. Relative retention plots of the PAHs of molecular weight 350. □ = Benzo[*pqr*]naphtho[8,1,2*bcd*]perylene; ○ = benzo[*a*]coronene; ○ = phenanthro[1,9,10,8*fghij*]perylene.

shown in Figs. 2–8. The seven sets of data are divided into groups according to molecular weight to facilitate comparison of isomers or other PAHs of similar carbon number. From the prior work it was known that three types of behavior were possible: PAHs could always be either planar or non-planar or only become non-planar at higher concentrations of the strong solvent. All three were seen in this work.

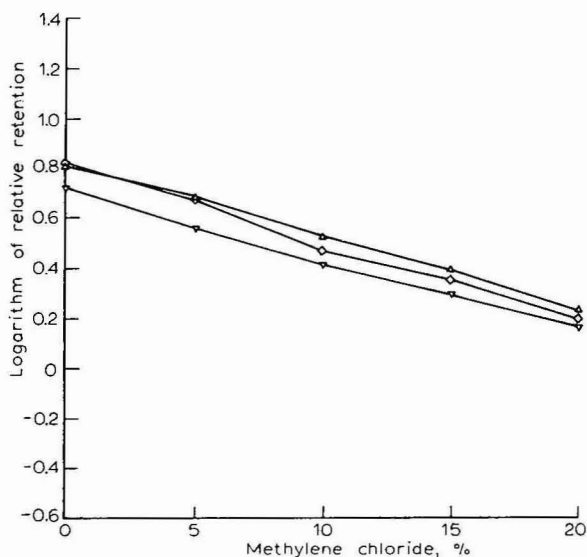


Fig. 5. Relative retention plots of the PAHs of molecular weight 374–376. ▽ = Naphtho[8,1,2*abc*]coronene; ◇ = dibenzo[*bc,ef*]coronene; △ = phenaleno[1,9*ab*]perylene.

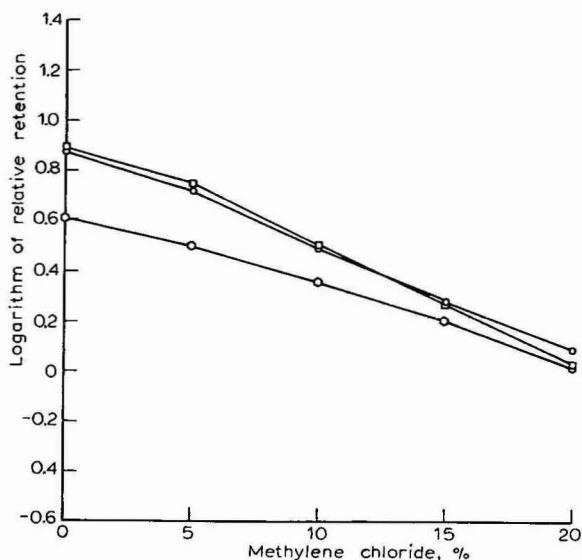


Fig. 6. Relative retention plots of the PAHs at molecular weight 376. □ = Tribenzo[de,kl,rs]pentaphene; ○ = pyranthrene; ◇ = tribenzo[a,cd,m]perylene.

Most of the molecules appeared to remain in a planar conformation in all the solvent mixtures, as evidenced by their approximately linear plots. Their UV spectra had shifts in the band positions, but no changes in band shape or the number of bands. Coronene and ovalene (compounds 3 and 18) behaved this way. In contrast, the plots for some of the PAHs showed some curvature. Benzo[rs]pentaphene and

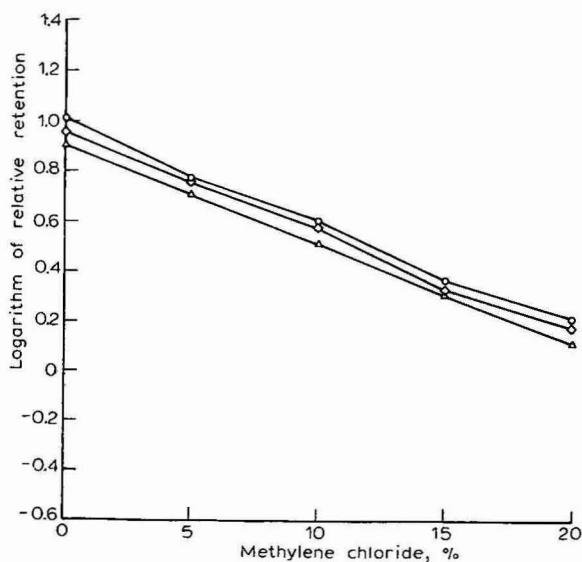


Fig. 7. Relative retention plots of the PAHs of molecular weights 398-400. △ = Ovalene; ◇ = naphtho[2,3a]coronene; ○ = dinbenzo[a,j]coronene.

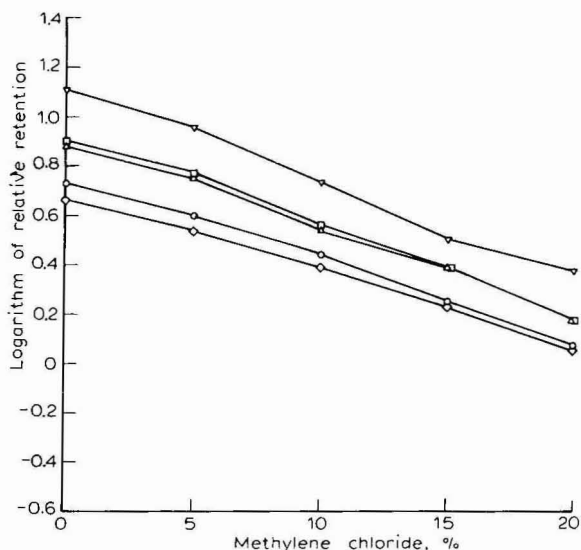


Fig. 8. Relative retention plots of the PAHs of molecular weights 424–426. ▽ = Benzo[cd]chryseno[4,5,6,7fghijk]perylene; ◇ = tetrabenzo[a,cd,j,lm]perylene; △ = benzo[rs]t-phenanthro[1,10,9,cde]pentaphene; □ = dibenzo[a,cd]naphtho[1,8,jk]perylene; ○ = tetrabenzo[de,hi,op,st]pentacene.

benzo[b]perylene (compounds 4 and 5, Fig. 2), at a molecular weight of 302, are an example of the different types of behavior seen for an isomeric pair. Benzo[b]perylene had a significantly curved plot, while benzo[rs]t-pentaphene gave an almost linear one. A curve plot was also observed for several of the other PAHs.

Another important trend was observed with tetrabenzo[a,cd,j,lm]perylene and tetrabenzo[de,hi,op,st]pentacene (compounds 23 and 26, Fig. 8). These molecules appeared to be so sterically strained that even in *n*-hexane they were non-planar. Their retention times were drastically smaller than other PAHs of similar molecular weight, but their unchanging non-planar conformation in all the solvent mixtures produced an approximately linear plot. The only way of identifying this type of behavior was comparison to other PAHs of the same carbon number. The non-planar PAHs' retentions were much less than the planar PAHs of the same carbon number. By contrast to those two strained, non-planar PAHs, compound 22 (with the same number of carbons) eluted much later. The two isomers of molecular weight 424, compounds 21 and 22, had identical retention behavior within experimental error; so only the line for compound 22 is shown in Fig. 8 for the two compounds.

In general, those PAHs whose UV spectra had shallow valleys between their highest wavelength absorbance bands appeared to elute earlier than expected. A correlation between these properties can be made. A parameter called the "shallowness factor" for a PAH was defined as the ratio of the average of the intensities of the two highest wavelength absorbance maxima and the intensity of the corresponding absorbance minimum. As the value of shallowness factor approached one, the spectral valley became smaller. The values for a particular set of PAHs in a particular solvent mixture can be compared with their relative retentions from an isocratic chromatographic run using the same solvent mixture. This experiment was performed

TABLE II
CORRELATION OF RETENTION TIME AND SHALLOWNESS FACTOR

Compound number	Relative retention	Shallowness factor
22	2.399	3.27
25	1.510	2.21
24	1.484	2.10
26	1.192	1.42
23	1.148	1.35

using spectra collected both on-the-fly, using the photodiode array detector during the separations, and statically with solutions of the individual PAHs in the different solvent mixtures. The two experimental approaches yielded similar values, but the values from the static measurements were much more precise. Table II is a comparison between the relative retention times in *n*-hexane–methylene chloride (90:10) for the 34-carbon PAHs and the shallowness factor values found statically in the same solvent mixture. The shallowness factor values are precise to 0.02 units. It was seen that the shallower PAHs elute the earliest. To a lesser degree, this trend was also seen for the other sets of PAHs.

In our earlier reversed-phase work, a PAH was found that had spectral differences in weak and strong solvents⁹. The absorbance band for benzo[*rst*]phenanthro[1,10,9*cde*]pentaphene (compound 24), around 475 nm, underwent a band-shape change so that rather than the one large absorbance band seen in methylene chloride, the compound in *n*-hexane or methanol showed two smaller ones. In the current work, similar comparison spectra were obtained for another five of the PAHs. These were chosen because they had the greatest anomalous elution behaviors for PAHs that had not been studied in our earlier work. The two solvent mixtures used for the spectral comparisons were *n*-hexane–methylene chloride (90:10) and 100% methylene chloride. These PAHs showed two types of differences when the spectra in the two solvent mixtures were compared. First, the depth of the valley

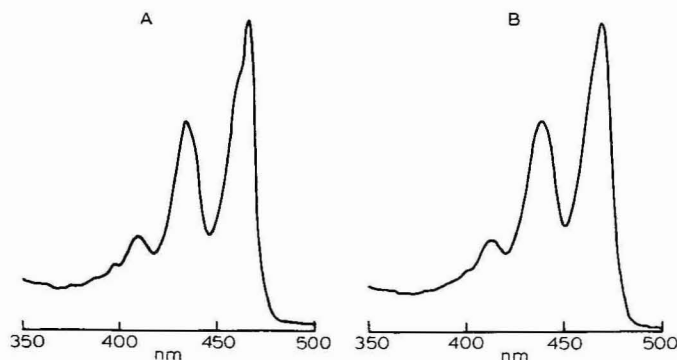


Fig. 9. Comparison spectra of naphtho[8,1,2*bcd*]perylene showing the changes in band-shape and shallowness with higher methylene chloride concentrations: (A) *n*-hexane–methylene chloride (90:10) and (B) 100% methylene chloride.

between the two highest wavelength absorbance bands was less in methylene chloride than in *n*-hexane. Secondly, some of these PAHs showed varying degrees of band shape changes similar to those seen previously with compound 24. The spectra of naphtho[8,1,2*bcd*]perylene, compound 8, are shown in Fig. 9. The change in the shallowness of the minimum, as well as the band shape changes, is seen. The shallowness factors for these six PAHs in the two solvents are shown in Table III. The values seen in methylene chloride were consistently lower than the values found in the predominantly *n*-hexane solution. This was only seen for the PAHs that had anomalous elution behavior. The values for the PAHs that had sharper absorbance bands and "normal" elution behavior, such as coronene or ovalene, differed by 0.008 units or less for the two solvents, with the greater value not always being the *n*-hexane one.

In addition to these spectral and chromatographic traits, these PAHs were also more soluble in *n*-hexane than isomers that had sharper spectral bands and longer retention times. This would also support the premise that these molecules are non-planar because they would also be less ordered crystallographically than the planar PAHs, if the solid state structure is similar to the solvated structure.

For the aminopropyl column, the three types of solution behavior of these PAHs caused any single isomeric set to have a wide range of retention times. Large overlaps with the other isomeric sets resulted. Thus any prediction of retention times by the number of rings or π electrons or by molecular shape were not possible.

This division of PAHs into classes based on the degree of planarity in solution is similar to the divisions made by Boschi *et al.*¹³ in their photoelectron spectroscopic study of the gas phase behavior of PAHs. The width of the photoelectron transitions were broader in sterically strained PAHs than those in the spectra of unstrained PAHs.

The nitropropyl-bonded packing column was more retentive than the aminopropyl-bonded phase; so slightly higher concentrations of methylene chloride could be used. The nitropropyl phase had an almost identical selectivity for separating isomers compared to the aminopropyl phase. Small differences in retention order, however, existed. This was seen especially at the higher methylene chloride concentrations. With the nitropropyl phase and its higher concentrations of methylene chloride, two pairs of closely eluting compounds reversed elution order compared to that seen with the aminopropyl phase. The ratios of the relative retention values in the various solvent mixtures for these pairs on the nitropropyl column are shown in

TABLE III
COMPARISON OF SHALLOWSNESS FACTOR IN DIFFERENT SOLVENTS

Compound number	<i>n</i> -Hexane	Methylene chloride
5	2.12	1.91
8	2.85	2.56
11	1.64	1.32
15	2.73	2.69
24	2.13	2.02
26	1.44	1.32

TABLE IV
RELATIVE RETENTION RATIOS INDICATING ELUTION ORDER CHANGES

<i>Methylene chloride (%)</i>	<i>Compounds 7 and 8</i>	<i>Compounds 12 and 14</i>	<i>Compounds 15 and 16</i>
5	0.943	0.959	0.889
10	0.971	1.016	0.936
15	1.002	1.052	0.953
20	1.066	1.087	0.987
25	1.093	1.115	1.010

Table IV. Values are also given for a third pair (compounds 7 and 8) which showed an elution order change on both columns. With lower methylene chloride concentrations, the elution order with the nitropropyl phase for all three pairs was the same as those seen with the aminopropyl phase. Since the ratios were less than one at lower concentrations and then became greater at higher concentrations, a change in elution order occurred that was caused by the use of greater proportions of methylene chloride possible with the nitropropyl column. Each of the PAHs that had been the later eluting compound at lower methylene chloride concentrations had a shallower spectrum than the earlier eluting one, indicating a greater susceptibility towards a non-planar structure. At higher concentrations of strong solvent, they went non-planar and eluted earlier than the other member of the pair.

The TENF column was extremely retaining, allowing runs at 100% methylene chloride. Only about half of the compounds eluted, even under these conditions. Those that did elute showed an order that paralleled our earlier reversed-phase studies. The highly strained nine-ring PAHs tetrabenzo[*a,cd,j,lm*]perylene and tetrabenzo[*de,hi,op,st*]pentacene (compounds 23 and 26) eluted before the much smaller benzo[*ghi*]perylene (compound 2). This was the most extreme example of the solvated structure effecting elution behavior, but compounds 5, 6, 8, 11, 14, 15, 17, 24, and 25 also showed earlier elution than expected when compared to isomers that are not sterically strained.

CONCLUSION

For each of the three columns examined, the solvent induced non-planarity of some PAHs caused the retention time range of an isomer set to be very large. The overlap between the isomer sets was then great enough to make any correlations between the number of π electrons or rings and the retention times impossible. Thus the use of parameters, such as the length-to-breadth ratio, appears to be valid only for the planar PAHs. The wide range of elution behavior was caused by three apparent types conformational behavior: (1) PAHs that were planar in all solvent mixtures and had predictable retention times that correlated with their ring number, (2) PAHs that were non-planar in all solvent mixtures and eluted much earlier than expected when compared to the planar PAHs, and (3) some PAHs which changed their degree of planarity with solvent composition so that their retention times could not be predicted by comparison to the planar PAHs. The degree of this non-planarity, and thus

the degree of earlier-than-expected chromatographic elution, was evidenced by the shallowness of the UV absorbance minima in the spectra of the PAHs. This amount of spectral shallowness changed with solvent in parallel fashion to the retention behavior changes. The degree of earlier-than-expected elution or the changes in elution order could be estimated by the UV spectra of the PAHs.

The use of gradient elution in PAH analyses must be carefully evaluated. The changing solvent composition can have a dramatic effect on retention order; so the identification of each peak must be verified. Single-wavelength detectors would not easily follow these changes. The separation of two or more closely eluting peaks could be accomplished by either a weaker or a stronger solvent mixture as well as the choice of different solvents, depending on which classes of PAHs are present.

The results from this new series of chromatographic experiments indicate that the use of retention time alone as an identifying parameter in HPLC for the larger PAHs is not valid, but its use for comparison to standard material would be appropriate if the reproducibility of the mobile phase composition is high enough to control the degree of non-planarity induced by the mobile phase. Primary identification of the PAHs must still be by comparison to standards and by spectral characterization.

ACKNOWLEDGEMENT

We thank Chevron Research Company for permission to publish this work.

REFERENCES

- 1 E. Clar, *The Aromatic Sextet*, Wiley-Interscience, New York, 1972.
- 2 R. B. Sleight, *J. Chromatogr.*, 83 (1973) 31.
- 3 S. A. Wise, W. J. Bennett and W. E. May, in A. Bjorsted and A. J. Dennis (Editors), *Polynuclear Aromatic Hydrocarbons: Chemistry and Biological Effects*, Batelle Press, Columbus, OH, 1980, p. 791.
- 4 M. Novotny, M. Lee and K. Bartle, *J. Chromatogr. Sci.*, 12 (1974) 606.
- 5 M. Novotny, in E. Grushka (Editor), *Bonded Stationary Phases in Chromatography*, Ann Arbor Sci. Publ., Ann Arbor, MI, 1974, p. 199.
- 6 S. A. Wise, W. J. Bonnett, F. R. Guenther and W. E. May, *J. Chromatogr. Sci.*, 19 (1981) 457.
- 7 K. Jinno and M. Okamoto, *Chromatographia*, 18 (1984) 495.
- 8 J. C. Fetzer and W. R. Biggs, *J. Chromatogr.*, 295 (1984) 161.
- 9 J. C. Fetzer and W. R. Biggs, *J. Chromatogr.*, 322 (1985) 275.
- 10 E. Clar, *Polycyclic Hydrocarbons*, Vol. 1, Academic Press, New York, 1964, Ch. 16.
- 11 J. L. Glajch, E. I. du Pont de Nemours and Company, personal communication, 1985.
- 12 L. R. Snyder and J. J. Kirkland, *Introduction to Modern Liquid Chromatography*, 2nd Edition, Wiley-Interscience, New York, 1979, pp. 587-588.
- 13 R. Boschi, E. Clar and W. Schmidt, *J. Chem. Phys.*, 60 (1974) 4406.

CHROM. 17 994

NOBLE, DIATOMIC AND ALIPHATIC GAS ANALYSIS BY AQUEOUS HIGH-PERFORMANCE LIQUID CHROMATOGRAPHY

JOHN O. BAKER*, MELVIN P. TUCKER and MICHAEL E. HIMMEL

Biotechnology Branch, Solar Fuels Division, Solar Energy Research Institute, 1617 Cole Boulevard, Golden, CO 80401 (U.S.A.)

(First received May 28th, 1985; revised manuscript received June 28th, 1985)

SUMMARY

Dissolved non-polar gases (five noble, three diatomic, and four unbranched aliphatic hydrocarbon gases) were resolved by aqueous high-performance liquid chromatography using an ion-moderated partition chromatography column (Bio-Rad HPX-87P) originally designed for monosaccharide analysis. The dissolved-gas peaks, which were detected and quantitated by high-sensitivity refractive-index detection, are eluted at 25°C in the order Ne, He, N₂, H₂, O₂, Ar, CH₄, Kr, Xe, C₂H₆, C₃H₈, *n*-C₄H₁₀. Based on the general elution order, and on the temperature dependences (4–72°C) of elution times for the individual gases, a mixed chromatographic mechanism is proposed, in which separation of the gases results from a mixture of size-exclusion, ion-ion-induced dipole, and classical hydrophobic effects, plus a second type of “hydrophobic” effect involving binding of the clathrate hydrate cages surrounding non-polar solutes to similar cages formed around hydrocarbon portions of the column packing material.

INTRODUCTION

Our laboratory routinely monitors enzymatic digestion of cellulosic biomass through analysis by high-performance liquid chromatography (HPLC) of the soluble sugars produced, using a Bio-Rad HPX-87P carbohydrate analysis column with deionized water as eluent and with refractive index (RI) detection. During these analyses we observed baseline perturbations in the form of negative RI peaks in the glucose-xylose-galactose region of the chromatograms. A few simple experiments revealed that the occurrence of the negative peaks was related to the entrainment of air in the injected sample. Sample injections known to have contained actual air bubbles resulted in unusually large negative peaks, whereas injection of water degassed by boiling resulted in positive RI peaks at the same positions on the chromatogram. In this latter case, the sample injected apparently contained less dissolved air than did the mobile phase, since although the filtered, deionized water used for the mobile phase had been degassed prior to being placed in the solvent reservoir, it had not been maintained rigorously gas free after that time.

It was not especially surprising that differences in the dissolved-gas levels of aqueous mobile phase and injected aqueous sample should result in peaks detectable by RI monitoring, since the solution of gas in water is known to result in a decrease in the density of the water¹. What was remarkable, however, was that entrapment of air in the injected sample resulted in not one, but two, well-defined, reproducible, and reasonably well-resolved peaks. Since the ratio of the areas of the two peaks was approximately 4:1, it occurred to us that the column might be separating nitrogen and oxygen, which are present in the atmosphere at approximately the same ratio. Preliminary experiments involving purging of samples with helium and nitrogen confirmed that this was indeed the case.

A number of studies have dealt with problems such as bubble related noise, baseline drift, and reduction in detector response caused in liquid chromatography (LC) and HPLC detection by the presence in the mobile phase of dissolved gases in general² and oxygen in particular²⁻⁵. To the best of our knowledge, however, there have been no reports of the separations of dissolved permanent gases by aqueous chromatography.

The observation that individual gases were separated by the column meant that the phenomenon of the negative peaks was of considerable interest in itself, in addition to being of practical importance in connection with analysis of monosaccharide and other solutes conveniently followed using RI detection. The practical importance of the gas peaks is of course that, with the advent of high-sensitivity RI detectors capable of being operated usefully at full-scale expansions of $0.25 \cdot 10^{-5}$ RI units (RIU) or even $0.125 \cdot 10^{-5}$ RIU, baseline perturbations that were mere annoyances in chromatography using less sensitive detection now become a major factor in determining the lower limit of quantitation for certain solutes. In the system we use for monosaccharide analysis, the solutes the quantitations of which are most interfered with are xylose and galactose, important constituents of fibrous biomass. The separation of three permanent gases (including helium) that do not react with water and are relatively inert with respect to the column packing material is also of considerable interest in terms of chromatographic theory. In order to determine whether the separation was general for dissolved permanent gases, we designed and had fabricated a solvent reservoir that maintains the mobile phase rigorously gas-free, thus giving a consistent baseline for gas-peak analysis, and then proceeded with determination of the chromatographic characteristics of three diatomic, five noble, and four hydrocarbon gases. The results demonstrate that aqueous HPLC can be used to separate and quantitate dissolved gases. A rationale is presented which correlates separation of the gases with known molecular properties of the solutes.

EXPERIMENTAL

Instrumentation

The chromatographic system used in these experiments consisted of a Beckman Model 100 A pump delivering eluent (deionized, degassed water) through a Beckman/Rheodyne Model 210 injection valve, to a Bio-Rad carbohydrate analysis precolumn and lead-loaded (Aminex HPX-87P) carbohydrate analysis column (300×7.8 mm). Column and precolumn were water-jacketed and controlled at various operating temperatures from 4°C to 72°C by a Forma Model 2006 refrigerated water

circulator. Detection of peaks was by means of a Hewlett-Packard high-sensitivity RI detector (Erma Instruments) used routinely at attenuations of 1.0 to 0.25 RIU per 10-mV full-scale output. Data were collected using a Shimadzu Model CR 1-A integrating recorder. A 0.250-ml sample loop was used for all injections. Gastight® (Hamilton) syringes and Mininert® syringe valves were purchased from Alltech.

Thoroughly degassed eluent (deionized water) was provided by a Pyrex reservoir (custom-fabricated from a 2000-ml suction flask) that permitted continuous gentle boiling of the eluent, with steam release through a constricted vent to prevent back-diffusion of air into the reservoir flask. Degassed water was pumped from the reservoir through stainless-steel tubing introduced through a custom side-arm; this design left the neck of the flask itself available for replenishing the water supply by adding filtered and degassed (boiled) water during extended chromatographic runs. The tubing that carried the eluent from reservoir to pump inlet was of stainless steel, Swage-Lok-connected, to avoid problems due to the oxygen- and nitrogen-permeability of tubing formed of PTFE or other flexible materials commonly used for HPLC eluent inlet lines.

Materials

Nitrogen, oxygen, helium, argon and hydrogen (ultra-high-purity, > 99.999%), neon (research grade, > 99.998%), ethane (C.P., 99.2%), propane and butane (instrument grade, 99.5%) were all purchased in high-pressure steel cylinders from Scientific Gas Products. Methane (> 99.99%) was obtained from Liquid Carbonic. Krypton and xenon (both 99.995%) were purchased in 1-l glass flasks from Scott Specialty Gases. The deuterium oxide used as a marker for total column volume was from Sigma.

Sample preparation for retention time studies

Solutions of all gases, except krypton, xenon and air, were prepared simply by bubbling the gas through a small quantity of Millipore-filtered deionized water. Samples of krypton and xenon were prepared by withdrawing 4 ml of the gas from the septum-capped glass vial into a 10-ml Gastight syringe fitted with a Mininert syringe valve and a 6-in. 20-gauge septum-taper needle, and containing 2 ml of deionized, degassed water. [Degassed water (4 ml) had been injected immediately before from the syringe into the flask to give the flask a slight overpressure.] The valve-sealed syringe was then attached to a laboratory rotator for 20 min to provide thorough equilibration of gas and water, after which the injection was made directly from the syringe. Samples of deionized, filtered water saturated with air were prepared simply by vortexing the water sample in contact with the atmosphere.

Standards for quantitation of dissolved gases

The apparatus shown schematically in Fig. 1 was used to prepare, simultaneously and separately, supplies of deionized water saturated at 25°C and ambient pressure with either helium (G_1) or argon (G_2). Each gas was first saturated with water vapor by bubbling through vigorously stirred water in a 250-ml flask containing a filter-paper wick, and then bubbled into the sample preparation flask, which was also vigorously stirred with a PTFE-coated magnetic bar. Both of the water-saturating chambers and both of the sample preparation chambers were maintained at

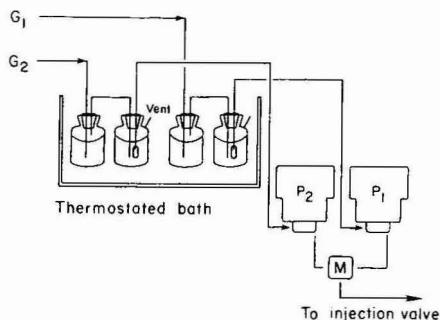


Fig. 1. Apparatus used to generate standard solutions for quantitation of dissolved gases. Aqueous solutions of two different gases in varying ratios are prepared by adjusting the relative rates at which two HPLC pumps (P_1 and P_2) deliver saturated (25°C , 1 atm) solutions of each of two gases (G_1 and G_2) to the mixing chamber M. (See text for further details.)

25°C in a water bath; both sample preparation chambers were vented to the atmosphere through water traps (not shown) with 2-cm heads of water. Gas-saturated water was withdrawn from each sample vessel via stainless-steel tubing (1/8-in. O.D.) by one of two HPLC pumps, P_1 and P_2 (Waters Assoc., Model 6000A solvent delivery systems). The output from pump P_1 was connected to the mixing chamber at the outlet of pump P_2 . The combined output of the two pumps was connected directly to the injection valve of the HPLC column through 4 ft. of 0.010-in. I.D. stainless-steel tubing. Samples of water at a variety of precisely-known degrees of saturation (with respect to a solution saturated with each gas at 25°C , ambient pressure) were prepared by varying the pumping speed of the two pumps (total flow-rate 1.0 ml/min). The mixing chamber and sample loop were flushed for a minimum of 6 min at each pump-speed ratio before the sample was injected onto the column. Gas saturation of the water in each sample preparation chamber was confirmed by observation of peaks of constant size for samples prepared with only one sample-mixing pump running, and injected at 15-min intervals over a period of an hour. For the gas-quantitation studies, the column operating temperature was 60°C .

RESULTS

Figs. 2–4 illustrate the separation of three series of permanent gases by an HPX-87P (Bio-Rad) carbohydrate analysis column, operated at 60°C with degassed, deionized water as eluent. Fig. 2 shows the separation of the principal constituents of air, which was the initial observation leading to this study. The third diatomic gas used in this study, hydrogen, has a retention time of 31.6 min at 60°C with a 0.3 ml/min flow-rate. Hydrogen (not shown) therefore is eluted so shortly after nitrogen that it is not resolved from nitrogen at 60°C and is poorly resolved from oxygen.

Of the five noble gases, four (argon, krypton, xenon, and helium or neon) can be resolved with baseline separation (Fig. 3). Helium and neon however, are eluted so close together that no separate peaks, or even shoulders are obtainable. In the composite chromatographic pattern shown in Fig. 3, the peaks for helium, neon, argon and krypton are negative peaks; that is, they were recorded with the polarity

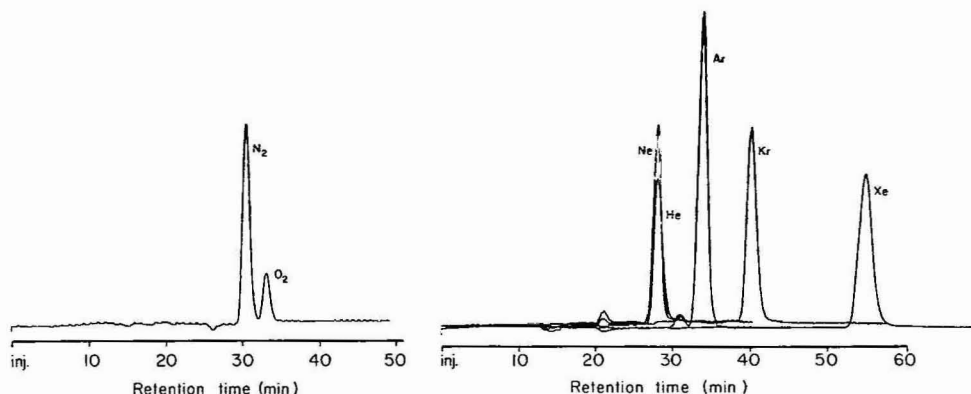


Fig. 2. Chromatography on the HPX-87P of a 0.25-ml sample of deionized water saturated with air at ambient conditions. Flow-rate, 0.3 ml/min; column temperature, 60°C; detector sensitivity, $0.25 \cdot 10^{-5}$ RIU full scale, detector polarity reversed.

Fig. 3. Superimposed chromatograms (HPX-87P) of five noble gases. Operating conditions same as Fig. 2, except that for xenon, polarity was normal and detector sensitivity was $1.0 \cdot 10^{-5}$ RIU full scale.

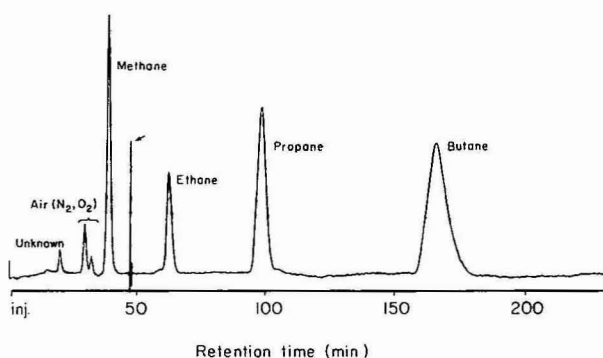


Fig. 4. Co-chromatography of four hydrocarbon gases. Detector polarity was reversed for methane, switched to "normal" for the remaining three gases. The spike at approximately 47 min (arrow) resulted from polarity change and baseline readjustment.

of the RI detector reversed. The xenon chromatogram, however, was monitored using normal detector polarity, and a detector sensitivity setting one-fourth of that used for the other noble gases. Whereas dissolving any of the four lighter noble gases in water results in a solution with RI less than that of pure water, a solution of xenon in water has an RI higher than that of water, as is the case for sugars, fatty acids and others of the more usual RI-detectable solutes. A similar division in terms of effect on RI is seen in Fig. 4, which shows a chromatogram at 60°C of the four *n*-alkanes that are gases under normal conditions. Here, methane is detected as a negative peak, but the three larger members of the series produce positive RI peaks. Like the noble gases (Fig. 3) the *n*-alkanes are eluted from the column in order of increasing molecular size. Deuterium oxide, used as an RI-detectable marker for a solute neither adsorbed nor sterically excluded by the column, had a retention time of 34.5 min at 60°C, 0.3 ml/min.

The highly stable, reproducible RI baseline provided by use of thoroughly degassed water as eluent allows the quantitation of dissolved permanent gases by measurement of peak areas. Fig. 5 shows standard curves constructed for helium and argon using as samples mixtures in varying ratios of saturated (25°C, 1 atm) water solutions of the two gases. Samples were mixed using the system shown schematically in Fig. 1 and described in the Experimental section. From the regression lines in Fig. 5 we see that for a given degree of saturation of the sample at 25°C, 1 atm partial pressure, the ratio of peak areas for argon and helium is 2.88. The ratio of the water solubility of argon to that of helium under these conditions is, however, 3.57 (ref. 6). On a molar basis, therefore, the (negative) RI response of argon is only 80.6% of that of helium.

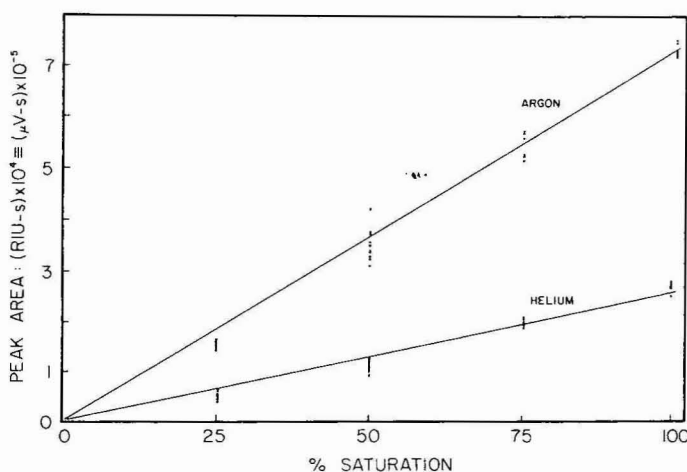


Fig. 5. Standard curves for quantitation of dissolved helium and argon. Samples prepared as described in Experimental section, using the apparatus shown schematically in Fig. 1.

The dependence of elution times on column operating temperature is shown in Figs. 6–8. Both the diatomic gases (Fig. 6) and the “noble”, or helium-group gases (Fig. 7) have relatively simple temperature dependences, with elution times uniformly increasing as temperature is increased. The differences in slope between the diatomic and noble gases are more apparent than real, arising from the fact that, for the sake of clarity and to facilitate comparisons within the groups, the diatomic and noble gas elution time–temperature profiles have been plotted separately with different abscissa scales. In fact, the temperature dependences of elution for the two groups are quite similar; oxygen essentially co-elutes with argon over the temperature range studied, for instance.

The temperature dependence of elution time for the smallest of the aliphatic series, methane, also does not vary strikingly from that of a noble gas with a similar average elution time; over most of the temperature range, the elution behavior of methane is quite similar to that of krypton. As the number of carbon atoms is increased, the remaining members of the *n*-alkane series begin to show temperature

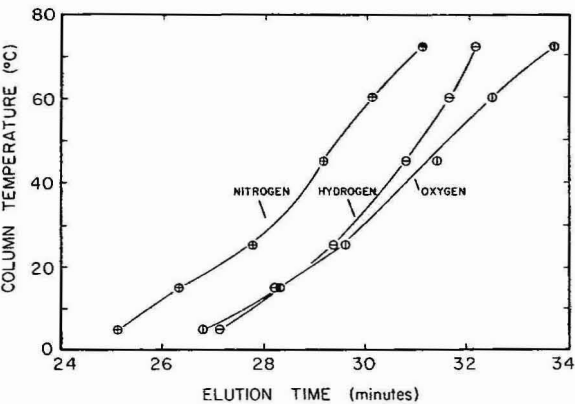


Fig. 6. Dependence of elution time on column operating temperatures for three diatomic gases. Flow-rate, 0.3 ml/min.

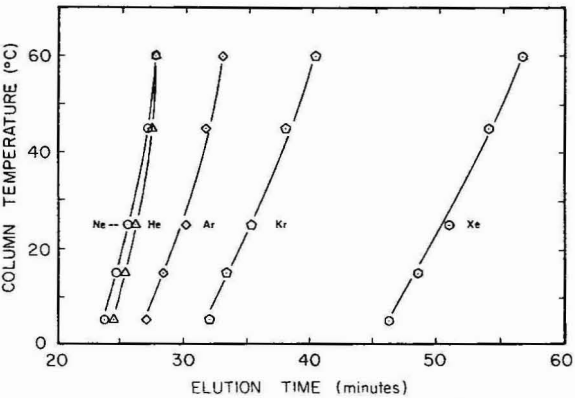


Fig. 7. Temperature dependence of elution time for five noble gases. Flow-rate, 0.3 ml/min.

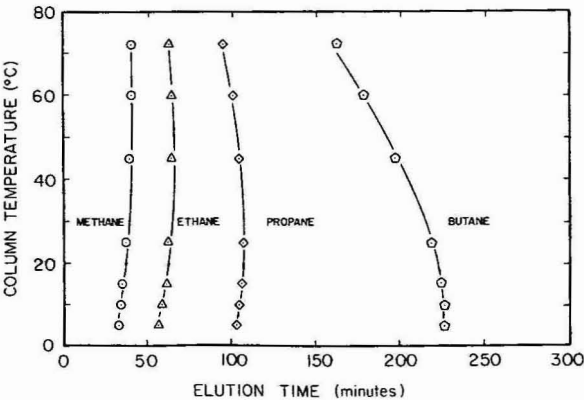


Fig. 8. Temperature dependence of elution time for four paraffin hydrocarbon gases. Flow-rate, 0.3 ml/min.

dependences significantly different from that of the noble and diatomic gases. Although the elution time-temperature profile for ethane (Fig. 8) differs very little from that for methane, it is quite different from that for xenon, a noble gas eluting in the same general region of the chromatogram. The shapes of the curves for propane and butane are even more strikingly different from those for the noble and diatomic gases. As the column temperature is increased from 4°C, the elution time for ethane first increases, up to about 25°C, and then remains relatively constant up to 72°C. The elution time for propane increases with temperature up to approximately 25°C, but then decreases significantly as the temperature is raised further. The elution time for butane is relatively independent of temperature from 4 to 10°C, but above 10°C the elution time decreases markedly as temperature is increased. Although the temperature dependence of butane elution differs noticeably from that of methane, and from that of the noble and diatomic gases, there is no evidence (Figs. 7 and 8) of a sharp break in behavior, but rather a smooth transition from one shape of temperature dependence to another.

Not only are the noble and aliphatic gases eluted in order of increasing molecular size when considered as separate groups, but the molecular size and elution time data pairs for the two groups mesh comfortably to form a smooth progression of increasing elution time with increasing molecular size. (At 60°C helium and neon are co-eluted, but at lower temperatures, at which a difference in elution times can be shown by injections of the two gases separately, the gas that is eluted first is neon, which, though a heavier molecule, has the smaller Van der Waals radius⁷⁻⁹).

The diatomic gases considered as a group do not follow the "smallest-first-off" rule obeyed by the other two groups. Nitrogen, the diatomic molecule with the largest molecular volume as indicated by the empirical term b from the Van der Waals equation of state⁹ is eluted earliest, while hydrogen, with the smallest volume of the three by a considerable margin, is eluted between nitrogen and oxygen over most of the temperature range. When the elution behavior of the diatomic gases is considered along with that of the noble and aliphatic gases, however, the diatomic molecules, in spite of the contrary ordering among themselves, do fall as a group in the general area of the elution time-temperature diagram they would be expected to occupy on the basis of the behavior of the other two groups.

The chromatographic behavior at 25°C of the solutes studied can be correlated with several of their molecular properties (Table I). In Fig. 9, the mean molecular polarizabilities¹⁰⁻¹² of the noble, diatomic, and aliphatic hydrocarbon gases, when plotted against retention time, fall along a smooth curve with an apparent intercept on the retention time axis at 24.8 min. When the value of this intercept, which corresponds to the elution time of a completely non-polarizable solute, is taken as t_{\min} in eqn. 1

$$K_d = \frac{t_R - t_{\min}}{t_{2H_2O} - t_{\min}} \quad (1)$$

the cube root^{13,14} of the resulting chromatographic partition coefficient, (K_d) is a linear function of the molecular polarizability (Fig. 10). Here, t_R is the retention time for a given solute and t_{2H_2O} is the elution time for a solute neither adsorbed on the column material nor excluded from the pore volume.

Solubility data available in the literature^{6,16-19} permit calculation of partition

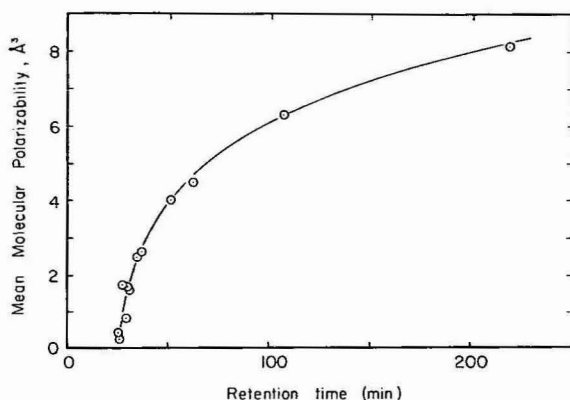


Fig. 9. Relationship between retention time (flow-rate, 0.3 ml/min, 25°C) and the mean molecular polarizability (refs. 6-8) for all twelve gases studied. In order of increasing polarizability, the gases are: He, Ne, H₂, Ar, O₂, N₂, CH₄, Kr, Xe, C₂H₆, C₃H₈ and *n*-C₄H₁₀.

TABLE I

CORRELATION OF SEVERAL CHROMATOGRAPHIC RETENTION PARAMETERS FROM EQN. 1* WITH POLARIZABILITY (Å³) AND MOLAR VOLUME (VAN DER WAALS *b*, l/mole)

Parameters	Correlation coefficient
Polarizability vs. $K_d^{1/3}$	0.9900
<i>b</i> vs. $\log t_R$	0.9879
<i>b</i> vs. $K_d^{1/3}$	0.9843
Polarizability vs. $\log t_R$	0.9788
<i>b</i> vs. K_d	0.9572**
Polarizability vs. $\log K_d$	0.9510**
<i>b</i> vs. $\log K_d$	0.9207**
Polarizability vs. t_R	0.9001**
Polarizability vs. K_d	0.9001**

* $t_{2H_2O} = 34.5$ min; $t_{min} = 24.8$ min.

** Show distinct curvature.

coefficients¹⁵ for the systems hexane–water and octanol–water, for most of the solutes in the present study. The partition coefficient $P_{organic}$ is calculated as the ratio, at 25°C, of solubility in the organic solvent to the solubility in water, with the partial pressure of the solute equal to 1 atm in both cases. P_{hexane} , the partition coefficient calculated with *n*-hexane as organic reference phase, is plotted against retention time (Fig. 11) for all of the solutes in this study except ethane, propane, and butane. Least-squares linear regression analysis of these data results in the best-fit straight line shown, with correlation coefficient r equal to 0.9631. A similar plot (not shown) with *n*-octanol as reference phase also shows a reasonably linear relationship ($r = 0.9653$, Table II). When the data in Fig. 11, for the *n*-hexane–water system, are replotted with the inclusion of data for ethane, the plot is significantly curved, with an r value of only 0.9315. Apparently the chromatographic retention of the noble and diatomic gases and methane is directly proportional to classical measures of “hydrophobicity”, but the relationship breaks down for the higher hydrocarbons.

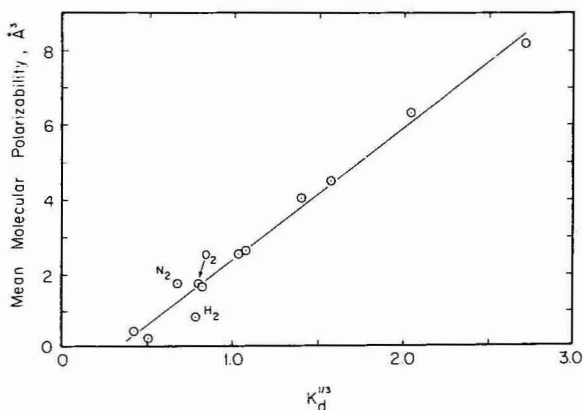


Fig. 10. Linear correlation between mean molecular polarizability and the cube root of the chromatographic partition coefficient K_d . The partition coefficient was calculated using eqn. 1, with the values 24.8 min and 34.8 min used for t_{\min} and t_{2H_2O} , respectively.

TABLE II

CORRELATIONS OF RETENTION TIME (t_R) WITH ORGANIC-WATER PARTITION COEFFICIENTS (P_{organic})

Partition coefficient	Correlation coefficient
P_{hexane}	0.9631*
P_{octanol}	0.9653**
P_{hexane}	0.9979***
P_{octanol}	0.9969§

* Noble and diatomic gases plus methane.

** Noble and diatomic gases (except xenon and hydrogen) plus methane.

*** Noble gases plus methane.

§ Noble gases (except xenon) plus methane. (Octanol solubility data not available for xenon.)

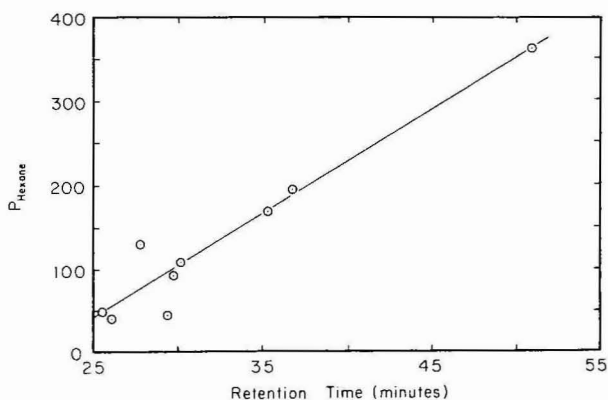


Fig. 11. Relationship between the hexane-water partition coefficient and retention time at 25°C for nine gases (those shown in Figs. 9 and 10, minus ethane, propane and butane). Partition coefficients calculated from solubility data found in refs. 6, 17 and 19.

When only the spherical or roughly spherical gases (*i.e.*, the noble gases plus methane) are considered, plots of molecular polarizability *vs.* $K_d^{1/3}$, and plots of P_{hexane} and P_{octanol} *vs.* retention time all show excellent linearity (Table II). The relationship shown in Fig. 10 between polarizability and $K_d^{1/3}$, is however the only relationship of those tested that exhibits good linearity for the entire collection of gases tested—the five noble gases, three diatomic gases, and four hydrocarbons.

For purposes of comparison with the results obtained with the HPX-87P column, brief studies were made of the chromatography of a small selection of gases on two other HPLC columns, both of which are designed purely for size-exclusion chromatography. With the Toyo Soda G2000PW (polyacrylamide bead) column and deionized, degassed water (0.3 ml/min) as eluent, neon, nitrogen, oxygen, $^2\text{H}_2\text{O}$ and methane eluted in the same order as on the HPX-87P. For columns of comparable dimensions (HPX-87P, 300×7.8 mm I.D.; G2000PW, 300×7.5 mm I.D.), however, resolution was considerably poorer on the G2000PW. Injection of an air-saturated sample produced two relatively broad and poorly-resolved peaks at 41.6 min (nitrogen) and 46 min (oxygen); use of two G2000PW columns in series was required for resolution comparable to that of the sharper peaks obtained on the HPX-87P. The silica based-bead Toyo Soda G3000SW (300×7.5 mm I.D.) on the other hand, yielded an elution order distinctly different from that of the HPX-87P. Air (73.1 min) and methane (67–68 min) both were eluted after $^2\text{H}_2\text{O}$ (51.3 min). The two major components of air were not resolved at all, a single broad peak being obtained.

DISCUSSION

Quantitative applications

In the analysis of gases dissolved in water or aqueous solutions, the aqueous HPLC method described here offers at least one significant advantage with respect to other methods such as gas chromatography (GC). Whereas GC requires the establishment of a head space, equilibration of this space with the liquid, and back calculation from the composition of the head space to that presumed to have existed in the original liquid, the aqueous HPLC method allows direct injection of the liquid sample itself. The preparation of appropriate standards (Fig. 5) will then allow direct determination of each dissolved gas. This method should be especially useful in measurement of the more dilute gas solutions in water, for which direct injection of solution into a GC column would entail injection of unacceptably large amounts of water.

Mechanism of the separation

The separation of dissolved inert gases by the HPX-87P column is not readily explicable in terms of any single retention mechanism; instead, a combination of mechanisms must be invoked to explain the observed patterns. Of the variety of interactions made possible by the chemical nature of the column packing, four seem capable of making significant contributions to the retention of these neutral solutes:

- (1) The bound heavy metal ion (Pb^{2+}), which contributes ion–dipole (ligand-exchange) interactions to the separation of monosaccharides, should be capable of ion–ion-induced dipole interactions in the chromatography of non-polar molecules.
- (2) The polystyrene backbone contributes the potential for classical hydrophobic interactions.

(3) A second, indirect type of hydrophobic bonding, involving interactions between clathrate-hydrate shells around different non-polar groups or molecules, may be important, especially for the larger aliphatic hydrocarbon solutes tested.

(4) The overall elution pattern, primarily determined by a combination of the three effects listed above, may be overlaid by minor effects due to size exclusion processes resulting from bead porosity. We shall examine these potential retention mechanisms further.

The overall behavior of neutral molecules in this system is consistent with general adsorptive mechanisms. There is some element of size-exclusion, in that some of the solutes are eluted before $^2\text{H}_2\text{O}$, which serves as a marker for V_t , the elution position of a solute that is neither adsorbed on the packing material nor sterically excluded from the pore volume of the beads. The void volume, V_0 cannot be determined with confidence, however, because of the several retention mechanisms that are almost certainly operating. Although size-exclusion effects may contribute to the chromatographic behavior of all of the neutral, non-polar solutes studied, the separation appears to be based for the most part on adsorptive, and not size-exclusion processes. For a series composed of the noble gases and the aliphatic hydrocarbons, the gases are eluted in order of increasing molecular size—the reverse of what would be expected for pure size-exclusion chromatography. In addition, from a theoretical point of view, eight of the twelve gases investigated (the four smaller noble gases, the three diatomic gases, and methane) are believed to exist in aqueous solution primarily as “guest” molecules in the same clathrate-hydrate structure—a “cage” formed by twenty water molecules hydrogen-bonded to each other and located approximately at the vertices of a regular pentagonal dodecahedron^{20–23}. This twelve-sided structure will be some 11–12 Å in average diameter and may therefore contribute to the elution of some of the solutes at earlier times than would be predicted in terms of size exclusion, based on the relative Van der Waals dimensions of the solutes with respect to those of $^2\text{H}_2\text{O}$. The enclosure of eight of the gas molecules in a package of relatively invariant size can also be expected to damp out any differences in chromatographic behavior that might have been expected from size-exclusion effects. Xenon, the largest of the noble gases studied, is more likely to be found in a larger, fourteen-sided cage in water^{24–26}. The larger hydrocarbon gases are too large to fit into the dodecahedral cage. These have been shown, through X-ray crystallographic, NMR, and low-temperature dielectric relaxation studies^{23,27,28} to occupy tetradecehedral (ethane)²³ and hexadecahedral (propane and butane)^{23,27,28} cages in crystalline hydrates. Again, the gas molecules that occupy the larger cages (and therefore have larger effective sizes in solution) are found to elute from the column later, not earlier, than those molecules found in smaller cavities (Figs. 3 and 4). The separation of these gases must therefore be explained primarily in terms of effects other than size-exclusion.

Dependence of the retention time on polarizability (Figs. 9 and 10) is consistent with general adsorptive phenomena, in particular with ion-ion-induced dipole interactions. Such interactions, which in this case can be ascribed to either the bound Pb^{2+} ions or to the sulfonic acid groups of the resin, are directly proportional to the polarizability of the neutral molecule, proportional to the square of the charge on the ion, and inversely proportional to the fourth power of the distance, r , between the nuclei²⁹. The increase in retention time with increasing temperature that is shown

by the diatomic and noble gases (Figs. 6 and 7) may be due in part to an increase in the strength of such interactions. The decrease in the dielectric constant of water with increasing temperature³⁰ will increase the strength of electrostatic interactions in general. Probably more important in this case, though, is an effect due to the combination of the strong (r^{-4}) dependence of ion-ion-induced dipole interactions on internuclear distance²⁹, and to the structuring of water around non-polar solutes²⁰. In order for the non-polar solute to approach sufficiently close to the stationary ion for induced-dipole effects to be significant, the clathrate "cage" about the solute must be disrupted. The rate of this disruption will be increased, and the position of the equilibrium³¹ between "hydrophobically solvated" and "free" inert solute will be shifted toward "free" solute as the temperature is increased. A certain damping effect on the magnitude of the changes with temperature is to be expected, since the more polarizable solutes (those capable of stronger interactions with the ion) are also those that form the more stable clathrate cages, due to stronger Van der Waals interactions with the water molecules forming the cage³².

A similar elution order (neon, nitrogen, oxygen, $^2\text{H}_2\text{O}$, methane) was obtained with the Toyo Soda G2000PW column, which is a polyacrylamide-based size-exclusion column not advertized as containing heavy metal ions. These results might seem to indicate that separation of gases by the HPX-87P can be explained without reference to ion-ion-induced dipole interactions. A cautionary note should be interjected here, however. It has recently been pointed out that some commercial silica-gel size-exclusion packing materials contain significant [up to 0.3% (w/w)] contaminations of heavy metals, and that the presence of these metals can profoundly affect chromatographic performance^{33,34}. The sand from which the silica-gel was manufactured is cited as the major source of the contaminant, but metal contamination from derivatizing reagents used in manufacture has also been listed as a possible source³⁴. This last consideration could apply to resin-based gels as well as to silica-based gels. Since no effort was made to render the G2000PW and G3000SW rigorously metal-free prior to use, metal ion interactions with solutes remain as a possible contributor to separations by these columns.

Fig. 11 suggests another possible contributor to the overall adsorptive retention of non-polar solutes by the HPX-87P packing material. For methane and the noble and diatomic gases, retention time shows a reasonably good linear proportionality to P_{hexane} , the calculated (see figure legend) partition coefficient for the system hexane-water at 25°C and 1 atm partial pressure of the gaseous solute. As was the case in the plot of $K_d^{1/3}$ versus retention time, nitrogen and hydrogen are the poorly-fitting solutes. With the elimination of these two data points, the fit for oxygen, methane, and the noble gases becomes excellent, with $r = 0.9978$. (More will be said about the behavior of hydrogen and nitrogen later in the discussion.) For the remaining solutes in Fig. 11, the data are consistent with the existence of significant hydrophobic bonding between the solutes and the aromatic-aliphatic backbone of the resin beads. According to this idea, the solutes leave the aqueous phase and are "dissolved", with direct Van der Waals contact between solute and resin material, in the polystyrene-divinylbenzene copolymer. The possibility of reversed-phase partitioning by this type of column packing has been noted previously in connection with separations of fatty acids by Jupille *et al.*³⁵.

The linear relationship of retention time and P_{hexane} breaks down for the ali-

phatics larger than methane. The addition of data for ethane to that plotted in Fig. 11 would result in a distinct upward curve of the plot to the right of xenon; the retention times for the larger aliphatics do not increase with P_{hexane} in proportion to the increases seen for the smaller gases. This is understandable since the solubilities of the paraffin hydrocarbons increase very rapidly as the solute becomes more similar to hexane. Hexane is simply too similar to the aliphatic solutes to serve as a good model, with respect to these solutes, of a "hydrophobic milieu" in general, or of the styrene-divinylbenzene copolymer in particular.

The strengths of "hydrophobic" interactions in aqueous solution have been shown to increase with increasing temperature^{20,36,37}; the increased retention times shown at higher temperatures by the diatomic and noble gases are therefore quite consistent with a substantial contribution of such binding to the retention mechanism. One aspect of the temperature dependence of inert-gas chromatography on the HPX-87P column that is not, however, explained by the interactions described so far is the temperature dependence of the elutions of *n*-butane and *n*-propane, and to a lesser extent, that of ethane. As the column operating temperature is raised from 4°C, methane, ethane, and propane first show increasing retention times, but above 25°C, an opposing (retention-time shortening) tendency effectively halts the lengthening of retention time for methane, and actually causes the retention times for ethane and propane to shorten as column temperature is increased further. This latter temperature effect is even more pronounced in the case of butane, to the extent that even at 4–10°C, there is no interval over which retention time clearly increases with temperature. Instead, as temperature is increased, the retention time for butane decreases steadily from its maximum at 4–10°C to a retention time at 72°C that is only 72% as long as that at the lowest temperatures studied. This type of temperature dependence is not predicted on the basis of either of the two adsorptive mechanisms proposed so far; both ion-ion-induced dipole interactions and classical hydrophobic bonding would be expected to increase in strength with increasing temperature^{20,30,38}.

The temperature dependence of butane elution, and the similar, though less pronounced "anomalous" behavior of the other aliphatics can be explained on the basis of a second type of "hydrophobic bonding". Stillinger²¹ has proposed that at least part of "hydrophobic bonding", may be due to the tendency of clathrate "cages", whether occupied by a "guest" molecule or empty, to share edges or faces^{21,22,39}. Whereas the type of hydrophobic bonding discussed earlier involves direct solute-solute (Van der Waals) contact and interaction, this second type of bonding is indirect, involving water-water interactions between molecules in the cages around the two solute molecules. Solute molecules "bonded" in this fashion inhabit adjacent, face-sharing and mutually-stabilizing clathrate structures.

Clathrate cages are likely to be formed, not only around isolated non-polar molecules, but also around the hydrocarbon portions of the packing material. Face-sharing interactions between the clathrate sheath around the packing material and the clathrate cages of dissolved gas molecules should result in retention of the gas molecules on the column, with the extent of retention of a given gas depending both on the strength of interactions between clathrate cages and upon the stability of the solute cage itself³¹. It is possible that the longer retention times of the larger hydrocarbons are due to more extensive interaction between the packing-material hydrate

sheath and the larger and less convex⁴⁰ sides of the clathrate cages surrounding the larger hydrocarbons. The shortening of the retention times for hydrocarbons at higher temperatures may result from greater disruption of the more extended clathrate structures. The fact that butane retention is far more sensitive to temperature than is retention of the smaller hydrocarbons may simply indicate that the overall retention mechanism for butane has a much larger contribution from clathrate-clathrate interactions, and thus has more to lose when these interactions are disrupted. It may also be that the butane clathrate cage itself is less stable than the cages enclosing the smaller molecules. This last possibility is difficult to evaluate on the basis of available information, but the results of NMR and dielectric relaxation studies^{27,28} and phase diagram studies⁴¹⁻⁴³ of natural gas hydrates provide reason for believing that this may be the case.

The retention model proposed above could with some justification be considered a specific case of the more general liquid-liquid partition effect suggested by Samuelson⁴⁴ as the primary retention mechanism in cation-form ion exchange chromatography with aqueous-organic mobile phase. Although water is the only component of the mobile phase here, the formation of the clathrate sheath around hydrophobic portions of the packing results in two distinct water phases—bound, stationary (clathrate) water and mobile, bulk water.

Earlier in the discussion the statement was made that the separation of gases on the HPX-87P will have to be explained on the basis of principles other than those of size-exclusion. While generally true, this statement requires some qualification, particularly in the case of diatomic gases hydrogen, nitrogen and oxygen. In Fig. 10 it can be seen that nitrogen elutes earlier, and hydrogen later, than would be predicted for these two gases on the basis of their polarizabilities as compared with those of the other ten gases studied. One possible explanation for this observation is to be found in the partial molar volumes of the gases in water at 25°C. Oxygen has a partial molar volume in the same range as those of argon and krypton (32.6–33.2 cm³/mole)¹ with the partial molar volume for helium being slightly smaller (29.7 cm³/mole)⁴⁵. The partial molar volume of hydrogen (26.7 cm³/mole)¹ is significantly smaller than that for the oxygen, argon, krypton group, and that of nitrogen (35.7 cm³/mole) is larger. This ordering of the partial molar volumes is consistent with the supposition that oxygen, argon, and krypton fit comfortably into dodecahedral clathrate cages, while nitrogen may spend at least part of the time in a larger (tetradecahedral) cage. Hydrogen, appears to spend a significant portion of time in a more compact solvation structure which can be thought of as resulting from the collapse of the dodecahedral structure. Both the “late” elution of hydrogen (compared with that predicted by polarizability correlations) and the “early” elution of nitrogen can be rationalized on the basis of size-exclusion effects due to the different effective sizes of these gas molecules and their attendant solvent cages. While the overall chromatographic behavior of the twelve gases is best correlated with molecular polarizabilities or organic-water partition coefficients, these correlations probably are overlaid by some size-exclusion effects. For pairs of gases such as oxygen and nitrogen, in which the molecular polarizabilities are essentially the same (1.70 and 1.73 Å³, respectively), the size-exclusion effects may well dictate the order of elution.

The foregoing description of a possible mixed mechanism for the separation of dissolved gases by the HPX-87P is summarized in eqn. 2.

$$V_e = V_t - K_{EX}V_p + K_{PO}V_s + K_{HP}V_s + K_{CL}V_s \quad (2)$$

In eqn. 2 V_e , the measured elution volume for a given solute, is depicted as the sum of five terms that reflect the various retention/exclusion mechanisms discussed above. The first two terms represent size-exclusion phenomena; V_t is the total volume available to the solvent (measured by injection of $^2\text{H}_2\text{O}$ in this instance) and is equal to the geometric volume of the column, *minus* the volume actually occupied on a molecular level by the packing material itself (V_s). K_{EX} represents the proportion of the total pore volume (V_p) from which a given solute (gas molecule plus hydrate shell) is sterically excluded. Since for a mechanism involving adsorptive as well as size-exclusion effects, exclusion of a solute from a portion of the pore volume results in denial of access to some of the adsorptive interaction sites, this term also represents losses in adsorptive retention. For this reason, K_{EX} may have values greater than 1.

K_{PO} is proportional to the strength of ion-ion-induced dipole interactions between the solute and packing material Pb^{2+} ions. K_{HP} is proportional to the strength of classical hydrophobic (direct contact) interactions between the solute and the resin hydrocarbon backbone. K_{CL} is a measure of the strength of water-water interactions between the clathrate hydrate shells around the solute molecules and the hydrate sheath around the hydrocarbon portions of the packing material.

The mixed retention mechanism described above is of course rather speculative, and is presented not as a finished analysis but as a starting point for further discussion of the observed separations.

ACKNOWLEDGEMENTS

This work was supported by the Office of Alcohol Fuels of the Department of Energy under WPA No. 349. The authors also wish to thank Dr. P. G. Squire for valuable conversations during the development of the manuscript.

REFERENCES

- 1 J. C. Moore, R. Battino, T. R. Rettich, Y. P. Handa and E. Wilhelm, *J. Chem. Eng. Data*, 27 (1982) 22-24.
- 2 S. R. Bakalyar, M. P. T. Bradley and R. Hanganen, *J. Chromatogr.*, 158 (1978) 277-293.
- 3 M. E. Rollie, C.-N. Ho and I. M. Warner, *Anal. Chem.*, 55 (1983) 2445-2448.
- 4 R. E. Reim, *Anal. Chem.*, 55 (1983) 1188-1191.
- 5 W. A. MacCrehan and W. E. May, *Anal. Chem.*, 56 (1984) 625-628.
- 6 B. B. Benson and D. Krause, Jr., *J. Chem. Phys.*, 64 (1976) 689-709.
- 7 H. A. Stuart, *Die Struktur des Freien Molekuls*. Springer, Berlin, 1952.
- 8 G. A. Cook, in G. A. Cook (Editor), *Argon, Helium, and the Rare Gases*, Vol. 1, Interscience, New York, 1961, p. 13.
- 9 R. C. Weast (Editor), *Handbook of Chemistry and Physics*, 55th ed., Chemical Rubber Company, Cleveland, OH, 1974, p. D-157.
- 10 A. H. Cockett and K. C. Smith, in J. C. Bailar (Editor), *Comprehensive Inorganic Chemistry*, Vol. 1, Pergamon, Oxford, 1973, p. 179.
- 11 R. H. Boyd and L. Kesner, *J. Chem. Phys.*, 72 (1980) 2179-2190.
- 12 R. H. Cole and J. S. Coles, *Physical Principles of Chemistry*, W. H. Freeman, San Francisco, 1964.
- 13 J. Porath and P. Flodin, *Nature (London)*, 183 (1959) 1657.
- 14 P. G. Squire, *Arch. Biochem. Biophys.*, 107 (1964) 471.
- 15 A. Leo, C. Hansch and D. Elkins, *Chem. Rev.*, 71 (1971) 525-616.
- 16 R. J. Wilcock, R. Battino and E. Wilhelm, *J. Chem. Thermodyn.*, 9 (1977) 111-115.

- 17 E. Wilhelm and R. Battino, *Chem. Rev.*, 73 (1973) 1-9.
- 18 R. J. Wilcock, R. Battino, W. F. Danforth and E. Wilhelm, *J. Chem. Thermodyn.*, 10 (1978) 817-822.
- 19 C. McAuliffe, *J. Phys. Chem.*, 70 (1966) 1267-1275.
- 20 C. Tanford, *The Hydrophobic Effect*, Wiley-Interscience, New York, 1973, pp. 24-35.
- 21 F. H. Stillinger, *Science*, 209 (1980) 451-457.
- 22 F. H. Stillinger, *Phil. Trans. R. Soc. London Ser. B*, 278 (1977) 97-112.
- 23 D. W. Davidson, in F. Franks (Editor), *Water: A Comprehensive Treatise*, Vol. 2, Plenum, New York, 1973, pp. 115-234.
- 24 J. A. Ripmeester and D. W. Davidson, *Bull. Magn. Reson.*, 2 (1980) 139.
- 25 J. A. Ripmeester and D. W. Davidson, *J. Mol. Struct.*, 75 (1981) 67.
- 26 G. H. Cady, *J. Chem. Educ.*, 60 (1983) 915-918.
- 27 D. W. Davidson, S. K. Garg, S. R. Gough, R. E. Hawkins and J. A. Ripmeester, *Can. J. Chem.*, 55 (1977) 3641-3650.
- 28 D. W. Davidson and J. A. Ripmeester, *J. Glaciol.*, 21 (1978) 33-49.
- 29 J. E. Huheey, *Inorganic Chemistry: Principles of Structure and Reactivity*, Harper and Row, New York, 1972, p. 191.
- 30 W. J. Hamer (compiler), in R. C. Weast (Editor), *Handbook of Chemistry and Physics*, 55th Ed., Chemical Rubber Company, Cleveland, OH, 1974, p. E-61.
- 31 A. Hvidt, *Biochim. Biophys. Acta*, 537 (1978) 374-379.
- 32 L. Pauling, *Science*, 134 (1961) 15-21.
- 33 M. Verzele and C. Dewaele, *J. Chromatogr.*, 217 (1981) 399-404.
- 34 M. Verzele, *LC, Liq. Chromatogr. HPLC Mag.*, 1 (1984) 217-218.
- 35 T. Jupille, M. Gray, B. Black and M. Gould, *Am. Lab.*, 13, No. 8 (1981) 80-86.
- 36 A. Ben-Naim, *Hydrophobic Interactions*, Plenum Press, New York, 1980.
- 37 A. Ben-Naim, in R. A. Horne (Editor), *Water and Aqueous Solutions: Structure, Thermodynamics, and Transport Processes*, Wiley-Interscience, New York, 1972, pp. 425-464.
- 38 Cs. Horváth, W. Melander and I. Molnár, *J. Chromatogr.*, 125 (1976) 129-156.
- 39 R. J. Speedy and M. Mezei, *J. Phys. Chem.*, 89 (1985) 171-175.
- 40 W. F. Claussen and G. D. Polglase, *J. Am. Chem. Soc.*, 74 (1952) 4817-4819.
- 41 V. T. John and G. D. Holder, *J. Chem. Eng. Data*, 27 (1982) 18-21.
- 42 F. H. Dotterweich, *Petrol. Eng.*, 13 (1942) 83-84, 87.
- 43 O. L. Roberts, E. R. Brownscombe and L. S. Howe, *Oil Gas J.*, 39 (30) (1940) 37-40, 43.
- 44 O. Samuelson, *Adv. Chromatogr. (N.Y.)*, 16 (1978) 113-149.
- 45 T. Enns, P. F. Scholander and E. D. Bradstreet, *J. Phys. Chem.*, 69 (1965) 389.

CHROM. 17 960

PROTEIN PRECIPITATION INDUCED BY A TEXTILE DYE

PRECIPITATION OF HUMAN PLASMINOGEN IN THE PRESENCE OF PROCION RED HE3B

O. BERTRAND*, S. COCHET and Y. KROVIARSKI

INSERM U. 160, Hopital Beaujon, F-92118 Clichy Cedex (France)

A. TRUSKOLASKI

INSERM U. 24, Hopital Beaujon, F-92118 Clichy Cedex (France)

and

P. BOIVIN

INSERM U. 160, Hopital Beaujon, F-92118 Clichy Cedex (France)

(Received June 7th, 1985)

SUMMARY

It was demonstrated that human purified plasminogen was precipitated in the presence of the textile dye Procion Red HE3B. The amount of precipitated plasminogen was dependent upon the molar ratio between the dye and protein and seemed to be independent of the protein concentration. A certain amount of dye was coprecipitated with the protein; this was shown also to be related to the dye-to-protein molar ratio. The precipitation of plasminogen induced by the dye was shown to have a pH optimum and to involve ionic and hydrophobic interactions. Procedures were devised which enabled the recovery of precipitated plasminogen in a soluble and non-denatured form totally free from dye. However, the precipitation of plasminogen by Procion Red HE3B could not be used as a single-step purification procedure from a heterogeneous starting material like plasma because of coprecipitation of other proteins. Nevertheless it is suggested that frequently there is a chance that a given protein will be precipitated by a given dye and therefore that protein precipitation by dyes could be a useful complementary method for the purification of proteins.

INTRODUCTION

The interaction of plasminogen with the dye Procion Red HE3B was first demonstrated by Harris and Byfield¹ who discovered that a column of this dye immobilized on agarose gel could extract plasminogen from serum. We wanted to study in more detail the interaction between the dye and protein. We observed that Procion Red HE3B could induce plasminogen precipitation. The present paper deals with a thorough study of the phenomenon and of its potential for the purification of proteins.

Protein precipitation induced by dyes has already been described: for instance, fibrinogen can readily be precipitated with nitroblue tetrazolium^{2,3}. Polylysine can be precipitated with methyl orange⁴ or trypan blue⁵; this effect forms the basis of a sensitive assay of this homopolyamino acid. Precipitation by the acridine dye rivanol was described more than 30 years ago^{6,7} and has since become widely used for protein fractionation, even on an industrial scale⁸.

Other workers have induced protein precipitation by using chemically synthesized derivatives of dyes: for instance, Haeckel *et al.*⁹, in one of the earliest studies to recognize Cibacron Blue as a pseudo affinity ligand, noted that pyruvate kinase from yeast could be precipitated by Dextran Blue. More recently, dyes were applied to the elegant principle of affinity precipitation¹⁰: by grafting Cibacron F3G A at both ends of a spacer, Lowe and Pearson¹¹ obtained a bifunctional ligand which was shown to precipitate lactate dehydrogenase.

MATERIALS AND METHODS

Most chemicals used in this study were bought from Merck (Darmstadt, R.F.G.) or Carlo Erba (Milano, Italy). The ion exchangers were from IBF (Gennevilliers, France), DEAE-Trisacryl, or from Whatman (Maidstone, U.K.), DE 23; lysine agarose and Cibacron Blue agarose were prepared according to standard methods.

Procion Red HE3B was a gift from ICI France (Clamart). Its purity was tested by thin-layer chromatography on silica gel plates in the solvent system butanol-propanol-water (20:40:40, v/v/v) derived from Small *et al.*¹²; one major spot (R_F 0.55) was seen. The dye was also subjected to analytical high-performance liquid chromatography (HPLC) on a LiChrosorb RP-18 column (25 × 0.46 cm, Merck). The conditions for this separation were essentially those given in ref. 13. After injection the column was developed at 1 ml/min with a 60-min linear gradient between the initial buffer (10 ml of acetic acid and 5 ml of triethylamine made up to 1 l with water) and the final buffer (same composition as that of the initial one except that the adjustment of the volume was made with a mixture of equal parts of water and acetonitrile). The major peak represented more than 97% of the optical density, and was eluted at 85% of the gradient. These results prompted us to use the dye as supplied by the manufacturer for most of the described study. The concentrations of dye stock solutions were assayed by appropriate absorbance measurements. Spectra (recorded on a Beckman DU8 instrument against appropriate blanks) and extinction coefficient measurements were however obtained for a sample of lyophilized dye which had been filtered on a LH 20 column (Pharmacia, Uppsala, Sweden) equilibrated with water. It had been confirmed that this chromatography would ensure an efficient desalting of the dye, a precaution suggested in ref. 13.

Human plasminogen was purified from human fresh frozen plasma according to an automatic version¹⁴ of the standard affinity chromatography technique described by Deutsch and Mertz¹⁵. The purified protein comprised only the non-proteolyzed Glu form of plasminogen, as confirmed by polyacrylamide gel electrophoresis¹⁶. Plasminogen concentrations were determined by measuring the absorbance of solutions at 280 nm using $\epsilon_{1\text{cm}}^{1\%} = 17^{17}$, and occasionally by immunodiffusion using immunoplate (Behring, Marburg, F.R.G.).

Purified plasminogen was iodinated with 1,3,4,6-tetrachloro-3,6-diphenylglycoluril (Iodogen)¹⁸ as recommended by the manufacturer (Pierce, Rockford, IL, U.S.A.): 1.4 ml of Iodogen solution (1 mg/ml) in methylene chloride were placed in a screw-cap tube (100 × 18 mm); the solvent was evaporated in a gentle stream of nitrogen. The dry tube was then rinsed with buffer (50 mM Tris-chloride pH 7.00 containing 0.2 M sodium chloride) Plasminogen (1.4 mg in 1 ml of the same buffer) was added to the tube and thereafter 0.5 mCi of Na¹²⁵I (CEA, Orsay, France). The tube was then left standing in an ice-bath for 1 h; the protein solution was then removed by pipette and deposited onto a column of lysine agarose. The retained plasminogen was eluted with ϵ -aminocaproate and finally freed from the latter by gel filtration on Sephadex G-25. The recovered iodinated plasminogen (specific activity 0.12 mCi/mg) was pooled and stored frozen in aliquots.

Quantitative study of the precipitation of plasminogen induced by Procion Red HE3B

In order to study easily the precipitation reaction, it was conducted with plasminogen solutions that were appropriately spiked with iodinated plasminogen. The reactions were conducted in small polypropylene tubes by adding Procion Red HE3B (as a concentrated stock solution) to the plasminogen solution (usually 0.5 ml), mixing on a Vortex and letting the mixture stand at 4°C for 1 h. It was checked several times that this duration was sufficient; in any case, no more precipitate could be formed after this period had elapsed even when the precipitation conditions were not optimal, e.g., at alkaline pH. The whole tube was then counted in a gamma counter (Intertechnique GC 3000) and then centrifuged at 10 000 g for 5 min in an Eppendorf centrifuge. The supernatant was carefully withdrawn with a fine Pasteur pipette. Gamma counting of the supernatant and/or precipitate gave a precise quantitative evaluation of the precipitated protein: the amount of dye in the precipitate was usu-

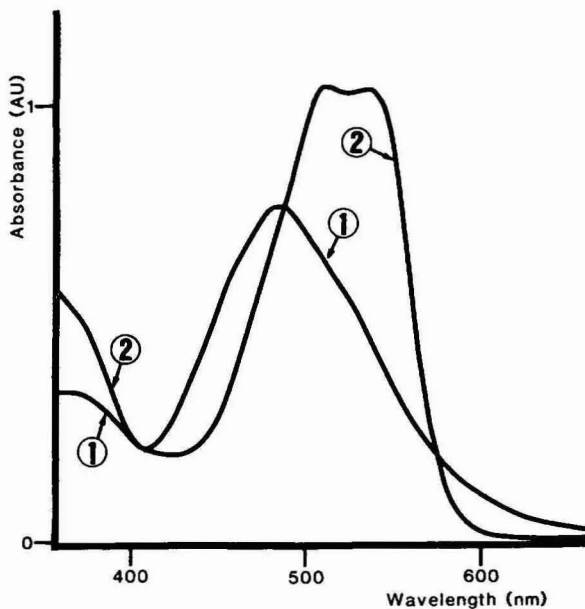


Fig. 1. Absorbance spectra of Procion Red HE3B dissolved in 50 mM sodium acetate pH 4.5 containing 0.2 M sodium chloride (curve 2) and dissolved in 1.25 M sodium hydroxide containing 8 M urea (curve 1).

ally determined by measuring the optical density of the precipitate redissolved in 1.25 *M* sodium hydroxide containing 8 *M* urea.

RESULTS AND DISCUSSION

Absorbance spectra of Procion Red HE3B

The absorbance spectrum of Procion Red HE3B dissolved in 50 mM sodium acetate buffer pH 4.5 containing 0.2 *M* sodium chloride is shown in Fig. 1 (curve 2). Extinction coefficient was measured at the wavelength of 530 nm. A value of 32 500 l mol⁻¹ cm⁻¹ was found which is in reasonable agreement with other published values¹³. The corresponding spectrum of Procion Red HE3B dissolved in 1.25 *M* sodium hydroxide containing 8 *M* urea is also shown in Fig. 1 (curve 1); the absorbance maximum is at 486 nm; the extinction coefficient at this wavelength was found to be 20 500 l mol⁻¹ cm⁻¹. We confirmed that the presence of plasminogen along with dye in 1.25 *M* sodium hydroxide containing 8 *M* urea had no significant effect either on the position of the absorbance maximum or on the extinction coefficient value; also that the absorbance of the dye dissolved in the different solvents and at the concentrations used followed the Beer Lambert law¹⁹.

Effect of pH

The effect of the pH on the reaction was studied with two different dye-to-protein molar ratios in a buffer containing 100 mmol/l of Tris base, glycine, disodium

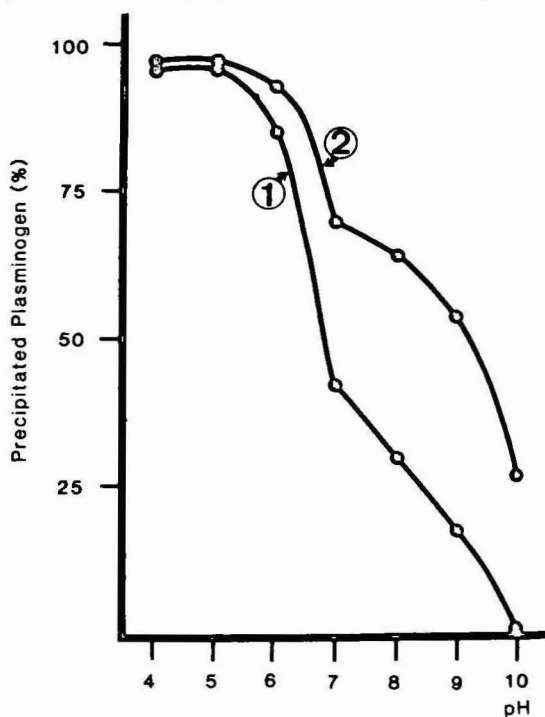


Fig. 2. Influence of pH on the precipitation of plasminogen induced by Procion Red HE3B. The buffer is given in the text. Two different dye-to-protein molar ratios were used: 13, curve 1; 33, curve 2.

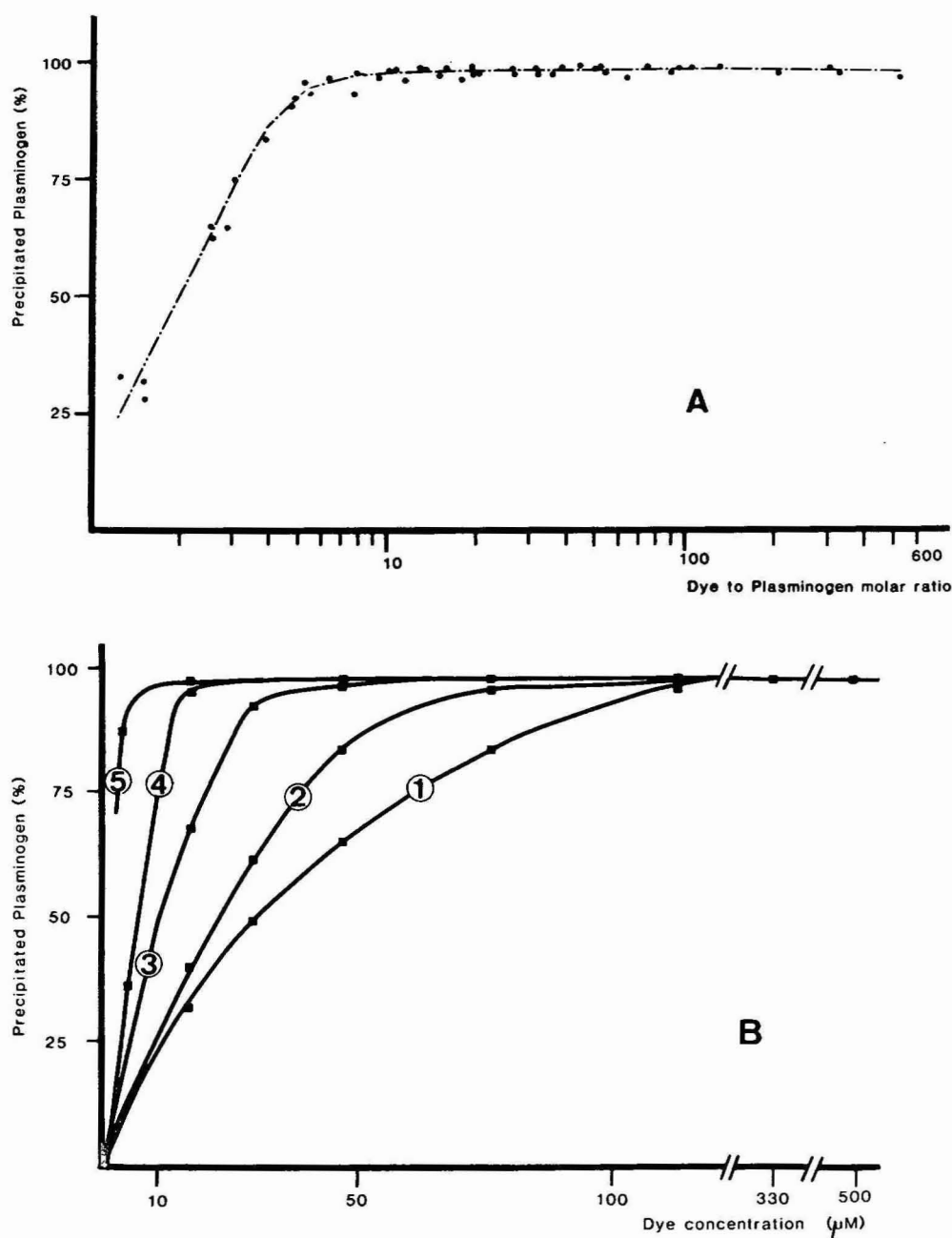


Fig. 3. A, Effect of the dye-to-plasminogen molar ratio on precipitation of the protein induced by the dye. Precipitation reactions were conducted in standard buffer as described in Materials and methods. B, variation of plasminogen precipitation with the concentration of the dye. Final concentrations of plasminogen in the precipitation medium were 45, 109, 218, 436 and 855 μ g/ml for curves 5-1, respectively. In A the same experimental data as in B, as well as data obtained at final plasminogen concentrations of 1.35 and 0.020 mg/ml, were used.

hydrogenphosphate and sodium chloride which had been adjusted to the desired pH by use of hydrochloric acid or sodium hydroxide. Fig. 2 shows that the optimum pH for precipitation is situated between 4 and 5. Hence most of the quantitative studies described later were done in 50 mM sodium acetate pH 4.5 buffer containing 0.2 M sodium chloride, which will be referred to hereafter as the standard buffer. The sulphate groups of Procion Red are likely to carry a negative charge at $\text{pH} \geq 4.00$; thus, because of a pH optimum, it seems tempting to think that the interaction of the dye with plasminogen which ends in precipitation is at least partly due to interactions between the negative charges of the dye and positive charges on the plasminogen molecule, positive charges which do progressively disappear when the pH is increased. It has to be pointed out that when the molar ratio of the dye to plasminogen is increased, a shoulder appears on the descending limb of the precipitation *versus* pH curve; such a shoulder could well be explained by the formation at high dye-to-protein molar ratios of new interacting positive charges of higher pK than the former ones.

Effect of the molar ratio of dye to plasminogen on precipitation

Fig. 3B shows a family of curves illustrating the variation of the amount of precipitated plasminogen with the dye concentration at several different plasminogen concentrations. The curve in Fig. 3A shows the corresponding variation with the molar ratio of dye to plasminogen. This curve demonstrates that when the molar

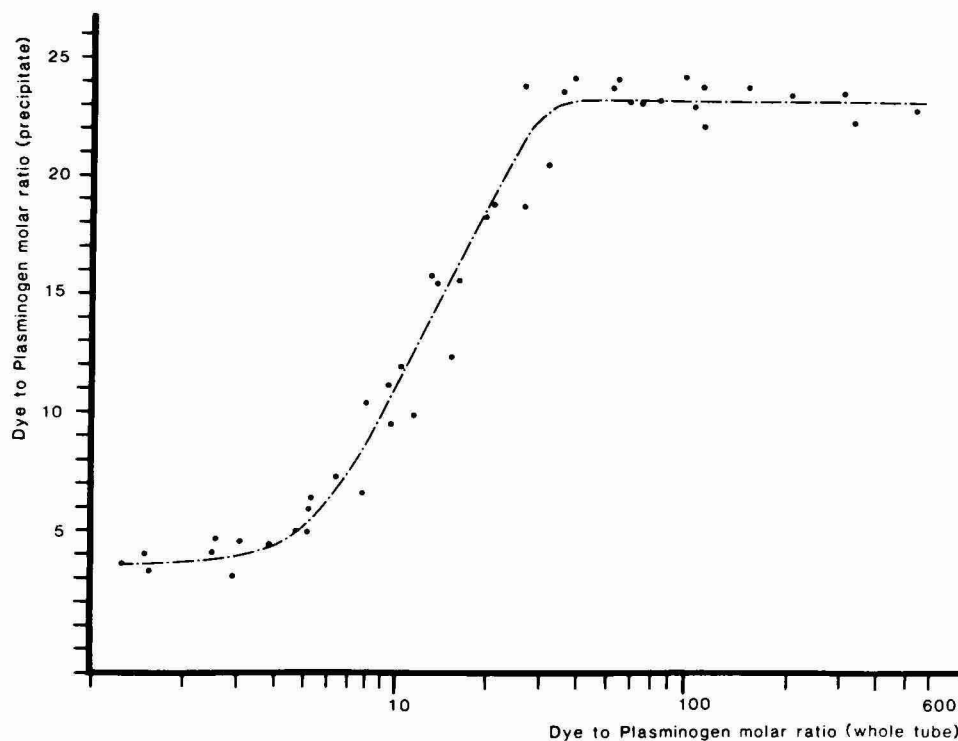


Fig. 4. Dye-to-protein molar ratio found in the precipitate as a function of the corresponding ratio used for the precipitation reaction. The experiments used were the same as those in Fig. 3.

ratio is equal or greater than 6 practically all the plasminogen is quantitatively precipitated.

Also, by mere visual inspection of the tubes in which the precipitations were conducted it was obvious that if plasminogen was indeed precipitated by the dye, the dye was also precipitated by the protein; the supernatants (at least for low molar ratios of dye to protein) were evidently much less coloured than the tube contents at the onset of the reaction. In order to be able to describe quantitatively the phenomenon, the amount of Procion Red HE3B present in the precipitate was evaluated as described in Materials and Methods.

Fig. 4 shows the variations of the molar ratio of dye to protein found in the precipitate with the dye/protein molar ratio used for the reaction. It is seen that at low molar ratios approximately four molecules of Procion Red are present in the precipitate, together with one molecule of plasminogen. When the molar ratio of Procion Red to plasminogen is increased, additional sites of the plasminogen molecule are involved up to an upper limit of 24 sites per molecule.

Influence of ionic strength on precipitation induced by the dye

The study of the optimum pH for precipitation of plasminogen by the dye had suggested that electrostatic interactions between charges of opposite signs played a rôle in the precipitation reaction. Hence an influence of the ionic strength was expected.

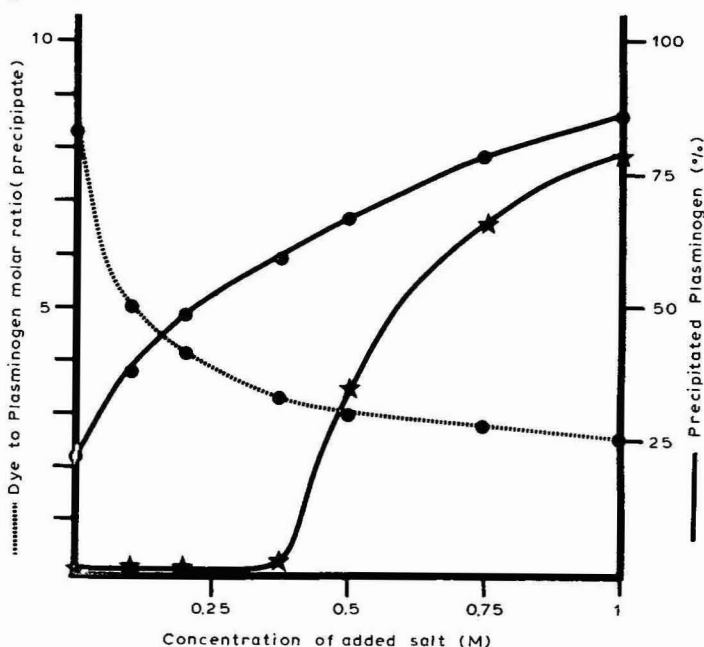


Fig. 5. Effect of sodium chloride molarity on the precipitation of plasminogen induced by the dye. The buffer was 50 mM sodium acetate pH 4.5. Filled circles correspond to experimental values which were obtained with a protein concentration of 0.9 mg/ml and a dye-to-protein molar ratio of 2.2. The dotted line shows the dye-to-plasminogen molar ratio found in the precipitate. Plasminogen was also partially precipitated in the absence of the dye (★) when the sodium chloride molarity was sufficiently high. Plasminogen concentration 0.9 mg/ml.

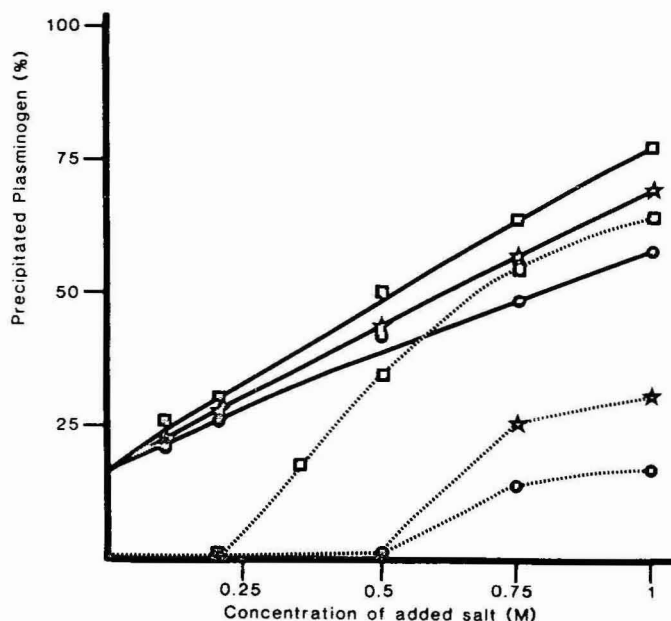


Fig. 6. Effect of different salts on the precipitation of plasminogen induced by Procion Red HE3B. The buffer was as in Fig. 5. The plasminogen concentration was 0.6 mg/ml and the dye-to-protein molar ratio was 1.4. Observed values in the presence of the dye are shown by the continuous lines and in the absence of the dye by the dotted lines. The experimental points are for potassium chloride (■), sodium chloride (★) and lithium chloride (●).

Fig. 5 shows the experimental variation of the amount of plasminogen precipitated when the molarity of sodium chloride in the precipitation medium was varied from 0 to 1 M. Clearly, precipitation of plasminogen by the dye increases with increasing molarity of sodium chloride. Noteworthy also is the fact that at higher than 0.3 M sodium chloride significant amounts of plasminogen are precipitated even in the absence of dye, due to the salting-out effect of sodium chloride. If one looks at the dye-to-protein molar ratio found in the precipitate, it is clear that this diminishes with increasing molarity of salt, this being more significant as long as no salting out of plasminogen (without dye) is likely to occur. Hence it could be tentatively concluded that an increasing concentration of sodium chloride, on the one hand, impairs fixation of the dye on the plasminogen molecule, in accord with a weakening of electrostatic bonds with increasing ionic strength, but on the other hand, a salting-out effect results in easier precipitation of plasminogen which has bound dye molecules.

The existence of a salting-out mechanism is substantiated by experiments with different salts, the results of which are shown in Fig. 6; clearly, the effect of a salt on plasminogen precipitation is correlated with its position in the lyotropic series²⁰.

Effect of ϵ -aminocaproate and related compounds on precipitation induced by dye

Plasminogen is known to bind ϵ -aminocaproate (EACA): both the number of binding sites and the dissociation constant have been established, as well as their location in the plasminogen molecule^{21,22}. This ligand is used to elute plasminogen

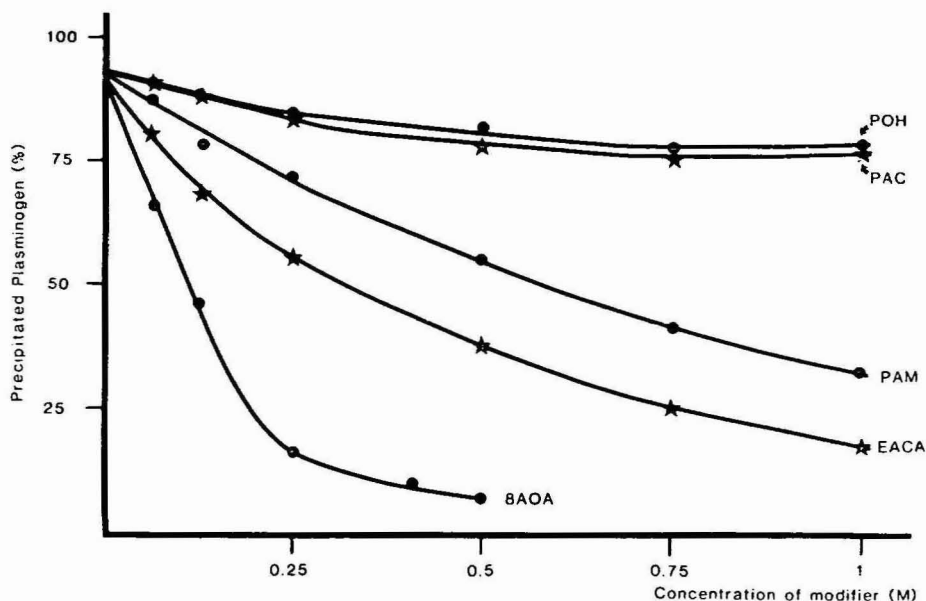


Fig. 7. Effect of varying the concentration of several organic components added to the precipitation mixture. Precipitation was conducted in the standard buffer with a dye-to-protein molar ratio of 14 (plasminogen concentration 0.44 mg/ml). Modifiers: EACA = ϵ -aminocaproate; POH = propanol; PAC = propionic acid; PAM = propylamine; 8AOA = 8-amino-1-octanoic acid.

from lysine agarose affinity chromatography columns¹⁵; it can be used also for desorption of plasminogen bound to fibrin²³. It was therefore interesting to determine whether there was an effect on precipitation induced by the dye. The results are shown in Fig. 7: obviously EACA interacts with and reduces plasminogen precipitation. This was somewhat unexpected because it had been noted by Harris and Byfield¹ that EACA could not be used for elution of bound plasminogen from columns of immobilized Procion Red HE3B. However, it has to be pointed out that the concentrations of EACA which had a definite effect on plasminogen precipitation by the dye were much higher than those used for desorption of plasminogen from lysine agarose columns¹⁵ or from fibrin²³. Hence it could be postulated that the effect of EACA on precipitation was not mediated by its specific interaction on the plasminogen surface at its dedicated place²² but was less specific: moreover it was found that 8-amino-1-octanoic acid, which is a very poor ligand for plasminogen²¹, is more effective than EACA for reducing the amount of precipitation induced by the dye. It could therefore be thought, for instance, that EACA or 8-amino-1-octanoic acid interferes with the precipitation reaction because their carboxylic group could compete with the dye for the postulated positive sites on the surface of the plasminogen molecule, or their positive amino groups could pair with sulphonate groups on the Procion Red molecule and so hinder interaction of the dye with plasminogen. In order to verify these hypotheses we have looked at the effects of propionic acid, propanol and propylamine on the precipitation. The experiments show definitely (see Fig. 7) that precipitation is more effectively prevented if the organic modifier bears an amine group. This suggests that at least part of the effect is mediated through the onset of ion-pair interactions with the sulphonate groups of the dye.

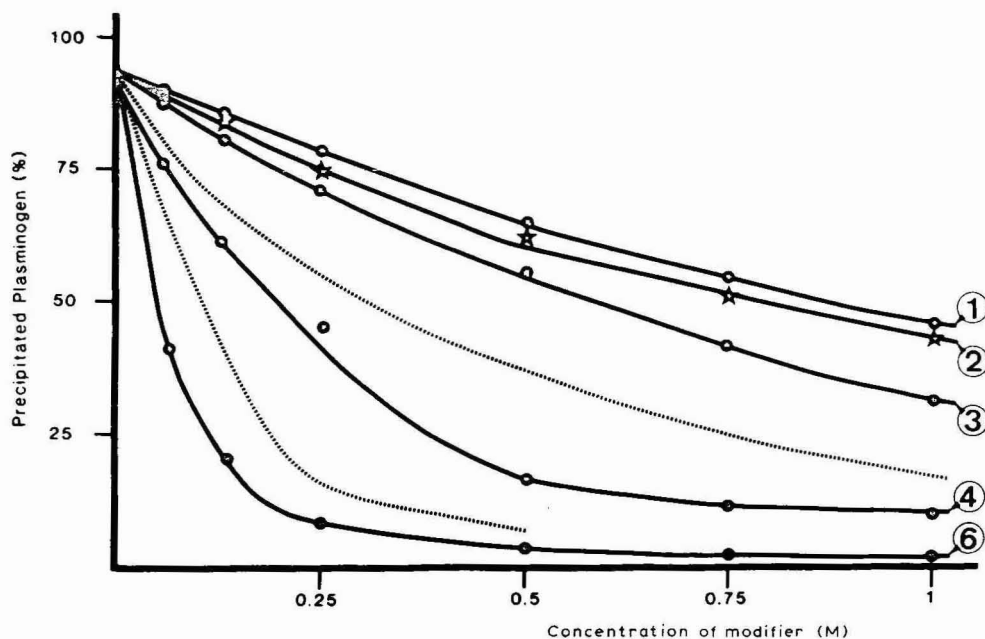


Fig. 8. Effect of several aliphatic amines on the precipitation of plasminogen induced by Procion Red HE3B. The precipitation conditions were as in Fig. 7. The number of carbon atoms in the amines are shown on the curves. Experimental curves (but not the experimental points) obtained with EACA and 8-amino-1-octanoic acid, already shown in Fig. 7, are also reported (dotted lines).

Noteworthy also is the fact that aliphatic amines are more effective in preventing precipitation the larger is the aliphatic chain (Fig. 8). In fact, if one uses the sets of hydrophobic fragmental constants defined by Rekker²⁴ to compute a hydrophobicity index for each of the amine-bearing organics, it is clear that the ability to prevent precipitation increases with increasing hydrophobicity of the modifier. This highlights the rôle played by hydrophobic interactions in the dye-induced precipitation of plasminogen.

Precipitation of plasminogen from plasma by dye

The mixing of dye and plasma at pH 4.5 resulted in easily visible precipitates even at a low dye-to-plasminogen molar ratio. However, the spiking of plasma with radioactive plasminogen showed that the formed precipitate did not contain plasminogen unless the dye-to-plasminogen molar ratio was ≥ 6000 (see Fig. 9). This was attributed above all to the large amounts of albumin present in the plasma: examination by sodium dodecyl sulphate (SDS) gel electrophoresis of the precipitates obtained when the dye-to-plasminogen molar ratio was lower than 3000 showed the presence of albumin as the major protein (albumin was the only visible band after Coomassie blue staining when 30 μ g of protein had been loaded onto the gel); also when human serum albumin was added to purified plasminogen at a final concentration similar to the one in the experiment with plasma, it was obvious that high dye-to-plasminogen molar ratios were also needed to precipitate plasminogen quan-

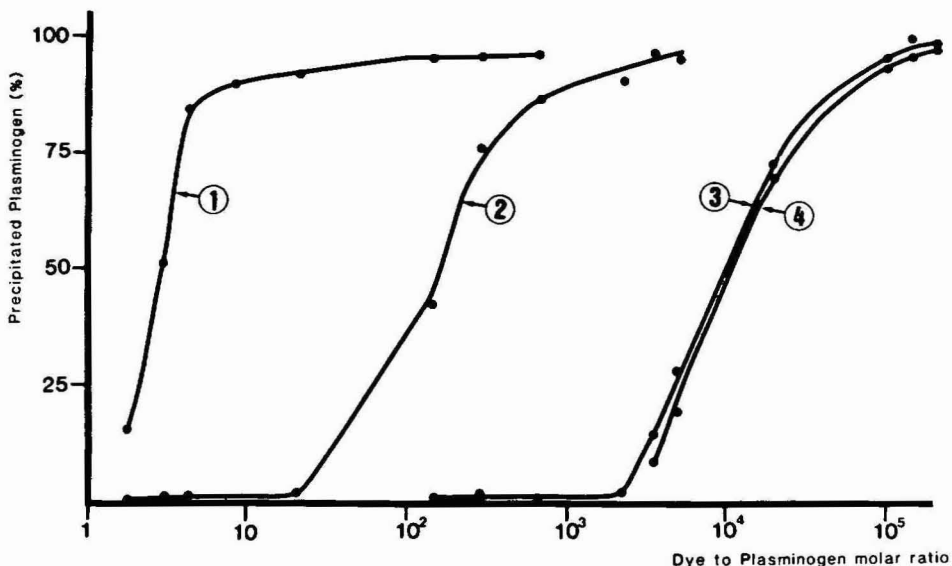


Fig. 9. Precipitation of plasminogen induced by Procion Red HE3B. Curves: 1, purified plasminogen dissolved in standard buffer; 2, albumin-depleted plasma (20 ml of plasma filtered through a column, 40×3.8 cm, filled with Cibacron Blue agarose equilibrated in 50 mM Tris-chloride buffer pH 8.5; breakthrough peak containing plasminogen adjusted to pH 4.5 after addition of sodium acetate); 3, plasma equilibrated in standard buffer by gel filtration on a Sephadex G-25 column of appropriate volume; 4, purified plasminogen mixed in standard buffer with human serum albumin (45 mg/ml). The plasminogen concentrations were adjusted by appropriate dilutions to the same value, 0.021 mg/ml.

titatively. On the other hand, by depleting the plasma of albumin using chromatography on Cibacron Blue agarose, it was possible to precipitate plasminogen quantitatively with lower dye-to-plasminogen molar ratios (see Fig. 9).

Here one can recall that the interference of albumin in the interaction between a dye and another protein has already been observed: for instance, it was noted that the presaturation of Cibacron Blue agarose columns with albumin increased the purification of nitrate reductase from *Chlorella*²⁵, and the presence of albumin weakened the interactions of interleukin 2 with Cibacron Blue agarose²⁶. The presence of albumin was shown to influence heavily the partitioning of prealbumin to an upper phase containing Remazol Yellow covalently linked to polyethylene glycol²⁷.

Obviously the fact that albumin is precipitated from the plasma by Procion Red HE3B sooner than plasminogen suggests that the latter protein could be substantially purified by fractional precipitation. Indeed preliminary experiments have shown that this is possible. Nevertheless, for reasons which will be discussed later, it doesn't appear that this could become a practical purification method for this protein.

Conditions for disruption of dye binding to plasminogen

The complete solubilization of the precipitated plasminogen was easily obtained as described in Materials and Methods by using 1.25 M sodium hydroxide containing 8 M urea. However this mixture is likely to denature protein and cannot

be used for preparative purposes. The complete and rapid dissolution of the precipitate was also obtained by using hexylamine titrated with hydrochloric acid to pH 8.3 at concentrations of 0.5 *M* or higher. It is noteworthy that when the tube containing the redissolved precipitate was left in the cold a new precipitate formed. This second precipitate was shown not to contain protein (provided that the final protein concentration was lower than 0.5 mg/ml), but only dye driven out of its interaction with plasminogen and finally out of the solution, presumably because of ion pairing with the organic base.

Gel filtration of the supernatant of this second precipitate (conducted on a Sephadex G-25 column of appropriate volume, equilibrated in 0.5 *M* hexylamine adjusted to pH 8.3 with hydrochloric acid) was ineffective in disrupting tight binding of the dye to plasminogen: dye and protein were eluted together at the void volume of the column. In contrast, by depositing the "second supernatant" on columns of DEAE-Trisacryl or DEAE-cellulose it was possible to obtain an effective separation of the dye and protein; plasminogen did not bind to the column but the dye was quantitatively retained. A 1-ml column of DEAE-Trisacryl or DE-23 equilibrated in the previously mentioned 0.5 *M* hexylamine buffer could bind more than 6 μmol of dye before the dye appeared in the eluate at a concentration of $0.6 \cdot 10^{-6}$ *M*. It is worth mentioning also that plasminogen could be freed from dye by chromatography on lysine agarose: when the second supernatant was deposited on a lysine agarose column both the dye and protein were retained; plasminogen was selectively eluted by EACA and recovered totally free from dye as shown by absorbance measurements at 530 nm. It has to be pointed out that when such chromatography was applied to a precipitate prepared from plasma, the plasminogen obtained at the end of the procedure was not only totally free from dye but was also purified from the other proteins which had been coprecipitated by the dye.

It is worth mentioning that plasminogen samples which had been precipitated and redissolved according to the previously described procedure were found to be fully activatable with urokinase or streptokinase in the same way as were samples of purified plasminogen which had not been submitted to the precipitation-redissolution procedure.

CONCLUSIONS

The experiments described demonstrate that plasminogen is precipitated by Procion Red HE3B. The precipitation is thought to involve ionic interactions between charges of opposite signs, and interactions of an hydrophobic character. The exact molecular mechanism of the precipitation is however obscure. It is worth noting that Procion Red HE3B is a relatively wide molecule bearing six sulphonate groups. One could postulate that precipitation of plasminogen is induced because several dye molecules bridge together a large number of plasminogen molecules. A similar explanation was presented for precipitation induced by charged polymers (for instance, precipitation of proteases by polyacrylic acid²⁸), but if this explanation were correct an influence of the plasminogen concentration would be observed: a decrease in the plasminogen concentration would probably induce a diminution of the precipitation induced by the dye; experimentally, at least in the range of plasminogen concentrations used (20 $\mu\text{g/ml}$ to 1.35 mg/ml), the plasminogen concentration had no effect on

the percentage of precipitation, the important parameter being the dye-to-plasminogen molar ratio. Moreover it was possible to precipitate plasminogen with Procion Red H3B²⁹, another dye which can be described as a half Procion Red HE3B (structures of the two dyes are described in ref. 30). The H3B Red bears only three sulfonate groups which are clustered together and therefore it does not seem capable of "bridging together" a large number of plasminogen molecules.

The most likely explanation of the ability of the dye to precipitate plasminogen seems to lie in the fact that once a sufficient number of dye molecules are linked to one plasminogen molecule the surface hydrophobicity of the latter is modified, aggregation with other molecules can occur and precipitation follows. The precipitation itself depends also on the salt composition of the surrounding medium and/or the presence of organic modifiers.

We have seen that the dye precipitates not only plasminogen but also albumin from plasma and that moreover because of a tight binding of the dye and plasminogen a subsequent chromatographic step is necessary to free the protein from the dye. Therefore we cannot confidently claim that precipitation by Procion Red HE3B will be of practical benefit for the large scale purification of plasminogen.

Nevertheless it is anticipated that more or less selective protein precipitation induced by dyes could be more than a biochemical curiosity and could be established as an authentic purification method. Indeed from the work of Lowe and Pearson¹¹ it can be anticipated that every protein which has at least two affinity sites for one dye can be precipitated by grafting this dye at both ends of a spacer; our results and other work²⁻⁸ have shown that precipitation can be induced in a simpler way by use of unmodified pure dyes.

Here it has to be emphasized that most dyes (and not only Procion Red HE3B and some other dyes²⁻⁸ can be seen to be endowed with a "precipitating" potential; recently, Scopes³¹ had written that a "wide variety of organic compounds possessing dual functions of hydrophobicity and polarity could cause precipitation". Indeed most textile dyes possess these "dual functions of hydrophobicity and polarity".

In the light of experience with pseudo affinity chromatography on immobilized dyes, one can infer that finding a useful dye for precipitating a given protein will be essentially a matter of trial and error¹³. Maybe it will be useful³² to find a pair of dyes, one of which precipitates most proteins of the crude extract but not the target protein and the other which precipitates some of them including the protein of interest.

It should be emphasized that the ease of disruption of the interaction between the precipitant and protein will have to be considered; the existence of too tight a binding between the precipitant and the target protein (as is the case between plasminogen and Procion Red HE3B) will probably be a disadvantage for preparative applications of the method.

ACKNOWLEDGEMENTS

Support from University Paris VII (UER Xavier Bichat) and from the Association pour la Recherche en Structure Protéique is gratefully acknowledged. Thanks are due also to ICI France for generous gifts of dyes.

REFERENCES

- 1 N. D. Harris and P. G. H. Byfield, *FEBS Lett.*, 103 (1979) 162–164.
- 2 A. W. Segal and A. J. Levi, *Clin. Sci. Mol. Med.*, 45 (1973) 817–826.
- 3 V. Vila, E. Raganon, F. Llopis and J. Aznar, *Clin. Chim. Acta*, 138 (1984) 215–219.
- 4 R. F. Itzhaki, *Anal. Biochem.*, 50 (1972) 569–574.
- 5 W. C. Shen, D. Yang and H. J. P. Ryser, *Anal. Biochem.*, 142 (1984) 521–524.
- 6 O. C. Gorodskaja, *Biokhimiya (Moscow)*, 15 (1950) 507–508.
- 7 J. Horejši and R. Smetana, *Acta Med. Scand.*, 155 (1956) 65–70.
- 8 M. Steinbuch, in J. M. Curling (Editor), *Methods of Plasma Protein Fractionation*, Academic Press, London, 1980.
- 9 R. Haeckel, B. Hess, W. Lauterborn and K. H. Wuster, *Hoppe-Seyler's Z. Physiol. Chem.*, 349 (1968) 699–714.
- 10 P. O. Larsson and K. Mosbach, *FEBS Lett.*, 98 (1978) 333–338.
- 11 C. R. Lowe and J. C. Pearson, in I. M. Chaiken, M. Wilchek and I. Parikh (Editors), *Affinity Chromatography and Biological Recognition*, Academic Press, London, 1983.
- 12 D. A. P. Small, C. R. Lowe, A. Atkinson and C. J. Bruton, *Eur. J. Biochem.*, 128 (1982) 119.
- 13 C. R. Lowe and J. C. Pearson, *Methods Enzymol.*, 104 (1984) 97–113.
- 14 O. Bertrand, S. Cochet, Y. Krowiarski and P. Boivin, *Haemostasis*, 14 (1984) 132 Abstract 243.
- 15 D. G. Deutsch and E. T. Mertz, *Science (Washington, D.C.)*, 170 (1970) 1095–1096.
- 16 U. K. Laemmli, *Nature (London)*, 227 (1970) 680–685.
- 17 K. C. Robbins and L. Summaria, *Methods Enzymol.*, 19 (1970) 184–199.
- 18 P. J. Fraker and J. C. Speck, *Biochem. Biophys. Res. Commun.*, 80 (1978) 849–857.
- 19 J. Frenzel, K. Nissler, W. Schellenberger, G. Koppenschlager and E. Hoffmann, *Biomed. Biochim. Acta*, 43 (1984) 413–418.
- 20 M. T. Record, Jr., C. F. Anderson and T. M. Lohman, *Q. Rev. Biophys.*, 11 (1978) 103–178.
- 21 F. J. Castellino and J. R. Powell, *Methods Enzymol.*, 80 (1981) 365–378.
- 22 Z. Vali and L. Patthy, *J. Biol. Chem.*, 257 (1982) 2104–2110.
- 23 J. C. Lormeau, J. Choay, J. Goulay, E. Sache and E. G. Vairel, *Ann. Pharm. Fr.*, 34 (1976) 287–296.
- 24 R. F. Rekker, *The Hydrophobic Fragmental Constant*, Elsevier, Amsterdam, 1977, p. 48.
- 25 G. Birkenmeier, B. Tschechonien and G. Koppenschlager, *FEBS Lett.*, 174 (1984) 162–166.
- 26 R. Fagnani, H. L. Cooper and J. Mendelsohn, *Anal. Biochem.*, 142 (1984) 487–496.
- 27 C. S. Ramadoss, J. Steczko, J. W. Uhlig and B. Axelrod, *Anal. Biochem.*, 130 (1983) 481–484.
- 28 J. C. Caygill, D. J. Moore and L. Kanagasabapathy, *Enzyme Microb. Technol.*, 5 (1983) 365–368.
- 29 O. Bertrand, S. Cochet and Y. Krowiarski, unpublished results.
- 30 G. Birkenmeier, E. Usbeck, L. Saro and G. Koppenschlager, *J. Chromatogr.*, 265 (1983) 27–35.
- 31 R. Scopes, *Protein Purification. Principles and Practice*, Springer, Berlin, 1982.
- 32 Y. Hey and P. D. G. Dean, *Biochem. J.*, 209 (1983) 363–371.

CHROM. 17 939

THE OCCURRENCE AND ORIGIN OF SYSTEM PEAKS IN NON-SUPPRESSED ION CHROMATOGRAPHY OF INORGANIC ANIONS WITH INDIRECT ULTRAVIOLET ABSORPTION DETECTION*

P. E. JACKSON and P. R. HADDAD*

Department of Analytical Chemistry, University of New South Wales, P.O. Box 1, Kensington, N.S.W. 2033 (Australia)

(Received June 5th, 1985)

SUMMARY

Chromatograms obtained for inorganic anions using non-suppressed ion chromatography with indirect UV absorption detection show two extraneous peaks; a non-retained peak (called the injection peak) and a late eluting peak (called the system peak). Experimental studies are reported which show that the system peak is governed by the sample concentration, the injected volume of sample, the nature of the sample ion, the sample pH and the eluent concentration and pH. A mechanism for the generation of injection and system peaks is presented which proposes that the injection peak is due to eluent dilution effects combined with the displacement of adsorbed eluent anions by the injected sample. The system peak is attributed to adsorption and desorption of neutral eluent molecules from the column surface which are retained by a reversed-phase mechanism on the unfunctionalised portions of the anion-exchange column. Evidence is presented to support this proposal. System peaks may be eliminated using an eluent pH such that no neutral eluent molecules are present.

INTRODUCTION

The determination of inorganic anions by non-suppressed ion chromatography generally involves the use of a low-capacity anion-exchange column combined with an eluent consisting of a dilute solution of an aromatic acid anion such as benzoate or phthalate^{1,2}. Detection methods include conductivity³ and indirect UV absorption^{4,5}. In the latter approach, the absorbance of the eluent is monitored and solute ions are detected by the decrease in absorbance resulting from displacement of eluent ions from the mobile phase by eluted ions. For convenience, the recorder polarity is usually arranged so that a positive peak corresponds to a decrease in absorbance. Indirect UV absorption detection has been shown to be a very sensitive detection

* Presented in part at the 8th Australian Symposium on Analytical Chemistry, Melbourne, Australia, April, 1985.

mode⁵ and has the advantage of being applicable to conventional high-performance liquid chromatographic (HPLC) instrumentation.

Chromatograms obtained with indirect UV absorption detection are characterised by the presence of two extraneous peaks. The first of these peaks elutes early in the chromatogram and is generally referred to as the "injection" or "solvent" peak⁶, whereas the second peak is later eluting and is often described as a "system" peak⁷. The system peak can cause several chromatographic problems including co-elution with solute peaks⁸, incorrect assignment of peak identities, unnecessarily lengthy run times or ghosting in subsequent chromatograms⁹ and erroneous quantitation of some solutes^{8,10}. The outcome of these effects is that the appearance of a system peak imposes a severe limitation on the utility of indirect UV absorption detection in ion chromatography.

In this paper, we report a study of the parameters which influence the retention time and magnitude of the system peak. A mechanism for the formation of the system peak in non-suppressed ion chromatography with indirect UV absorption detection is proposed. The results described were obtained using phthalate eluents in conjunction with several different low-capacity anion-exchange columns.

EXPERIMENTAL

Instrumentation and reagents

The liquid chromatograph used consisted of a Waters Assoc. (Milford, MA, U.S.A.) Model M6000 pump, Model U6K injector, Model M450 variable-wave-length UV detector and Model M730 data module. Three low-capacity anion-exchange columns were used: a Vydac 302 IC 4.6 anion chromatography column (Separations Group, Hesperia, CA, U.S.A.), 250 × 4.6 mm I.D.; a Bio-Gel TSK IC Anion PW column (Bio-Rad Labs., Richmond, CA, U.S.A.), 50 × 4.6 mm I.D.; and a PRP-X100 ion chromatography column (Hamilton, Reno, NV, U.S.A.), 150 × 4.1 mm I.D.

All reagents were of the highest available purity. Standard solutions (1000 ppm) of inorganic anions were prepared by dissolving weighed amounts of the sodium salts in water purified on a Millipore (Bedford, MA, U.S.A.) Milli-Q water purification system. The standard solution (1000 ppm) of nitric acid was prepared by dilution of the concentrated acid.

Chromatographic procedures

Mobile phases were prepared using analytical grade phthalic acid or potassium hydrogen phthalate, dissolved in water from the Milli-Q water purification system. The pH of each mobile phase was adjusted by dropwise addition of 1 M sodium hydroxide. All mobile phases were filtered through a 0.45- μ m filter and degassed in an ultrasonic bath prior to use. Further chromatographic conditions are given in the figure captions.

RESULTS AND DISCUSSION

Occurrence of system peaks

A typical chromatogram obtained for a mixture of inorganic anions separated

on a low-capacity anion-exchange column with phthalate as eluent and using indirect UV absorption detection is shown in Fig. 1. This chromatogram exhibits decreases in eluent absorbance (displayed as positive peaks) corresponding to elution of the solute ions and also contains two further peaks, namely the injection peak and the system peak. Both of these latter peaks may be positive or negative in direction, depending on the conditions used.

In the experimental work described in this paper, the characteristics of the late eluting system peak were studied and qualitative information on the characteristics of the injection peak was also obtained. A quantitative study of the injection peak observed with conductivity detection has previously been reported by Hershcovitz *et al.*⁶.

Effect of eluent parameters on the system peak

If the eluent concentration was maintained at a constant value, changes in the eluent pH produced marked changes in the system peak. The retention time of the system peak showed a general increase with increasing pH (Fig. 2) and the height of the system peak became progressively smaller. At pH 7 and higher pH values, no system peak was observed. With the phthalate eluents used, it is noteworthy that above pH 7, the eluent contained only doubly ionised phthalate ($pK_{a1} = 2.95$, $pK_{a2} = 5.41$). The above observations are in agreement with those reported by Okada and

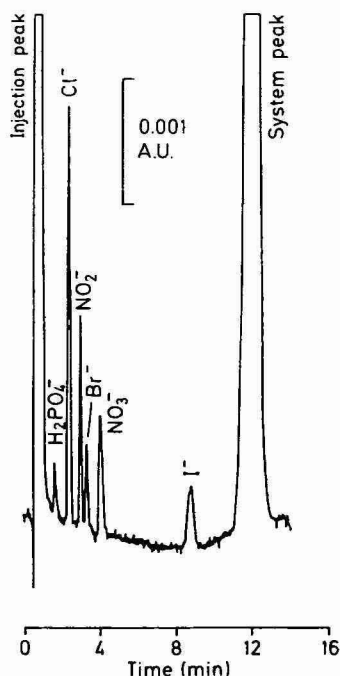


Fig. 1. Ion chromatogram showing injection and system peaks observed with indirect UV absorption detection. Conditions: Column, Vydac 302 IC 250 \times 4.6 mm I.D.; eluent, 2.5 mM potassium hydrogen phthalate at pH 4.0; flow-rate, 2.0 ml/min; injection volume, 250 μ l; detection by UV absorption at 285 nm; solute concentrations, 100–400 ppb. [The American billion (10^9) is meant.]

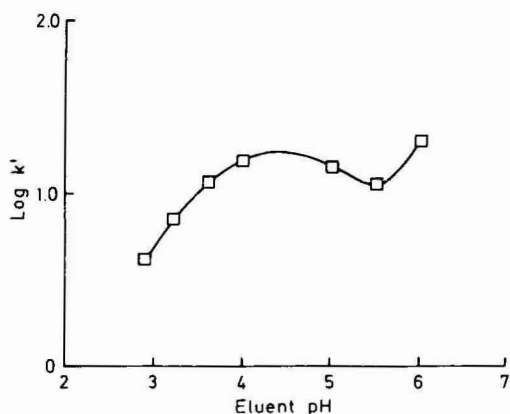


Fig. 2. Variation of the logarithm of capacity factor for the system peak with mobile phase pH. Conditions: column, Bio-Gel TSK Anion PW, 50×4.6 mm I.D.; eluent, 1.2 mM potassium hydrogen phthalate; flow-rate, 1.4 ml/min; detector sensitivity, 0.04 a.u.f.s.

Kuwamoto¹¹ for tartrate eluents ($pK_{a1} = 3.04$, $pK_{a2} = 4.37$), which showed no system peak at pH values of 5 or higher.

A plot of the logarithm of the capacity factor of the system peak *versus* the logarithm of eluent concentration was constructed at constant eluent pH. This plot is given in Fig. 3, from which it can be seen that a linear relationship existed between $\log k'$ and $\log [\text{eluent}]$. This result agrees with previous measurements made with a silica based anion-exchange column using phthalate eluents¹².

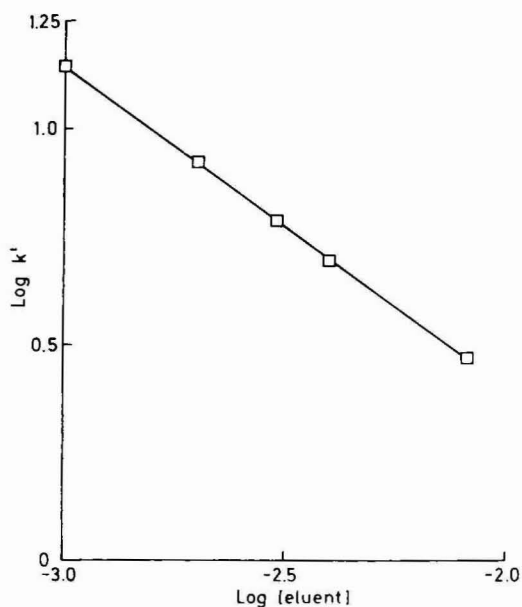


Fig. 3. Effect of eluent concentration on the capacity factor of the system peak. Conditions: as for Fig. 2 except that a mobile phase pH of 5.5 was used.

Effect of sample parameters on the system peak

When deionised water was injected, a positive system peak was observed, with the magnitude of this peak being proportional to the injected volume. The tendency for the system peak to increase with larger injection volumes was also observed when a solute was injected. Fig. 4 illustrates the effect of injecting water and also 1 μg of nitrite ion, using injection volumes of 10 μl or 100 μl . The height of the nitrite peak was the same for both injection volumes, but a larger system peak was observed for the 100- μl injection.

Fig. 5 shows the effect of increasing the sample concentration whilst maintaining a constant injection volume of 10 μl . As the concentration of nitrite ion was increased from 100 to 1000 ppm, the system peak changed from a slight positive peak to a small negative peak. These results indicate that increased sample concentrations tended to result in a more negative system peak.

The nature of the solute anion used was also found to have a significant effect on the system peak. For example, at identical concentrations of 1000 ppm, the height of the system peak for various univalent anions followed the order chloride > nitrite > nitrate > bromide > iodide. It is noteworthy that the heights of the analytical peaks for these solutes followed the same order, suggesting that this effect results chiefly from the differing molecular weights of the species involved. Indeed, the trend

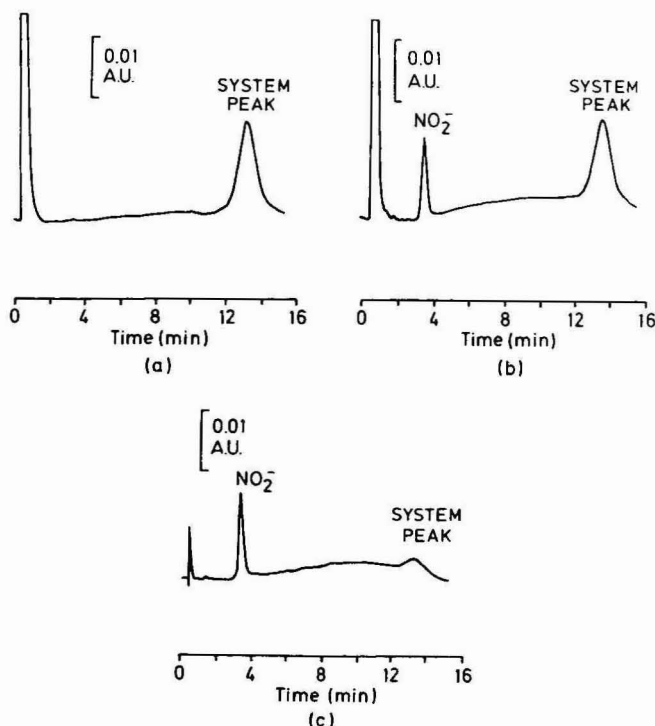


Fig. 4. Effect of sample injection volume on the system peak. (a) 100 μl deionised water, (b) 100 μl 10 ppm nitrite, (c) 10 μl 100 ppm nitrite. Conditions: column, Bio-Gel TSK Anion PW, 50 \times 4.6 mm I.D.; eluent, 3.2 mM potassium hydrogen phthalate at pH 4.2; flow-rate, 1.2 ml/min; detection, UV absorption at 295 nm, 0.1 a.u.f.s.

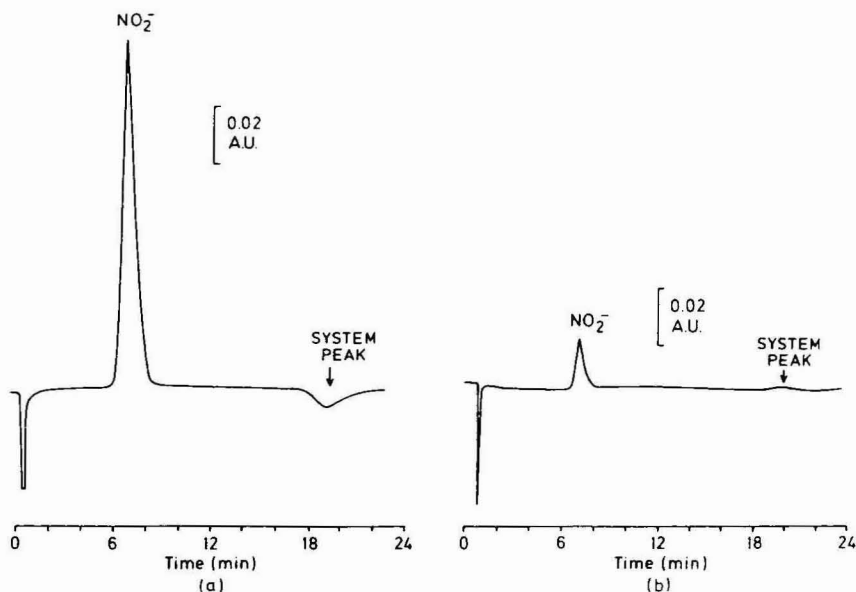


Fig. 5. Effect of sample concentration on the system peak. (a) 100 ppm nitrite, (b) 1000 ppm nitrite. Conditions: eluent, 1.2 mM potassium hydrogen phthalate at pH 4.2; flow-rate, 1.2 ml/min; detection, UV absorption at 265 nm, 0.2 a.u.f.s.; injection volume, 10 μl ; other conditions as for Fig. 2.

described above was not apparent when solutions of identical molar concentrations were used.

A further aspect pertaining to the nature of the solute ion was the tendency for some solutes to exhibit retention times close to that of the system peak. Sulphate ion was most troublesome in this regard and under a wide range of mobile phase conditions, sulphate partly co-eluted with the system peak (Fig. 6). Resolution of

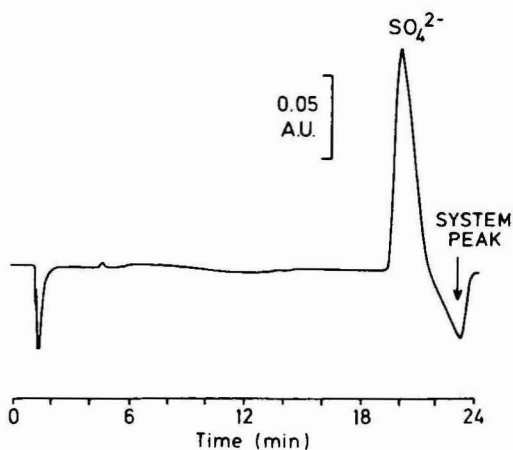


Fig. 6. Co-elution of the system peak with sulphate. Conditions: column, Vydac 302 IC 250 \times 4.6 mm I.D.; eluent, 4.0 mM potassium hydrogen phthalate at pH 4.2; flow-rate, 2.0 ml/min; detection, UV absorption at 295 nm, 0.4 a.u.f.s.; sample, 10 μl 1000 ppm sulphate.

sulphate and the system peak was possible only at relatively high values of eluent pH, under which conditions sulphate could be eluted before the system peak.

The pH of the injected sample was found to exert a large effect on the system peak. The factor of importance here was the disparity between the pH values of the eluent and sample. When the sample was more acidic than the eluent, the height of the system peak was decreased, whilst samples more alkaline than the eluent caused an increase in the system peak. The greater the disparity between the sample and eluent pH values, the greater was the observed effect.

This behaviour was illustrated by injection of carbonate, phosphate, nitrate and nitric acid into a phthalate eluent at pH 4.2. Both carbonate and phosphate gave large, positive system peaks (Fig. 7) since both samples (pH 11 and 12, respectively) were considerably more alkaline than the eluent. It is also noteworthy that no analytical peak was observed for carbonate and an early eluting peak was observed for phosphate. Consideration of the buffering capacity of the eluent and the acid dissociation constants for carbonic and phosphoric acids suggests that carbonate would be fully protonated and phosphate would be partly protonated to form dihydrogen phosphate. The protonated carbonic acid would be expected to elute with the injection peak and would not be detected using indirect UV absorption detection. Similarly, dihydrogen phosphate would be expected to elute early in the chromatogram, as shown in Fig. 7. This figure also highlights the possibility of incorrect assignment of peak identity resulting from the appearance of a system peak. Since divalent carbonate ion was injected in Fig. 7a, it would not be unreasonable for the late eluting system peak to be assigned to carbonate.

When nitrate ion and nitric acid were separately injected into a phthalate eluent

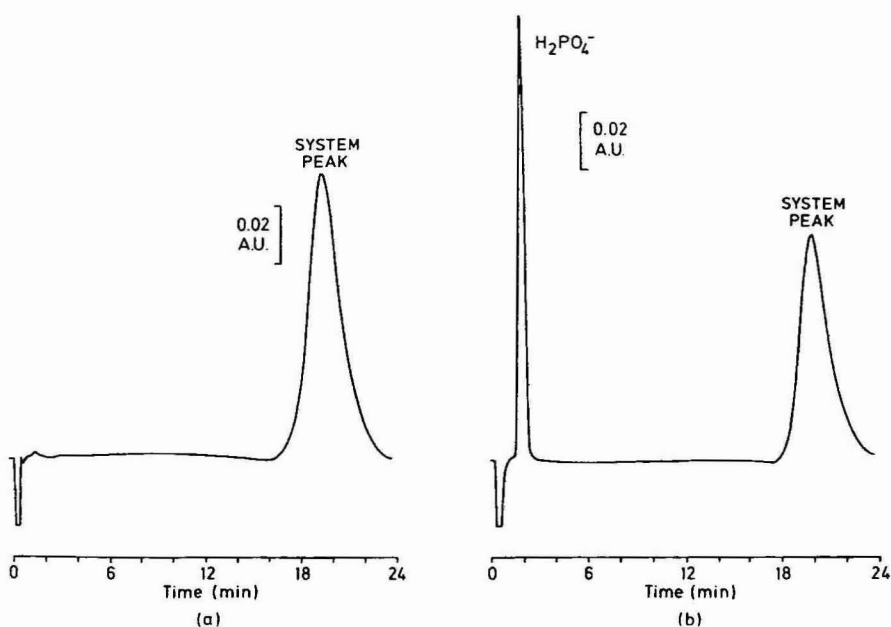


Fig. 7. System peaks resulting from injection of basic solutes. (a) 10 μl 1000 ppm carbonate (b) 10 μl 1000 ppm phosphate. Conditions: as for Fig. 5.

at pH 4.2, the system peak for the acidic sample was considerably more negative than that observed for nitrate ion (Fig. 8). The analytical peak for nitrate was independent of the sample pH.

The effect of sample pH on the system peak was also evident when solutions of phthalate were injected into the same phthalate eluent used in the above studies. If the pH of the phthalate sample was identical to that of the eluent, no system peak was observed. Alternatively, samples more acidic (e.g. phthalic acid at pH 3) or more alkaline (e.g. phthalate at pH 7.0) produced negative and positive system peaks, respectively, when injected into a phthalate eluent at pH 4.2.

Possible models for system peak formation

The preceding discussion has illustrated that the system peak was influenced by a considerable number of factors, and these effects may be summarised as follows: (1) The retention time of the system peak showed a general increase with eluent pH. (2) The height of the system peak reduced with increasing eluent pH. Eluents of pH greater than 6.5 gave no system peak. (3) The logarithm of the capacity factor for the system peak was linearly related to the logarithm of the eluent concentration, at constant pH. (4) For constant amounts of sample, an increase in the injected volume of sample produced a positive change in the system peak. (5) At constant injection volumes, an increase in sample concentration produced a negative change in the system peak. (6) Samples more alkaline than the eluent produced positive system peaks, whereas samples more acidic than the eluent gave negative system peaks. The magnitude of the system peak produced by this effect was dependent on the pH difference between the sample and eluent.

It is clear that these effects could combine to produce either positive or negative

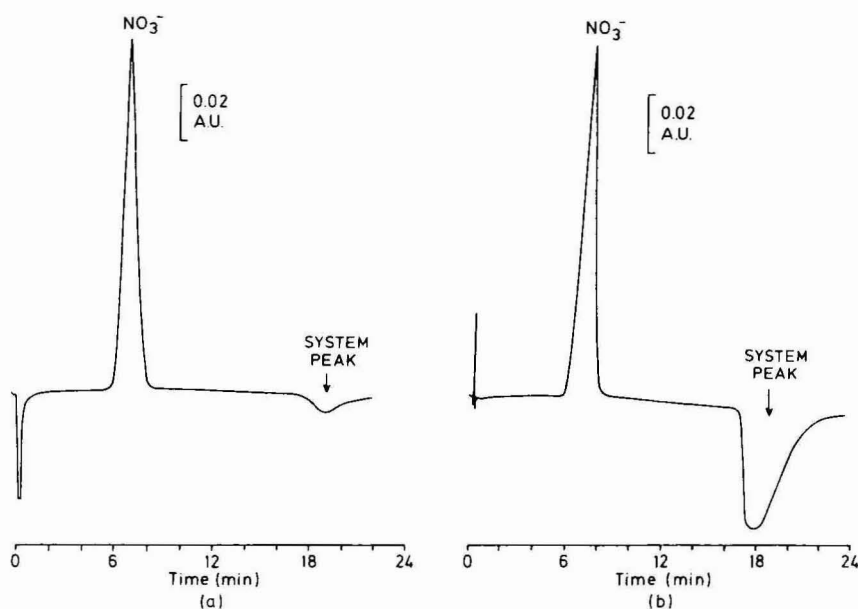


Fig. 8. System peak resulting from injection of an acidic sample. (a) 10 μ l 1000 ppm nitrate (b) 10 μ l 1000 ppm nitrate injected as nitric acid. Conditions: as for Fig. 5.

system peaks and under conditions where opposing effects were counterbalanced, the system peak could be absent.

General trends in the behaviour of the injection peak were also apparent from the studies conducted on the system peak. These trends are summarised below: (1) The retention time of the injection peak was independent of the sample pH and the eluent concentration. (2) For constant amounts of sample, the height of the injection peak increased with increasing injected volume of the sample. (3) At constant injection volumes, an increase in sample concentration produced a negative change in the injection peak.

As with the system peak, the injection peak resulting from these trends could be positive or negative in direction (see Figs. 4–8), or absent from the chromatogram.

Two somewhat opposing models have been advanced to explain the injection and system peaks. The first model proposes that the injection peak results from ion-exclusion of sample cations from the anion-exchange column and the system peak is due to an "anion absent effect" which compensates for disturbance of the eluent-column equilibrium caused by passage of the injection peak through the column¹¹. An essential feature of this model is that the eluent ions displaced from the column after injection of sample anions do not travel through the column with the injection peak. In contrast, the second model proposes that these displaced eluent anions are unretained on the column and elute with the injection peak⁶. The height of the injection peak is determined by a combination of the displaced eluent anion effect and the dilution factor resulting from the sample injection volume. The system peak may be considered to be due to elution of the neutral, protonated form of the eluent which traverses the column by a reversed-phase mechanism².

A detailed study of the "anion absent effect" has been reported for tartaric acid eluents used with conductivity or indirect UV absorption detection¹¹. On the other hand, the alternative mechanism proposed above has also been supported by a quantitative study of the injection peak⁶ in which the calculations made were based on the assumption that displaced eluent anions eluted with the injection peak.

The results of the present study are generally supportive of the proposal that both eluent anions and neutral eluent molecules are displaced from the column on injection of the sample. The eluent anions are unretained on the column and elute with the injection peak, whereas the neutral eluent molecules elute slowly under a reversed-phase mechanism and appear as a positive or negative system peak. The only evidence contrary to this proposal is Fig. 3, where the linear relationship observed between $\log [\text{eluent}]$ and $\log k'$ for the system peak is similar to that reported for anionic solutes retained via an ion-exchange mechanism¹². On the other hand, it is important to note that the system peak was found to disappear at eluent pH values of about 6.5; that is, under conditions where the eluent was completely ionised. At these pH values, the absence of any neutral eluent molecules would account for the lack of a system peak under the mechanism proposed above, whereas the presence of an abundance of eluent anions would suggest that if an "anion absent effect" model was in operation, a system peak should still occur. An additional factor was that only a single system peak was observed for eluents containing both divalent and monovalent eluent anions. Under these conditions, two system peaks might be expected with the "anion absent effect" model.

The eluent acid effect

In order to investigate further whether the system peak was the result of reversed-phase elution of the neutral (*i.e.* acidic) form of the eluent, additional experiments were undertaken. These experiments were based on the assumption that a system peak resulting from reversed-phase retention would exhibit strong dependence on the nature of the packing material and would show predictable retention behaviour when organic modifiers were added to the mobile phase.

The dependence of system peak retention on the nature of the packing material was evaluated using three different low-capacity anion-exchange columns. Each column contained quaternary ammonium ion-exchange functionalities bonded to different types of material: silica (Vydac 302 IC), polymethacrylate (Bio-Gel TSK Anion PW) or styrene-divinylbenzene copolymer (Hamilton PRP X100). Of these materials, the styrene-divinylbenzene copolymer ion-exchange resin was expected to show the greatest reversed-phase characteristics since the neutral polymer has frequently been used as a reversed-phase packing¹³. Using phthalate eluents of identical pH, the eluent concentration and flow-rate was adjusted so that chloride ion showed equal retention on each column. In this way, the balance between eluent strength and the ion-exchange capacity of the column was approximately equal for the three columns. Table I gives the chromatographic conditions used and also lists the retention time for the system peak observed with each column. The styrene-divinylbenzene copolymer column showed much greater retention of the system peak than the other two columns.

The effect of addition of organic modifiers to mobile phases used with the styrene-divinylbenzene copolymer column was studied in a similar manner to that described above. Here, a series of phthalate mobile phases at constant pH and containing increasing percentages of methanol were prepared, with the phthalate concentration for each eluent being adjusted so that chloride ion gave an identical retention time with each eluent. In this way, the ion-exchange elution strengths of all of these eluents were equivalent. A plot of the logarithm of the capacity factor for the system peak *versus* the percentage of methanol was prepared (Fig. 9), revealing that a linear relationship was followed. This behaviour was indicative that the retention of the system peak was subject to a reversed-phase mechanism¹⁴.

The effect of injection of organic modifiers onto a column equilibrated with an aqueous phthalate eluent was also studied. Fig. 10 shows the system peaks ob-

TABLE I

RETENTION TIMES FOR SYSTEM PEAKS ON VARIOUS LOW CAPACITY ANION-EXCHANGE COLUMNS

Phthalate eluents (pH 4.2) were used at the concentrations and flow-rates indicated.

Column	Eluent concentration (mM)	Flow-rate (ml/min)	Retention time (min)	
			Chloride	System peak
Vydac 302 IC	3.0	2.0	4.37	19.00
Bio-Gel TSK Anion PW	3.0	0.8	4.43	20.39
Hamilton PRP X100	1.5	1.9	4.34	47.67

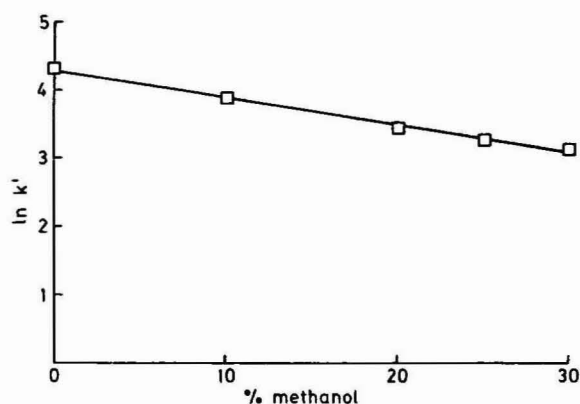


Fig. 9. Variation of the capacity factor for the system peak with the percentage of methanol in the mobile phase. Conditions: column, Hamilton PRP X100, 150 \times 4.1 mm I.D.; eluent, potassium hydrogen phthalate at pH 4.2 containing the indicated percentages of methanol. The eluent concentrations were adjusted so that chloride ion gave the same retention time for all eluents.

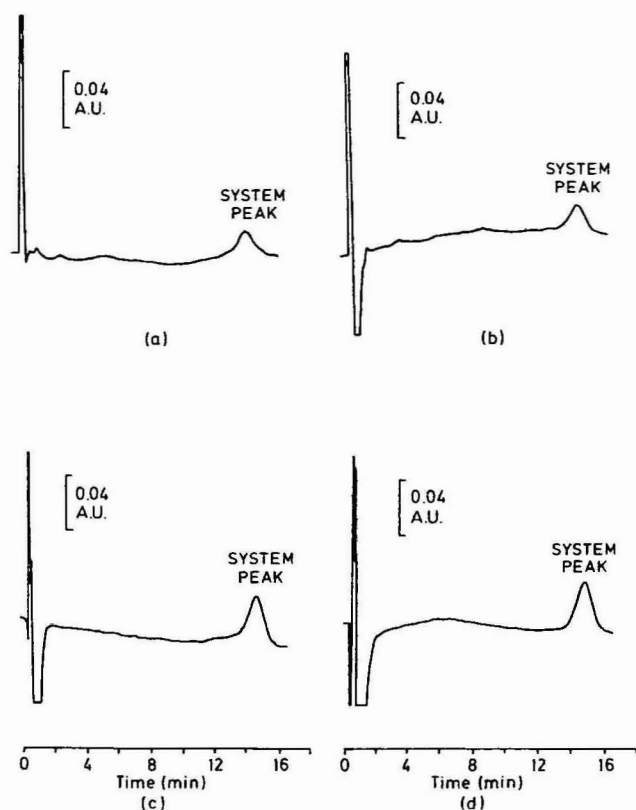


Fig. 10. System peaks induced by injection of organic modifiers. (a) 25 μ l deionised water. (b) 25 μ l methanol, (c) 25 μ l acetonitrile, (d) 25 μ l tetrahydrofuran. Conditions: column, Bio-Gel TSK Anion PW, 50 \times 4.6 mm I.D.; eluent, 2.0 mM potassium hydrogen phthalate at pH 4.2; flow-rate, 1.2 ml/min; detection, UV absorption at 265 nm, 0.4 a.u.f.s.

tained when 25- μ l volumes of water, methanol, acetonitrile and tetrahydrofuran were injected onto the polymethacrylate column. This figure illustrates that the size of the system peak increased when the organic modifiers were injected and this effect may be attributed to greater desorption of bound neutral eluent molecules from the column surface.

CONCLUSIONS

The injection peak in non-suppressed ion chromatography using indirect UV absorption detection is considered to arise from a combination of a decreased absorbance due to eluent dilution resulting from the injected sample solvent and an increased absorbance caused by eluent anions displaced by initial binding of the sample anions onto the column. This peak elutes at the unretained volume of the column and its height is dependent on sample concentration and the injected sample volume. The injection peak may be positive or negative.

The system peak is considered to arise from the elution of neutral, protonated eluent molecules desorbed from the column surface during sample injection. These eluent acid molecules traverse the column by a reversed-phase mechanism in which they are continually adsorbed onto and desorbed from the unfunctionalised regions of the packing material. With the low capacity columns used, as much as 85% of the surface area of the packing material is free of anion-exchange functionalities¹⁵. If the eluent pH is raised to a level where the eluent is completely ionised, then the system peak is eliminated.

Injection of water causes both dilution of the eluent and desorption of the eluent acid. The resultant system peak is therefore positive (*i.e.* decreased absorbance) since the eluent acid concentration resulting from this effect will never reach the equilibrium level found in the bulk eluent. When a solute ion is injected, both of the abovementioned effects occur, however the effect of the ionic strength of the sample on the initial desorption of eluent acid must also be considered. High ionic strength samples will tend to favour increased adsorption of eluent acid molecules on the column. The resulting system peak can therefore be positive or negative, depending on the injection volume, the sample concentration and the nature of the injected anion.

Sample pH effects result from changes in the mobile phase concentration of eluent acid arising from acid-base reactions. Samples more alkaline than the eluent will cause an initial rapid decrease of protonated eluent molecules in the mobile phase, leading to a positive system peak. The opposite effect occurs when an acidic sample is injected and a negative system peak results.

ACKNOWLEDGEMENTS

We thank Waters Associates (Sydney) for generous support and Mr. A. Heckenberg for helpful discussions.

REFERENCES

- 1 D. T. Gjerde, J. S. Fritz and G. Schmuckler, *J. Chromatogr.*, 186 (1979) 509.
- 2 J. S. Fritz, D. L. DuVal and R. E. Barron, *Anal. Chem.*, 56 (1984) 1177.
- 3 J. E. Girard and J. A. Glatz, *Am. Lab.*, 13 (1981) 26.
- 4 P. R. Haddad and A. L. Heckenberg, *J. Chromatogr.*, 252 (1982) 177.
- 5 H. Small and T. E. Miller, Jr., *Anal. Chem.*, 54 (1982) 462.
- 6 H. Hershcovitz, Ch. Yarnitzky and G. Schmuckler, *J. Chromatogr.*, 244 (1982) 217.
- 7 M. Denkert, L. Hackzell, G. Schill and E. Sjogren, *J. Chromatogr.*, 218 (1981) 31.
- 8 A. L. Heckenberg and P. R. Haddad, *J. Chromatogr.*, 299 (1984) 301.
- 9 C. A. Hordijk, C. P. C. M. Hagenaars and Th. E. Cappenberg, *J. Microbiol. Methods*, 2 (1984) 49.
- 10 T. Okada and T. Kuwamoto, *J. Chromatogr.*, 284 (1984) 149.
- 11 T. Okada and T. Kuwamoto, *Anal. Chem.*, 56 (1984) 2073.
- 12 P. R. Haddad and C. E. Cowie, *J. Chromatogr.*, 303 (1984) 321.
- 13 D. P. Lee, *J. Chromatogr. Sci.*, 20 (1982) 203.
- 14 C. Horvath and W. Melander, *J. Chromatogr. Sci.*, 15 (1977) 393.
- 15 D. P. Lee, *J. Chromatogr. Sci.*, 22 (1984) 327.

CHROM. 17 982

PERFORMANCE CHARACTERISTICS OF SOME COMMERCIALY AVAILABLE LOW-CAPACITY ANION-EXCHANGE COLUMNS SUITABLE FOR NON-SUPPRESSED ION CHROMATOGRAPHY

P. R. HADDAD*, P. E. JACKSON and A. L. HECKENBERG

Department of Analytical Chemistry, University of New South Wales, P.O. Box 1, Kensington, N.S.W. 2033 (Australia)

(Received June 25th, 1985)

SUMMARY

Five commercial low-capacity anion-exchange columns (Vydac 302 IC 4.6, Interaction ION-100, Hamilton PRP-X100, Bio-Gel TSK IC-Anion-PW and Waters IC Pak A) were compared in terms of their performance characteristics when used for non-suppressed ion chromatography with conductivity detection. Chromatograms were obtained with the manufacturer's recommended eluent and a phthalate eluent designed to give optimal chromatographic performance within the constraints of reasonable run times and acceptable peak shapes for later eluting peaks. These chromatograms were used to provide data on column efficiency, peak asymmetry and resolution of three critical solute pairs. With the exception of the Interaction column, all columns gave acceptable resolution of a standard mixture of seven anions. Choice between columns should be based on such factors as the types and relative concentrations of sample anions, the sample and eluent pH, the percentage of organic modifier to be used in the eluent and the cost of the columns.

INTRODUCTION

Early anion-exchange columns employed in high-performance liquid chromatographic (HPLC) applications were of relatively high ion-exchange capacity (*e.g.* 1 mequiv./g) and were generally used for the separation of organic ionic species¹. These columns have proved to be unsuitable for application to inorganic anions due to the fact that their high ion-exchange capacities necessitated use of eluents with ionic strengths sufficiently high to prohibit conductivity detection being employed. For this reason, a number of low-capacity anion-exchange materials were developed for ion chromatography of inorganic anions with conductivity detection.

The rationale used was that these columns could be employed with dilute eluents of low background conductivity, which in turn would permit the use of conductivity detection. Gjerde *et al.*^{2,3} synthesised a number of low-capacity anion exchangers which when used with eluents comprising a dilute solution of an aromatic acid such as benzoate, provided the first example of single-column anion chromato-

TABLE I
DESCRIPTION AND SPECIFICATIONS OF THE LOW-CAPACITY ANION-EXCHANGE COLUMNS USED IN THIS STUDY

Column	Dimensions (mm)	pH range	Upper pressure limit (p.s.i.)	Maximum flow- rate (ml/min)	Maximum organic modifier (%)	Ion-exchange capacity (μ equiv./g)	Particle size (μ m)	Type of packing material
Vydac 302 IC 4.6	250 \times 4.6	2-6	5000	—*	100	100	20	Spherical silica with bonded quaternary groups
Interaction ION-100	50 \times 3.2	0-14	1400	1.0	10	100	10	Neutral hydrophilic macro- porous resin with covalently bound quaternary ammonium groups.
Hamilton PRP-X100	150 \times 4.1	1-13	5000	8.0	100	200	10	Highly cross-linked poly- styrene-divinylbenzene coated with quaternary ammonium groups
Bio-Gel TSK Anion PW	50 \times 4.6	1-12	—*	2.0	20	30	10	Polymethacrylate gel coated with quaternary ammonium groups
Waters IC Pak A	50 \times 4.6	1-12	1000	1.2	20	30	10	Polymethacrylate gel coated with quaternary ammonium groups

* No data available.

graphy. These resins however exhibited poor chromatographic efficiencies, but nevertheless illustrated the potential of this approach.

Several alternative anion-exchange materials have since become commercially available and in this paper, the chromatographic performance of the most commonly used columns is assessed in terms of efficiency, resolution, susceptibility to overloading, selectivity and their ability to perform a separation of seven standard anions. A variety of eluents was used for this study, but in all cases, conductivity detection was employed.

EXPERIMENTAL

Instrumentation

The liquid chromatograph used consisted of a Waters Assoc. (Milford, MA, U.S.A.) Model M590 pump, Model U6K injector, Model M430 conductivity detector and Model M730 data module.

Columns

The columns used in this study were as follows: (1) Vydac 302 IC 4.6 anion chromatography column, 250 × 4.6 mm I.D. (Separations Group, Hesperia, CA, U.S.A.); serial number 831205.4. (2) Interaction ION-100 column, 50 × 3.2 mm I.D. (Interaction Chemicals, Mountain View, CA, U.S.A.); serial number 15-149-3. (3) Hamilton PRP-X100 ion chromatography column, 150 × 4.1 mm I.D. (Hamilton Company, Reno, NV, U.S.A.); serial number 79434. (4) Bio-Gel TSK IC-Anion-PW column, 50 × 4.6 mm I.D. (Bio-Rad labs., Richmond, CA, U.S.A.); serial number 10533. (5) Waters IC Pak-A anion column, 50 × 4.6 mm I.D. (Waters Assoc.); Serial number T42431 21.

Reagents and procedures

All reagents were of the highest available purity and standard solutions of the inorganic anions were prepared by dissolving weighed amounts of the sodium salts in water purified with a Millipore (Bedford, MA, U.S.A.) Milli Q water purification system.

The mobile phases were prepared using analytical grade reagents, chromatographic grade organic solvents and pure water. Mobile phases were filtered through a 0.45- μ m filter and degassed in an ultrasonic bath before use.

RESULTS

Column description

The physical dimensions, operating pH range, flow or pressure limitations, permissible percentage of organic modifier, ion-exchange capacity, particle size and a description of the packing material for each column are listed in Table I. One of the columns (Vydac) was packed with a silica-based material, whereas the remainder were resin-based ion exchangers. Stainless steel was used as the column construction material in all cases except the Bio-Gel TSK column which was constructed of PTFE.

The columns used for this study were all newly purchased and each was supplied with a test chromatogram, with the exception of the Waters column which was

TABLE II
DATA FOR TEST CHROMATOGRAMS SUPPLIED BY COLUMN MANUFACTURERS

Column	Anions used in test mixture	Eluent	Flow-rate (ml/min)	Efficiency* (theoretical plates)
Vydac	Cl^- , NO_2^- , Br^- , NO_3^- , SO_4^{2-}	2 mM Phthalate, pH 5.0	2.0	4934 (NO_3^-)
Interaction	F^- , Cl^- , NO_2^- , Br^- , NO_3^- , SO_4^{2-}	1.2 mM Phthalate, pH 5.0	1.0	No value given
Hamilton	F^- , Cl^- , NO_2^- , Br^- , NO_3^-	2.0 mM Benzoate	2.0	3450 (NO_3^-)
Bio-Gel TSK	F^- , Cl^- , NO_2^- , Br^- , NO_3^- , PO_4^{3-} , SO_4^{2-}	1.3 mM Tetraborate, 5.8 mM boric acid, 1.3 mM gluconate, 5 g/l glycerin, 120 ml/l acetonitrile, 30 ml/l <i>n</i> -butanol, pH 8.5	1.2	944 (SO_4^{2-})

* The half-height method was used to calculate efficiency and the solute used for this calculation is shown in brackets.

provided with a guaranteed minimum value of efficiency (900 theoretical plates). Data from the test chromatograms are summarised in Table II and the actual chromatograms are shown in Fig. 1. These test chromatograms were repeated using the manufacturer's recommended eluents and the instrumentation described in the experimental section. In all cases, measured efficiencies were in close agreement with the supplied values listed in Table II.

Performance characteristics

A standard mixture containing 100 ppm each of fluoride, chloride, nitrite, bromide, nitrate, sulphate and iodide was selected for the evaluation of column performance. Two sample injection volumes were used; 10 μl and 100 μl . The first of these injection volumes corresponded to 7 μg of sample and represented a typical working range for the columns, whereas the larger injection volume corresponded to 70 μg of sample, which was expected to cause overloading of some of the columns. The onset of column overloading is an important factor in the analysis of samples which contain ions at widely varying concentrations. The chromatograms obtained with the above standard mixture using the manufacturer's recommended eluent (see Table II) were used to calculate the column efficiency (at capacity factors of 5 and 10), the resolution of three critical peak pairs and the peak asymmetry at two levels of sample loading for each column. The results are given in Table III.

Experience in this laboratory has indicated that phthalate eluents gave optimal separations with most low-capacity anion-exchange columns. Furthermore, use of a common eluent would facilitate comparison of the columns. The eluent concentration and pH was adjusted for each column so that the total time taken for elution of the mixture was approximately equal. In addition, every attempt was made to maximise the resolution of earlier eluting peaks, whilst at the same time ensuring that adequate peak shape was obtained for late eluting species. The chromatograms obtained are

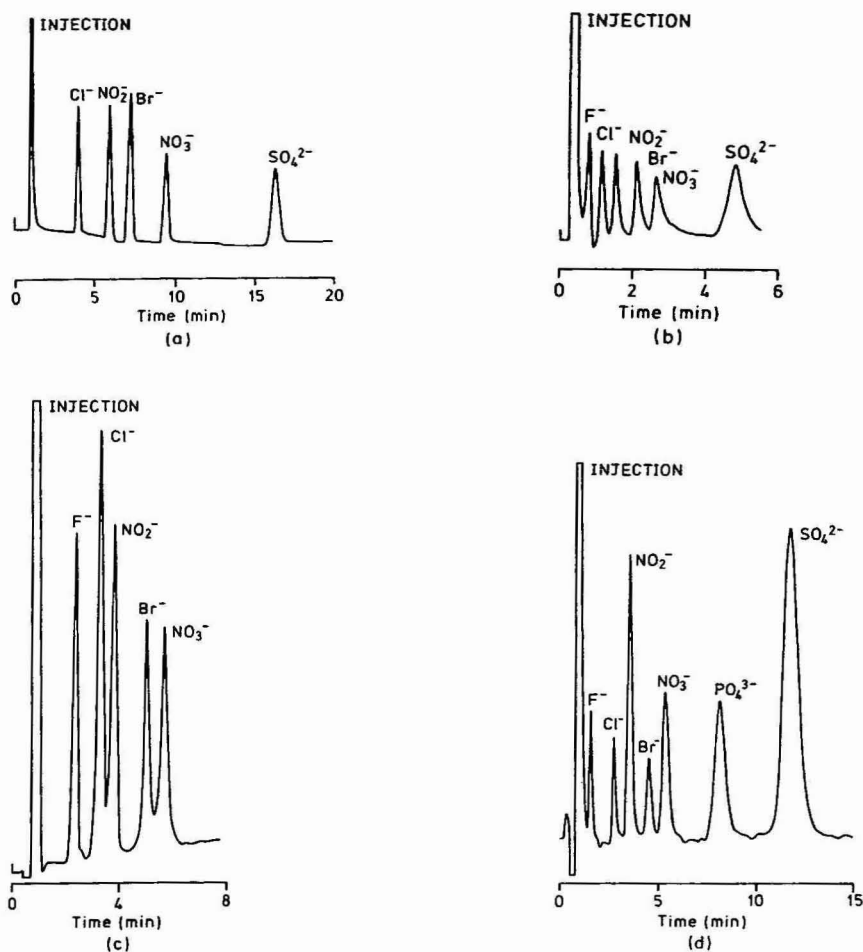


Fig. 1. Manufacturer's test chromatograms. (a) Vydac 302 IC 4.6, (b) Interaction ION-100, (c) Hamilton PRP-X100, (d) Bio-Gel TSK-IC-Anion PW. Conditions: Eluents and flow-rates are given in Table II. Conductivity detection was used in all cases.

given in Fig. 2 and efficiency and resolution data calculated from these chromatograms are listed in Table IV.

DISCUSSION

Type of packing material

The column packing materials may be broadly divided into silica-based and resin-based types, with the majority of columns tested falling into the latter category. Use of a silica material provides excellent rigidity of the packing and hence tolerance of high back-pressures and flow-rates, but creates problems with eluent pH limitations and a tendency to adsorb strongly fluoride ion, making it difficult to determine this ion.

TABLE III
PERFORMANCE CHARACTERISTICS FOR SEPARATION OF A STANDARD ANION MIXTURE USING TEST CONDITIONS RECOMMENDED BY COLUMN MANUFACTURERS

Chromatographic conditions are listed in Table II, except for the Waters column for which an eluent containing 1.5 mM tetraborate, 5.8 mM boric acid, 1.3 mM gluconate, 5 g/l glycerin and 120 ml/l acetonitrile was used.

Column	Retention times (min)							Efficiency* (theoretical plates per column)	Theoretical plates per meter ($k' = 5$)	Peak asymmetry** for nitrate		Resolution (R_s)			
	F ⁻	Cl ⁻	NO ₂ ⁻	Br ⁻	NO ₃ ⁻	SO ₄ ²⁻	I ⁻			7- μ g loading	70- μ g loading	Cl ⁻ /NO ₂ ⁻	NO ₂ ⁻ /Br ⁻	Br ⁻ /NO ₃ ⁻	
	$k' = 5 \quad k' = 10$														
Vydac	—***	4.33	6.17	6.65	8.55	12.84	20.34	3609	1554	13 084	1.07	0.41	2.24	0.80	2.44
Interaction	0.97	1.30	1.54	2.12	2.55	5.97	10.41	618	373	12 360	1.33	0.42	0.58	0.85	0.96
Hamilton	2.90	4.10	4.68	5.92	6.70	16.51	20.18	3450	3217	22 999	1.68	1.10	0.92	2.13	0.94
Bio-Gel TSK	1.46	2.49	3.12	3.95	4.59	10.18	11.40	934	898	18 680	1.17	0.72	0.90	1.10	0.89
Waters	1.57	2.73	3.39	4.17	4.83	14.20	10.46	1276	1220	25 520	1.02	0.57	1.69	1.89	1.39

* Efficiency was calculated using the 5σ method.

** Calculated according to Saunders⁷.

*** No peak observed.

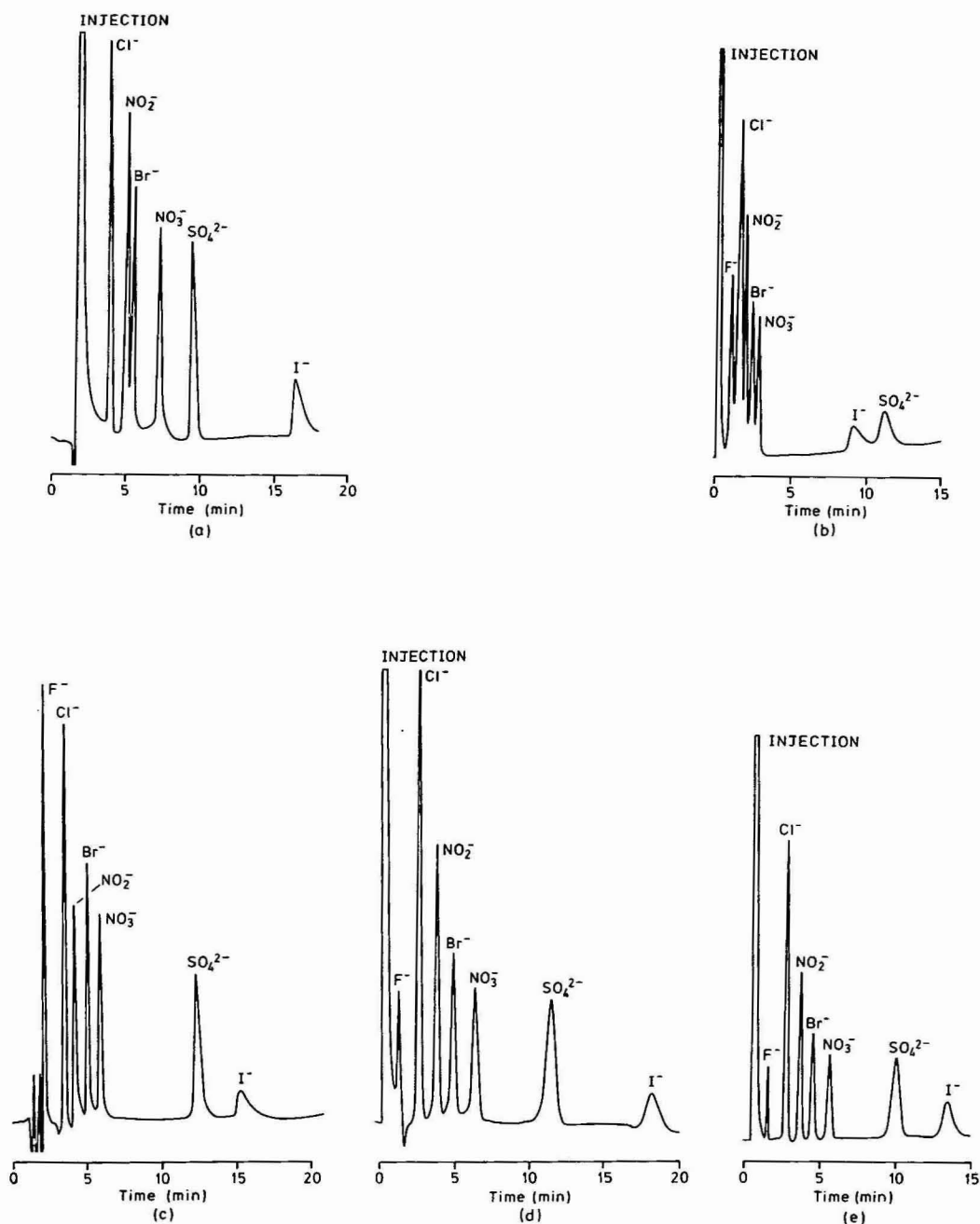


Fig. 2. Chromatograms obtained with optimised phthalate eluents. (a) Vydac 302 IC 4.6, (b) Interaction ION-100, (c) Hamilton PRP-X100, (d) Bio-Gel TSK IC-Anion-PW, (e) Waters IC Pak A. Conditions: Eluents, potassium hydrogen phthalate solutions at the following concentrations and pH values: (a) 3 mM, pH 5.3, (b) 1 mM, pH 4.1, (c) 1 mM, pH 5.5, (d) 1 mM, pH 5.3, (e) 1 mM, pH 7.0. Flow-rates (ml/min): (a) 2.0, (b) 1.0, (c) 2.0, (d) 1.2, (e) 1.2. Sample: 10 μ l of a mixture containing 100 ppm each of the indicated anions.

TABLE IV

EFFICIENCY AND RESOLUTION DATA FOR OPTIMISED PHTHALATE ELUENTS

Chromatographic conditions and actual chromatograms used for data calculations are given in Fig. 2.

Column	Efficiency*		Resolution (R_s)		
	Theoretical plates per column	Theoretical plates per meter	Cl^-/NO_2^-	NO_2^-/Br^-	Br^-/NO_3^-
Vydac	4163	16 652	1.97	0.73	2.09
Interaction	605	12 100	0.75	0.91	0.87
Hamilton	2356	15 706	1.28	1.76	1.62
Bio-Gel TSK	959	19 180	1.92	1.62	2.03
Waters	1306	26 120	2.37	2.05	2.64

* Calculated for nitrate ion using the 5σ method.

The pH limitation towards alkaline eluents is imposed by the solubility of the silica material and represents a serious drawback to the use of silica-based columns in anion chromatography. In the first place, the use of eluents with pH values greater than 6 is often necessary for the elimination of interfering "system" peaks⁴. Such system peaks are especially prevalent when phthalate eluents are employed with indirect UV absorption detection. In addition, some of the eluents known to be useful for anion chromatography are quite strongly alkaline, for example, 0.5 mM potassium hydroxide⁵ and the gluconate-borate eluent described in Table II. Secondly, it is often advantageous, and in some cases essential, to operate at high eluent pH in order to obtain satisfactory peaks for species which are subject to protolytic equilibria. For example, bicarbonate ion can be determined only with eluents of pH greater than approximately 6.5 and useful selectivity effects can be achieved for phosphate, oxalate etc. using eluent pH changes. Any restriction on the range of eluent pH values must necessarily inhibit exploitation of these effects. Resin-based columns therefore offer considerable advantages in this respect. It should be stressed here that the wide pH limits for resin-based columns shown in Table I may be quite temperature sensitive. For example, experience in our laboratory with the Hamilton column has shown that when eluents were used at temperatures exceeding 30°C, column lifetime was dramatically reduced if eluent pH values above 8 were employed.

Whilst resin-based columns offer advantages in terms of eluent pH, they lack the packing rigidity of silica-based materials. Examination of Table I indicates that with the exception of the Hamilton column, severe restrictions exist regarding the maximum pressures and flow-rates which can be used with the resin-based columns. These restrictions in turn lead to the necessity for short columns to be used. The polystyrene-divinylbenzene resin employed in the Hamilton column appears to have good pressure stability and may be used at relatively high flow-rates.

The addition of organic modifiers to the aqueous mobile phases typically used in anion chromatography may be desirable. The possible benefits which could arise are selectivity effects due to the influence of organic modifier solvation effects on the ion-exchange equilibria, or prevention of the adsorption of non-polar sample components on the column packing material. This latter effect may result in column

poisoning and we have found that the Hamilton column is particularly susceptible in this regard, undoubtedly due to the reversed-phase nature of the polystyrene-divinylbenzene material used⁶. The tolerance of the anion-exchange resins to organic modifiers is therefore of some importance, and Table I shows that a considerable range exists for this parameter.

Ion-exchange capacity

In single-column (non-suppressed) ion chromatography, the sensitivity of detection is usually determined by the background conductivity of the eluent since the detector signal is essentially the difference between the conductivities of the eluent anion and the solute anion. The eluent concentration (and hence conductivity) required for efficient separation is related to the total ion-exchange capacity of the column and this is governed by the column dimensions and the exchange capacity of the packing material. When phthalate eluents were used, the eluent strengths (taking into account the eluent pH and concentration) increased in the following column order: Interaction < Bio-Gel TSK < Waters < Hamilton < Vydac. Detection sensitivity was equivalent for the Waters, Bio-Gel TSK and Hamilton columns, with the Vydac and Interaction columns giving reduced sensitivities due to high eluent strength and poor efficiency, respectively.

Column performance characteristics

When the manufacturer's recommended eluent was used for the separation of the standard anion mixture, the results given in Table III were obtained. The longer columns (Vydac and Hamilton) gave the highest numbers of theoretical plates per column, but when efficiency was expressed as theoretical plates per meter, the Waters column gave the highest value. Comparison of the column efficiency values calculated at capacity factors of 5 and 10 shows that the Vydac and Interaction columns exhibited a large decrease in efficiency for longer retained peaks.

The resolution values given in Table III reflect the ability of each column to resolve three closely eluting peak pairs in the standard anion mixture. The selectivity differences which existed between the columns were reflected by the fact that the worst resolved peak pair differed from column to column. For example, nitrite and bromide were poorly resolved on the Vydac column, whereas chloride and nitrite, as well as bromide and nitrate, were poorly resolved with the Hamilton column. The Waters column provided the best overall resolution.

A further selectivity effect was also observed. In general, all of the solutes tested eluted in the same order (Table III), with the exception of iodide and sulphate which showed a reversal of retention order on the Waters column. This effect disappeared when the Waters column was used with a phthalate eluent (see Fig. 2e), but was observed when the Interaction column was used with a phthalate eluent of lower pH than that employed in the manufacturers test chromatogram (see Fig. 2b). However it is fair to say that all of the columns tested showed similar overall selectivity.

The peak asymmetry values shown in Table III illustrate that the columns examined were easily overloaded, with severely fronted peaks observed for a column loading of 70 μ g of sample. Despite this peak distortion, the test mixture was still adequately resolved on all columns except the Interaction column.

The chromatograms obtained with optimised phthalate eluents (Fig. 2) provide a convenient means to compare the column performances. It should be remembered that the concentration and pH of each phthalate eluent was selected so that the overall length of each chromatogram was similar, and that acceptable peak shapes were obtained for the later eluting species (iodide and sulphate). The latter condition required that the chromatogram obtained for the Interaction column was somewhat shorter than those for the other columns, leading to a tendency for the early eluting peaks to be poorly resolved. The data given in Table IV show that with the exception of the Hamilton column, the numbers of theoretical plates per column obtained with the optimised phthalate eluents were approximately equal to, or higher than, the values observed using the manufacturer's recommended eluent (see Table III). Comparison of Tables III and IV also shows that the resolution of critical peak pairs was significantly better with the phthalate eluents than with the manufacturer's recommended eluent, for all columns except the Vydac column.

CONCLUSIONS

Of the five columns tested, four (Vydac, Hamilton, Bio-Gel TSK and Waters) gave adequate separation of the seven standard anions. Elution order was almost identical with all columns, showing that the selectivities of the columns were very similar.

The choice of column for a particular separation is dependent on such factors as the types and relative concentrations of sample anions, the sample pH and the desired eluent pH, the percentage of organic modifier required in the eluent and in view of the wide variation in prices for the columns, cost.

REFERENCES

- 1 P. R. Haddad and A. L. Heckenberg, *J. Chromatogr.*, 300 (1984) 357.
- 2 D. T. Gjerde, J. S. Fritz and G. Schmuckler, *J. Chromatogr.*, 186 (1979) 509.
- 3 D. T. Gjerde, G. Schmuckler and J. S. Fritz, *J. Chromatogr.*, 187 (1980) 35.
- 4 P. E. Jackson and P. R. Haddad, *J. Chromatogr.*, 346 (1985) 125.
- 5 T. Okada and T. Kuwamoto, *Anal. Chem.*, 57 (1985) 258.
- 6 D. P. Lee, *J. Chromatogr. Sci.*, 22 (1984) 327.
- 7 D. L. Saunders, *J. Chromatogr. Sci.*, 15 (1977) 372.

CHROM. 17 985

THE PERFORMANCE OF SOME CELL DESIGNS FOR LASER-INDUCED FLUORESCENCE DETECTION IN OPEN-TUBULAR LIQUID CHROMATOGRAPHY*

H. P. M. VAN VLIET* and H. POPPE

University of Amsterdam, Analytical Department, Nwe Achtergracht 166, 1018 WV Amsterdam (The Netherlands)

(First received October 22nd, 1984; revised manuscript received June 25th, 1985)

SUMMARY

The applicability of fluorescence detection in miniaturized cells using a helium–cadmium laser as the excitation source at 325 nm to open-tubular liquid chromatography has been studied. The investigated cells were fused-silica capillaries of 25 and 10 μm I.D., comprising part of the column or being coupled separately to it, and a sheath flow cell. The volume standard deviation of the various cells was found to be 0.1–2 nl which makes them suitable for the above purpose. The mass detection limits were found to be in the attogram range. However, the concentration detection limits, were found to be one to two orders of magnitude higher than those obtainable with conventional sized fluorescence detectors. This is mainly caused by the instability of the laser.

INTRODUCTION

The advantages of open tubular liquid chromatography (OT-LC) with respect to separation speed and efficiency can be exploited only when the external contribution to peak broadening is kept to the order of a few nanolitres^{1,2}. As far as the injection volume is concerned, this is easily achieved by using split injection techniques. However, due to optical problems involved when using conventional light sources, a decrease in the cell volume is not possible without a severe loss in sensitivity. Fluorescence detection can be carried out successfully with laser excitation^{3,4} because of the possibility to focus all of the available radiation in extremely small volumes.

In OT-LC the values of the time constants are not critical. From the data of Knox and Gilbert¹, it can be derived that the standard deviations will be over 1 s, thus allowing a minimum time constant (T_{RC}) of 0.3 s. In this respect the situation is comparable to that in conventional high-performance liquid chromatography (HPLC).

* The main part of this paper was presented at the 8th International Symposium on Column Liquid Chromatography, New York, May 20–25, 1984.

In this work we have investigated the limitations of laser fluorescence detectors with respect to extra peak broadening and detection limits. We decided to use a relatively simple and inexpensive laser which might be considered for a more general application in the near future. The study involved the evaluation of three cell designs, *viz.*, on-column detection, fused-silica capillary cells and a sheath flow cell.

MATERIALS AND METHODS

Chemicals

The solvents used were analytical and Uvasol grade methanol from Baker (Phillipsburgh, NJ, U.S.A.) and Merck (Darmstadt, F.R.G.) respectively, and deionized water, filtered through a PSC filter assembly (Barnstead, Boston, MA, U.S.A.). Prior to use, all solvents were degassed by vacuum suction over 0.5- μ m acetate filters (Millipore, Bedford, MA, U.S.A.).

The test compounds used were anthracene, fluoranthene, pyrene, fluorescein (Janssen, Beerse, Belgium) and quinine sulphate (BDH, Poole, U.K.). Stock solutions of the polycyclic aromatic hydrocarbons (PAHs) were prepared in methanol, the quinine sulphate was dissolved in 0.1 *N* sulphuric acid and the fluorescein was dissolved in methanol–1 *M* sodium hydroxide (1:1). Spectral data for the PAHs were taken from ref. 5.

Apparatus

Fig. 1 shows the general experimental set-up. The system consisted of a Series 4100 constant-flow pump (Varian, Walnut Creek, CA, U.S.A.), a Model 7120 central-port injection valve (Rheodyne, Berkeley, CA, U.S.A.), a home-made splitting device, fused-silica capillaries of different lengths and internal diameters (SGE, Ringwood, Victoria, Australia) and various home-made detection cells, which will be described below.

As a light source, a Model 4110 H-uv helium–cadmium laser (Liconix, Sunnyvale, CA, U.S.A.) was employed, operated at 325 nm. At this wavelength the specified minimum power is 2.5 mW. However, after about 1000 h of use, the power had decreased to *ca.* 1.2 mW. Tube replacement became necessary after about 1700 h of operation, due to the formation of so-called colour centres in the brewster win-

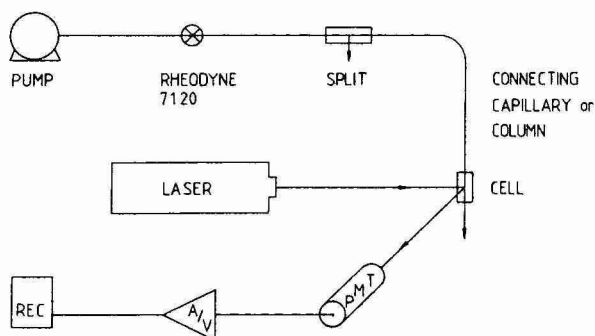


Fig. 1. Diagram of the experimental set-up. A bandpass filter and an appropriate lens were inserted in the laser beam. At the emission side, a lens and a monochromator or a cut-off filter were used. A/V = Current-to-voltage convertor; REC = recorder.

dows, because of the UV absorption by these centres, laser action at the 325-nm line ceases. The line at 442 nm is hardly affected by this effect⁶.

Optics

A 325-nm bandpass filter was inserted in the laser beam. In order to focus the beam an appropriate quartz lens was used. The focal length, f , was calculated from the specified full angle divergence, θ , of the laser using the approximate equation

$$f = 2r/\theta \quad (1)$$

in which r is the radius of the illuminated spot⁷. The desired radius can be derived from the size and geometry of the cell used, *e.g.*, for a cylindrical fused-silica cell r should be smaller than the internal radius.

The light emitted under a 90° angle was collected by a fresnel lens, $f = 16$ mm and aperture 0.6, then passed through a 420-nm cut-off filter or a Model 82-410 Ebert monochromator (Jarrell-Ash, Waltham, MA, U.S.A.) and the intensity was measured with a Type 6255 S photomultiplier tube (PMT) (EMI, Hayes, U.K.). The resulting current was converted into a voltage by means of a Diomod 72-W amplifier (Knick, Berlin, F.R.G.) with adjustable low-pass filter and gain.

Cell designs

Three cell designs were investigated: a fused-silica tube which forms the end of the open-tubular column (on-column detection), a separate piece of fused-silica capillary, coupled to the end of the column (coupled cell) and a sheath flow cell.

On-column detection. In this detection mode the laser beam is focused on the end of a fused-silica column, the protective polymer layer of which has been burned off over a short distance. It can be used only if the stationary phase is sufficiently transparent at the excitation and emission wavelengths.

Coupled cells. Coupled cells can be used either when the stationary phase is not sufficiently transparent or when the path length of the light becomes unfavourably short due to the use of columns having small internal diameters. The coupled cells were prepared by cutting an appropriate length of tubing, typically 15 mm, and burning off the polymer layer over the last 5 mm. Connections were made with a 1/32-in. T-type zero dead-volume connector with "FS" vespel adapters (Valco, Houston, TX, U.S.A.). Cells with internal diameters of 25 and 10 μm were investigated.

Sheath flow cell. The principle of the sheath flow cell is that the column effluent, entering a quartz cuvette, is surrounded by a concentric second stream of liquid. Provided that the flow is laminar, no noticeable diffusion will occur over a certain distance. The use of the sheath flow cell was expected to result in a low background signal and background noise, because reflection and scattering at the windows are far removed from the measurement area. On the other hand, the manipulation of this cell was expected to be more complicated than that of a fused-silica cell.

The design of the sheath flow cell, which is well known from flow cytometry⁸, was adopted from the cells described by Hershberger *et al.*^{9,10} and John *et al.*¹¹. A view of the cell is shown in Fig. 2. Contrary to the situation in microbore HPLC, in OT-LC the use of a connecting capillary between the column and the cell is not necessary. The column is simply inserted into the flow assembly and the laser beam

is focused through the quartz window onto a point which is typically 3 mm above the column end. The aim of the design was to have a flexible system, in which the outer, shield or sheath entry tube can easily be replaced in order to allow adjustment of the outlet diameter. Also the inner or effluent entry tube can easily be centered in the outer tube. The sheath flow was delivered by a syringe-type LDP 13A constant-flow pump (Labotron, Gelting, F.R.G.).

Splitting device

Splitting devices were constructed using Swagelock 1/16-in. three-way unions. The connection between the valve and the union was made by stainless-steel tubing (1/16 in. O.D., 0.5 mm I.D.). The fused-silica column was inserted all the way through the union and the tubing, as close as possible to the valve rotor. It was sealed at the union using appropriately drilled PTFE "no-hole" ferrules. A capillary restriction was connected to the remaining end of the three-way union. The splitting ratio was varied by adjusting the length and/or the internal diameter of this restriction.

Using splitting ratios of up to 1:1000, the external broadening due to the mixing chamber, present at the top of the column, could easily be minimized. When a splitting device is used the fused-silica columns are effectively operated at constant pressure. The pump delivers a constant flow to the splitting point. This flow is mainly diverted to the restriction and the permeability of the latter and the preset flow-rate determine the inlet pressure of the column.

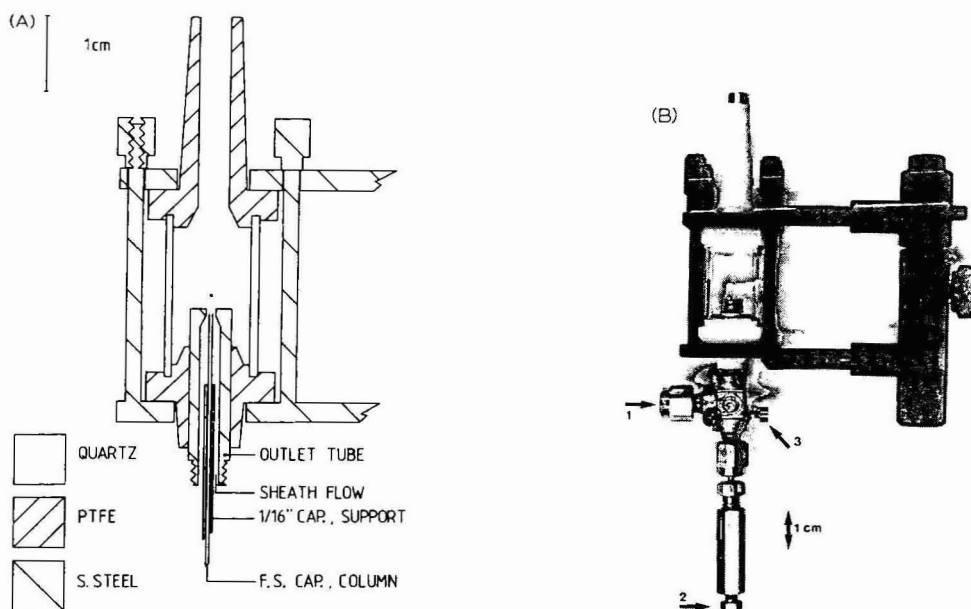


Fig. 2. A, Diagram of the assembly of the sheath flow cell, which is connected to a positioner. Of the flow assembly, only the outlet tube, with a capillary column, is shown. This assembly can easily be removed from the cell assembly by pulling it out of the PTFE holder. B, Picture of the total sheath flow cell. 1 = Sheath flow entry; 2 = column connection (microbore) or column insertion (OT-LC), 3 = screws to adjust the position of the 1/16-in. capillary support.

Columns

As the most stringent requirements on external peak broadening apply to unrestrained peaks, the columns in our experiments did not contain a stationary phase. The dimensions of the fused-silica columns were 450 cm \times 25 μ m I.D. and 185 cm \times 10 μ m I.D., referred to as the 25- and the 10- μ m column. Over the investigated range of linear velocities, the columns had volume standard deviations of 5–10 nl and of 0.2–0.5 nl respectively.

Procedure

Prior to the actual experiments, 175 μ l of a concentrated fluorescein or pyrene solution were injected. Optical alignment was achieved by adjusting the positions of the parts of the system with home-made positioners in order to obtain the maximum signal. Peak widths were measured at 0.6 of the maximum height. The reported sigma values were calculated as half this peak width.

The performance of the detection modes was tested first by using the 25- μ m and then the 10- μ m column, the latter providing a more demanding test. The coupled and sheath flow cells were tested by comparing the obtained plate height (H) vs. linear velocity (u) plot with the plot resulting from the use of on-column detection, assuming that this detection mode would not result in any noticeable extra peak broadening. This assumption was checked by comparing the results to the theoretically expected plate heights, which can be calculated using the Golay¹² and Wilke–Chang^{13,14} equations. The volume standard deviation of the external peak broadening can then be calculated according to

$$\sigma_v = \pi r_c^2 \sqrt{L(H_{\text{obs}} - H_{\text{calc}})} \quad (2)$$

in which r_c is the internal diameter of the column, L is its length and H_{obs} and H_{calc} are the observed and calculated plate heights respectively.

The detection limits, taken as three times the standard deviation of the noise (σ_N), were determined by injecting 175 μ l of a solution of the compound of interest and measuring the height of the resulting block in the chromatogram. Noise levels were measured by recording the baseline over 1-min intervals and taking the average of six measurements of the peak-to-peak signal as $4\sigma_N$.

RESULTS AND DISCUSSION

Injection volume

In the set-up shown in Fig. 1 the 25- μ m column was installed and the splitting ratio set at 1:360. By partially filling the loop the effective injection volume was varied from 22 to 0.6 nl. The maximum allowable injection volume was determined by measuring the peak width in the on-column detection mode. The results are shown in Table I. It was concluded that an injection volume of 1 nl results in a negligible contribution to the external peak broadening in this system. For practical reasons, the splitting ratio was altered to about 1:800.

With the 10- μ m column the maximum allowable injection volume was likewise determined to be 100 pl.

TABLE I

PEAK WIDTH AS A FUNCTION OF THE INJECTION VOLUME ON A CAPILLARY COLUMN

Column: 450 cm \times 25 μ m, fused silica. Splitting ratio: 1:356. u = 28.5 mm/s. Test compound: fluorescein. Mobile phase: methanol–water (80:20, v/v). On-column detection. Eff. V_{inj} is the effective injection volume, σ_t and σ_v are the peak standard deviations in time and volume units.

Total V_{inj} (μ l)	Eff. V_{inj} (nl)	t_R (s)	σ_t (s)	σ_v (nl)
8	22	158	3.7	52
4	11	158	3.5	49
2	5.6	158	3.4	47
1	2.8	158	2.9	41
0.5	1.4	159	2.5	35
0.3	0.8	159	2.2	31
0.2	0.6	159	2.2	31

Performance of the cells

On-column detection. Using the 25- μ m column, the theoretical H vs. u curve was calculated for methanol as a mobile phase. Next, the curve was obtained experimentally. The results shown in Fig. 3 and Table II for fluoranthene indicate the good agreement between calculated and observed values. Using eqn. 2 it can be calculated that the difference between the calculated and observed plate height corresponds to an extra volume standard deviation of 2–3 nl over the investigated linear velocity range.

A comparable agreement was found when anthracene was used as the solute and when the mobile phase was changed to methanol–water (80:20, v/v). In Fig. 4 chromatograms are shown for fluoranthene on the 25- μ m column, recorded with different time constants.

Similar experiments were carried out with the 10- μ m column. The corresponding H vs. u data are shown in Fig. 5 and Table III. The difference between the observed and calculated values corresponds to an extra volume standard deviation of only 0.1–0.2 nl.

From these results it can be concluded that on-column detection fulfils the requirements as far as external broadening is concerned.

Coupled cells. A fused-silica cell having an internal diameter of 25 μ m, pre-

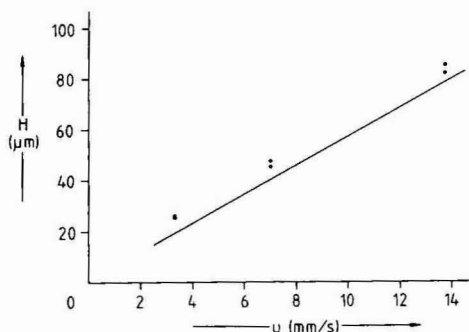


Fig. 3. Plot of H versus u for fluoranthene on a 450 cm \times 25 μ m column. Injection volume: 1 nl. Mobile phase: methanol. \bullet , Observed plate height; —, calculated plate height. On-column detection mode.

TABLE II

CALCULATED AND OBSERVED PLATE HEIGHTS IN OT-LC FOR SEVERAL DETECTION MODES USING 25- μm I.D. CELLSColumn: 450 cm \times 25 μm . Solvent: methanol. Solute: fluoranthene. u_s and u_c are the linear velocities of sheath and column flow, respectively.

u (mm/s)	H (μm)					u_s/u_c for sheath flow cell
	Calculated	Observed				
			On-column detection	Coupled cell	Sheath flow cell	
13.7	79	82	86	127*	0.8	
13.7	79	86	90	111*	0.8	
7.0	41	46	47	41	1.6	
7.0	41	48	46	45	1.6	
3.3	19	27	26	23	3.1	
3.3	19	27	24	22	3.1	

* Caused by too low a flow-rate.

pared as described above, was connected to the 25- μm capillary column. The determined plate heights are shown in Table II. Compared to on-column detection, the use of a coupled cell has no adverse effect on the efficiency of this system, *i.e.*, the average extra deviation was less than 1 nl.

Next a fused-silica cell with an internal diameter of 10 μm was connected to the 10- μm column. As shown in Table III, a significant increase in the plate height was observed compared to on-column detection. The increase amounts to an extra-

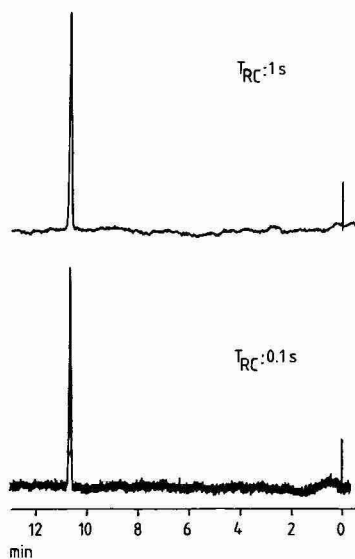


Fig. 4. Chromatograms of 2.5 pg fluoranthene on a 450 cm \times 25 μm column. Injection volume: 1 nl. Mobile phase: methanol. Detection limits: for $T_{RC} = 1$ s, 25 fg ($N = 77\,000$); for $T_{RC} = 0.1$ s, 75 fg ($N = 96\,000$).

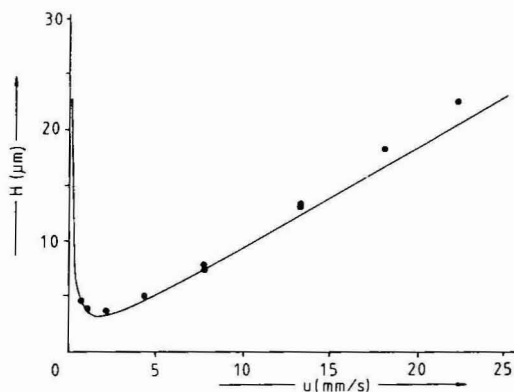


Fig. 5. Plot of H versus u for fluoranthene on a $185\text{ cm} \times 10\text{ }\mu\text{m}$ column. Injection volume: 100 μl . Other details as in Fig. 3.

column volume deviation of 0.1–0.3 nl. By applying the exponentially modified gaussian peak model¹⁵, it was found that the additional broadening is that expected of an ideal mixing chamber having a volume of 0.4 nl¹⁶. It can be assumed that the dead volume in the connector is the cause of this effect. With small internal diameters it becomes increasingly difficult to avoid a significant dead volume in the connector. The wall becomes relatively thick and the capillaries cannot be cut exactly flat and perpendicularly. The fact that effects of the magnitude of 0.4 nl can easily be measured with the present equipment indicates the excellent performance of the system with respect to external broadening.

It can be concluded that 25- μm coupled cells can be used when column standard deviations are greater than 5 nl, and that 10- μm coupled cells give rise to a low

TABLE III

CALCULATED AND OBSERVED PLATE HEIGHTS IN OT-HPLC FOR SEVERAL DETECTION MODES USING 10- μm I.D. CELLS

Column: $185\text{ cm} \times 10\text{ }\mu\text{m}$. Solvent: methanol. Solute: fluoranthene. Each value is the average from at least two measurements.

u (mm/s)	H (μm)		u_s/u_c for sheath flow cell		
	Calculated	Observed			
		On-column detection	Coupled cell	Sheath flow cell	
22.9	21			60*	0.9
22.9	21	24	27	25	1.8
17.9	16	18	22	18	2.4
13.2	12	13	19	14	3.2
8.8	8	8	11	9	4.8
4.4	4	5	6	5	9.6

* Caused by too low a flow-rate.

but significant extra peak broadening when the column volume standard deviation is less than about 1 nl.

Sheath flow cell. The plate heights determined for fluoranthene as solute and methanol as mobile phase are shown in Tables II and III for the 25- and 10- μm column respectively. These results show that the ratio of the linear velocities of the sheath and column flow should be greater than 1. We presume that this is related to the relatively thick wall of the fused-silica capillaries, and found similar behaviour when 1/16-in. steel tubing with an internal diameter of 0.25 mm was used as the column outlet under microbore conditions. However, after tapering the end of the tube to a needle point, under those conditions an increase of only about 10% was found at a velocity ratio of 0.25¹⁷.

Under OT-LC conditions excellent results are obtained when the sheath flow is large enough. The extra-volume deviations in comparison to on-column detection correspond to only 0.2–1 nl. However, a few drawbacks should be mentioned. It was found that a change in the velocity of the sheath flow often causes a change in the position of the column flow in the cell, resulting in misalignment of the optical system. This effect is probably due to imperfections in the concentricity of the inlet and outer tube at the cell entrance. Because of the small column dimensions, the optical alignment has to be very precise and this leads to a rather laborious procedure. When fused-silica cells are used the alignment is relatively easy, because the position of the liquid is fixed and not influenced by stream patterns. Also, great care has to be taken to cut the end of the column at a right angle. A badly cut tip invariably causes turbulence and contamination of the bulk of the liquid in the cell.

Signal

The optical and electrical paths were followed with the sheath flow cell, and the monochromator replaced by the cut-off filter. For each stage the expected photon, electron or voltage level was calculated. The resulting flow scheme is given in Table IV. Although the numbers are only indicative of the order of magnitude, because of the various uncertainties, it can be concluded that the observed signal corresponds to the expected value. Also it can be seen that the photon collection efficiency in this early design is rather low. In the present system the efficiency is 16%. However, as will be shown, under the present conditions the collection efficiency has no direct effect on the detection limit.

For fluoranthene a linear relationship between the concentration and peak height was obtained over at least four orders of magnitude ($r = 0.9997$, $n = 11$), using the 25- μm column and the sheath flow cell.

Noise and detection limit

Given a certain calibration factor, the detection limit is determined by the noise level. In order to find the predominant source of noise, measurements were carried out for each subsequent element of the system. This was done with PMT cathode voltages between -550 and -800 V, which were shown in preliminary experiments to be the most satisfactory. By operation of the system in the absence of laser excitation and a voltage on the PMT, it was ascertained that the amplifier and recorder noise could be neglected. Next it was verified that the proportional noise in the photometric system (PMT and high voltage supply) was negligible as well. This was

TABLE IV
ENERGY FLOW SCHEME

Test compound: fluoranthene. PMT cathode voltage: -560 V without monochromator. Abbreviations and symbols: Eff = efficiency; P = laser power; T = transmitters; Φ = fluorescence quantum yield; c = concentration; l = length; G = gain.

$P = 1.2$ mW	Laser	$2.0 \cdot 10^{15}$ photons/s
$T(\text{tl}) = 60\%$	Filter, lenses and cuvette	$1.2 \cdot 10^{15}$ photons/s
$\Phi = 0.3$	Fluorescence	$7.4 \cdot 10^9$ photons/s
$\epsilon = 6500$ l/mol/cm		
$c = 1.37 \cdot 10^{-7}$ M		
$l = 10^{-2}$ cm		
Eff = 8%	Photon capture	$5.9 \cdot 10^8$ photons/s
Eff = 8%	PMT	$7.5 \cdot 10^{11}$ electrons/s
$G = 1.6 \cdot 10^4$		
$1 \text{ A} \cdot \text{s} = 6.24 \cdot 10^{18}$ electrons		$1.2 \cdot 10^{-7}$ A
$G = 10^{-7}$ A/V	A-V converter	1.2 V
Experimentally found		1.1 V

done with a cell filled with pure solvent. After turning on the laser, the background signal was measured and the total variance of the noise determined. Then the PMT was illuminated with a light-emitting diode fed from a constant-current source and at the same signal level the variance was again determined. From these experiments it could be concluded that the instability of the laser radiation constitutes the predominant contribution to the observed noise.

In Table V the detection limits and signals for several fused-silica cells are compared, including some cells used in microbore scale experiments. It can be concluded that there is no difference in detection limit between cells with diameters of 10 – 100 μm . Also, the calibration factor decreases when the tube diameter becomes smaller than the laser spot size.

Since in our system the laser is the main contributor to the noise, a decrease in the background signal can be expected to exert a direct influence on the detection

TABLE V
DETECTION LIMITS FOR QUININE SULPHATE USING SEVERAL FUSED-SILICA CELLS

$T_{\text{RC}} = 1$ s; $V_{\text{PMT}} = 700$ V; em 420 nm cut-off filter. Solvent: methanol–water (60:40, v/v). For other conditions see text.

Cell diameter (μm)	V_{PMT} (V)	$f_{\text{laser lens}}$ (mm)	Detection limit (10^{-9} mol/l)	Signal (mV)
100	600	100	4	—
50	600	75	3	50
50	700	75	2	—
25	600	50	3	48
25	700	50	2	—
10	600	50	3	12

limit. Fluorescing impurities in the solvents were found to contribute to the background. Also scattered light could be suppressed by inserting and optimizing an aperture in the emitted light path. In this way the detection limits were improved by one order of magnitude. The detection limit for fluoranthene was 1×10^{-9} mol/l. However, no differences were found between the silica cells and the sheath flow cell, and similar results were obtained when the cut-off filter was replaced by the monochromator. It is concluded that at present the use of the sheath flow cell offers no advantage over fused-silica cells.

The laser instability can be compensated for by correcting the signal for laser fluctuations, measured independently. In such a "double beam" instrument the correction can be made by subtracting¹⁸ or, better, ratioing the two photocurrents. Preliminary results with such a system were obtained both with analogue (home-built) and digital (home-modified) circuits. With the latter an approximately eight-fold improvement was typically observed.

The approach of Folestad *et al.*¹⁹ of collecting the emitted radiation in a direction out of the plane through the laser axis and perpendicular to the capillary did not result in an improvement of the detection limit in our system.

The concentration detection limits, obtained as described above, are about the same as those reported by Guthrie *et al.*¹⁸. The data of Folestad *et al.*¹⁹ correspond to a substantially lower detection limit of about 5×10^{-14} mol/l for fluoranthene. However, this result was obtained with a far more powerful and expensive laser and with the free falling jet cell which at the moment is not compatible with the flow-rates in microbore and OT-LC work.

CONCLUSIONS

From the results obtained we conclude that both the coupled cell and the sheath flow cell can be used as an alternative to on-column detection. Because the volume standard deviations can be well below 1 nl, all three detection modes can meet the requirements for external peak broadening in OT-LC.

The mass detection limits are impressively low. For example, at the concentration detection limit of 10^{-9} mol/l, 0.1 ag of fluoranthene is present in the illuminated volume of a 10- μ m cell. A more realistic figure is obtained by considering the amount of fluoranthene present in four volume standard deviations of the chromatographic system when the peak crest is at the concentration detection limit. In the case of the 10- μ m column, with a linear velocity of 23 mm/s and on-column detection, 240 ag fluoranthene are present in such a volume.

However, the concentration detection limit itself is more relevant. Our values are higher than those obtained with the best available conventional HPLC fluorimeters, using cells of 3–10 μ l. Because of this loss in sensitivity we do not recommend the present system for microbore work. In such cases, when an external peak broadening of 0.5–1 μ l is allowed, it is easier to use a conventional detector with a 3- μ l cell and about a three-fold make-up flow. For OT-LC a somewhat lower concentration detection limit is allowable, since the first aim of this technique is to generate more plates in a shorter time than is possible with other forms of HPLC.

The applicability of the present system is therefore limited to open-tubular columns and packed capillaries. Since no differences were found in the detection limit

and in the background signal, our first choice would be on-column detection or the use of coupled cells, these being the simplest to use. In view of the extremely small volume deviations obtained, down to 0.1 nl, we may paraphrase Knox and Gilbert¹ by concluding that there are more than excellent prospects for capillary LC.

The laser employed has the advantage of being a relatively inexpensive instrument. On the other hand, the availability of only two lines, 325 and 442 nm, limits the number of fluorophores that can be detected. However, for a large number of fluorimetric detection schemes, pre- or post-column derivatization is used. Many of the customary reagents, such as dansyl chloride, dansyl chloride and *o*-phthalaldehyde, are suitable for excitation at 325 nm, while Gluckman *et al.*²⁰ showed the applicability of coumarin based reagents with an excitation maximum near 325 nm. We are currently investigating the possibilities of post-column reaction detection on the OT-LC scale²¹.

ACKNOWLEDGEMENT

J. Kraak and J. Kuysten are acknowledged for helpful discussions and the latter also for assistance with the digital experiments. The optical components were skilfully made by H. Brugman.

REFERENCES

- 1 J. H. Knox and M. T. Gilbert, *J. Chromatogr.*, 186 (1979) 405.
- 2 J. C. Sternberg, *Adv. Chromatogr.*, 2 (1966) 205.
- 3 M. Novotny, *Anal. Chem.*, 53 (1981) 1294A.
- 4 R. Green, *Anal. Chem.*, 55 (1983) 20A.
- 5 I. B. Berlman, *Handbook of Fluorescence Spectra of Aromatic Molecules*, Academic Press, New York, 2nd ed., 1971.
- 6 Optilas bv, Alphen a/d Rijn, The Netherlands, personal communication.
- 7 P. B. Huff, B. J. Tromberg and M. J. Sepaniak, *Anal. Chem.*, 54 (1982) 946.
- 8 D. Pinkel, *Anal. Chem.*, 54 (1982) 503A.
- 9 L. W. Hershberger, J. B. Callis and G. D. Christian, *Anal. Chem.*, 51 (1979) 1444.
- 10 L. W. Hershberger, J. B. Callis and G. D. Christian, *Anal. Chem.*, 53 (1981) 971.
- 11 P. John, E. R. McQuart and I. Souter, *Analyst (London)*, 107 (1982) 221.
- 12 M. J. Golay, in D. H. Desty (Editor), *Gas Chromatography 1958*, Butterworth, London, 1959, p. 36.
- 13 C. R. Wilke and P. Chang, *Am. Inst. Chem. Eng. J.*, 1 (1955) 264.
- 14 S. Bretsznajder, *Prediction of Transport and Other Physical Properties of Fluids*, Pergamon Press, Oxford, 1971, pp. 33–39, 358–383.
- 15 W. W. Yau, *Anal. Chem.*, 49 (1977) 395.
- 16 W. M. A. Niessen, H. P. M. van Vliet and H. Poppe, *Chromatographia*, 20 (1985) 357.
- 17 H. P. M. van Vliet and H. Poppe, in preparation.
- 18 E. J. Guthrie, J. W. Jorgenson and P. R. Dluznieski, *J. Chromatogr. Sci.*, 22 (1984) 171.
- 19 S. Folestad, L. Johnson, B. Josefsson and B. Galle, *Anal. Chem.*, 54 (1982) 925.
- 20 J. Gluckman, D. Shelly and M. Novotny, *J. Chromatogr.*, 317 (1984) 443.
- 21 H. P. M. van Vliet, G. J. M. Bruin, J. C. Kraak and H. Poppe, in preparation.

CHROM. 17 933

DIRECT COUPLING OF MICRO HIGH-PERFORMANCE LIQUID CHROMATOGRAPHY WITH FAST ATOM BOMBARDMENT MASS SPECTROMETRY

YUKIO ITO, TOYOHIDE TAKEUCHI* and DAIDO ISHII

Department of Applied Chemistry, Faculty of Engineering, Nagoya University, Chikusa-ku, Nagoya-shi, 464 (Japan)

MASASHI GOTO

Research Center for Resource and Energy Conservation, Nagoya University, Chikusa-ku, Nagoya-shi, 464 (Japan)

(Received May 28th, 1985)

SUMMARY

An interface for direct coupling of micro high-performance liquid chromatography with fast atom bombardment mass spectrometry has been developed. The interface was made of fused-silica capillary tubing, the end of which was attached to a stainless-steel frit. The mobile phase contained glycerol, which functioned as the matrix, and the solvent was immediately vaporized on the surface of the frit. The argon beam stroke the surface of the frit and its position was adjusted so that the solute could be effectively ionized. The performance of the interface was examined using bile acids as the test solutes.

INTRODUCTION

Various methods for coupling liquid chromatography (LC) and mass spectrometry (MS) have been investigated, involving direct introduction accompanied by chemical ionization¹, a thermospray method^{2,3}, a moving-belt method⁴, etc. However, these ionization techniques are unsuitable for high-molecular-weight compounds, which have been successfully analysed by fast atom bombardment MS (FABMS) and secondary-ion MS (SIMS). A few reports have dealt with the direct combination of LC with FABMS or SIMS^{5,6}, but techniques have been restricted to the moving-belt method owing to obstruction by the mobile phase solvent. Micro high-performance LC (micro HPLC) can overcome this problem. Micro HPLC combines well with MS because of the low flow-rates of the mobile phase^{7,8}.

This paper describes the direct coupling of micro HPLC with FABMS using a new interface.

EXPERIMENTAL

Mass spectrometer

A JMS-DX 300 double-focusing mass spectrometer (JEOL, Tokyo, Japan) was employed without any modification. The argon beam energy was 6 kV and the ion source temperature was kept at 100°C. The interface was introduced from the side of the direct introduction system of the mass spectrometer.

LC-MS interface

The structure of the interface for micro HPLC-FABMS is illustrated in Fig. 1. The interface is made of fused-silica capillary tubing, 40 μm I.D. and 0.19 mm O.D. (Scientific Glass Engineering, Melbourne, Australia), which was glued into the stainless-steel tubing, 0.19 mm I.D. and 0.41 mm O.D. (Hakkoshoji, Tokyo, Japan), with epoxy-resin adhesive. The latter tubing was glued in glass tubing, 0.5 mm I.D. and 3 mm O.D., with epoxyresin adhesive for insulation. The stainless-steel frit (2 μm porosity) was attached to the outlet of the interface tubing, and only the rim of the frit was glued to the cross-section of the glass tubing. The small-diameter (1/16 in.) frit was cut from a thin plate (0.33 mm thick) in the laboratory.

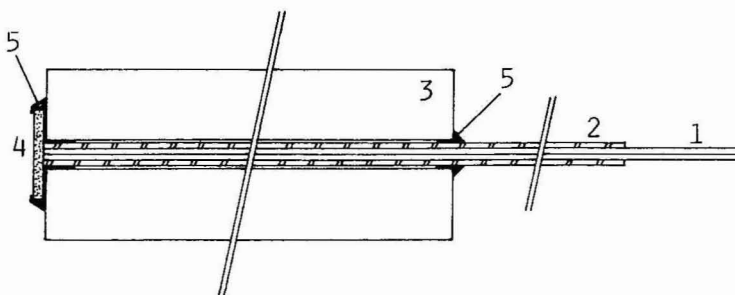


Fig. 1. Structure of the interface. 1 = Fused-silica tubing (40 μm I.D., 0.19 mm O.D.); 2 = stainless-steel tubing (0.19 mm I.D., 0.41 mm O.D.); 3 = glass tubing (0.5 mm I.D., 3 mm O.D.); 4 = stainless-steel frit; 5 = epoxy-resin adhesive.

The effluent from the column passes through the 40 μm I.D. fused-silica capillary and reaches the porous frit. The mobile phase solvent is immediately vaporized on the surface of the frit, and the solute and the matrix (glycerol) are left on the surface and are subjected to bombardment by the argon beam. The solute can be effectively dispersed in the matrix by premixing glycerol with the mobile phase.

Micro HPLC apparatus

A micro HPLC system was assembled from Micro Feeder MF-2 (Azumadenkikogyo, Tokyo, Japan) equipped with a gas-tight syringe MS-GAN 025 (Terumo, Tokyo, Japan) as a pump, an ML-422 micro valve injector (0.02 μl ; Jasco, Tokyo, Japan), a fused-silica column (50 \times 0.26 mm I.D.) packed with ODS-Hypersil-5 (5 μm ; Shandon, Runcorn, U.K.) and a UVIDEC-100 II UV spectrophotometer (Jasco) equipped with a small-volume (0.05 μl) flow cell, as shown in Fig. 2. Line filters (2 μm) are placed between the LC pump and the injector and between the column and

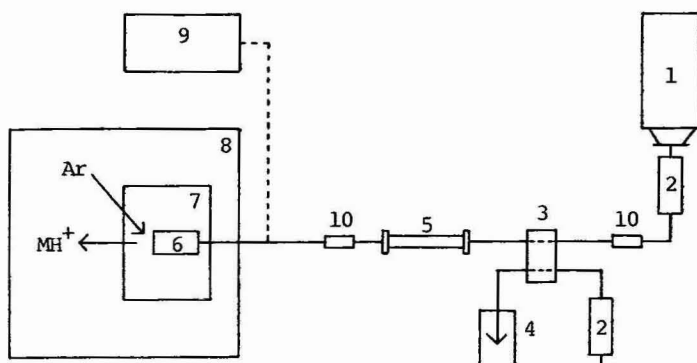


Fig. 2. Diagram of the apparatus. 1 = Micro Feeder; 2 = gas-tight syringe; 3 = sample injector; 4 = waste reservoir; 5 = separation column; 6 = interface; 7 = ion source; 8 = mass spectrometer; 9 = UV spectrophotometer; 10 = line filters.

the interface, in order to filter the mobile phase and the column effluent. The line filters are composed of unions in which a laboratory-cut stainless-steel thin frit is placed. A 1/16 in. union was used for the former line filter and a 1/32 in. union for the latter. The separation column was prepared as described previously⁹.

Reagents

HPLC-grade distilled water, acetonitrile, glycerol and ammonium bicarbonate were supplied by Wako (Osaka, Japan). The mobile phase and the sample solution were filtered with a membrane filter (0.45 μm) before use. Bile acids were supplied from Sigma (St. Louis, MO, U.S.A.) or P-L Biochemicals (Milwaukee, WI, U.S.A.).

RESULTS AND DISCUSSION

In FABMS the solute must be dispersed in a matrix such as glycerol, so that it can be effectively ionized. The solute is manually mixed with the matrix in a batch process, which is unsuitable for HPLC-FABMS coupling. Premixing of glycerol with the mobile phase permits on-line dispersion of the solute in the matrix and allows the solute to be loaded with the sample injector. The concentration of glycerol in the mobile phase affects the sensitivity and the retention of the solute.

The mobile phase was a mixture of glycerol and ethanol. The ion current of glycerol was increased as the proportion of glycerol increased up to 15%, which indicates that the sensitivity increases as the proportion of glycerol increases. The ion current of glycerol in the mobile phase containing 15% glycerol was 1.2–1.3 times greater than in the mobile phase containing 10% glycerol. However, glycerol increased the viscosity of the mobile phase, and thus a proportion of 10% was selected for this work.

The flow-rate of the mobile phase should be carefully chosen because it strongly affects the pressure in the mass spectrometer. Ideally the vaporization rate of the glycerol should be the same as the rate of supply. When the flow-rate was 0.52 $\mu\text{l}/\text{min}$, the pressure around the inlet of the diffusion pump was quite stable ($7 \cdot 10^{-6}$ – $8 \cdot 10^{-6}$

Torr). Higher flow-rates of the mobile phase led to infavourable observations, such as unstable vaporization or electric discharge in the ion gun. These problems will be overcome by improving the vacuum system.

Fig. 3 demonstrates the repeated ion monitoring of 20 ng of sodium taurocholate (mol. wt. 537) without the separation column. The peak width obtained with FABMS detection was around twice that obtained with UV detection, and tailing was observed in the former. These deteriorations may be due to band spreading of the solute on the frit and the slow ionization speed. The reproducibility of the peak height was satisfactory. The signal at m/z 369 corresponds to the protonated tetramer of glycerol and shows the stability of ionization. It should be noted that the ion current of glycerol is decreased when the solute is ionized.

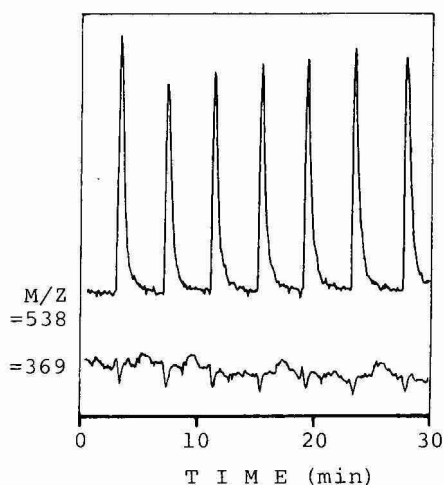


Fig. 3. Ion monitoring of bile acid and glycerol. Upper trace, m/z 538; lower trace, m/z 369. Mobile phase, glycerol-acetonitrile-water (10:27:63); flow-rate, 0.52 $\mu\text{l}/\text{min}$; sample, 20 ng of sodium taurocholate.

Fig. 4 demonstrates the separation of sodium taurocholate and sodium taurodeoxycholate (50 ng of each injected). The reconstructed ion chromatogram (RIC) and mass chromatograms are shown in the figure. The signals at m/z 516 and m/z 500 correspond to protonated taurocholic acid and protonated taurodeoxycholic acid, respectively. The RIC range was set at 450–560 in order to avoid interference from signals due to the glycerol background. Fig. 4 also shows a chromatogram obtained with UV detection. Band broadening or tailing observed with FABMS detection will be improved by adjusting the structure of the interface, the amount of glycerol used and the energy of bombarding particles.

This system allows the subtraction of the background interference due to the matrix from the solute signal, leading to high sensitivity. Figs. 5 and 6 show mass spectra of sodium taurocholate and sodium taurodeoxycholate, respectively. These spectra give structural information and are nearly the same as those obtained with the conventional off-line batch method.

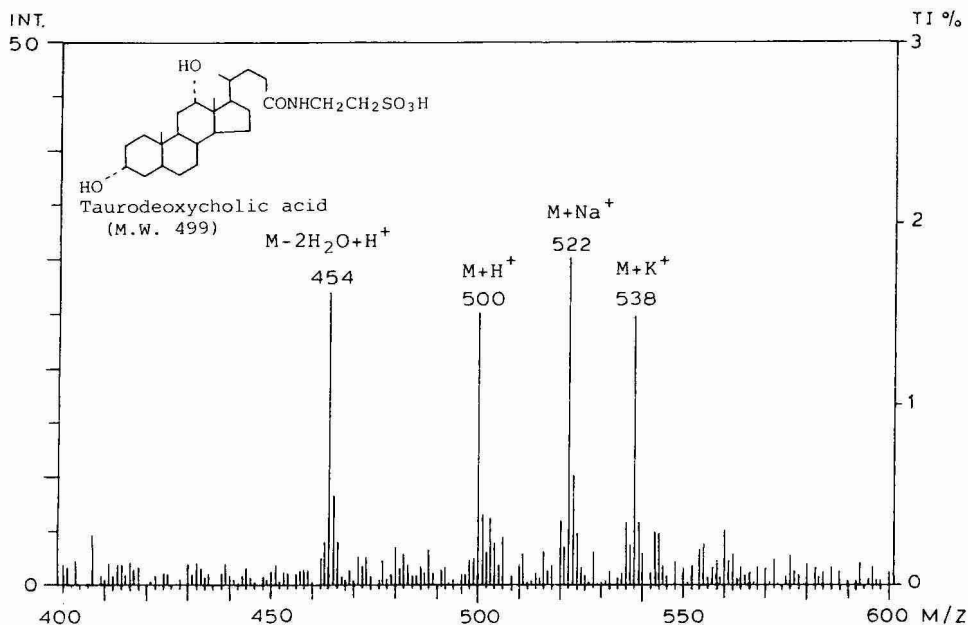


Fig. 6. Mass spectrum of sodium taurodeoxycholate. Operating conditions as in Fig. 4.

CONCLUSION

The developed interface allows the coupling of micro HPLC and FABMS, with the mobile phase premixed with the matrix. The pressure in the ion source could be kept stable. The method will also be suitable as a new sample introduction method for FABMS.

REFERENCES

- 1 J. A. Apffel, U. A. Th. Brinkman and R. W. Frei, *Anal. Chem.*, 55 (1983) 2280.
- 2 C. R. Blakely and M. L. Vestal, *Anal. Chem.*, 55 (1983) 750.
- 3 T. R. Covey, J. B. Crowther, E. A. Dewey and J. D. Henion, *Anal. Chem.*, 57 (1985) 474.
- 4 M. J. Hayes, E. P. Lankmayer, D. Vouros, B. L. Karger and J. M. McGuire, *Anal. Chem.*, 55 (1983) 1745.
- 5 R. D. Smith, J. E. Burger and A. Johnson, *Anal. Chem.*, 53 (1981) 1603.
- 6 P. Dobberstein, G. Korte, G. Meyerhoff and R. Pesch, *Int. J. Mass Spectrom. Ion Phys.*, 46 (1983) 185.
- 7 T. Takeuchi, Y. Hirata and Y. Okumura, *Anal. Chem.*, 50 (1978) 657.
- 8 Y. Yoshida, H. Yoshida, S. Tsuge, T. Takeuchi and K. Mochizuki, *J. High Resolut. Chromatogr. Chromatogr. Commun.*, 3 (1980) 16.
- 9 T. Takeuchi and D. Ishii, *J. Chromatogr.*, 213 (1981) 25.

CHROM. 17 957

MULTICHANNEL SPECTROPHOTOMETRIC DETECTOR FOR FUSED-SILICA CAPILLARY TUBE ISOTACHOPHORESIS

MASASHI GOTO*

Research Center for Resource and Energy Conservation, Nagoya University, Chikusa-ku, Nagoya-shi 464 (Japan)

and

KATSUTOSHI IRINO and DAIDO ISHII

Department of Applied Chemistry, Faculty of Engineering, Nagoya University, Chikusa-ku, Nagoya-shi 464 (Japan)

(Received June 7th, 1985)

SUMMARY

Isotachophoresis carried out in a 0.25 mm I.D. fused-silica capillary tube yielded high resolution. The use of an ultraviolet visible multichannel spectrophotometer with photodiode array as detector together with a cross flow cell (volume 0.01 μ l) was investigated. The system enables excellent resolution of organic acids and nucleotides, and was applied to micro spectrophotometric identification of the iron(II)-*o*-phenanthroline complex.

INTRODUCTION

In capillary tube isotachophoresis, thermal, conductivity, potential gradient and single-wavelength UV absorption detectors are usually used. However, all these detectors are generally unsatisfactory for identifying the species of each zone. Multichannel photodiode array UV-visible detectors have recently been developed and used in high-performance liquid chromatography (HPLC)¹. They enable multi-wavelength detection and yield spectral information in a single chromatographic analysis. We have developed a multichannel spectrophotometric detector with parallel and cross flow cells for micro HPLC^{2,3}.

In isotachophoresis, PTFE (polytetrafluoroethylene) and FEP (fluorinated ethylene-propylene) tubes with an inside diameter of *ca.* 0.5 mm are commonly used for the migration tube. A decrease in the inside diameter of the migration tube will result in a decrease in the temperature difference between the centre of the tube and the wall, and the temperature profile will thus decrease. Moreover, the absolute increase in temperature is smaller, which reduces the convective disturbances. Therefore the use of narrow-bore tubes with smaller inside diameters will increase the resolution⁴.

In the present work, a fused-silica capillary tube of 0.25 mm I.D. was used as

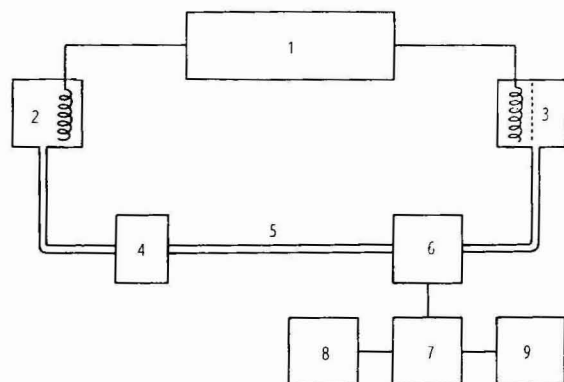


Fig. 1. Block diagram of the apparatus. 1 = Constant power supply; 2 = leading electrolyte; 3 = terminating electrolyte; 4 = sample injection port; 5 = capillary migration tube; 6 = multichannel photodiode array UV-visible detector; 7 = micro computer; 8 = monitorscope; 9 = plotter.

the migration tube in isotachophoresis, and a miniaturized multichannel photodiode array UV-visible detector was developed for capillary tube isotachophoresis. The system was applied to the analysis of real samples and to the micro spectrophotometric identification of the components.

EXPERIMENTAL

A block diagram of the apparatus is shown in Fig. 1. For isotachophoresis, an IP-2A instrument (Shimazu Seisakusho, Kyoto, Japan) was employed after replacing a FEP tube of 0.50 mm I.D. with a fused-silica tube of *ca.* 0.25 mm I.D. as the migration tube. The fused-silica tubing was obtained from SGE (Melbourne, Australia). For detection, a micro gate photodiode array detector MGPD, a micro computer MC-800, a monitorscope MC-910 and a plotter MC-920 (all from Union Gi-

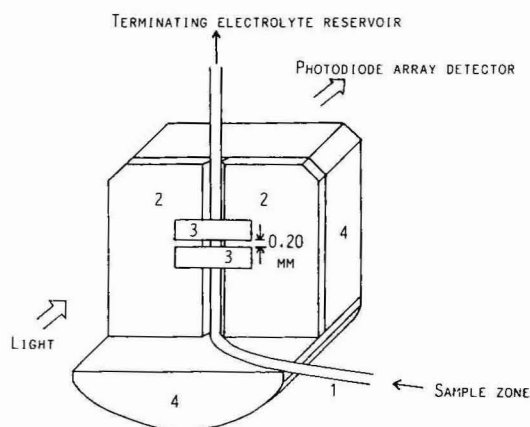


Fig. 2. Schematic diagram of the micro cross flow cell for capillary isotachophoresis. 1 = Fused-silica capillary tube (0.25 mm I.D.); 2 = stainless-steel slit block; 3 = aluminium slit tape; 4 = stainless-steel cell block.

ken, Osaka, Japan) were used. The MGPD system comprised 840 active photodiode array elements, two of which controlled each channel. Its spectral range and bandwidth were 200–800 nm and 1.4 nm, respectively.

Most UV-visible detectors used in conventional HPLC have a parallel flow cell, in which the light path is parallel to the direction of flow, and the typical cell volume of conventional flow cells is 8 μ l (light pathlength 10 mm). On the other hand, a cross flow cell is chiefly employed in micro HPLC to reduce the cell volume. The structure of the micro cross flow cell employed in isotachopheresis is illustrated in Fig. 2. Two stainless-steel slit blocks were fixed on the stainless-steel cell block, having a hole in the centre for the light path and a horizontal slit width of *ca.* 0.20 mm. The material coating the fused-silica capillary migration tube (0.25 mm I.D.) was removed near the outlet parts by use of a small flame, and the capillary was mounted between the two stainless-steel slit blocks. The vertical slit width was set at *ca.* 0.20 mm by two aluminium slit tapes. Thus, the cell volume was reduced to 0.01 μ l and the maximum light pathlength reduced to 0.25 mm, leading to a decrease in the observed light intensity. The latter problem was solved in this MGPD system by decreasing the number of optical parts such as lenses and mirrors, and reducing the distance between the light source and the flow cell and that between the flow cell and the grating.

For anion analysis, 0.01 *M* hydrochloric acid, β -alanine, Triton X-100 (pH 3.6) and 0.01 *M* sodium *n*-caproate (pH 7.5) were used for the leading and terminating electrolytes, respectively. Seven organic acids, maleic, fumaric, salicylic, phthalic, lactic, *p*-aminosalicylic and benzoic acid, and three nucleotides, adenosine 5'-monophosphate (AMP), adenosine 5'-diphosphate (ADP) and adenosine 5'-triphosphate (ATP), were used for the anion standard samples. Commercially available apple juice (30%) and cosmetic lotion were employed as the real samples without any pretreatment. For cation analysis, 0.005 *M* potassium acetate, acetic acid (pH 5.0) and 0.005 *M* γ -amino-*n*-butyric acid (pH 5.0) were used for the leading and terminating electrolytes, respectively. Iron(II)-*o*-phenanthroline complex (10 μ M) was prepared by mixing 0.01 *N* iron(II) ammonium sulphate and 0.01 *M* *o*-phenanthroline in the ratio of 1:4, and diluting in distilled and deionized water.

Sodium *n*-caproate, *p*-aminosalicylic acid and *o*-phenanthroline were purchased from Tokyo Chemical Industry (Tokyo, Japan), Kishida Chemical Industry (Osaka, Japan) and E. Merck (F.R.G.), respectively. Other reagents were obtained from Wako Chemical Industries (Osaka, Japan).

RESULTS AND DISCUSSION

Isotachopheretic separation with fused-silica capillary tube

Verheggen *et al.*⁴ demonstrated the importance of the inside diameter of the migration tube by using PTFE tubing. They tested PTFE narrow-bore tube with approximate inside diameters of 0.4, 0.2 and 0.1 mm, and found that with an I.D. of *ca.* 0.2 mm to be almost optimal, owing to the construction of the injection system and conductivity detector. On the other hand, the electroosmotic flow at low (centimolar) concentrations of electrolyte was found to be far from negligible with Pyrex glass tubes having inside diameters smaller than 0.4 mm. Since fused-silica tubing is suitable for "on line" UV detection, we tried to use a narrow-bore fused-silica tube

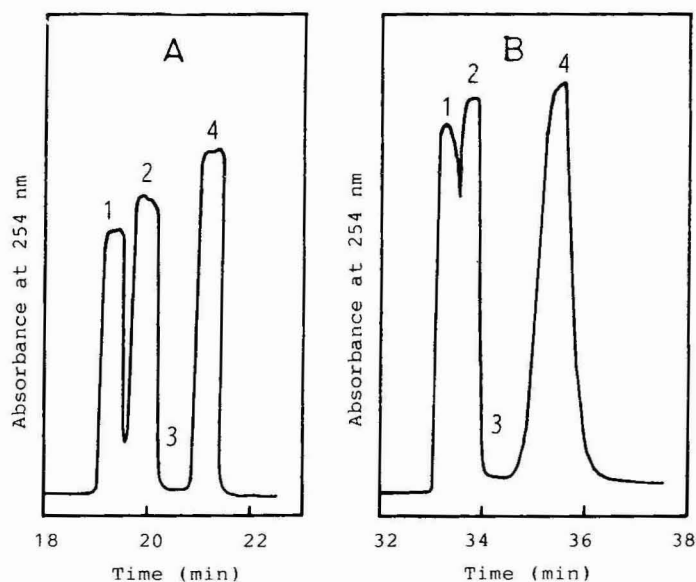


Fig. 3. Comparison of isotachophoretic separation with different migration tubes. A, Fused-silica tubing (200×0.25 mm I.D.); B, FEP tubing (75×0.50 mm I.D.). Zones: 1 = ATP; 2 = ADP; 3 = succinic acid; 4 = AMP. Sample amount injected: $2 \mu\text{l}$ of each 500 ppm mixture. Migration current: $25 \mu\text{A}$. Slit diameter: 0.17 mm (A), 0.30 mm (B).

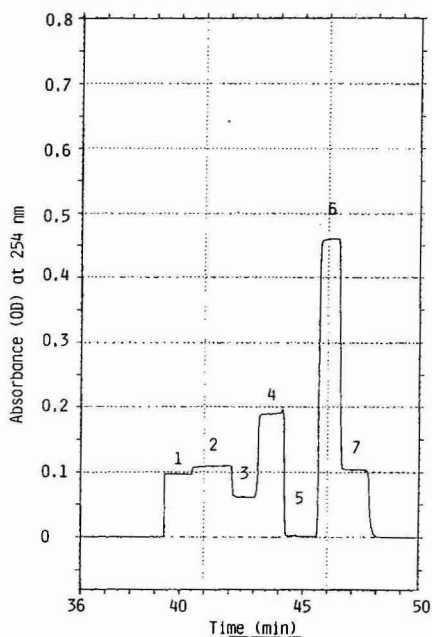


Fig. 4. Isotachophoretic separation of a standard mixture of seven organic acids with a fused-silica capillary tube. Zones: 1 = maleic acid; 2 = fumaric acid; 3 = salicylic acid; 4 = phthalic acid; 5 = lactic acid; 6 = *p*-aminosalicylic acid; 7 = benzoic acid. Sample amount injected: $2 \mu\text{l}$ of each 500 ppm mixture. Leading electrolyte: 0.01 *M* hydrochloric acid, β -alanine, Triton X-100 (pH 3.6). Terminating electrolyte 0.01 *M* sodium *n*-caproate (pH 7.5). Migration current: $25 \mu\text{A}$. Migration tube: fused-silica tubing $\times 0.25$ mm I.D.).

as the migration tube. Fig. 3 shows a comparison of isotachopherograms of a mixture of AMP, ADP, ATP and succinic acid with a FEP tube of *ca.* 0.50 mm I.D. and a fused-silica tube of *ca.* 0.25 mm I.D. In this case, a conventional single-wavelength UV detector UVD-10A (Shimazu Seisakusho) was used for zone detection with slit diameters of 0.30 mm for the FEP tube and 0.17 mm for the fused-silica tube. Clearly, the use of the fused-silica tube increased the resolution at a shorter analytical time, compared with that of the conventional FEP tube.

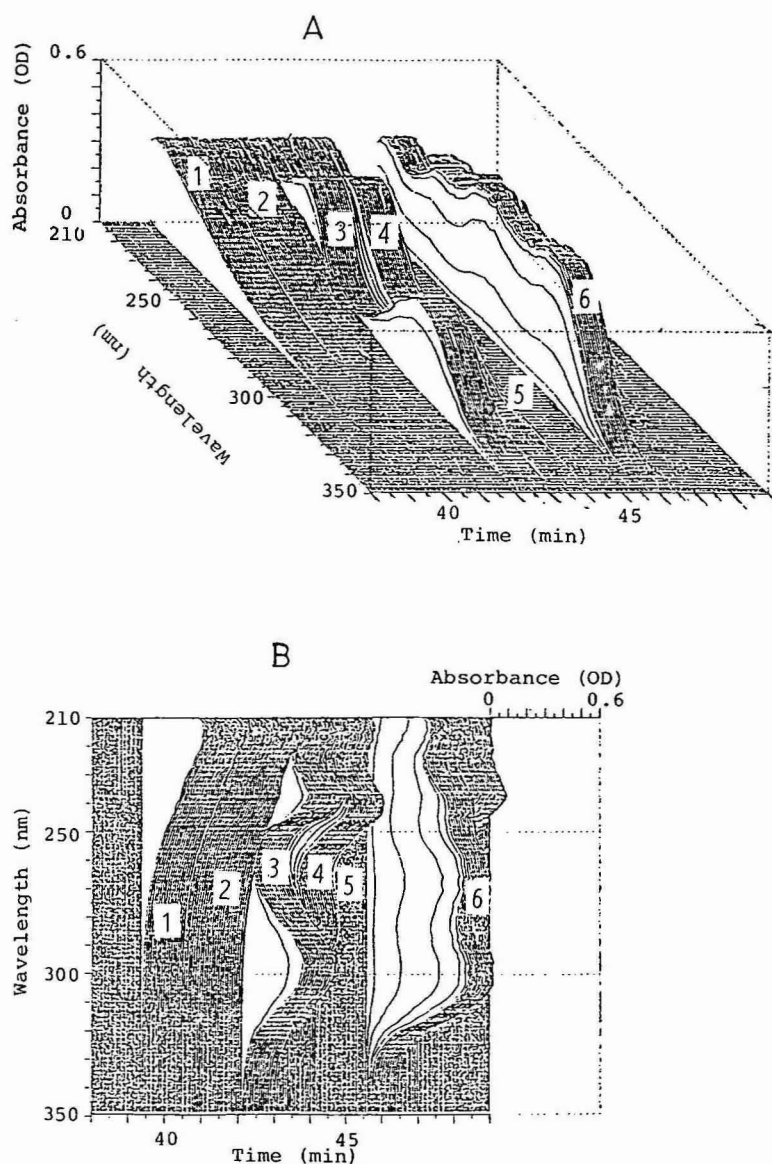


Fig. 5.

(Continued on p. 172)

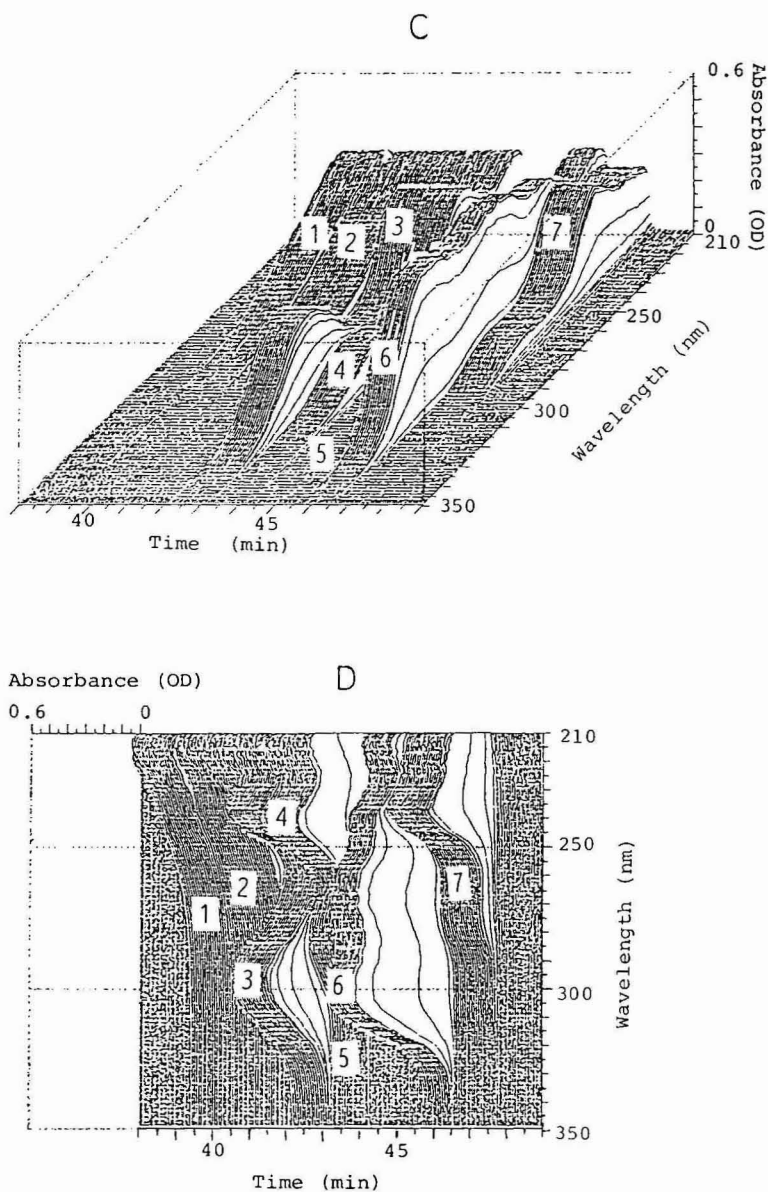


Fig. 5. Different three-dimensional isotachopherograms of a standard mixture of seven organic acids. A, Forward three-dimensional plot at 45°; B, forward plot at 90°; C, backward plot at 45°; D, backward plot at 90°. The number of zones and experimental conditions are as in Fig. 4.

Multichannel spectrophotometric detection in isotachopheresis

An isotachopheretic separation of a standard mixture of organic acids was carried out in a fused-silica tube (500 × 0.25 mm I.D.) by using the multichannel photodiode array UV-visible detector and a cross flow cell (volume 0.01 μ l). Fig. 4

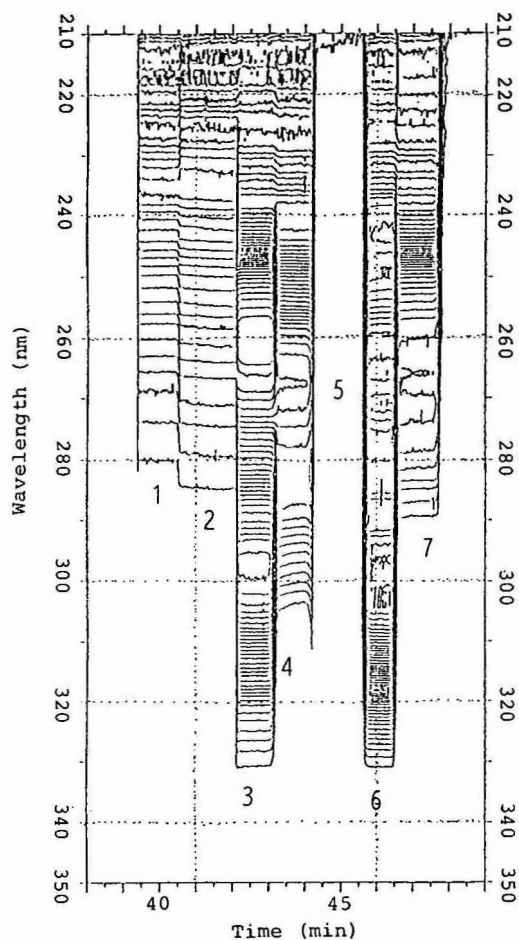


Fig. 6. Contour plot for isotachopheresis of a standard mixture of seven organic acids. The number of zones and experimental conditions are as in Fig. 4. Absorbance step: 0.01.

shows the conventional isotachopherogram monitored at a single wavelength, 254 nm. The seven organic acids were very well separated in the fused-silica capillary tube at a migration current of 25 μ A. However, it is rather difficult to identify each migration zone, except for lactic acid which has no UV absorption, from the isotachopherogram at the single wavelength. Fig. 5 shows three-dimensional isotachopherograms obtained in the proposed system: A and B are the forward isotachopherograms, C and D the backward isotachopherograms; A and C are the 45° angle plots, B and D the 90° angle plots, respectively. Thus, the addition of the wavelength axis to the absorbance and time axes in the isotachopherogram dramatically improves the identification within each migration zone. The zone of benzoic acid could not be found in the forward isotachopherograms, since the UV absorbance of *p*-aminosalicylic acid was too large, while it was clearly seen in the backward isotachopherograms. The 45° angle plots were useful for basic quantitative and qualitative information, while the 90° angle plots gave exact qualitative information. Fig. 6 shows

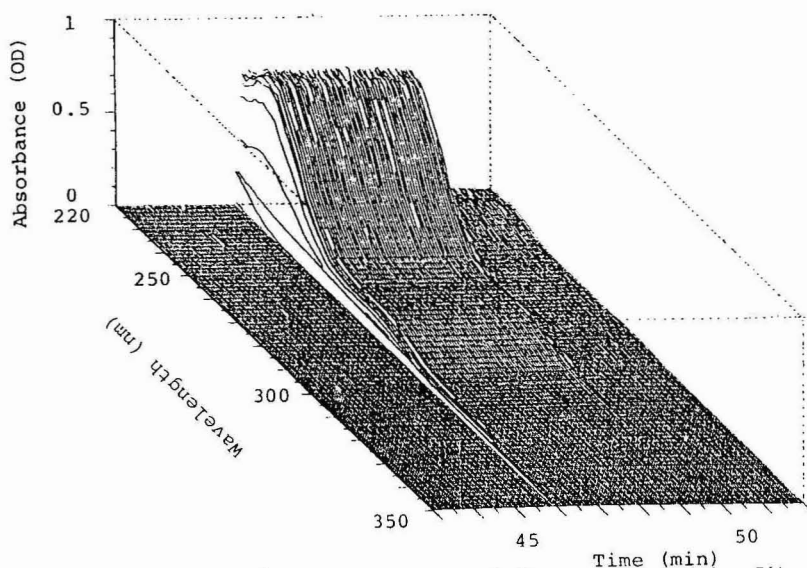


Fig. 7. Multichannel spectrophotometric detection of benzoic acid in a cosmetic lotion. Sample amount injected: $1\ \mu\text{l}$ of raw cosmetic lotion. Other experimental conditions as in Fig. 4.

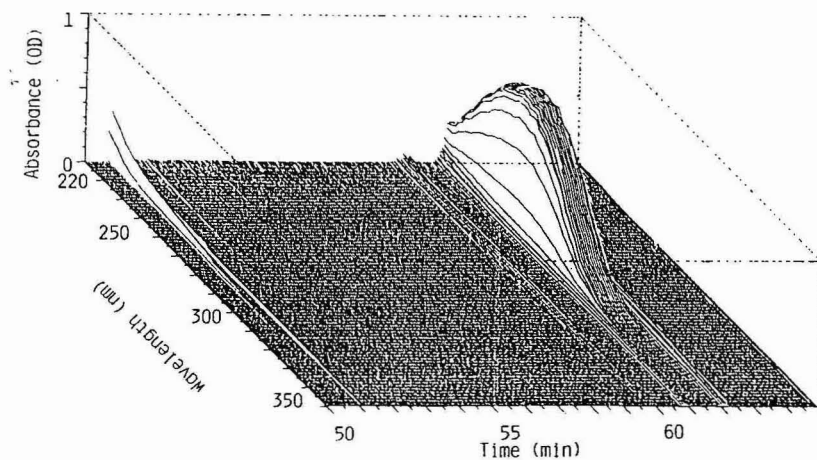


Fig. 8. Multichannel spectrophotometric detection of ascorbic acid in apple juice. Sample amount injected: $2\ \mu\text{l}$ of raw apple juice (30%). Other experimental conditions as in Fig. 4.

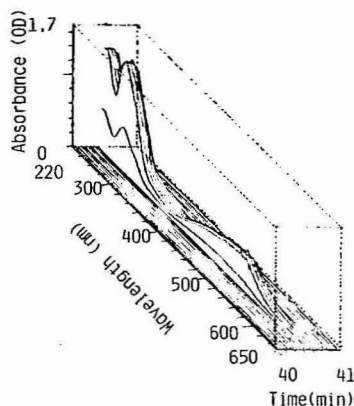


Fig. 9. Three-dimensional isotachopherogram of the iron(II)-*o*-phenanthroline complex obtained with a fused-silica capillary tube. Sample amount injected: 10 μl of 10 μM (5.6 ng as iron). Leading electrolyte: 0.005 *M* potassium acetate, acetic acid (pH 5.0). Terminating electrolyte: 0.005 *M* γ -amino-*n*-butyric acid, acetic acid (pH 5.0). Migration current: 25 μA . Migration tube: fused-silica tubing (500 \times 0.25 mm I.D.).

contour plots at absorbance steps of 0.01 units for isotachopheresis of the organic acid mixture. It should be noted that a rectangular shape is characteristic in isotachopheresis, while a founded shape is observed in HPLC. This plot was useful to check the purity of each migration zone.

The proposed system was applied to the determination of organic acids in real samples. Figs. 7 and 8 show the three-dimensional isotachopherograms at 45° angle of cosmetic lotion and apple juice (30%) directly injected into the described system. Benzoic acid and ascorbic acid in each sample could clearly be identified by using the UV absorption spectra.

Application to micro spectrophotometric identification of samples

According to the Kohlrausch equation, in isotachopheresis, the sample injected can be concentrated or diluted to an extent related mainly to the concentration of leading ion used. The proposed system was applied to a very dilute sample in order to obtain the complete UV-visible spectrum by means of isotachopheretic concentration. Fig. 9 shows the three-dimensional isotachopherogram of 10 μl of 10 μM iron(II)-*o*-phenanthroline complex which could be separated from excess of *o*-phenanthroline. In this case, 10 μl of sample were concentrated to about 0.2 μl by isotachopheresis. As shown in Fig. 9, four complete absorption spectra were obtained with a sample ammount of only 5.6 ng (as iron).

CONCLUSIONS

The use of a fused-silica capillary tube with an inside diameter smaller than the *ca.* 0.5 mm commonly used improves the resolution without an appreciable electroosmotic flow. A multichannel photodiode array detector can be employed. A cross flow cell of volume only 0.01 μl is sufficient to detect migration zones, since the sample is generally concentrated by migration in isotachopheresis, while it is diluted by diffusion in HPLC or zone electrophoresis.

The system can be applied to micro spectrophotometric identification of samples; a full UV-visible absorption spectrum of iron(II)-*o*-phenanthroline can be obtained with a sample amount of *ca.* 1 ng (as iron).

ACKNOWLEDGEMENT

The authors thank Dr. H. Sasagawa of Union Giken for his technical assistance.

REFERENCES

- 1 B. G. Wills, *Application Notes*, No. 295-5, Hewlett-Packard, Palo Alto, CA, 1980.
- 2 T. Takeuchi and D. Ishii, *J. Chromatogr.*, 288 (1984) 451.
- 3 D. Ishii, M. Goto and T. Takeuchi, *J. Chromatogr.*, 316 (1984) 441.
- 4 T. P. E. M. Verheggen, F. E. P. Mikkers and F. M. Everaerts, *J. Chromatogr.*, 132 (1977) 205.

CHROM. 17 977

QUANTITATIVE ANALYSIS OF HYDROCARBONS IN GASOLINES BY CAPILLARY GAS-LIQUID CHROMATOGRAPHY

II. ISOTHERMAL AND TEMPERATURE-PROGRAMMED ANALYSES

E. MATISOVÁ* and J. KRUPČÍK

*Department of Analytical Chemistry, Faculty of Chemical Technology, Slovak Technical University, Jánska
1, 812 37 Bratislava (Czechoslovakia)*

P. ČELLÁR

Slovnaft AV VVZ, Vlčie hrdlo, 824 12 Bratislava (Czechoslovakia)

and

A. KOČAN

*Research Institute of Preventive Medicine, Department of Mass Spectrometry, Limbova 14, 833 01 Bratislava
(Czechoslovakia)*

(First received May 15th, 1985; revised manuscript received June 17th, 1985)

SUMMARY

Quantitative analysis of the gasoline fraction of crude oil (paraffins, branched paraffins, aromatics and naphthenes) and structure group analysis has been performed by high resolution capillary gas chromatography using squalane columns with different film thicknesses under temperature-programmed conditions. The results obtained were compared with those from isothermal analysis. "The modified standard addition method" was used. The contents of aromatic hydrocarbons determined on a polar stationary phase, SP-2340, were in good agreement with those obtained on squalane.

INTRODUCTION

High resolution capillary gas chromatography (HRCGC) approaches the ultimate goal of a petroleum chemist, *i.e.*, complete component analysis, and provides the petrochemical engineer with the information and knowledge required to convert crude petroleum into profitable products. It is one of the few techniques capable of distinguishing between paraffins and naphthenes, thus providing a true PONA (paraffins, olefins, naphthenes and aromatics) analysis which is often required in the control of gasoline production. The disadvantage of this approach is that every peak must be identified in the chromatogram or at least classified according to the chemical group to which it belongs.

Though squalane has certain shortcomings as a liquid phase for capillary columns, *e.g.*, low maximum operating conditions and it is difficult to prepare a stable

column when using glass or fused-silica tubing^{1,2}, it has been used in the analysis of hydrocarbons because of its high selectivity towards hydrocarbons and the wealth of retention data already published. Most published data on the retention properties of hydrocarbons in the gasoline range have been obtained under isothermal conditions³⁻⁸. However, economics demands shorter analyses. Therefore, most practical analyses are temperature programmed⁹⁻¹². Most hydrocarbons exhibit a change in retention relative to say, the normal hydrocarbons as the temperature is changed. The practical result is that the relative elution times and even the elution order can change with different chromatographic conditions¹¹.

Recently Johansen *et al.*¹³ published a method of analysis of complex gasoline samples on an OV-101 capillary column under temperature-programmed conditions using modern sophisticated laboratory data systems. However, an identification based only on the so-called relative retention time obtained under the actual temperature-programmed conditions might be insufficient for a sample of unknown composition.

The combination of a gas chromatograph, a mass spectrometer and a computer is the premier technique for identifying or at least classifying unknown peaks in a chromatogram¹¹. Some difficulties in the identification of hydrocarbons may arise from the similarity of the mass spectra of isomeric hydrocarbons.

In our previous paper¹⁴ we elucidated further the composition of the gasoline fraction of crude oil using HRCGC and by carrying out the identification on the basis of retention data and gas chromatography-mass spectrometry (GC-MS). We pointed out the problems connected with generally acknowledged methods of quantitative analysis of gasolines. The aim of the present study was to compare the capillary GC analysis of the gasoline fraction of crude oil under isothermal and temperature-programmed conditions.

EXPERIMENTAL

Measurements were performed by two methods. In the first method a Hewlett-Packard 58 80 A gas chromatograph equipped with an integrator C R1 A (Shimadzu, Japan) and a metal capillary column (100 m × 0.25 mm I.D.) with a thick film of squalane (0.5 µm) was employed. Helium was the carrier gas. A temperature programme of 40–110°C with a gradient of 0.3°C/min was used. GC-MS measurements were performed using an HP 59 95 instrument under similar chromatographic conditions.

In the second method a Carlo Erba gas chromatograph equipped with an integrator Autolab 6 300 and a glass capillary column (98 m × 0.25 mm I.D.) with a thin film of squalane (0.1 µm) was employed. Hydrogen was the carrier gas. Both isothermal conditions (57.8°C) and temperature-programmed conditions (isothermal at 40°C up to the elution of *n*-heptane, then programmed to 80°C at a rate of 0.8°C/min, finally isothermal at 80°C) were used. A fused-silica capillary column (60 m × 0.25 mm I.D.) containing SP-2340 and nitrogen as carrier gas at 80°C was also employed.

Both chromatographs were equipped with a flame ionization detector and an inlet stream splitter.

A gasoline fraction of crude oil enriched with higher boiling hydrocarbons was analysed and was injected with a 1-µl Hamilton syringe.

Peak areas were measured as either the digital integration response, or the retention time, t_R in mm, multiplied by the peak height, h also in mm.

RESULTS AND DISCUSSION

In our previous paper we used "the modified standard addition method" for the isothermal quantitative analysis of hydrocarbons in gasolines and showed that this method gives more correct results than does "the area per cent technique". Both methods are based on the assumption that the relative weight responses (RWR) of hydrocarbons are nearly constant for the whole series of hydrocarbons^{10,16-18}. "The modified standard addition method" does not require the elution of all components from the column and in contrast to "the standard addition method" does not require precise and reproducible injection. The sum of the determined contents of hydrocarbons in a gasoline sample may be far from 100%, as is always the case in "the area per cent technique", where there are large errors due to the presence of very small peaks below the flame ionization detection limit. Therefore, we have used "the modified standard addition method" for quantitative analysis of hydrocarbons also under temperature-programmed conditions.

Quantitative analysis of hydrocarbons on squalane

A temperature programme was used to shorten the analysis time for gasoline, and the results obtained were compared with those of isothermal analysis. Two methods were applied: a lower temperature gradient (0.3°C/min) and a column with a thick film of squalane; and a higher temperature gradient (0.8°C/min) and a column of comparable length but with a thin film of squalane. The starting temperature was 40°C. To avoid column bleeding in a glass capillary column with a thin film of squalane, the final temperature was 80°C. Therefore, a part of the analysis was performed under isothermal conditions. The number of unresolved peaks and the analysis time are highly dependent on the temperature gradient used. The C₈-C₁₀ *n*-alkanes were used as standards. To avoid peaks discrimination at the split injection compounds peak area was always related to the peak area of the near eluting standard.

The results of the temperature-programmed quantitative analysis of hydrocarbons are given in Table I, and chromatograms of the separation of gasoline constituents are given in Figs. 1, 2. The component numbering is as in Table I. The compound identification was performed by GC-MS with the help of GC and GC-MS under isothermal conditions. In Table I are included also the results of quantitative analysis under isothermal conditions (57.8°C) on a thin film column.

On the basis of these results the following conclusions can be drawn. The analysis time for gasoline up to the elution of *n*-decane on a metal capillary column with a thick film of squalane is relatively long, 173 min, and is similar to that for a published isothermal analysis of gasoline on a high resolution capillary column, 180 min¹⁴. However, the number of unresolved peaks is significantly increased using temperature programming. The analysis time was lower on the thin film column either under temperature-programmed (63 min) or isothermal conditions (68 min). The number of unresolved peaks under temperature-programmed conditions was even higher as on a thick film column of comparable length. Thus, the best peak resolution was obtained under isothermal conditions, though many peaks still re-

TABLE I

RESULTS OF THE QUANTITATIVE ANALYSIS OF GASOLINE ON SQUALANE BY THE MODIFIED STANDARD ADDITION METHOD

Temperature programmes: TP-1, 40–110°C, 0.3°C/min, TP-2, isothermally at 40°C up to *n*-C₇, then 40–80°C at 0.8°C/min, isothermally at 80°C; each using digital integration. Isothermal analyses at 57.8°C; peaks areas from $t_R \times h$.

Peak No.	Component	Weight %		
		TP-1	TP-2	Isothermal
2	2-Methylbutane	0.035	0.033	0.038
3	<i>n</i> -Pentane	0.200	0.186	0.209
4	2,2-Dimethylbutane	0.005	0.005	—
5	Cyclopentane	0.122	0.112	0.109
6	2,3-Dimethylbutane	0.080	0.074	} 0.998
7	2-Methylpentane	0.809	0.834	
8	3-Methylpentane	0.623	0.657	0.746
9	<i>n</i> -Hexane	2.059	2.122	2.433
10	2,2-Dimethylpentane	} 1.449	} 1.395	} 1.567
11	Methylcyclopentane			
12	2,4-Dimethylpentane	0.106	0.095	
13	Benzene	0.113	0.111	0.121
14	3,3-Dimethylpentane	0.012	0.014	0.015
15	Cyclohexane	1.043	0.965	1.054
16	2-Methylhexane	1.180	1.238	1.396
17	2,3-Dimethylpentane	} 0.551	} 0.578	0.550
18	1,1-Dimethylcyclopentane			0.040
19	3-Methylhexane	1.746	1.886	2.107
20	1(<i>cis</i>),3-Dimethylcyclopentane	0.575	0.554	0.623
21	3-Ethylpentane	} 0.713	} 0.707	0.227
22	1(<i>trans</i>),3-Dimethylcyclopentane			0.608
23	1(<i>trans</i>),2-Dimethylcyclopentane	1.213	1.206	1.372
24	<i>n</i> -Heptane	4.629	4.841	5.477
25	2,2-Dimethylhexane	} 0.248	} 0.226	0.020
26	1(<i>cis</i>),2-Dimethylcyclopentane			0.226
27	1,1,3-Trimethylcyclopentane	0.150	0.155	0.149
28	Methylcyclohexane	3.295	3.346	3.781
29	2,5-Dimethylhexane	0.290	0.281	0.325
30	2,4-Dimethylhexane	0.335	} 1.363	0.352
31	Ethylcyclopentane	1.052		1.149
32	1(<i>trans</i>),2(<i>cis</i>),4-Trimethylcyclopentane	0.535	0.520	0.575
33	3,3-Dimethylhexane	} 1.205	0.007	0.033
34	Toluene		1.265	1.469
35	1(<i>trans</i>),2(<i>cis</i>),3-Trimethylcyclopentane	0.746	0.730	0.820
36	2,3,4-Trimethylpentane	0.090	0.085	0.092
37	2,3-Dimethylhexane	0.295	0.340	0.307
38	2-Methyl-3-ethylpentane	0.196	0.244	0.194
39	1,1,2-Trimethylcyclopentane	0.106	} 2.756	} 3.046
40	2-Methylheptane	2.629		
41	4-Methylheptane	0.778	0.766	0.872
42	3,4-Dimethylhexane	0.175	0.168	0.153
43	3-Methylheptane	1.780	1.855	1.794
44	3-Methyl-3-ethylpentane	} 0.049	0.029	0.052
45	1(<i>cis</i>),2(<i>trans</i>),4-Trimethylcyclopentane		} 0.030	0.039
46	Naphthene	0.041		0.026

TABLE I (continued)

Peak No.	Component	Weight %		
		TP-1	TP-2	Isothermal
47	1(<i>cis</i>),2(<i>trans</i>),3-Trimethylcyclopentane	0.205	0.190	0.201
48	1(<i>cis</i>),3-Dimethylcyclohexane	1.456	1.477	} 1.212
49	1(<i>trans</i>),4-Dimethylcyclohexane	0.164	0.121	
50	1,1-Dimethylcyclohexane	0.512	0.467	0.665
51	1-Methyl-2(<i>trans</i>)-ethylcyclopentane	0.413	0.470	0.517
52	1-Methyl-3(<i>cis</i>)-ethylcyclopentane	1.157	1.049	1.270
53	1-Methyl-1-ethylcyclopentane	0.137	0.113	0.103
54	<i>n</i> -Octane	5.771	6.132	6.164
55	1(<i>cis</i>),2(<i>cis</i>),3-Trimethylcyclopentane + 1(<i>trans</i>),2-dimethylcyclohexane	1.003	0.749	1.053
56	1(<i>cis</i>),4-Dimethylcyclohexane + 1(<i>trans</i>),3-dimethylcyclohexane	0.274	} 0.244	} 0.222
57	Branched paraffin			
58	Branched paraffin	—	0.017	0.016
59	2,3,5-Trimethylhexane	} 0.264	} 0.170	0.082
60	Isopropylcyclopentane			0.174
61	Branched paraffin	—	} 0.023	—
62	Branched paraffin	—		—
63	2,2-Dimethylheptane	} 0.066	0.038	0.025
64	Naphthene		0.063	0.034
65	2,4-Dimethylheptane	} 0.457	0.285	0.278
66	1-Methyl-2(<i>cis</i>)-ethylcyclopentane		0.135	0.158
67	Branched paraffin	—	—	—
68	2,2,3-Trimethylhexane	0.033	} 0.089	0.032
69	Naphthene	0.053		} 1.324
70	2,6-Dimethylheptane	} 1.249	} 1.416	
71	Naphthene			} 0.027
72	1(<i>cis</i>),2-Dimethylcyclohexane	} 0.914	} 0.707	} 0.839
73	<i>n</i> -Propylcyclopentane			
74	2,5-Dimethylheptane	0.470		0.461
75	3,5-Dimethylheptane	0.142	} 3.064	0.133
76	Ethylbenzene	} 2.399		} 2.266
77	Ethylcyclohexane			
78	3,3-Dimethylheptane	0.026	} 0.026	0.029
79	Branched paraffin	0.010		—
80	Naphthene	} 1.331		0.190
81	Naphthene		} 1.457	1.288
82	1,1,3-Trimethylcyclohexane	0.307		0.274
83	Branched paraffin	0.116		0.112
84	1(<i>cis</i>),3(<i>cis</i>),5-Trimethylcyclohexane	} 0.427	0.196	} 0.310
85	Branched paraffin		0.499	
86	Branched paraffin	0.030	0.032	0.010
87	Cycloalkane + <i>p</i> -xylene	} 0.829	} 0.793	0.465
88	Branched paraffin			0.382
89	<i>m</i> -Xylene	1.128	1.159	1.327
90	Branched paraffin	—	—	—
91	Branched paraffin	0.642		0.640
92	Branched paraffin	0.010	0.690	0.011
93	Branched paraffin	} 0.493	0.113	0.203
94	Naphthene		0.165	0.317
95	1(<i>trans</i>),2(<i>cis</i>),4-Trimethylcyclohexane	0.212	0.268	0.172

(Continued on p. 182)

TABLE I (continued)

Peak No.	Component	Weight %		
		TP-1	TP-2	Isothermal
96	1(<i>trans</i>),2(<i>trans</i>),4-Trimethylcyclohexane + 1(<i>trans</i>),3(<i>trans</i>),5-trimethylcyclohexane	0.309	0.300	0.255
97	4-Methyloctane	0.911	1.016	0.890
98	2-Methyloctane	1.070	1.112	1.056
99	Naphthene	0.135	*	0.084
100	Naphthene	} 0.310	} 0.147	0.084
101	Ethylheptane			0.157
102	<i>o</i> -Xylene	} 2.593	1.017	} 2.551
103	3-Methyloctane		1.606	
104	Naphthene			0.237
105	Branched paraffin	0.031	—	0.013
106	Naphthene	0.081	0.064	0.064
107	Naphthene	0.014	0.022	0.013
108	Naphthene	} 0.103	} 0.094	} 0.079
109	Naphthene			
110	Naphthene	0.066	0.054	0.053
111	1(<i>trans</i>),2(<i>cis</i>),3-Trimethylcyclohexane	0.107	0.095	0.094
112	1,1,2-Trimethylcyclohexane + 3,3-diethylpentane (5:1)	0.542	0.627	0.492
113	1(<i>cis</i>),2(<i>trans</i>),4-Trimethylcyclohexane	} 0.400	} 0.273	} 0.290
114	Branched paraffin			
115	1(<i>cis</i>),2(<i>cis</i>),4-Trimethylcyclohexane + 1(<i>cis</i>),3(<i>cis</i>),4-trimethylcyclohexane	0.266	} 0.197	0.223
116	Naphthene	0.029		0.028
117	Naphthene	} 0.230	} 0.217	} 0.159
118	Naphthene			
119	Methylethylcyclohexane	0.510	} 0.447	0.424
120	Naphthene	0.075		0.029
121	Naphthene	0.081	} 0.880	0.015
122	Isopropylbenzene	} 0.739		} 0.583
123	Naphthene			
124	Naphthene	—	0.016	—
125	Naphthene	} 5.470	0.089	0.046
126	<i>n</i> -Nonane		5.455	5.068
127	Naphthene	0.170	0.116	0.110
128	Naphthene	—	—	—
129	Naphthene + branched paraffin (1:1)	—	—	—
130	Naphthene	—	—	—
131	Naphthene	—	—	—
132	Naphthene	} 0.196	} 0.355	} 0.065
133	Naphthene			
134	Branched paraffin	} 0.071	} 0.355	} 0.033
135	Branched paraffin			
136	Naphthene	0.258		0.299
137	Naphthene	—	—	—
138	Naphthene	} 0.349	} 0.208	} 0.067
139	Naphthene			
140	Branched paraffin			0.085
141	Naphthene	} 0.532	} 0.385	} 0.461
142	Naphthene			

TABLE I (continued)

Peak No.	Component	Weight %		
		TP-1	TP-2	Isothermal
143	Naphthene	—	0.200	0.017
144	Naphthene	—		
145	Branched paraffin	0.230	0.063	0.141
146	Naphthene	0.049		
147	Naphthene		0.123	0.036
148	Naphthene	0.062		
149	Branched paraffin		0.099	0.255
150	Naphthene	1.002		
151	Naphthene		0.381	0.249
152	Branched paraffin	0.078		
153	<i>n</i> -Propyl benzene		0.924	0.986
154	Naphthene	—		
155	Branched paraffin	0.104	0.089	0.076
156	Branched paraffin			
157	Naphthene	1.289	0.714	0.663
158	C ₉ naphthene			
159	C ₉ naphthene	0.094	1.203	
160	Naphthene			1.482
161	2,6-Dimethyloctane	—	—	
162	Branched paraffin	0.324	0.088	0.020
163	Branched paraffin			
164	Branched paraffin	0.101	0.102	
165	Branched paraffin			0.610
166	2,5-Dimethyloctane	0.588	0.375	
167	1-Methyl-3-ethylbenzene			0.713
168	1-Methyl-4-ethylbenzene	0.382	0.220	
169	Naphthene			0.132
170	Naphthene	0.050	0.107	
171	C ₁₀ branched paraffin			0.097
172	Branched paraffin	—	—	
173	Branched paraffin	0.138	0.046	0.044
174	C ₁₀ branched paraffin	0.087	0.046	0.044
175	Naphthene			
176	Branched paraffin	—	0.031	—
177	Branched paraffin	—	—	—
178	Branched paraffin	—	—	—
179	Naphthene	0.095	0.080	0.060
180	Naphthene			
181	Naphthene	0.197	—	—
182	Branched paraffin	—	—	—
183	Branched paraffin	—	—	—
184	Branched paraffin	—	—	—
185	1-Methyl-2-ethylbenzene	0.583	0.760	0.615
186	Branched paraffin	0.301	0.119	0.190
187	Branched paraffin	0.049	—	
188	Branched paraffin	—	—	—
189	Naphthene	0.257	0.056	—
190	Naphthene			
191	1,3,5-Trimethylbenzene	0.193	0.203	0.173
192	Branched paraffin	—	—	—
193	Branched paraffin	**	0.177	0.125
194	Branched paraffin	—	—	—

(Continued on p. 184)

TABLE I (continued)

Peak No.	Component	Weight %			
		TP-1	TP-2	Isothermal	
195	Naphthene	} 0.736	0.316	0.252	
196	4-Methylnonane		} 0.739	0.637	
197	<i>tert.</i> -Butylbenzene	} 0.077			
198	Naphthene		} 1.123	} 0.106	—
199	Naphthene				
200	2-Methylnonane	} 0.104	0.738	0.579	
201	Naphthene		0.133	0.132	
202	C ₁₀ naphthene	} 0.060	} 0.116	} 0.053	
203	Naphthene				
204	Naphthene	} 0.056	} 0.082	} 0.040	
205	Naphthene				
206	Naphthene	—	—	—	
207	3-Methylnonane	0.755	0.506	0.414	
208	Naphthene	0.026	} 0.164	} 0.052	
209	Naphthene	0.114			
210	1,2,4-Trimethylbenzene	0.770	0.734	0.679	
211	Branched paraffin	—	—	—	
212	Naphthene	} 0.065	0.017	—	
213	Branched paraffin		} 0.198	—	
214	<i>sec.</i> -Butylbenzene	0.166		0.146	
215	Branched paraffin	} 0.186	—	—	
216	Naphthene		} 0.369	0.148	
217	Naphthene	0.238		0.208	
218	Naphthene	0.165	0.160	0.120	
219	Branched paraffin	0.087	—	—	
220	Naphthene	0.101	0.098	0.031	
221	Branched paraffin	—	—	—	
222	Two naphthenes	0.174	} 0.304	} 0.186	
223	Branched paraffin	—			
224	Naphthene	0.042	} 0.091	0.033	
225	Naphthene	} 0.190		} 0.020	
226	Branched paraffin				
227	Branched paraffin	} 0.108	} 0.067	} 0.033	
228	Naphthene				
229	Naphthene	} 0.147	} 0.200	} 0.167	
230	Naphthene				
231	Branched paraffin	—	—	—	
232	Branched paraffin	—	0.034	—	
233	Naphthene	0.318	0.305	0.277	
234	1,2,3-Trimethylbenzene	—	0.034	—	
235	Branched paraffin	0.092	0.069	0.065	
236	1-Methyl-4-isopropylbenzene	0.048	0.049	} 2.148	
237	Branched paraffin	2.513	2.317		
238	<i>n</i> -Decane				

* Co-eluted with peak 97.

** Co-eluted with peaks 189, 190.

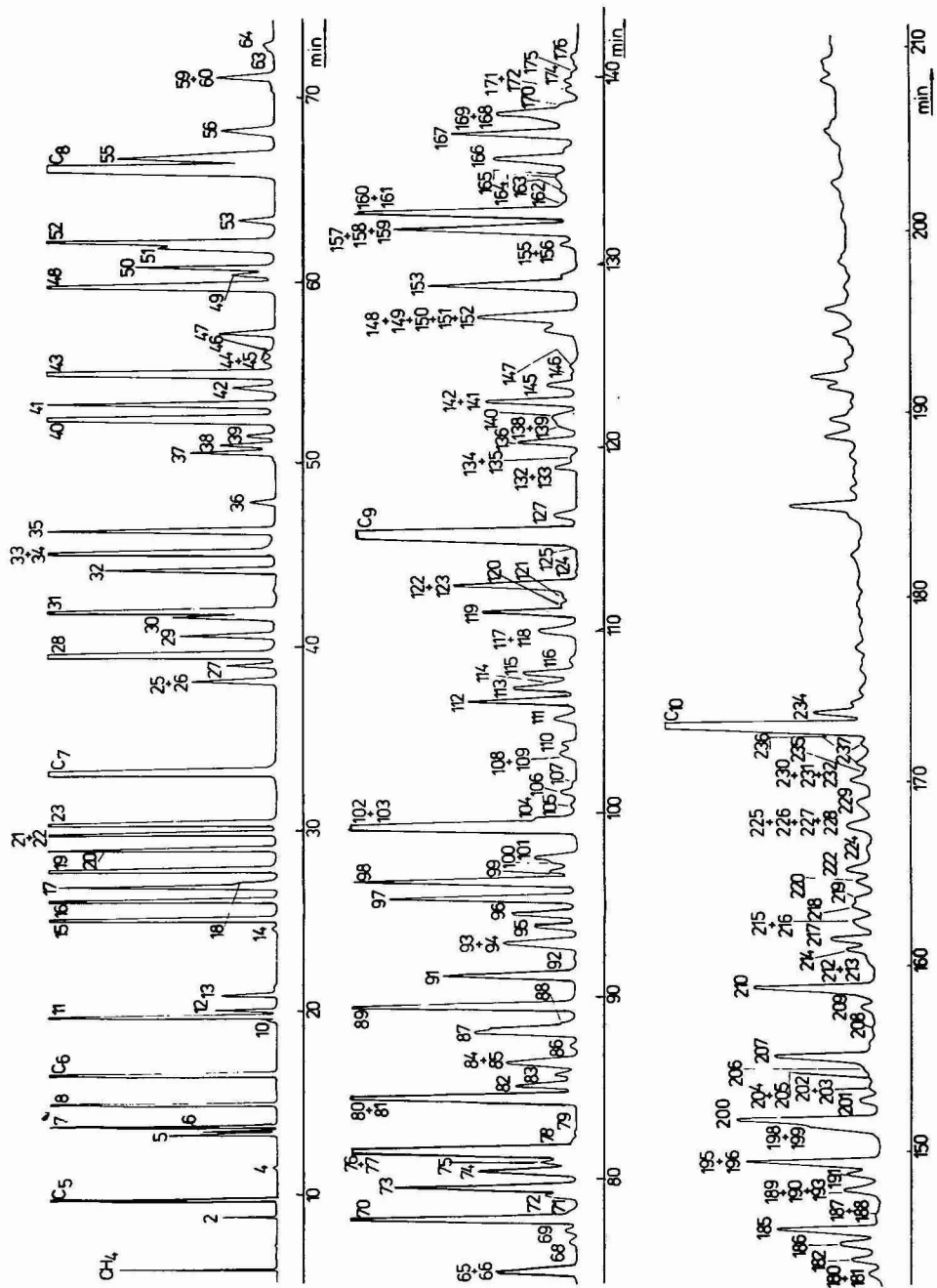


Fig. 1. Chromatogram of the separation of the hydrocarbon constituents of the gasoline fraction of crude oil on a metal capillary column containing a thick film of squalene under temperature-programmed conditions. For experimental details, see text.

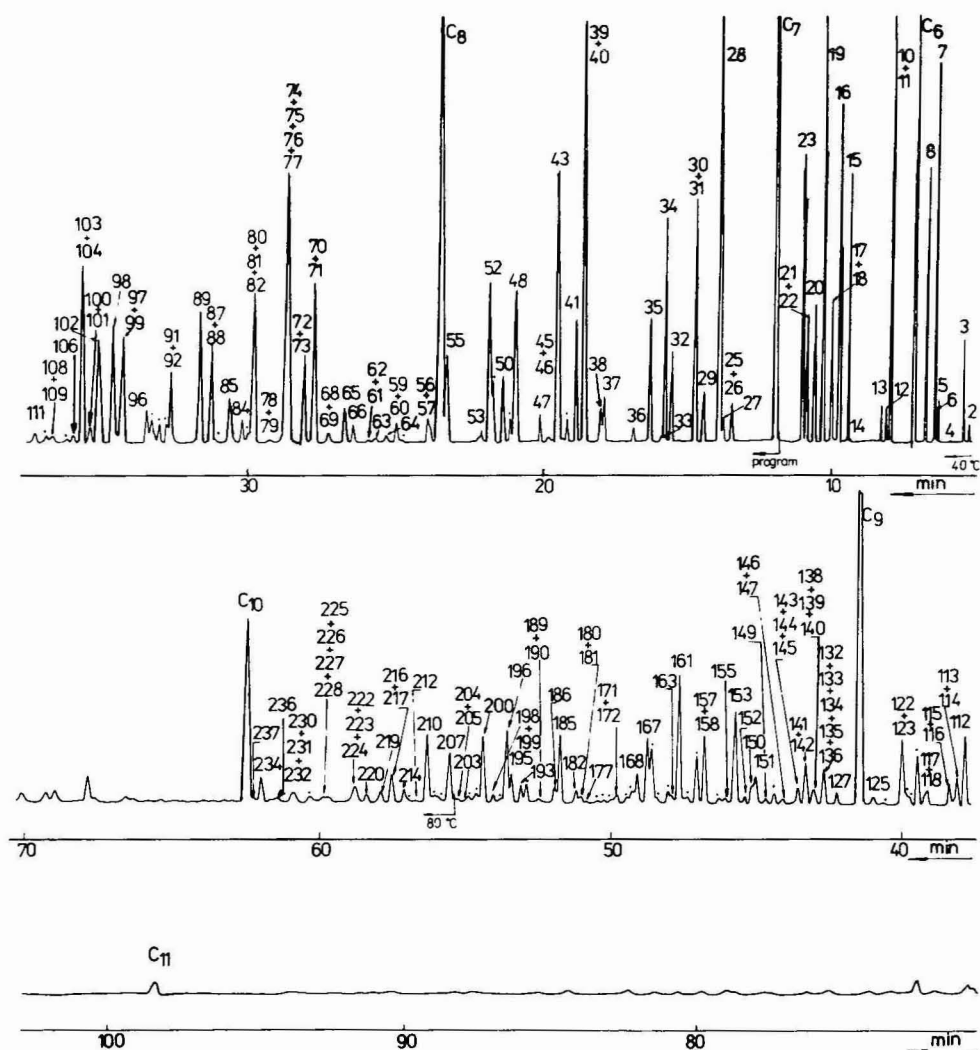


Fig. 2. Chromatogram of the separation of the hydrocarbon constituents of the gasoline fraction of crude oil on a glass capillary column containing a thin film of squalane under temperature-programmed conditions. For experimental details, see text.

TABLE II

GROUP ANALYSIS OF GASOLINE ON SQUALANE BY THE MODIFIED STANDARD ADDITION METHOD

Chromatographic conditions as in Table I.

Compounds	Weight %		
	TP-1	TP-2	Isothermal
<i>n</i> -Paraffins	20.512	21.053	21.473
Branched paraffins	25.984	25.789	25.324
Aromatics	9.198	9.552	8.957
Naphthenes	31.733	29.260	30.148

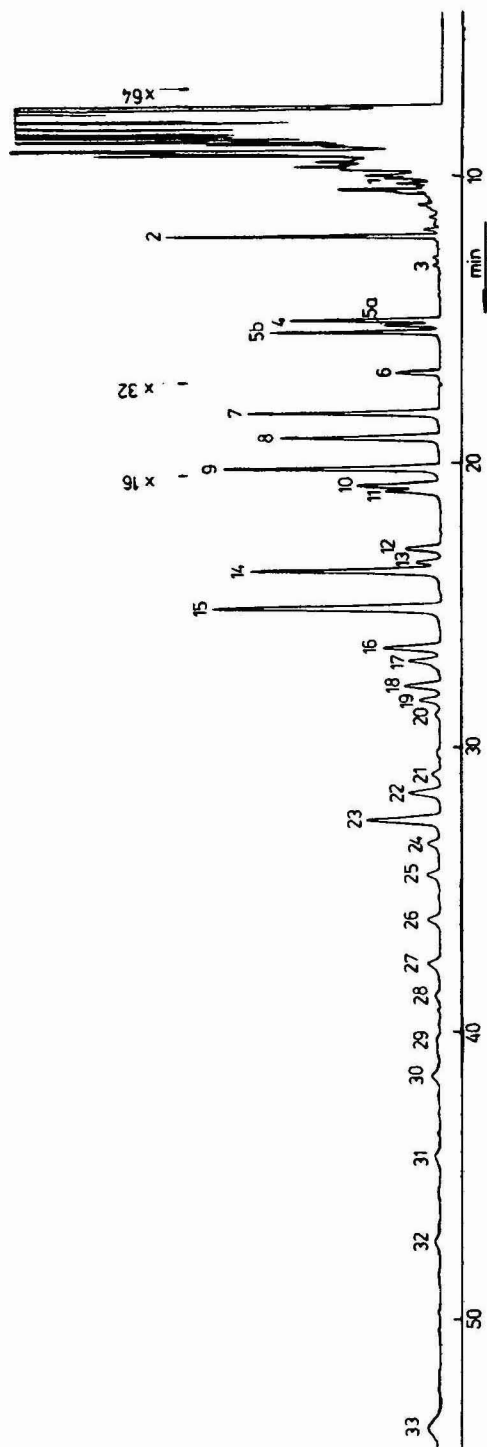


Fig. 3. Chromatogram of the separation of the aromatics in the gasoline fraction of crude oil on SP-2340 in a fused-silica capillary column at 80°C and with a nitrogen pressure of 0.9 atm.

mained unresolved in comparison to published results¹⁴. The qualitative¹⁹ and the preceding quantitative analysis in both isothermal and temperature programmed analysis was difficult when peaks overlapped, which was often the case. It is evident that for sufficient component separation and for the preceding group analysis it is necessary to optimize the experimental conditions, such as column length (efficiency), film thickness, temperature gradient, time of analysis, etc., with respect to the number of resolved peaks.

Comparing the weight per cent of the constituents determined under temperature-programmed conditions, where the peak areas were evaluated by digital integration, and the weight per cent under isothermal conditions, where the peak areas

TABLE III

RESULTS OF THE QUANTITATIVE ANALYSIS OF AROMATICS IN GASOLINE ON SP-2340 BY THE MODIFIED STANDARD ADDITION METHOD

Peak No.	Compound	Weight %
1	Benzene	0.177
2	Toluene	1.578
3	Decahydronaphthalene	0.035
4	Ethylbenzene	1.078
5a	<i>p</i> -Xylene	0.383
5b	<i>m</i> -Xylene	1.260
6	Isopropylbenzene	0.357
7	<i>o</i> -Xylene	0.841
8	<i>n</i> -Propylbenzene	0.729
9	1,3- + 1,4-Methylethylbenzene	1.042
10	1,3,5-Trimethylbenzene	0.204
11	<i>sec.</i> -Butylbenzene	0.135
12	1-Methyl-4-isopropylbenzene	0.096
13	Methylisopropylbenzene	0.066
14	1-Methyl-2-ethylbenzene	0.540
15	1,2,4-Trimethylbenzene	0.686
16	Methylpropylbenzene	0.176
17	Diethylbenzene	0.094
18	<i>n</i> -Butylbenzene	0.119
19	Diethylbenzene	0.070
20	Branched C ₁₁ alkylbenzene	0.016
21	1,2-Diethylbenzene	0.028
22	1-Methyl-2-propylbenzene	0.118
23	1,2,3-Trimethylbenzene	0.286
24	Dimethylethylbenzene	0.045
25	Dimethylethylbenzene	0.051
26	Tetramethylbenzene	0.053
27	Indane	0.055
28	Methylindane	0.024
29	Tetramethylbenzene	0.018
30	Methylindane	0.040
31	Dimethylethylbenzene	0.030
32	C ₁₀ alkylbenzene	0.032
33	C ₁₀ alkylbenzene	0.073
Σ Aromatics		10.535

were evaluated by the $t_R \cdot h$ method, it is seen that the per cent of low boiling compounds determined by the latter method is slightly higher and of high boiling compounds lower than those determined with temperature programming and digital integration.

The components not given in Table I were either below the limit of detection under the given conditions or they were coeluted with other peaks, which was difficult to observe at their very low concentrations (less than 0.010%).

The results of the group analysis of hydrocarbons eluted up to *n*-decane on squalane are given in Table II. When peaks overlapped, their quantitative analysis was made according to the known proportion of constituents in peaks, determined either from isothermal analysis, when peaks were resolved, or from GC-MS measurements, when peaks were not due to isomers.

Quantitative analysis of aromatic hydrocarbons on SP-2340

The aromatic hydrocarbon content was determined also on the polar stationary phase SP-2340. Due to the high efficiency of the fused-silica column, it was possible to analyse also higher boiling aromatics with lower weights per cent than on the metal capillary column with 1,2,3-tris(cyanoethoxy)propane¹⁴. A chromatogram of the separation of hydrocarbons in gasoline on SP-2340 in a fused-silica capillary column at 80°C and with a nitrogen pressure of 0.9 atm is shown in Fig. 3. The component numbering is as in Table III; GC-MS was used for compound identification.

TABLE IV

RESULTS (WEIGHT %) OF THE QUANTITATIVE ANALYSIS OF AROMATICS IN GASOLINE ON SQUALANE AND SP-2340

Chromatographic conditions as in Table I; on SP 2340, peak areas were determined as $t_R \times h$.

Compound	Squalane			SP 2340
	TP-1	TP-2	Isothermal	
Benzene	0.113	0.111	0.121	0.177
Toluene	1.154	1.265	1.469	1.578
Ethylbenzene	1.007	1.022	0.952	1.078
<i>p</i> -Xylene	0.307	0.293	0.289	0.383
<i>m</i> -Xylene	1.128	1.159	1.327	1.260
<i>o</i> -Xylene	0.838	1.017	0.886	0.841
Isopropylbenzene	0.402	0.401	0.317	0.357
<i>n</i> -Propylbenzene	0.924	0.986	0.731	0.729
1-Methyl-3-ethylbenzene	0.713	0.670	0.673	} 1.042
1-Methyl-4-ethylbenzene	0.490	0.382	0.220	
1-Methyl-2-ethylbenzene	0.583	0.760	0.615	0.540
1,3,5-Trimethylbenzene	0.193	0.203	0.173	0.204
<i>tert.</i> -Butylbenzene	—	0.027	0.017	—
1,2,4-Trimethylbenzene	0.770	0.734	0.679	0.686
<i>sec.</i> -Butylbenzene	0.166	0.148	0.146	0.135
1,2,3-Trimethylbenzene	0.318	0.305	0.277	0.286
1-Methyl-4-isopropylbenzene	0.092	0.069	0.065	0.096
Σ Aromatics	9.198	9.552	8.957	9.392

The content of aromatics obtained on SP-2340 was calculated using the modified standard addition method¹⁴ with ethylbenzene as the standard. The results of the quantitative analysis of individual aromatic hydrocarbons in gasoline are given in Table III.

In Table IV are summarized the results of quantitative analysis of aromatics in gasoline eluted up to *n*-decane on squalane (temperature-programmed and isothermal analysis) and on SP-2340. The results are in relatively good agreement.

ACKNOWLEDGEMENT

The authors thank Dr. W. Supina, Supelco, Bellefonte, U.S.A. for a gift of the SP-2340 column.

REFERENCES

- 1 W. G. Jennings, *Gas Chromatography with Glass Capillary Columns*, Academic Press, New York, 2nd ed., 1980, p. 294.
- 2 C. F. Chien, M. M. Kopečňi and R. J. Laub, *J. High Resolut. Chromatogr. Chromatogr. Commun.*, 4 (1981) 539.
- 3 D. A. Tourres, *J. Chromatogr.*, 30 (1967) 357.
- 4 J. A. Rijks and C. A. Cramers, *Chromatographia*, 7 (1974) 215.
- 5 A. Matukuma, in C. L. A. Harbourn and R. Stock (Editors), *Gas Chromatography 1968*, Institute of Petroleum, London, 1969.
- 6 O. E. Schupp, III and J. S. Lewis (Editors), *Gas Chromatographic Data Compilation*, American Society for Testing and Materials, Philadelphia, PA, ASTM D 25 A, 1967.
- 7 O. E. Schupp, III and J. S. Lewis (Editors), *Gas Chromatographic Data Compilation, Supplement I*, American Society for Testing and Materials, Philadelphia, PA, ASTM AMD 25 A S-1, 1971.
- 8 H. Schröder, *J. High Resolut. Chromatogr. Chromatogr. Commun.*, 3 (1980) 38, 95, 199, 362.
- 9 L. R. Durrett, L. M. Taylor, C. F. Wantland and I. Dvoretzky, *Anal. Chem.*, 35 (1963) 637.
- 10 W. N. Sanders and J. B. Maynard, *Anal. Chem.*, 40 (1968) 527.
- 11 I. M. Whittemore, in K. H. Altgelt and T. H. Gouw (Editors), *Chromatography in Petroleum Analysis*, Marcel Dekker, New York, 1979, pp. 50–70.
- 12 E. R. Adlard, A. W. Bowen and D. G. Salmon, *J. Chromatogr.*, 186 (1979) 207.
- 13 N. G. Johansen, L. S. Ettre and R. L. Miller, *J. Chromatogr.*, 256 (1983) 393.
- 14 E. Matisová, J. Krupčík, P. Čellár and J. Garaj, *J. Chromatogr.*, 303 (1984) 151.
- 15 L. Durrett, M. C. Simmons and I. Dvoretzky, *Prepr. Div. Petrol. Amer. Chem. Soc.*, 6 (1961) 63.
- 16 L. S. Ettre, *J. Chromatogr.*, 8 (1962) 525.
- 17 W. A. Dietz, *J. Gas Chromatogr.*, 5 (1967) 68.
- 18 W. G. Jennings, *J. Chromatogr. Sci.*, 13 (1975) 185.
- 19 J. Krupčík, unpublished results.

CHROM. 17 929

CAPILLARY GAS CHROMATOGRAPHIC METHOD FOR THE DETERMINATION OF COMPLEX MIXTURE OF ISOCYANATES AND AMINES

G. SKARPING*, L. RENMAN and C. SANGÖ

Department of Technical Analytical Chemistry, Lund Institute of Technology, Chemical Center, P.O. Box 124, S-221 00 Lund (Sweden)

and

L. MATHIASSEN and M. DALENE

Department of Analytical Chemistry, University of Lund, Chemical Center, P.O. Box 124, S-221 00 Lund (Sweden)

(Received May 28th, 1985)

SUMMARY

A capillary gas chromatographic method using nitrogen-selective detection was developed for the analysis of complex mixtures of isocyanates and amines in air. The isocyanate group was converted directly in the air sampling step into urethane by reaction with ethanol using potassium hydroxide as a catalyst. The amine group was converted into an amide using pentafluoropropionic anhydride in an extractive derivatization procedure. The complex pattern of air pollutants after thermal degradation of a polyurethane polymer, based on toluene diisocyanate (TDI) and 3,3'-dichloro-4,4'-diaminodiphenylmethane (MOCA), was investigated. Substantial amounts of amines, isocyanates and aminoisocyanates, molecules containing both an amine and an isocyanate group, were found. Consideration must be given to these findings when using current methods for isocyanate and amine determination. The detection limits for isocyanates, amines and aminoisocyanates, essentially depending on the nitrogen content of the molecule, were about equal and in the order of 40–80 fmol.

INTRODUCTION

Isocyanates and amines are the predominant pollutants in many workplace atmospheres and various methods for their determination have been developed.

Isocyanates are most frequently determined, after derivatization to urea derivatives, by high-performance liquid chromatography (HPLC) with UV^{1–4}, fluorescence^{2,5,6} or electrochemical detection^{7,8}. The choice of a strongly UV-absorbing or fluorescing agent in the derivatization step has permitted the trace analysis of both aromatic and aliphatic isocyanates. Aromatic amines present in samples have sometimes been simultaneously determined⁴. Direct analysis of free isocyanates by gas chromatography (GC) on packed columns using electron-capture detectors has been

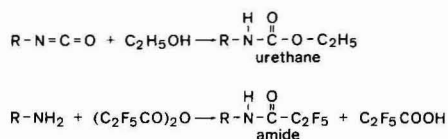
discussed^{9,10}. A capillary GC method using electron-capture and nitrogen-selective detector has recently been reported¹¹.

GC has been the preferred method for the analysis of amines. Direct analyses of free amines¹²⁻¹⁵ and also after a derivatization step have been described^{16,17}. GC methods for total isocyanate monomer determination based on hydrolysis in acidic solutions have been presented¹⁸⁻²¹; they give the sum of the concentration of each isocyanate and its corresponding hydrolysed product.

Mixtures of isocyanates and amines in air may be very complex, especially following the thermal degradation of polyurethanes. The possible conversion of isocyanates to the corresponding primary amines by hydrolysis makes the sampling and analysis even more complicated. There is still a great need for methods that give high selectivity and low detection limits and where as many components as possible are determined simultaneously.

Here we describe a glass capillary GC method that permits the simultaneous determination of isocyanate monomers, primary and secondary amines and partially hydrolysed isocyanates. Air samples are collected in alkaline ethanol solutions and the sample work-up procedure includes two derivatization steps; in the first the isocyanate groups are derivatized with ethanol to form urethane groups and in the second the amine groups are derivatized with pentafluoropropionic acid anhydride to give the corresponding amide groups. The resulting toluene solution is finally analysed by capillary GC with nitrogen-selective detection.

The derivatization reactions are illustrated below.



R = alkyl or aryl

EXPERIMENTAL

Equipment

A Carlo Erba Fractovap Model 4160 gas chromatograph with on-column injection and a flame ionization detector and a Varian Model 3700 gas chromatograph, equipped with a Varian thermionic specific detector (TSD) and a Carlo Erba on-column injection system were used. Typical settings for the detector were as follows: gas flow-rates, 4.0 ml/min of hydrogen and 180 ml/min of air; bead heating current, 5.3 scale divisions; bias voltage, -10 V; and detector temperature, 290°C. The carrier gas was helium at an inlet pressure of 1.0 kg/cm², dried over molecular sieve 5A and deoxygenated using an "Indicating Oxytrap" (Chrompack, Middelburg, The Netherlands). Chromatograms were recorded on Servogor Model 310 recorders, and a Hewlett-Packard Model 3390A integrator was used for peak evaluation. A Finnigan Model 4021 gas chromatograph-mass spectrometer was used in the electron impact (EI) and ammonia chemical ionization (CI) modes with positive ion monitoring for structure confirmations. A Rotavapor-M (Büchi Laboratorium Technik, Plawil, Switzerland) connected to an aspiration pump was used for evaporation.

Column preparation

Duran 50 borosilicate glass capillary columns were drawn on a Carlo Erba GCDM Model 60 glass capillary-drawing machine and leached according to Grob and Grob²². The columns were dried by nitrogen purging for 2 h at 250°C. Deactivation was achieved by dynamic coating with a plug of 1,3-divinyldimethylsilazane followed by flame-sealing and thermal treatment at 350°C overnight. After rinsing with toluene, methanol and diethyl ether, PS-255 stationary phase (Fluka, Buchs, Switzerland) was applied by static coating from pentane solutions to produce a 0.75- μ m stationary phase thickness. The stationary phase was then cross-linked with azo-*tert*.-butane according to Wright *et al.*²³.

Chemicals

The substances investigated were 2,4-toluene diisocyanate (2,4-TDI), 2,6-toluene diisocyanate (2,6-TDI), hexamethylene diisocyanate, isophorone diisocyanates, phenyl isocyanate, 1-naphthyl isocyanate, 2,4-toluenediamine (2,4-TDA), 2,6-toluenediamine (2,6-TDA), hexamethylenediamine, isophoronediamines, aniline, 1-naphthylamine, 3,3'-dichloro-4,4'-diaminodiphenylmethane and *o*-chloroaniline and the interfering substances considered were N-methylmorpholine, 1,4-diazabicyclo[2.2.2]octane (DABCO), dimethylethylamine, diethylamine, aniline and phenol. They were obtained from the following suppliers: E. Merck, Darmstadt, FRG (2,4- and 2,6-TDA hexamethylenediamine, 2,4-TDI, hexamethylene diisocyanate, isophorone diisocyanate, dimethylethylamine and 1-naphthyl isocyanate); Aldrich-Europe, Beerse Belgium (2,6-TDI) ICN Pharmaceuticals, Plainview, NJ, U.S.A. (isophoronediamine); Fluka, Buchs, Switzerland (N-methylmorpholine, DABCO and 1-naphthylamine); Mallinckrodt, St. Louis, MO, U.S.A. (aniline); and BDH, Poole, U.K. (diethylamine and phenol).

Isooctane and toluene were of glass-distilled grade from Rathburn Chemicals (Walkerburn, U.K.). Ethanol of spectroscopic grade was obtained from Kemetyl (Sweden). Pentafluoropropionic anhydride was obtained from Pierce (Rockford, IL, U.S.A.) and azo-*tert*.-butane from Alfa Products (Thiokol, Ventron Division, Danvers, MA, U.S.A.). The stationary phase PS-255 was obtained from Fluka and 1,3-divinyldimethylsilazane from Petrarch Systems (Bristol, PA, U.S.A.).

Procedure

Preparation of standards. Isocyanate standards (urethanes) were prepared by reaction of 30 mg of the isocyanates in 25 ml of ethanol at 60°C. For aromatic isocyanates a reaction time of 15 min was used and for aliphatic isocyanates 2 h. Standards were diluted with toluene prior to the GC analysis. The standards were stable for at least 3 weeks when stored in a refrigerator.

For amine standards (amides), 1 ml of toluene and 20 μ l of pentafluoropropionic anhydride were placed in a test-tube containing 0.1 μ mol of amine in 1 ml of 1 M phosphate buffer (pH 7) and the test-tube was immediately shaken vigorously for 1 min. The toluene layer containing the amide derivative was separated and stored in a refrigerator. The standards were stable for at least 3 weeks.

Sampling. An air sampling procedure was simulated as follows. A 10-ml volume of 0.2% (w/v) ethanolic potassium hydroxide solution was poured into a midjet impinger flask. Isocyanates dissolved in isooctane (7 ng/ μ l) were injected into a glass

tube connected to the impinger inlet. The isooctane volume was varied between 20 and 100 μl . The tube was carefully heated, while air was drawn through it into the absorbing solution at a flow-rate of 1 l/min for 5 min. The concentration of isocyanates in the absorbing solution after sampling was in the range 14–70 ng/ml. The procedure was applied to 2,4- and 2,6-TDI and hexamethylene diisocyanate.

Work-up procedure before GC analysis. A 30- μl volume of phosphoric acid was added to 10 ml of absorption solution in an impinger flask. The solvent was slowly evaporated to dryness at 20°C during a period of *ca.* 15 min, then 1 ml of 1 M phosphate buffer (pH 7), 1 ml of toluene and 20 μl of pentafluoropropionic anhydride were added. The mixture was instantly shaken for 1 min, transferred into a small test-tube and the toluene layer analysed by GC.

RESULTS

Standards

Isocyanate derivatives (urethanes). Standards were prepared as described above and the conversion to urethanes was followed by GC. Aliquots of an ethanolic solution (0.5 μl) were removed and injected on-column on to a glass capillary column with chemically bonded PS-255 stationary phase and detected with a flame ionization detector.

The chromatograms in Fig. 1 illustrate the course of the uncatalysed reaction between hexamethylene diisocyanate and ethanol. At room temperature the reaction rate is slow (Fig. 1A). However, if the temperature is increased to 60°C the reaction is complete within 2 h (Fig. 1C). The reaction rates are, as expected, higher for aromatic than for aliphatic isocyanates. For 2,4- and 2,6-TDI less than 5 min are needed to complete the reaction. In all instances the reaction was complete within 2 h, hexamethylene diisocyanate having the lowest reaction rate.

Amine derivatives (amides). Extractive derivatization of amines with pentafluoropropionic anhydride is discussed elsewhere²⁴. Complete reaction was achieved within 1 min. The amides formed were stable in toluene solution for at least 3 weeks at nmol/ml concentrations.

Sample preparation prior to GC analysis

Operations included are air sampling of isocyanates/amines, addition of phosphoric acid to the sampling solution (0.2% potassium hydroxide in ethanol), solvent evaporation, extraction with toluene and, for sample components containing primary amino groups, derivatization with pentafluoropropionic anhydride in connection with the extraction step.

Air sampling. The reaction between isocyanates and ethanol with ethanol as absorption medium on air sampling has been discussed by Nieminen *et al.*⁴. They showed that addition of 0.2% potassium hydroxide to the ethanol effectively catalysed the reaction with aromatic isocyanates and made side-reactions negligible. We found that the same applies to aliphatic isocyanates. To determine the influence of moisture and oxygen on the sampling of isocyanates/amines in alkaline ethanolic solution, the sampling period was varied between 5 and 20 min with an air flow-rate of 1 l/min, a relative humidity of about 50% and an absorption volume of 10 ml. No significant differences were found.

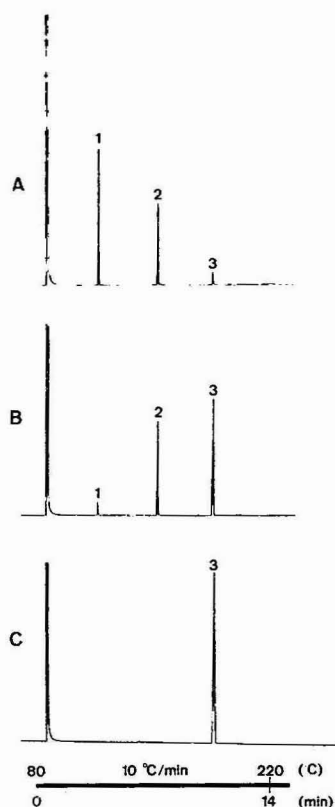


Fig. 1. Urethane formation from hexamethylene diisocyanate (1.2 mg/ml) in ethanolic solution. Chromatogram A was obtained after 40 min at 25°C, B after 30 min at 60°C and C after 120 min at 60°C. (1) Hexamethylene diisocyanate; (2) partially reacted hexamethylene diisocyanate; (3) totally reacted hexamethylene diisocyanate. On-column injection of 0.5 μ l of ethanolic solution. Column: 10 m \times 0.32 mm I.D. Duran 50 glass capillary, 1,3-divinyltetramethyldisilazane-deactivated, with PS-255 as the stationary phase; film thickness, 0.75 μ m. Temperature programming as shown. Carrier gas: helium at 0.5 kg/cm². Flame ionization detection.

Addition of phosphoric acid. In order to neutralize the potassium hydroxide, about 15 μ l of phosphoric acid are needed under the conditions described under Experimental. This gives satisfactory results for the analysis of the urethanes. If amines are to be analysed simultaneously, the amount of phosphoric acid is increased to 30 μ l to prevent losses of amines during the evaporation step. A modification of the procedure with addition of phosphoric acid immediately after sampling for 5 min and after a delay period of 30 min before the work-up procedure did not give significant losses. This shows that the urethane formation reaction is complete within minutes in alkalized ethanol.

Extraction. The extraction efficiency for the urethanes and amides was studied by shaking standards in toluene for 10 min with 1 M phosphate buffer (pH 7) and comparing the concentrations of the derivatives in the toluene layer before and after this operation. A 100% extraction efficiency was found for all isocyanate and amine derivatives.

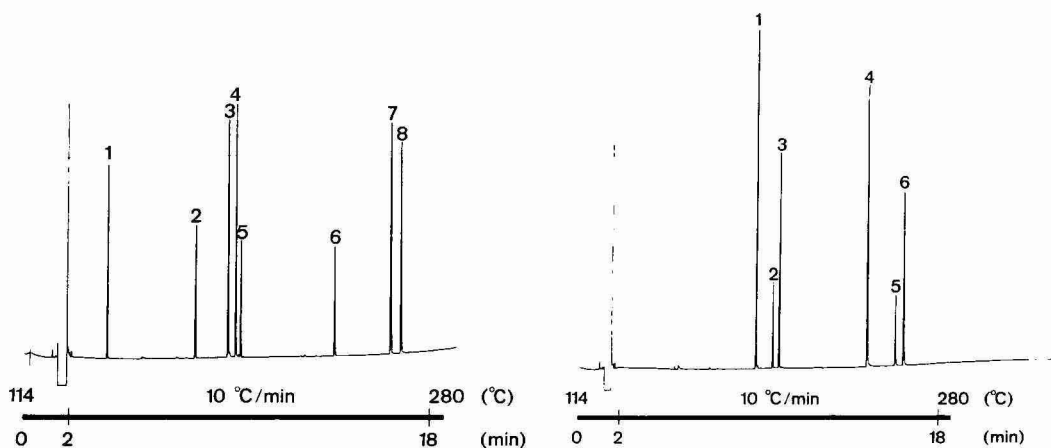


Fig. 2. Chromatogram of pentafluoropropionic derivatives of aromatic amines and ethanol derivatives of aromatic isocyanates (urethanes). On-column injection of 1 μ l of a 4 pmol/ μ l toluene solution of derivatives of (1) aniline, (2) phenyl isocyanate, (3) 2,6-TDA, (4) 2,4-TDA, (5) 1-naphthylamine, (6) 1-naphthyl isocyanate, (7) 2,6-TDI and (8) 2,4-TDI. Column: 15 m \times 0.32 mm I.D. Duran 50 glass capillary, 1,3-divinyltetramethyldisilazane-deactivated, with PS-255 as the stationary phase; film thickness, 0.75 μ m. Temperature programming as shown. Carrier gas: helium at 1.0 kg/cm². Nitrogen-sensitive detector (Varian TSD) with bead heating current 5.3 scale divisions, bias voltage -10 V, detector temperature 290°C, hydrogen at 4.0 ml/min, air at 400 ml/min and nitrogen make-up gas at 5 ml/min. Attenuation: $4 \cdot 10^{-12}$ A f.s.

Fig. 3. Chromatogram of pentafluoropropionic derivatives of aliphatic amines and ethanol derivatives of aliphatic isocyanates (urethanes). On-column injection of 1 μ l of a 4 pmol/ μ l toluene solution of derivatives of (1) hexamethylenediamine, (2 and 3) isomers of isophoronediamine, (4) hexamethylene diisocyanate, and (5 and 6) isomers of isophorone diisocyanates. Chromatographic conditions as in Fig. 2.

Chromatography

The chromatographic behaviour of the urethanes and amides is shown in Figs. 2 and 3. The good resolution obtained between urethanes and amides is important when both types of compounds occur simultaneously. The use of an apolar stationary phase with a relatively high film thickness offers the best resolution.

Quantification

Quantification was based on peak-height measurement and comparison with external standards. The overall yield did not significantly differ from 100% in any case when the work-up procedure was executed within 1 h after the sampling. The precision at a concentration of 0.7 ng/ μ l was *ca.* 5% for five samples. The contribution to the precision from the chromatographic run alone was typically less than 2% for both urethanes and amides with triple injections at a concentration of 400 pg/ μ l.

Air sampling of toluene diisocyanates, some of the most important isocyanates with respect to occupational health, was further studied according to the procedure described under Experimental. The variation of the peak height with concentration of 2,4-TDA and 2,4-TDI is shown in Fig. 4. The concentration range investigated, 140–700 pg/ μ l, corresponds to isocyanate concentrations in air of 0.4–2 times the

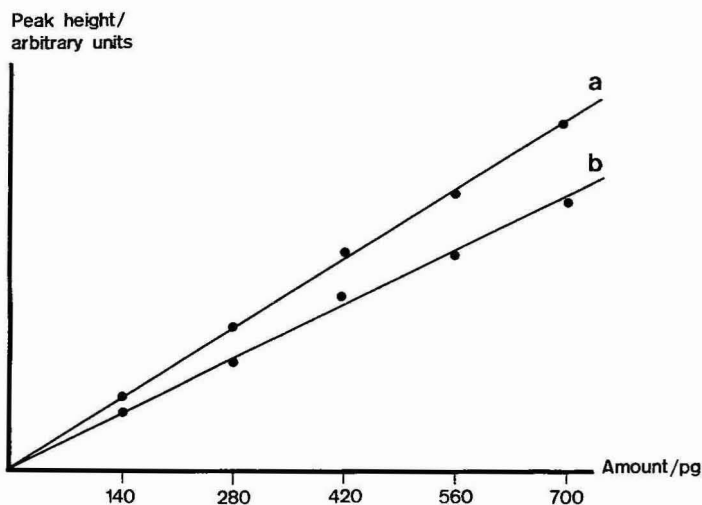


Fig. 4. Calibration plot for (a) 2,6-TDA and (b) 2,6-TDI as amide and urethane derivatives. Volume injected, 1 μ l. Chromatographic conditions as in Fig. 2.

Swedish Threshold Limit Value (0.01 ppm, 5-min sampling period). A corresponding plot for 2,6-TDA and 2,6-TDI shows identical slopes and zero intercepts.

Detection limits

As the chromatographic behaviour of both urethanes and amides is good, the detection limits for the derivatives are similar, depending essentially on the nitrogen content of the derivatives when using a nitrogen-selective detector. It is about 80 fmol for substances with one nitrogen atom and about 40 fmol for those with two nitrogen atoms (1- μ l injection, on-column), and decreases slightly with increasing retention times for the molecules eluted. For toluene diurethanes these figures correspond to 4 fmol.

Interferences

2,4- and 2,6-TDI and 2,4- and 2,6-TDA were chosen as model substances. The interfering substances investigated (see *Chemicals*) are expected to occur as pollutants in work atmospheres.

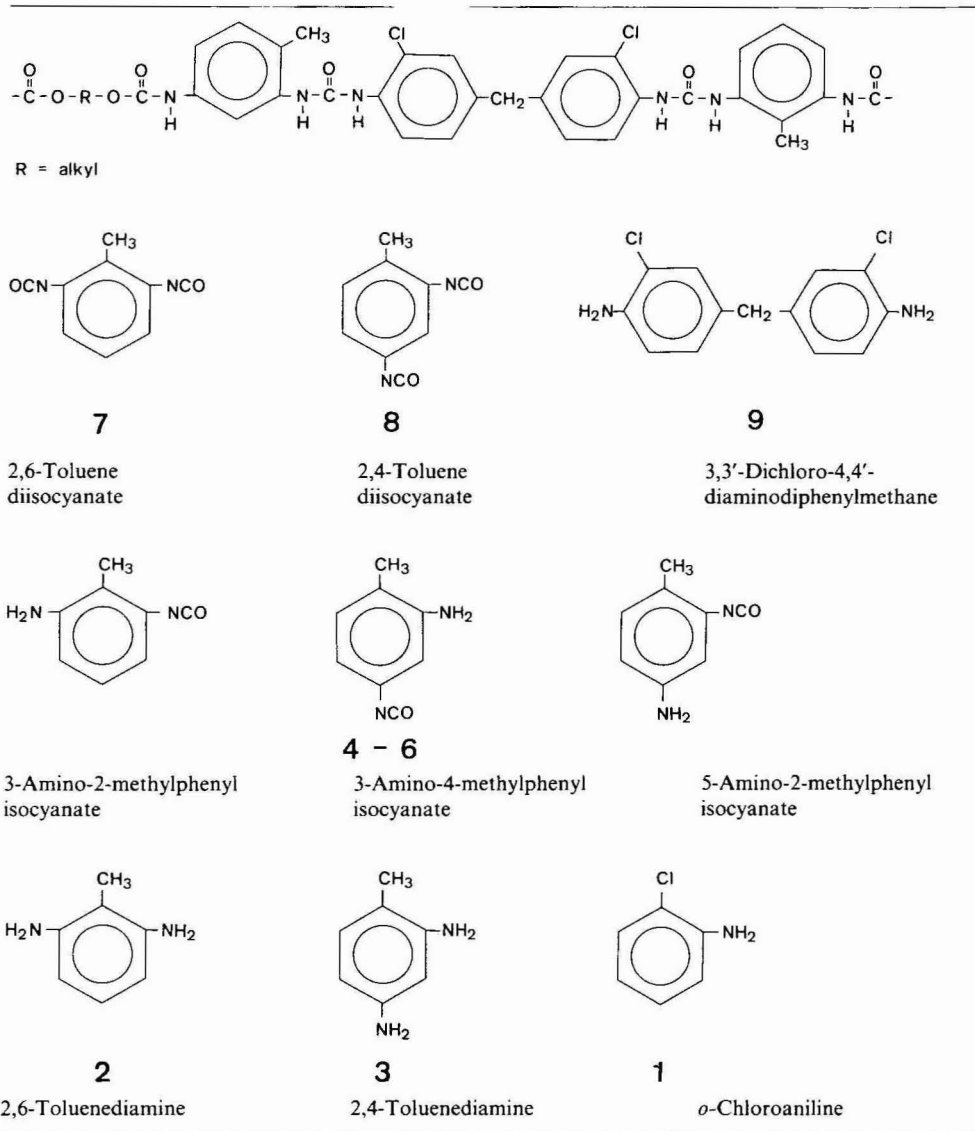
Air sampling of isocyanates was performed as described under Experimental. The amount of isocyanates corresponds to an air concentration of 0.01 ppm, which with an air volume of 5 l gives a concentration of 35 ng/ml in the 10-ml sampling solution (0.2% potassium hydroxide in ethanol). Toluenediamines were added to the sampling solution to give the same concentrations together with a 1000-fold relative molar amount of interfering substances. Air sampling, the work-up procedure and analysis as described under Experimental were performed within 4 h.

The yield of urethanes did not differ significantly from 100% in any instance, when compared with standards. Only with diethylamine as an interfering substance did we find a slight decrease (*ca.* 10%) in the yield of the amides. An increase in the amount of the reagent (anhydride) did not improve the yield. When the diethylamine

TABLE I

SCHEMATIC REPRESENTATION OF AN ADIPRENE POLYMER AND EXPECTED DEGRADATION PRODUCTS

The numbers of the compounds refer to the chromatogram in Fig. 5.



to isocyanate ratio was decreased by a factor of 10, the amides also gave a yield of 100%.

Stability test

In order to test the stability of the urethanes and amines present in the sampling

solution, the same procedure for analysis was used as in the interference test above. Model substances, sample concentrations and interfering substance concentrations were as above, except the diethylamine concentration, which according to the results above was decreased 10-fold. Solutions were allowed to stand for 3 weeks in daylight or darkness at room temperature (about 22°C).

We found the urethanes to be stable in all instances. However, the investigated toluenediamines were found to be stable for such a long period only in the absence of interfering substances. With interfering substances present, only small fractions (less than 10%) of the amines could be detected after derivatization to the corresponding amides.

Another problem with alkaline solutions containing interfering substances in large amounts is that these substances may decompose on standing, resulting in the occurrence of substances that interfere with the chromatographic separation. However, the urethanes appear late in the chromatograms, in contrast to most of the decomposition products emanating from interfering substances. Only in one instance, aniline, did an overlapping peak appear for 2,4-toluenediurethane. In this instance the peak height for the 2,6-isomer was unaffected. The 2,4-isomer is therefore probably also stable.

Application

Thermal degradation of polymeric material may occur in many situations, and the knowledge of the type and concentrations of the degradation products in air and hence the risks of exposure is very limited. The reason for this is mainly the complex pollutant pattern and the accompanying need for powerful analytical separation methods.

In this application we studied the thermal degradation of a polyurethane, Adiprene, formed by the reaction of a prepolymer of 2,4- and 2,6-TDI with 3,3'-dichloro-4,4'-diaminodiphenylmethane (MOCA) as curing agent. Possible degradation patterns have been discussed elsewhere^{25,26}. The most important fragmentation products of occupational health interest to be expected are isocyanates, amines and degradation compounds containing both isocyanate and amine functional groups (see Table I).

Two polymers based on Adiprene L-42 and Adiprene L-325 (DuPont, Wilmington, DE, U.S.A.) were investigated. The thermal degradation experiment was performed as follows: 5 mg of the polymer were placed in a glass tube and air at a flow-rate of 1 l/min was led through the tube into a midjet impinger containing 10 ml of alkaline ethanol absorption solution. The glass tube was heated from 20 to 350°C during a period of 10 min, which also was the total sampling time. The resulting samples were pre-treated and analysed by GC as described above.

Fig. 5 shows a typical chromatogram obtained using a nitrogen-selective detector. Thermal degradation of the polymers may result in three isomeric aminoisocyanates (see Table I). The amount of aminoisocyanates compared with the total amount of nitrogen-containing degradation products in the chromatogram was calculated to be in the order of 35%, assuming the same detector response per mole of substance. The corresponding fractional amounts were *ca.* 5% for TDA, 23% for TDI, 30% for MOCA and 7% for *o*-chloroaniline. The two Adiprene polymers gave the same patterns but with different relative amounts.

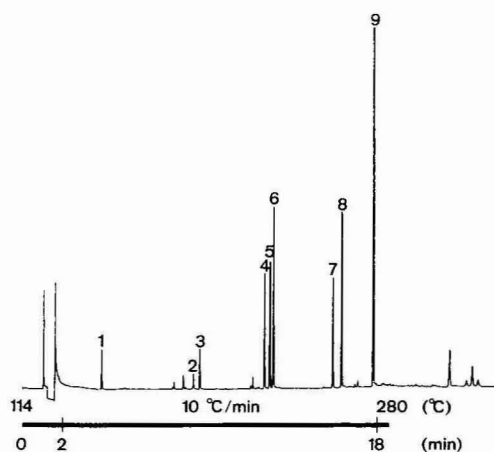


Fig. 5. Chromatogram of derivatized thermal degradation products from a polyurethane polymer (Adiprene). Amine groups derivatized with pentafluoropropionic anhydride and isocyanate groups with ethanol. On-column injection of 1 μ l toluene solution of derivatives of (1) *o*-chloroaniline, (2) 2,6-TDA, (3) 2,4-TDA, (4–6) aminoisocyanates, (7) 2,6-TDI, (8) 2,4-TDI and (9) 3,3'-dichloro-4,4'-diaminodiphenylmethane. Compounds are illustrated in Table I. Attenuation: $32 \cdot 10^{-12}$ A f.s. Chromatographic conditions as in Fig. 2.

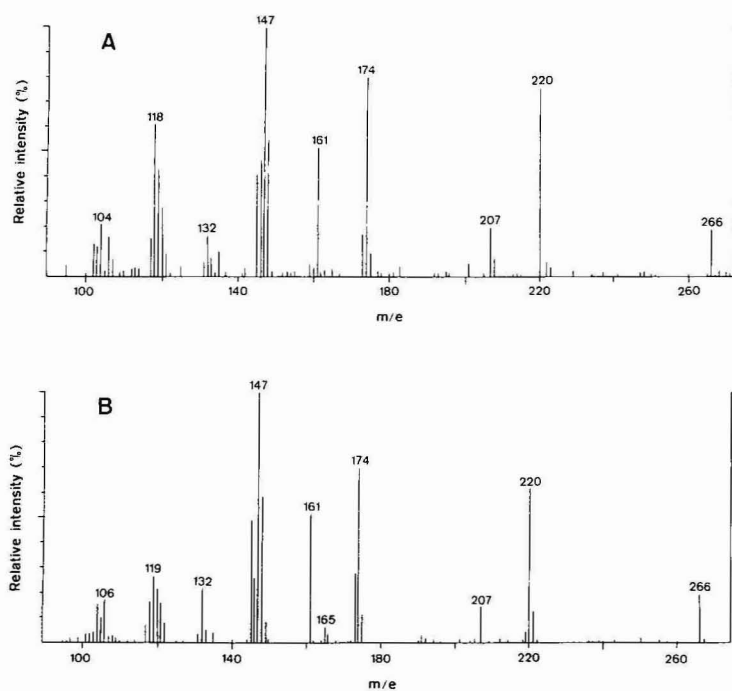


Fig. 6. Mass spectra of the ethanol derivatives of (A) 2,6- and (B) 2,4-TDI (2,6- and 2,4-toluene diurethanes) obtained by electron-impact ionization and positive ion monitoring.

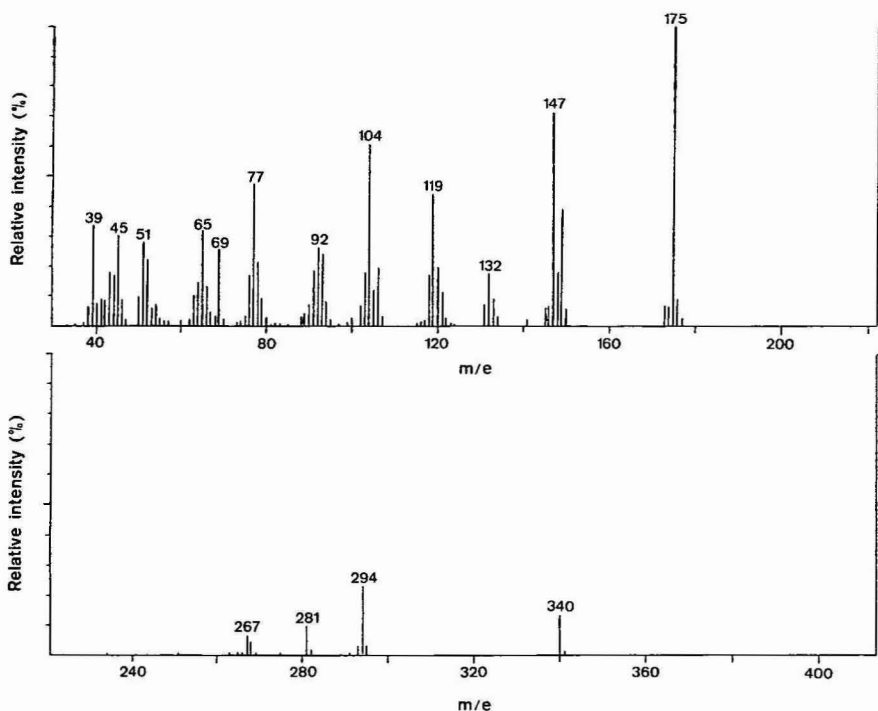


Fig. 7. Mass spectrum of ethanol and pentafluoropropionic derivatives of a monoaminotoluene monoisocyanate obtained by electron-impact ionization and positive ion monitoring (peak 4 in Fig. 5).

The peaks in Fig. 5 were identified by comparison with standards and further confirmed by mass spectrometry. A complementary approach is to use a dual detection system with nitrogen-selective and electron-capture detector¹⁶.

Mass spectrometry

The mass spectra of amides formed by the reaction between pentafluoropropionic anhydride and the amines in Fig. 5 have been discussed elsewhere²⁷. Mass spectra of the present diurethanes and of mixed compounds containing both urethane and amide groups are briefly discussed below.

Electron-impact (EI) mass spectra of the two 2,4- and 2,6-toluene diurethanes are shown in Fig. 6. The fragmentation patterns for the two isomers are very similar with the molecular ion M with m/e 266. Mass spectra for the monoaminotoluene monoisocyanate derivatives were obtained utilizing both electron impact as well as chemical ionization (CI) with ammonia. Figs. 7 and 8 show mass spectra for one of the derivatives (peak 4 in Fig. 5) in the EI and CI modes. The mass spectra for all these derivatives are similar, with abundant ions for EI with m/e 340, 294, 175 and 147 and for CI with m/e 358, 341 and 279. The peak with m/e 340 in EI corresponds to the expected molecular weight. According to ref. 28, characteristic peaks in the ammonia CI spectrum are $(M + H)$ and $(M + NH_4)$, which with a molecular weight of 340 will give the peaks obtained with m/e 341 and 358, respectively.

Typical fragmentation peaks of urethanes when using the EI mode are an

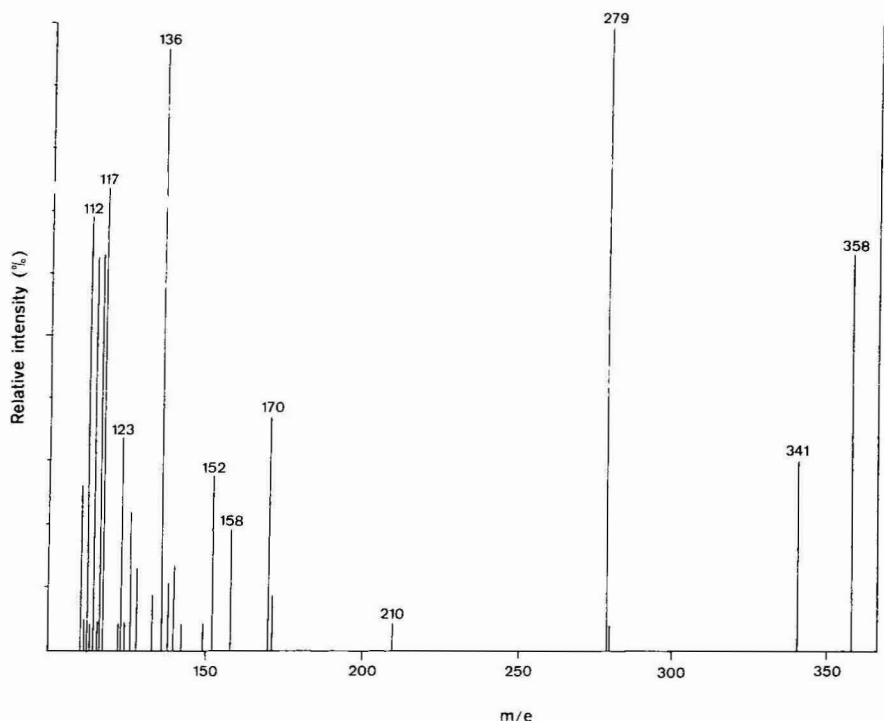


Fig. 8. Mass spectrum of ethanol and pentafluoropropionic derivatives of an aminoisocyanate obtained by chemical ionization with ammonia and positive ion monitoring (peak 4 in Fig. 5).

($M - 46$) peak with the loss of C_2H_5OH and an ($M - 59$) peak with the loss of CO_2 and CH_3^{\cdot} (ref. 29). These fragments are found in the EI spectra of 2,4- and 2,6-toluene diurethanes in Fig. 6 at m/e 220 and 207, respectively, and also in the spectra of the aminoisocyanates (see Fig. 7) at m/e 294 and 281, respectively. The loss of C_2H_5OH in phenylurethane results in phenyl isocyanate²⁹. The loss of two C_2H_5OH groups from toluene diurethanes should give toluene diisocyanates at m/e 174 ($M - 92$). This fragment is also found and gives one of the most abundant peaks. The occurrence of this fragment is probably due to both thermal- and EI-induced fragmentation²⁹. In a similar way a simultaneous fragmentation of amide and methane groups in the aminoisocyanate derivatives with a loss of C_2F_5 from the amide group and a loss of C_2H_2OH from the urethane group will give the peak with m/e 175 in Fig. 7.

C_2F_5 fragments with m/e 119 and CF_3 fragments with m/e 69 have been observed previously in the EI mass spectra of pentafluoropropionic diamides of 2,4- and 2,6-TDI²⁷. These fragments also appear in the spectrum of the aminoisocyanates. However, it should be noted that a peak with m/e 119 is also present in the spectra of the diurethanes in Fig. 6A and B.

DISCUSSION

The hydrolysis of isocyanates and thermal degradation of polyurethanes has

been studied in some detail over several years in our laboratories^{26,30,31} and the work reported here is a continuation of these investigations.

The method described allows the simultaneous determination of aliphatic and aromatic isocyanates and amines and of aminoisocyanates (see Fig. 5). In the HPLC method using UV detection described by Nieminen *et al.*⁴, where isocyanates are determined as urethanes and amines as free amines, only UV-absorbing compounds can be simultaneously determined. In other HPLC methods based on derivatization of the isocyanate group with strongly UV-absorbing or fluorescing agents, aliphatic isocyanates can also be determined, whereas aliphatic amines still remain undetected and aromatic amines often co-elute with the reagent.

A distinct advantage of the present method is the high resolution and the possibility of mass spectrometric detection, which greatly facilitates the identification of eluted compounds.

The simultaneous occurrence of isocyanates and corresponding fully hydrolysed amines in air has been investigated previously³². Discrimination between the two types of substances was indirectly accomplished by a combination of two analytical methods. The isocyanates were determined by HPLC after derivatization and UV detection and the sum of the isocyanates and corresponding amines by GC as perfluoro fatty acid amides after sampling in acidic solutions. This approach may cause errors, however, if aminoisocyanates are present as these are hydrolysed to diamines. On thermal degradation of polyurethanes, the amounts of aminoisocyanates may widely over-range those of diamines. When such samples are collected in acidic solutions, the concentrations of diamines will obviously be markedly over-estimated.

The roughly equal sensitivity for all derivatives with the GC method using nitrogen-selective detection described here compares favourably with that obtained by HPLC, where the sensitivity varies with the type of substance. The detection limits are comparable to those obtained by HPLC. Further, the selectivity with the nitrogen-selective detector is superior to that with HPLC detectors.

The results obtained in the interference and stability tests show that the method presented here can be used as a routine method for isocyanate determination. Nieminen *et al.*⁴ also found that the isocyanate derivatives showed excellent stability in the sampling solution. The matrix in their samples, however, was not described. For amine determinations the sample storage is critical. We have shown that if the sample work-up procedure starts shortly after the completed sampling period, as much as a 1000-fold molar amount of tertiary amines may be present without disturbing the determination of the primary amines as amide derivatives. However, after storing such solutions in darkness at room temperature for 3 weeks only about 10% of the initial amine concentrations could be found. Further improvements directed towards better stability of the amines in the sampling solution are necessary if this method is to be used as a routine method for the determination of primary and secondary amines, as the period between sampling and analysis may often be several weeks. To avoid side-reactions, the reaction rate between isocyanates and ethanol was increased by using potassium hydroxide. Nieminen *et al.*⁴ have discussed the merits of this catalyst, and other catalysts have been discussed by Farkas and Mills³³. The choice of another catalyst such as an organotin compound may enhance the stability of amines in the absorbing solution.

ACKNOWLEDGEMENT

We thank Professor Bengt Smith for valuable discussions concerning this work.

REFERENCES

- 1 K. L. Dunlap, R. L. Sandridge and J. Keller, *Anal. Chem.*, 48 (1976) 497.
- 2 C. Sangö and E. Zimerson, *J. Liquid Chromatogr.*, 3 (1980) 971.
- 3 D. A. Bagon and C. J. Purnell, *J. Chromatogr.*, 190 (1980) 75.
- 4 E. H. Nieminen, L. H. Saarinen and J. T. Laakso, *J. Liquid Chromatogr.*, 6 (1983) 453.
- 5 S. P. Levine, J. H. Hoggatt, E. Chladek, G. Jungclaus and J. L. Gerlock, *Anal. Chem.*, 51 (1979) 1106.
- 6 L. H. Kormos, R. L. Sandridge and J. Keller, *Anal. Chem.*, 53 (1981) 1122.
- 7 C. J. Warwick, D. A. Bagon and C. J. Purnell, *Analyst (London)*, 106 (1981) 676.
- 8 S. D. Meyer and D. E. Tallman, *Anal. Chim. Acta*, 146 (1983) 227.
- 9 B. B. Wheals and J. Thomson, *Chem. Ind. (London)*, 6 (1969) 753.
- 10 G. W. Schanche and E. R. Hermann, *Amer. Ind. Hyg. Ass. J.*, 35 (1974) 47.
- 11 G. Skarping, B. E. F. Smith and M. Dalene, *J. Chromatogr.*, 331 (1985) 331.
- 12 A. Di Corcia and R. Samperi, *Anal. Chem.*, 46 (1974) 977.
- 13 M. Dalene, L. Mathiasson and J. Å. Jönsson, *J. Chromatogr.*, 207 (1981) 37.
- 14 G. Audunsson and L. Mathiasson, *J. Chromatogr.*, 315 (1984) 299.
- 15 L. Mathiasson and P. Lövkvist, *J. Chromatogr.*, 217 (1981) 177.
- 16 G. Skarping, L. Renman and M. Dalene, *J. Chromatogr.*, 270 (1983) 207.
- 17 M. Dalene, T. Lundh and L. Mathiasson, *J. Chromatogr.*, 322 (1985) 169.
- 18 G. F. Ebell, D. E. Fleming, J. H. Genovese and G. A. Taylor, *Ann. Occup. Hyg.*, 23 (1980) 185.
- 19 G. Skarping, C. Sangö and B. E. F. Smith, *J. Chromatogr.*, 208 (1981) 313.
- 20 G. G. Esposito and T. W. Dolzine, *Anal. Chem.*, 54 (1982) 1572.
- 21 G. Audunsson and L. Mathiasson, *J. Chromatogr.*, 261 (1983) 253.
- 22 K. Grob and G. Grob, *J. High Resolut. Chromatogr. Chromatogr. Commun.*, 2 (1979) 677.
- 23 B. W. Wright, P. A. Peaden and M. L. Lee and T. J. Stark, *J. Chromatogr.*, 248 (1982) 17.
- 24 L. Renman, *J. Chromatogr.*, submitted for publication.
- 25 C. Reed, *Brit. Polym. J.*, 6 (1974) 1.
- 26 L. Renman, C. Sangö and G. Skarping, *Am. Ind. Hyg. Assoc. J.*, submitted for publication.
- 27 G. Skarping, L. Renman and B. E. F. Smith, *J. Chromatogr.*, 267 (1983) 315.
- 28 A. Maquestiacci, R. Flammang and L. Nielsen, *Org. Mass Spectrom.*, 15 (1980) 376.
- 29 H. Budzikiewicz, C. Djerassi and D. H. Williams, *Mass Spectrometry of Organic Compounds*, Holden-Day, San Francisco, 1967, pp. 500–502.
- 30 *Project Nos. ASF 81-0718, ASF 82-0527 and ASF 81-0499*, Swedish Work Environment Fund, Stockholm (in Swedish).
- 31 L. Belin, U. Wass, G. Audunsson and L. Mathiasson, *Brit. J. Ind. Med.*, 40 (1983) 251.
- 32 C. Rosenberg, *Analyst (London)*, 109 (1984) 1.
- 33 A. Farkas and G. A. Mills, *Advan. Catal.*, 13 (1962) 393.

CHROM. 17 970

AN IMPROVED SOLVENT-EXTRACTION BASED PROCEDURE FOR THE GAS CHROMATOGRAPHIC ANALYSIS OF RESIN AND FATTY ACIDS IN PULP MILL EFFLUENTS

R. H. VOSS* and A. RAPSOMATIOTIS*

Pulp and Paper Research Institute of Canada, 570 St. John's Boulevard, Pointe Claire, Quebec H9R 3J9 (Canada)

(Received June 13th, 1985)

SUMMARY

An analytical procedure for the determination of resin and fatty acids in pulp mill effluents is described. The procedure involves isolation of the resin and fatty acids from the effluent sample by solvent extraction with an equal volume of methyl *tert.*-butyl ether under alkaline (pH 9) conditions, derivatization of the extract with diazomethane, and subsequent analysis of the methylated extracts by gas chromatography on a 25 m × 0.20 mm I.D. OV-17 fused-silica capillary column using a flame ionization detector. The method of isolation, that is, extraction of the effluent sample at pH 9 with an equal volume of solvent, is a key feature of the new analytical procedure. These conditions overcome many of the major problems commonly associated with the application of a solvent extraction isolation technique to pulp mill effluents, such as emulsion formation, lignin precipitation, and resin acid isomerization.

INTRODUCTION

Extensive research over the past ten years, particularly that done by British Columbia Research in Canada, has established that resin acids and, to a lesser extent, unsaturated fatty acids are major contributors to the toxicity of softwood pulp and paper mill effluents to fish^{1–5} as determined from acute lethal bioassays using salmonoid fish species (trout and salmon). Consequently, the availability of analytical methods for determining resin and fatty acids (RFA) is essential for controlling the discharge of these compounds to the environment and assessing their biological effect.

Although analytical methods utilizing high-performance liquid chromatography show some promise for determining RFA in pulp mill effluents^{6–8}, analysis by gas chromatography (GC) still remains the method of choice for a detailed characterization of the RFA constituents in pulp and paper mill effluents. Almost all GC

* Present address: Waters Scientific Ltd., Lachine, Quebec, Canada.

procedures in use today for RFA analysis in pulp mill effluents have evolved from two distinct methods which were first developed in the early 1970s, one by the National Council of the Paper Industry for Air and Stream Improvement (NCASI)^{9,10} in the U.S.A. and the other by British Columbia Research (BCR)^{11,12} in Canada. The fundamental difference between the NCASI and BCR procedures was the method of isolation. The NCASI procedure used solvent extraction of the acidified (pH 2–3) effluent with diethyl ether, whereas, the BCR procedure removed the RFA from the effluent under alkaline (pH 9–10) conditions by adsorption onto a porous polymeric resin (XAD-2). In both cases, the final step of the analysis involved packed column GC of the methyl ester derivatives of the isolated RFA which were prepared by reaction with diazomethane. Over the past ten years, the analytical methods for RFA determination in pulp mill effluents have been improved or modified, principally by incorporating many of the latest developments in analytical instrumentation for chromatographic separation and detection such as high-resolution capillary GC^{13–16} and combined GC–mass spectrometry (MS)^{17–19}. However, the methods used to isolate the RFA from the effluent samples have essentially remained the same, that is, diethyl ether extraction or XAD-2 resin sorption.

The isolation method chosen for a given analysis is important as it defines the maximum recovery of the analytes of interest, as well as possible co-extractives that may interfere with the quantitative analytical step. If the isolation methods used in the BCR and NCASI procedures gave equivalent results, then either would be an acceptable component of an analytical procedure designed for RFA analysis. However, it is this aspect of the procedures which has become a major source of disagreement among analysts involved with the determination of RFA in pulp mill effluents.

Rogers and Mahood²⁰ and Claeys and Owens²¹ evaluated the use of XAD resins for the analysis of RFA in pulp mill effluents. Both groups reached similar conclusions, namely, that the NCASI solvent extraction technique should be used for routine quantitative determinations of RFA in pulp mill effluents. The use of XAD resins was recommended for qualitative analyses of effluents and for environmental studies involving the processing of large sample volumes such as highly dilute samples of receiving waters or pulp mill effluents from which toxicants are to be recovered.

Although BCR workers reported optimum recovery by XAD resin when the pH of the effluent sample was adjusted to about^{9,11,13,14}, Claeys and Owens²¹ and Rogers and Mahood²⁰ reported that the best results were achieved with XAD resins when processing acidified (pH 3) samples. Claeys and Owens²¹ found an average efficiency of only 23% for the XAD-2 extraction of resin acids from a sample of biologically treated kraft mill effluent at adsorption pH values of 6.4–10. Upon acidification of the sample to pH 3 the efficiency improved to about 90%. Claeys' findings with respect to the effect of pH were consistent with the results reported earlier by Junk *et al.*²² who found that a mixture of organic acids, including oleic acid, at the 10–50 µg/l level could be quantitatively recovered from distilled water provided that the sample was acidified (5 ml of hydrochloric acid per liter of sample). Otherwise, a low recovery (*e.g.*, 32% for oleic acid) was observed.

From a recent evaluation of the applicability of solvent extraction and XAD-2 adsorption for the isolation of resin acids from thermo-mechanical pulp (TMP) ef-

fluent before and after treatment by an activated sludge process, Richardson and Bloom²³ found that XAD-2 adsorption gave the best recovery. In addition, like BCR, they observed that a pH > 7 was required for the optimum recovery of resin acids from untreated TMP effluent by XAD-2 adsorption. Curiously, a pH of 5 was found to give the best recovery for the treated effluent samples.

Recently BCR and NCASI participated in a split-sample program of analysis of pulp mill effluents for the purpose of comparing the results obtained by their respective analytical procedures¹⁹. The BCR resin sorption procedure gave 20–40% lower results for resin acid constituents than the NCASI solvent extraction procedure. In general, the BCR procedure provided higher concentrations of fatty acids. In contrast, in an earlier study¹⁴ BCR had found that the recovery of RFA from a sample of softwood bleached kraft pulp mill effluent by the resin sorption method was approximately twice that obtained by ethyl ether extraction. The poor agreement found between the two methods in the recent cooperative study¹⁹ cannot, however, be attributed solely to the different isolation procedures (*i.e.*, XAD-2 adsorption and solvent extraction). There were other procedural differences in the methods particularly with respect to sample preservation and separation–measurement methods which could have influenced the results. After sample preparation, the BCR method used capillary GC with flame ionization detection (FID) for the subsequent analysis, whereas, the NCASI procedure used packed column GC and MS as detection system. The NCASI report¹⁹ from this interlaboratory study recommended that further development and improvement of the analytical methodologies was necessary in order to provide more reliable analytical results.

In principle, solvent extraction should provide a simpler and faster method of isolation for wastewater samples. However, the solvent extraction method has its problems. Direct solvent extraction of pulp mill effluent samples produces foaming emulsions^{10,12,14,17–19,23} which can make the sample work-up step more difficult (*e.g.*, by requiring centrifugation to break the emulsion) and can result in low recoveries and poor precision for the RFA analysis. In fact, the absence of emulsion problems is one of the major arguments in favour of using resin sorption methodology in place of solvent extraction procedures for the analysis of organic compounds in wastewaters²⁴. Emulsion problems can be reduced by making the effluent very acidic (pH 2–3) prior to extraction¹⁰ as in the NCASI procedure^{9,10,16,17,19}, however, this can lead to additional problems such as isomerization of some of the resin acid constituents^{19,23}, particularly levopimaric acid, and precipitation of lignin residues which can impede the recovery of the RFA from the effluent samples. McMahon²⁵ recently reported the application of a petroleum ether–acetone–methanol (PAM) extraction procedure for the analysis of the RFA in kraft mill internal process streams. Emulsions can be more severe for process streams where the lignin content is relatively high. Using the PAM solvent system, McMahon was able to eliminate emulsions in the extraction of acidified process effluents. Claeys *et al.*¹⁹ applied McMahon's procedure to the analysis of biologically treated pulp mill effluents and found that it did not provide a significant improvement in RFA recovery compared to the NCASI diethyl ether extraction procedure. A similar approach, using the solvent system hexane–acetone–methanol, has been developed at our institute²⁶ for the analysis of acidic and neutral extractives in sulphite-mechanical pulps and process streams. This approach, however, requires repetitive extraction which results in extended sample

preparation time particularly when applied to very dilute effluent streams.

This paper describes a solvent-extraction based GC procedure for the determination of RFA in pulp mill effluents. This new procedure overcomes many of the major problems commonly associated with the application of this isolation technique to pulp mill effluents such as emulsion formation, lignin residue precipitation and resin acid isomerization.

EXPERIMENTAL

Analytical procedure

The effluent sample (50 ml of biotreated effluent or typically 10 ml of untreated effluent diluted to 50 ml with distilled water) was spiked with heptadecanoic acid (50 μ l of a 0.208 μ g/ μ l solution in dimethyl sulfoxide). The heptadecanoic acid was included as a surrogate for RFA and served as an indicator of potential problems with respect to recovery and/or derivatization. Then, after adjusting the pH of the effluent sample to pH 9 using 0.5 *M* sodium hydroxide, the sample was extracted once with an equal volume (*i.e.*, 50 ml) of methyl *tert.*-butyl ether (MTBE) (Burdick & Jackson, distilled-in-glass) in a 125-ml separatory funnel. The solvent extract was transferred to a 50-ml round-bottomed flask having a graduated conical tip²² and concentrated to approximately 0.3 ml using a vacuum rotary evaporator at 25–30°C. To the concentrate were added 100 μ l of methanol (which served as a catalyst for the subsequent esterification step²⁷) containing 22.6 μ g of propyl dehydroabietate as an internal standard and approximately 0.6 ml of diethyl ether. The resulting mixture was methylated by bubbling continuously generated diazomethane through the solution (using a diazomethane generating system similar to that described by Levitt²⁸) until the yellow colour of excess diazomethane persisted for at least 5 min. Finally, the methylated extract was concentrated to 0.2 ml using a gentle stream of nitrogen, and a 2- μ l aliquot was analyzed by split capillary GC with FID.

Chromatographic analyses were made using a Hewlett-Packard Model 5880A gas chromatograph and a 25 m \times 0.20 mm I.D. fused-silica capillary column (Hewlett-Packard) wall-coated with cross-linked 50% phenylmethyl silicone (OV-17 type) phase of 0.17- μ m film thickness. The GC conditions were as follows: column temperature was held at 150°C for 1 min then programmed to 200°C at 10°C/min followed immediately by a 2°C/min increase to 260°C; injector, 250°C; detector, 270°C; carrier gas, helium at 173 kPa; split injection (1:13 split ratio). Compound concentrations were estimated on the basis of electronically-integrated GC peak areas relative to the internal standard (propyl dehydroabietate). An assumed relative response factor of 1.0 was used for each RFA. This is consistent with the values near unity which have previously been reported for many of these compounds^{9,10,29–31}.

Samples

A sample of effluent, collected from the outlet of a (5-day) aerated lagoon treatment system of a softwood bleached kraft mill located in eastern Canada, was used for the development and evaluation of the analytical procedure for RFA determination. Although the level of RFA in this combined bleached kraft mill effluent (BKME) after biological treatment was relatively low (total concentration about 50 μ g/l), the background level was further reduced by passing the (pH-unadjusted) ef-

fluent sample through a column containing XAD-2 resin. By using the XAD-treated effluent for method validation, the correction required for background levels was minimized, particularly for RFA at relatively low concentration levels. Yet, at the same time, this approach provided an effluent sample whose matrix was on the whole much the same (particularly with respect to relatively high-molecular-weight lignin residues and inorganic constituents) as the effluent without XAD-2 treatment.

To demonstrate the application of the RFA method, samples of BKME entering and leaving a (5-day) aerated lagoon treatment system were collected from a second softwood bleached kraft pulp mill site in eastern Canada.

Standards

The unsaturated fatty acid standards, oleic (*cis*-9-octadecenoic) and linoleic (9,12-octadecadienoic) acid, were obtained from Alltech (Deerfield, IL, U.S.A.). Standards of the resin acids (and chlorinated resin acids) commonly found in pulp mill effluents were purchased from BCR (Vancouver, Canada) with the exception of pimaric acid which was obtained from Chemicals Procurement Lab. (College Point, NY, U.S.A.). The propyl dehydroabietate internal standard¹⁹ was supplied by courtesy of L. LaFleur (NCASI, Corvallis, OR, U.S.A.).

RESULTS AND DISCUSSION

Method development and evaluation

During the course of exploratory work on the extraction of a sample of BKME with MTBE, we discovered that problematic emulsions could be eliminated provided that a volume of MTBE solvent approximately equal to or greater than the volume of the effluent sample was used. Otherwise, emulsions would form. The benefit of emulsion retardation by extracting with an equal volume of solvent was also observed when extractions were made using diethyl ether.

The recovery of RFA from an effluent sample by a single extraction with an equal volume of MTBE and the influence of effluent pH on the recovery were examined in subsequent experiments. For these studies, an XAD-2 treated lagoon outlet sample (see Experimental) spiked with known amounts of a mixture of RFA was used. The stock spiking solution prepared in dimethyl sulfoxide contained two unsaturated fatty acids, oleic and linoleic acid, and two representative resin acids, isopimaric acid and dehydroabietic acid (Fig. 1).

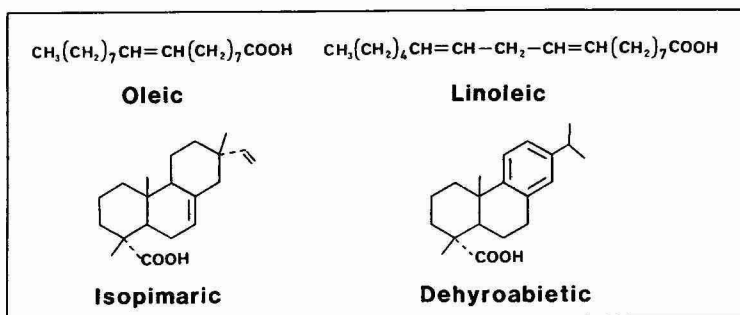


Fig. 1. Structures of representative RFA constituents of softwood pulp mill effluents.

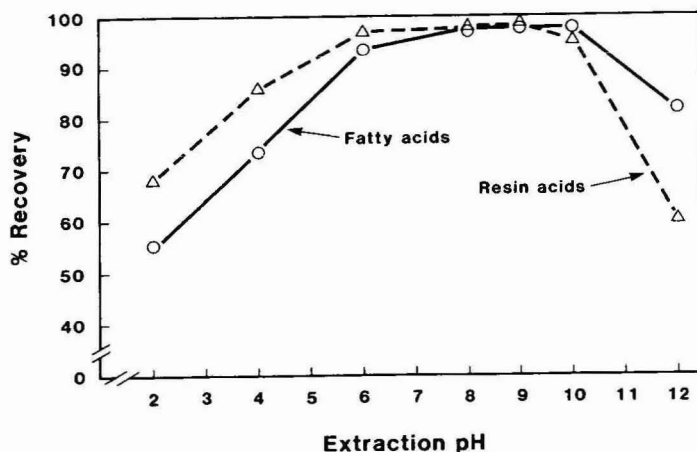


Fig. 2. Influence of effluent sample pH on the recovery of resin acids (isopimaric + dehydroabietic) and fatty acids (oleic + linoleic) from a spiked effluent sample by a single extraction with an equal volume of MTBE.

A series of spiked effluent samples, adjusted to various pH values, were extracted twice with a volume of solvent (MTBE) equal to the effluent volume (50 ml). The two extracts were worked up and analyzed separately for RFA. Percent recovery was then calculated from the ratio of the amount of RFA found from the first extraction to the sum of the amounts from the first and second extractions. The results from a study of the influence of effluent pH on the recovery of RFA in the range of pH 2–12 revealed, as shown in Fig. 2, that a maximum recovery (98%) of RFA was obtained at approximately pH 8–9. Interestingly, BCR had observed a similar optimum pH for the recovery of RFA by the resin sorption isolation technique^{11,14}. Our results indicated that the recovery by solvent extraction fell off appreciably at effluent pH values less than about pH 6 and greater than approximately pH 10. At low pH, such as pH 2, the recovery of resin acids was poor (*ca.* 68%) although somewhat better than for fatty acids (*ca.* 55%). Conversely, at relatively high pH, such as pH 12, the recovery of the fatty acids (*ca.* 81%) was higher than for the resin acids (*ca.* 60%). The low pH results are consistent with the observation by NCASI that their diethyl ether extraction procedure (at pH 2) appeared to give low recoveries for the fatty acids¹⁹.

Intuitively, one might have expected an optimum recovery of the acidic RFA compounds at low pH and this presumably is a reason, along with reduced emulsion formation¹⁰, that strongly acidic conditions have been chosen in the past for RFA isolation from pulp mill effluents by solvent concentration. Yet, in contrast, our results (Fig. 2) reveal that poor RFA recovery will be obtained under strongly acidic conditions. One possible explanation for the decreased recovery of RFA from pulp mill effluents by solvent extraction under acidic conditions is that the RFA compounds become bound to the relatively high-molecular-weight lignin residues in the effluent, much in the same manner that various authors have shown that hydrophobic pollutants can bind to dissolved humic materials (*e.g.*, see Landrum *et al.*³² and references cited therein). For example, Hassett and Anderson³³ have observed that

the recovery of cholesterol from water samples by liquid-liquid extraction was lower in the presence of dissolved humic materials. Carter and Suffet³⁴ recently found that the binding of DDT by humic materials increases at lower pH levels. Their explanation for the pH effect was that the humic polymer becomes less hydrophilic and consequently more able to bind hydrophobic compounds as its charge becomes neutralized with decreasing pH. Similarly, one can speculate that at lower pH the possibility of binding of RFA by dissolved lignin material in pulp mill effluents can be enhanced because of increases in the hydrophobic character of both the lignin material and the RFA constituents. Our finding, from additional experiments, that RFA compounds were quantitatively recovered when spiked into distilled water and extracted in the range of pH 2 to 7, lends support to the above hypothesis.

Regardless of the mechanisms responsible for the pH effects observed, this study does illustrate the importance of establishing the recovery of an analytical method by using an actual sample of the type to which the analysis is subsequently to be applied. Otherwise, possible matrix effects which can interfere with the analyte recovery may go undetected as, for example, when distilled water¹⁸ is used to assess recovery.

An additional benefit of extracting the effluent samples at pH 9, instead of at pH 2 as in the NCASI procedure, is that the amount of extraneous (often non-volatile) organic material extracted from the effluent sample is very much reduced. Thus, the effluent extracts obtained from the pH 9 extractions can probably be analyzed by splitless capillary GC without additional clean-up such as by silica gel chromatography^{16,25}.

The procedure presented in this report can also be modified to incorporate the ethylation procedure recently described by LaFleur *et al.*¹⁶ which uses triethyloxonium tetrafluoroborate.

The precision of the analytical method was determined by performing five replicate analyses of (XAD-2 treated) BKME lagoon outlet effluent spiked with our four-component RFA mixture at two different concentration levels, 200 ppb* and 20 ppb of each RFA constituent.

The precision (percent relative standard deviation) of analysis was found to be $\pm 5\%$ and $\pm 2\%$ for the fatty acids and resin acids, respectively, at the high (200 ppb) concentration level and $\pm 10\%$ and $\pm 3\%$, respectively, at the low (20 ppb) concentration level.

The detection limit of the method was determined to be approximately 5 ppb by performing split capillary GC-FID analysis of a series of solutions corresponding to concentrations of 20, 10, 5, 2.5 and 1.25 ppb of each of the four RFA used for spiking.

If required, a lower detection limit can be attained by extracting larger volumes of sample and/or by using the splitless GC injection technique in place of the split injection mode.

Method application

Fig. 3 illustrates the application of the analytical method described in this paper to the determination of the RFA content of combined pulp mill effluent en-

* The American billion (10^9) is used throughout the article.

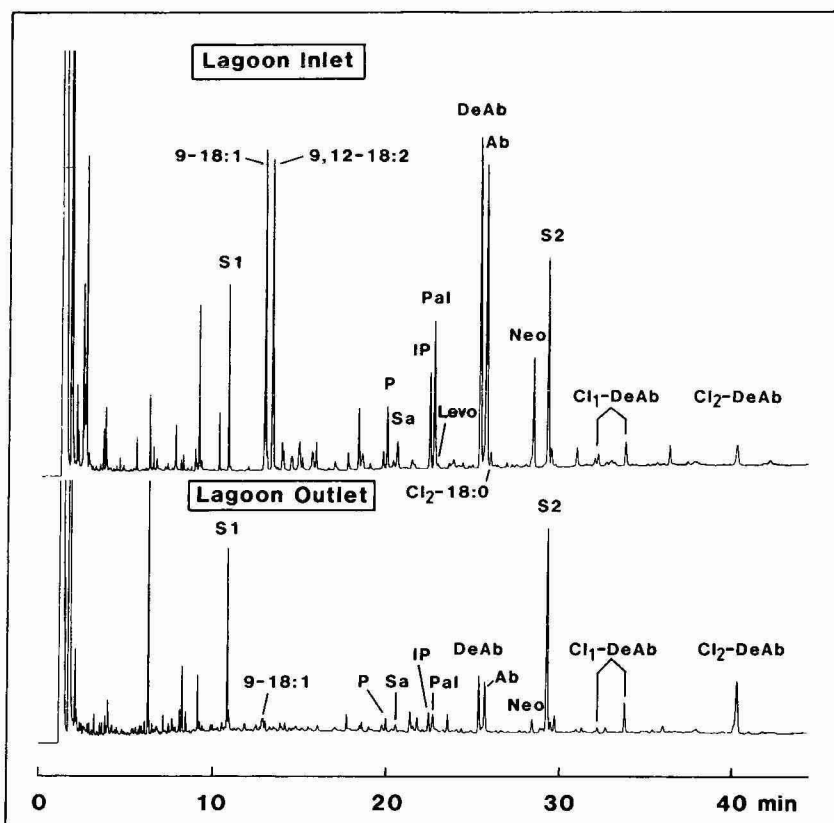


Fig. 3. Capillary GC-FID chromatograms of methylated extracts of combined bleached kraft mill effluent going into and coming out of an aerated lagoon treatment system. (RFA abbreviated notations as in Table I; S1 = surrogate compound, heptadecanoic acid; S2 = internal standard, propyl dehydroabietate).

tering and leaving the (5-day) aerated lagoon treatment system of a softwood bleached kraft pulp mill. In comparing the GC profiles for the lagoon inlet and outlet samples, it should be kept in mind that five times less sample was taken for analysis of the inlet sample. As shown, all of the major RFA constituents in the effluent samples were adequately resolved on the OV-17 type fused-silica capillary column. Of particular interest is the separation of the methyl esters of palustric and levopimaric acid. The resolution of this pair of acids has not been possible on non-polar (methyl silicone) type columns (*e.g.*, SE-30, OV-101, SE-54)^{30,31,35} except at relatively low column temperatures³⁰ which would make the analysis impractical because of the increased analysis time. Using a glass capillary column coated with 1,4-butanediol succinate (BDS), Holmbom^{15,35} has been able to satisfactorily resolve all of the major RFA components including the levopimaric-palustric pair. However, this column does not seem to be appropriate for the analysis of both non-chlorinated and chlorinated resin acids (*i.e.*, monochloro- and dichlorodehydroabietic acids) because of the excessively long retention time of the latter compounds on the BDS column.

TABLE I

CONCENTRATIONS OF RESIN AND FATTY ACIDS FOUND IN SOFTWOOD BLEACHED KRAFT MILL EFFLUENT ENTERING AND LEAVING A 5-DAY AERATED LAGOON TREATMENT SYSTEM

Acid	Concentration ($\mu\text{g/l}$)	
	Inlet	Outlet
<i>Fatty acids</i>		
Oleic (9-18:1)*	2450	21
Linoleic (9,12-18:1)	2890	—***
9,10-Dichlorostearic (Cl_2 -18:0)	34	—
<i>Resin Acids</i>		
Pimaric (P)	612	25
Sandaracopimaric (Sa)	322	19
Isopimaric (IP)	977	39
Palustric (Pal)	1510	54
Levopimaric (Lev)	71	6
Dehydroabietic (DeAb)	3860	126
Abietic (Ab)	3650	114
Neoabietic (Neo)	1300	36
Monochlorodehydroabietic** (Cl_1 -DeAb)	477	89
12,14-Dichlorodehydroabietic (Cl_2 -DeAb)	339	188
Total	18 492	719

* Shorthand notation for unchlorinated RFA as in ref. 35.

** Sum of two isomers, 12- and 14-chlorodehydroabietic acid.

*** Not detected.

The quantitative results given in Table I indicate that this aerated lagoon's removal efficiency for RFA compounds was approximately 96%. RFA removal efficiencies of >90% are not uncommon for well-operated aerated lagoons^{13,14,36,37}.

REFERENCES

- 1 J. M. Leach and A. N. Thakore, *J. Fish. Res. Board Can.*, 30 (1973) 479.
- 2 I. H. Rogers, *Pulp Pap. Mag. Can.*, 74, 9 (1973) 111.
- 3 J. M. Leach and A. N. Thakore, *Prog. Water Technol.*, 9 (1978) 787.
- 4 I. H. Rogers, H. Mahood, J. Servizi and R. Gordon, *Pulp Pap. Can.*, 80, 9 (1979) 94.
- 5 C. C. Walden and T. E. Howard, *Pulp Pap. Can.*, 82, 4 (1981) 115.
- 6 R. D. Mortimer, *The Analysis of Resin and Fatty Acids in Mill Effluents by High Performance Liquid Chromatography*, Environmental Protection Service, Environment Canada, Ottawa, CPAR Project Report No. 829-1, 1979.
- 7 R. K. Symons, *J. Liq. Chromatogr.*, 4 (1981) 1807.
- 8 D. E. Richardson, B. V. O'Grady and J. B. Bremner, *J. Chromatogr.*, 268 (1983) 341.
- 9 Anon., *Natl. Counc. Pap. Ind. Air Stream Improv., Stream Improv. Tech. Bull. No. 258*, 1972.
- 10 R. R. Claeys, *Natl. Counc. Pap. Ind. Air Stream Improv., Stream Improv. Tech. Bull. No. 281*, 1975.
- 11 J. M. Leach and A. N. Thakore, *Isolation and Analysis of Toxic Constituents of Kraft Pulp Mill Effluents, Prepr. Pap., 4th Air Stream Improv. Conf.*—*Can. Pulp. Pap. Assoc., Tech. Sec., St. Andrews, N.B., Sept. 11-13, 1973*, p. 63.
- 12 J. M. Leach and A. N. Thakore, *Isolation of the Toxic Constituents of Kraft Pulp Mill Effluents*, Environmental Protection Service, Environment Canada, Ottawa, CPAR Project Report No. 11-5, 1974.

- 13 L. T. K. Chung, H. P. Meier and J. M. Leach, *Tappi*, 62, 12 (1979) 71.
- 14 J. M. Leach and L. T. K. Chung, *Development of a Chemical Toxicity Assay for Pulp Mill Effluents*, National Technical Information Service, Springfield, VA, Report No. EPA-600-2-80-206, 1980.
- 15 B. Holmbom, *Pap. Puu*, 62 (1980) 523.
- 16 L. E. LaFleur, K. Ramage and T. M. Bousquet, *Procedures for the Analysis of Resin and Fatty Acids in Pulp Mill Effluents*, *Abstr. Pap.*, 67th Ann. Conf., Environ. Div., Chem. Inst. Can., Montreal, Quebec, June 3-6, 1984, *Abstr. EN* 1-3.
- 17 R. R. Claeys and L. E. LaFleur, *Natl. Counc. Pap. Ind. Air. Stream Improv.*, *Stream Improv. Tech. Bull. No. 343*, 1981.
- 18 V. E. Turoski, M. E. Kuehnl and B. F. Vincent, *Tappi*, 64, 5 (1981) 117.
- 19 R. Claeys, L. LaFleur, V. Elia and A. L. Caron, *Natl. Counc. Pap. Ind. Air Stream Improv.*, *Tech. Bull. No. 397*, 1983.
- 20 I. H. Rogers and H. W. Mahood, *Fish. Mar. Serv. Can. Tech. Rep. No. 730*, 1977.
- 21 R. R. Claeys and E. Owens, *Natl. Counc. Pap. Ind. Air Stream Improv.*, *Stream Improv. Tech. Bull. No. 302*, 1978.
- 22 G. A. Junk, J. J. Richard, M. D. Grieser, D. Witiak, J. L. Witiak, M. D. Arguello, R. Vick, H. J. Svec, J. S. Fritz and G. V. Calder, *J. Chromatogr.*, 99 (1974) 745.
- 23 D. E. Richardson and H. Bloom, *Appita*, 35 (1982) 477.
- 24 G. A. Junk, *Synthetic Polymers for Accumulating Organic Compounds from Water*, *Abstr. Pap.*, 188th Natl. Meet., Div. Environ. Chem., Am. Chem. Soc., Philadelphia, PA, Aug. 26-31, 1984, p. 249.
- 25 D. H. McMahon, *Tappi*, 63, 9 (1980) 101.
- 26 J. T. Wearing, M. D. Ouchi, R. D. Mortimer, T. G. Kovacs and A. Wong, *J. Pulp Pap. Sci.*, 10 (1984) J 178.
- 27 H. Schlenk and J. L. Gellerman, *Anal. Chem.*, 32 (1960) 1412.
- 28 M. J. Levitt, *Anal. Chem.*, 45 (1973) 618.
- 29 D. F. Zinkel and C. C. Engler, *J. Chromatogr.*, 136 (1977) 245.
- 30 D. O. Foster and D. F. Zinkel, *J. Chromatogr.*, 248 (1982) 89.
- 31 G. M. Dorris, M. Douek and L. H. Allen, *J. Am. Oil. Chem. Soc.*, 59 (1982) 494.
- 32 P. F. Landrum, S. R. Nihart, B. J. Eadie and W. S. Gardner, *Environ. Sci. Technol.*, 18 (1984) 187.
- 33 J. P. Hassett and M. A. Anderson, *Environ. Sci. Technol.*, 13 (1979) 1526.
- 34 C. W. Carter and I. H. Suffet, *Environ. Sci. Technol.*, 11 (1982) 735.
- 35 B. Holmbom, *J. Am. Oil Chem. Soc.*, 54 (1977) 289.
- 36 K. Chandrasekaran, R. Reis, G. Tanner and H. Rogers, *Pulp Pap. Can.*, 79, 10 (1978) 65.
- 37 D. B. Easty, L. G. Borchardt and B. A. Wabers, *Tappi*, 61, 10 (1978) 57.

CHROM. 17 930

PENTAFLUOROBENZYL *p*-TOLUENESULPHONATE AS A NEW DERIVATIZING REAGENT FOR GAS CHROMATOGRAPHIC DETERMINATION OF ANIONS

KOICHI FUNAZO*

Department of Chemistry, Osaka Prefectural Technical College, Saiwai-cho 26-12, Neyagawa, Osaka 572 (Japan)

MINORU TANAKA, KAZUHIRO MORITA, MITSUO KAMINO and TOSHIYUKI SHONO

Department of Applied Chemistry, Faculty of Engineering, Osaka University, Yamada-oka, Suita, Osaka 565 (Japan)

and

HSIN-LUNG WU

School of Pharmacy, Kaohsiung Medical College, Kaohsiung 800 (Taiwan)

(Received May 28th, 1985)

SUMMARY

A new derivatizing agent, pentafluorobenzyl *p*-toluenesulphonate, has been synthesized, which is designed to enhance the volatility of analytes and introduce a detector-oriented tag into the molecules for gas chromatography (GC) with electron-capture detection. The derivatization of several inorganic anions was studied, and a new GC method for their simultaneous determination has been developed. Bromide, iodide, cyanide, thiocyanate, nitrite, nitrate and sulphide can be simultaneously derivatized to their pentafluorobenzyl derivatives using tetra-*n*-amylammonium chloride as the phase transfer catalyst. The derivatives were subsequently determined by GC with flame ionization detection. This method has also been applied to the determination of carboxylic acids or phenols, the derivatives of which were identified using mass spectrometry. The derivatives from bromide, iodide, cyanide, thiocyanate, nitrite, nitrate and sulphide were pentafluorobenzyl bromide, pentafluorobenzyl iodide, pentafluorobenzyl cyanide, pentafluorobenzyl thiocyanate, α -nitro-2,3,4,5,6-pentafluorotoluene, pentafluorobenzyl nitrate and bis(pentafluorobenzyl) sulphide, respectively. The effects of added acid or base, and of the reaction time, on the pentafluorobenzylation are discussed.

INTRODUCTION

Gas chromatography (GC) is a valuable technique for determining volatile organic and inorganic compounds because of its unmatched separating power. By use of derivatization, furthermore, this technique can be extended to the determination of non-volatile and thermally unstable compounds. Derivatization has been used not only to increase the volatility of compounds but also to introduce a detec-

tor-oriented tag into the molecules. Electron-capture detection (ECD) has been studied in conjunction with derivatization, due to its very high sensitivity¹, and various derivatizing agents have been developed for electron-capture GC.

We are interested in GC of inorganic anions, which is still a relatively new and far from thoroughly investigated discipline because of the non-volatility of inorganic anions and the failure to find suitable methods of chemical derivatization. Nevertheless, some procedures have been reported for GC of inorganic anions²⁻⁵. The majority of these procedures are for the determination of individual inorganic anions, while only a few are for their simultaneous determination. Chloride, bromide and iodide, for instance, were reported to be simultaneously determined by GC, based on the addition of hydrogen halides to epoxides^{6,7}. Silylation was also applied to the simultaneous GC determination of several inorganic oxyanions⁸⁻¹⁰. In that method, the anions were desiccated as their tetraalkylammonium salts before silylation. Faigle and Klockow¹¹ reported a procedure for the simultaneous determination of nitrate, sulphate and phosphate as their *n*-butyl esters formed by reaction with *n*-butyl iodide. MacGee and Allen¹² described the determination of four halides: they were converted into their tetraalkylammonium salts on an ion-exchange resin and then into the corresponding alkyl halides by thermal decomposition in the injection port of the gas chromatograph. This method was modified by using an alkyl sulphonate, such as *n*-butyl *p*-toluenesulphonate¹³ or *n*-decyl methanesulphonate¹⁴, as the alkylating agent. In this case, the inorganic anions must first be isolated or dried before alkylation because the derivatization takes place in the water-free organic solvent. We have improved this method, which is complicated and time-consuming: aqueous bromide, iodide, thiocyanate and nitrate were extracted into the organic layer from the aqueous one as their tetraalkylammonium salts and then *n*-butylated with *n*-butyl *p*-toluenesulphonate¹⁵.

All the methods described above are not very sensitive, because the use of flame ionization detection (FID) or thermal conductivity detection (TCD) could not be avoided, owing to the introduction of the hydrocarbon moieties from the derivatizing agents. Therefore, in order to use ECD, which is much more sensitive than FID or TCD, we have attempted pentafluorobenzoylation of inorganic anions instead of *n*-butylation in our previous method¹⁵ and synthesized a new derivatizing agent, pentafluorobenzyl *p*-toluenesulphonate (TsO-PFB). Its applicability to the simultaneous determination of inorganic anions by GC has been investigated. Organic anions, such as carboxylates and phenolates, have also been derivatized with TsO-PFB. This paper describes a preliminary study of the simultaneous determination of inorganic or organic anions at relatively high concentrations using FID. The final objective of this work is, of course, to develop a new GC method for the simultaneous determination of trace inorganic or organic anions by using ECD.

EXPERIMENTAL

Apparatus

A Yanaco G-180 gas chromatograph equipped with a dual FID system (Yanagimoto, Kyoto, Japan) was used together with a stainless-steel coiled tube (4 m × 3 mm I.D.) as separation column. The liquid phase and column temperature employed in determining each inorganic anion are given in Table I. For simultaneous

TABLE I

GC CONDITIONS AND CORRELATION COEFFICIENTS OF CALIBRATION CURVES FOR DETERMINATION OF INORGANIC ANIONS

Anion	Liquid phase	Column temp. (°C)	Internal standard and concentration (M)	Correlation coefficient	Concentration range (ppm)
Br ⁻	5% OV-225	120	Benzyl bromide (0.01)	0.9991	30–300
I ⁻	5% OV-225	120	Iodobenzene (0.05)	0.9996	50–500
CN ⁻	5% OV-225	180	Tribromobenzene (0.01)	0.9952	10–100
SCN ⁻	5% OV-225	180	Tribromobenzene (0.01)	0.9997	20–200
NO ₂ ⁻	5% DC-550	120	Iodobenzene (0.01)	0.9993	45–450
NO ₃ ⁻	5% DC-550	155	<i>p</i> -Dibromobenzene (0.01)	0.9990	25–250
S ²⁻	5% OV-225	200	Tribromobenzene (0.005)	0.9985	6.5–65
Cl ⁻	5% PEG-HT	110	<i>p</i> -Dichlorobenzene (0.05)	0.9992	35–350

determinations, the column was packed with 5% OV-225 (2.5 m) + 5% OV-210 (1.5 m). The liquid phases 5% OV-225 and 3% OV-17 were used in the determination of individual organic anions and for their simultaneous determination, respectively. The column packing materials, 5% OV-225, 5% OV-210, 3% OV-17, 5% DC-550 and 5% PEG-HT on Uniport HP (60–80 mesh) were obtained from Gasukuro Kogyo (Tokyo, Japan). Nitrogen was used as the carrier gas at a constant flow-rate of 30 ml/min. The injection port and detector temperatures were maintained at 250°C. A Shimadzu Chromatopac C-R1B data processor was used as the recorder and integrator.

A Hitachi RMU-6E mass spectrometer was employed with an ionization source temperature of 200°C, an electron energy of 70 eV and an acceleration energy of 1.8 kV.

Reagents

Analytical-reagent grade tetra-*n*-butylammonium hydrogensulphate (TBAHS) was obtained from Tokyo Kasei (Tokyo, Japan), and commercial grade tetra-*n*-amylammonium chloride (TAAC) from Wako (Osaka, Japan). The new derivatizing agent, TsO-PFB, was prepared from *p*-toluenesulphonyl chloride and pentafluorobenzyl alcohol by a modification of the literature method¹⁶ and recrystallized from methanol. It was identified by mass spectrometry and infrared spectrophotometry (Fig. 1). The inorganic anions were used as their sodium or potassium salts of analytical reagent grade. Dichloromethane and deionized water were distilled before use for analysis. All other chemicals were also of analytical-reagent grade.

Procedure

The procedure for the simultaneous determination of bromide, iodide, cyanide, thiocyanate, nitrite, nitrate and sulphide was as follows. A brown-coloured test-tube with a screw cap (*ca.* 10 ml) was used as the reaction vessel in order to protect the contents from the light. To 1.0 ml of a reference standard solution containing the seven inorganic anions were added 0.2 ml of a 0.1 M aqueous solution of TAAC and 1.0 ml of a 0.1 M solution of TsO-PFB in dichloromethane. The vessel was sealed

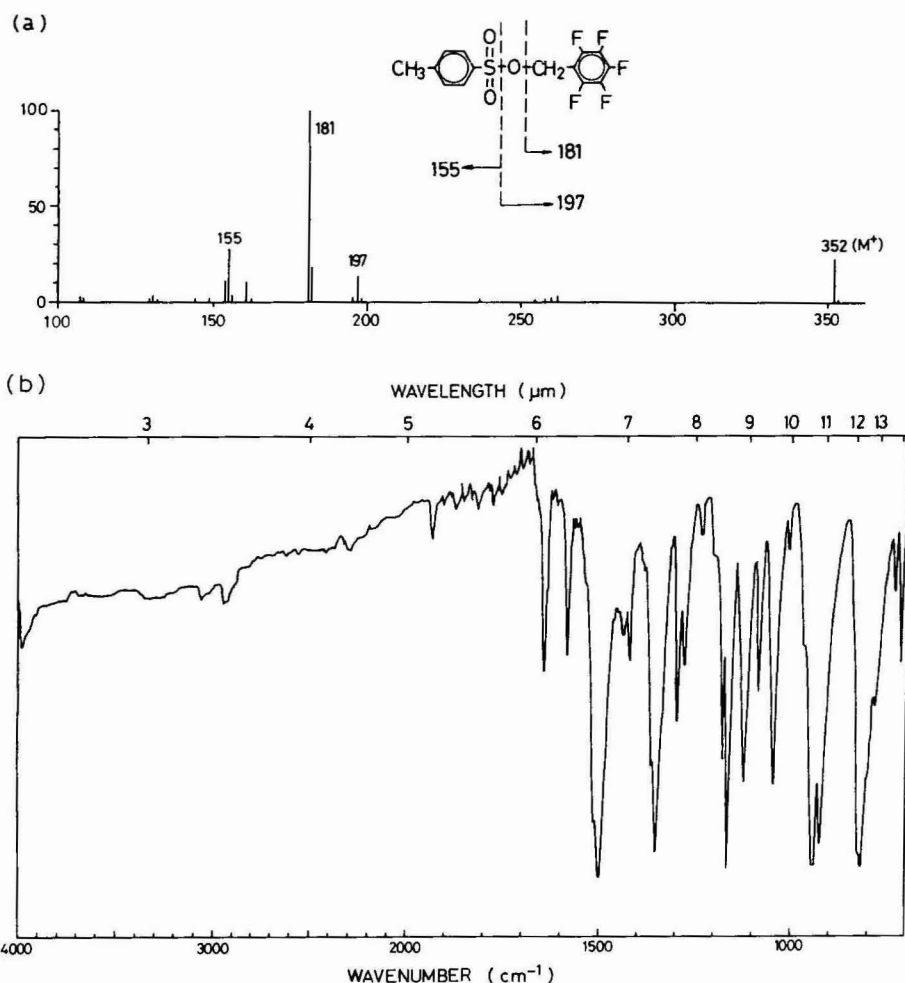


Fig. 1. Mass (a) and infrared (b) spectra of TsO-PFB.

tightly with the stopper and shaken mechanically for 30 min at room temperature. The organic layer was then separated from the aqueous one, and an aliquot of it (0.5 μ l) was injected into the gas chromatograph. For the determination of the individual anions, the dichloromethane solution of TsO-PFB contained an internal standard as listed in Table I.

The procedure for determining carboxylic acids or phenols was different from the above. To 1.0 ml of a reference standard solution containing carboxylic acids or phenols was added 0.5 ml of a 0.1 *M* aqueous solution of TAAC, 0.1 ml of a buffer solution pH 12.0 comprising 0.05 *M* disodium hydrogenphosphate and 0.0432 *M* sodium hydroxide and 1.0 ml of a 0.05 *M* solution of TsO-PFB in dichloromethane. Then the reaction vessel was shaken for 2 h (carboxylic acids) or for 1 h (phenols). For determinations of the individual carboxylic acids or phenols, 0.5 ml of dichloromethane were further added, which contained an internal standard as listed in Table II.

TABLE II

GC CONDITIONS AND CORRELATION COEFFICIENTS OF CALIBRATION CURVES FOR DETERMINATION OF CARBOXYLIC ACIDS OR PHENOLS

Internal standards: BDCB = 1-bromo-2,4-dichlorobenzene; DBB = *p*-dibromobenzene; TCB = 1,2,3,4-tetrachlorobenzene.

Carboxylic acid or phenol	Column temp. (°C)	Internal standard and concentration (mM)	Correlation coefficient
<i>n</i> -Butyric acid	160	BDCB (6.6)	0.9994
<i>n</i> -Valeric acid	170	DBB (5.0)	0.9988
Isovaleric acid	170	TCB (10.0)	0.9992
<i>n</i> -Caproic acid	170	DBB (5.0)	0.9985
Isocaproic acid	170	DBB (5.0)	0.9982
<i>n</i> -Heptanoic acid	180	TCB (8.0)	0.9993
<i>n</i> -Caprylic acid	180	TCB (8.0)	0.9987
Phenol	180	TCB (5.0)	0.9983
<i>o</i> -Cresol	180	TCB (8.0)	0.9990
<i>m</i> -Cresol	180	TCB (8.0)	0.9992
<i>p</i> -Cresol	180	TCB (8.0)	0.9983
2,4-Xylenol	190	TCB (8.0)	0.9996
2,6-Xylenol	190	TCB (8.0)	0.9986
3,4-Xylenol	190	TCB (8.0)	0.9992
3,5-Xylenol	190	TCB (8.0)	0.9995
<i>o</i> -Methoxyphenol	190	TCB (8.0)	0.9996

RESULTS AND DISCUSSION

Pentafluorobenzylation of inorganic anions

Fig. 1 shows the mass and infrared spectra of TsO-PFB synthesized. The mass peaks at m/e 352 and 181 correspond to the parent ion and base ion equivalent to the fragment $C_6F_5CH_2^+$, and infrared bands at 1170 and 1360 cm^{-1} are characteristic of the symmetric and antisymmetric vibrations of $S(=O)_2$, respectively.

In order to estimate the ability of TsO-PFB to pentafluorobenzylate inorganic anions, the derivatization reaction was performed as described in the Experimental section for bromide, iodide, cyanide, thiocyanate, nitrite, nitrate sulphide, cyanate, sulphate, carbonate, phosphate and phosphite. For the first seven anions from bromide to sulphide, the GC peaks seemed to correspond to the PFB derivatives of the anions. However, the other anions did not give GC peaks. Therefore, further studies were carried out only for the seven anions.

The PFB derivatives of the inorganic anions were identified as follows. An authentic sample of the PFB derivative of each anion was synthesized by scaling up the reaction and was examined by mass spectrometry after purification. From the mass spectra obtained, the PFB derivatives of bromide, iodide, cyanide, nitrite, nitrate and sulphide were assigned as pentafluorobenzyl bromide (PFB-Br), pentafluorobenzyl iodide (PFB-I), pentafluorobenzyl cyanide (PFB-CN), α -nitro-2,3,4,5,6-pentafluorotoluene (PFB-NO₂), pentafluorobenzyl nitrate (PFB-ONO₂) and bis(pentafluorobenzyl) sulphide [(PFB)₂S], respectively. From its mass spectrum, the PFB derivative of thiocyanate (Fig. 2) seemed to be pentafluorobenzyl thiocyanate (PFB-

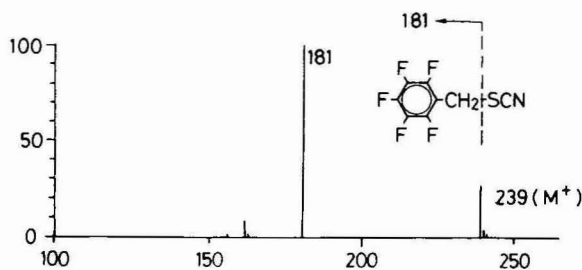


Fig. 2. Mass spectrum of the PFB derivative of thiocyanate.

SCN) or pentafluorobenzyl isothiocyanate. Based on the qualitative test of alkyl thiocyanate or isothiocyanate reported by Kemp¹⁷, the PFB derivative of thiocyanate was identified as PFB-SCN. Bromide, iodide, cyanide, nitrate and sulphide are each converted into only one PFB derivative under the various conditions tested. However, depending on the derivatization conditions, nitrite or thiocyanate gives two PFB derivatives, *i.e.*, PFB-NO₂ or PFB-ONO₂ for nitrite or PFB-SCN and/or (PFB)₂S for thiocyanate.

Optimum derivatization conditions for inorganic anions

The effect on the derivatization of added acid or base was examined using TBAHS or TAAC as the phase transfer catalyst. To 1.0 ml of a 0.05 *M* aqueous solution of each inorganic anion were added 0.5 ml sulphuric acid or potassium hydroxide at different concentrations, 0.2 ml of a 0.1 *M* aqueous solution of the phase transfer catalyst and 1.0 ml of a 0.1 *M* solution of TsO-PFB in dichloromethane. Then the derivatization was performed by shaking for 1 h. Fig. 3 shows the results; the derivatization yield (the overall yield containing the extraction yield) plotted on the ordinate was measured as follows. The peak area of the PFB derivative produced from each anion at 0.05 *M* was compared with that of a standard solution. The latter contained each authentic PFB derivative at a concentration of 0.05 *M*, corresponding to a derivatization yield of 100%.

When TBAHS is the phase transfer catalyst (Fig. 3a), nitrite is derivatized mainly to PFB-ONO₂ (●) and slightly to PFB-NO₂ (○), independent of the concentration of the added acid or base. In an acidic medium, thiocyanate is derivatized to PFB-SCN (○) in quite high yield, but to (PFB)₂S (●) in relatively low yields in a basic medium. Similar behaviour for thiocyanate is also observed when using TAAC (Fig. 3b). The optimum pH for the derivatization of nitrate and sulphide was achieved by adding 8.0 *M* potassium hydroxide. However, this is not the case for the derivatization of thiocyanate. Consequently, the optimum pH for the simultaneous determination of the seven anions cannot be found when TBAHS is used as the phase transfer catalyst.

Fig. 3b shows the results of the effect of added acid or base on the derivatization with TAAC. Nitrite is derivatized to PFB-NO₂ (○) when neither sulphuric acid nor potassium hydroxide is added. Thiocyanate is derivatized to PFB-SCN (○) in an acidic or neutral medium, in quantitative yield. It is also clear that neither the addition of sulphuric acid nor potassium hydroxide leads to the optimum pH. This suggests that simultaneous determination is possible by using TAAC as the

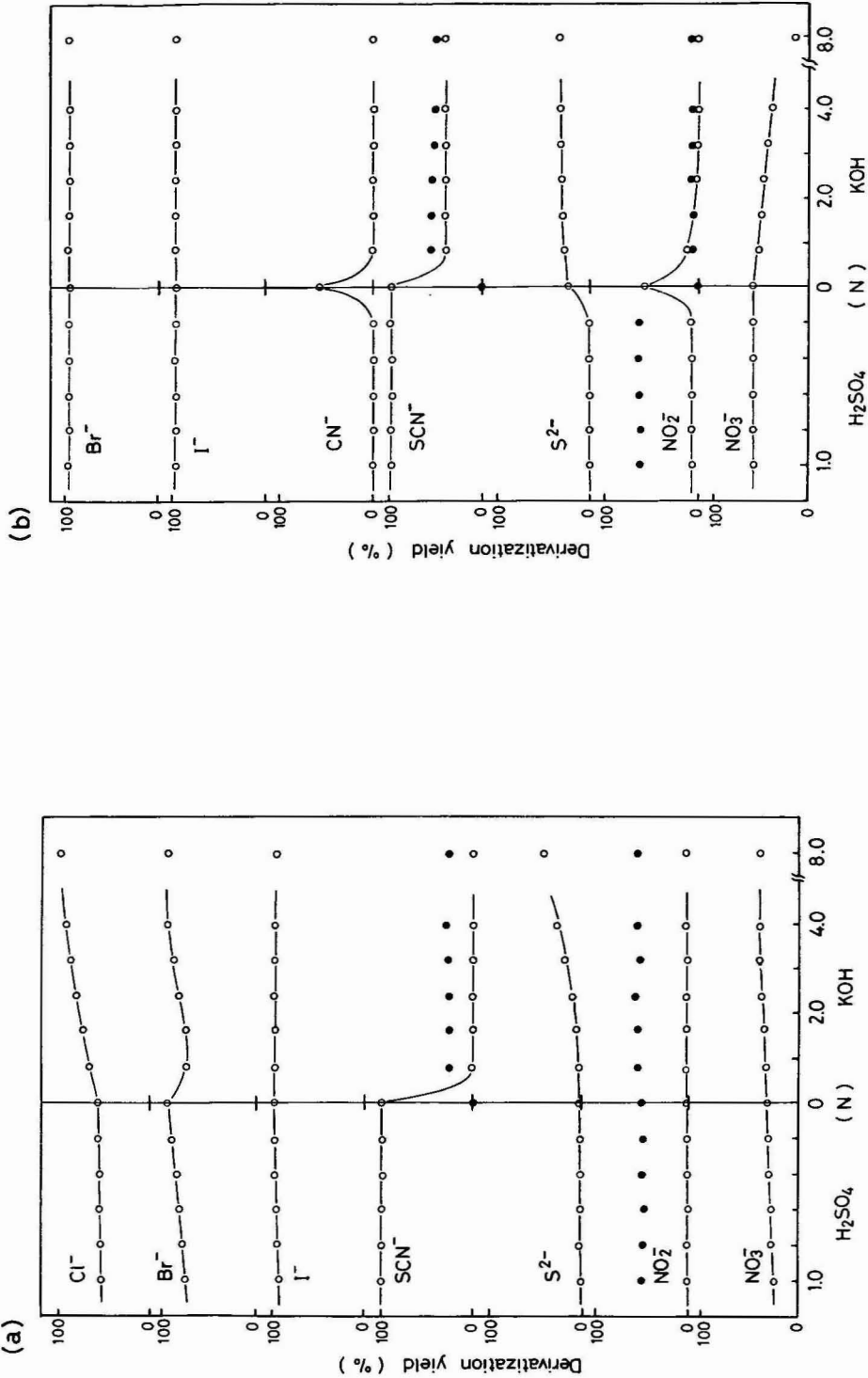


Fig. 3. Effect of added acid or base on the derivatization of inorganic anions, using TBAHS (a) or TAAC (b) as the phase transfer catalyst.

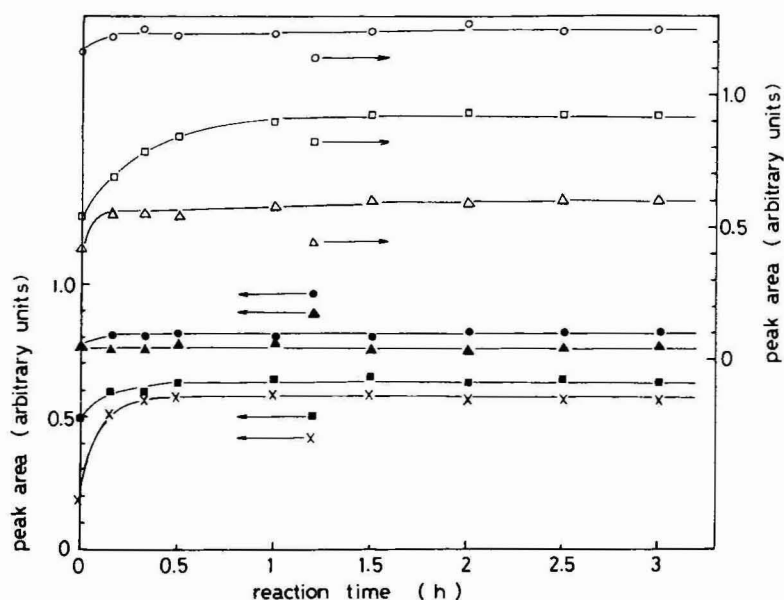


Fig. 4. Effect of reaction time on the derivatization of inorganic anions. Anions: ○ = bromide; ● = iodide; △ = cyanide; ▲ = thiocyanate; □ = nitrite; ■ = nitrate; × = sulphide.

phase transfer catalyst. Therefore, further work was carried out with TAAC, adding neither the acid nor the base.

The effect of reaction time on the derivatization was also examined at the optimum pH. The results are shown in Fig. 4; about 30 min are required for plateau formation with all the PFB derivatives. A period of 30 min was therefore set as the derivatization time.

Analytical calibration and gas chromatogram

The application of the method to the determination of the seven inorganic anions was evaluated. Ten different concentrations of the reference standard solutions containing each anion were quantitated in order to construct a calibration curve

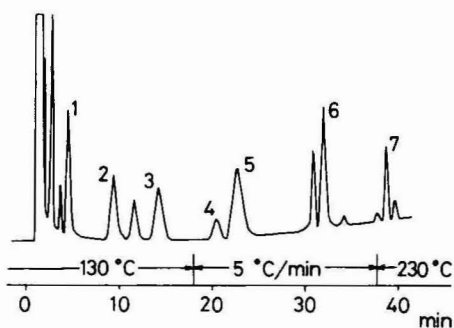


Fig. 5. Gas chromatogram for the simultaneous determination of seven inorganic anions. Peaks: 1 = bromide; 2 = iodide; 3 = nitrate; 4 = nitrite; 5 = cyanide; 6 = thiocyanate; 7 = sulphide.

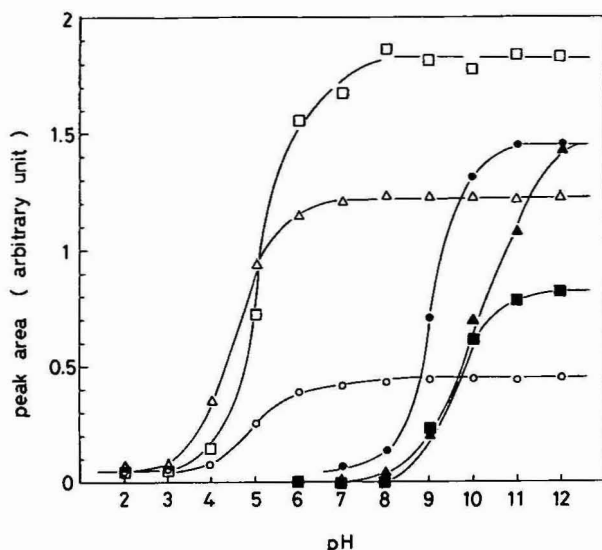


Fig. 6. Effect of pH on the derivatization of carboxylic acids or phenols. Analytes: ○ = *n*-butyric acid; △ = *n*-valeric acid; □ = isocaproic acid; ● = phenol; ▲ = *o*-cresol; ■ = 2,6-xyleneol.

of the amount of each anion *versus* the ratio of the peak area of the corresponding PFB derivative to that of the internal standard. Straight lines were obtained passing through the origin. The correlation coefficients and the determination ranges are given in Table I.

Fig. 5 shows the gas chromatogram obtained for the simultaneous determination of the seven inorganic anions. The resolution of the seven PFB derivatives is very difficult on a column containing only one liquid phase. Therefore, we used a column packed with OV-225 and OV-210, with temperature-programming. For the determination of individual anions, the organic layer is subjected to isothermal GC at the column temperature given in Table I, and the resulting PFB derivative determined by an internal standard method.

Derivatization of carboxylic acids or phenols

The derivatization method described for the inorganic anions was also applied to the determination of organic anions. In addition to the carboxylic acids and the phenols listed in Table II, formic, acetic and propionic acids were examined, but were not derivatized in relatively high yields under various reaction conditions. The derivatization was performed at various pH values by using buffer solutions, according to the procedure described in the Experimental section. Fig. 6 shows some of the results, which indicate that the derivatization yields for the carboxylic acids and the phenols become constant at pH higher than 7 and 12, respectively. Therefore, a buffer solution of pH 12 was used. The reaction time was set at 120 min for the derivatization of carboxylic acids and at 60 min for that of phenols.

Fig. 7 shows typical gas chromatograms for the mixtures of PFB derivatives obtained under the optimum reaction conditions. Good resolution of the derivatives of carboxylic acids or phenols is achieved on the column of 3% OV-17, except for

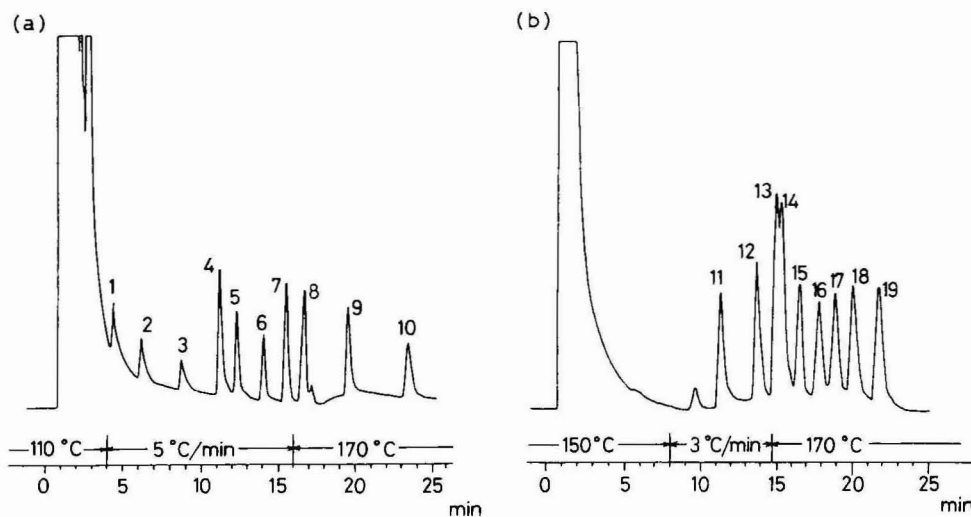


Fig. 7. Gas chromatograms for the simultaneous determination of carboxylic acids (a) and phenols (b). Peaks: 1 = formic acid; 2 = acetic acid; 3 = propionic acid; 4 = *n*-butyric acid; 5 = isovaleric acid; 6 = *n*-valeric acid; 7 = isocaproic acid; 8 = *n*-caproic acid; 9 = *n*-heptanoic acid; 10 = *n*-caprylic acid; 11 = phenol; 12 = *o*-cresol; 13 = *m*-cresol; 14 = *p*-cresol; 15 = 2,6-xyleneol; 16 = 2,4-xyleneol; 17 = 3,5-xyleneol; 18 = *o*-methoxyphenol; 19 = 3,4-xyleneol.

m- and *p*-cresol (Fig. 7b). In Fig. 7a, formic, acetic and propionic acids are included, though they give low derivatization yields. Calibration curves for all the acids (except for these three) and phenols were constructed over the concentration range 0.20–2.0 mM. They were all straight lines passing through the origin, and the correlation coefficients are given in Table II. The derivatives of carboxylic acids and phenols were also identified by mass spectrometry, as with those of inorganic anions. The carboxylic acids are derivatized as their PFB esters, and the phenols as their PFB ethers.

CONCLUSIONS

It is found that inorganic anions, *i.e.*, bromide, iodide, cyanide, thiocyanate, nitrite, nitrate and sulphide, can be simultaneously determined by pentafluorobenzylation with TsO-PFB and TAAC followed by GC-FID. Furthermore, chloride is also pentafluorobenzylated; however, it cannot be determined when TAAC is used as the phase transfer catalyst, because TAAC possesses chloride as a counter anion. In the determination of chloride, 8.0 M potassium hydroxide aqueous solution (0.5 ml) was added to the solution containing chloride, which was then derivatized using TBAHS instead of TAAC as described for the other seven inorganic anions. The GC conditions and the correlation coefficient of the calibration curve for chloride are also given in Table I together with those of the other inorganic anions.

The present technique based on pentafluorobenzylation is an ECD-oriented derivatization designed to enhance the sensitivity. The development of this method for the simultaneous determination of trace inorganic or organic anions by GC-ECD is under investigation.

ACKNOWLEDGEMENT

This work was partially supported by a Grant-in-Aid for Scientific Research from the Ministry of Education of Japan.

REFERENCES

- 1 C. F. Poole and A. Zlatkis, *Anal. Chem.*, 52 (1980) 1002A.
- 2 J. A. Rodringuea-Vázquez, *Anal. Chim. Acta*, 73 (1974) 1.
- 3 J. Drozd, *J. Chromatogr.*, 113 (1976) 303.
- 4 W. C. Butts, in K. Blau and G. S. King (Editors), *Handbook of Derivatives of Chromatography*, Heyden & Son, London, 1978, p. 411.
- 5 M. Tanaka and T. Shono, *Kagaku (Kyoto)*, 36 (1981) 149.
- 6 H. A. Russel, *Angew. Chem., Int. Ed. Engl.*, 9 (1970) 392.
- 7 B. Vierkorn-Rudolph and K. Bächmann, *J. Chromatogr.*, 217 (1981) 311.
- 8 W. C. Butts, *Anal. Lett.*, 3 (1970) 29.
- 9 W. C. Butts and W. Rainey, Jr., *Anal. Chem.*, 43 (1971) 538.
- 10 T. P. Mawhinney, *Anal. Lett.*, 16 (1983) 159.
- 11 W. Faigle and D. Klockow, *Z. Anal. Chem.*, 306 (1981) 190.
- 12 J. MacGee and K. G. Allen, *Anal. Chem.*, 42 (1970) 1672.
- 13 W. M. Moore, *Anal. Chem.*, 54 (1982) 602.
- 14 W. Faigle and D. Klockow, *Z. Anal. Chem.*, 310 (1982) 33.
- 15 K. Funazo, H.-L. Wu, K. Morita, M. Tanaka and T. Shono, *J. Chromatogr.*, 319 (1985) 143.
- 16 A. H. Blatt (Editor), *Org. Synth.*, Collect. Vol. 1 (1956) 145.
- 17 W. E. Kemp, *Analyst (London)*, 64 (1939) 658.

CHROM. 17 935

3-BROMOMETHYL-6,7-DIMETHOXY-1-METHYL-2(1*H*)-QUINOXALINONE AS A NEW FLUORESCENCE DERIVATIZATION REAGENT FOR CARBOXYLIC ACIDS IN HIGH-PERFORMANCE LIQUID CHROMATOGRAPHY

MASATOSHI YAMAGUCHI, SHUJI HARA, REIKO MATSUNAGA and MASARU NAKAMURA

Faculty of Pharmaceutical Sciences, Fukuoka University, Nanakuma, Jonan-ku, Fukuoka 814-01 (Japan)
and

YOSUKE OHKURA*

Faculty of Pharmaceutical Sciences, Kyushu University 62, Maidashi, Higashi-ku, Fukuoka 812 (Japan)

(Received May 20th, 1985)

SUMMARY

3-Bromomethyl-6,7-dimethoxy-1-methyl-2(1*H*)-quinoxalinone was found to be a selective and highly sensitive fluorescence derivatization reagent for carboxylic acids in high-performance liquid chromatography. Its reactivity was investigated for various linear C₃–C₂₀ saturated fatty acids. The reagent reacts with the fatty acids in acetonitrile in the presence of 18-crown-6 and potassium carbonate to produce the corresponding fluorescent esters, which can be separated on a reversed-phase column, Radial-Pak C₁₈ cartridge, with gradient elution using 57–100% (v/v) aqueous methanol; the detection limits for the acids were 0.3–1 fmol for an injection volume of 5 μ l. The reagent also reacts with unsaturated fatty, dicarboxylic, aromatic carboxylic and hydroxycarboxylic acids and acidic nucleotides to form fluorescent derivatives. α -Keto acids and α -amino acids do not give fluorescent derivatives under these conditions.

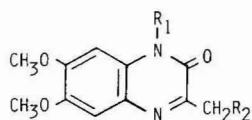
INTRODUCTION

Many fluorescence derivatization agents have been developed for the determination of carboxylic acids by high-performance liquid chromatography (HPLC), e.g., 4-hydroxymethyl-7-methoxy¹, 4-diazomethyl-7-methoxy², 4-bromomethyl-6,7-dimethoxy³ and 4-bromomethyl-7-methoxycoumarins (Br-MMCs)^{4–6}, N,N'-dicyclohexyl-O-(7-methoxycoumarin-4-yl)methylisourea⁷, 8-(chloromethyl)-⁸, 9-(hydroxymethyl)-⁹ and 9-aminophenanthrene¹⁰, 9-anthryldiazomethane^{11,12}, 9,10-diaminophenanthrene¹³, *p*-(9-anthroyl)phenacyl bromide¹⁴, 1-aminoethyl-4-dimethylaminonaphthalene¹⁵ and 1-bromoacetylpyrene¹⁶. HPLC methods with these reagents are fairly sensitive but, in general, do not permit the determination of carboxylic acids at sub-femtomol level. Of these reagents, Br-MMC may be most suit-

able, because it has the smallest molecular size. Thus, Br-MMC has been most widely used for the determination of carboxylic acids. However, the fluorescence intensities of the MMC derivatives of carboxylic acids are greatly influenced by the solvent. Furthermore, the fluorescence intensities of these derivatives depend on the kind of carboxylic acids¹⁷. 9,10-Diaminophenanthrene derivatives are also subject to solvent effects¹³. Thus, these disadvantages make it difficult to separate various carboxylic acids using gradient elution and determine them simultaneously at the same detector sensitivity.

Recently, a fluorimetric HPLC method for the determination of carboxylic acids using 4-bromomethyl-7-acetoxycoumarin (Br-MAC) has been developed¹⁸. It is based on the reaction of Br-MAC with carboxylic acids to give esters, which are then separated by HPLC. The derivatives in the eluates are hydrolyzed by an alkaline solution in a post-column system and the resulting fluorescence is detected. The method is very sensitive and does not suffer from the above disadvantages, but requires both pre- and post-column techniques.

We have reported that pyruvic acid reacts with 1,2-diamino-4,5-dimethoxybenzene (DDB) in acidic solution to form a highly fluorescent product, 6,7-dimethoxy-3-methyl-2(1*H*)-quinoxalinone (DQ)^{19,20}. Recently, we found that 6,7-dimethoxy-1,3-dimethyl-2(1*H*)-quinoxalinone (DDQ), a methylation product of DQ, gives a more intense fluorescence. Thus 3-bromomethyl-6,7-dimethoxy-1-methyl-2(1*H*)-quinoxalinone (Br-DMEQ) was synthesized as a fluorescence derivatization reagent for carboxylic acids. In order to investigate its reactivity with carboxylic acids, linear saturated C₃–C₂₀ fatty acids have been employed as model carboxyl compounds. Br-DMEQ reacts with the fatty acids in acetonitrile or acetone in the presence of 18-crown-6 and potassium carbonate to produce the corresponding fluorescent esters. The esters are separated on a reversed-phase column with gradient elution using aqueous methanol. The reactivity of Br-DMEQ with various carboxylic acids (unsaturated fatty, dicarboxylic, hydroxycarboxylic, aromatic carboxylic, α -keto and α -amino acids) and acidic nucleosides has also been studied.



$R_1=R_2=H$: DQ; $R_1=CH_3$, $R_2=H$: DDQ

$R_1=CH_3$, $R_2=Br$: Br-DMEQ

EXPERIMENTAL

Apparatus

Uncorrected fluorescence spectra and intensities were measured with a Hitachi MPF-2A spectrofluorimeter in 10 × 10 mm quartz cells; spectral bandwidths of 6 nm were used in both the excitation and emission monochromators.

Infrared (IR) spectra were recorded with a Shimadzu 430 spectrophotometer using potassium bromide pellets. ¹H and ¹³C nuclear magnetic resonance (NMR) spectra were obtained with Hitachi R-22 and JEOL FX-100 spectrometers at 90 and

25.1 MHz, respectively, using a *ca.* 5% (w/v) solution of [$^2\text{H}_6$]dimethylsulphoxide (DMSO- d_6) containing tetramethylsilane as an internal standard. The splitting patterns were designated as follows: s, singlet; d, doublet; t, triplet; q, quartet. In ^{13}C NMR spectra, signals were assigned by both the complete decoupling and off-resonance decoupling techniques. Electron impact mass spectra were taken with a JEOL DX-300 spectrometer. The pH was measured with a Hitachi-Horiba M-7 pH meter at *ca.* 25°C. Uncorrected melting points were measured with a Yazawa melting point apparatus.

Materials and reagents

All chemicals were of analytical reagent grade, unless noted otherwise. Deionized and distilled water was used. Acetonitrile and acetone for the derivatization reaction were refluxed over calcium hydroxide for more than 10 h and distilled through a 120-cm column filled with helical coils. The solvents were used within 2 days, because they were contaminated with some fatty acids present in air. Propionic (C_3), butyric (C_4), valeric (C_5), caproic (C_6), caprylic (C_8), capric (C_{10}), lauric (C_{12}), myristic (C_{14}), palmitic (C_{16}), margaric (C_{17}), stearic (C_{18}) and arachidic (C_{20}) acids were purchased from Sigma (St. Louis, MO, U.S.A.).

Synthesis of Br-DMEQ

DQ was prepared by the reaction of pyruvic acid with DDB as described previously²⁰. DQ (1 g, 4.5 mmol) in 50 ml of anhydrous methanol was treated with an ethereal diazomethane solution prepared by the established method²¹. The reaction mixture was evaporated to dryness *in vacuo*. The residue dissolved in 5 ml of ethyl acetate was purified by column chromatography (25 \times 3.5 cm I.D.) on silica gel 60 (*ca.* 130 g, 70–230 mesh; Japan Merck, Tokyo, Japan) with *n*-hexane–ethyl acetate (1:3, v/v) as eluent, to give DDQ (380 mg, 1.6 mmol) as yellow needles, m.p. 170–171°C. IR $\nu_{\text{max}}^{\text{KBr}}$ (cm^{-1}): 1640 (C=O); 1620 (aromatic C=N). ^1H NMR (DMSO- d_6): δ 2.39 (3H, s, C- CH_3); 3.61 (3H, s, N- CH_3); 3.83 and 3.94 (each 3H, each s, O- CH_3); 7.21 and 6.91 (each 1H, each s, aromatic H). ^{13}C NMR (DMSO- d_6): δ 20.7 (q), 29.1 (q), 55.9 (q), 56.2 (q), 97.5 (q), 110.6 (d), 126.1 (s), 128.0 (s), 145.6 (s), 150.9 (s), 153.8 (s), 154.3 (s). Analysis (%) calculated for $\text{C}_{12}\text{H}_{14}\text{N}_2\text{O}_3$: C, 61.53; H, 6.02; N, 11.96; found: C, 61.71; H, 6.11; N, 11.77. MS: m/z 234 (M^+); 219 ($\text{M}^+ - \text{CH}_3$); 163 ($\text{M}^+ - \text{CH}_3 - \text{CH}_3\text{O}$). DDQ was stable in the crystalline state for at least a year in daylight at room temperature.

To a solution of DDQ (350 mg, 1.5 mmol) in 3 ml of acetic acid placed in 20-ml screw-capped test-tube were added *ca.* 350 mg of anhydrous sodium acetate and 2 ml of 1.5 *M* bromine in acetic acid. The tube was tightly closed and heated at 100°C for *ca.* 15 min, then cooled. The precipitates formed on adding *ca.* 10 ml of diethyl ether were removed by filtration and washed two or three times with small portions of ether. The combined filtrates and washings were evaporated to dryness. The residue dissolved in 5 ml of ethyl acetate was chromatographed on silica gel 60 (*ca.* 130 g, 70–230 mesh, Japan Merck; column size, 25 \times 3.5 cm I.D.) with ether. The main fraction was concentrated to dryness and the residue was recrystallized from *n*-hexane–ethyl acetate (1:1, v/v) to give Br-DMEQ (110 mg, 0.6 mmol) as yellow needles, m.p. 161–163°C. IR $\nu_{\text{max}}^{\text{KBr}}$ (cm^{-1}): 1640 (C=O); 1620 (aromatic C=N). ^1H NMR (DMSO- d_6): δ 3.71 (3H, s, N- CH_3); 3.93 and 4.01 (each 3H, each

s, O-CH₃); 4.62 (2H, s, CH₂-Br); 6.64 and 7.24 (each 1H, each s), aromatic H). ¹³C NMR (DMSO-d₆) :δ 25.5 (t), 29.5 (q), 56.2 (q), 56.8 (q), 98.1 (q), 111.1 (d), 127.0 (s), 128.8 (s), 146.1 (s), 151.3 (s), 154.4 (s), 155.0 (s). Analysis (%) calculated for C₁₂H₁₃BrN₂O₃: C, 46.03; H, 4.18; N, 8.95; found: C, 46.40; H, 4.12; N, 8.63. MS: *m/z* 312 and 314 (M⁺); 297 and 299 (M⁺ - CH₃). Br-DMEQ was stable in the crystalline state for a year or longer when kept dry in the dark at room temperature. The reagent dissolved in acetonitrile could be used for more than a week when stored in a refrigerator at 5°C.

Derivatization procedure

To *ca.* 100 mg of finely powdered potassium carbonate placed in a PTFE screw-capped test-tube were added 0.5 ml of a test solution of fatty acids in acetonitrile, 0.25 ml each of 3.8 mM 18-crown-6 and 0.8 mM Br-DMEQ (both in acetonitrile). The tube was tightly closed and heated at 80°C for 20 min in the dark. After cooling, 5 μl of the reaction mixture were injected into the chromatograph. For the reagent blank, 0.5 ml of acetonitrile in place of 0.5 ml of a test solution were subjected to the same procedure.

HPLC apparatus and conditions

A Hitachi 655A high-performance liquid chromatograph equipped with a high-pressure sample injector and a Hitachi F1000 fluorescence spectrometer equipped with a 12-μl flow cell operating at the excitation wavelength of 370 nm and the emission wavelength of 450 nm were used. The column was a Radial-Pak C₁₈ cartridge (100 × 4 mm I.D., particle size 10 μm; Waters Assoc., Milford, MA, U.S.A.). It can be used for more than 1000 injections with only a small decrease in the theoretical plate number. The column temperature was ambient (20–27°C). For the separation of the DMEQ derivatives of fatty acids, a gradient elution with 57–100% (v/v) aqueous methanol (Fig. 1) was carried out by using a Hitachi 833A solvent-

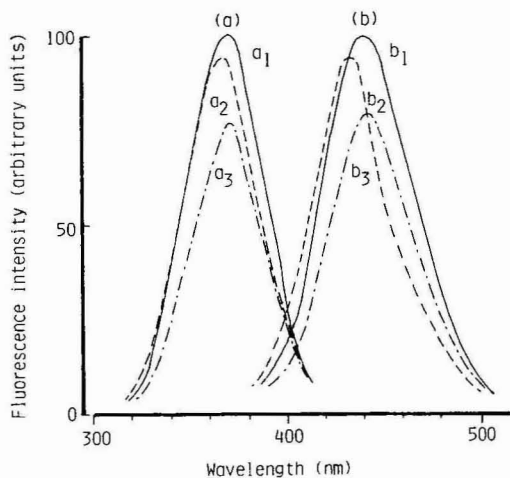


Fig. 1. Fluorescence excitation (a) and emission (b) spectra of DDQ (1.0 nmol/ml) in methanol (a₁, b₁), acetonitrile (a₂, b₂) and water (a₃, b₃).

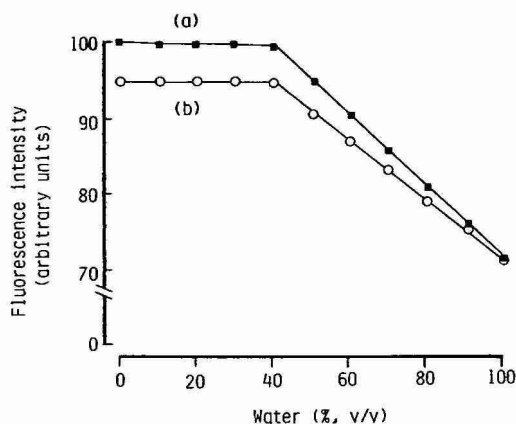


Fig. 2. Effect of water concentration in aqueous methanol (a) and aqueous acetonitrile (b) on the fluorescence intensity of DDQ (1.0 nmol/ml). The fluorescence intensity was measured at the excitation and emission maxima.

gradient device. The flow-rate was 2.0 ml/min. Peak areas were measured on a Waters QA-1 Data System.

RESULTS AND DISCUSSION

Fluorescence properties of DDQ and Br-DMEQ

The fluorescence properties of DDQ and Br-DMEQ in methanol, acetonitrile, water and their mixtures, which have widely been used as mobile phases in reversed-phase chromatography, were examined to find a suitable mobile phase for the HPLC separation of DMEQ derivatives of the fatty acids.

The fluorescence excitation (maximum, 370 nm) and emission (maximum, 450 nm) spectra of DDQ in methanol were practically identical with those in water (Fig. 1). The maxima in aqueous methanol were independent of the concentration of water. On the other hand, the fluorescence excitation and emission maxima (363 nm and 429 nm, respectively) in acetonitrile were slightly blue-shifted compared with those

TABLE I

FLUORESCENCE INTENSITY OF DDQ (1.0 nmol/ml) DISSOLVED IN THE BRITTON-ROBINSON BUFFER AT VARIOUS pH VALUES

The fluorescence intensity was measured at the excitation and emission maxima. The intensity at pH 7.0 was taken as 100.

pH	Relative fluorescence intensity	pH	Relative fluorescence intensity
2.0	52	6.0	96
3.0	84	7.0–12.0	100
4.0	92	7.0–12.0	
5.0	95	7.0–12.0	

in methanol and water (Fig. 1). The fluorescence intensity was almost maximum and constant at water concentrations of 0–40% (v/v) in both aqueous methanol and acetonitrile, but was slightly decreased in proportion to the water concentration at >40% (v/v) (Fig. 2). The most intense and constant fluorescence of DDQ occurred in neutral and alkaline solution (Table I). These results suggest that aqueous methanol is suitable as a mobile phase in reversed-phase chromatography of DMEQ derivatives of fatty acids with gradient elution.

The fluorescence excitation and emission spectra of Br-DMEQ in methanol and acetonitrile were almost identical to those of DDQ. However, the fluorescence intensity of Br-DMEQ in these solvents was much lower than that of DDQ, probably due to the heavy atom effect of bromine; the intensity of Br-DMEQ was *ca.* one tenth of that of DDQ.

Separation of DMEQ derivatives of fatty acids

The simultaneous separation of DMEQ derivatives of (C_3 – C_{20}) fatty acids was studied on a reversed-phase column, Radial-Pak C_{18} cartridge, with aqueous methanol. Methanol–water (95:5, v/v) gave a complete separation of DMEQ derivatives of (C_{10} – C_{20}) long chain fatty acids, though the peaks for (C_3 – C_8) short chain fatty acids were almost overlapped with that for Br-DMEQ. When methanol–water (57:43, v/v) was used, DMEQ derivatives of the short chain fatty acids were completely separated, but those of the long chain fatty acids were eluted late with peak broad-

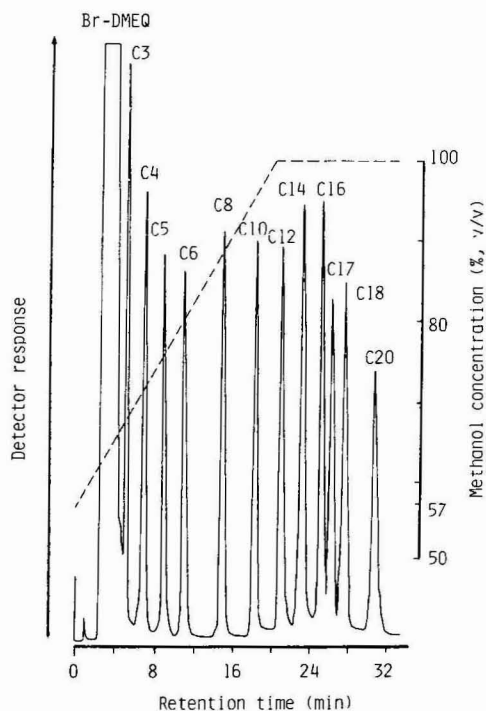


Fig. 3. Chromatogram of DMEQ derivatives of C_3 – C_{20} acids. A portion (0.5 ml) of a standard mixture of the acids (each 1.0 nmol/ml) was treated according to the described procedure.

TABLE II

RELATIONSHIPS BETWEEN THE CARBON NUMBERS OF LINEAR SATURATED FATTY ACIDS AND THE PEAK AREAS IN THE CHROMATOGRAMS

A portion (0.5 ml) of a standard mixture of C₃–C₂₀ acids (each 1.0 nmol/ml) was treated according to the described procedure. The peak area obtained with propionic acid was taken as 100.

Carbon number	Peak area	Carbon number	Peak area
3	100	12	84
4	92	14	82
5	80	16	75
6	83	17	77
8	85	18	75
10	82	20	73

ening. Gradient elution with aqueous methanol served to minimize the elution times and also sharpen the peaks. Fig. 3 shows a typical chromatogram obtained with a gradient of methanol between 57 and 100% (v/v) in the mobile phase. All the peaks were completely separated within 32 min. The change in methanol concentration actually had no effect on the fluorescence excitation and emission maximum wavelengths and intensities of the DMEQ derivatives of all the fatty acids; the spectra were virtually identical with those of DDQ.

The peak areas were slightly decreased for fatty acids with higher carbon numbers (Table II). This means that the individual fatty acids may be determined at almost the same sensitivity. On the other hand, the fluorescence intensity of MMC derivatives of fatty acids greatly varies depending on the individual fatty acids¹⁷.

Derivatization conditions

The conditions were examined using a mixture of the fatty acids (each 1.0 nmol/ml). The most intense peaks were obtained at concentrations greater than *ca.* 3.0 mM of the reagent solution for all the fatty acids; 3.8 mM was used in subsequent work.

18-Crown-6 and potassium carbonate have been used to facilitate the derivatization of fatty acids with reagents having bromomethyl groups^{1-3,6,14,16,18}. Maximum and constant peak areas could be attained at 18-crown-6 concentrations in the solution in the range 2.0–5.0 M for C₃–C₅ short chain fatty acids, and in the range 3.0–5.0 mM for C₁₀–C₂₀ long chain fatty acids; 10 mM was selected as optimum for the simultaneous derivatization of all the fatty acids. The peak areas for the fatty acids were maximal and constant at amounts of potassium carbonate higher than 20 and 150 mg for the short and the long chain fatty acids, respectively; 100 mg were employed in subsequent work.

The derivatization reaction of butyric acid with Br-DMEQ apparently occurred even at moderately low temperatures; higher temperatures allowed the fluorescence to develop more rapidly (Fig. 4). However, at 100°C, the peak areas were decreased at heating times of 10 min or longer. At 80°C, the peak areas for all the fatty acids were almost maximal after heating for 20 min. Thus, heating for 20 min at 80°C was employed in subsequent work. The derivatization reaction proceeded

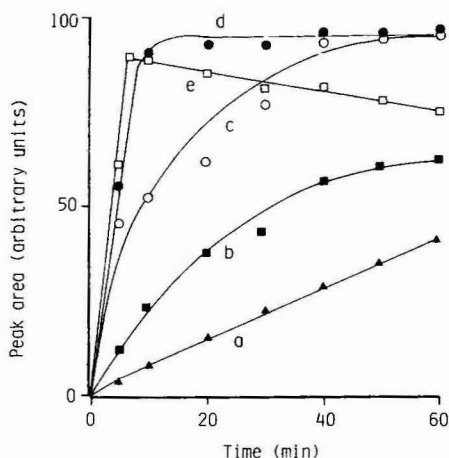


Fig. 4. Effect of reaction time and temperature on the peak area. Portions (0.5 ml) of butyric acid (1.0 nmol/ml) were treated according to the described procedure. Temperatures: a, 20; b, 37; c, 50; d, 80; e, 100°C.

effectively in acetonitrile or acetone; acetonitrile was utilized because of its easy purification. The DMEQ derivatives in the final mixture were stable for at least 72 h in daylight at room temperature.

Precision, calibration and detection limit

The precision was established by repeated determination using a standard mix-

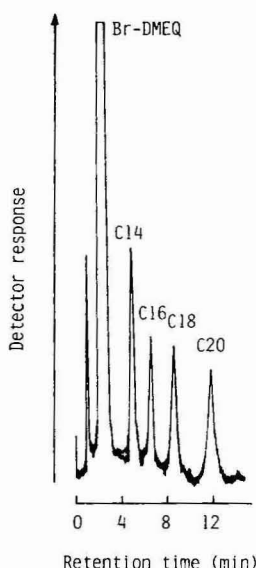


Fig. 5. Chromatogram of DMEQ derivatives of C_{14} – C_{20} acids. A portion (0.5 ml) of a standard mixture of the acids (each 1.0 nmol/ml) was treated according to the derivatization procedure. The reaction mixture was diluted 1000 times in acetonitrile and applied onto the chromatograph. HPLC conditions: mobile phase, methanol–water (95:5, v/v); for the other conditions, see Experimental.

TABLE III

COMPOUNDS WHICH REACT WITH Br-DMEQ TO PRODUCE FLUORESCENT ESTERS, AND THEIR RETENTION TIMES

Portions (0.5 ml) of 1.0 nmol/ml solutions of the compounds were treated according to the described procedure.

<i>Compound</i>	<i>Retention time (min)</i>	<i>Compound</i>	<i>Retention time (min)</i>
<i>Unsaturated fatty acids</i>		<i>Aromatic carboxylic acids</i>	
Myristoleic acid	20.7	Benzoic acid	9.4
Palmitoleic acid	22.2	Salicylic acid	7.1
Linolenic acid	22.2	<i>p</i> -Aminobenzoic acid*	17.0
Arachidonic acid	22.3	<i>Nucleosides</i>	
Linoleic acid	22.4	Uridine	13.7
Oleic acid	23.8	Deoxyuridine	14.1
<i>Dicarboxylic acids</i>		Thymidine	15.2
Oxalic acid	1.0	<i>Miscellaneous</i>	
Malonic acid	1.3	Imidazole-4-acetic acid	8.3
Succinic acid	1.5	1-Methyl-4-imidazoleacetic acid	7.9
Adipic acid	1.8	Glucuronic acid*	10.2
<i>Hydroxycarboxylic acids</i>			
Lactic acid	3.7		
Malic acid	1.2		

* Linear gradient elution with aqueous methanol during 30 min [methanol concentration (% v/v): initial, 30; final, 70] was used for the HPLC separation of DMEQ derivatives of these compounds. When the mobile phase in the described procedure was used, DMEQ derivatives of these compounds were not separated from Br-DMEQ.

ture of fatty acids (each 2.0 pmol/ml). The coefficients of variation did not exceed 2.0% for all the fatty acids examined ($n = 10$ in each case).

The relationships between the peak areas and the amounts of the individual fatty acids were linear from 50 fmol to at least 100 pmol per injection volume (5 μ l).

To ascertain the sensitivity, a standard mixture of C₁₄–C₂₀ acids was treated according to the described procedure and the reaction mixture was successively diluted in acetonitrile and subjected to HPLC. Fig. 5 shows a chromatogram in which each peak corresponds to 5.0 fmol of fatty acid. It indicates that the detection limits for the fatty acids are 0.3–1 fmol at a signal-to-noise ratio of 2. The sensitivity is at least 100 times higher than that of the method with Br-MMC, and *ca.* 10 times higher than that with Br-MAC.

Reaction of Br-DMEQ with compounds other than linear saturated fatty acids

Many unsaturated fatty, dicarboxylic, hydroxycarboxylic and aromatic carboxylic acids and acidic nucleosides react with Br-DMEQ under the derivatization conditions described, to produce fluorescent derivatives which can be separated by HPLC. The retention times for the DMEQ derivatives of the compounds are shown in Table III. α -Keto acids (pyruvic, α -ketoglutaric, α -ketocaproic, α -ketovaleric and phenylpyruvic acids) and seventeen different α -amino acids did not fluoresce. Other substances such as alcohols, sugars, amines, aldehydes, ketones, phenols and sulphhydryl compounds gave no fluorescent derivatives under these conditions. These

observations suggest that the reagent is selective for carboxylic acids and compounds with active imino hydrogen. It is considered that the reactivity of Br-DMEQ is very similar to that of Br-MAC and Br-MMC.

Br-DMEQ as a fluorescence derivatization reagent should be useful for the detection of carboxylic acids of biological importance at the femtomol level by HPLC using gradient elution.

REFERENCES

- 1 S. Goya, A. Takadate, H. Fujino and M. Irikura, *Yakugaku Zasshi*, 101 (1981) 1064.
- 2 A. Takadate, T. Tahara, H. Fujino and S. Goya, *Chem. Pharm. Bull.*, 30 (1982) 4120.
- 3 R. Farinotti, Ph. Siard, J. Bousson, S. Kirkiacharian, B. Valeur and G. Mahuzier, *J. Chromatogr.*, 269 (1983) 81.
- 4 W. Dungen, *Anal. Chem.*, 49 (1977) 442.
- 5 W. Dungen, A. Mayer, K. E. Muller, R. Pietshmann, C. Plachetta, R. Sehr and H. Tuss, *Z. Anal. Chem.*, 288 (1977) 361.
- 6 J. F. Lawrence, *J. Chromatogr. Sci.*, 17 (1979) 147.
- 7 S. Goya, A. Takadate, H. Fujino and T. Tanaka, *Yakugaku Zasshi*, 100 (1980) 744.
- 8 W. D. Korte, *J. Chromatogr.*, 243 (1982) 153.
- 9 H. Lingeman, A. Hulshoff, W. J. M. Underberg and F. B. J. M. Offermann, *J. Chromatogr.*, 290 (1984) 215.
- 10 M. Ikeda, K. Shimada, T. Sakaguchi and U. Matsumoto, *J. Chromatogr.*, 305 (1984) 261.
- 11 N. Nimura and T. Kinoshita, *Anal. Lett.*, 13 (1980) 191.
- 12 S. A. Baker, J. A. Monti, S. T. Christain, F. Benington and R. D. Morin, *Anal. Biochem.*, 107 (1980) 116.
- 13 J. B. F. Lloyd, *J. Chromatogr.*, 189 (1980) 359.
- 14 W. D. Watkins and M. B. Peterson, *Anal. Biochem.*, 124 (1982) 30.
- 15 J. Goto, N. Goto, A. Hikichi, T. Nishimaki and T. Nambara, *Anal. Chim. Acta*, 120 (1980) 187.
- 16 S. Kamada, M. Maeda and A. Tsuji, *J. Chromatogr.*, 272 (1983) 29.
- 17 J. B. F. Lloyd, *J. Chromatogr.*, 178 (1979) 249.
- 18 H. Tsuchiya, T. Hayashi, H. Naruse and N. Takagi, *J. Chromatogr.*, 234 (1984) 121.
- 19 S. Hara, Y. Takemori, T. Iwata, M. Yamaguchi, M. Nakamura and Y. Ohkura, *Anal. Chim. Acta*, in press.
- 20 S. Hara, M. Yamaguchi, M. Nakamura and Y. Ohkura, *Chem. Pharm. Bull.*, 35 (1985) 3493.
- 21 H. Schlenk and J. L. Gellerman, *Anal. Chem.*, 32 (1960) 1412.

CHROM. 17 996

DECAPRENO- β -CAROTENE AS AN INTERNAL STANDARD FOR THE QUANTIFICATION OF THE HYDROCARBON CAROTENOIDS BY HIGH-PERFORMANCE LIQUID CHROMATOGRAPHY

FREDERICK KHACHIK* and GARY R. BEECHER

U.S. Department of Agriculture, Agricultural Research Service, Beltsville Human Nutrition Research Center, Nutrient Composition Laboratory, Building 161, BARC-East, Beltsville, MD 20705 (U.S.A.)

(First received May 15th, 1985; revised manuscript received June 20th, 1985)

SUMMARY

The application of decapreno- β -carotene as an internal standard in quantification of the hydrocarbon carotenoids extracted from raw carrots has been thoroughly examined. Decapreno- β -carotene is a C₅₀ β -carotene that has most of the requirements of an internal standard and it can be commercially synthesized in high purity. An isocratic high-performance liquid chromatographic (HPLC) system has been developed that separated all-*trans*- α -carotene, all-*trans*- β -carotene, and its 15,15'-*cis*-isomer from this internal standard. Quantitative determination of the hydrocarbon carotenoids in carrots by HPLC using the internal standard technique gave values for α - and β -carotene similar to those obtained from α - and β -carotene standards alone.

INTRODUCTION

Numerous analytical methods for the separation and quantification of the naturally occurring carotenoids have been described in the literature. Most of the carotenoid data in food composition tables have been generated using AOAC analytical procedures which lack analytical specificity¹. The use of new separation techniques and chemical instrumentation for generating detailed analytical information in regard to the carotenoid content of foods has become increasingly important. High-performance liquid chromatography (HPLC) has been shown to be the most efficient technique for the analysis of the complex mixture of plant carotenoids²⁻⁷. The separation and the analysis of carotenoids by HPLC minimizes the isomerization and decomposition of these light, heat, and air sensitive compounds. Accurate characterization of specific carotenoids in food is important in refining our understanding of the relation between ingestion of dietary fruits and vegetables and human cancer. The observed protective effect seen in epidemiologic studies to date has been attributed to β -carotene and, as a result, several human intervention studies using synthetic β -carotene have been initiated to confirm this hypothesis^{8,9}. Since the preparation of carotenoid samples for HPLC analysis requires extensive extraction and work-up

procedures that can be accompanied by various analytical errors, the use of an internal standard is very essential. Many examples have appeared in the literature of the separation and quantification of the plant carotenoids by HPLC; however, few of these have employed an internal standard. Stancher and Zonta⁵ have employed azobenzene as an internal standard for quantitative determination of β -carotene and vitamin A in Taleggio cheese extract by HPLC. The light absorption of azobenzene and its HPLC retention time on a normal phase silica column are compatible with that of β -carotene. However, on a C₁₈ reversed-phase column azobenzene elutes much faster than α - and β -carotene and is not suitable as an internal standard. Furthermore, azobenzene is not structurally close to carotenoids and is expected to have different solubility and chromatographic behavior, which may result in its limited application as an internal standard. β -Apo-8'-carotenal has been used as an internal standard in the separation and quantification of citrus carotenoids by reversed-phase HPLC⁶. We have also found that this compound is an appropriate internal standard for the quantification of the oxygenated carotenoids (xanthophylls) extracted from a number of fruits and vegetables¹⁰. Since the HPLC retention time of β -apo-8'-carotenal is much shorter than that of α - and β -carotene, this compound fails to serve as an internal standard for the quantification of the hydrocarbon carotenoids. The most interesting application has recently been reported by Driskell *et al.*¹¹, who have described a procedure for quantitative determination of β -carotene in human serum using (2*R*,2'*R*)-2,2'-dimethyl- β -carotene (Fig. 1) as an internal standard.

Although dimethyl- β -carotene has many attractive features as an internal standard, it is not stable more than two weeks at -70°C , as reported by the authors¹¹. The preparation of small quantities of this compound requires elaborate synthesis, which also contributes to its lack of commercial availability^{12,13}. We propose the use of decapreno- β -carotene (Fig. 1) as an internal standard for the quantification of the hydrocarbon carotenoids. We have shown that this compound has most of the requirements of an internal standard for the quantification of α - and β -carotene extracted from raw carrots. Decapreno- β -carotene is a C₅₀ β -carotene that contains two isoprene units more than that of β -carotene and can be synthesized commercially in high purity.

EXPERIMENTAL*

Apparatus

A Beckman Model 114M ternary solvent delivery system equipped with a Beckman Model 421 controller was interfaced into a Hewlett-Packard 1040A rapid-scanning UV-VIS photodiode array detector. The data were stored and processed by means of a Hewlett-Packard 85-B computing system which was operated with a Hewlett-Packard Model-9121 disc drive and a Model 7470 A plotter. The chromatographic runs were monitored at 450 nm for α - and β -carotene and at 500 nm for the internal standard. The absorption spectra of the carotenoids were recorded between 200 and 600 nm as frequent as 1 scan/5 s (maximum scanning capability = 1 scan/100

* Mention of a trademark or proprietary product does not constitute a guarantee or warranty of the product by the U.S. Department of Agriculture, and does not imply its approval to the exclusion of other products that may also be suitable.

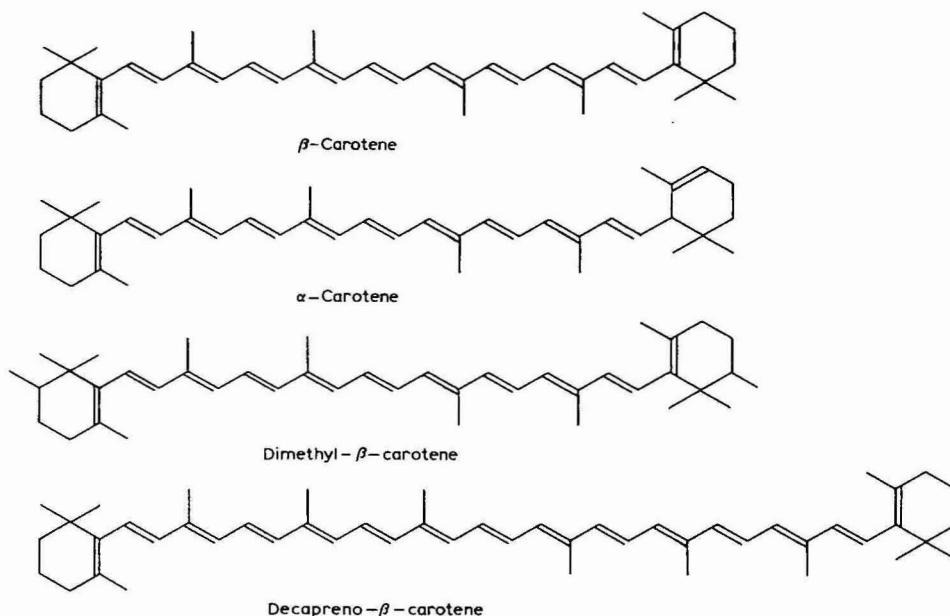


Fig. 1. Molecular structures of β -carotene, α -carotene, (2*R*,2'*R*)-2,2'-dimethyl- β -carotene, and decapreno- β -carotene.

ms). The HP-85B computer with a built-in integration program was used to evaluate the peak area and peak heights.

Column

Separations were performed on a stainless-steel (25 cm \times 4.6 mm I.D.) Microsorb C₁₈ (5- μ m spherical particles) column (Rainin Instrument) which was protected with a Brownlee guard cartridge (3 cm \times 4.6 mm I.D.) packed with Spheri-5 C₁₈ (5- μ m particle size). Analysis of food samples often required frequent changes of the guard cartridge and frequent reversed flushing of the pre-column with methanol and methylene chloride-hexane (1:1).

Reagents and material

The reference samples of α - and β -carotene (Sigma, St. Louis, MO, U.S.A.) were used without further purification. 15,15'-*cis*- β -Carotene was a gift from Hoffmann-LaRoche (Basel, Switzerland). An original sample of decapreno- β -carotene (internal standard) was obtained from Professor A. G. Andrewes but subsequently this compound was synthesized in large quantities in our laboratory. HPLC-grade solvents, methanol, acetonitrile, methylene chloride, and hexane (Fisher Scientific, Pittsburgh, PA, U.S.A.) were used without further purification. Carrots were purchased fresh from local supermarkets on the day of the analysis.

Chromatographic procedure

An isocratic system of methanol (22%, pump A), acetonitrile (55%, pump C), and methylene chloride-hexane (1:1) (23%, pump B) effected the separations of α -

and β -carotene and the internal standard in 23 min. The column flow-rate was 0.70 ml/min. Scans of the absorption spectra provided about 8 to 10 data points on each of the peaks as they were eluted from the HPLC column.

Extraction

The extraction procedure was similar to that employed by Bushway and Wilson⁴ for the extraction of fruits and vegetables. The internal standard (5 to 6 mg) was added to a 10 g sample of carrots, 20 g of anhydrous sodium sulfate, and 1.0 g magnesium carbonate contained in a Waring blender. The resulting mixture was extracted with 150 ml of tetrahydrofuran at a moderate speed for 5 min. The extract was filtered *in vacuo* and the solid materials were re-extracted with tetrahydrofuran until the resulting filtrate was colorless (four extractions were sufficient to remove all the carotenes). The solvent was removed on a rotary evaporator at 30°C and the concentrated carrot filtrate (50 ml) was partitioned into petroleum ether (100 ml) and water (100 ml). The water layer was washed with petroleum ether several times and the resulting organic layers were combined, dried over sodium sulfate and evaporated to dryness. The residue was transferred to a 50-ml volumetric flask using hexane. Samples were injected (20 μ l) in duplicate for the HPLC analysis.

Synthesis of decapreno- β -carotene

Decapreno- β -carotene has been synthesized by three different methods: the Grignard reaction that follows the building principle of $C_{21} + C_8 + C_{21}$ developed by Karrer and Eugster¹⁴; the enol ether condensation that was employed by Isler *et al.*¹⁵ using a $C_{19} + C_{12} + C_{19}$ building scheme, and finally the condensation of vitamin A aldehyde with a Wittig compound prepared from a C_{10} diol. We have employed the last method that has been developed by Surmatis and Ofner¹⁶ to prepare gram quantities of the decapreno- β -carotene, as shown in Fig. 2.

Vitamin A aldehyde (retinal) was purchased commercially (Aldrich) and the C_{10} Wittig compound (II) was prepared according to the method of Strong¹⁷ and Surmatis and Ofner¹⁶. To effect the condensation to C_{50} β -carotene, the C_{10} Wittig (II) was added to a stirred solution of phenyllithium in ethyl ether, followed by the addition of vitamin A aldehyde. As methanol was added decapreno- β -carotene was obtained in 38% yield as a dark, violet crystalline solid which was recrystallized from methanol and methylene chloride. Alternatively, the Wittig compound of the acetylenic C_{10} diene (III) prepared in a similar manner as that of (II) was condensed with all-*trans*-retinal to form the dehydro C_{50} carotenoid (IV) in 42% yield. Selective reduction of (IV) followed by isomerization afforded all-*trans*-decapreno- β -carotene (V) in 69% yield. The UV-VIS absorption spectra of the product V were identical with the reported literature spectra of the decapreno- β -carotene¹⁴ and that of an authentic sample of this compound provided by Professor Arthur G. Andrewes. The absorption spectrum of the decapreno- β -carotene (Fig. 3) in the HPLC solvent system had a maximum at 502 nm.

The internal standard was shown to be pure by plotting the peak ratios at various wavelengths. The purity of the internal standard was further ascertained by the evaluation of at least ten absorption spectra of this compound monitored by the rapid scanning detector. In all cases the absorption maximum remained at 502 nm and all spectra were superimposable.

Qualitative identification of the carotenoids

All-*trans*- α - and β -carotene were identified by comparison of their chromatographic retention times as well as their absorption spectra (Fig. 4) with those of the reference samples. 15,15'-*cis*- β -Carotene was identified from its absorption spectrum which contained a strong *cis*-peak in the near UV region at 334 nm (characteristic of the central *cis*-isomers of carotenoids)¹⁸. The chromatographic retention time and the absorption spectrum of the 15,15'-*cis*- β -carotene were also identical with that of an authentic sample of this compound gifted by Hoffman LaRoche.

Standard solutions and quantitative evaluation

Three stock solutions were prepared by dissolving 10 mg of all-*trans*- α -carotene, 12 mg of all-*trans*- β -carotene, and 37 mg of the internal standard in 100 ml of hexane. Aliquots of 1–3 ml of the stock solution of β -carotene were mixed with 5 ml of the stock solution of the internal standard into separate 10-ml volumetric flasks and the flasks were brought to volume with hexane. The standard solutions for α -carotene were similarly prepared by mixing 1–3-ml aliquots of this compound with 5 ml of the internal standard solution into separate 10-ml volumetric flasks. Samples were injected (20 μ l) in duplicate onto the chromatograph and the peak areas of α - and β -carotene and the internal standard were integrated. The response factors of the individual carotenoids were also obtained from separate injections of their stock solutions at various concentrations. The standard curves were obtained by plotting the area ratio of α - and β -carotene to the internal standard *versus* the concentration

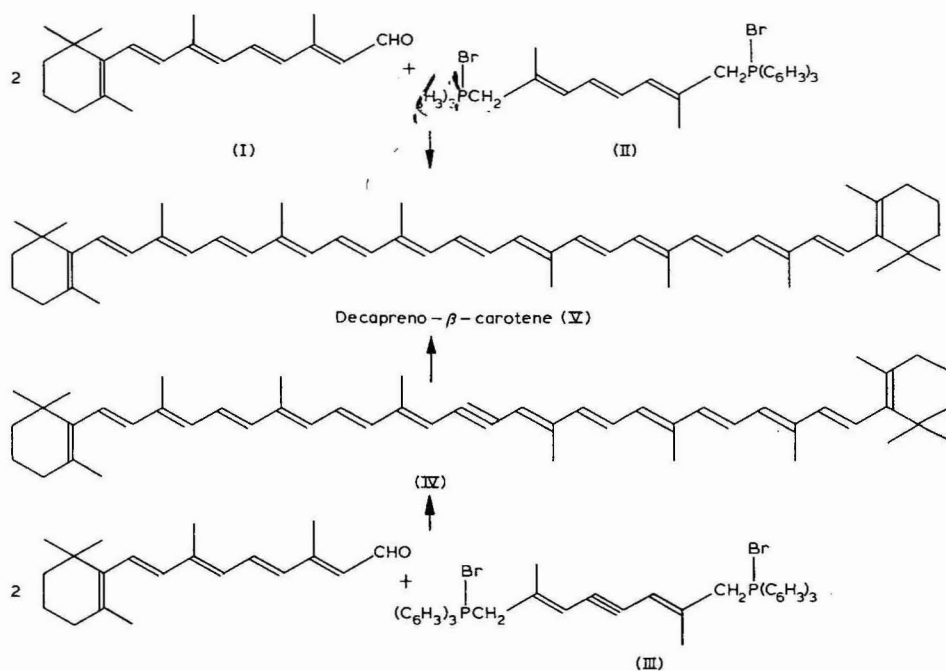


Fig. 2. Chemical synthesis of all-*trans*-decapreno- β -carotene according to the method of Surmatis and Ofner¹⁶.

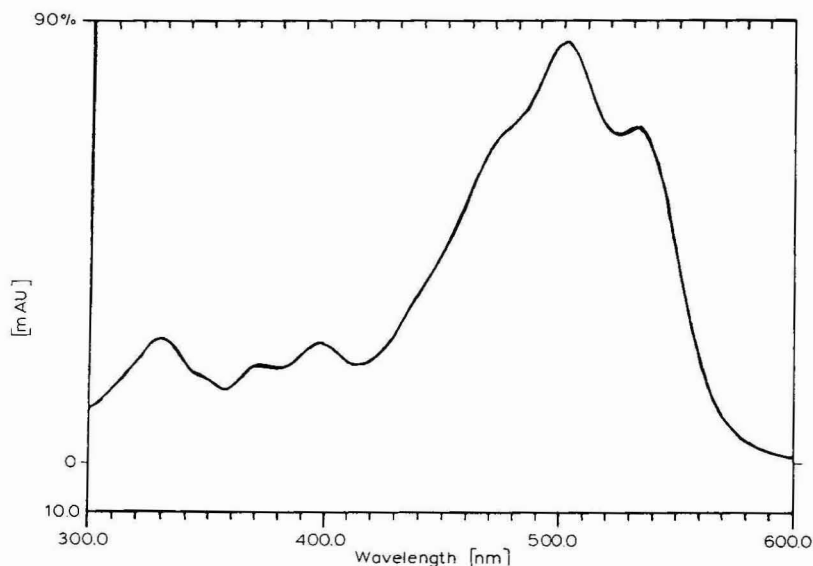


Fig. 3. Absorption spectrum of all-*trans*-decapreno- β -carotene ($\lambda_{\text{max}} = 502$ nm) in the HPLC solvent system methanol-acetonitrile-methylenechloride-hexane (22:55:11.5:11.5).

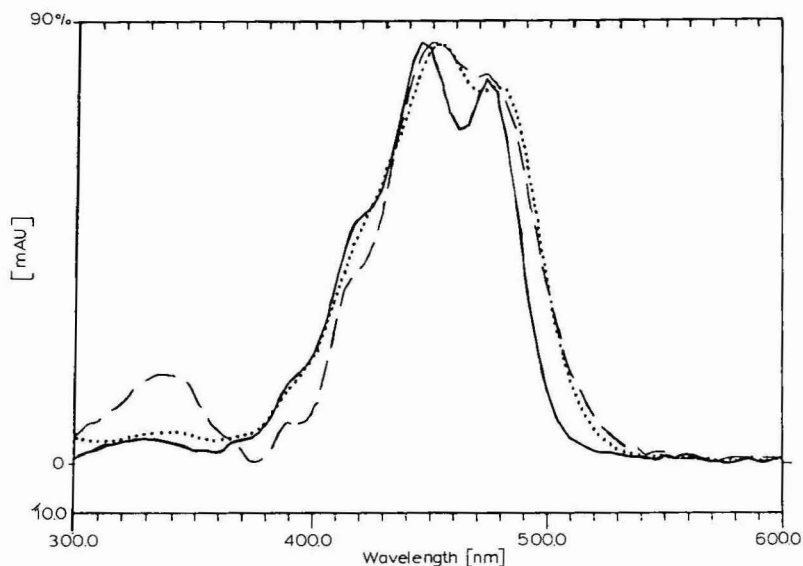


Fig. 4. Absorption spectra of all-*trans*- α -carotene (—) ($\lambda = 446$ nm), all-*trans*- β -carotene (.....) ($\lambda = 454$ nm), and 15,15'-*cis*- β -carotene (---) ($\lambda = 450$ nm) in the HPLC solvent system methanol-acetonitrile-methylenechloride-hexane (22:55:11.5:11.5).

of the individual carotenes. The quantification of the hydrocarbon carotenoids in raw carrot extract was based on the evaluation of the area ratio of α - and β -carotene peaks to the area of the internal standard peak with the area ratios obtained from the standard curves.

RESULTS AND DISCUSSION

A typical chromatographic profile of a raw carrot extract containing decapreno- β -carotene (internal standard) is shown in Fig. 5. An isocratic system of methanol-acetonitrile-methylene chloride-hexane (22:55:11.5:11.5) has been employed to separate all-*trans*- α -carotene (peak A), all-*trans*- β -carotene (peak B), and 15,15'-*cis*- β -carotene (peak C, appearing as a shoulder on the all-*trans*- β -carotene peak) from the internal standard (peak D). Decapreno- β -carotene is the last eluting peak and it does not interfere with the α - and β -carotene peaks. For most of the other fruits and vegetables studied, particularly the green vegetables, the carotenoids that elute last on a C_{18} reversed-phase column are all-*trans*- β -carotene and its 15,15'-*cis*-isomer¹⁹. Therefore, the application of decapreno- β -carotene as an internal standard for the quantification of the hydrocarbon carotenoids is not limited to carrots and it can be extended to other fruits and vegetables. Decapreno- β -carotene has also been found suitable for the determination of α - and β -carotene in human serum²⁰. There are several advantages that make this C_{50} β -carotene an attractive internal standard for the determination of α - and β -carotene. These are as follows: (a) it elutes after all-*trans*- α - and β -carotene on the C_{18} reversed-phase HPLC column; (b) it is not naturally occurring and can be readily synthesized on a large scale in high purity; (c) it has similar solubility behavior as that of α - and β -carotene and it can be added to the fruits and vegetables at the extraction stage; (d) it is stable relative to α - and β -carotene and it does not undergo degradation or stereoisomerization in the extracting solvents within the analysis time.

The recovery studies on decapreno- β -carotene indicated that the solubility behavior of this compound is very similar to that of α - and β -carotene. The average

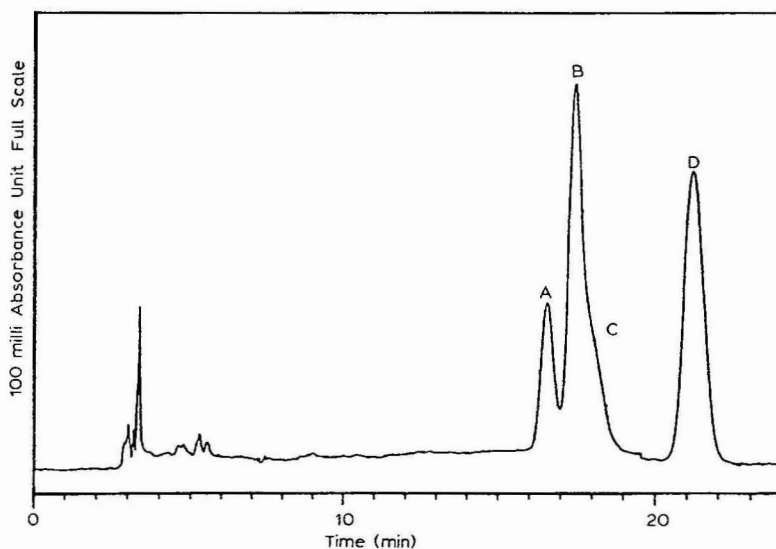


Fig. 5. HPLC profile of raw carrot extract containing all-*trans*-decapreno- β -carotene as an internal standard. Chromatographic conditions described in text. Peaks: A = all-*trans*- α -carotene, B = all-*trans*- β -carotene, C = 15,15'-*cis*- β -carotene, D = all-*trans*-decapreno- β -carotene (internal standard).

TABLE I
RECOVERY OF DECAPRENO- β -CAROTENE FROM CARROT EXTRACTS

Weight (mg) of internal standard added	Weight (mg) of internal standard recovered	Recovery (%) [*]
5.2	5.0	96.2
5.5	5.3	96.4
5.8	5.7	98.3

^{*} Relative standard deviation is 1.2%.

recovery of decapreno- β -carotene from carrot extracts was more than 96% (Table I). These results have been based on the weight of the internal standard before and after extraction as determined by the HPLC peak area of the internal standard.

The calibration curves obtained from a plot of the area ratios of α - and β -carotene peaks to that of the internal standard against the concentrations of these carotenes (Fig. 6) gave good linearity over a wide range of concentration and had a relative standard deviation of 3.3% for α -carotene and 3.4% for β -carotene. Since 15,15'-*cis*- β -carotene was not resolved and it appeared as a tailing shoulder on all-*trans*- β -carotene peak, the area corresponding to this *cis*-isomer was included in the integration of the all-*trans*- β -carotene. Therefore, in quantification of the total carotenoids in raw carrots, it has been assumed that the 15,15'-*cis*- β -carotene would exhibit a similar chromatographic response to its all-*trans*-isomer.

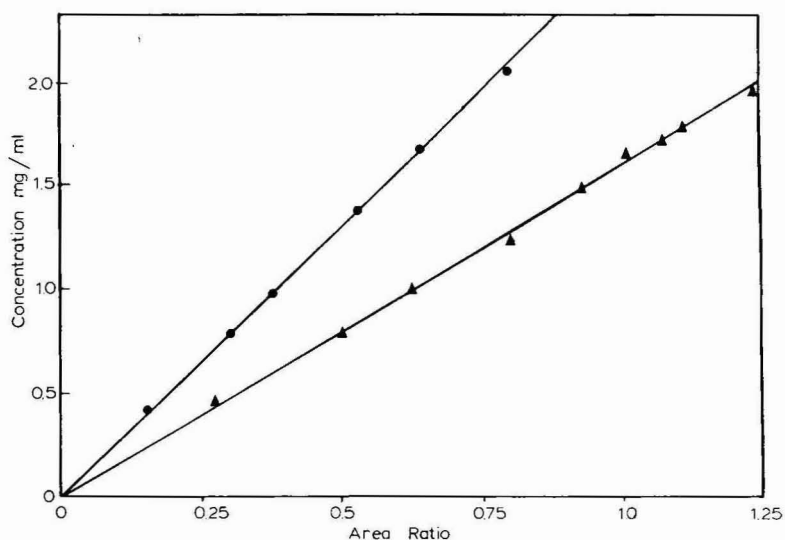


Fig. 6. Plots of the standard curves for α - and β -carotene. ●, Concentration of α -carotene (mg/ml) versus area ratio of α -carotene-internal standard, coefficient of variation 3.3%. ▲, Concentration of β -carotene (mg/ml) versus area ratio of β -carotene-internal standard, coefficient of variation 3.4%. [Coefficient of variation = (standard deviation/mean) \times 100].

It is not clear at this point whether the presence of the *cis*-isomer of β -carotene in raw carrots is an artifact due to extraction and/or chromatography. There have been literature reports^{21,22} that have described the separation of mono and di-*cis*-isomers of β -carotene by HPLC. These reports have indicated that the *cis*-isomers are stable enough in solvents such as hexane, acetone, and chloroform to allow their isolation and characterization.

The carotenoid content of five separate batches of raw carrots has been determined using the internal standard technique. The relative standard deviations for α -carotene, β -carotene, and total carotenes were 7, 2.5, and 3.6% respectively. The discrepancy within these data is consistent with the usually observed large variability of carrot samples. The quantitative determination of all-*trans*- α - and all-*trans*- β -carotene employing decapreno- β -carotene as an internal standard is in good agreement with the values obtained for these carotenes based only on the response factor of α - and β -carotene standard solutions (data not shown). The total carotene content of carrots using the internal standard was in the range of 16.44–17.92 mg/100 g which is consistent with the total carotene content of raw carrots reported by HPLC (6.6–18.4 mg/100 g)⁴ and colorimetric methods (6–21 mg/100 g)²³.

The reproducibility of our results within the same series of samples indicates that the decapreno- β -carotene can be employed as an internal standard to generate reliable quantitative data on the hydrocarbon carotenoids. Since the HPLC analysis of carotenoids is usually accompanied by extraction and sample pretreatment where variable recoveries of these compounds may occur, we strongly recommend the use of an internal standard to compensate for various analytical errors. The accuracy of this approach is obviously dependent on the structure equivalence of the carotenoids of interest and the internal standard. We have shown that decapreno- β -carotene is a suitable internal standard for the quantitative determination of α - and β -carotene. However, the development of other internal standards for quantification of various classes of carotenoids may be necessary.

ACKNOWLEDGEMENTS

We would like to thank Professor Arthur G. Andrewes for providing us with an authentic sample of the decapreno- β -carotene. Thanks are also due to Professors H. J. Mayer and Chr. Suter of Hoffmann-LaRoche for their generous gift of a number of carotenoid samples including 15,15'-*cis*- β -carotene. Partial support by the National Cancer Institute through reimbursable agreement Y01-CN-30609 is acknowledged.

REFERENCES

- 1 G. R. Beecher and F. Khachik, *JNCI, J. Natl. Cancer Inst.*, 73 (1984) 1397.
- 2 I. Stewart, *J. Assoc. Off. Anal. Chem.*, 60 (1977) 132.
- 3 Y.-P. C. Hsieh and M. Karel, *J. Chromatogr.*, 259 (1983) 515.
- 4 R. J. Bushway and A. M. Wilson, *Can. Inst. Food Sci. Technol. J.*, 15 (1982) 165.
- 5 B. Stancher and F. Zonta, *J. Chromatogr.*, 238 (1982) 217.
- 6 G. Noga and F. Lenz, *Chromatographia*, 17 (1983) 139.
- 7 O. H. Will III and M. Ruddat, *J. Liquid Chromatogr.*, 2 (1984) 610.
- 8 R. B. Shekelle, M. Lepper, S. Liu, P. Oglesby, A. M. Shryock and J. Stamler, *Lancet*, ii (1981) 1185.
- 9 R. Peto, R. Doll, J. D. Buckley and M. B. Sporn, *Nature (London)*, 290 (1981) 201.

- 10 F. Khachik and G. R. Beecher, *Application of a multiwavelength scanning UV/visible HPLC detector to the chromatographic resolution and identification of naturally occurring carotenoids, presented at the 36th Pittsburgh Conference on Analytical and Applied Spectroscopy, New Orleans, LA, February 25–March 1, 1985.*
- 11 W. J. Driskell, M. M. Bashor and J. W. Neese, *Clin. Chem.*, 29 (1983) 1042.
- 12 C. H. Eugster, A. H. Trivedi and P. Karrer, *Helv. Chim. Acta*, 38 (1955) 1359.
- 13 A. G. Andrewes, S. Liaaen-Jensen and G. Borch, *Acta Chem. Scand.*, B28 (1974) 737.
- 14 P. Karrer and C. H. Eugster, *Helv. Chim. Acta*, 34 (1951) 28.
- 15 O. Isler, M. Montavon, R. Ruegg and P. Zeller, *Justus Liebigs Ann. Chem.*, 603 (1957) 129.
- 16 J. D. Surmatis and A. Ofner, *J. Org. Chem.*, 26 (1961) 1171.
- 17 F. M. Strong, *J. Am. Chem. Soc.*, 70 (1948) 154.
- 18 W. Vetter, G. Englert, N. Rigassi and U. Schwieter, in O. Isler (Editor), *Carotenoids*, Birkhauser Verlag, Basel, 1971, p. 198.
- 19 F. Khachik and G. R. Beecher, *Application of HPLC/scanning UV-visible detection for identification and quantification of carotenoids in fruits and vegetables, presented at the 7th International Symposia on Carotenoids, Munich, August 27–31, 1984.*
- 20 W. J. Driskell, personal communication.
- 21 M. Vecchi, G. Englert, R. Maurer and V. Meduna, *Helv. Chim. Acta*, 64 (1981) 2746.
- 22 K. Tsukida, K. Saiki, T. Takii and Y. Koyama, *J. Chromatogr.*, 245 (1982) 359.
- 23 S. W. Souci, W. Fachmann and H. Kraut, *Food Composition and Nutrition Tables 1981/1982*, Wissenschaftliche Verlagsgesellschaft, Stuttgart, 1981.

CHROM. 17 995

A COMBINED RECYCLING AFFINITY COLUMN-FILTRATION TECHNIQUE

JAMES P. CHARLTON

Department of Biochemistry, Box 440, University of Virginia School of Medicine, Charlottesville, VA 22908 (U.S.A.)

(First received May 29th, 1985; revised manuscript received June 20th, 1985)

SUMMARY

A new preparative purification technique for biological macromolecules is developed by combining the affinity column chromatography and the membrane filtration technique. A unique feature of the affinity column-filtration apparatus is that the filtrate from the filtration unit is recycled back to the inlet of the affinity column, thus decreasing considerably the total amount of ligands required for the affinity column. A second important feature is that the pump which connects the affinity column and the filtration unit is monitored by an infrared sensor device on the filtration cell; consequently, the flow of the column eluent into the filtration unit is controlled automatically by the solution height in the filtration cell. Highly homogeneous regulatory subunits of type I cAMP-dependent protein kinase from rabbit skeletal muscle are demonstrated to be obtainable by the new purification technique. Thus, this apparatus could have important applications in the purification of a wide range of biological macromolecules. A test for estimating affinity bound proteins is also discussed.

INTRODUCTION

Affinity chromatography involves the covalent attachment of a ligand onto an insoluble polymer (*e.g.* agarose) which can be packed as the stationary support into a chromatographic column. Because of the specific binding that occurs between the covalently attached ligand and a particular enzyme, the affinity column can absorb selectively the particular enzyme from a mixture of proteins passed through it. Subsequent elution of the adsorbed enzyme can be achieved by eluting the affinity column with buffer solutions of high ionic strength or denaturants which can perturb the affinity of the enzyme for the covalently attached ligand resulting in dissociation of the enzyme-ligand complex. Alternatively, elution of the tightly adsorbed enzyme from insoluble supports can be achieved by using a solution containing a high concentration either of the ligand or a ligand analogue which can compete with the covalently attached ligand for the enzyme.

The importance of using a ligand analogue in affinity chromatography is most

evident in cases where the binding affinity of protein to ligands is particularly strong. For example, the affinity of the regulatory subunit of cAMP-dependent protein kinase for cAMP is extremely high¹, and the ligand analogue, 1,N⁶-ethenoadenosine 3',5'-cyclic monophosphate, has been successfully employed for eluting the regulatory subunit from an affinity column packed with cAMP-Sepharose². A drawback of this method is that, in order to wash off the adsorbed enzymes for a reasonably good yield, a large volume of the ligand analogue containing eluant is sometimes needed. This can be particularly painful, if the ligand analogue has to be synthesized chemically or if it is very expensive. In this communication, a method is described to circumvent this need of a large amount of ligand analogue by recycling the eluant in a closed system.

EXPERIMENTAL PROCEDURES

Materials

Epoxy-activated Sepharose 6B was obtained from Pharmacia. ACA-44 ultragel was supplied by LKB. Phenylmethylsulfonylfluoride (PMSF), cAMP and its analogue, 1,N⁶-etheno-cAMP, were products of Sigma. Other chemicals and solvents were of reagent grade. Filtration cell (Model 10) and microporous filters (YM-10) were purchased from Amicon.

Methods

8-Bromo-cAMP and 8-(β -hydroxyethylthio)-cAMP were prepared following the procedure of Muneyama *et al.*³, and 8-(β -hydroxyethylthio)-cAMP was subsequently used together with epoxy-activated Sepharose 6B to synthesize the cAMP affinity matrix⁴.

The cAMP-dependent protein kinase I from rabbit skeletal muscle was purified to the stage of DEAE-cellulose chromatography using the procedure of Huang and Huang⁵.

The affinity column-filtration apparatus

A new affinity column filtration apparatus, shown diagrammatically in Fig. 1, was constructed for the continuous depletion of adsorbed enzymes, the regulatory subunit of cAMP-dependent protein kinase I in this case, from the cAMP affinity matrix by the recycled ligand analogue, 1,N⁶-etheno-cAMP, containing eluent. The apparatus consisted of an affinity column packed with cAMP-affinity matrix. A pump connects the column outlet to the filtration unit, and the on/off switch of the pump is controlled automatically through an amplifier by an infrared sensor attached to the filtration unit, shown in detail in Fig. 1. The column eluant is pumped into the filtration unit and it is stirred constantly by a magnetic bar. The solvent and small molecules including the free ligand analogue in the filtration unit are forced to pass through the filter membrane by a constant pressure (*ca.* 35 p.s.i.) provided by a nitrogen tank equipped with a regulator valve; hence, the regulatory subunit-cAMP analogue complex was separated and concentrated in the filtration unit. The solution in the filtration cell is monitored by an infrared sensor which, in turn, regulates the on/off switch at the pump connecting the column and the filtration unit. When the solution is lowered to below the level where the infrared sensor is positioned, the

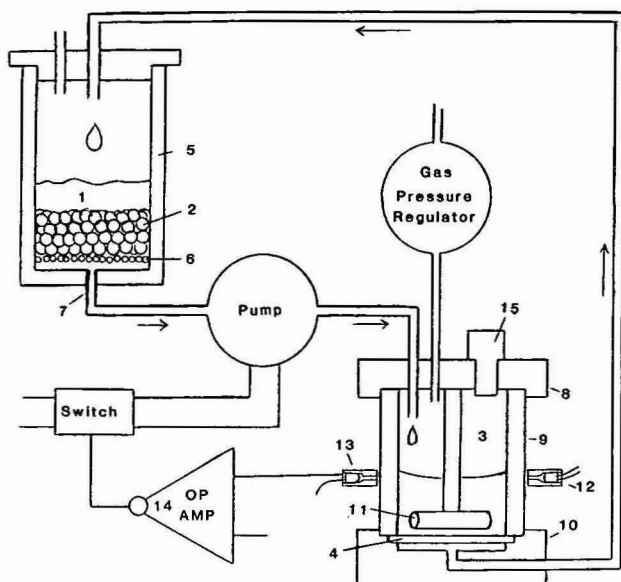


Fig. 1. Affinity column-filtration apparatus. The solvent (1) passes through a bed of affinity beads (2) complexed with the macromolecules for which they are specific. The solvent is pumped into a pressurized chamber (3) where the solvent and other small molecules, such as ligands, are forced by the pressure through a molecular filter (4). Larger biological macromolecules are retained by the filter. The solvent, depleted of macromolecules, is returned to the bed of beads where more macromolecules are dissolved. 5 = Column vessel, 6 = nylon screen, 7 = column outlet, 8-10 = pressure chamber components, 11 = the magnetic stir bar, 12 = the infrared emitting diode and collimator, 13 = the receiving collimator and infrared triggered transistor, 14 = an electrical operational amplifier, and 15 = a plug in the opening used for the removal of the macromolecule concentrate. The flow-rate of solvent in the system is limited by the permeability of and the area of the filter. The area of the filter in the design of the apparatus is limited because small volumes cannot efficiently be collected from the surface of a large filter. Macromolecules will plug the filter if a certain pressure is exceeded. This pressure is dependent on, among other things, the concentration and the character of the macromolecule. The stir bar keeps the concentration of the macromolecule from going high at the surface of the membrane and allows the filter to be operated at a higher pressure without stopping up. The filter cannot be forced by a pump to pass a higher flow-rate than that which is optimal for a given macromolecule. In the apparatus shown, the variations of the pump-rate is cushioned by the gas in the pressure cell. The pressure in the cell is held constant by a source of pressurized gas and a gas pressure regulator. The pump has a higher flow-rate than that of the filter and is switched on and off by a switch which is controlled by the level of solution in the pressure cell. An infrared beam from the diode senses the presence of the solution in the cell by the solution deflecting the beam off of the infrared phototransistor which activates the amplifier which operates the switch and pump.

solution does not refract the incident infrared beam into, and hence ceases to activate, the phototransistor in the sensor. Consequently, the pump is switched on and the column eluant is pumped into the filtration unit. The filtrate from the filtration unit is recycled back to the inlet of the affinity column as illustrated in Fig. 1.

Purification of the regulatory subunit of cAMP-dependent protein kinase I from rabbit skeletal muscle

Prior to the mixing of cAMP-Sepharose affinity beads with crude protein kinase I preparation after the DEAE-cellulose fractionation step, the cAMP-Sepharose

beads were washed extensively with distilled water. Pilot experiments were first carried out in the cold room at 0°C as follows. To a series of known volume of crude protein kinase solution, a fixed amount of washed cAMP-Sepharose affinity beads was added. After rotating the mixture in a mechanical rotator for 15 min, the beads were allowed to sediment. Aliquots from the supernatant in various tubes were assayed for protein kinase activity in the presence and absence of cAMP, and the sedimented Sepharose affinity beads also were subjected to protein assay. If the supernatant in one of the pilot tubes showed the same enzymatic activity of protein kinase in the presence and absence of cAMP, and the volume of crude solution was also maximal, this volume was also minimal where the affinity beads were shown to have a maximum of bound proteins. The ratio of the mass of Sepharose affinity beads to the volume of crude protein kinase solution in this tube was determined and used subsequently for the preparative separation of the regulatory subunit of cAMP-dependent protein kinase I.

For a large scale purification, an appropriate amount of slurried Sepharose affinity beads was added to the crude DEAE-cellulose fraction of protein kinase with rapid mixing at 0°C. After rotating for 30 min, the Sepharose affinity beads were then allowed to sediment, and the supernatant was removed. The chromatographic column (3 cm in diameter) of the affinity column-filtration apparatus described earlier was then loaded, in the cold room at 0°C. The sedimented beads were washed, at 0°C, exhaustively over a fine nylon mesh, which had been pretreated with silicone, with 0.5 M sodium chloride and with PMSF in buffer R consisting of 10 mM morpholinoethanesulfonic acid (MES)-10 mM Tris-1 mM EDTA-1 mM dithiothreitol-10 mM methylamine at pH 6.5. A 14-ml aliquot of 0.5 M sodium chloride buffer R containing 5 mM cAMP analogue, 1,N⁶-etheno-cAMP, at pH 6.5, was then applied to elute the regulatory subunit, and the column's outlet was coupled to the pump which, in turn, was connected to the inlet of the filtration unit. The pump, infrared beam, the sensor and the magnetic bar were switched on, and the affinity purifications were performed automatically at 0°C. In the apparatus, the regulatory subunit-cAMP analogue complex was constantly collected and concentrated on top of the filtration membrane. In addition, the unbound cAMP analogue in the filtrate was recycled back to the inlet of the chromatographic column to further elute the regulatory subunit. This type of affinity column-filtration apparatus thus provided a novel means for a combined powerful separation method for enzymes and the recycling of the expensive ligand analogues.

The concentrated regulatory subunit-cAMP analogue complex (15-30 mg in 1 ml) collected in the filtration cell was removed and then subjected to gel-filtration chromatography on an ACA-44 column (115 × 1.5 cm I.D.) which had been washed and equilibrated with buffer R containing 0.1 M sodium chloride. Following application of the sample, regulatory subunits were eluted from the ACA-44 column with the same buffered sodium chloride solution, and the eluant was collected drop-wise in a fraction collector.

Protein kinase assay. Protein kinase activity was assayed radioisotopically. The assay solution (total volume 90 µl) contained 5 µmol glycylglycine buffer (pH 7.0), 0.05 mg histone type IIA substrate, 3 nmol [γ -³²P]ATP (specific radioactivity 50-100 c.p.m. per pmol), 0.5 µmol magnesium dichloride, and cAMP (0.1 nmol) if added. The enzymatic reaction was initiated by adding a portion (10 µl) of protein kinase

solution. Following incubation at 30°C for 10 min, an aliquot (75 μ l) was precipitated onto a piece of filter paper and washed in 10% (w/v) trichloroacetic acid; the paper was dried and counted for radioactivity (32 P) as described by Huang and Huang⁵.

Other techniques. Protein was determined spectroscopically by the method of Bradford⁶. The presence of bound regulatory subunit on the Sepharose affinity bead was detected as follows: An aliquot (5–10 mg) of the damp caked, washed regulatory subunit containing Sepharose affinity beads was loaded into a small disposal plastic column (3 ml, Quik-sep column, Isolab). The column was washed first with buffer R containing 0.5 M sodium chloride and then with distilled water. The washed Sepharose affinity beads were washed rapidly with 0.3 ml freshly prepared Bradford reagent two times. The Sepharose affinity beads were then stirred gently in the presence of another volume of Bradford reagent for at least 2 min, and the Sepharose affinity beads were allowed to drain. The beads were washed several times with 1 ml of distilled water followed by draining off the water. At this stage, the blue color of the column bed indicated the presence of bound regulatory subunit on the Sepharose affinity beads. In fact, the blue dye can be eluted off the column with 95% ethanol, and the absorbance of the dye-ethanol eluant at 595 nm can be determined. From the final results obtained with the affinity column-filtration apparatus, one can estimate the total amount of protein originally adsorbed on a given weight of Sepharose affinity beads. Based on the amount of bound protein per mg of Sepharose affinity beads and the absorbance, at 595 nm, of the dye eluted off the small plastic column packed with a known amount of Sepharose affinity beads, one can estimate empirically the amount of bound protein absorbed per mg of Sepharose affinity beads in subsequent experiments simply by determining the absorbance of the dye-ethanol eluant at 595 nm.

Silicone treatment. A 2–5 ml of silicone solution, a 95% ethanol solution saturated with high-vacuum silicone grease (Dow Corning), was used to rinse the glass or plastic surface as described earlier.

Sodium dodecyl sulphate-polyacrylamide gel electrophoresis (SDS-PAGE) was performed in 0.2 M Tris-0.2 M acetate buffer, pH 6.4, containing 0.1% SDS on 5.3% polyacrylamide gel as described previously².

RESULTS AND DISCUSSION

The regulatory subunits of cAMP-dependent protein kinase I from rabbit skeletal muscle prepared before and after the affinity column-filtration step were analyzed by SDS-PAGE as shown in Fig. 2. Before the affinity column-filtration step, the preparation is seen to contain heterogenous collections of many polypeptide bands, whereas the sample after the purification step using the affinity column-filtration apparatus shows a single, intense electrophoretic band of apparent molecular weight 48 000, a band that has been observed for the regulatory subunit of cAMP-dependent protein kinase I⁵. This result demonstrates that the affinity column-filtration apparatus has a high separation efficacy for the enzyme or protein purification.

The elution profile from the affinity column-filtration apparatus for homogenous regulatory subunits of the type 1 rabbit skeletal muscle protein kinase is presented in Fig. 3. Complete depletion of the bound regulatory subunits (13 mg) from the Sepharose affinity beads (5 ml) by the recycled 1,N⁶-etheno-cAMP (initial

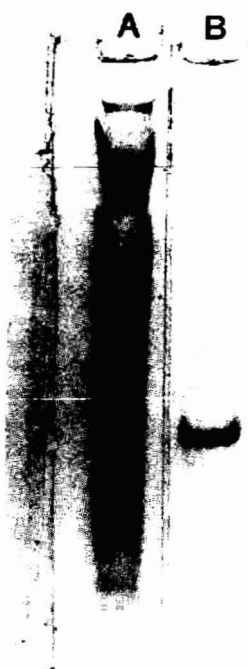


Fig. 2. Lane A, SDS-PAGE of cAMP dependent protein kinase type I from rabbit skeletal muscle purified through the DEAE step. Lane B, Purification of the material in lane 1 by the affinity column-filtration apparatus showing a single intense staining band of protein with an apparent molecular weight of 48 000 daltons. This band is the cAMP binding regulatory subunit of the protein kinase which was present at a low concentration in the material shown in lane 1.

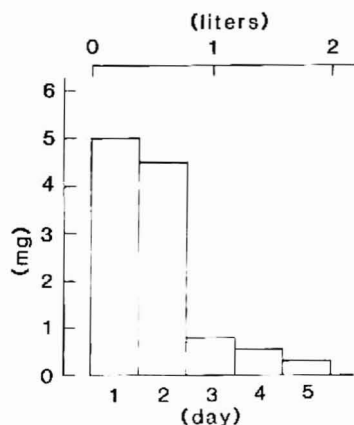


Fig. 3. A typical separation. An amount of 2.55 kg of rabbit muscle was purified through the DEAE step. Wet cake cAMP affinity beads (5 g) were added to the 600 ml DEAE fraction and the cAMP binding protein was purified as in the text. The bar graph shows the yield per day in milligrams. Also shown is an approximate volume of solution recirculated on to the column.

concentration 2 mM) is observed to require more than a week with an approximate flow-rate of 0.3 ml/min at 0°C. However, more than 80% of total bound protein are eluted off during the first 4-day period.

From theoretical considerations one can predict the aspects of a given elution. The rate of production of an enzyme in moles per unit of time, R , is related to the saturation of the immobile ligand by the formula

$$R = K \frac{[EL]}{[L]}$$

where $[EL]$ is the concentration of the insoluble ligand complexed with the enzyme, and $[L]$ is the concentration of the insoluble ligand that is unoccupied by the enzyme. Furthermore, the proportionality constant, K , is related to the flow-rate as follows

$$K = [L_1] \frac{K_1}{K_2} (dv/dt)$$

where $[L_1]$ is the concentration in moles per liter of the free soluble ligand or ligand analogue in the solution of the system; K_1 is the dissociation constant for the enzyme from the immobile ligand; K_2 is the dissociation constant of the enzyme from the soluble ligand; dv/dt the flow-rate in liters per unit of time.

The rate of production R can also be shown, theoretically, when the beads are only fractionally loaded, to decay exponentially with time. Experimentally, shown in Fig. 3, an exponential decay in the production of the regulator subunit of protein kinase can be seen from days 2 through 5.

To obtain the most rapid recovery of the macromolecule, the immobilized ligand should be nearly saturated with the macromolecule. If the macromolecule bound to the immobilized ligand $[EL]$ is a fraction of the immobilized ligand $[L]$ the rate of production will be correspondingly small. The elution shown in Fig. 3 was from initially saturated affinity beads.

To keep recovery times as short as possible the flow-rate dv/dt should be as large as possible for the amount of the immobilized ligand. Short columns with relatively large diameters should be used and large area filters should be used consistent with the more limited recoverability of the enzyme off of a large filter.

The amount of bound protein on the cAMP-Sepharose affinity beads can be increased by adding 1 mM of MgATP into the crude enzyme preparation after the DEAE-cellulose fractionation step and by incubating the crude enzyme preparation and the Sepharose affinity bead overnight, at 0°C, in the presence of PMSF, a protease inhibitor. It is well established that MgATP is required for the dissociation and association of the cAMP-dependent protein kinase and its subunits^{2,7}. The association-dissociation equilibria of protein kinase and its subunits may be necessary prior to the binding of the regulatory subunit to the cAMP-Sepharose affinity bead.

The main emphasis of this communication is to report on the development of an affinity column-filtration apparatus for the separation of biological macromolecules such as enzymes or proteins. Although only one type of affinity matrix to purify a particular enzyme subunit is discussed here, the range of potential applications of

the affinity column-filtration apparatus can be greatly extended, if different types of affinity matrix are used in the apparatus under various conditions. An important feature of the new apparatus involves the recycling of the ligand analogues; hence, this apparatus is particularly useful for preparative fractionations of proteins or enzymes involving the use of expensive ligands.

ACKNOWLEDGEMENTS

The author thanks Dr. L. C. Huang and Dr. C. Huang for their support and discussions. This work was supported in part by Grant GM-17452 from National Institutes of Health, U.S. Public Health Service.

REFERENCES

- 1 J. A. Beavo, P. J. Bechtel and E. G. Krebs, *Adv. Cyclic Nucleotide Res.*, 5 (1975) 241.
- 2 J. P. Charlton, C. Huang and L. C. Huang, *Biochem. J.*, 209 (1983) 581.
- 3 K. Muneyama, R. J. Bauer, D. A. Shuman, R. K. Robins and L. N. Simon, *Biochemistry*, 10 (1971) 2390.
- 4 W. Weber, C.-W. Vogel and H. Hilz, *FEBS Lett.*, 99 (1979) 62.
- 5 L. C. Huang and C. Huang, *Biochemistry*, 14 (1975) 68.
- 6 M. M. Bradford, *Anal. Biochem.*, 72 (1976) 248.
- 7 V. Chau, L. C. Huang, G. Romero, R. L. Biltonen and C. Huang, *Biochemistry*, 19 (1980) 924.

CHROM. 17 954

THREE INDEPENDENT METHODS FOR QUANTITATIVE DETERMINATION OF OCTYL COVALENTLY COUPLED TO SEPHAROSE CL-4B

BO-LENNART JOHANSSON* and INGRID DREVIN

Pharmacia AB, Biotechnology, Department of Quality Control, S-751 82 Uppsala 1 (Sweden)

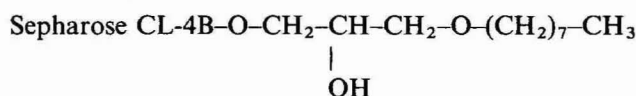
(Received June 7th, 1985)

SUMMARY

Quantification of the octyl content in Octyl-Sepharose CL-4B was accomplished by three independent methods. Firstly, the ^1H NMR spectrum was registered on a deuterium chloride hydrolysed gel. Secondly, gas chromatography was applied to the ether-linked ligands cleaved by boron tribromide. Finally, the gel was combusted to carbon dioxide and elemental carbon analysis was performed. The results from the three methods indicate only random errors at a confidence level of 95%. All developed methods are therefore usable for the determination of the ligand content.

INTRODUCTION

Octyl-Sepharose CL-4B gel is frequently used for hydrophobic interaction chromatography of proteins and peptides¹⁻⁴. The gel is synthesized by the reaction of octyl glycidyl ether with Sepharose CL-4B to give the partial structure:



The accurate determination of the amount of coupled octyl is highly important. The quality control of each production batch demands precise analytical methods as does the proof of ligand leakage from the support. When investigating the effect of ligand coverage on separation accurate determinations are also required.

A gas chromatographic (GC) method for the quantitative determination of octyl on Octyl-Sepharose CL-4B based on the ether cleavage by boron tribromide has recently been presented⁵. In order to adapt this method to a dried gel and to optimize and simplify the cleavage procedure this method has now been reinvestigated.

For comparison a ^1H NMR method has been developed in which the degree of substitution is evaluated by the standard addition of octanol to a solubilized Octyl-Sepharose CL-4B. Earlier, a ^1H NMR method for the determination of the ligand

content was described⁶. However, it suffers from some severe drawbacks, exemplified by the requirement of precise knowledge of the gel matrix for correct interpretation.

A third independent method, which is based on the determination of the carbon content of the substituted and unsubstituted Sepharose CL-4B, has also been developed. This method supports the reliability of the two others.

EXPERIMENTAL

Chemicals and apparatus

2-Bromooctane, 4-bromooctane, boron tribromide, and octyl- β -D-glucopyranoside were of purum quality. Dichloromethane, methanol, dodecane, octanol and 1-bromooctane were of p.a. quality. Deuterium chloride and [$^2\text{H}_6$]dimethylsulphoxide (isotopic purity >99.5%) were from Ciba-Geigy (Basle, Switzerland). Octyl-Sepharose CL-4B and Sepharose CL-4B were obtained from Pharmacia (Uppsala, Sweden).

An HP 5790 gas chromatograph equipped with a flame ionization detector was used. The samples (1 μl) were injected onto a glass column (2 m \times 4 mm I.D.) packed with 10% Apiezon L on Chromosorb W HP (80–100 mesh). The carrier gas flow-rate was 30 ml/min, the oven temperature 145°C, and the injector and detector temperatures 180°C and 200°C, respectively.

The NMR spectra were recorded with a Jeol FX 200 instrument at 199.5 Hz. In the pulsed NMR experiments the number of pulses was 100, the pulse time 7 μsec , the pulse delay 20 sec, the acquisition time 2 sec, and the delay between pulse and acquisition was 50 μsec . The spectral range explored was 2000 Hz.

Determination of the degree of substitution by gas chromatography

Preparation of the gel. About 10 ml of Octyl-Sepharose CL-4B were transferred to a glass filter funnel (G-4), washed with water, shrunk with acetone and finally dried at 105°C for 15 h. The dry gel was then kept in an desiccator.

Cleavage. About 40 mg of the dry gel were placed in a 10-ml measuring flask together with 500 μl of dichloromethane and kept at 25°C. The reaction was started with 800 μl of a solution of boron tribromide (1.38 mmol) in dichloromethane, which was freshly prepared every week, protected from moisture and stored at -30°C . After a reaction time of 30 min, unchanged boron tribromide was destroyed by hydrolysis with 800 μl of a 10% sodium hydroxide solution in water, and 20 μmol of *n*-dodecane were added as internal standard followed by dilution in methanol to volume.

The cleavage of a model substance, octyl- β -D-glucopyranoside, was performed in the same way.

For determination of the cleavage products standard solutions of 4-bromooctane, 2-bromooctane, 1-bromooctane and octanol in methanol were prepared in the concentration range 0.1–5 mM. All solutions were 2 mM in dodecane.

Determination of the degree of substitution by ^1H NMR spectroscopy

The gel was prepared as above, and 20 mg of the dried gel were hydrolysed with 200 μl of 38% deuterium chloride at 70°C for 35 sec. The hydrolysed gel was cooled in an ice-bath for 1 min, after which 2.00 ml of [$^2\text{H}_6$]dimethylsulphoxide

(DMSO-d₆) were added. From this mixture two samples of 1.00 ml each were taken. To one of the samples 100 μ l of DMSO-d₆ were added and to the other 100 μ l of DMSO-d₆ containing 10 μ mol of octanol. NMR spectra were registered on these solutions. Standard solutions of octanol in DMSO-d₆ in the concentration range 2–20 mM were registered in the same way. The peaks from the H_A, H_B and H_C protons were integrated. The internal standard was isotopic impurities of DMSO-d₆ (Fig. 1).

The relaxation time for octanol and the isotopic impurities of DMSO-d₆ were measured in different surroundings by the inversion recovery method⁷.

Determination of the degree of substitution by carbon analysis

Octyl-Sepharose CL-4B and the underivatized gel (Sepharose CL-4B) used as basic material for the substituted gel were washed and dried as above. The content of carbon was then determined on both gels.

Calculation. The amount of octyl glycidyl ether (X) in milligrams coupled to 100 mg of Sepharose CL-4B was calculated from the following equation:

$$Z = \frac{100 \left(Y + \frac{132.12}{186.30} X \right)}{(100 + X)} \quad (1)$$

Rearrangement of this equation yields.

$$X = \frac{100 (Z - Y)}{(70.92 - Z)} \quad (2)$$

where Y and Z are the degrees of carbon content in weight per cent of Sepharose CL-4B and Octyl-Sepharose CL-4B, respectively. The molecular weight of octyl glycidyl ether is 186.30 g/mol and the weight of the carbon atoms in the same ether is 132.12 g/mol. The degree of substitution (S) in μ mole/mg can be thus written as:

$$S = \frac{X \cdot 10^3}{186.30 (100 + X)} \quad (3)$$

RESULTS AND DISCUSSION

Description of the methods and the sampling procedure

The three independent methods for the determination of the ligand content in Octyl-Sepharose CL-4B were developed to investigate and identify errors and to work out one accurate method. The methods were chosen to be chemically and physically disparate so that interfering factors would affect the results in different ways. In the NMR method only the glycoside bonds are cleaved, whereas the GC method is based on the disruption of the ligand from the matrix. The third method implies total combustion of Octyl-Sepharose CL-4B to carbon dioxide.

In the determination of ligand density, sampling of substituted agarose gels normally means that a certain settled gel volume is taken^{5,8}. This sampling procedure

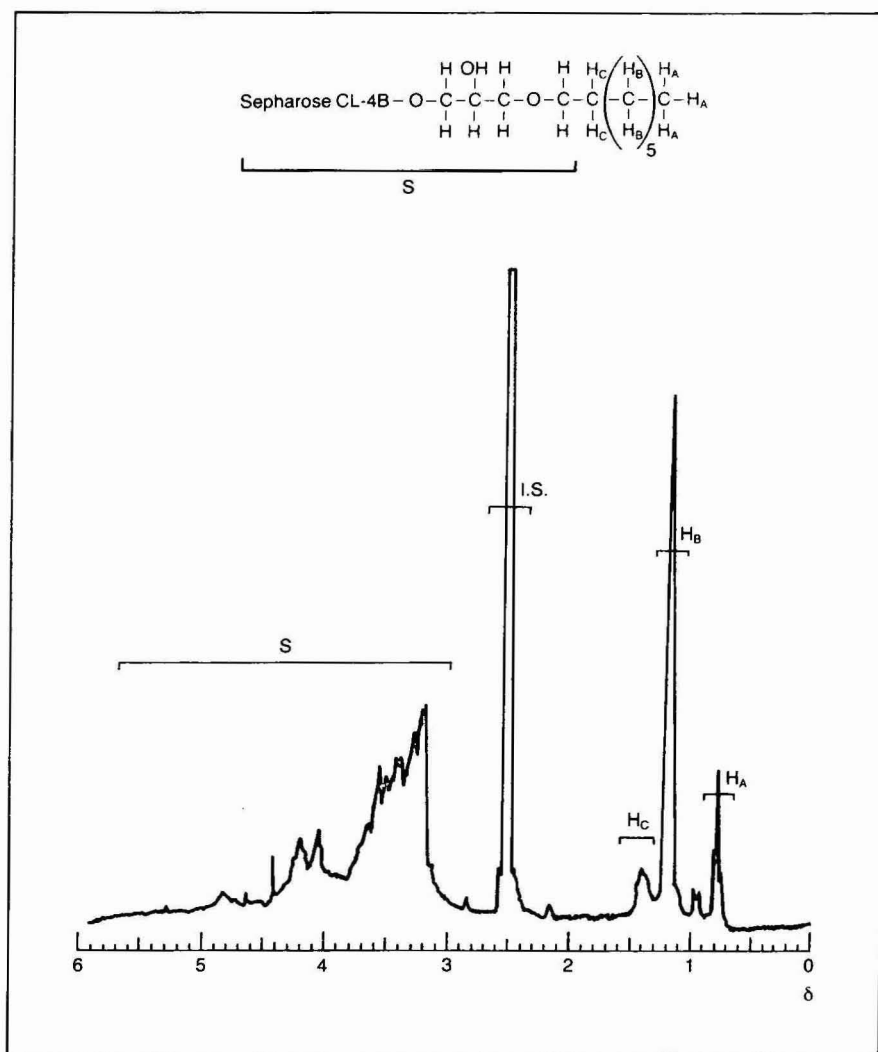


Fig. 1. NMR spectrum of partially hydrolysed Octyl-Sepharose CL-4B in DMSO- d_6 . The small amount of DMSO- d_6 containing ^1H was used as internal standard.

is unreliable because the gel volume varies with the hydrostatic pressure when the gel is settled, the choice of solvent and other parameters which influence the swelling of the gel (e.g. time for swelling, temperature, salt content)⁹. In this study these errors have been circumvented since the ligand density was analysed on a dried gel. The dry weight of Octyl-Sepharose CL-4B is *ca.* 40 mg/ml settled gel, which can be used if a rough estimation of the density is wanted per millilitre of settled gel.

NMR spectroscopy

The acidic hydrolysis of Octyl-Sepharose CL-4B as described above splits the agarose gel into shorter polygalactanes, which are soluble in DMSO- d_6 . The NMR

TABLE I

RELAXATION TIMES OF THE INTERNAL STANDARD AND THE LIGAND IN DIFFERENT SURROUNDINGS

Compound	Relaxation time (min)	
	CH ₂ protons	CH ₃ protons
DMSO-d ₆ in the sample solution*		7.5**
Octanol dissolved in DMSO-d ₆	1.5	2.6
Octanol dissolved in hydrolysed Sepharose CL-4B	0.9	1.9
Octyl in the sample solution*	0.5***	1.5§

* See Experimental for details.

** Internal standard in Fig. 1.

*** H_B and H_C in Fig. 1.§ H_A in Fig. 1.

spectrum of such a solution is shown in Fig. 1. For determination of the amount of octyl groups the peaks from the H_A, H_B and H_C protons are integrated and summed. However, this integral includes a small peak at $\delta = 1$, which emanates from the gel matrix (Fig. 1). The magnitude of this peak is *ca.* 5% of the total integral and is therefore subtracted during the calculation of the ligand content.

Since the relaxation time of free octanol differs from that of octyl groups bonded to galactose residues (Table I), it is important to use a pulse delay long enough to allow all the octyl groups to relax. The value of pulse delay chosen here (20 sec) also allows the DMSO impurities used as internal standard to relax towards their equilibrium value (Table I).

The calibration graph of octanol was found to be linear with an intercept at origo.

The degree of substitution was determined by this NMR method for five dif-

TABLE II

QUANTITATIVE DETERMINATION OF THE LIGAND IN DIFFERENT BATCHES OF OCTYL-SEPHAROSE CL-4B WITH THREE INDEPENDENT METHODS

Year of production	Batch No.	Degree of substitution* ($\mu\text{mol}/\text{mg}$ dry gel)		
		Gas chromatography	NMR spectroscopy	Carbon analysis
1977	3375	1.07 \pm 0.06		
1977	9080	0.69 \pm 0.06	0.69 \pm 0.08	
1979	11143	0.80 \pm 0.06		
1981	18580	0.90 \pm 0.06	0.87 \pm 0.07	1.01 \pm 0.07
1982	24768	0.99 \pm 0.06		
1983	28565	0.84 \pm 0.06	0.77 \pm 0.08	
1983	32349	1.01 \pm 0.06	1.01 \pm 0.08	1.00 \pm 0.07
1984	33653	1.12 \pm 0.06	1.11 \pm 0.07	1.11 \pm 0.07

* Values reported with a confidence interval of $t = 95\%$; see text for details.

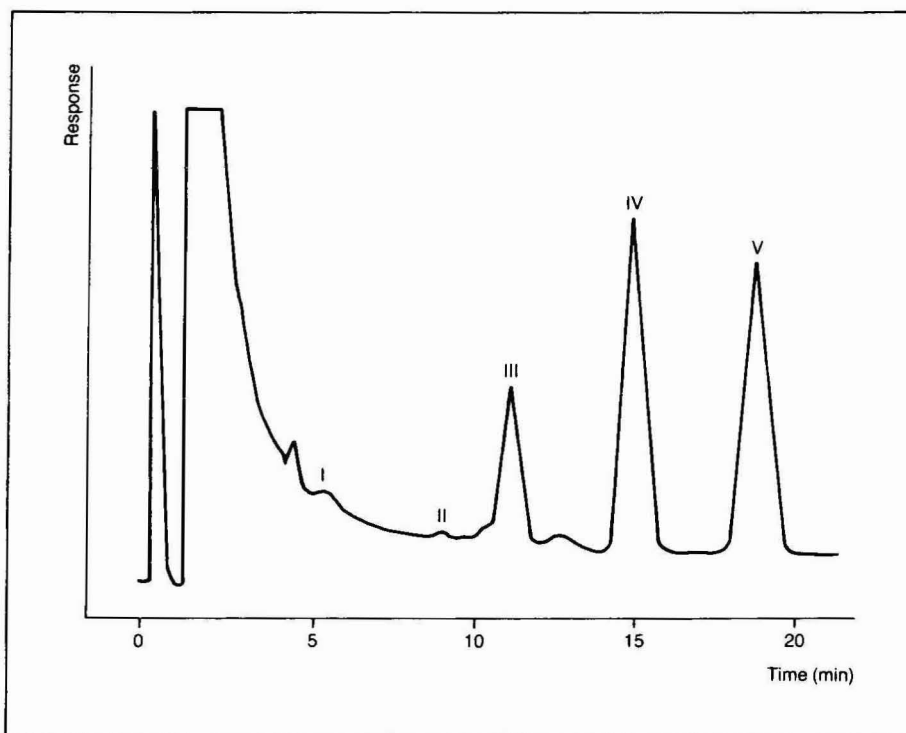


Fig. 2. Gas chromatogram of the cleavage of 40 mg of dry Octyl-Sepharose CL-4B using 1.38 mmol boron tribromide. Peaks: I = 4-bromooctane; II = octanol; III = 2-bromooctane; IV = 1-bromooctane; V = dodecane.

ferent batches of Octyl-Sepharose CL-4B (Table II) and gave a pooled standard deviation of 0.05 ($n = 12$).

Gas chromatography

Cleavage products. When octyl- β -D-glucopyranoside is cleaved by boron tribromide the products are octanol, 2-bromooctane, 1-bromooctane and small amounts of 4-bromooctane, as confirmed by comparison with the retention time of standards.

The cleavage pattern is the same when Octyl-Sepharose is cleaved (Fig. 2), but the proportions of the products may differ when the cleavage time or the amount of boron tribromide is changed (Figs. 3 and 4). However, the minor product 4-bromooctane is always less than 1% of the octyl-containing products.

Cleavage conditions. Complete cleavage of 25 μ mol of octyl- β -D-glucopyranoside is achieved when the amount of boron tribromide is greater than 400 μ mol (Fig. 3). This corresponds to an eight-fold excess of boron tribromide over reactive groups in the octyl- β -D-glucopyranoside.

To obtain quantitative cleavage when 25 μ mol of octyl- β -D-glucopyranoside are cleaved together with 40 mg of dry Sepharose CL-4B, the amount of boron tribromide has to be increased to a ten-fold excess (500 μ mol), and for quantitative

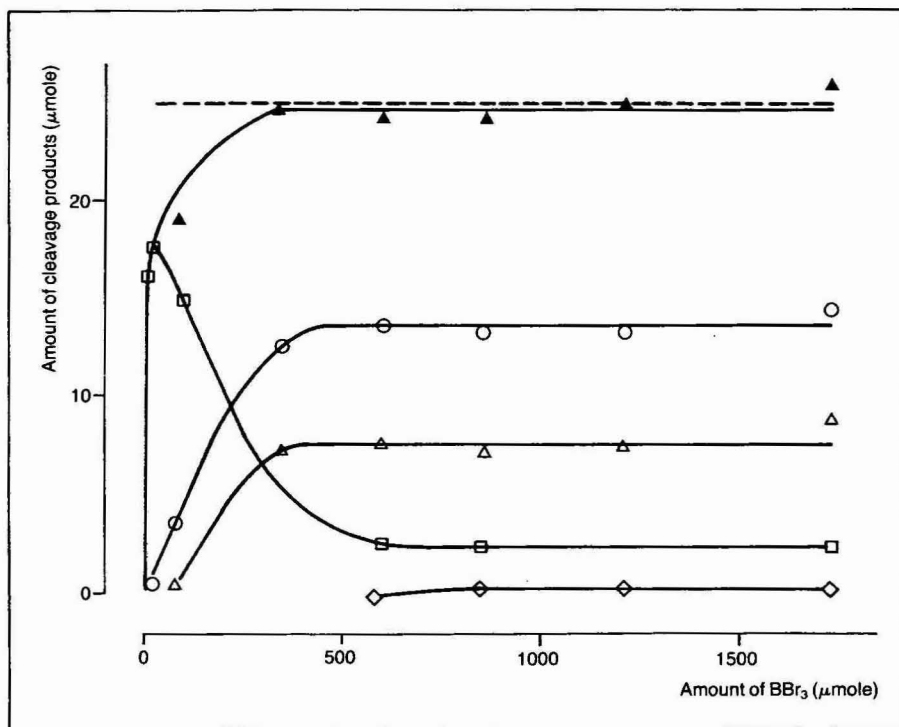


Fig. 3. Yield of products from the cleavage of 25 μmol of octyl- β -D-glucopyranoside by different amounts of boron tribromide after a cleavage time of 30 min. \diamond = Amount of 4-bromooctane; \square = amount of octanol; \triangle = amount of 2-bromooctane; \circ = amount of 1-bromooctane; \blacktriangle = total amount of cleavage products. The dashed line represents 100% recovery.

cleavage of 40 mg of Octyl-Sepharose CL-4B 1000 μmol of tribromide were needed (Fig. 4). This consumption of boron tribromide of the agarose matrix has been pointed out previously^{5,10}.

As depicted in Fig. 5, a time of 30 min is enough to achieve total cleavage of Octyl-Sepharose CL-4B or octyl- β -D-glucopyranoside.

Estimation of the degree of substitution. The amount of octyl groups coupled to Sepharose CL-4B was evaluated from the amounts of octanol, 2-bromooctane and 1-bromooctane produced. These compounds give linear correlations between the concentration and the ratio of the area of the sample peak to that of the internal standard. All calibration graphs have intercepts at origo. A series of eight different batches of Octyl-Sepharose CL-4B has been investigated (Table II). These tests were performed by three different people and a pooled standard deviation of 0.06 ($n = 32$) was obtained.

Carbon analysis

The degree of substitution was determined by carbon analysis on three batches of Octyl-Sepharose CL-4B (Table II). A pooled standard deviation of 0.03 ($n = 6$) was obtained.

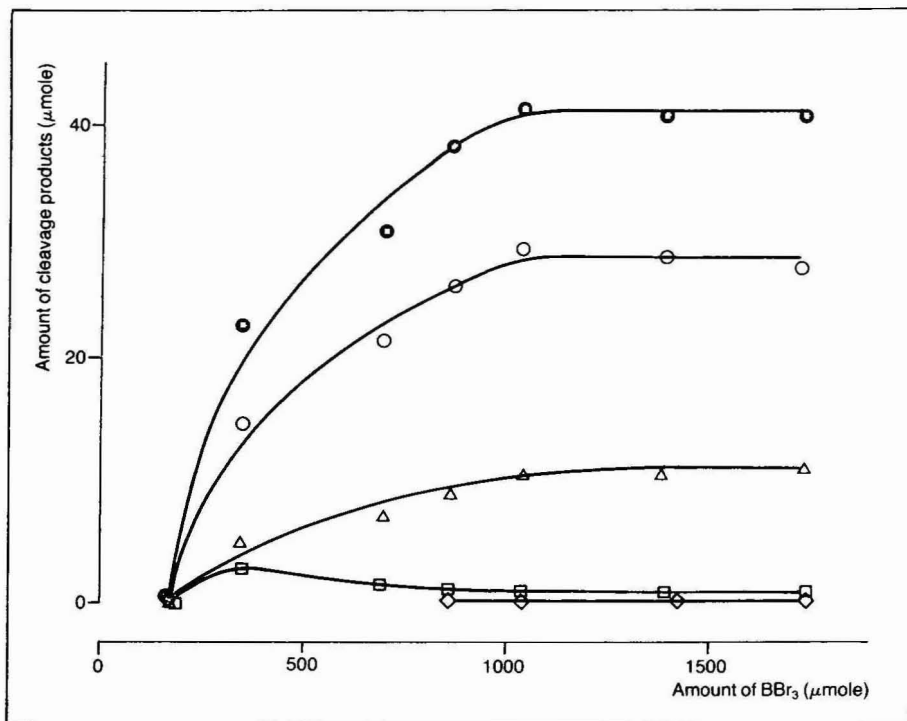


Fig. 4. Yield of products from the cleavage of 40 mg of dry Octyl-Sepharose CL-4B batch No. 32349 by different amounts of boron tribromide after a cleavage time of 30 min. \diamond = Amount of 4-bromooctane; \square = amount of octanol; \triangle = amount of 2-bromooctane; \circ = amount of 1-bromooctane; \bullet = total amount of cleavage products.

CONCLUSIONS

Comparison of the ligand densities determined by the three methods show that they consistently yield results showing only random differences at 95% confidence level (Table II). Therefore it is a reasonable assumption that no significant systematic errors are present. All three methods are consequently usable for the determination of the octyl content in Octyl-Sepharose CL-4B.

The uncertainty in the carbon analysis ($\pm 0.05\%$ C) and the fact that the carbon contents in unsubstituted and substituted Sepharose CL-4B are of the same magnitude makes this method unreliable at low ligand contents. Elemental analysis is therefore normally used where the immobilized ligand contains an element not represented in the gel matrix¹¹. However, in many cases the carbon analysis is sufficiently accurate, especially if the carbon content in the ligand is high and the ligand is of high molecular weight.

One of the main limitations of the NMR method is the inherent lack of sensitivity. Therefore, the method of choice, if low ligand contents are to be analysed, is the GC method.

The GC method is now used in the authors' laboratory for quality control of

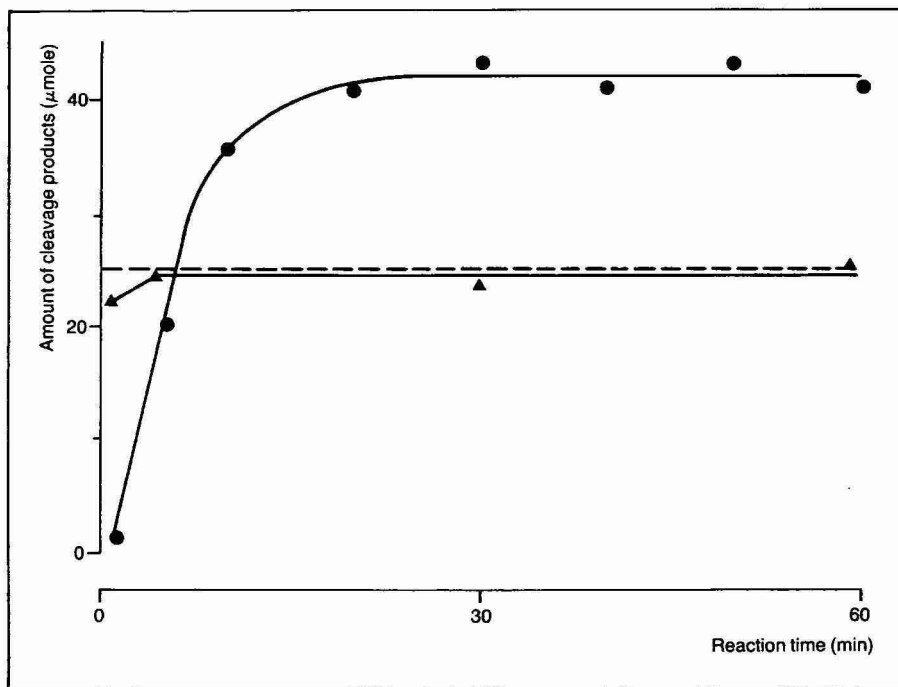


Fig. 5. The time dependence of the total yield of products from the cleavage of 25 μmol of octyl- β -D-glucopyranoside (▲) and 40 mg of dry Octyl-Sepharose CL-4B batch No. 32349 (●). The dashed line represents 100% recovery of the cleavage of 25 μmol of octyl- β -D-glucopyranoside.

the ligand content in Octyl-Sepharose CL-4B. This choice is based on the fact that the GC method also is used for other ligands¹⁰.

ACKNOWLEDGEMENT

The authors thank Mr. Sven-Olof Larsson at Pharmacia for recording the proton NMR spectra.

REFERENCES

- 1 S. Rosén, *Biochim. Biophys. Acta*, 523 (1978) 3124.
- 2 J.-C. Jansson and T. Låås, in R. Epton (Editor), *Chromatography of Synthetic and Biological Polymers*, Vol. 2, Ellis Horwood, Chichester, 1978, p. 60.
- 3 P. Strop, D. Cechová and V. Tomasek, *J. Chromatogr.*, 259 (1983) 255.
- 4 W. J. Gelsema, C. L. De Ligny, W. M. Blanken, R. J. Hamer, A. M. P. Roozen and I. A. Bakker, *J. Chromatogr.*, 196 (1980) 51.
- 5 H.-G. Genieser, D. Gabel and B. Jastorff, *J. Chromatogr.*, 215 (1981) 235.
- 6 J. Rosengren, S. Pålman, M. Glad and S. Hjertén, *Biochim. Biophys. Acta*, 412 (1975) 51.
- 7 R. J. Abraham and P. Loftus, *Proton and Carbon-13 NMR Spectroscopy*, Heyden, London, 1978, p. 122.
- 8 T. K. Korpela, *J. Chromatogr.*, 242 (1982) 33.
- 9 J. K. Inman, *Methods Enzymol.*, 34B (1974) 56.
- 10 I. Drevin and B.-L. Johansson, *J. Chromatogr.*, 295 (1984) 210.
- 11 C. R. Lowe, *An Introduction to Affinity Chromatography*, Elsevier Biomedical Press, New York, 1979, pp. 395–399.

CHROM. 17 978

ADAPTATION OF THE EQUIPMENT FOR HIGH-PERFORMANCE ELECTROPHORESIS TO ISOELECTRIC FOCUSING

STELLAN HJERTÉN* and MING-DE ZHU*

Institute of Biochemistry, University of Uppsala, Biomedical Center, P.O. Box 576, S-751 23 Uppsala (Sweden)

(Received June 25th, 1985)

SUMMARY

Fast and reproducible isoelectric focusing experiments have been performed in glass capillaries of 0.2 mm I.D., wall thickness 0.1 mm, and length 120 mm. These narrow, thin-walled tubes permit rapid removal of the Joule heat to allow high voltages (3000 V) and short run times. The experiments were carried out in equipment designed for high-performance electrophoresis. The protein zones were detected by on- or off-tube measurements of their UV absorption. This detection technique requires that the proteins can be mobilized following the isoelectric focusing step. This mobilization has been achieved either by pumping the zones past the stationary UV monitor (with the voltage applied to avoid zonal broadening during the elution) or by electrophoretic elution, accomplished by replacing the acid at the anode by a base (or the base at the cathode by an acid), which caused the pH gradient—and thereby the proteins—to move in the tube. The electrophoretic mobilization procedure is more universal because it is also applicable when the focusing is performed in a gel.

INTRODUCTION

Two types of apparatus for high-performance electrophoresis (HPE) have been described, one for analytical^{1,2} and one for micropreparative as well as analytical experiments^{3–5}. In the former version we use an on-tube and in the latter an off-tube detection technique. The HPE equipment can be employed not only for zone electrophoresis^{1–5} but also for displacement electrophoresis⁶. In this paper we show that the application range can be extended to include isoelectric focusing. Since the HPE apparatus can detect only migrating solute zones we had to develop methods to mobilize the train of focused zones, preferably without impairment of the resolution obtained in the focusing step. In this paper two such mobilization methods will be described.

* Permanent address: Central laboratory, Academy of Traditional Chinese Medicine, Beijing, China.

MATERIALS AND EQUIPMENT

Human transferrin was a gift from KABI/Vitrum, Stockholm, Sweden. Hemoglobin was prepared from outdated human erythrocytes. The carrier ampholytes (Pharmalyte™, pH 3–10) were bought from Pharmacia, Uppsala, Sweden. The protein zones in the electrophoresis tube were recorded either on-tube as they migrated electrophoretically past a detector consisting of a monochromator giving an 0.2–0.3-mm wide UV beam, which passed through the electrophoresis tube onto a photomultiplier connected to a recorder^{1,2}, or off-tube as they left electrophoretically the capillary tube and were transferred to a high-performance liquid chromatographic (HPLC) detector by an HPLC pump⁴.

EXPERIMENTAL AND RESULTS

Isoelectric focusing and subsequent mobilization of the protein zones by hydrodynamic flow (Method A)

The electrophoresis tube had the dimensions 0.2 I.D. × 0.4 O.D. × 120 mm. Its inside wall was coated with methylcellulose (as described on p. 163 in ref. 7) to eliminate zone distortion caused by electroendosmosis and possible adsorption of the solutes (proteins) to the tube wall (an equation showing the favourable effect of methylcellulose is given on pp. 171 and 172 in the same reference). The electrophoresis tube was then filled with a 1% solution of Pharmalyte (pH 3–10) containing hemoglobin and transferrin. Phosphoric acid (0.02 M) served as anolyte and sodium hydroxide (0.02 M) as catholyte. The focusing was conducted at 1000 V for 7 min (the current decreased from 40 to 15 μ A) and then at 3000 V for 13 min (visual inspection of the hemoglobin zones showed that a steady state had been attained after this time). A pump connected to the cathodic end of the electrophoresis tube via a T-tube was then started to deliver 0.02 M phosphoric acid into the electrophoresis tube at a rate of *ca.* 0.05 μ l/min. The free end of the T-tube, closed with a dialysis membrane to prevent non-controllable liquid flow in the electrophoresis tube, was immersed in the cathodic vessel during both the focusing and the mobilization steps. The protein zones were monitored at 280 nm as they were pumped past the stationary UV detector (Fig. 1). The voltage (3000 V) was maintained during the pumping in order to eliminate distortion of the zones.

Isoelectric focusing and subsequent electrophoretic mobilization of the protein zones (Method B)

The methylcellulose-coated electrophoresis tube had the same dimensions as the tube employed in the above experiment, and the same sample, Pharmalyte, anolyte and catholyte were used. An agarose gel plug (*ca.* 3 mm long) at the cathodic end of the electrophoresis tube eliminated the risk of hydrodynamic flow in the tube. At a voltage of 1200 V the proteins became focused within 20 min. The phosphoric acid in the anode vessel was then replaced by 0.02 M sodium hydroxide and the voltage was increased to 3000 V. The current was initially 14 μ A, increased gradually during the mobilization, was *ca.* 30 μ A when the last peak had passed the detector and then continued to increase thereafter. All protein zones had passed the detector (280 nm) after electrophoresis for *ca.* 15 min. The electropherogram is shown in Fig. 2a.



Fig. 1. Elution of focused protein zones by hydrodynamic flow and monitoring by on-tube detection. The sample consisted of 10 μg of human hemoglobin (Hb) and 15 μg of human transferrin (Tr). The experiment was carried out in the HPE equipment^{1,2}. The protein zones were recorded as they passed a stationary UV detector monitoring at 280 nm.

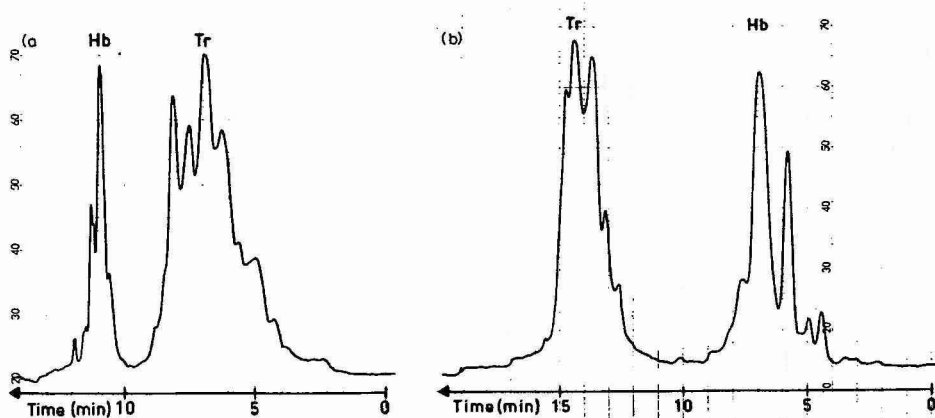


Fig. 2. Electrophoretic elution of focused protein zones and their monitoring by on-tube detection. The same sample and equipment were used as in the experiment shown in Fig. 1. The elution was achieved by replacing the acid at the anode with a base (a), or the base at the cathode with an acid (b).

To determine whether alterations in the protein pattern and in the pH gradient occur during the mobilization of the protein zones, the above experiment was repeated in the free-zone electrophoresis apparatus, where stabilization against convection is achieved by slow rotation (40 rpm) of the horizontal quartz electrophoresis tube ($380 \times 3 \text{ I.D.} \times 8 \text{ mm O.D.}$) around its long axis⁷. The latter apparatus is very suitable for this type of measurement since it permits scanning of the protein pattern at any time during both the focusing and the mobilization and also allows one to withdraw zones from the tube after completion of a run, for instance, for pH measurements. The result of such an analysis is shown in Fig. 3. As curve I indicates, the pH gradient in the electrophoresis tube extended from 7.0 to 9.6 at the moment when the transferrin zone had just migrated out of the tube. This experiment was carried out overnight at a constant voltage of 500 V.

The experiment shown in Fig. 2a was repeated, with the difference that the

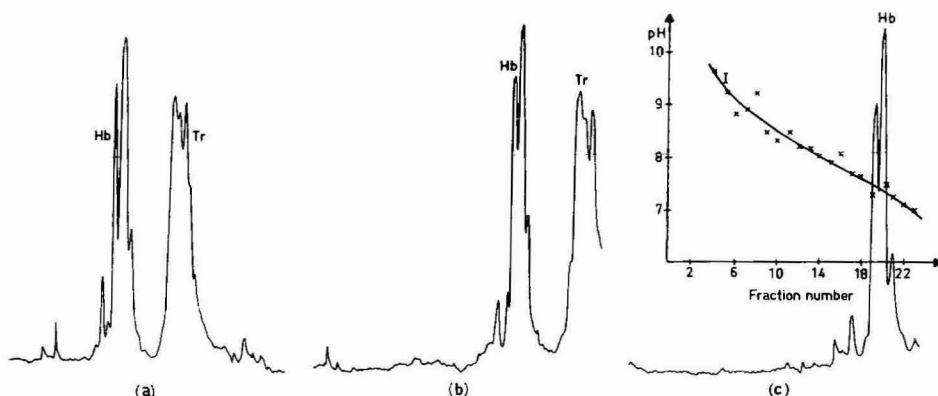


Fig. 3. Isoelectric focusing (a) of the same proteins as were used in the experiment shown in Fig. 2 and subsequent elution of the protein zones by replacing the acid at the anode by a base (b, c). The experiment was carried out in the free-zone electrophoresis apparatus⁷. After completion of the run, 1-cm fractions were withdrawn from the revolving electrophoresis tube for pH measurements (curve 1).

mobilization step was performed with 0.02 *M* phosphoric acid in both the electrode vessels (Fig. 2b). When this experiment was performed in the above free-zone electrophoresis apparatus, the pH gradient extended from 3.0 to 7.5 at the moment when the hemoglobin left the electrophoresis tube.

Electrophoretic elution of focused zones is applicable both in free solution (Figs. 2a and 2b) and in gel media. The example shown in Fig. 4 refers to an experiment performed under the same conditions as that shown in Fig. 2a, with the difference that the focusing was done in a polyacrylamide gel of the composition $T = 3\%$; $C = 3\%$ (for definition of these parameters, see ref. 8), rather than in free solution.

In all the above experiments the protein zones were monitored by an on-tube detection method. However, a pattern similar to that shown in Fig. 2a was obtained when the experiment was repeated with off-tube detection³. The pump delivered 0.02 *M* sodium hydroxide to the flow cuvette of the HPLC detector at a rate of 0.15 ml/min.

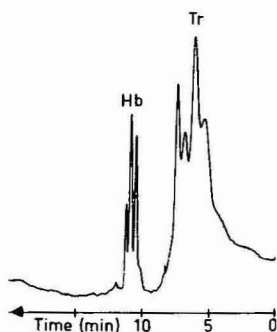


Fig. 4. An isoelectric focusing experiment similar to that shown in Fig. 2a, with the main difference that it was performed in a polyacrylamide gel instead of in free solution.

DISCUSSION

In 1976 McCormick *et al.*⁹ and in 1978 McCormick *et al.*¹⁰ showed that, following isoelectric focusing, "selective zone recovery could be achieved by transposition of the gels into either isoelectric ampholytes or charged buffers". We believe that this paper is the first to describe successful one-step mobilization of all the isoelectrically focused protein zones by changing the composition of the electrode solutions. Although our studies on mobilization of the train of focused proteins by changing the composition of the anolyte or catholyte originated from attempts to use the HPE electrophoresis equipment for isoelectric focusing, the mobilization technique described can be adapted to runs in other types of column as well.

For a discussion of the mobilization of the protein zones following the focusing step we refer to the experiment presented in Fig. 2a. When the acid at the anode is replaced by sodium hydroxide, the hydroxyl ions begin to migrate through the electrophoresis tube toward the anode and the sodium ions at the anode begin to move toward the cathode. The migrating sodium ions will cause a continuous increase in the conductivity of the solution in the electrophoresis tube, and the migrating hydroxyl ions an increase in both conductivity and pH. The change in pH will not be abrupt because the carrier ampholytes have a good buffering capacity. (Since the hydrogen ions in the sodium hydroxide solution are present at much lower concentration than the hydroxyl ions, they will contribute much less than the hydroxyl ions to a change in pH and conductivity in the electrophoresis tube, and can therefore be neglected in this discussion.) When the ampholytes and the proteins are titrated by the migrating hydroxyl ions they become negatively charged and will move towards the anode in agreement with Fig. 3. The above-mentioned increase in conductivity caused by the sodium and hydroxyl ions, and strengthened by the charged ampholytes, is manifested as an increase in the current (at constant voltage) during the mobilization process.

It is premature to discuss whether elution by hydrodynamic flow (Fig. 1) or by electrophoresis (Figs. 2 and 4) gives the higher resolution. However, a comparison of these figures does not reveal any large differences in the separation pattern.

In Fig. 2a the resolution of the transferrin components is better than in Fig. 2b, whereas the hemoglobin components are resolved better in Fig. 2b. If this reflects a general phenomenon one should perform the mobilization of the proteins toward both the positive and the negative pole to see which procedure gives the higher resolution.

To judge from Fig. 3 the resolution is not affected much during the mobilization of the protein zones. This is in agreement with the observation that hemoglobin is positioned in the moving pH gradient at a pH close to its isoelectric point, which is *ca.* 7.0; (see curve I in Fig. 3c).

Elution of separated protein zones by hydrodynamic flow (Method A above) is of course, not applicable if the capillary tube contains a gel. In such cases one can use the alternative technique and perform the mobilization by changing the composition of the catholyte or anolyte (Method B above). We have used the latter technique when the isoelectric focusing was carried out in a polyacrylamide gel (Fig. 4).

In agreement with observations made by other authors¹¹⁻¹⁴, both transferrin

and hemoglobin appeared in multiple forms upon isoelectric focusing (Figs. 1–4). Since we have not taken any precautions to prevent release of iron from the transferrin, some of the transferrin peaks obtained may correspond to molecules with reduced iron content. Since the focusing experiments (including the mobilization step) performed in the free-zone electrophoresis equipment took much longer (run over-night) than those carried out in the HPE equipment (*ca.* 30 min), the differences between the protein patterns obtained with these different types of apparatus (Fig. 3 and Figs. 1, 2 and 4, respectively) can possibly be ascribed to transferrin molecules with different numbers of iron atoms.

Perhaps the HPE apparatus with the off-tube detection system gives electropherograms with somewhat lower resolution than the apparatus with on-tube monitoring. On the other hand, the former apparatus has the advantage that it permits recovery of the separated proteins and can thus be used for micropreparative runs.

In this paper we have shown the potentialities of a hydrodynamic and an electrophoretic method to mobilize the pH gradient and the focused proteins. Both methods permit rapid detection of the protein zones without time-consuming staining. Therefore we feel it is important to publish the results at this early stage in the development of the methods, even if much remains to be investigated.

ACKNOWLEDGEMENTS

The authors are much indebted to Mrs. Karin Elenbring for very skilful technical assistance. The work was supported by the Swedish Natural Science Research Council.

REFERENCES

- 1 S. Hjertén, *J. Chromatogr.*, 270 (1983) 1–6.
- 2 S. Hjertén, in H. Hirai (Editor), *Electrophoresis '83*, Walter de Gruyter, Berlin, 1984, pp. 71–79.
- 3 M.-d. Zhu and S. Hjertén, in V. Neuhoff (Editor), *Electrophoresis '84*, Verlag Chemie, Weinheim, 1984, pp. 110–113.
- 4 S. Hjertén and M.-d. Zhu, *Pure Appl. Chem.*, (1985) in press.
- 5 S. Hjertén and M.-d. Zhu, *J. Chromatogr.*, 327 (1985) 157–164.
- 6 S. Hjertén and M.-d. Zhu, in H. Peeters (Editor), *Protides of the Biological Fluids*, Pergamon, in press.
- 7 S. Hjertén, *Chromatogr. Rev.*, 9 (1967) 122–219.
- 8 S. Hjertén, *Arch. Biochem. Biophys.*, Suppl. 1 (1962) 147–151.
- 9 A. McCormick, L. E. Miles and A. Chrambach, *Anal. Biochem.*, 75 (1976) 314–324.
- 10 A. McCormick, H. Wachslight and A. Chrambach, *Anal. Biochem.*, 85 (1978) 209–218.
- 11 H. Stibler, *J. Neurol. Sci.*, 36 (1978) 273–288.
- 12 H. Stibler, *J. Neurol. Sci.*, 42 (1979) 275–281.
- 13 O. Vesterberg and U. Breig, *J. Immunol. Meth.*, 46 (1981) 53–62.
- 14 O. Vesterberg, *Biochim. Biophys. Acta*, 257 (1972) 11–19.

CHROM. 17 941

ISOTACHOPHORETIC CONTROL OF PEPTIDE SYNTHESIS AND PURIFICATION

A NOVEL APPROACH USING ULTRAVIOLET DETECTION AT 206 nm

PETER STEHLE* and PETER FÜRST

Institute for Biological Chemistry and Nutrition, University of Hohenheim, Stuttgart 70 (F.R.G.)

(Received June 3rd, 1985)

SUMMARY

The synthesis and purification of two glutamine-containing dipeptides were controlled by applying analytical capillary isotachopheresis. The use of a newly developed detector block allowed conductivity detection and, for the first time, UV measurement at 206 nm. This system facilitates qualitative and quantitative analysis of peptides not absorbing at 254 and 280 nm in amounts of less than 200 ng, thereby permitting a direct classification of the sample ions analysed. Optimization of peptide synthesis is significantly improved by this novel method, which enables simultaneous monitoring of the reaction products and contaminating inorganic ions during synthesis and purification.

INTRODUCTION

In a previous communication, synthesis of peptides containing glutamine (Gln) and tyrosine (Tyr) was described¹, and in subsequent reports the potential use of analytical capillary isotachopheresis in characterizing these synthetic products was emphasized^{2,3}. In the present study, the synthesis and purification of two Gln-containing dipeptides, L-alanyl-L-glutamine (Ala-Gln) and L-aspartyl-L-glutamine (Asp-Gln) were isotachophoretically controlled using conductivity and UV detection. A newly developed detector block allowed measurements of the UV signal not only at the commonly used wavelengths (254 and 280 nm), but also at 206 nm, which is especially suited for peptide bonds. This novel method of detection enabled satisfactory analysis of peptide material in amounts less than 200 ng, which is not feasible with the commonly used detector systems. The use of the proposed detector block facilitates detection of peptides not absorbing at 254 and 280 nm. Thus, this new qualitative and quantitative approach may represent a novel method for controlling peptide synthesis and purification procedures.

EXPERIMENTAL

Peptide synthesis and purification

Ala-Gln and Asp-Gln were synthesized by the N-carboxy anhydride (NCA) method described previously^{1,4}. The synthesized peptides were purified by repeated gel filtration on Sephadex G-10 (Pharmacia, Uppsala, Sweden)¹. Crude materials, intermediates and end products were isotachophoretically analysed in concentrations and amounts given in the figures.

Analytical isotachopheresis

Analytical isotachopheresis was performed by using a LKB 2127 Tachophor equipped with an automatic driving current control unit. Separations were made in a PTFE capillary (230 × 0.55 mm I.D.) attached to a newly developed detector block (LKB 2127-140), allowing detection of the linear conductivity signal and UV absorption at 254/280 nm and 206 nm. Mercury (254 nm) and iodine (206 nm) were used as light sources. The detection signals were monitored by employing a two-channel recorder (Kipp & Zonen, Delft, The Netherlands) with a chart speed of 6 cm/min. The separations required *ca.* 10 min and the detection current was 60 μ A.

The operational systems used are outlined in Table I. These solutions were prepared from analytical grade chemicals provided by E. Merck (Darmstadt, F.R.G.) and Sigma (St. Louis, MO, U.S.A.) as previously described^{2,3}.

As reference, aqueous solutions of alanine (Ala) and aspartic acid (Asp) (E. Merck) as well as glutamine (Gln) and L-alanyl-L-alanine (Ala-Ala) (Sigma) were investigated alone or in doping experiments.

RESULTS

Control of peptide synthesis

Three crude specimens of Ala-Gln derived under various synthesis conditions were analysed with electrolyte system 1 (Table I). The respective isotachopherograms are shown in Fig. 1. Using conductivity detection and UV measurement at 254 nm (Fig. 1A) analyses of the crude products revealed at least five non-UV-absorbing

TABLE I
OPERATIONAL SYSTEMS FOR ANIONIC ANALYSIS

MES = Morpholinoethanesulphonic acid; ammediol = 2-amino-2-methyl-1,3-propanediol; HPMC = hydroxypropylmethylcellulose.

	<i>Leading electrolyte</i>	<i>Terminating electrolyte</i>
System 1	0.005 M MES Ammediol 0.4% HPMC pH 9.1	0.01 M β -alanine Ammediol Ba(OH) ₂ pH \approx 10
System 2	0.01 M Cl ⁻ Bis-Tris 0.4% HPMC pH 6.0	0.01 M MES Tris pH \approx 6

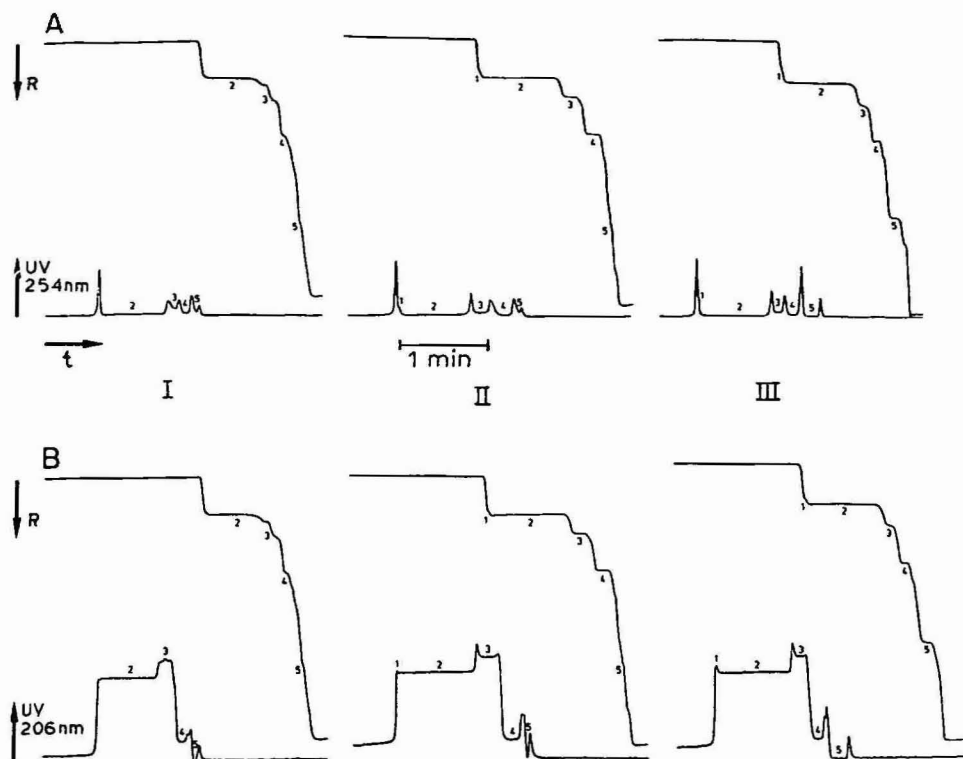


Fig. 1. Isotachopheretic analyses (electrolyte system 1) of three different crude samples of Ala-Gln (I-III): UV detection at 254 nm (A) and 206 nm (B). For each separation, 20 μ l were injected, corresponding to 8.68 μ g of material. Key: 1 = Ala-Ala; 2 = Ala-Gln; 3 = unknown peptide(s); 4 = Gln; 5 = Ala.

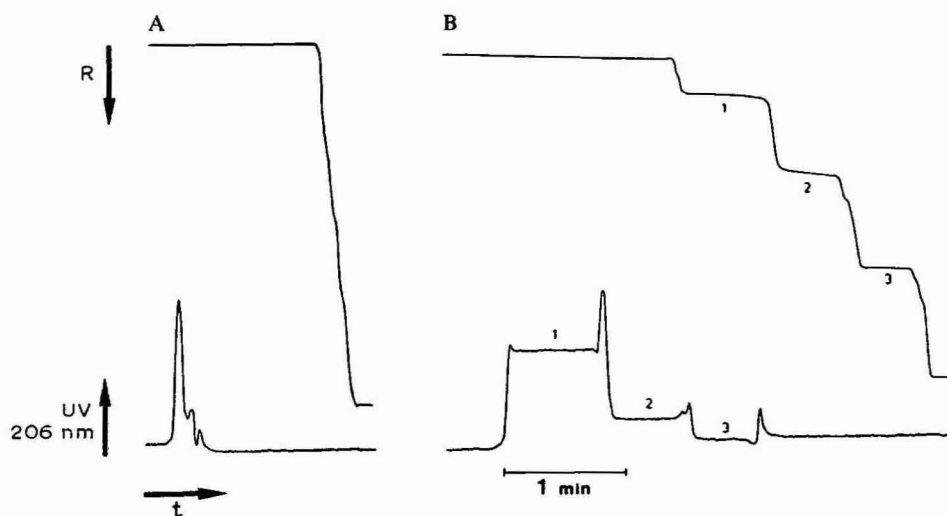


Fig. 2. Isotachopheretic analysis (electrolyte system 1) of a reference mixture of Ala-Ala (1), Gln (2) and Ala (3). (A) electrolyte system; (B) reference mixture (2.5 μ l injected, corresponding to 0.80 μ g of Ala-Ala, 0.73 μ g of Gln and 0.45 μ g of Ala).

zones, as indicated by the conductivity signal. Four of these zones exhibited characteristic UV levels with a detection wavelength of 206 nm (Fig. 1B). As shown, the main zone as well as two minor zones revealed high UV absorption, obviously suggesting that they correspond to peptide material. One other minor zone, showing a lower UV absorption, may represent unchanged starting material. These assumptions were verified by analysing reference substances (Fig. 2). Compared with the isotachopheretic pattern of electrolyte system 1 (A), analysis of an equimolar standard mixture (B) resulted in two UV-absorbing zones and one non-UV-absorbing zone, corresponding to the dipeptide Ala-Ala and the free amino acids Gln and Ala.

Analyses of three different crude samples of Asp-Gln were performed by applying electrolyte system 2 (Table I) showing five discrete separated zones in various amounts (Fig. 3). None of these compounds exhibited UV absorption at 254 nm (Fig. 3A), whereas characteristic UV levels compared with the leading ion were measured at 206 nm (Fig. 3B). The main synthesis product, as well as three minor unidentified side products, showed high UV absorption, suggesting the presence of peptide bond(s) in these compounds, whereas the fifth zone exhibited low UV absorption. This latter zone was identified as free Asp by analysing the reference substance. The isotachopherograms of the electrolyte system alone (A) and of a standard solution of Asp (B) are depicted in Fig. 4.

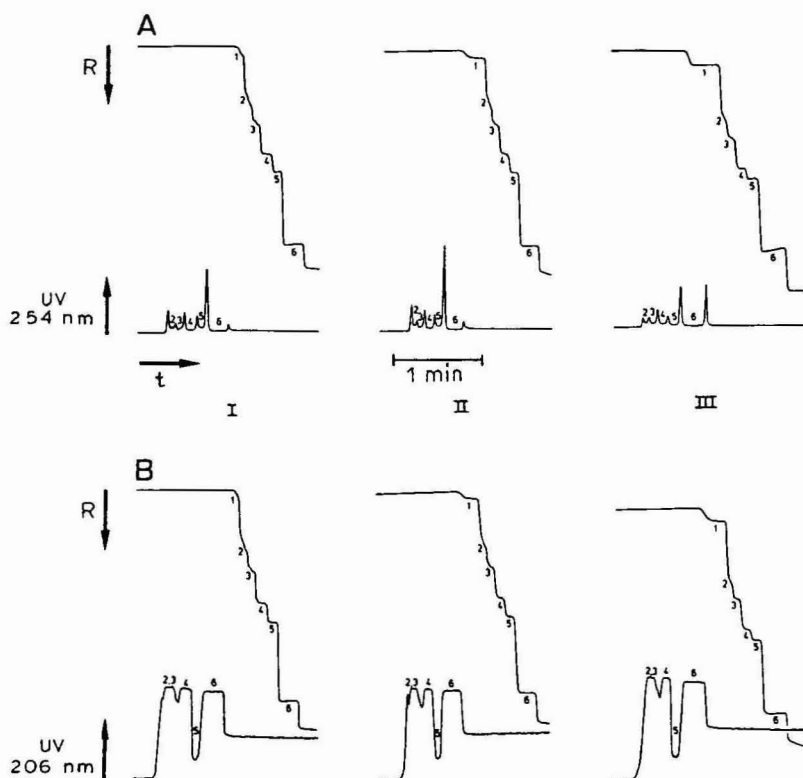


Fig. 3. Isotachopheretic analyses (electrolyte system 2) of three different crude samples of Asp-Gln (I-III): UV detection at 254 nm (A) and 206 nm (B). For each separation, 10 μ l were injected, corresponding to 5.49 μ g of material. Key: 1 = sulphate; 2, 3, 4 = unknown peptides; 5 = Asp; 6 = Asp-Gln.

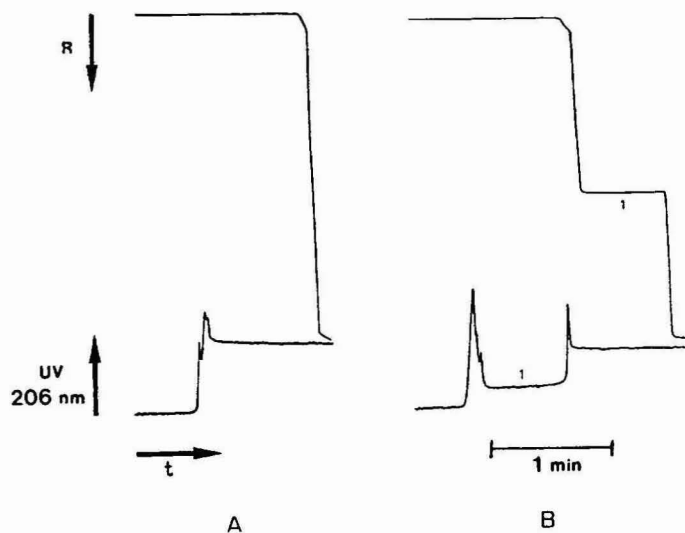


Fig. 4. Isotachopheretic analysis (electrolyte system 2) of a reference solution of Asp (1). (A) electrolyte system; (B) reference solution (10 μ l injected, corresponding to 2.66 μ g of Asp).

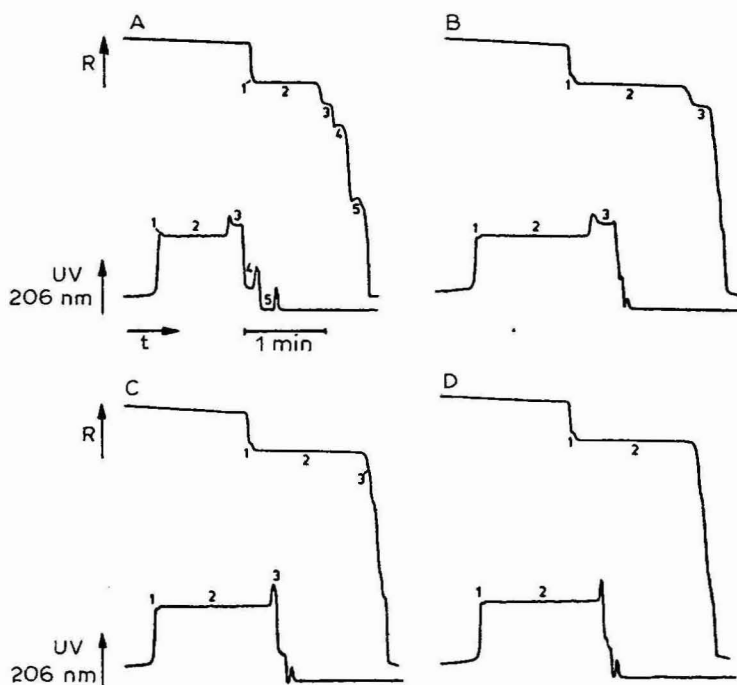


Fig. 5. Isotachopheretic analyses (electrolyte system 1) of Ala-Gln before (A) and after (B-D) the different purification steps. Key as in Fig. 1. For each separation 20 μ l were injected, corresponding to 8.68 μ g of material.

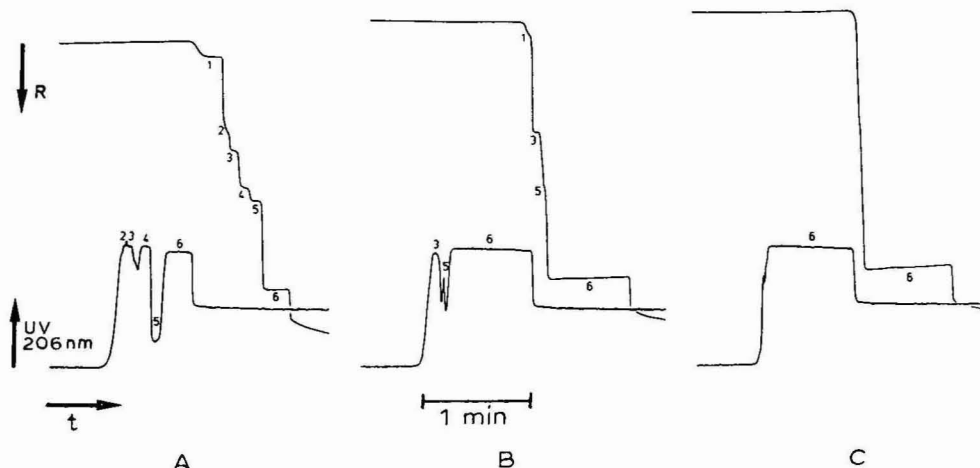


Fig. 6. Isotachopheretic analyses (electrolyte system 2) of Asp-Gln before (A) and after (B,C) the different purification steps. Key as in Fig. 3. For each separation 10 μ l were injected, corresponding to 5.49 μ g of material.

In all Asp-Gln fractions analysed a further zone, only detectable in the conductivity signal, was observed. This suggested the presence of contaminating sulphate derived from the peptide synthesis procedure.

Control of purification process

The crude material and the different peptide fractions obtained during the development of purification of Ala-Gln were analysed by conductivity detection and UV measurement at 206 nm. The respective isotachopherograms are shown in Fig. 5. Compared with the analysis of the crude material (A), both free amino acids Ala and Gln could be removed during the first gel-chromatographic purification step (B). Furthermore, the zone length for the main product was markedly increased, and moderate increases were also noted for Ala-Ala and the unidentified side product. This might be due to simultaneous removal of salts during the first purification step. The majority of the two contaminating products could be removed by applying further gel filtration purification steps (C,D). In the final product an enrichment of Ala-Gln of approaching 100% could be achieved. Only traces of Ala-Ala were detectable.

The crude material (A) and the different purified peptide fractions (B,C) of Asp-Gln were analysed similarly but with electrolyte system 2 (Table I), as illustrated in Fig. 6. No free Asp and only small amounts of contaminating peptides could be detected after the first purification step. After the second gel-chromatographic separation an enrichment of approaching 100% was observed for Asp-Gln.

DISCUSSION

Although in several investigations analytical capillary isotachopheresis was found to be a promising tool in qualitative and quantitative analyses of synthetic^{2,3,5-9}

and naturally occurring¹⁰⁻¹⁶ peptides, only a few investigators have applied this method as a control in peptide purification process¹⁷⁻²⁰.

Kopwille *et al.* analysed the crude material as well as peptide-containing fractions obtained during the purification of synthetic tetradeca-, deca- and undecapeptides¹⁷⁻¹⁹. Friedel and Holloway employed analytical isotachopheresis in the analysis of intermediates and end products during synthesis of a pentapeptide²⁰. In these studies detection was made by monitoring thermometric and UV signals. Owing to the relatively low sensitivity of thermometric detection, high amounts (*ca.* 30 μ g) of peptide material were necessary to obtain satisfactory results. Additionally, the characteristic wave form of the thermometric signal rendered a quantitative and qualitative evaluation difficult. Thus, only the enrichment of the main products during the purification process could be followed. In these studies the UV absorption was monitored at 254 nm and/or 280 nm, so only peptides containing aromatic amino acids and cystine revealed characteristic UV absorption.

In general, *s.c.* "marker or separation peaks" (presumably due to different refractive indexes of the separated zones) mark the respective zone boundaries of non-UV-absorbing solutes allowing evaluation of the UV signal. Nevertheless, in certain operational systems no such "marker peaks" are detectable, thereby invalidating evaluation of the UV signal^{21,22}. Furthermore, lack of characteristic UV levels at 254/280 nm complicates the identification and classification of unknown sample compounds.

Up to date, measurement of UV absorption at lower wavelengths has not been feasible, since in all commercially available built-in UV detectors the signal was measured directly through the capillary wall. Thus, the high absorption and dispersion of the capillary material (generally PTFE) hindered the use of wavelengths below 230 nm. In the present study, a new commercially available detector block was applied, which allowed concomitant conductivity and UV measurements. The great improvement of the new UV detector lies in the fact that the fibre optics lead the light directly into the interior of the liquid system. This results in a significantly lower loss of UV light intensity compared with the previous types of capillary plate. Consequently, this new detector block facilitates UV measurement at 206 nm.

A limiting factor in using UV detection at 206 nm is the considerably increased absorption of the buffer solutions at this wavelength. As demonstrated by Verheggen *et al.*²³, operational systems at alkaline pH including chloride or MES as leading and Ammediol or Tris as counter ion show low absorption at 206 nm. In contrast, anionic operational systems at pH 6 with histidine as counter ion are not suitable, owing to the strong absorption of this amino acid at lower wavelengths²³. Therefore, preparing an operational system at pH 6, we replaced histidine with Bis-Tris (pK_a 6.5) which showed a high buffer capacity at this pH value and low UV absorption at 206 nm (Figs. 3, 4 and 6).

The advantage of measuring UV absorption at 206 nm compared with 254 nm is illustrated in Figs. 1 and 3, which show that analyses of both Gln-containing peptides at 254 nm revealed several non-UV-absorbing zones. Since no characteristic UV levels could be measured at this wavelength, no information about the chemical structure of the separated compounds could be obtained. Consequently, for further characterization of sample ions suitable reference substances are required. In contrast, UV detection at 206 nm facilitates a direct classification of the sample ions,

enabling a direct differentiation between peptides formed during synthesis and unchanged starting materials (Figs. 1 and 3). This is of great importance in the optimization of peptide synthesis by the modification of reaction variables: pH, temperature and especially starting amino acid material.

According to the high absorption coefficient of peptide bonds at 206 nm²⁴, all zones with high UV absorption must correspond to peptides, whereas all zones with lower or no UV absorption could be unreacted free amino acids, as verified when analysing the respective standard mixtures shown in Figs. 2 and 4, respectively. Indeed, it is evident that the characteristic conductivity step heights and UV levels derived on the one hand from the crude preparations and on the other hand from the standard substances are identical. The main Gln-containing products could be identified and characterized after purification, as previously described¹.

Apart from the qualitative approach, isotachopheresis provides quantitative information about the composition of the samples analysed^{2,3,12,13,21}. In this context one should remember that the concentrations of the zones are directly related to the concentration of the leading ion²¹. Thus, the ratio of the main peptide formed to remaining starting material and side products can be estimated by measuring single zone lengths and total zone length, respectively. Calculation of this ratio may serve as a guideline to define optimum conditions for synthesis (Figs. 1 and 3) and purification (Figs. 5 and 6).

This quantitative approach underlines the obvious advantage of isotachopheresis compared with high-performance liquid chromatography (HPLC), which requires the use of suitable reference substances for a proper quantitative evaluation of analysed material. Indeed, the major advantages of isotachopheresis over HPLC lie in the facts that no processing of samples is necessary prior to analysis⁹ and that simultaneous detection of contaminating ions is feasible²⁵. This latter advantage is emphasized in Figs. 3 and 6, which show the presence of contaminating sulphate acquired from sulphuric acid in the reaction mixture used for peptide synthesis.

In the present study, the simultaneous use of unspecific conductivity detection and UV monitoring at 206 nm obviously increased the resolution and sensitivity compared with previously used detection systems, enabling quantitative measurement of peptide material in amounts of less than 200 ng. Thus, the introduction of the new detector block and its subsequent application might ameliorate the control of synthesis and purification procedures in peptide chemistry.

ACKNOWLEDGEMENTS

This work was supported by Arbeitsgemeinschaft Industrieller Forschungsvereinigungen (AIF, Nr. 5986). The kind support from Pfrimmer and Co. (Erlangen, F.R.G.) is gratefully acknowledged.

REFERENCES

- 1 P. Stehle, B. Kühne, W. Kubin, P. Fürst and P. Pfaender, *J. Appl. Biochem.*, 4 (1982) 280.
- 2 P. Stehle, B. Kühne, P. Pfaender and P. Fürst, *J. Chromatogr.*, 249 (1982) 408.
- 3 P. Stehle, P. Pfaender and P. Fürst, *J. Chromatogr.*, 294 (1984) 507.
- 4 P. Pfaender, H. Pratzel, H. Blecher, G. Gorka and G. Hansen, in Y. Wolman (Editor), *Peptides 1974*, Wiley, New York, Toronto and Israel Universities Press, 1975, pp. 137–140.

- 5 A. Kopwillem, F. Chillemi, A. B. Bosisio-Righetti and P. G. Righetti, *Protides Biol. Fluids*, 21 (1974) 657.
- 6 A. J. P. Martin and F. Hampson, in P. G. Righetti (Editor), *Progress in Isoelectric Focusing and Isotachophoresis*, North Holland, Amsterdam, Oxford, 1975, pp. 327–350.
- 7 F. M. Everaerts, M. Geurts, F. E. P. Mikkers and Th. P. E. M. Verheggen, *J. Chromatogr.*, 119 (1976) 129.
- 8 H. Miyazaki and K. Katoh, *J. Chromatogr.*, 119 (1976) 369.
- 9 C. J. Holloway and V. Pingoud, *Electrophoresis*, 2 (1981) 127.
- 10 L. Pradayrol, J. A. Chayvialle, M. Carlquist and V. Mutt, *Biochem. Biophys. Res. Commun.*, 85 (1978) 701.
- 11 M. Carlquist, V. Mutt and H. Jönrvall, *FEBS Lett.*, 108 (1979) 457.
- 12 L. Zimmerman, A. Baldesten, J. Bergström and P. Fürst, *Clin. Nephrol.*, 13 (1980) 183.
- 13 L. Zimmerman, P. Fürst, J. Bergström and H. Jönrvall, *Clin. Nephrol.*, 14 (1980) 107.
- 14 J. Gróf and J. Menyhárt, in F. M. Everaerts (Editor), *Analytical Isotachophoresis*, Elsevier, Amsterdam, 1981, pp. 99–107.
- 15 H. Kodama and S. Uasa, *J. Chromatogr.*, 163 (1979) 300.
- 16 H. Mikasa, K. Sasaki and H. Kodama, *J. Chromatogr.*, 305 (1984) 204.
- 17 A. Kopwillem, R. Lundin and H. Sievertsson, *LKB Application Note*, 159 (1974).
- 18 A. Kopwillem, U. Moberg, G. Westin-Sjödahl, R. Lundin and H. Sievertsson, *Anal. Biochem.*, 67 (1975) 166.
- 19 A. Kopwillem, *Protides Biol. Fluids*, 22 (1975) 715.
- 20 K. Friedel and C. J. Holloway, *Electrophoresis*, 2 (1981) 116.
- 21 F. M. Everaerts, J. L. Beckers and Th. P. E. M. Verheggen (Editors), *Isotachophoresis: Theory, Instrumentation and Applications*, Elsevier, Amsterdam, Oxford, New York, 1976.
- 22 P. Stehle, *Thesis*, University of Hohenheim, Stuttgart-Hohenheim, F.R.G.
- 23 Th. P. E. M. Verheggen, F. M. Everaerts and J. C. Reijenga, *J. Chromatogr.*, 320 (1985) 99.
- 24 K. Lübke, E. Schröder and G. Kloss (Editors), *Chemie und Biochemie der Aminosäuren, Peptide und Proteine II*, Thieme Verlag, Stuttgart, 1975, pp. 180–182.
- 25 J. W. Van Nispen, P. S. L. Janssen, B. C. Goverde, J. C. M. Schierders, F. Van Dinther and J. A. J. Hannink, *Int. J. Peptide Protein Res.*, 17 (1981) 256.

CHROM. 17 983

QUANTITATION OF LONG-CHAIN ALKYL BENZENES IN ENVIRONMENTAL SAMPLES BY SILICA GEL COLUMN CHROMATOGRAPHY AND HIGH-RESOLUTION GAS CHROMATOGRAPHY

HIDESHIGE TAKADA* and RYOSHI ISHIWATARI

Department of Chemistry, Faculty of Science, Tokyo Metropolitan University, Fukazawa, Setagaya-ku, Tokyo 158 (Japan)

(First received February 12th, 1985; revised manuscript received June 17th, 1985)

SUMMARY

A high-resolution (capillary) gas chromatographic method with preceding separation by silica gel column chromatography was established for quantitation of alkylbenzenes with normal C_{10} – C_{14} and branched C_{11} – C_{13} alkyl chains in sediment and suspended matter. This method is applicable to environmental samples containing nanogram amounts of alkylbenzenes per gram of sample (dry weight). The recoveries of alkylbenzenes are 81–94% and the reproducibility is good (relative standard deviation less than 12%).

INTRODUCTION

The presence of anthropogenic hydrocarbons in recent marine and coastal sediments has been reported by many authors^{1–7}. We recently found a series of alkylbenzenes with C_{10} – C_{14} alkyl chains in coastal (Tokyo Bay) and river sediments and proposed that these alkylbenzenes are supplied into the sediments by the use of synthetic detergents (ABS) which contain trace amounts of alkylbenzenes as contamination⁸. A similar idea was presented by Eganhouse *et al.*⁹ for the alkylbenzenes in the sediments of the coastal zone of southern California. Therefore, these long-chain alkylbenzenes (hereafter described as C_{10} – C_{14} alkylbenzenes) can be used as a good tracer of pollution by synthetic detergents and/or domestic wastes in the aquatic environment.

In the case of environmental samples, it is generally difficult to separate C_{10} – C_{14} alkylbenzenes from aliphatic and aromatic hydrocarbons because the former are present in smaller amounts than the latter. In this context, only one paper¹⁰ has reported quantitative analyses of this type of alkylbenzenes in mixtures of organic compounds in environmental samples. Two different methods were employed: silver nitrate thin-layer chromatography (TLC) to isolate the alkylbenzene fraction from the total lipid extract, and direct analysis of hydrocarbon fractions by high-resolution gas chromatography–mass spectrometry (GC–MS) without separating these alkylbenzenes from other hydrocarbons. However, TLC is generally not suitable for

routine analyses and may not be appropriate for analysis of environmental samples. We considered column chromatography to be better than TLC.

The purpose of the present study was to establish conditions for isolating C₁₀–C₁₄ alkylbenzenes by the use of silica gel column chromatography, with pre-treatment, which can be applied to environmental (sediment and suspended matter) samples.

EXPERIMENTAL

Chemicals

All organic solvents used in this study were redistilled in an all-glass still. Activated copper was prepared according to the procedure of Blumer¹¹ and stored in benzene. Florisil (100–200 mesh, Wako Fine Chemicals) was washed with benzene–methanol (6:4), heated at 155–160°C for 5 h and stored in benzene. Silica gel (100–200 mesh; Mallinckrodt) was baked at 450°C, heated at 155–160°C for 5 h and stored in *n*-hexane.

The following standards were obtained commercially and used without further purification: 1-phenyloctane (1-C₈AB), 1-phenylnonane (1-C₉AB), 1-phenyldecane (1-C₁₀AB), 1-phenylundecane (1-C₁₁AB), 1-phenyldodecane (1-C₁₂AB), 1-phenyltridecane (1-C₁₃AB), 1-phenyltetradecane (1-C₁₄AB), biphenyl, acenaphthene, fluorene, pyrene, phenanthrene, benzo[*a*]fluorene, chrysene, benzo[*a*]pyrene, perylene, coronene, *n*-docosane, 1-docosene and *n*-dotriacontane.

A standard mixture of linear alkylbenzenes with known isomeric composition was supplied by Misubishi Petrochemical Company and used for the identification of alkylbenzenes from environmental samples. A standard mixture of branched alkylbenzenes was prepared by extracting alkylbenzenes with *n*-hexane from a synthetic detergent (Neopelex No. 6) containing branched alkylbenzene sulphonates (hard-type ABS), which was supplied by Kao Corporation.

Environmental samples

Three kinds of environmental samples (two river sediments, river suspended matter and bay sediment) were used. The river sediments were taken from River Tamagawa and River Arakawa with an Ekman dredge in 1983. The suspended matter was taken by filtering 200 l of river-water (River Tamagawa) through a pre-baked glass fibre filter (GF/C, pore size 0.6 µm). Rivers Tamagawa and Arakawa were representative of polluted rivers in Japan, flowing through or adjacent to the Tokyo city area into Tokyo Bay. The population of the drainage basin is approximately 3 and 0.5 million, respectively¹².

The Tokyo Bay sediment sample was collected with a dredge near the central part of the bay (location 2) in 1981 and stored at –20°C until use. The area of Tokyo Bay is approximately 1200 km² and the population of its drainage basin is 23 million¹².

Extraction and isolation procedures

Fig. 1 gives an outline of the procedures for extraction and isolation of alkylbenzene from environmental samples. A freeze-dried sediment sample (ca. 5 g) was Soxhlet-extracted in a glass-fibre thimble with 150 ml of benzene–methanol (6:4) for

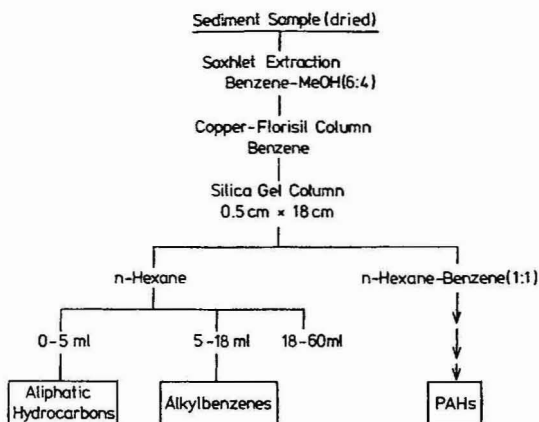


Fig. 1. Analytical procedure for alkylbenzenes.

18 h. In the case of samples of suspended matter, a freeze-dried glass-fibre filter containing the suspended matter was Soxhlet-extracted with 1.5 l of benzene-methanol (6:4) for 18 h. The organic solvent extract was concentrated to dryness in a rotary evaporator at 30°C and then taken up in 5 ml of benzene. Elemental sulphur in the extract was removed as copper sulphide by addition of 0.5 g of activated copper. The extract in benzene was then applied on a Florisil column (8 × 1.0 cm I.D.) for removal of copper sulphide and polar material (pigments). The first 30 ml of benzene eluate was taken and evaporated to dryness in a rotary evaporator at 30°C.

The eluate was taken up in 0.3 ml of *n*-hexane and then subjected to silica gel column chromatography using a 18 × 0.5 cm I.D. column. A slight pressure of nitrogen gas was employed, giving a flow-rate of *ca.* 0.2 ml/min. *n*-Hexane was used as an eluent to give three fractions: 0–5 ml, 5–18 ml and 18–60 ml. Then, 6 ml of *n*-hexane-benzene (1:1) was used to elute polycyclic aromatic hydrocarbons (PAHs). The second *n*-hexane fraction was shown to contain C₁₀–C₁₄ alkylbenzenes.

Qualification and quantitation

The second *n*-hexane fraction (alkylbenzene fraction) was evaporated just to dryness under reduced pressure at 30°C and taken up in an appropriate volume (50–100 µl) of isooctane solution containing biphenyl (13 mg/ml) as an internal standard. A small portion (2 µl) was then injected for GC on a Hewlett-Packard 5880A gas chromatograph equipped with a flame ionization detector. A 25 m × 0.3 mm I.D. fused-silica capillary column coated with SE-54 was used for the analysis under the following conditions: detector temperature, 310°C; injector temperature, 300°C; initial column temperature, 50°C, isothermal for 2 min, then programmed to 120°C at 30°C/min, to 200°C at 3°C/min and then to 300°C at 30°C/min and maintained for 20 min; helium carrier gas flow-rate, 1.5 ml/min; splitless injection.

Linear alkylbenzenes were identified by MS as well as by coinjection with the standard mixture of linear alkylbenzenes for GC. The mass spectra were recorded with a Shimadzu-LKB 9000 GC-MS system. The operating conditions were as fol-

lows: GC column, 25 m \times 0.3 mm I.D., fused silica coated with SE-54; injector temperature, 280°C; oven temperature programmed from 100 to 300°C at 6°C/min, helium carrier gas pressure at column head, 0.6 kg/cm²; MS in the electron impact (EI) mode at 70 eV with scanning from 50 to 400 a.m.u.; temperature of ionization chamber, 330°C.

Branched alkylbenzenes were identified by coinjection with the standard mixture of branched alkylbenzenes which had been identified by GC-MS.

All quantitative data were obtained by measuring GC peak areas using a Hewlett-Packard 5880A Series GC Terminal integrator. Biphenyl was used as an internal standard for the quantification of C₁₀-C₁₄ alkylbenzenes. Their concentrations were calculated by using the response factors of 1-C₁₀AB, 1-C₁₁AB, 1-C₁₂AB, 1-C₁₃AB and 1-C₁₄AB relative to biphenyl and assuming that the relative response factors of C₁₀ABs is the same that of 1-C₁₀AB, C₁₁ABs that of 1-C₁₁AB, C₁₂ABs that of 1-C₁₂AB, C₁₃ABs that of 1-C₁₃AB and C₁₄ABs that of 1-C₁₄AB, respectively. The response factors of 1-C₁₀AB, 1-C₁₁AB, 1-C₁₂AB, 1-C₁₃AB and 1-C₁₄AB relative to biphenyl were determined separately using authentic alkylbenzene standards.

RESULTS AND DISCUSSION

Isolation of alkylbenzenes by silica gel column chromatography

In general, a benzene-methanol (6:4) extract of a sediment sample contains a large amount of polar materials (mainly chlorophyll pigments). Since these polar materials interfere with the isolation of alkylbenzenes in silica gel column chromatography, a Florisil column was used to remove them. The appropriate conditions are given in the Experimental section.

The optimum conditions for silica gel chromatography of the alkylbenzenes was examined by using a mixture of standard *n*-alkanes, *n*-alkenes, alkylbenzenes and PAHs (each 10 μ g) dissolved in 0.3 μ l of *n*-hexane. This was applied on a silica gel column (18 \times 0.5 cm I.D.) and eluted with *n*-hexane at a flow-rate of 0.2 ml/min. A 1- or 2-ml volume of eluate was taken and evaporated just to dryness under a stream of nitrogen, and then immediately taken up in an appropriate volume of *n*-hexane. A small portion (2 μ l) was then subjected to GC for determination of the

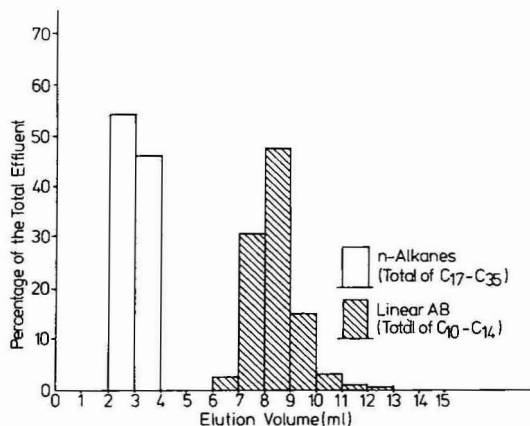


Fig. 2. Elution diagram of *n*-alkanes and alkylbenzenes extracted from River Tamagawa sediment.

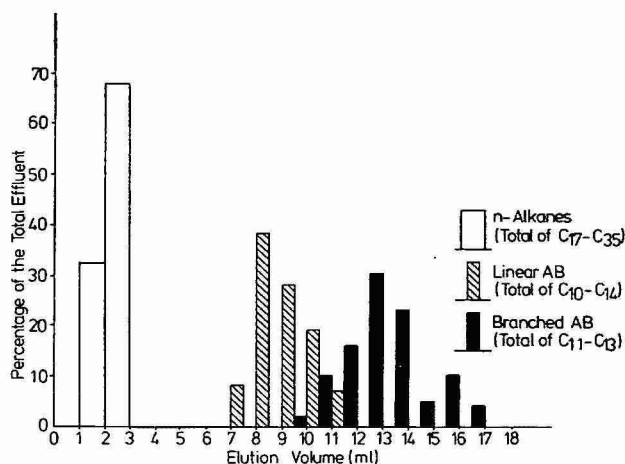


Fig. 3. Elution diagram of *n*-alkanes and alkylbenzenes extracted from Tokyo Bay sediment.

ABs. The results indicated that *n*-alkanes and *n*-alkene were eluted in the first 4 ml, alkylbenzenes between 7 and 13 ml and PAHs were eluted after 70 ml.

In order to test whether the above elution conditions were also valid for sediment extracts, a sediment extract from River Tamagawa (location: Rokugo) was applied on a silica gel column. Fig. 2 illustrates the elution curve obtained. This indicates that the elution volumes of linear alkylbenzenes in the sediment extract are almost the same as those for the standards. Similar results were obtained for an extract from Tokyo Bay sediment (Fig. 3). In this case, the elution volumes of linear ABs as well as branched ABs were determined because branched ABs were present in sufficient amounts. Consequently, aliphatic hydrocarbons were eluted in the first 4 ml of *n*-hexane, linear ABs in the second 7–11 ml and branched ABs in 10–17 ml. The elution volume of PAHs was larger than 70 ml. The alkylbenzene fraction ob-

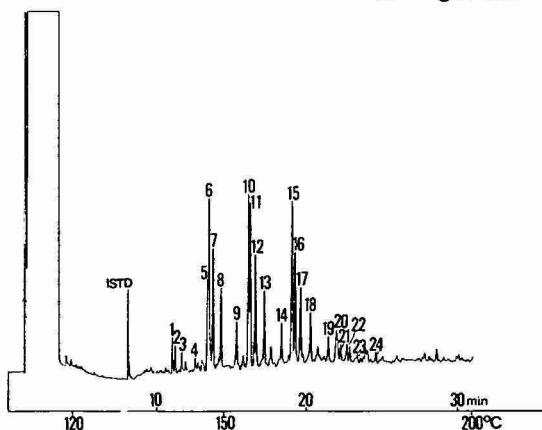


Fig. 4. Capillary gas chromatogram of alkylbenzenes extracted from River Tamagawa sediment. Numbers refer to the compounds listed in Table I. ISTD = Biphenyl as an internal standard. GC conditions: 25 m \times 0.3 mm I.D. Fused-silica capillary column coated with SE-54; 0.7 atm helium as carrier gas; flame ionization detector; splitless mode; column temperature 50°C for the initial 2 min, then programmed to 120°C at a rate of 30°C/min, to 200°C at a rate of 3°C/min and then to 300°C at a rate of 30°C/min.

tained by this procedure is pure enough for quantitation by GC, as shown in Fig. 4. Thus, it was concluded that the second 5–18 ml of *n*-hexane eluate corresponds to the alkylbenzene (linear as well as branched) fraction.

Retention indices of alkylbenzenes

Retention indices of alkylbenzenes were calculated for GC identification. 1-C₈AB, 1-C₉AB, 1-C₁₀AB, 1-C₁₁AB, 1-C₁₂AB, 1-C₁₃AB and 1-C₁₄AB were used as the internal standards for determining retention indices of alkylbenzenes, and their retention indices are defined as 80.00, 90.00, 100.00, 110.00, 120.00, 130.00 and 140.00, respectively. The retention index, *I*, is defined as

$$I = 10 \times \frac{RT(\text{substance}) - RT(1-C_n\text{AB})}{RT(1-C_{n+1}\text{AB}) - RT(1-C_n\text{AB})} + 10n$$

where RT(substance) is the retention time of the substance for which the retention index is to be determined, RT(1-C_{*n*}AB) and RT(1-C_{*n*+1}AB) are the retention times

TABLE I
LINEAR ALKYL BENZENES IDENTIFIED IN A TAMAGAWA SEDIMENT SAMPLE

Peak No.	Compound	Retention* index	Concentration	
			Average (ng/g dry sediment)	R.S.D.* (%)
1	5-C ₁₀ AB	86.70	114	9
2	4-C ₁₀ AB	87.54	123	9
3	3-C ₁₀ AB	89.37	70	8
4	2-C ₁₀ AB	92.84	67	1
5	6-C ₁₁ AB	95.92	233	} 11
6	5-C ₁₁ AB	96.20	531	
7	4-C ₁₁ AB	97.15	354	
8	3-C ₁₁ AB	99.15	244	13
9	2-C ₁₁ AB	102.71	237	15
10	6-C ₁₂ AB	105.31	642	9
11	5-C ₁₂ AB	105.76	547	10
12	4-C ₁₂ AB	106.90	440	12
13	3-C ₁₂ AB	108.95	272	10
14	2-C ₁₂ AB	112.63	205	10
15	7-/6-C ₁₃ AB	114.75	748	10
16	5-C ₁₃ AB	115.42	446	10
17	4-C ₁₃ AB	116.59	284	12
18	3-C ₁₃ AB	118.81	193	10
19	2-C ₁₃ AB	122.52	147	5
20	7-/6-C ₁₄ AB	124.20	315	8
21	5-C ₁₄ AB	125.01	86	10
22	4-C ₁₄ AB	126.37	96	14
23	3-C ₁₄ AB	128.67	53	3
24	2-C ₁₄ AB	132.46	69	5
	Total		6516	

* Average calculated from five determinations.

** Triplicate analyses; R.S.D. = relative standard deviation.

for the internal standards which bracket the substance of interest and n is alkyl carbon number of the alkylbenzene internal standard eluted prior to the substance of interest.

Table I gives retention indices for linear alkylbenzenes from River Tamagawa (location: Rokugo) sediment. These alkylbenzenes had been identified by MS and coinjection with the standard alkylbenzenes in GC, as mentioned before (see Experimental section). The reproducibility of the retention indices was within 0.07 for five replicate analyses of the sediment extracts.

TABLE II

ALKYLBENZENE CONCENTRATIONS (ng/g DRY MATERIAL) IN ENVIRONMENTAL SAMPLES

Linear alkylbenzenes		Recent sediment		Suspended solid
Peak No.	Compound	R. Arakawa (Shinkasai-bashi)	Tokyo Bay	R. Tamagawa (Chofu-seki)
1	5-C ₁₀ AB	46	25	103
2	4-C ₁₀ AB	37	6	8
3	3-C ₁₀ AB	38	4	34
4	2-C ₁₀ AB	63	19	—*
5	6-C ₁₁ AB	156	142	591
6	5-C ₁₁ AB	279	96	1126
7	4-C ₁₁ AB	187	50	841
8	3-C ₁₁ AB	168	55	423
9	2-C ₁₁ AB	276	n.d.**	310
10	6-C ₁₂ AB	353	206	2375
11	5-C ₁₂ AB	286	130	2075
12	4-C ₁₂ AB	240	86	1450
13	3-C ₁₂ AB	178	38	900
14	2-C ₁₂ AB	123	5	680
15	7-/6-C ₁₃ AB	385	306	4288
16	5-C ₁₃ AB	245	218	2488
17	4-C ₁₃ AB	157	99	1638
18	3-C ₁₃ AB	144	38	1613
19	2-C ₁₃ AB	113	22	1099
20	7-/6-C ₁₄ AB	302	224	1689
21	5-C ₁₄ AB	110	68	678
22	4-C ₁₄ AB	31	58	490
23	3-C ₁₄ AB	47	13	469
24	2-C ₁₄ AB	54	5	278
Total		4009	1913	25 650
Branched alkylbenzenes				
	C ₁₁ AB	40	55	—
	C ₁₂ AB	907	1471	—
	C ₁₃ AB	175	485	—
	Total	1122	1983	—

* Not detected.

** Not determined.

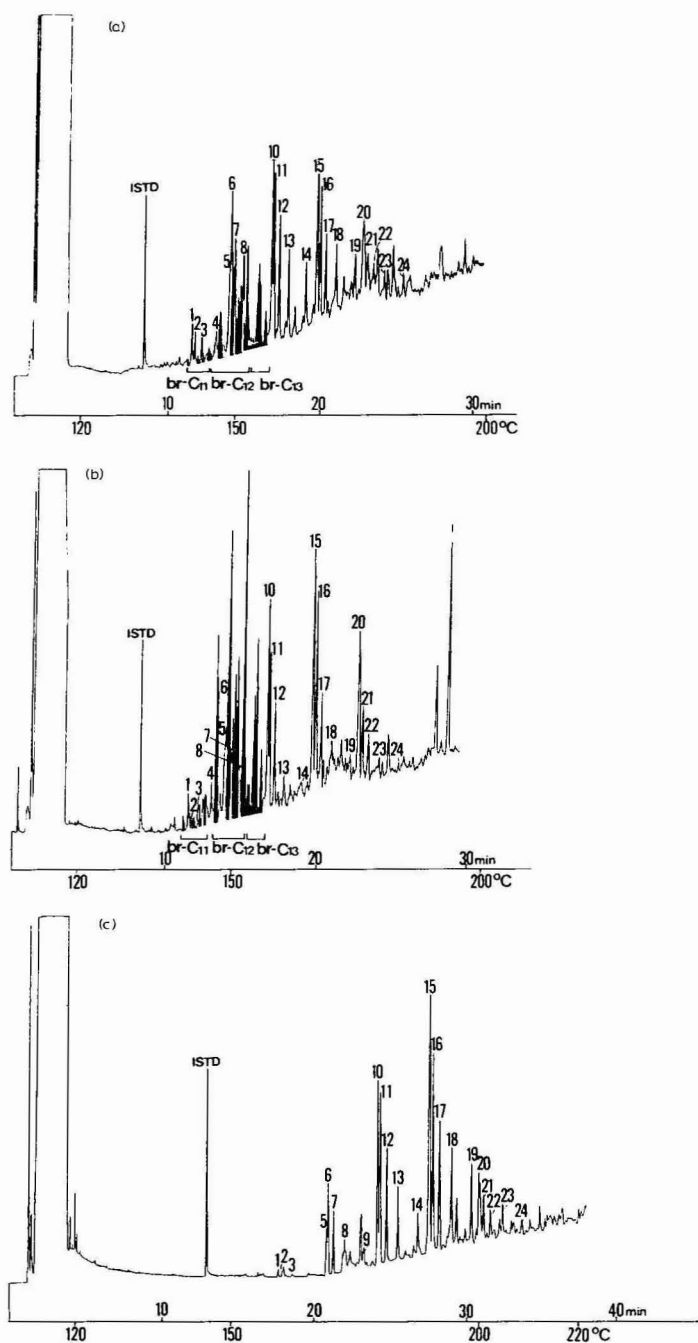


Fig. 5. Capillary gas chromatograms of alkylbenzenes extracted from River Arakawa sediment (a), Tokyo Bay sediment (b) and River Tamagawa suspended matter (c). Numbers refer to the compounds listed in Table I. Shaded peaks correspond to branched alkylbenzenes. Br-C₁₁ = Alkylbenzenes with branched C₁₁ chain; br-C₁₂ with branched C₁₂ chain and br-C₁₃ with branched C₁₃ chain. GC conditions as in Fig. 4.

Calibration curve

The linearity of the calibration curve for GC analysis was examined by using a mixture of equal concentrations (2–50 mg/l) of standard 1-C₁₀, 1-C₁₁, 1-C₁₂ and 1-C₁₃ alkylbenzenes in isooctane. A 2- μ l volume of each solution was injected. A linear relationship was obtained between the GC response and the amount of alkylbenzenes injected. The detection limit is 0.1 ng of alkylbenzenes. As described below, a common sediment sample contains 1–1000 ng of linear alkylbenzene per g dry material. Thus the calibration curve for alkylbenzenes can be used for their determination in sediment samples.

Recovery and reproducibility

The recovery of alkylbenzenes was determined by duplicate analyses of a sediment sample (River Tamagawa: Rokugo). A mixture of equal amounts (2.5 μ g in 25

TABLE III
ALKYLBENZENES IDENTIFIED IN ENVIRONMENTAL SAMPLES

Peak No.	Identification	Retention index*
b-1	Branched: C ₉ AB	79.93
b-2	Branched: C ₁₂ AB	85.38
1	Linear: 5-C ₁₀ AB	86.70
b-3	Branched: C ₁₁ AB	87.06
2	Linear: 4-C ₁₀ AB	87.54
b-4	Branched: C ₁₁ AB	87.96
b-5	Branched: C ₁₁ AB	88.36
3/b-6	Linear: 3-C ₁₀ AB/branched: C ₁₁ AB	89.37
b-7	Branched: C ₁₁ AB	89.80
b-8	Branched: C ₁₂ AB	91.30
b-9	Branched: C ₁₂ AB	91.73
4/b-10	Linear: 2-C ₁₀ AB/branched: C ₁₂ AB	92.84
b-11	Branched: C ₁₂ AB	93.79
b-12	Branched: C ₁₂ AB	94.03
b-13	Branched: C ₁₂ AB	94.74
5	Linear: 6-C ₁₁ AB	95.92
6	Linear: 5-C ₁₁ AB	96.20
b-14	Branched: C ₁₂ AB	96.54
7	Linear: 4-C ₁₁ AB	97.16
b-15	Branched: C ₁₂ AB	97.55
b-16	Branched: C ₁₂ AB	98.06
b-17	Branched: C ₁₂ AB	98.67
8	Linear: 3-C ₁₁ AB	99.16
b-18	Branched: C ₁₂ AB	100.27
b-19	Branched: C ₁₃ AB	101.20
b-20	Branched: C ₁₃ AB	101.53
b-21	Branched: C ₁₃ AB	102.46
9	Linear: 2-C ₁₁ AB	102.71
b-22	Branched: C ₁₃ AB	102.95
b-23	Branched: C ₁₃ AB	104.01
b-24	Branched: C ₁₃ AB	104.58
10	Linear: 6-C ₁₂ AB	105.31

* Average of alkylbenzenes extracted from River Arakawa and Tokyo Bay sediments. The variation is within 0.18.

μl *n*-hexane) of 1-C₁₀, 1-C₁₁, 1-C₁₂ and 1-C₁₃ alkylbenzenes was added to the organic solvent extracts from 5 g of the sediment sample and analyzed by GC after taking all steps of the analytical procedure. The recoveries were 94 ± 4 , 84 ± 5 , 89 ± 3 and $81 \pm 2\%$ for 1-C₁₀AB, 1-C₁₁AB, 1-C₁₂AB and 1-C₁₃AB, which is satisfactory for their quantitation.

The reproducibility was determined by triplicate analyses of a well homogenized sediment sample (River Tamagawa: Rokugo) containing 0.05–0.7 μg of the individual alkylbenzenes per g dry sediment. The results are shown in Table I (concentrations and relative standard deviations). The reproducibility is satisfactory.

Application to environmental samples

The analytical method described is currently being used in our laboratory for studying the behaviour of alkylbenzenes in the aquatic environment. Table II shows the analytical results for alkylbenzenes in representative river sediment, bay sediment and river suspended matter to illustrate the feasibility of the present method. As shown in Fig. 5, linear C₁₀–C₁₄ alkylbenzenes are detected in all these samples. Isomers which differ in the position of substitution of the benzene ring are well separated. The relative composition of the linear alkylbenzenes in these samples is similar, C₁₂ and C₁₃ homologues being the most abundant and C₁₀ and C₁₄ homologues being minor constituents. The total amount of linear alkylbenzenes in the sediment samples is 1.9–7.1 μg per g dry sample and quite high (26 μg per g dry sample) for the suspended matter. The concentration of linear alkylbenzenes in the sediment sample is the same as of PAHs.

In contrast to the River Tamagawa sediment sample, branched alkylbenzenes were detected in the sediment samples from River Arakawa and Tokyo Bay, in concentrations of 0.4–2.0 μg per g dry sample; C₁₁–C₁₃ alkylbenzenes are present, C₁₂ being predominant. As shown in Table III, most of the branched alkylbenzenes fall in the same range on the gas chromatograms as the linear C₁₀ and C₁₁ alkylbenzenes, but are separated from them.

ACKNOWLEDGEMENTS

This work was partly supported by the Ministry of Education, Science and Culture, Japan (Grant No. 58030062, 59030064) and The Tokyo Foundation for the Better Environment (Grant No. 5724).

REFERENCES

- 1 J. W. Farrington and B. W. Tripp, *Geochim. Cosmochim. Acta*, 41 (1977) 1627.
- 2 P. Gearing, J. N. Gearing, T. F. Lytle and J. S. Lytle, *Geochim. Cosmochim. Acta*, 40 (1976) 1005.
- 3 W. Giger, M. Reonhard, C. Schaffner and W. Stumm, *Environ. Sci. Technol.*, 8 (1974) 454.
- 4 A. C. Hurtt and J. G. Quinn, *Environ. Sci. Technol.*, 13 (1979) 829.
- 5 S. G. Wakeham and R. Carpenter, *Limnol. Oceanogr.*, 21 (1976) 711.
- 6 R. E. Laflamme and R. A. Hites, *Geochim. Cosmochim. Acta*, 42 (1978) 289.
- 7 S. J. Yun, R. Ishiwatari, M. Shioya and E. Matsumoto, *Chikyu Kagaku (Geochemistry)*, 17 (1983) 53.
- 8 R. Ishiwatari, H. Takada, S. J. Yun and E. Matsumoto, *Nature (London)*, 301 (1983) 599.
- 9 R. P. Eganhouse, D. L. Blumfeld and I. R. Kaplan, *Environ. Sci. Technol.*, 17 (1983) 523.
- 10 R. P. Eganhouse, E. C. Ruth and I. R. Kaplan, *Anal. Chem.*, 55 (1983) 2120.
- 11 M. Blumer, *Anal. Chem.*, 29 (1957) 1039.
- 12 *Data of quality of riverine and estuarine waters in Tokyo (in Japanese)*, Tokyo Metropolitan Bureau of Environmental Protection, 1981, p. 90.

CHROM. 17 936

ISOLATION AND QUANTITATIVE ANALYSIS OF PHOSPHATIDYLGLYCEROL AND GLYCOLIPID MOLECULAR SPECIES USING REVERSED-PHASE HIGH-PERFORMANCE LIQUID CHROMATOGRAPHY WITH FLAME IONIZATION DETECTION

LAURENCE A. SMITH*, HELEN A. NORMAN, SUNG HO CHO, and GUY A. THOMPSON, Jr.
Department of Botany, University of Texas, Austin, TX 78713 (U.S.A.)

(First received March 20th, 1985; revised manuscript received May 30th, 1985)

SUMMARY

Conditions are described for the quantitative analysis of phosphatidylglycerol and plant glycolipid molecular species by reversed-phase high-performance liquid chromatography employing a commercially available flame ionization detector. Direct detection on a mass basis overcomes the problem of poor detectability found with most natural lipids. Effective mobile phases composed primarily of volatile solvents are described. Splitting of the column eluate stream allows a portion of each individual molecular species to be recovered for other types of analysis.

INTRODUCTION

Although the potential of high-performance liquid chromatography (HPLC) for resolving complex mixtures of biological compounds is abundantly documented, application of HPLC towards lipids has been hindered due to the poor detectability of these compounds in column eluates. Of those HPLC analyses of underivatized lipids that have been reported, UV detection in the 200–205-nm range was typically the method of choice^{1–4}. This type of detection has severe limitations. First, UV-absorbing mobile phases may not be used. Second, even in the 200–205-nm region, only lipids containing unsaturated alkyl chains or other less common absorbing groups can be detected. As most natural lipid classes are composed of a mixture of molecular species* differing in their degree of saturation, those lipid classes which include a large proportion of highly unsaturated molecular species would show a stronger absorbance than those which do not. For this reason, quantification of natural lipid mixtures using UV detection is impractical.

The determination of molecular species of individual phospholipid classes raises special problems as the more saturated molecular species may not be detected by UV at all. To circumvent this problem, the few successful HPLC quantitative

* Molecular species within a certain lipid class are identical except for having different combinations of fatty acids bound at the *sn*-1 and *sn*-2 positions of their glycerol moiety.

analyses reported have involved conversion of lipids under study to colored derivatives for improved detectability². A different type of detection system, therefore, is clearly needed if the potential resolving power of HPLC for lipid analyses is to be fully utilized.

Fortunately, there have been several successful attempts at designing a more universal detector. One such success, described by Charlesworth, is a mass detector based on light scattering detection⁵, and several reports applying this detector to lipid separations show great promise for its future use⁶⁻⁸. An alternative type of mass detection features deposition of the column eluate on a moving wire or belt which, after evaporation of the mobile phase, is passed on for mass spectrometry or flame ionization detection (FID)⁹. The FID response has been shown to be proportional to the mass of the compounds eluted¹⁰. A slightly modified system utilizing a moving belt of woven quartz fibers has also been described¹¹. In this system, the column eluate is applied to the circular quartz belt as a fine jet stream. The elevated temperature of the belt housing removes the solvent, leaving the sample solute behind to pass through the detector flame. The belt then passes through a hotter oxygen-hydrogen flame for cleaning prior to application of additional column eluate. Recently, this FID system has become commercially available at a cost comparable with that of other HPLC detectors.

In this report, the application of the revolving belt flame ionization detector towards analyzing the molecular species composition of membrane lipids is examined. Detection limits and the amount of sample needed to conduct a typical analysis are presented, and the ability to utilize eluate splitting techniques for sample collection and/or independent analysis, the limitations imposed by the use of this detector, and its potential for use in lipid analysis are discussed.

EXPERIMENTAL

Isolation of phosphatidylglycerol and glycolipid classes

Phosphatidylglycerol (PG), digalactosyldiglyceride (DGDG), and monogalactosyldiglyceride (MGDG) were isolated from *Dunaliella salina* chloroplast lipid extracts by silicic acid column chromatography and thin-layer chromatography (TLC) procedures previously described¹². TLC was performed on silica gel H using chloroform-acetic acid-methanol-water (75:25:5:2.2, v/v/v/v) as the developing solvent. After dissipation of solvent vapors under nitrogen, the resolved components were eluted from the silica gel using chloroform-methanol-water (3:5:1, v/v/v). MGDG and DGDG extracts were adjusted to give proportions of chloroform-methanol-0.1 M potassium chloride (2:3.5:4). The lower phase was then dried under a stream of nitrogen. PG extracts were purified in the same way but replacing potassium chloride with water in the wash. Sugar analyses were conducted using the method of Dubois *et al.*¹³ and lipid phosphorus was determined using the method of Bartlett¹⁴ as modified by Marinetti¹⁵.

HPLC analysis

HPLC analyses were conducted utilizing a BAS Model PM 30-A dual piston pump, a Rheodyne Model 7125 syringe-loading sample injector with a 20- μ l loop, and a 25 cm \times 4.6 mm I.D. Rainin Microsorb (5 μ m) reversed-phase column. A

0.5- μ m pore size prefilter was placed between the injector and the column. Molecular species were detected by a Tracor 945 flame ionization LC detector (Tracor Instruments, Austin, TX, U.S.A.) at a block temperature of 160°C, and elution profiles were recorded and integrated by an HP 3390A integrator (Hewlett-Packard, Avondale, PA, U.S.A.). HPLC grade methanol, acetonitrile, water (Fisher Scientific), 1-ethylpropylamine and acetic acid (Aldrich) were utilized in mobile phases. A Milton Roy spectromonitor D variable-wavelength UV detector (Milton Roy, Riviera Beach, FL, U.S.A.) was also employed at a wavelength of 205 nm where stated for certain HPLC applications. In analyses where 60% of the column eluate was split away for collection, a pump flow-rate of 1.9 ml/min was utilized to maintain a solvent delivery of 0.76 ml/min to the revolving quartz belt. A pump flow-rate of 0.8 ml/min was used for analyses without eluate splitting.

Gas chromatographic analysis

Gas chromatographic (GC) analyses were conducted on a Varian 3700 gas chromatograph equipped with an SP 2330 capillary column (10 m \times 0.25 mm I.D.) (Sulpeco, Bellefonte, PA, U.S.A.) and a flame ionization detector. Integration of GC peaks was performed utilizing a CSI-204 integrator (Columbia Scientific, Austin, TX, U.S.A.). Molecular species resolved by HPLC were concentrated under nitrogen, and fatty acid methyl esters of these lipids were prepared directly with boron trifluoride-methanol (Sigma, St. Louis, MO, U.S.A.)¹⁶. These were analyzed isothermally at 170°C. The analysis of PG molecular species was conducted on the trimethylsilyl (TMS) derivatives of diacylglycerols prepared by phospholipase C hydrolysis according to Lynch and Thompson¹⁷.

RESULTS

HPLC with FID

A primary requirement of the revolving belt flame ionization detector is evaporative removal of mobile phase from the belt without loss of the sample solute. Although this requirement would suggest that the detector would be more suitable in normal-phase applications where organic mobile phases are employed, reversed-phase applications can be obtained for lipids if methanol, acetonitrile, and other relatively volatile solvents are the primary constituents in the mobile phase. Evaporation must be accomplished within the 8 sec time span required for the belt to transport eluate from its application point to the detecting flame, and even though the temperature of the belt during this transport can be adjusted between 80 and 210°C, we have found that no mobile phase components should have boiling points greater than 100°C. Furthermore, satisfactory baselines can be obtained only if components with boiling points close to 100°C are present in concentrations that are less than 20% of the total volume. This mobile phase volatility requirement, then, is restricting in that a number of buffers, ion pairing agents, or salts normally used in reversed-phase applications cannot be used with this detector. For example, we have found that 30 mM choline chloride and potassium phosphate buffer, both of which have been previously employed in HPLC separations of lipids^{3,18} are not suitable for use with the flame ionization detector because they give excessively high background noise.

Another problem encountered with FID is the inadequate electronic noise filtering capability for use with strip chart recorders. High and low filter settings were not sufficient to reduce sharp baseline spikes observed at low attenuation settings when mobile phases for molecular species were employed. This was overcome, however, by utilizing the HP 3390-A integrator at a peak width setting of 0.64 min, which enabled sufficient filtering for relatively flat baselines. There was no observable loss in resolution due to this high filtering or use of FID when separation profiles were compared with profiles of the same lipid mixture obtained using UV detection and no integration (Fig. 1). This comparison also illustrates the major advantage of FID over UV detection, namely the measurement of individual components on a mass basis for quantification. Thus, peaks 4 and 8, which contained approximately the same masses of glycolipids (Table I), displayed this faithfully in the FID profile (Fig. 1A) but not in the UV profile (Fig. 1B) because peak 8 contained relatively saturated lipids. We have previously employed UV detection in conjunction with a quantitative analysis of these same *Dunaliella* glycolipids, but in that study, quantification was achieved through the time consuming GC analysis of fatty acid methyl esters prepared from each eluted peak after the addition of an internal standard¹⁸

Eluate stream splitting

The development of HPLC separations is ideally accomplished through the

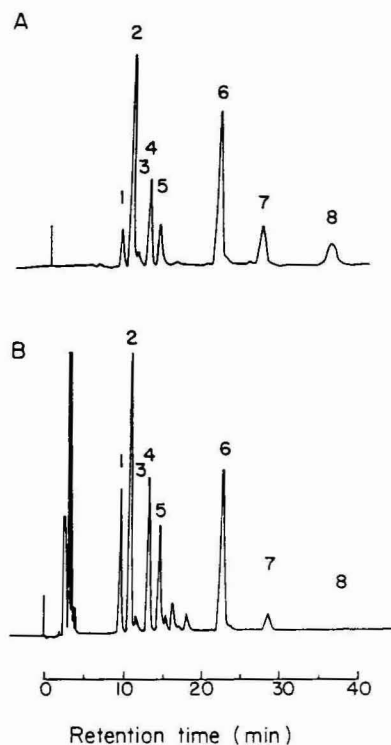


Fig. 1. Reversed-phase HPLC separation of DGDG molecular species utilizing methanol-water (96:4; v/v) as mobile phase. The molecular species resolved were detected by FID (A) and UV (205 nm) (B). Peak identification is given in Table I.

TABLE I

MOLECULAR SPECIES COMPOSITION OF DGDG FROM *DUNALIELLA SALINA*

Peak number	Peak retention time (min)	Fatty acid* composition	Percentage of total DGDG molecular species
1	8.8	18:3/16:4**	5.7 ± 0.4
2	9.8	18:3/16:3 (isomer***)	21.7 ± 0.3
3	11.0	18:3/16:3	1.1 ± 0.2
4	12.5	18:3/16:2; 18:2/16:3 (isomer)	12.9 ± 0.7
5	13.9	18:3/18:3	8.3 ± 0.5
6	21.2	18:3/16:0	28.9 ± 1.1
7	27.2	18:2/16:0	11.1 ± 0.2
8	35.5	18:1/16:0	10.3 ± 0.2

* In the shorthand numbering system used to identify fatty acids the number preceding the colon represents the number of carbon atoms and that following the colon indicates the number of double bonds present.

** The fatty acids separated by a slash represent the components in the *sn*-1 and *sn*-2 positions, respectively, of the molecular species.

*** Believed to be a different isomer from the other 16:3 shown.

§ Trace.

use of pure standards to discern elution order and resolution. The commercial availability of naturally occurring molecular species standards within any given class of lipids, however, is very limited. It will normally be necessary, therefore, to split away a portion of the column effluent prior to flame ionization in order to identify the eluted compounds and evaluate the degree of resolution. A splitting capability also allows the collection of specified portions of each peak for radioactivity analysis or other uses.

In order to accomplish stream splitting prior to FID, we found it necessary to increase the pump flow-rate from the standard to 1.0 ml/min. For example, if only 40% of the column eluate was directed to the detector, and the remaining 60% was split away for collection, then the pump flow-rate had to be increased to 1.9 ml/min in order to maintain the minimum flow-rate to the FID system of 0.7 ml/min required to provide a jet stream of mobile phase for uniform application to the revolving belt. Development of the splitting technique also required delaying the eluate diverted to the fraction collector from emerging into the collection tube until shortly after the equivalent portion directed to the FID system had been dried and passed through the detecting flame. The delay could be varied by changing the length or internal diameter of the collection tubing and measured by connecting a UV detector to its outlet. Once the proper delay was obtained, UV-absorbing glycolipids were injected to evaluate potential band spreading of that portion of eluate diverted through the collection tubing. Satisfactory delays without any detectable band spreading were indicated when a comparison of the FID and UV detector elution profiles showed no differences in peak resolution (data not shown).

HPLC-FID analysis of glycolipid molecular species

The reversed-phase separation and FID of molecular species of chloroplast DGDG from *Dunaliella salina* utilizing methanol-water (96:4; v/v) as the mobile

phase is shown in Fig. 1. The molecular species were identified by stream splitting and collection of each eluted peak followed by a fatty acid GC analysis. These results showed that almost all peaks consisted of one molecular species (Table I) and that this chloroplast lipid was a complex mixture of at least nine molecular species. Approximately 29% of DGDG consisted of the 18:3/16:0 molecular species while the next most abundant component (21.7%) was the 18:3/16:3 (isomer) molecular species. The only peak found to contain more than one molecular species in the chloroplast DGDG analysis was the fourth eluting peak, composed of a combination of the 18:3/16:2 and 18:2/16:3 (isomer) molecular species. The relative amounts (% w/w) of the major fatty acids of DGDG [16:0 (29%), 16:3 isomer (12%), 18:2 (9%) and 18:3 (39%)] as determined by GC analysis of fatty acid methyl esters¹² were in good agreement with total levels calculated from the weights of the separated molecular species [*i.e.* 16:0 (25%), 16:3 isomer (12%), 18:2 (8%) and 18:3 (40%)]. Levels of minor fatty acid components also correspond well. This confirmed the accuracy of quantitation by HPLC-FID analysis.

Analysis of MGDG molecular species could be accomplished with the same mobile phase. Peak integration during this separation showed that of the four peaks detected by FID, approximately 87% of the total sample was the 18:3/16:4 MGDG molecular species while approximately 10% consisted of a combination of 18:3/16:3 and 18:2/16:4 molecular species (data not shown).

The elution of the individual molecular species of both glycolipids followed the order reported for HPLC separations of other complex lipid molecular species^{2,19}. That is, elution time increased with both fatty acyl carbon chain length and the degree of unsaturation.

The relative amounts of each molecular species present in the two glycolipid classes, as determined by FID, was substantiated by total fatty acid analysis of MGDG and DGDG (data not shown) and previous results reported by this lab for these particular *Dunaliella* glycolipids separated by HPLC using a mobile phase containing non-volatile components¹⁸. Injection of glycolipids at various concentrations showed that reproducible quantitation of the resolved molecular species could be accomplished using a minimum of 75 nmol of chloroplast DGDG or MGDG. Based on this amount, the quantitation limit of minor species contributing only 1–2% of total glycolipid mass (Table I) was approximately 1.2–1.4 nmol. Routine analyses, however, were usually conducted on 0.3–1.4 μ mol of each glycolipid class. This working range insured that enough material could be collected by stream splitting for radioactivity counting or GC analysis, while accurate detection could be accomplished on the remaining eluate going to the FID.

HPLC-FID analysis of PG

The reversed-phase separation of *Dunaliella salina* chloroplast PG molecular species was achieved with a mobile phase consisting of 1-ethylpropylamine-acetic acid-methanol-acetonitrile (0.3:0.5:34.7:64.5, v/v/v/v) (Fig. 2). By employing stream splitting and collecting 60% of each peak prior to FID, it was possible to show by a GC analysis of the fatty acid methyl esters that the first and largest peak consisted of 18:3 and t16:1 (*trans*-4-3-hexadecenoic acid) in equimolar amounts. The second peak consisted of 18:2 and t16:1 fatty acids, while the third peak contained a mixture of 18:2 isomers paired with 16:0.

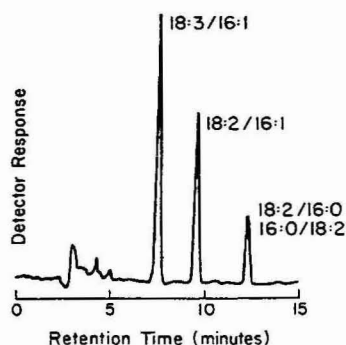


Fig. 2. Reversed-phase HPLC separation of PG molecular species utilizing 1-ethylpropylamine-acetic acid-methanol-acetonitrile (0.3:0.5:34.7:64.5, v/v/v/v) as mobile phase.

When 1-ethylpropylamine was eliminated from the mobile phase, none of the PG molecular species was eluted from the column. While the observed decrease in the column retention properties (capacity factors) after the addition of the 1-ethylpropylamine was clearly due to increased partitioning of PGs into the mobile phase relative to the C_{18} stationary phase, we could not definitely attribute this change to a specific effect such as ion-pairing and sample- C_{18} interactions. The substitution of shorter chain alkylamines, such as triethylamine, did not result in reduced elution times, while the utilization of longer chain amines (*e.g.* hexylamine, octylamine) was precluded since the high boiling point of these compounds resulted in incomplete evaporation from the revolving FID belt. Moreover, studies on separations of neutralized PG species could not be accomplished as the pK_a of the ionizable lipid phosphate group (pK_a 1–2) is too low to be within a safe pH working range for these columns. Due to these difficulties, no further investigation on this interaction was conducted.

The ability to quantitate molecular species accurately by HPLC-FID detection

TABLE II

MOLECULAR SPECIES COMPOSITION OF PG FROM *DUNALIELLA SALINA* AS DETERMINED BY GC AND BY HPLC

PG molecular species*	Percentage of total PG			
	GC	HPLC		
		Total PG injected (nmol)		
		50	31	13
18:3/16:1	62.2 ± 1.1	63.4 ± 0.5	63.3 ± 0.9	63.5 ± 1.0
18:2/16:1	28.2 ± 0.6	26.3 ± 0.2	26.8 ± 0.7	26.5 ± 0.8
18:2/16:0; 16:0/18:2**	9.6 ± 1.2	10.0 ± 0.8	9.9 ± 0.6	10.0 ± 0.6

* The fatty acids separated by a slash represent the components in the *sn*-1 and *sn*-2 positions, respectively, of the molecular species.

** The reverse isomers 18:2/16:0 and 16:0/18:2 are not separated in these conditions. The eluted HPLC peak was a combination of 18:2^{d9,12}/16:0, 16:0/18:2^{d6,9}, and 16:0/18:2^{d9,12}.

was investigated in detail using the chloroplast PGs. Relative amounts of component molecular species were determined directly by integration of peaks during HPLC-FID and independently by GC analysis of the TMS derivatives of PG-derived diacylglycerols¹⁷ using the same lipid preparation. Comparison of these results (Table II) indicates that accurate quantitation can be obtained utilizing HPLC-FID. The direct HPLC method offers a major advantage over previous GC analyses in that the lengthy preparation of volatile derivatives is avoided, hence reducing the risk of selective losses due, for example, to oxidation of polyunsaturated fatty acids or incomplete hydrolysis by phospholipase C. Quantitation could be accomplished on a minimum of 13 nmol of total chloroplast PG, indicating that the quantitation limit for one molecular species is approximately 1.3 nmol. Routine analyses, however, were conducted on 30–50 nmol of PG. As shown in Table II, relative peak areas remained essentially the same over this working range.

DISCUSSION

Results of these studies have shown that the revolving belt flame ionization detector can be utilized effectively for the detection of various lipid molecular species separated by HPLC. Quantitative information on the relative amounts of the resolved molecular species present within a lipid class can be readily obtained by direct peak integration without the necessity of first computing response factors for each species. The lower detection limits for quantitation by HPLC-FID were found to be approximately 1.2–1.4 nmol DGDG, enough sample must be injected so that the smallest molecular species-contained peak to be quantitated is present in at least this amount. It was also determined that peak ratios remain the same over a wide range of concentrations (at least one order of magnitude) of glycolipid injected, illustrating that FID can be used effectively within this range.

PG, MGDG, and DGDG are major plant lipids of higher and lower plant chloroplasts²⁰, and the elucidation of their metabolism, as well as those of additional complex lipid classes, is a primary interest in this laboratory. Preliminary studies have already indicated that a simple modification of the mobile phase employed for the separation of a PG molecular species will permit the separation of phosphatidylcholine and phosphatidylethanolamine molecular species. It should be possible to develop completely volatile mobile phases effective for HPLC-FID separation of most biologically important lipids.

ACKNOWLEDGEMENTS

This work was supported in part by Grant PCM-800289 from the National Science Foundation and Grant F-350 from the Robert A. Welch Foundation. L.A.S. is a Postdoctoral Trainee on a National Cancer Institute Training Program (1 T32 CA09182). H.A.N. is a Robert A. Welch Postdoctoral Fellow.

REFERENCES

- 1 Y. Nakagawa and L. A. Horrocks, *J. Lipid Res.*, 24 (1983) 1268–1275.
- 2 M. Batley, N. H. Packer and J. W. Redmond, *Biochim. Biophys. Acta*, 710 (1982) 400–405.
- 3 G. M. Patton, J. M. Fasulo and S. J. Robins, *J. Lipid Res.*, 23 (1982) 190–196.

- 4 F. B. Jungalwala, J. E. Evans and R. H. McCluer, *Biochem. J.*, 155 (1976) 55–60.
- 5 J. M. Charlesworth, *Anal. Chem.*, 50 (1978) 1414–1420.
- 6 A. Stolyhwo, H. Colin, M. Martin and G. Guiochon, *J. Chromatogr.*, 288 (1984) 253–275.
- 7 A. Stolyhwo, H. Colin and G. Guiochon, *J. Chromatogr.*, 265 (1983) 1–18.
- 8 R. Macrae, L. C. Trugo and J. Dick, *Chromatographia*, 15 (1982) 476–478.
- 9 O. S. Privett and W. L. Erdahl, *Methods Enzymol.*, 72 (1981) 56–108.
- 10 F. C. Phillips, W. L. Erdahl, J. A. Schmit and O. S. Privett, *Lipids*, 19 (1984) 880–887.
- 11 J. J. Szakasits and R. E. Robinson, *Anal. Chem.*, 46 (12) (1974) 1648–1653.
- 12 D. V. Lynch and G. A. Thompson, Jr., *Plant Physiol.*, 69 (1982) 1369–1375.
- 13 M. Dubois, K. A. Gilles, J. K. Hamilton, P. A. Rebers and F. Smith, *Anal. Chem.*, 28 (1956) 50–56.
- 14 G. R. Bartlett, *J. Biol. Chem.*, 234 (1959) 446–468.
- 15 J. Marinetti, *J. Lipid Res.*, 3 (1962) 1–20.
- 16 W. R. Morrison and L. M. Smith, *J. Lipid Res.*, 5 (1964) 600–608.
- 17 D. V. Lynch and G. A. Thompson, Jr., *Plant Physiol.*, 74 (1984) 193–197.
- 18 D. V. Lynch, R. E. Gundersen and G. A. Thompson, Jr., *Plant Physiol.*, 72 (1983) 903–905.
- 19 F. B. Jungalwala, V. Hayssen, J. M. Pasquini and R. H. McCluer, *J. Lipid Res.*, 20 (1979) 579–587.
- 20 J. L. Harwood, in P. K. Stumpf (Editor), *The Biochemistry of Plants, Vol. 4, Lipids: Structure and Function*, Academic Press, New York, 1980, pp. 1–55.

CHROM. 17 947

SIMULTANEOUS DETERMINATION OF FREE AND CONJUGATED ECDYSTEROIDS BY LIQUID CHROMATOGRAPHY

S. SCALIA*

Institute of Pharmaceutical Chemistry, University of Ferrara, Via Scandiana 21, 44100 Ferrara (Italy)
and

E. D. MORGAN

Department of Chemistry, University of Keele, Keele, Staffordshire ST5 5BG (U.K.)

(Received June 5th, 1985)

SUMMARY

A high-performance liquid chromatographic procedure has been developed for the simultaneous assay of the major free ecdysteroids (insect moulting hormones) and the corresponding ecdysteroid 22-phosphates found in *Schistocerca gregaria* eggs. No preliminary fractionation into the free and conjugated hormones was required. An Ultrasphere ODS column with ultraviolet detection and a methanol-phosphate buffer gradient elution were used. The retention time of the conjugates was dependent on the sodium phosphate concentration in the mobile phase. The unconjugated and conjugated ecdysteroids were determined directly after aqueous methanol extraction and Sep-Pak C₁₈ cartridge purification.

INTRODUCTION

The occurrence of ecdysteroids (insect moulting hormones) in the eggs of a number of insect species has been demonstrated by several authors^{1–5}. In most cases it has been shown that the hormones were synthesized in the adult ovaries and then transferred to the eggs^{2,6–8}.

The major ecdysteroids identified in newly laid eggs of the desert locust (*Schistocerca gregaria*) are ecdysone, 2-deoxyecdysone and 20-hydroxyecdysone^{4,5,9}, all present in the free form, but also and chiefly (90% of the total) as polar conjugates hydrolysable with a crude enzyme preparation from the snail *Helix pomatia*. The conjugated ecdysteroids have been chemically identified^{10,11} as ecdysteroid 22-phosphate esters by fast atom bombardment mass spectrometry and ¹H, ¹³C and ³¹P NMR spectroscopy.

Towards the end of *S. gregaria* embryogenesis a variety of ecdysteroid conjugates and metabolites have been identified¹² in addition to the maternal free and conjugated hormones. This group is not included in the present study.

During egg development in *S. gregaria* a fluctuation of the titre of both the free and conjugated ecdysteroids has been reported^{4,5,7,13}, and the variation of hor-

none levels correlated with distinct stages of embryogenesis^{5,13}. Hence the assay of ecdysteroids in the maturing eggs is important for understanding the physiology of the insect embryo development.

Previously the chromatographic resolution of free and conjugated ecdysteroids from insect material has required a preliminary separation of the two classes of steroids, by solvent partition^{4,5,14}, thin-layer chromatography (TLC)^{2,3,15}, Sep-Pak C₁₈ cartridge¹⁶, C₁₈ bonded phase² or silicic acid⁹ columns. The conjugates were then hydrolysed with *Helix pomatia* enzymes to release the ecdysteroid moieties which were determined by high-performance liquid chromatography (HPLC) with UV detection^{5,9,16} or by electron-capture gas chromatography after derivatization^{4,17}.

From our work¹⁸ and that of others^{11,12} it has been shown that the conjugated ecdysteroids can be directly resolved by HPLC without prior enzymatic hydrolysis, after removal of the free hormones.

However, none of these methods can resolve the free and conjugated ecdysteroids by a single HPLC injection.

A method is described here for the simultaneous separation of ecdysone, 2-deoxyecdysone, 20-hydroxyecdysone and of the corresponding 22-phosphate esters by reversed-phase HPLC (RP-HPLC). The application of this new chromatographic system to the quantitation of the unconjugated and conjugated hormones in the maturing eggs of the desert locust is also reported.

EXPERIMENTAL

Materials

Eggs were obtained from a colony of *S. gregaria* Forskal reared as described previously⁵. Under the conditions chosen for the incubation of the eggs, they hatched at day 15.

HPLC grade methanol and water were purchased from Farmitalia Carlo Erba (Milano, Italy). All other chemicals were of analytical grade (Farmitalia). *Helix pomatia* aryl-sulphatase preparation was obtained from Sigma (St. Louis, MO, U.S.A.).

Ecdysone and 20-hydroxyecdysone were gifts from Dr. C. Casagrande (Simes, Milano, Italy), 2-deoxyecdysone from Dr. D. H. S. Horn (C.S.I.R.O., Melbourne, Australia). Conjugated ecdysone, 20-hydroxyecdysone and 2-deoxyecdysone were isolated from newly laid eggs of *S. gregaria* as described previously¹⁸.

Methods

Sample processing. Each batch of eggs (2 g) was homogenized in methanol-water (8:2) with a blender. The first three supernatants after centrifugation (1000 g for 10 min, at 20°C) were combined and evaporated *in vacuo* at 40°C. The residue obtained was suspended in 7 ml of methanol-water (80:20) and injected into a Sep-Pak C₁₈ cartridge (Waters Assoc., Milford, MA, U.S.A.) to remove non-polar contaminants. The eluate from the Sep-Pak was reduced to dryness, redissolved in a known volume of the initial mobile phase (500 µl) and a portion of this solution (5 µl) was injected into the HPLC column.

Chromatography. The HPLC analyses were performed with a Jasco apparatus (Model BIP-I pump, Model GP-A40 solvent programmer and Model UVDEC-100-V variable-wavelength detector; Jasco, Tokyo, Japan) linked to a sample-injec-

tion valve (Rheodyne, Cotati, U.S.A.) and a chromatographic data processor (Chromatopac C-R3A; Shimadzu, Kyoto, Japan). The detector was set to 244 nm.

Free and conjugated ecdysteroids were separated on a 150 × 4.6 mm I.D. stainless-steel column pre-packed with 5- μ m particles of Ultrasphere ODS (Alltech, Eke, Belgium) and eluted with a linear gradient, in two steps, of methanol–aqueous buffer at a flow-rate of 0.9 ml/min. Solvent A was 5 mM sodium phosphate buffer (pH 6.8) and solvent B was methanol. The gradient programme used was according to the following scheme:

15% $\xrightarrow{\text{linear (8 min)}}$ 40% $\xrightarrow{\text{isocratic (9 min)}}$ 40% $\xrightarrow{\text{linear (6 min)}}$ 60% B

The elution programme was begun 0.5 min before sample injection. The eluents were filtered and degassed with helium before use. The chromatograph was operated at room temperature.

The ecdysteroid peaks were quantified using the integrator which was calibrated with standard solutions of pure ecdysone, 2-deoxyecdysone and 20-hydroxyecdysone.

The analysis of the free ecdysteroids was carried out on two different types of HPLC systems: (a) a reversed-phase column (Servachrom RP-18; 250 × 4.5 mm I.D., particle size 5 μ m; Serva Feinbiochemica, Heidelberg, F.R.G.) run under isocratic conditions (methanol–water, 60:40) at a flow-rate of 0.8 ml/min, and (b) an adsorption column (LiChrosorb Si 60, 250 × 4.5 mm I.D., particle size 5 μ m; Merck, Darmstadt, F.R.G.) eluted with methylene chloride–methanol–water (150:25:2) at a flow-rate of 1.2 ml/min.

Trimethylsilyl ether derivatives of the free ecdysteroids were obtained as described elsewhere⁴ and chromatographed with a Fractovap 4200 gas chromatograph (Carlo Erba) fitted with a flame ionization detector. The glass column, 1.8 m × 2 mm I.D., was packed with 1.5% OV-101 on Supelcoport (Supelco, Bellefonte, PA, U.S.A.). The operating conditions were: column temperature, 285°C; injector port temperature, 295°C; detector temperature, 300°C; carrier gas (nitrogen) flow-rate, 30 ml/min.

Identification of ecdysteroids. The free ecdysteroids were identified by co-chromatography with authentic compounds on two different chromatographic systems (reversed-phase and adsorption columns) and by comparison of the gas chromatographic retention times of their trimethylsilyl ether derivatives with those of silylated standard compounds.

The conjugated ecdysteroid fractions were desalted on Sep-Pak C₁₈¹⁰, hydrolysed with *H. pomatia* enzymes and the released ecdysteroids purified as described previously¹⁸. The identity of the individual hormones obtained in this way was determined as described above.

RESULTS

RP-HPLC

A chromatogram of a typical separation of 20-hydroxyecdysone, ecdysone, 2-deoxyecdysone and the corresponding 22-phosphate ester conjugates using the sys-

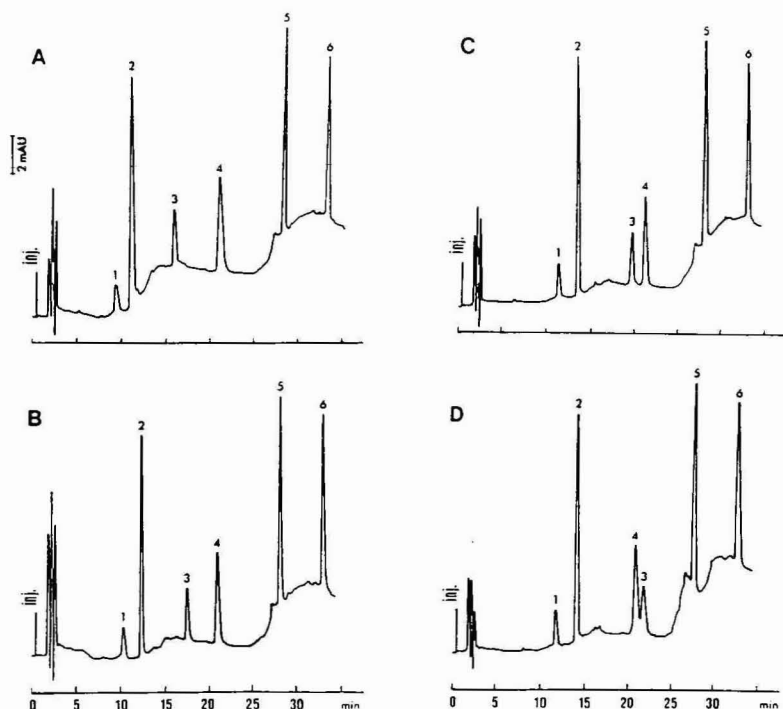


Fig. 1. Elution profiles of ecdysteroids and their phosphate conjugates on an Ultrasphere ODS column (150×4.6 mm I.D.). The separations were performed at a flow-rate of 0.9 ml/min with a linear gradient of methanol in 5 mM (A), 12.5 mM (B), 25 mM (C) and 50 mM (D) sodium phosphate buffer (pH 6.8). Solvent programme: 0 min, 15% methanol; 8 min, 40% methanol; 17 min, 40% methanol; and 23 min, 60% methanol. Detection: UV absorbance at 244 nm. Peaks: 1 = 20-hydroxyecdysone phosphate; 2 = ecdysone phosphate; 3 = 2-deoxyecdysone phosphate; 4 = 20-hydroxyecdysone; 5 = ecdysone; 6 = 2-deoxyecdysone.

tem described here is shown in Fig. 1A. Each of the three conjugates was resolved one from the other and from each of the corresponding unconjugated ecdysteroids on an Ultrasphere ODS column using a linear gradient in two steps of methanol in sodium phosphate buffer. When sodium phosphate was replaced by water in the mobile phase, the conjugates were eluted with the unretained solvent peak, whereas the free ecdysteroids showed the same retention times with either water or sodium phosphate (not shown).

The influence of the buffer concentration on the chromatography of the free ecdysteroids and of the conjugated pairs has been examined. The range of sodium phosphate concentrations studied was 5–50 mM. With increasing salt concentration in the mobile phase the retention volume for each conjugate increased while the retention of the unconjugated ecdysteroids was unaffected over the entire range of mobile phase salt concentrations (Fig. 1A–D). This is further illustrated in Table I where, for each sodium phosphate concentration, the retention volumes measured from the chromatograms in Fig. 1 are listed. The reversal in elution order for conjugated 2-deoxyecdysone and free 20-hydroxyecdysone occurring at a salt concentration of 50 mM reflects the increase in retention of the conjugated ecdysteroids.

TABLE I

EFFECT OF MOBILE PHASE SALT CONCENTRATION ON RP-HPLC OF FREE AND CONJUGATED ECDYSTEROIDS

Chromatographic conditions as in Fig. 1.

Sodium phosphate concentration (mM)	Retention volume (ml)					
	Ecdysteroid*					
	1	2	3	4	5	6
5 (Fig. 1A)	8.2	9.6	13.8	18.6	25.1	29.2
12.5 (Fig. 1B)	9.2	11.0	15.5	18.6	25.0	29.3
25 (Fig. 1C)	9.9	11.9	17.4	18.8	25.1	29.2
50 (Fig. 1D)	10.5	12.4	19.4	18.5	24.6	29.2

* Compounds 1-6 refer to the numbered peaks in Fig. 1.

The resolution of conjugated 2-deoxyecdysone and free 20-hydroxyecdysone decreased with increasing buffer concentration and the two hormones were not baseline separated at 50 mM sodium phosphate.

Application

We have used the 5 mM sodium phosphate-methanol gradient RP-HPLC system for the assay of the major free and conjugated hormones in eggs of *S. gregaria* at different stages of development, *i.e.*, 1-, 3- and 10-day old eggs. Each batch of egg pods was extracted as described in the Experimental section. The resulting solution, after passage through a Sep-Pak, was suitable for HPLC analysis without further purification. The conjugated and unconjugated hormones present were separated by RP-HPLC in a single pass and quantified by recording the UV absorbance of the column effluent. Representative chromatograms of extracts from 1- and 3-day old eggs are shown in Figs. 2 and 3, respectively.

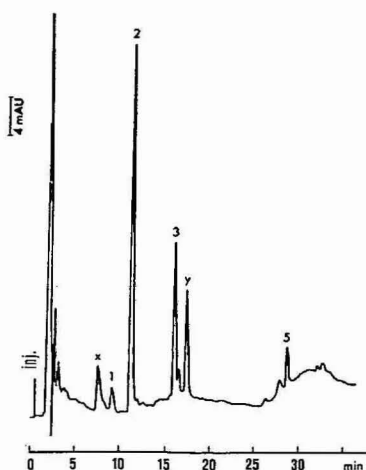


Fig. 2. Typical RP-HPLC separation of ecdysteroids from 1-day old eggs (2 g). Conditions as in Fig. 1A; peaks as in Fig. 1. X, Y = Unknown compounds, not ecdysteroids.

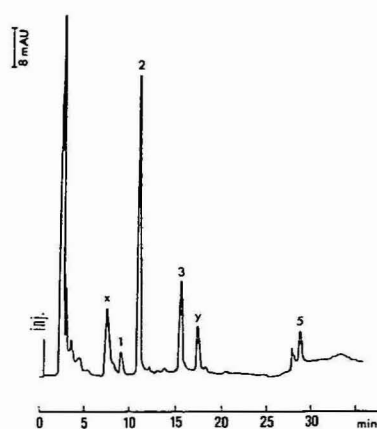


Fig. 3. Typical RP-HPLC separation of ecdysteroids from 3-day old eggs (3 g). Conditions as in Fig. 1A; peaks as in Figs. 1 and 2.

TABLE II

COMPARISON OF AMOUNTS OF ECDYSTEROIDS FOUND IN 1-DAY OLD *S. GREGARIA* EGGS BY THE PRESENT RP-HPLC METHOD AND BY THE PREVIOUS PROCEDURE⁵

Results are the average of two determinations.

Compound	Amount (ng per egg)	
	RP-HPLC	Previous procedure
Conjugated ecdysone	419	402
Conjugated 2-deoxyecdysone	168	155
Conjugated 20-hydroxyecdysone	32	36
Free ecdysone	31	29

The present method for the rapid and simultaneous determination of the levels of free and conjugated ecdysteroids in the eggs of *S. gregaria* was validated by comparison with the previously adopted procedure⁵ on the same sample of eggs. The two methods produced consistent results (see Table II), proving the validity of the RP-HPLC titre determination of the hormones.

In accordance with earlier reports^{5,13}, the amount of unconjugated 20-hydroxyecdysone and 2-deoxyecdysone was below the sensitivity of the method for the sample size available. The detection limit was 10 ng of ecdysteroid.

The identity of the compounds separated by gradient elution RP-HPLC was assigned by co-chromatography with authentic material and confirmed by collecting the different UV-absorbing peaks from the column. After hydrolysis of the conjugates, they were analysed isocratically on a reversed-phase column, on an adsorption column and after silylation by gas chromatography on an OV-101 column.

The simultaneous separation of ecdysteroids and of their conjugated forms was also accomplished for samples of 10-day old eggs (Fig. 4). Good agreement was again found between the results obtained by the method described here and by the

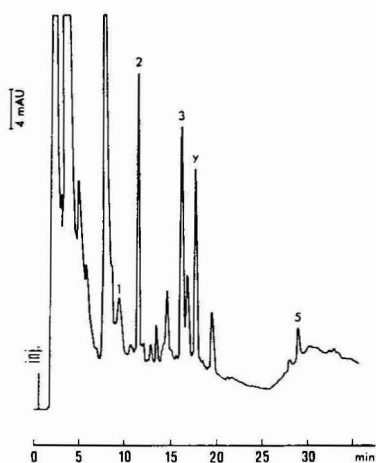


Fig. 4. Typical RP-HPLC separation of ecdysteroids from 10-day old eggs (2 g). Conditions as in Fig. 1A; peaks as in Figs. 1 and 2.

previously reported procedure⁵. The appearance of UV-absorbing substances in the elution profile of 10-day old eggs, in addition to those present in the chromatograms for 1- and 3-day old eggs, is consistent with the more complex pattern of ecdysteroid conjugates and metabolites^{1,2} found in late-stage embryos. The necessary reference compounds were not available for further identifications.

DISCUSSION

Until now the assay of unconjugated and conjugated ecdysteroids in biological material required separation of the two forms of the hormones by TLC^{2,3}, column chromatography^{2,9} or solvent partition^{4,5}. These methods are time-consuming in routine analysis and require several manipulations which represent a source of possible errors.

An HPLC method has been designed for the simultaneous determination of the free ecdysteroids and of the corresponding conjugates in *S. gregaria* eggs, which does not require prior group separation. The major ecdysteroids and their conjugated forms present in the eggs have been resolved in a single analysis by gradient elution RP-HPLC with the addition of sodium phosphate to the aqueous portion of the mobile phase. The absence of salt did not affect the chromatography of the free ecdysteroids, whereas poor retention was observed for the conjugates. The increase in retention of the conjugated ecdysteroids when sodium phosphate was present in the mobile phase can probably be traced to a neutralization of the ecdysteroid phosphate charge which increases the interaction of the hydrophobic portion of the steroid conjugates with the bonded phase.

The advantages offered by this new RP-HPLC procedure are the minimum sample preparation, circumventing preliminary separation and hydrolysis of the conjugates.

A number of UV-absorbing substances, which are not ecdysteroids, are present in the elution profile. Nevertheless the well separated peaks permit unequivocal identification, accurate and rapid quantification of the hormones, suitable for routine analysis.

ACKNOWLEDGEMENTS

We thank Drs. C. Casagrande and D. H. S. Horn for gifts of ecdysteroids, Drs. A. Sbrenna and G. Sbrenna (Institute of Zoology, Ferrara University, Italy) for providing *S. gregaria* eggs and Mrs. K. Geiger for assistance in preparing the manuscript.

REFERENCES

- 1 E. Ohnishi, T. Ohtaki and S. Fukuda, *Proc. Jpn. Acad.*, 47 (1971) 413.
- 2 T. H. Hsiao and C. Hsiao, *J. Insect Physiol.*, 25 (1979) 45.
- 3 M. Lagueux, C. Hetru, F. Goltzene, C. Kappler and J. A. Hoffmann, *J. Insect Physiol.*, 25 (1979) 709.
- 4 A. R. Gande and E. D. Morgan, *J. Insect Physiol.*, 25 (1979) 289.
- 5 S. Scalia and E. D. Morgan, *J. Insect Physiol.*, 28 (1982) 647.
- 6 A. R. Gande, E. D. Morgan and I. D. Wilson, *J. Insect Physiol.*, 25 (1979) 669.
- 7 L. N. Dinan and H. H. Rees, *Insect Biochem.*, 11 (1981) 255.

- 8 M. Lagueux, M. Hirn and J. A. Hoffmann, *J. Insect Physiol.*, 23 (1977) 109.
- 9 L. N. Dinan and H. H. Rees, *J. Insect Physiol.*, 27 (1981) 51.
- 10 R. E. Isaac, M. E. Rose, H. H. Rees and T. W. Goodwin, *J. Chem. Soc. Chem. Commun.*, (1982) 249.
- 11 R. E. Isaac, M. E. Rose, H. H. Rees and T. W. Goodwin, *Biochem. J.*, 213 (1983) 533.
- 12 R. E. Isaac and H. H. Rees, *Biochem. J.*, 221 (1984) 459.
- 13 S. Scalia, N. Gorini, A. Sbrenna-Micciarelli, G. Sbrenna and E. D. Morgan, *Acta Embryol. Morphol. Exper.*, 5 (1984) 131.
- 14 T. Mizuno and E. Ohnishi, *Devel. Growth Differ.*, 17 (1975) 219.
- 15 J. A. Hoffmann, J. Koolman, P. Karlson and P. Joly, *Gen. Comp. Endocrinol.*, 22 (1974) 90.
- 16 R. Lafont, J. L. Pennetier, M. Andrianjafintrimo, J. Claret, J. F. Modde and C. Blais, *J. Chromatogr.*, 236 (1982) 137.
- 17 E. D. Morgan and I. D. Wilson, in J. A. Hoffmann (Editor), *Progress in Ecdysone Research*, Elsevier, Amsterdam, 1980, p. 29.
- 18 S. Scalia and E. D. Morgan, *J. Chromatogr.*, 238 (1982) 457.

CHROM. 17 967

ISOLATION OF ERYTHROMYCINS AND RELATED SUBSTANCES FROM FERMENTATION RESIDUES OF *STREPTOMYCES ERYTHREUS* BY HIGH-PERFORMANCE LIQUID CHROMATOGRAPHY ON SILICA GEL

I. O. KIBWAGE*, G. JANSSEN, E. ROETS, J. HOOGMARTENS and H. VANDERHAEGHE

Katholieke Universiteit Leuven, Instituut voor Farmaceutische Wetenschappen, Laboratorium voor Farmaceutische Chemie, Van Evenstraat 4, B-3000 Leuven (Belgium)

(Received June 13th, 1985)

SUMMARY

Preparative high-performance liquid chromatography on silica gel allows the isolation of erythromycins and related substances from mother-liquor concentrates. Three mobile phases were used consecutively: A, ethyl acetate–methanol–25% ammonia (100:8:1, v/v); B, diethyl ether–methanol–25% ammonia (100:7:1, v/v) and C, dichloromethane–methanol–25% ammonia (100:5:0.5, v/v). The separation and purification was confirmed by thin-layer chromatography. Thirteen pure substances were isolated among which are erythromycins A, B, C and D, 8,9-anhydroerythromycin A-6,9-hemiketal, erythromycins A and C-6,9;6,12-spiroketal and N-demethylerythromycin A-6,9;9,12-spiroketal.

INTRODUCTION

It has been shown by high-performance liquid chromatography (HPLC)¹ and also by thin-layer chromatography (TLC)^{2,3} that commercially available erythromycin contains erythromycins B and C (EB, EC) besides the main component erythromycin A (EA). We wished to isolate these related substances in order to determine their response in the microbiological assay for this antibiotic. For this study we decided to isolate them from the mother-liquor concentrate from an industrial process.

Numerous methods have been employed to isolate erythromycin and related substances from the fermentation liquors of *Streptomyces erythreus*. The major metabolite, EA, is isolated by extraction and crystallization^{4,5}. From the filtrate, EB⁶ and EC⁵ have been obtained by use of countercurrent distribution. EA and EB have been separated on a column packed with cellulose⁶. Oleinick and Corcoran⁷ used consecutive columns of Amberlite IRC-50 resin and silica gel to separate labelled EA from mycelium-free fermentation beer. ED was isolated by chromatography on a column packed with Sephadex LH-20⁸. Columns packed with similar materials have been used to separate human EA metabolites^{9,10} and to fractionate erythromycin E from a chloroform extract of a *S. erythreus* mutant¹¹. Recently, preparative HPLC

has been used to isolate erythromycin F from a mother-liquor concentrate¹². Several other erythromycin-related glycosides and biosynthetic intermediates have been isolated from fermentation broths of blocked mutants¹³⁻¹⁸ of *S. erythreus*.

In this paper we report on the separation and purification of EA, EB, EC and ED from mother-liquor concentrates, using preparative HPLC on silica gel. A number of other substances were also isolated. Some were identified, the structures of others are still under investigation.

EXPERIMENTAL

Preparative HPLC

Instrumentation. The laboratory-assembled chromatograph was the same as that described for analytical work by Wouters *et al.*¹⁹. It has now been equipped with two Milton Roy Minipumps (Laboratory Data Control, Riviera Beach, FL, U.S.A.), a 10-ml loop and a Waters differential refractometer R403 (Waters Assoc., Milford, MA, U.S.A.). The detector attenuation was set at either X64 or X32 depending on the sample concentration.

Column and packing material. The column, 25 cm × 22.7 mm I.D. (Chrom-pack, Middelburg, The Netherlands), was packed in the laboratory with silica gel 60H, 15 µm, for TLC (E. Merck, Darmstadt, F.R.G.). Fine particles were removed by flotation in water as follows. Water (500 ml) was added to silica gel (75 g) in a 600-ml beaker (diameter 7.5 cm). The suspension was mechanically stirred for 5 min to obtain an homogeneous suspension. After standing for 2 h the supernatant was decanted. The procedure was repeated twice. The silica gel residue was filtered on a sintered glass filter (D4) and dried in an oven, first at 80°C for 1 day then at 120°C for 1 day. The dried silica was cooled in a desiccator, over phosphorus pentoxide, under vacuum.

Packing procedure. Silica (65 g) was slurried in 250 ml of carbon tetrachloride. The slurry was sonicated for 4 min and quickly introduced into the slurry reservoir, a 50 × 2.0 cm I.D. stainless-steel tube, fixed to the column. The reservoir was filled with carbon tetrachloride and the slurry was immediately packed into the column using a Haskel Pump Model DSTV-122 at a pressure of about 250 kg/cm² and with hexane as the pressurizing liquid. The reagent grade solvents were distilled from glass apparatus.

The column was tested by chromatography of a mixture of *o*-, *m*- and *p*-nitroanilines with dichloromethane, distilled over phosphorus pentoxide, as the mobile phase. The flow-rate was set at 15 ml/min. A column efficiency of 12 000 plates per metre was obtained, and a selectivity of 1.3 and a resolution of 2.33 was calculated for the last two peaks (*m*- and *p*-nitroanilines).

Solvents, mobile phases and operating conditions. Ethyl acetate (>99.5%), methanol (>99%), dichloromethane (>99%) (Janssen Chimica, Beerse, Belgium), and diethyl ether (Belgolabo, Overijse, Belgium) were distilled from glass apparatus. Dichloromethane was distilled over phosphorus pentoxide. Ammonia (25% pro analysi, E. Merck) was used. Three mobile phases were used: A, ethyl acetate-methanol-25% ammonia (100:8:1, v/v); B, diethyl ether-methanol-25% ammonia (100:7:1, v/v) and C, dichloromethane-methanol-25% ammonia (100:5:0.5, v/v). They were degassed for 10-15 min in an ultrasonic bath. When purifying smaller

fractions, the composition of the mobile phase, with respect to methanol and ammonia, was sometimes slightly modified to obtain better separation of close eluting impurities.

Samples were dissolved in the mobile phase to a concentration of not more than 500 mg per 10 ml and filtered through paper before injection. The flow-rate was set at 15 ml/min and the chart speed at 5 mm/min. The chromatograph was operated at room temperature.

Sample. Mother-liquor concentrates from the industrial production of erythromycin, obtained after crystallization of the majority of erythromycin, were donated by Roussel-Uclaf (Paris, France) and are herein referred to as MLC. Part (11 g) of the anhydroerythromycin A (erythromycin A-6,9;9,12-spiroketal) present was removed by twice crystallizing a 50-g sample of MLC from dichloromethane-hexane.

Thin-layer chromatography (TLC)

Pre-coated TLC plates, Stratochrom SIF₂₅₄ (Carlo Erba, Milan, Italy), and Silica gel 60F₂₅₄ (E. Merck) were used throughout. Three mobile phases were used: A, ethyl acetate-methanol-25% ammonia (85:10:5, v/v); B, diethyl ether-methanol-25% ammonia (90:9:2, v/v) and C, dichloromethane-methanol-25% ammonia (90:9:1.5, v/v). Samples in dichloromethane solutions were spotted in 10- μ g quantities for qualitative analysis and comparative evaluation, while 100- μ g quantities were used for purity tests. The spots were visualized by spraying with conc. sulphuric acid-2-methoxybenzaldehyde-ethanol (1:1:9, v/v) and heating at 110°C for 1 min. Details of these TLC methods have been described³.

Analytical HPLC

Instrumentation. The chromatographic system consisted of a Waters Model M-45 solvent-delivery system, a Pye Unicam LC 3 UV variable wavelength detector (Pye Unicam, Cambridge, U.K.) set at 215 nm and a Kipp and Zonen BD40 recorder (Kipp and Zonen, Delft, The Netherlands). The column was maintained at 40°C by means of a glass water-jacket connected to a water-circulating bath²⁰. The column, 25 cm \times 4.6 mm I.D. was packed in the laboratory with RoSiL C₁₈, 5 μ m (RSL-Alltech Europe, Eke, Belgium), following the packing procedure previously described²¹.

Solvent, mobile phase and operating conditions. Acetonitrile and methanol HPLC grade S were purchased from Rathburn Chemicals (Walkerburn, Scotland, U.K.). Analytical grade ammonium dihydrogen phosphate and diammonium hydrogen phosphate (E. Merck) were used to prepare 0.2 M phosphate buffer pH 7.0. Tetramethylammonium (TMA) hydroxide (20%, w/w in methanol) (Janssen Chimica) was diluted in water to prepare a 0.2 M TMA solution, and adjusted to pH 7.0 with phosphoric acid 85% (E. Merck). The mobile phase was acetonitrile-methanol-0.2 M TMA pH 7.0-0.2 M phosphate buffer pH 7.0-water (30:30:25:5:10, v/v) and was degassed by sonication. Samples were prepared by dissolving about 10 mg in 1 ml of acetonitrile-water (1:1). They were introduced onto the column using a Valco Model CV-6-uHPa-N60 sampling valve (Valco, Houston, TX, U.S.A.) equipped with a 20- μ l loop. The flow-rate was set at 1.0 ml/min and the chart speed at 5 mm/min. The retention times were measured manually.

Other analytical methods

Melting points (m.p) were determined in open capillary tubes using a Büchi Model SMP 20 apparatus (Büchi, Flawil, Switzerland). Ultraviolet (UV) absorption spectra of the compounds in methanol were recorded with a Beckman Model 25 spectrophotometer (Beckman Instruments, Fullerton, CA, U.S.A.). Optical rotations, $[\alpha]_D$, were obtained in methanol solutions using a Thorn-NPL automatic polarimeter Type 243 (Thorn Automation, Nottingham, U.K.). Infrared (IR) absorption spectra of potassium bromide pellets containing 1% (w/w) of sample were recorded on a Perkin-Elmer Model 197 IR spectrophotometer (Perkin-Elmer, Norwalk, CT, U.S.A.).

Mass spectra were recorded on a single-focusing AEI MS-12 mass spectrometer (Kratos, Manchester, U.K.) operated at an accelerating voltage of 8 kV, trap current 100 μ A, ionization energy 70 eV and ion-source temperature 150–190°C. Samples were introduced by the direct insertion probe. Exact mass measurements were performed by computer processing at a resolving power (10% valley) of 9000 using perfluorokerosene as the mass standard and a double-focusing AEI MS-902 S mass spectrometer (Kratos) equipped with a VG-2020 data system. The experimental conditions were the same as for the low resolution mass spectrometry (MS).

Proton magnetic resonance (PMR) spectra were obtained on a Varian XL 100 15 spectrometer (Varian, Palo Alto, CA, U.S.A.) using solutions in deuteriochloroform.

Reference samples

Erythromycin A was purified by five consecutive crystallizations of a commercial sample, twice from a 10% (w/v) solution in dichloromethane then three times in acetone–water (1:1). The crystals were left to dry in contact with the atmosphere, to obtain a pure dihydrate (m.p. 132–136°C). Erythromycin B was donated by Proter (Milan, Italy) and crystallized (m.p. 200–201.5°C) from acetone. Small quantities of impure samples of erythromycins C and D were donated by Abbott (North Chicago, IL, U.S.A.). The following reference compounds were prepared following procedures described in the literature: erythromycin A-6,9;9,12-spiroketal or anhydroerythromycin A (AEA)²², yield 64% (m.p. 146.5–149.5°C and at 161.5–162.5°C); 8,9-anhydroerythromycin A-6,9-hemiketal or erythromycin enol ether (EAEN)²³, yield 68% (m.p. 138–141.5°C); erythromycin B enol ether (EBEN)²³, yield 62% (m.p. 139–142°C); N-demethylerythromycin A (dMeEA)²⁴, yield, overall from EA, 73% (m.p. 144.5–147.5°C).

Anhydro-N-demethylerythromycin A (AdMeEA) was prepared following the procedure for the preparation of AEA. dMeEA (2 g) was suspended in 100 ml of water and dissolved by adding concentrated hydrochloric acid to pH 2.5. The solution was left at room temperature for 30 min. An excess of sodium carbonate was added and the mixture was extracted four times, each with 50 ml of dichloromethane. The organic layer was dried over anhydrous sodium sulphate and evaporated to dryness under reduced pressure, yielding 1.6 g of residue. The residue was dissolved in 5 ml of dichloromethane and 10 ml of *n*-pentane were added. The crystals which formed overnight at –15°C were collected to yield 1.1 g (yield 56%) of AdMeEA; R_F 0.27 (TLC, mobile phase, C); $[\alpha]_D^{25}$ – 43° (c = 1, methanol); m.p. 142.5–146.5°C.

Erythromycin C-6,9;9,12-spiroketal (AEC) was obtained following the pro-

cedure for preparing AdMeEA. EC (200 mg), obtained by preparative HPLC, was suspended in 10 ml of water and dissolved by adding concentrated hydrochloric acid to pH 2.5. The solution was left at room temperature for 30 min. The solution was diluted in 40 ml of water, an excess of sodium carbonate was then added and the mixture was extracted three times, each time with 25 ml of dichloromethane. The organic layer was dried over anhydrous sodium sulphate and evaporated to dryness under reduced pressure. AEC in the residue was purified by preparative HPLC with solvent system C, yielding 120 mg (yield 61.5%); R_F 0.28 (TLC, mobile phase C); $[\alpha]_D^{22} - 54^\circ$ ($c = 1$, methanol).

The structures of the examined reference compounds are shown in Fig. 1.

RESULTS AND DISCUSSION

Chromatography

Three different packing materials were evaluated for preparative HPLC. The silanized silica column had low capacity (≈ 50 mg of a simple mixture of erythromycins per injection) and gave inadequate separation of components. Similar problems were observed for macroporous poly(styrene-divinylbenzene) copolymer (XAD-2) used in the reversed-phase mode. The usefulness of silica gel in classical column chromatography^{6,7} and in TLC³ of erythromycins prompted us to investigate silica packed columns. The development of mobile phase systems for such columns

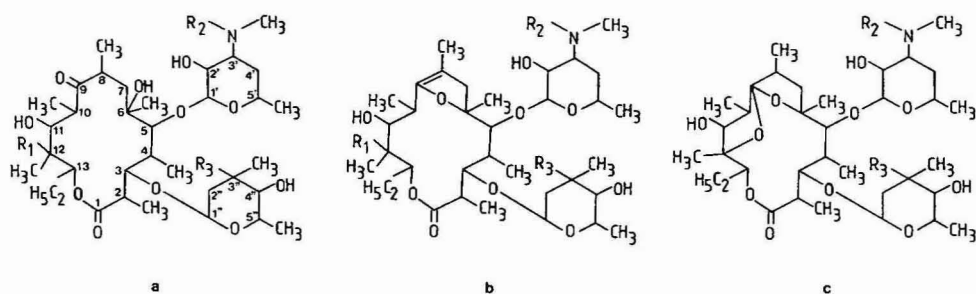


Fig. 1.

(a) Structures of erythromycins

Erythromycin A (EA)
Erythromycin B (EB)
Erythromycin C (EC)
Erythromycin D (ED)
N-Demethylethromycin A (dMeEA)

R ₁	R ₂	R ₃
OH	CH ₃	OCH ₃
H	CH ₃	OCH ₃
OH	CH ₃	OH
H	CH ₃	OH
OH	H	OCH ₃

(b) Structure of enol ether

8,9-Anhydroerythromycin A-6,9-hemiketal (EAEN)

OH	CH ₃	OCH ₃
----	-----------------	------------------

(c) Structures of spiroketals

Erythromycin A-6,9;9,12-spiroketal (AEA)
N-Demethylethromycin A-6,9;9,12-spiroketal (AdMeEA)
Erythromycin C-6,9;9,12-spiroketal (AEC)

—	CH ₃	OCH ₃
—	H	OCH ₃
—	CH ₃	OH

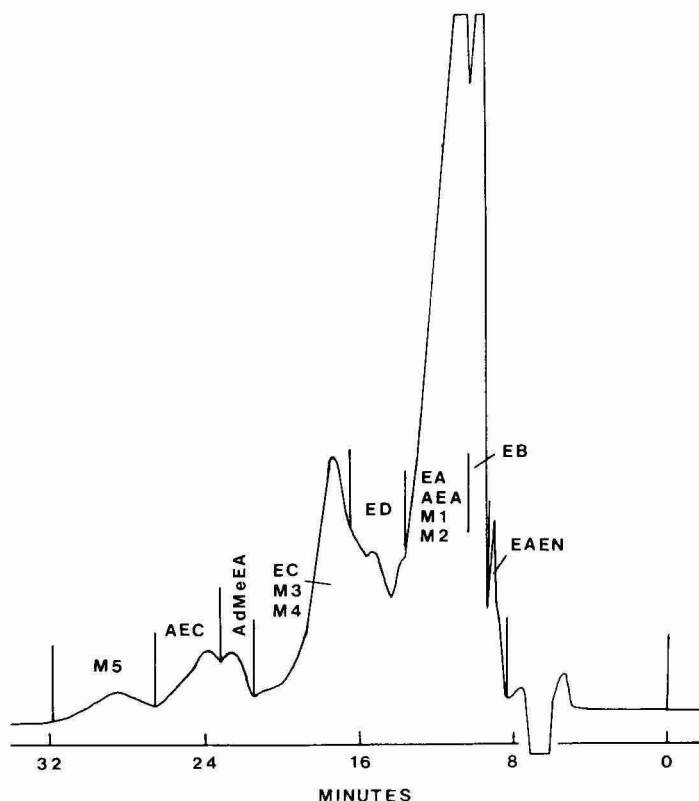


Fig. 2. Typical preparative high-performance liquid chromatogram of mother-liquor concentrates (MLC) of *S. Erythreus* on silica gel, 15 μ m (25 cm \times 22.7 mm I.D.). Mobile phase: ethyl acetate-methanol-25% ammonia (100:8:1, v/v). Flow-rate: 15 ml/min. Detection: refractive index. Sample load: 500 mg. EAEN = 8,9-Anhydroerythromycin A-6,9-hemiketal; EB = erythromycin B; EA = erythromycin A; AEA = erythromycin A-6,9,9,12-spiroketal; ED = erythromycin D; EC = erythromycin C; AdMeEA = N-demethylethromycin A-6,9,12-spiroketal; AEC = erythromycin C-6,9,9,12-spiroketal; M1-M5 = compounds of unknown structure.

was done using TLC plates. The details of the TLC investigations have been published³.

Small changes in the methanol and ammonia contents of some of the mobile phases gave suitable mobile phases for preparative HPLC. Details are given in the Experimental section. TLC was used in the follow up of the purification process. The capacity of silica gel packed columns (500 mg of erythromycins per injection) was ten times higher than that of reversed-phase materials, and afforded better separations. Furthermore the use of organic solvents in the mobile phases facilitates easier recovery of the isolated products by removal of solvents under reduced pressure. During the separation of substances from MLC, the mobile phases were used in the order in which they are listed in the Experimental section. With the first mobile phase the fractions were collected according to the chromatogram shown in Fig. 2. Similar fractions from about 80 runs (40 g of MLC) were pooled and chromatographed using the second mobile phase and so on. From the purer fractions, the major compound

was isolated by crystallization and the filtrate was discarded or used for further purification.

The order of use of the mobile phases has little effect on the final results. This was confirmed by carrying out an experiment with another fermentation residue. In this second experiment, the mobile phases were used in reverse order with some changes in methanol and ammonia content. The same substances as those obtained in the first separation were isolated but in different yields.

The columns used were found to be stable over 6 months of nearly continuous use.

In all, thirteen substances were isolated. Some other substances were detected but not isolated. The yields, chromatographic and some physical characteristics are shown in Table I. Those substances identified are listed with their names. Details of the identifications are presented below. An analytical HPLC chromatogram of a mixture of purified substances is shown in Fig. 3. M4 was not chromatographed because of the small amount of material available.

Identification of isolated substances

The identity of the eight compounds shown in Table I was established by comparison of their chromatographic and spectroscopic behaviour with those of reference substances. The data presented in the table and in the discussion below were obtained with the isolated compounds only. These data were identical to those obtained for the reference compounds. Mixtures of EAEN, AEA and AdMeEA and the corresponding reference substances gave no depression of the m.p.

The isolated substances can be divided into three groups: (a) the primary metabolic compounds EA, EB, EC and ED (Fig. 1a); (b) compounds formed by acid-catalysed transformation, EAEN, AEA, AEC and AdMeEA (Fig. 1b, c) and (c) compounds isolated but not identified (M1–M5) the identification of this latter group is currently being pursued.

In the group of erythromycins, identity was first determined by comparing TLC R_F values and HPLC retention times with those of reference samples. A very diagnostic feature of TLC is the colour reaction of the compounds with the spray reagent 2-methoxybenzaldehyde-sulphuric acid. EA and EC give greyish green spots whereas EB and ED give violet-blue spots. The UV spectra of methanolic solutions of the compounds show a maximum at about 280 nm; $A_{1\%}^{1\text{cm}} = 0.4$ (EA), 0.5 (EB), 0.4 (EC) and 0.6 (ED). The IR spectra of the compounds show bands at 3500–3400 (OH), 3000–2700 (CH_2 , CH_3), 1720 (lactone), 1700 (ketone), 1450 and 1375 cm^{-1} . The identity was confirmed by MS which gave prominent ions: molecular ion, m/z 733 (EA), 717 (EB), 719 (EC) and 703 (ED); desosamine, m/z 158 (EA, EB, EC and ED); cladinose, m/z 159 (EA and EB) and mycarose, m/z 145 (EC and ED). Owing to the composite nature of the ion at m/z 159²⁵, the presence of cladinose was verified by the presence of the ions at m/z 127²⁶ and 115, both related to the parent ion by appropriate metastable peaks.

In the group of compounds formed by acid-catalysed transformation, two types must be distinguished, the 8,9-anhydro 6,9-hemiketals (enol ethers) and the anhydro 6,9;9,12-spiroketals (spiroketals). The structures are shown in Fig. 1b and c respectively. Only one enol ether was isolated. TLC and HPLC showed it to be identical to the reference sample EAEN. The UV spectrum is transparent in the

TABLE I
SUBSTANCES ISOLATED FROM MOTHER-LIQUOR CONCENTRATES OF *S. ERYTHREUS* BY PREPARATIVE HPLC

M1-M5 = Products of unknown structure. NC = Not crystallized; ND = not determined.

Substance	Crystallizing solvent	Yield* (g)	M.p. (°C)	$[\alpha]_D^{20-22}$ (°)	TLC			HPLC [§]	
					R_f^{**}	Colour of spot***			
						A	B		C
Erythromycin A	Acetone-water	ND	132-136	-72	0.46	0.40	0.43	Greyish green	1.00
B	Acetone	2.9	200-201	-94 ^{§§}	0.50	0.45	0.44	Violet-blue	1.67
C	Acetone-water	0.95	200-202	ND	0.36	0.27	0.34	Greyish green	0.54
D	Acetone	0.26	ND	ND	0.43	0.32	0.37	Violet-blue	0.87
8,9-Anhydroerythromycin A-6,9-hemiketal (EAEN)	Ethanol	0.47	138-141.5	-43	0.53	0.60	0.53	Greyish green	2.99
Erythromycin A-6,9,12-spiroketal (AEA)	Dichloromethane-hexane	7.60	146.5-149.5 and 161.5-162.5	-55	0.43	0.43	0.38	Greyish green	1.23
N-Demethylethromycin A-6,9,12-spiroketal (AdMeEA)	Dichloromethane-pentane	0.32	142.5-146.5	-13	0.34	0.32	0.27	Greyish green	0.70
Erythromycin C-6,9,12-spiroketal (AEC)	Acetonitrile	0.47	140.5-144.5	-54 ^{§§}	0.31	0.27	0.28	Greyish green	0.76
M1	Acetonitrile	0.25	135-136.5 and 185-187	-24	0.44	0.40	0.39	Greyish yellow	0.44
M2	Acetonitrile	0.90	131-136	-45	0.44	0.37	0.44	Yellowish brown	1.43
M3	Acetonitrile	0.30	222-223	-14	0.36	0.28	0.26	Yellowish brown	1.35
M4	NC	0.02	ND	ND	0.34	0.23	0.33	Grey	ND
M5	NC	0.04	ND	ND	0.31	0.21	0.22	Yellowish brown	0.81

* Yields are from 40 g of MLC.

** Mobile phases: A, ethyl acetate-methanol-25% ammonia (85:10:5, v/v); B, diethyl ether-methanol-25% ammonia (90:9:2, v/v); C, dichloromethane-methanol-25% ammonia (90:9:1.5, v/v).

*** Spray reagent: concentrated sulphuric acid-2-methoxybenzaldehyde-ethanol (1:1:9, v/v).

§ Column RoSiL C₁₈, 5 μ m (25 cm \times 4-6 mm I.D.), at 40°C. Mobile phase: acetonitrile-methanol-0.2 M tetramethylammonium phosphate pH 7.0-0.2 M phosphate buffer pH 7.0-water (30:30:25:5:10, v/v). Relative retentions are given.

§§ Concentration is 0.5% (w/w).

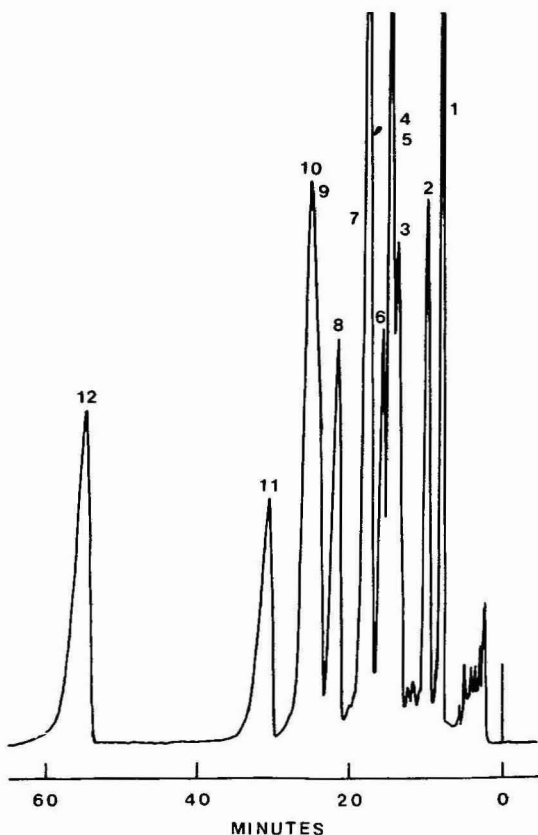


Fig. 3. Reversed-phase HPLC chromatogram of a mixture of compounds isolated from mother-liquor concentrates (MCL) of *S. erythreus* on RoSiL C₁₈, 5 μ m (25 cm \times 4.6 mm I.D.), at 40°C. Mobile phase: acetonitrile-methanol-0.2 M tetramethylammonium phosphate pH 7.0-0.2 M phosphate buffer pH 7.0-water (30:30:25:5:10, v/v). Flow-rate: 1 ml/min. Detection at 215 nm. Peaks: 1 = M1; 2 = EC; 3 = AdMeEA; 4 = AEC; 5 = M5; 6 = ED; 7 = EA; 8 = AEA; 9 = M3; 10 = M2; 11 = EB; 12 = EAEN. M4 was not chromatographed because of the lack of material.

ketone-absorbing region (280 nm) but shows a maximum at 212 nm ($A_{1\text{cm}}^{1\%} = 102$) which is about six times more intense than that obtained with EA (207 nm, $A_{1\text{cm}}^{1\%} = 15.5$). The IR spectrum shows absorption bands at 3500-3400 (OH), 3000-2700 (CH₂, CH₃), 1720 (lactone), 1450, 1375, 1275 and 1160 cm⁻¹. The mass spectrum exhibits the molecular ion at m/z 715, C₃₇H₆₅NO₁₂ (calculated: 715.4506, found: 715.4438), with other peaks at m/z 159 (cladinose) and m/z 158 (desosamine). A prominent fragment ion, m/z 434, C₂₁H₄₀NO₈ (calculated: 434.2753, found: 434.2750), is formed by loss of the C6-C10 part of the macrolide ring from the molecular ion with back transfer of a hydrogen to yield m/z 592, C₂₉H₅₄NO₁₁ (calculated: 592.3696, found: 592.3684), followed by loss of the cladinosyl moiety and gain of a hydrogen. Both fragmentations are supported by the presence of appropriate metastable peaks. This fragmentation is characteristic of compounds containing the 8,9-anhydroerythronolide-6,9-hemiketal structure²⁷.

Although EBEN could have been formed under the same conditions as for EAEN, none was isolated.

Three spiroketals were isolated, *i.e.*, AEA, AEC and AdMeEA. AEA is present in the greatest amount, although it was partly removed from the MLC by crystallization. EB and ED cannot form spiroketals because they lack a hydroxyl group at the C12 position. The identity of the three compounds was first established by TLC and HPLC in comparison with reference samples. The UV spectra of the compounds are transparent in the ketone-absorbing region (280 nm). The IR spectra show absorption bands at 3500–3400 (OH), 3000–2700 (CH₂, CH₃), 1720 (lactone), 1450, 1375, 1160 and 905 cm⁻¹. The band at 905 cm⁻¹ has been attributed to the spiroketal structure⁹. The mass spectra show the molecular ion at *m/z* 715 (AEA), C₃₇H₆₅NO₁₂ (calculated: 715.4506, found: 715.4466), 701 (AEC) and 701 (AdMeEA), C₃₆H₆₃NO₁₂ (calculated: 701.4350, found: 701.4315). AEA gives fragments for desosamine (*m/z* 158) and cladinose (*m/z* 159). AEC and AdMeEA are differentiated by fragments assigned to the sugar moieties: AEC gives *m/z* 145 (mycarose) and *m/z* 158 (desosamine), whereas AdMeEA gives *m/z* 144 (N-demethyldesosamine) and *m/z* 159 (cladinose). A prominent characteristic fragment ion at *m/z* 341, C₁₈H₂₉O₆ (calculated: 341.1964, found 341.1970 for AEA, 341.1964 for AdMeEA), is common to the three compounds. It consists of the C1–C12 part of the aglycone and is formed by loss of the desosaminyloxy group and of propene (C₁₃–C₁₅) yielding the ion at *m/z* 499, C₂₆H₄₃O₉ (AEA and AdMeEA) (calculated: 499.2907, found: 499.2975 for AEA, 499.2904 for AdMeEA) and *m/z* 485 (AEC), followed by loss of the cladinosyl group and back transfer of a hydrogen as established by the presence of metastable peaks. An ion at *m/z* 341 also occurs in the mass spectrum of the 6,9;9,12-spiroketal of N-demethyl-N-propionylerythromycin A⁹. The identity of these compounds was further confirmed by PMR spectroscopy. The spectrum of AEA gives signals at 2.3 ppm [6H, N(CH₃)₂] and 3.3 ppm [3H, O–CH₃]. The spectrum of AEC lacks the latter signal, confirming that the neutral sugar is mycarose, whereas for AdMeEA the signal is present but the signal at 2.3 ppm [3H, N–CH₃] has half the intensity recorded for AEA. Additional proof of the AdMeEA structure was obtained by its methylation to AEA using formaldehyde and cyanoborohydride²⁸.

The isolation of numerous erythromycin-related glycosides has been mentioned in the literature. The presence of large amounts of AEA and AEC in filtrate residues has been reported⁸, but no systematic separation of these compounds has been published. To our knowledge, this is also the first time that AdMeEA has been detected and isolated from *S. erythreus* culture media.

The isolation of AdMeEA from MLC infers the presence of dMeEA in *S. erythreus* culture media. However, no dMeEA was isolated. The presence of dMeEA in commercial samples of erythromycin has been shown previously³. The rôle of dMeEA in culture media could be two-fold, either as a biosynthetic intermediate or as a product of EA metabolism by *S. erythreus*.

ACKNOWLEDGEMENTS

The authors thank Roussel-Uclaf (Paris, France) for the gift of mother-liquor concentrates, Proter (Milan, Italy) for the gift of the reference sample of erythromycin

B, Abbott (Chicago, U.S.A.) for the gift of reference samples of erythromycins C and D and RSL-Alltech (Eke, Belgium) for the gift of a sample of RoSiL C₁₈, 5 μ m. We also thank Dr. S. Toppet for PMR spectra, Dr. F. Compennolle and R. De Boer for mass measurements and Miss L. Van Meensel for secretarial assistance. I. O. Kibwage thanks Algemeen Bestuur van de Ontwikkelingssamenwerking of the Belgian Government for a scholarship.

REFERENCES

- 1 K. Tsuji and J. F. Goetz, *J. Chromatogr.*, 147 (1978) 359.
- 2 H. Vanderhaeghe and L. Kerremans, *J. Chromatogr.*, 193 (1980) 119.
- 3 I. O. Kibwage, E. Roets and J. Hoogmartens, *J. Chromatogr.*, 256 (1983) 164.
- 4 R. K. Clark, Jr., *Antibiot. Chemother.*, 3 (1953) 663.
- 5 P. F. Wiley, R. Gale, C. W. Pettinga and K. Gerzon, *J. Am. Chem. Soc.*, 79 (1957) 6074.
- 6 C. W. Pettinga, W. M. Stark and F. R. van Abeele, *J. Am. Chem. Soc.*, 76 (1954) 569.
- 7 N. L. Oleinick and J. W. Corcoran, *J. Biol. Chem.*, 244 (1969) 729.
- 8 J. Majer, J. R. Martin, R. S. Egan and J. W. Corcoran, *J. Am. Chem. Soc.*, 99 (1977) 1620.
- 9 J. Majer, R. S. Stanaszek, S. L. Mueller and G. Morti, *Drug Metab. Dispos.*, 6 (1978) 673.
- 10 J. Majer, *Antimicrob. Agents Chemother.*, 19 (1981) 628.
- 11 J. R. Martin, R. S. Egan, A. W. Goldstein and P. Collum, *Tetrahedron*, 31 (1975) 1985.
- 12 J. R. Martin, R. L. De Vault, A. C. Sinclair, R. S. Stanaszek and P. Johnson, *J. Antibiot.*, 35 (1982) 426.
- 13 J. R. Martin, T. J. Perun and R. L. Girolami, *Biochemistry*, 5 (1966) 2852.
- 14 J. R. Martin and W. Rosenbrook, *Biochemistry*, 6 (1967) 435.
- 15 J. R. Martin and T. J. Perun, *Biochemistry*, 7 (1968) 1728.
- 16 J. R. Martin and R. S. Egan, *Biochemistry*, 9 (1970) 3439.
- 17 J. R. Martin, T. J. Perun and R. S. Egan, *Tetrahedron*, 28 (1972) 2937.
- 18 P. Collum, R. S. Egan, A. W. Goldstein and J. R. Martin, *Tetrahedron*, 32 (1975) 2375.
- 19 I. Wouters, S. Hendrickx, E. Roets, J. Hoogmartens and H. Vanderhaeghe, *J. Chromatogr.*, 291 (1984) 59.
- 20 P. De Pourcq, J. Hoebus, E. Roets, J. Hoogmartens and H. Vanderhaeghe, *J. Chromatogr.*, 321 (1985) 441.
- 21 J. Hoogmartens, E. Roets, G. Janssen and H. Vanderhaeghe, *J. Chromatogr.*, 244 (1982) 299.
- 22 P. F. Wiley, K. Gerzon, E. H. Flynn, M. V. Sigal, O. Weaver, U. V. Quarck, R. R. Chauvette and R. Monahan, *J. Am. Chem. Soc.*, 79 (1957) 6062.
- 23 P. Kurath, P. H. Jones, R. S. Egan and T. J. Perun, *Experientia*, 27 (1971) 362.
- 24 E. H. Flynn, H. W. Murphy and R. E. McMahon, *J. Am. Chem. Soc.*, 77 (1955) 3104.
- 25 K. L. Rinehart, Jr., J. C. Cook, Jr., K. H. Maurer and U. Rapp, *J. Antibiot.*, 27 (1974) 1.
- 26 L. A. Mitscher, H. D. H. Showatter and R. L. Foltz, *J. Chem. Soc., Chem. Commun.*, (1972) 796.
- 27 G. Janssen, unpublished results.
- 28 R. F. Borch and A. I. Hassid, *J. Org. Chem.*, 37 (1972) 1673.

CHROM. 17 972

ISOLATION AND STEREOSPECIFIC DETERMINATION OF THE ENANTIOMERS OF OXINDAZAC BY DIRECT LIQUID CHROMATOGRAPHIC RESOLUTION ON TRIACETYLCELLULOSE

E. FRANCOTTE

Central Research Laboratories, Ciba-Geigy Limited, Basle (Switzerland)
and

H. STIERLIN* and J. W. FAIGLE

Research and Development, Pharmaceuticals Division, Ciba-Geigy Limited, Basle (Switzerland)
(Received June 17th, 1985)

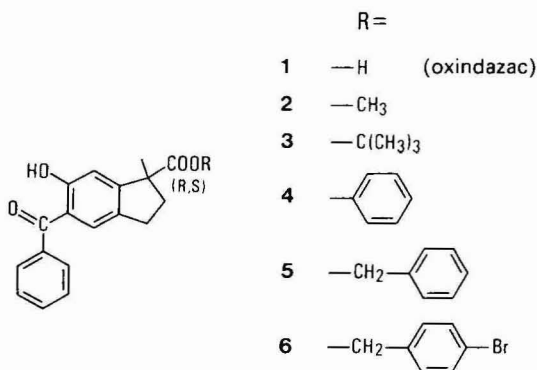
SUMMARY

The preparation of the optically pure enantiomers of the antiphlogistic trial drug oxindazac via liquid chromatographic resolution of the corresponding *tert.*-butyl or benzyl ester on triacetylcellulose is described. Cleavage of the optically pure enantiomeric esters to the acids proceeds without significant racemization. The methyl ester of oxindazac is also completely resolved on the same chiral phase. Whereas oxindazac racemizes easily upon derivatization to diastereomers, no racemization is observed upon methylation to the corresponding methyl ester with diazomethane. An inverse isotope dilution method has been developed to determine both enantiomers of the drug in biological fluids after administration of ^{14}C -labelled oxindazac. The enantiomers are converted into their methyl esters and separated on triacetylcellulose. Quantitation is performed by on-line UV detection at 290 nm and off-line radiometry. In the analysis of plasma samples, endogenous compounds do not interfere. The recoveries of [^{14}C]oxindazac from water, rat and human plasma were $99.6 \pm 1.8\%$ for the (+)- and $96.0 \pm 1.4\%$ for the (–)-enantiomer. The plasma concentrations and urinary excretion of the two enantiomers were determined in a human volunteer who had received 200 mg of racemic ^{14}C -labelled oxindazac.

INTRODUCTION

The analgesic and antiphlogistic trial drug oxindazac*, 5-benzoyl-2,3-dihydro-6-hydroxy-1H-indene-1-carboxylic acid, is a chiral compound¹. The centre of chirality at C-1 is in the α -position with respect to the carboxyl group and carries a very labile proton. The same structural element is present in several other non-steroidal anti-inflammatory drugs. They include arylpropionic acids such as ibuprofen, benoxaprofen and loxoprofen, and the indan-1-carboxylic acid clidanac^{2–5}. In this

* Code number used in previous publication (ref. 1): CGP 6258.



class of drugs the pharmacological activities seem to reside in the S-enantiomers^{6,7}. The disposition in the organism is normally stereoselective, enzymatic inversion of the R- to the S-form being one possible mechanism⁷.

Our first attempts to resolve the enantiomers of oxindazac were unsuccessful. It was not possible to apply the classical methods of preparation and resolution of diastereomers because of rapid racemization of the enantiomers, for instance upon derivatization with optically active reagents. The higher tendency to epimerize at the benzylic position of compound 1 in comparison with analogous drugs can be attributed to the combined inductive effects of the functional groups of 1.

Direct separation of enantiomers by liquid chromatography on a chiral stationary phase has become a promising alternative to the classical methods. Different types of chiral phases have been reported⁸⁻¹² and among them, microcrystalline triacetylcellulose has shown a very good stereoselective recognition for many aromatic compounds¹³⁻¹⁷. We found that several racemic esters of oxindazac can be completely resolved on triacetylcellulose columns. Based on this principle, we developed methods for both the preparative separation of the enantiomers of oxindazac and the determination of the enantiomeric composition of mixtures of them. The latter method, which combines liquid chromatography with inverse isotope dilution, was used in a study on the stereoselective kinetics of ¹⁴C-labelled oxindazac in man. This paper describes the development and application of the new methods.

EXPERIMENTAL

Chemicals

Oxindazac, CGP 6258 (Lot No. 800182), was prepared by Ciba-Geigy (Basle, Switzerland). It was labelled with ¹⁴C in the keto group (Batch No. Z.564.4F, Ciba-Geigy), specific radioactivity 18.9 kBq/mg and radiochemical purity *ca.* 99%, as ascertained by isotope dilution analysis and thin-layer chromatography (TLC) on silica gel (Si 60 F-254; Merck, Darmstadt, F.R.G.) in two chromatographic solvent systems: cyclohexane-dioxan-acetic acid (65:35:1, v/v/v) and *n*-heptane-1-propanol-acetic acid (85:15:1, v/v/v).

The solvents and chemicals used were all of reagent grade, obtained from Merck or Fluka (Buchs, Switzerland). Diethyl ether was distilled to remove the sta-

bilizer and was stored over magnesium sulphate; 1,2-dichloroethane was distilled before use. A phosphate buffer solution pH 6.9 (0.025 *M* disodium hydrogen phosphate + 0.025 *M* potassium dihydrogen phosphate in 1 l) and a solution of pH 2.06 (0.090 *M* potassium chloride + 0.010 *M* hydrochloric acid in 1 l) were used. Microcrystalline triacetylcellulose was prepared by acetylation of microcrystalline cellulose (Merck), following the procedure of Hesse and Hagel¹⁸. Diazomethane in diethyl ether was prepared in a special device¹⁹ from *N,N'*-dimethyl-*N,N'*-dinitrosoterephthalamide (Fluka) and 5 *M* sodium hydroxide.

Synthesis and cleavage of esters of oxindazac

The *tert.*-butyl ester 3 was prepared by reaction of 5 mmol of oxindazac with 6.1 mmol of *tert.*-butanol, 6.1 mmol of 1,1'-carbonyldiimidazole and a few drops of pyridine in 4 ml 1,2-dichloroethane at 70°C for 3 h. The reaction mixture was diluted in 20 ml 1,2-dichloroethane and washed with 1 *M* sodium hydroxide and 1 *M* hydrochloric acid, each 10 ml. The concentrated organic phase was chromatographed on a silica gel G (Merck) column of 30 × 4 cm with chloroform. The resulting yellowish oil was crystallized from methanol. Yield: 24%. M.p.: 107°C. ¹H NMR (deuteriochloroform): 12.12 (s, OH); 7.68, 7.59 and 7.51 (m, 5H, *o*-, *p*- and *m*-benzoyl H); 7.40 (s, H-4); 7.11 (s, H-7); 3.96 (t, H-1); 2.99 and 2.80 (m, 2H, H-3); 2.44 and 2.30 (m, 2H, H-2); 1.52 (s, 9H, CH₃).

The phenyl ester 4 was prepared by reaction of 1.4 mmol of oxindazac with 20 mmol of phenol and 1.3 mmol of 1,1'-carbonyldiimidazole and a few drops of pyridine in 2 ml 1,2-dichloroethane at 70°C for 2 h. Chromatography was performed as above, with chloroform as eluent. Recrystallization was from methanol. Yield: ca. 67%. M.p.: 105–106°C. ¹H NMR (deuteriochloroform): 12.12 (s, OH); 7.68, 7.60 and 7.52 (m, 5H, *o*-, *p*- and *m*-benzoyl H); 7.46 (s, H-4); 7.28 (s, H-7); 7.41, 7.25 and 7.12 (m, 5H, *m*-, *p*- and *o*-phenoxy H); 4.31 (t, H-1); 3.07 and 2.90 (m, 2H, H-3); 2.62 and 2.50 (m, 2H, H-2).

The benzyl ester 5 was prepared by reaction of 21.3 mmol of oxindazac with 87.7 mmol of benzyl bromide and 49.9 mmol of triethylamine in 40 ml 1,2-dichloroethane at 50°C for 15–20 min. The reaction mixture was diluted in 20 ml 1,2-dichloroethane, washed twice with water and the concentrated organic phase was chromatographed as described above, but with 1,2-dichloroethane as eluent. Recrystallization was from methanol or ethanol. Yield: ca. 90%. M.p.: 106–107°C. ¹H NMR (deuteriochloroform): 12.08 (s, OH); 7.67, 7.60 and 7.51 (m, 5H, *o*-, *p*- and *m*-benzoyl H); 7.40 (s, H-4); 7.38 (br s, 5H, phenyl H of benzyl); 7.11 (s, H-7); 5.23 and 5.18 (AB system, *J* = 13 Hz, OCH₂); 4.10 (t, H-1); 3.00 and 2.83 (m, 2H, H-3); 2.50 and 2.37 (m, 2H, H-2).

The *p*-bromobenzyl ester 6 was prepared by reaction of 0.7 mmol of oxindazac, dissolved in 2 ml acetone, with ca. 1.5 mmol of triethylamine and 0.7 mmol of *p*-bromobenzyl bromide in 3 ml acetone at 50°C for about 15 min and then for 4 h at room temperature. The reaction mixture was poured onto 50 ml water and then extracted with ca. 100 ml 1,2-dichloroethane. After drying over magnesium sulphate, the organic solvent was concentrated and the yellowish oil was crystallized from methanol. Crystals formed only on storing at –20°C. Yield: ca. 80%. M.p. 70–72°C. ¹H NMR (deuteriochloroform): 12.09 (s, OH); 7.66, 7.60 and 7.51 (m, 5H, *o*-, *p*- and *m*-benzoyl H); 7.52 and 7.25 (AA'BB' system, *p*-bromophenyl H); 7.42 (s, H-4); 7.08

(s, H-7); 5.18 and 5.11 (AB system, $J = 13$ Hz, OCH_2); 4.10 (t, H-1); 3.00 and 2.83 (m, 2H, H-3); 2.47 and 2.38 (m, 2H, H-2).

For the preparation of the methyl ester 2 on an analytical scale, 0.003–0.03 mmol of oxindazac were treated with a large excess of freshly prepared diazomethane (see above) in diethyl ether for about 15 min in an ultrasonic bath. For spectroscopic analysis, the ester was chromatographed on a LiChrosorb Si 60 column (see below) with cyclohexane–1,2-dichloroethane–tetrahydrofuran–acetic acid (55:40:4:1, v/v/v/v) as eluent. Yield: > 90%. M.p.: 89–90°C. ^1H NMR (deuteriochloroform): 12.10 (s, OH); 7.66, 7.59 and 7.51 (m, 5H, *o*-, *p*- and *m*-benzoyl H); 7.41 (s, H-4); 7.11 (s, H-7); 4.07 (t, H-1); 3.77 (s, OCH_3); 3.00 and 2.82 (m, 2H, H-3); 2.47 and 2.37 (m, 2H, H-2).

For hydrolysis of the *tert*.-butyl ester of oxindazac, 0.14 mmol of the ester 3 were dissolved in 10 ml 1,2-dichloroethane, *ca.* 1 mmol of trimethylsilyl iodide added and the mixture allowed to react for 10–15 min at room temperature. The deep red solution was shaken together with 50 ml water in a separating funnel for about 5 min, to hydrolyse the intermediate silyl ester. The water phase was extracted with 1,2-dichloroethane and the organic solvent was concentrated to dryness. After a second extraction the yield was nearly quantitative. The product was recrystallized from methanol.

The benzyl ester of oxindazac was cleaved by hydrogenation. A 0.7-mmol amount of the ester 5 was dissolved in 10 ml tetrahydrofuran, 20 mg of 5% palladium on carbon were added and hydrogen was bubbled through the mixture at 25°C and normal pressure for about 3 h. The gas consumption was 125% of theoretical. The catalyst was separated on a filter frit, and the concentrated organic solution was chromatographed on a silica gel G column (30 × 2 cm) with cyclohexane–1,2-dichloroethane–ethanol (50:40:10, v/v/v). Recrystallization was from 1,2-dichloroethane and a few drops of heptane. Yield: 45–65%.

Chromatographic conditions

Preparative chromatographic resolution of the *tert*.-butyl ester 3 was performed on a 60 × 5 cm glass column (Buechi, Uster, Switzerland). This column was slurry-packed with swollen microcrystalline triacetylcellulose (particle size 40–70 μm) in 95% ethanol at room temperature. A pressure of 4 kg cm^{-2} (flow-rate 300 ml h^{-1}) was applied and the eluate was detected by a UV-spectrophotometer (UV-120-02; Shimadzu, Tokyo, Japan) at 290 nm in series with a polarimeter (241 MC; Perkin-Elmer, Norwalk, CT, U.S.A.) at 365 nm. The benzyl ester 5 was resolved under the same conditions. Traces of base, which may cause racemization, have to be eliminated by washing the glassware with acetic acid and then acetone before use.

For the analytical chromatographic resolution of the esters of oxindazac, the same triacetylcellulose (particle size 25–32 μm) packed in a 18 × 1.3 cm or 60 × 1.3 cm glass column (Buechi) was used. The mobile phase, 95% ethanol, was pumped (Altex pump, Model 110; Kontron, Zürich, Switzerland) through the column at a flow-rate of 0.5 ml min^{-1} , so that a pressure of about 1.5 kg cm^{-2} was reached. The compound was detected and quantified on-line with a UV-detector at 290 nm (Uvikon 725, Kontron) connected to an integrating recorder (W & W 1100, Kontron).

To separate oxindazac from endogenous constituents in extracts of body fluids, chromatography on LiChrosorb Si 60 (Merck, 10 μm) was used. A stainless-

steel column (25 × 1 cm) was connected to a pre-column (4 × 0.4 cm), both packed with the same material. The chromatographic solvent cyclohexane–1,2-dichloroethane–acetic acid (80:18:2, v/v/v) was pumped through the column at a flow-rate of 4 ml min⁻¹. The pump, detection and quantification were as described above; the wavelength was set at 350 nm.

Polarimetry

The optical rotation was measured with a Model 241 MC polarimeter (Perkin-Elmer) equipped with a 5-ml cell of length 10 cm. The solvents used were chloroform and ethanol.

Inverse isotope dilution analysis (IDA)

To a 1-ml plasma sample containing ¹⁴C-labelled oxindazac was added an aqueous solution (1 ml) of the non-labelled racemic oxindazac (*ca.* 500 µg). After a homogeneous solution had been obtained, the sample was extracted with 100–150 ml dichloromethane at pH 2.06, and after concentration the analyte was treated with diazomethane as described above. The diethyl ether was evaporated and the dry residue was dissolved in 95% ethanol for separation on triacetylcellulose (column: 18 × 1.3 cm). The peaks corresponding to the two enantiomeric forms of the methyl ester were integrated and collected for off-line measurement of radioactivity. When urine samples were analysed, or when enzymatic hydrolysis with β-glucuronidase preceded the determination, an additional chromatographic purification on LiChrosorb Si 60 (see above) had to be included before the reaction with diazomethane and separation on triacetylcellulose.

Enzymatic hydrolysis

Enzymatic hydrolysis of conjugates in plasma and urine was performed with β-glucuronidase (*Escherichia coli*; Sigma, St. Louis, MO, U.S.A.) at pH 6.9 and 37°C for 3 h. For extraction with dichloromethane, the samples were adjusted to pH 2.06, and the extracts were chromatographed on LiChrosorb Si 60 (see above).

Calibration of the LC method used in IDA

Replicate samples containing various amounts of the racemic methyl ester of oxindazac were injected onto the triacetylcellulose column. The amounts ranged from 113 to 273 µg of each enantiomer. The two peaks were integrated, their areas summed and then divided by two. The range of the concentrations was chosen to encompass the expected concentrations of biological samples mixed with the carrier substance. Peak areas were determined automatically by the UV-detector and the integrator. Calibration curves were fitted by means of a computer program using a linear regression analysis.

Recovery of enantiomers from samples spiked with racemic [¹⁴C]oxindazac

Samples of 1 ml water, or 1 ml rat or human plasma, were spiked with about 7 or 11 µg of ¹⁴C-labelled oxindazac and submitted to IDA. The results obtained were compared with the amount of racemic [¹⁴C]oxindazac added to each sample to determine the recovery. It was assumed that synthetic [¹⁴C]oxindazac is a 1:1 mixture of the ¹⁴C-labelled (+)- and (–)-enantiomers.

Application

A single oral 200-mg dose of racemic ^{14}C -labelled oxindazac in a gelatine capsule was administered to a healthy male volunteer²⁰. Blood was withdrawn at 0, 0.5, 1, 2, 4, 6, 8, 12 and 24 h after dosing. Urine was collected in fractions during 2 days. Plasma was prepared from the heparinized blood samples and the carrier substance (non-labelled racemic oxindazac) was added immediately. Plasma specimens and urine were stored at -20°C until analysis.

Measurement of radioactivity

Radiometry was done by liquid scintillation counting as described elsewhere²¹.

RESULTS AND DISCUSSION

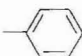
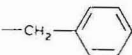
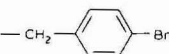
Preparation of the optically pure forms of oxindazac

The free acid 1 is only partially resolved by chromatography on triacetylcel-
lulose. By contrast, several esters of 1 are completely resolved on the same support.
The results are summarized in Table I. For a preparative isolation of the optically
pure forms of oxindazac, via direct chromatographic resolution of an ester derivative,
the *tert.*-butyl or benzyl ester is particularly suitable. They are easily cleaved under
mild conditions to yield again the free acid without racemization.

TABLE I

CHROMATOGRAPHIC RESOLUTION OF ESTERS OF OXINDAZAC ON TRIACETYLCEL-
LULOSE

Column: 60×1.3 cm. Eluent: 95% ethanol. Flow-rate: 30 ml h^{-1} .

Compound	R	Capacity factors		Separation factor, α	Resolution factor, R_s
		k_1^*	k_2		
2	$-\text{CH}_3$	2.67 (—)	4.16	1.56	2.1
3	$-\text{C}(\text{CH}_3)_3$	1.10 (—)	1.72	1.55	1.5
4		4.13 (—)	8.27	2.00	3.0
5		4.15 (—)	7.94	1.91	2.9
6		3.68 (—)	15.23	4.14	2.1

* Sign of the optical rotation of the first eluted enantiomer.

Chromatographic resolution of these two esters, 3 and 5, on a preparative scale (100–200 mg) gives in both cases the pure enantiomeric forms in very high yield (Fig. 1). The optical purity of the isolated enantiomeric esters was tested by re-injection of a sample on an analytical column. Only one peak was detected, indicating the optical purity and stability of the enantiomers. The properties of the enantiomers of the *tert.*-butyl and the benzyl ester are included in Table II.

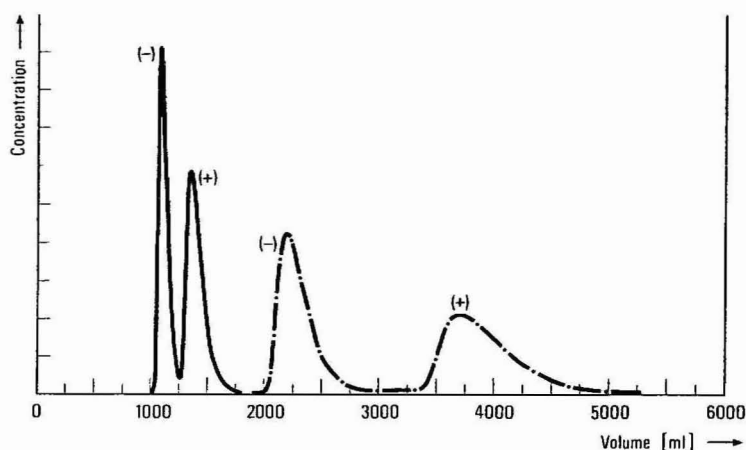


Fig. 1. Chromatographic resolution of 100 mg of compound 3 (—) and 200 mg of 5 (---) on a triacetylcellulose column (60 × 5 cm).

TABLE II

PROPERTIES OF THE ENANTIOMERS OF OXINDAZAC (I) AND ITS ESTERS 3 AND 5

Compound	m.p. (°C)	$[\alpha]_D^{24}$	$[\alpha]_{578}^{24}$	$[\alpha]_{546}^{24}$
1 (–)*	155–157	$-32 \pm 2^{**}$	$-34.8 \pm 2^{**}$	-43.2^{**}
1 (+)*	154–156	$+32 \pm 2^{***}$	$+34.5 \pm 2^{***}$	$+43.2^{***}$
3 (–)	106–107	$-37.6 \pm 2^{\S}$	$-40.6 \pm 2^{\S}$	$-50 \pm 2^{\S}$
3 (+)	106–107	$+39.5 \pm 2^{\S\S}$	$+42.6 \pm 2^{\S\S}$	$+52 \pm 2^{\S\S}$
5 (–)	119–123	$-66 \pm 2^{\S\S\S}$	$-71.3 \pm 2^{\S\S\S}$	$-85.6 \pm 2^{\S\S\S}$
5 (+)	119–122	$+70 \pm 2^{\dagger}$	$+73.7 \pm 2^{\dagger}$	$+88.2 \pm 2^{\dagger}$

* The absolute configuration is still unknown.

** c 0.373, chloroform.

*** c 0.368, chloroform.

\S c 0.946, ethanol.

$\S\S$ c 0.902, ethanol.

$\S\S\S$ c 0.188, ethanol.

\dagger c 0.186, ethanol.

By cleavage of the optically pure enantiomers of the *tert.*-butyl ester with trimethylsilyl iodide, or of the benzyl ester by hydrogenation, up to 90% of the corresponding pure enantiomeric forms of the free acid 1 are obtained.

Properties of the enantiomers of oxindazac

The properties of the enantiomers of oxindazac are given in Table II. The optical purity of the isolated enantiomers of oxindazac was confirmed as follows: reaction of the individual enantiomers with diazomethane gave the corresponding methyl esters. Upon chromatography on an analytical triacetylcellulose column, only one peak is observed for the (–)-enantiomer (Fig. 2b) and for the opposite (+)-enantiomer. The racemic methyl ester is completely resolved on the same column

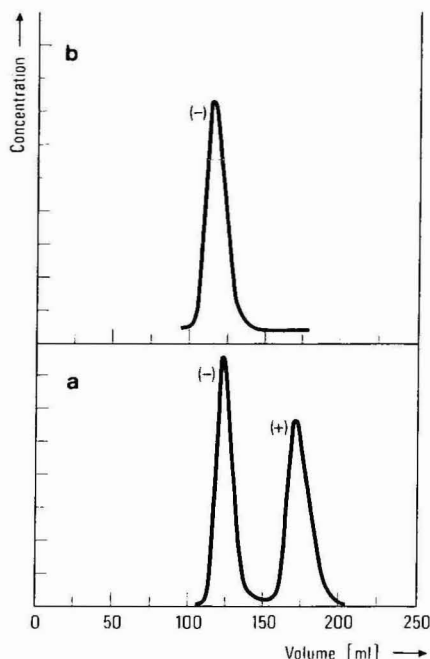


Fig. 2. Chromatography of the methyl ester of racemic oxindazac (a) and its (–)-enantiomer (b) on a triacetylcellulose column (60 × 1.3 cm).

(Fig. 2a). This demonstrates that cleavage of the *tert.*-butyl and benzyl esters, and esterification with diazomethane, proceed without significant racemization.

IDA method for measurement of the enantiomers of oxindazac

With the IDA method described here, it is possible to determine the enantiomeric composition of samples containing ^{14}C -labelled oxindazac. This method combines direct chromatographic resolution of the methyl ester 2, as shown in Fig. 2a, with the principle of inverse isotope dilution. Racemic, unlabelled oxindazac is added to the sample, acting as an ideal internal standard which allows correction for all losses preceding the actual measurement. The drug is extracted from the sample and treated with diazomethane. Ester formation is virtually quantitative, and no by-products are formed. The methyl ester is resolved by chromatography. The amount of each enantiomer can be determined from the spectrophotometric and radiometric results.

The analysis of blank samples of plasma from rat and man revealed that endogenous compounds do not interfere with the UV-detection of the enantiomeric esters. However, urine samples and plasma samples treated with β -glucuronidase gave rise to some interference. In these cases, the analyte extracted from the biological sample has to be purified on a LiChrosorb Si 60 column before methylation.

To demonstrate the absence of racemization, the optically pure enantiomers of compound 1 were taken through the individual steps of the analytical procedure. These steps include extraction at pH 2.06, enzymatic hydrolysis at pH 6.9, chro-

matography on LiChrosorb Si 60 and reaction with diazomethane. When checking the optical purity of the (+)- or the (–)-isomer, the content of the respective antipode was found to be 3% at the most.

Calibration and validation of the IDA method

Calibration of the spectrophotometric determination was performed with the racemic methyl ester 2. It was shown that both enantiomers possess the same photometric response. The calibration curves were linear; the reproducibility of the method expressed as the coefficient of variation (C.V.) was 0.4% for both enantiomers ($n = 7$).

Samples of water, rat plasma and human plasma, spiked with the usually occurring amounts of ^{14}C -labelled oxindazac, were analysed by the IDA assay for accuracy. The recoveries were $99.6 \pm 1.8\%$ for the (+)- and $96.0 \pm 1.4\%$ for the (–)-enantiomer ($n = 7$). The data were calculated with the assumption that synthetic [^{14}C]oxindazac is a 1:1 mixture of the two enantiomers. In fact, the sum of the individual values of (+)- and (–)-oxindazac resulted in means \pm C.V. of $97.8 \pm 1.4\%$ for the recovery of racemic oxindazac. The sensitivity of the method would be around $0.01 \mu\text{g/g}$ (0.04 nmol/g) when a specific radioactivity of *ca.* 19 kBq/mg is applied.

Kinetics of the enantiomers of ^{14}C -labelled oxindazac in man

The analytical assay was used to determine the pharmacokinetics of the enantiomers of oxindazac in a healthy human volunteer. He had received a single oral dose of 200 mg of racemic ^{14}C -labelled oxindazac. Plasma samples were analysed for total ^{14}C -labelled compounds and the (+)- and (–)-enantiomers (Fig. 3). The two optical isomers were determined in individual urine fractions and in the pooled urine (0–48 h) before and after enzymatic hydrolysis with β -glucuronidase (Table III). The results show stereoselective disposition of oxindazac in man; the underlying mechanism is still being unexplored.

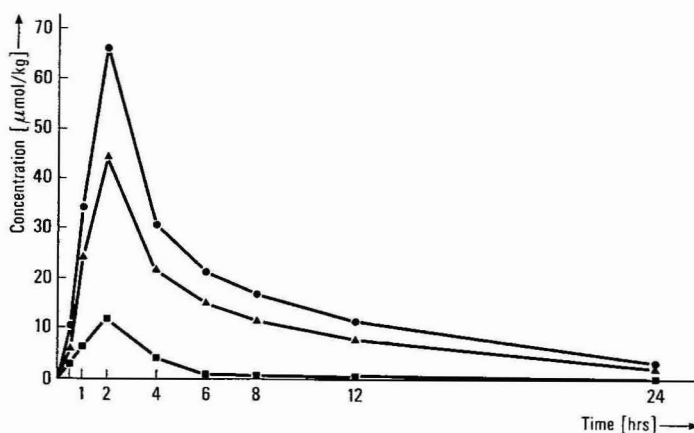


Fig. 3. Plasma concentrations of total ^{14}C -labelled compounds (●) and of the (+)- (■) and (–)-enantiomers (▲) of oxindazac after a single oral dose (200 mg) of ^{14}C -labelled drug to a healthy volunteer.

TABLE III

EXCRETION OF THE (+)- AND (-)-ENANTIOMERS OF OXINDAZAC IN URINE AFTER A SINGLE ORAL DOSE OF 200 mg OF ^{14}C -LABELLED DRUG TO A HEALTHY VOLUNTEER

Results are expressed as % of urinary ^{14}C .

Treatment of urine	Compound determined	% of urinary ^{14}C in individual urine fractions				
		0-6 h	6-12 h	12-24 h	24-48 h	0-48 h (Pool)
Untreated	(+)-Enantiomer	7.2	—*	—	—	7.7
	(-)-Enantiomer	5.4	—	—	—	5.9
	Total	12.6				13.6
Hydrolysed	(+)-Enantiomer	35.2	28.1	34.3	25.9	30.7
	(-)-Enantiomer	28.7	22.3	28.0	22.6	28.1
	Total	63.9	50.4	62.3	48.5	58.8

* Not determined.

The plasma concentrations of total oxindazac, calculated by summing the values for the two isomers, fit well the concentration patterns obtained in an earlier study in man¹. In the latter case, oxindazac was determined by a non-stereospecific gas-liquid chromatographic method.

CONCLUSION

By direct resolution of enantiomeric esters on triacetylcellulose, it is possible to isolate the optically pure forms of racemic oxindazac on a preparative scale. For analytical purposes, this chromatographic resolution is used together with the isotope dilution technique. The method is suitable for stereospecific measurement of the enantiomers of oxindazac in body fluids.

ACKNOWLEDGEMENTS

We are indebted to Dr. W. K  ng of Ciba-Geigy for providing ^{14}C -labelled oxindazac, and Dr. T. Winkler of Ciba-Geigy for recording and interpreting the NMR spectra. We gratefully acknowledge the excellent technical assistance of Mr. W. Gertsch.

REFERENCES

- 1 P. H. Degen and W. Schneider, *J. Chromatogr.*, 277 (1983) 361.
- 2 R. F. N. Mills, S. S. Adams, E. E. Cliffe, W. Dickinson and J. S. Nicholson, *Xenobiotica*, 3 (1973) 589.
- 3 C. H. Cashin, W. Dawson and E. A. Kitchen, *J. Pharm. Pharmacol.*, 29 (1977) 330.
- 4 S. Naruto, Y. Tanaka, R. Hayashi and A. Terada, *Chem. Pharm. Bull.*, 32 (1984) 258.
- 5 S. Tanayama, E. Tsuchida and Z. Suzuoki, *Xenobiotica*, 3 (1973) 643.
- 6 S. Tamura, S. Kuzuna and K. Kawai, *J. Pharm. Pharmacol.*, 33 (1981) 29.
- 7 A. J. Hutt and J. Caldwell, *J. Pharm. Pharmacol.*, 35 (1983) 693.

- 8 D. W. Armstrong, *J. Liq. Chromatogr.*, 7, Suppl. 2 (1984) 353.
- 9 S. Allenmark, *J. Biochem. Biophys. Methods*, 9 (1984) 1.
- 10 I. W. Wainer and T. D. Doyle, *LC, Liq. Chromatogr. HPLC Mag.*, 2 (1984) 88.
- 11 P. H. Pirkle and J. Finn, in J. Morrison (Editor), *Asymmetric Synthesis*, Vol. 1, Academic Press, New York, 1983, p. 87.
- 12 G. Blaschke, *Angew. Chem., Int. Ed. Engl.*, 19 (1980) 13.
- 13 G. Hesse and R. Hagel, *Justus Liebigs Ann. Chem.*, (1976) 996.
- 14 K. Schloegl and M. Widhalm, *Chem. Ber.*, 115 (1982) 3042.
- 15 K. Schloegl and M. Widhalm, *Monatsh. Chem.*, 115 (1984) 1113, and refs. cited therein.
- 16 G. Blaschke and H. Markgraf, *Arch. Pharm. (Weinheim Ger.)*, 317 (1984) 465.
- 17 H. Koller, K. H. Rimböck and A. Mannschreck, *J. Chromatogr.*, 282 (1983) 89.
- 18 G. Hesse and R. Hagel, *Chromatographia*, 6 (1973) 277.
- 19 H. M. Fales, T. M. Jaouni and J. F. Babashak, *Anal. Chem.*, 45 (1973) 2302.
- 20 H. Stierlin, J. W. Faigle, W. Küng and W. Theobald, in preparation.
- 21 W. Dieterle and J. W. Faigle, *J. Chromatogr.*, 259 (1983) 301.

CHROM. 17 976

STUDIES ON THE ANALYSIS OF FOOD ADDITIVES BY HIGH-PERFORMANCE LIQUID CHROMATOGRAPHY

V*. SIMULTANEOUS DETERMINATION OF PRESERVATIVES AND SACCHARIN IN FOODS BY ION-PAIR CHROMATOGRAPHY

HISAYA TERADA* and YOSHIO SAKABE

Nagoya City Health Research Institute, 1-11, Hagiya-cho, Mizuho-ku, Nagoya 467 (Japan)

(First received May 2nd, 1985; revised manuscript received June 17th, 1985)

SUMMARY

A high-performance liquid chromatographic method for the simultaneous determination of sorbic acid, benzoic acid, *p*-hydroxybenzoic acid and its methyl, ethyl, isopropyl, *n*-propyl, isobutyl, *n*-butyl esters and saccharin in foodstuffs is described. For good separations of these compounds, acetonitrile–water–0.2 *M* phosphate buffer pH 3.6 (7:12:1) containing 2 mM cetyltrimethylammonium bromide as an ion-pair reagent and a Nucleosil 5C18 column are required. A steam distillation method and a Sep-Pak C₁₈ cartridge method for the sample preparation are compared. The recoveries from a coffee drink were generally better than 93.8% and the relative standard deviations were 0.85–2.15% for the Sep-Pak C₁₈ cartridge method.

INTRODUCTION

Sorbic acid (SOA), benzoic acid (BA), the esters of *p*-hydroxybenzoic acid (ethyl-, isopropyl-, *n*-propyl-, isobutyl- and *n*-butyl-PHBA) and saccharin (SA) are commonly used food additives in Japan. Many methods for their analysis have been reported, including UV spectrophotometry¹, thin-layer chromatography (TLC)^{1,2}, gas chromatography (GC)¹ and high-performance liquid chromatography (HPLC)^{3–17}. However, TLC procedures are difficult to quantify accurately, and UV spectrophotometric and GC procedures require tedious pre-treatments and do not allow the simultaneous determination of these food additives. Although HPLC has great advantages over other conventional methods, simultaneous separations of these food additives is difficult because the polarities of SOA, BA and SA are extremely different from those of the esters of PHBA. Several reports have been made on simultaneous separations of these compounds using gradient elution^{9–14} or ion depression¹⁷. Recently, Aitzetmüller and Arzberger¹⁵ reported an isocratic method for the

* Part IV: H. Terada and Y. Sakabe, *Eisei Kagaku*, 29 (1983) 394.

simultaneous determination of preservatives in foods using normal phase HPLC

The use of ion-pair chromatography enables the highly polar compounds to be separated as weakly polar compounds. We previously reported¹⁶ an HPLC method for the determination of SOA, BA and SA this technique. However, the method could not to be applied to the esters of PHBA. The purpose of the present study was to investigate the chromatographic behaviour of the nine preservatives SOA, BA, PHBA, methyl-, ethyl-, isopropyl-, *n*-propyl-, isobutyl- and *n*-butyl-PHBA and to establish a method for the simultaneous determination of these compounds and SA in food products.

EXPERIMENTAL

Apparatus and reagents

The HPLC system consisted of a Twinkle pump (Jasco, Tokyo, Japan), a VL614 variable loop injector with a 100- μ l sample loop, a Uvidec 100 II UV detector operating at 235 nm and an U125M recorder (Nippon Denshi Kogaku, Kyoto, Japan). Separations were carried out by using stainless-steel columns (15 cm \times 4.3 mm I.D.; Umetani, Osaka, Japan) packed by the balanced slurry technique with LiChrosorb RP-18 (5 μ m) (E. Merck, Darmstadt, F.R.G.), Develosil ODS-5 (Nomura Kagaku, Seto, Japan) and Nucleosil 5C18 (Macherey-Nagel, Düren, F.R.G.), respectively. The columns were water-jacketed for temperature control (27°C). A Sep-Pak C₁₈ cartridge was obtained from Waters Assoc. (Milford, MA, U.S.A.).

PHBA, esters of PHBA, *n*-decyltrimethylammonium bromide (DTA), *n*-dodecyltrimethylammonium bromide (DDTA), *n*-tetradecyltrimethylammonium bromide (TTA) and cetyltrimethylammonium bromide (CTA) were purchased from Tokyo Kasei (Tokyo, Japan), SOA and BA from Katayama (Osaka, Japan) and SA from Wako (Osaka, Japan).

The phosphate buffer was prepared from 0.2 *M* potassium dihydrogen phosphate by titration to the required pH with 0.2 *M* phosphoric acid or 0.2 *M* dipotassium hydrogen phosphate. All the water used was purified by the Milli-Q water purification system (Millipore, Bedford, MA, U.S.A.).

Chromatographic procedure

Mobile phases were prepared by mixing the calculated amounts of acetonitrile, water, 0.2 *M* phosphate buffer and ion-pair reagents and degassed in an ultrasonic bath immediately before use. The operating conditions are given in the figure captions. The capacity factors were calculated from the equation

$$k' = (t_R - t_0)/t_0$$

where t_R is the retention time of the sample peak and t_0 is the retention time for a non-retained peak.

Sample preparations

Steam distillation method. To an accurately weighed quantity (*ca.* 10 g) of ground sample in a 500-ml kjeldahl flask, 60 g of sodium chloride, 150 ml of water and 10 ml of 15% tartaric acid were added. The mixture was then steam distilled at a rate of 10 ml/min until *ca.* 480 ml of distillate had been collected in a 500-ml

volumetric flask, the volume was adjusted with water. To aliquots (10 ml) of this solution in a 20-ml volumetric flask, 5 ml of acetonitrile were added and the volume was adjusted with water; 100 μ l of this solution were subjected to HPLC.

Quantitation was carried out using calibration graphs obtained from a standard solution (preservatives and SA in the concentration range 0.25–1.25 μ g in 1.0 ml of 25% aqueous acetonitrile).

Sep-Pak C_{18} cartridge method. To an accurately weighed quantity (ca. 2 g) of liquid sample in a 50-ml volumetric flask, 5 ml of 0.2 M phosphate buffer pH 3.0 and 5 ml of 5 mM CTA were added and the volume adjusted with water. After mixing the solution, 5 ml of the mixture were poured into a Sep-Pak C_{18} cartridge at a rate of 2 ml/min and the cartridge was washed with 10 ml of water. The cartridge was attached to a 20-ml glass syringe and pre-conditioned with 20 ml of methanol, 20 ml of water and 2 ml of 5 mM CTA prior to use. The preservatives and SA were eluted from the cartridge with 10 ml of acetonitrile–water (1:1) into a 20 ml volumetric flask and the volume was adjusted with water. Aliquots (100 μ l) of this solution were subjected to HPLC.

Quantitation was carried out using calibration graphs obtained from a standard solution which was treated with a Sep-Pak C_{18} cartridge according to the above analytical procedure.

RESULTS AND DISCUSSION

The influence of the support on the retention and the selectivity of the chromatographic system was studied using LiChrosorb RP-18, Develosil ODS-5 and Nucleosil 5C18 as supports. Although similar chromatographic behaviours were ob-

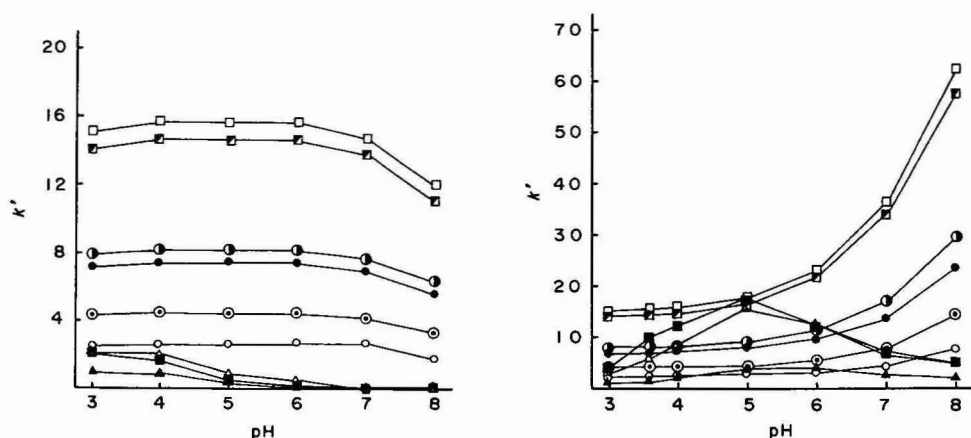


Fig. 1. Effect of the pH of the phosphate buffer added to the mobile phase containing no ion-pair reagent on the k' of the preservatives: \blacktriangle — \blacktriangle , PHBA; \triangle — \triangle , SOA; \blacksquare — \blacksquare , BA; \circ — \circ , methyl-PHBA; \odot — \odot , ethyl-PHBA; \bullet — \bullet , isopropyl-PHBA; \odot — \odot , *n*-propyl-PHBA; \blacksquare — \blacksquare , isobutyl-PHBA; \square — \square , *n*-butyl-PHBA. Operating conditions: column; Nucleosil 5C18 (15 cm \times 4.3 mm I.D.); mobile phase, acetonitrile–water–0.2 M phosphate buffer (7:12:1); column temperature, 27°C; flow-rate, 1.0 ml/min; detector, UV 235 nm.

Fig. 2. Effect of the pH of the phosphate buffer added to the mobile phase containing 2 mM CTA as an ion-pair reagent on the k' of the preservatives. Other details as in Fig. 1.

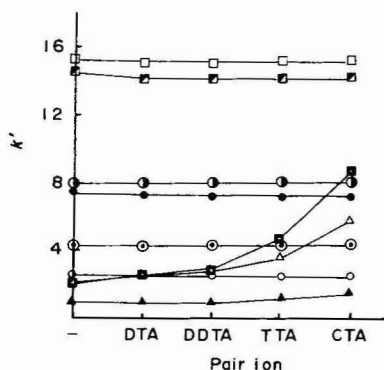


Fig. 3. Relationship between the alkyl chain length of the ion-pair reagent (2 mM) and k' of the preservatives. Mobile phase: acetonitrile–water–0.2 M phosphate buffer (pH 3.6) (7:12:1) containing 2 mM ion-pair reagent. Key to symbols as in Fig. 1.

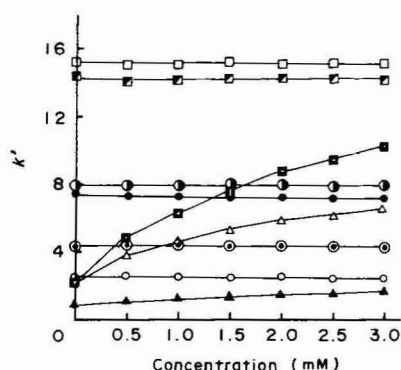


Fig. 4. Effect of the concentration of CTA on the k' of the preservatives. Mobile phase: acetonitrile–water–0.2 M phosphate buffer (pH 3.6) (7:12:1) containing 0–3.0 mM CTA. Key to symbols as in Fig. 1.

served, the LiChrosorb RP-18 and Develosil ODS-5 columns did not give a good separation of isobutyl-PHBA and *n*-butyl-PHBA. The Nucleosil 5C18 column, however, gave good separations of all compounds investigated. Therefore, it was adopted for further investigations.

Fig. 1 shows the effect of the pH of the phosphate buffer added to the mobile phase containing no ion-pair reagent on the capacity factors (k') of the preservatives. In the range pH 3–6, the k' values of each ester of PHBA were constant, but at pH > 7 they were slightly decreased. The k' values of the highly polar PHBA, SOA and BA also decreased with increasing pH. Fig. 2 shows the effect of the pH of the

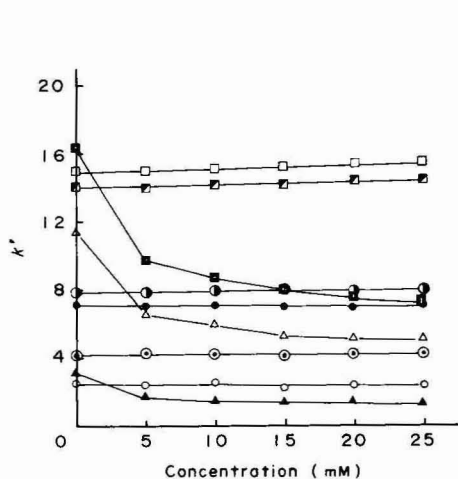


Fig. 5. Effect of the concentration of phosphate buffer pH 3.6 on the k' of the preservatives. Mobile phase: acetonitrile (35%, v/v)–water containing 0–25 mM phosphate buffer pH 3.6 and 2 mM CTA.

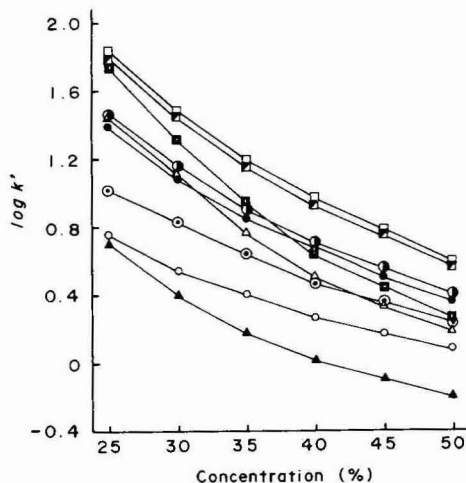


Fig. 6. Effect of the concentration of acetonitrile on the $\log k'$ of the preservatives. Mobile phase: acetonitrile (25–50%, v/v)–water containing 10 mM phosphate buffer pH 3.6 and 2 mM CTA.

phosphate buffer added to the mobile phase containing 2 mM CTA as an ion-pair reagent on the k' of the preservatives. The k' values for the esters of PHBA increased with increasing pH, in contrast to the behaviour in the mobile phase containing no ion-pair reagent. On the other hand, the k' of PHBA, SOA and BA had a maximum at pH 5.

Fig. 3 shows the relationship between the alkyl chain length of the ion-pair reagent and the k' of the preservatives. The k' values for the esters of PHBA were constant, regardless of the ion-pair reagents, but the values for PHBA, SOA and BA increased with increasing alkyl chain length of the ion-pair reagent.

Figs. 4–6 show the effect of the concentration of CTA, phosphate buffer pH 3.6 and acetonitrile, respectively, on the k' of the preservatives. The values for the esters of PHBA were independent of the concentration of CTA and slightly increased with increasing concentration of phosphate buffer, the values for PHBA, SOA and BA increased with increasing concentration of CTA and decreased with increasing concentration of phosphate buffer and the values for all the compounds decreased with increasing concentration of acetonitrile, especially in the case of the acids.

On the basis of these results, acetonitrile–water–0.2 M phosphate buffer pH 3.6 (7:12:1) containing 2 mM CTA was used as a mobile phase. Fig. 7 shows a typical chromatogram for a standard mixture. SA could be separated simultaneously under the same chromatographic conditions.

For the sample pre-treatment, a steam distillation method, commonly used to analyze preservatives such as SOA, BA and esters of PHBA¹, and a Sep-Pak C₁₈ cartridge method were employed. In previous studies, we established a method of preparation for SOA, BA and SA using a Sep-Pak C₁₈ cartridge¹⁶. The packing material of the Sep-Pak C₁₈ cartridge is similar to that present in the analytical

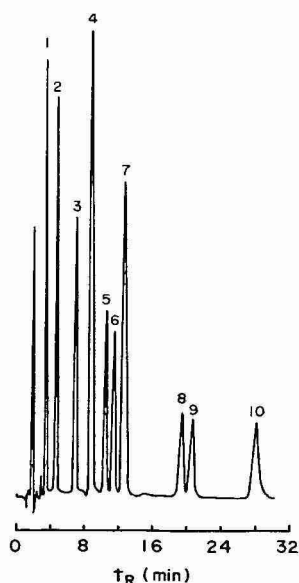


Fig. 7. Liquid Chromatogram obtained from a standard mixture (containing 0.1 $\mu\text{g/ml}$ of each compound): 1 = PHBA; 2 = methyl-PHBA; 3 = ethyl-PHBA; 4 = SOA; 5 = isopropyl-PHBA; 6 = *n*-propyl-PHBA; 7 = BA; 8 = isobutyl-PHBA; 9 = *n*-butyl-PHBA; 10 = SA.

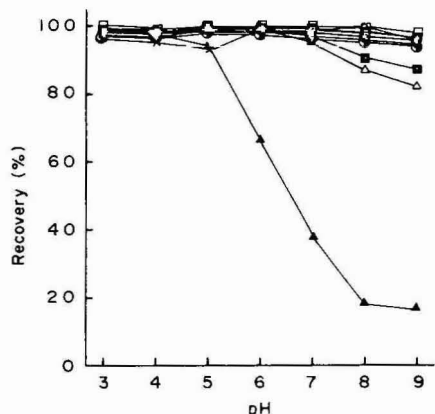


Fig. 8. Effect of the pH of the sample solution on the recoveries of the preservatives and SA (x) from a Sep-Pak C₁₈ cartridge. See Fig. 1 for key to symbols.

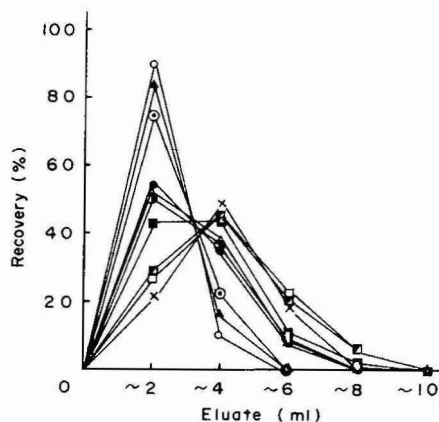


Fig. 9. Elution pattern of the preservatives and SA (x) from a Sep-Pak C₁₈ cartridge. See Fig. 1 for key to symbols.

column. Accordingly, not only the esters of PHBA but also the highly polar SOA, BA and SA can be adsorbed in the cartridge from aqueous solutions containing an ion-pair reagent such as CTA. Therefore, the method was modified for the preparation of PHBA and its esters.

Fig. 8 shows the effects of the pH of the sample solution on the recoveries of the preservatives and SA from a Sep-Pak C₁₈ cartridge. In the range pH 3–5, the recoveries were over 95%, but at pH > 6 for PHBA and 8 for SOA and BA the recoveries decreased. Consequently, 0.2 M phosphate buffer pH 3.0 was added to the sample solution in order to maintain in a pH < 5.

Fig. 9 shows the elution pattern of the preservatives and SA from a Sep-Pak C₁₈ cartridge. All of the compounds were eluted completely with 10 ml of acetonitrile–water (1:1).

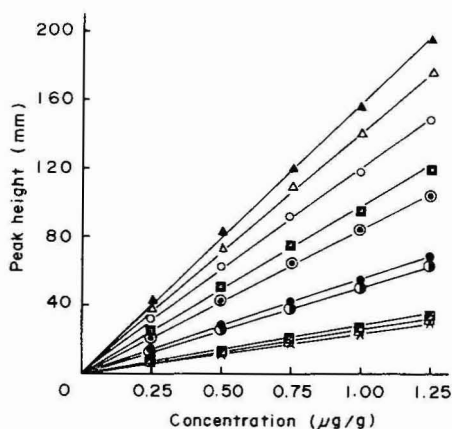


Fig. 10. Calibration curves of the preservatives and SA (x) obtained by use of the Sep-Pak C₁₈ cartridge method. See Fig. 1 for key to symbols.

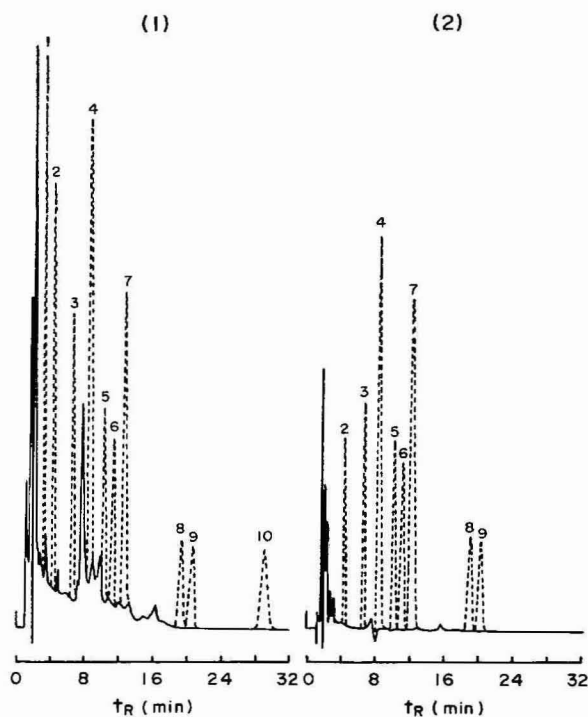


Fig. 11. Chromatograms obtained from a coffee drink prepared by use of the Sep-Pak C_{18} cartridge method (1) and the steam distillation method (2). Broken line: sample spiked with 100 $\mu\text{g/g}$ of the standard mixture. Peaks as in Fig. 7.

TABLE I

RECOVERIES OF THE PRESERVATIVES AND SA FROM A COFFEE DRINK

Methods: A = steam distillation method; B = Sep-Pak C_{18} cartridge method. C.V. = Coefficient of variation.

Compound	Method A		Method B	
	Recovery (%)	C.V. (%)	Recovery (%)	C.V. (%)
PHBA	—	—	100.3	1.01
SOA	76.1	5.97	101.6	0.90
BA	97.2	1.34	99.9	1.22
SA	—	—	102.4	1.18
Methyl-PHBA	32.6	8.05	99.0	1.14
Ethyl-PHBA	77.1	4.29	96.7	0.85
Isopropyl-PHBA	95.5	1.13	93.8	1.20
<i>n</i> -Propyl-PHBA	91.3	2.56	96.1	1.53
Isobutyl-PHBA	95.8	0.92	100.9	2.15
<i>n</i> -Butyl-PHBA	95.9	1.58	100.3	1.80

Fig. 10 shows the calibration curves of the preservatives and SA obtained by use of the Sep-Pak C₁₈ cartridge method. Linear plots of relative response passing through the origin were obtained for all of the compounds studied in the concentration range 0.25–1.25 µg in 1.0 ml of the solution subjected to HPLC.

Fig. 11 shows the chromatograms obtained from a coffee drink spiked with the preservatives and SA after treatment by the Sep-Pak C₁₈ cartridge method (1) and the steam distillation method (2).

In a recovery test, the steam distillation method and the Sep-Pak C₁₈ cartridge method were applied to a coffee drink spiked with the preservatives and SA each at a level of 100 µg/g. The reproducibility was determined by carrying out five identical analyses, and the results are summarized in Table I. The steam distillation method had a few advantages, namely it provided a cleaner sample solution that contained few interfering compounds, and it was applicable to samples of various types. Nevertheless, it was time-consuming and provided no recovery of PHBA and SA and low recoveries of SOA, methyl- and ethyl-PHBA. The Sep-Pak C₁₈ cartridge method generally provided better results.

The detection limits of the present method were 5 µg/g for PHBA, SOA, BA, methyl- and ethyl-PHBA and 10 µg/g for isopropyl-, *n*-propyl-, isobutyl-, *n*-butyl-PHBA and SA. They, however, could be enhanced for a specific analysis by using the appropriate absorption maximum (BA, 225 nm; SA, 205 nm; SOA, PHBA and the esters of PHBA, 260 nm), because the detector wavelength used, 235 nm, was a compromise made in order to detect all of the compounds concerned simultaneously.

REFERENCES

- 1 *Standard Methods of Analysis for Hygienic Chemists —with commentary*, Pharmaceutical Society of Japan, Kinbara, Tokyo, 1980, p. 296.
- 2 R. Duden, A. Fricker, R. Calverley, K. H. Park and V. M. Rios, *Z. Lebensm.-Unters.-Forsch.*, 151 (1973) 23.
- 3 J. J. Nelson, *J. Chromatogr. Sci.*, 11 (1973) 28.
- 4 H. Terada, K. Hisada, M. Asanoma, Y. Maruyama, T. Ishihara and Y. Sakabe, *Annu. Rep. Nagoya City Health Res. Inst.*, 23 (1976) 36.
- 5 M. Ueta and M. Mazaki, *J. Food Hyg. Soc. Jpn.*, 18 (1977) 278.
- 6 D. S. Smyly, B. B. Woodward and E. C. Conrad, *J. Assoc. Off. Anal. Chem.*, 59 (1976) 14.
- 7 Y. Kitada, K. Tamase, M. Sasaki, Y. Nishikawa and K. Tanigawa, *J. Food Hyg. Soc. Jpn.*, 21 (1980) 480.
- 8 A. W. Archer, *Analyst (London)*, 105 (1980) 407.
- 9 U. Leuenberger, R. Gauch and E. Baumgartner, *J. Chromatogr.*, 173 (1979) 343.
- 10 J. Hild and C. Gerty, *Z. Lebensm.-Unters.-Forsch.*, 170 (1980) 110.
- 11 A. Collinge and A. Noifalaise, *Anal. Chim. Acta*, 132 (1981) 201.
- 12 Y. Kitada, K. Tamase, K. Yamada, M. Sasaki and K. Tanigawa, *Naraken Eisei Kenkyujo Nenpo*, 15 (1981) 86; *C.A.*, 98 (1983) 52014a.
- 13 L. Gagliardi, A. Amato, A. Basili, G. Cavazzutti, E. Gattavecchia and D. Tonelli, *J. Chromatogr.*, 315 (1984) 465.
- 14 C. Gertz and K. Herrmann, *Dtsch. Lebensm.-Rundsch.*, 79 (1983) 331.
- 15 K. Aitzetmüller and E. Arzberger, *Z. Lebensm.-Unters.-Forsch.*, 178 (1984) 279.
- 16 H. Terada, K. Hisada, Y. Maruyama and Y. Sakabe, *Eisei Kagaku*, 29 (1983) 297.
- 17 H. Nakaguma, K. Tajima and T. Konishi, *Eisei Kagaku*, 31 (1985) 32.

CHROM. 17 988

Note

Preparation of glass and fused-silica capillary columns coated with immobilized XE-60

W. BLUM*

Zentrale Funktion Forschung, Ciba-Geigy AG, 4002 Basle (Switzerland)

and

K. GROB

GC-Laboratory, ETH Zürich, EAWAG, 8600 Dübendorf (Switzerland)

(Received June 27th, 1985)

The modification of deionized silica surfaces by persilylation with monofunctional silylating agents¹ results, in addition to increasing inertness, in a decreased surface energy. Consequently, subsequent coating is successful only with more or less apolar phases the surface tension of which allows a sufficiently homogeneous spreading on the modified support surface.

Procedures have been described² which to increase the surface energy by introducing dipoles, while preserving the inertness. Our attempts to use the recommended cyanopropylmethylcyclorosiloxanes for the persilylation of glass capillaries led to pyrolysis of the cyclorosiloxanes, resulting in dark brown deposits whenever the reaction was carried out at 350°C for several hours.

In order to interpret this observation, we have to start with the assumption that a cyclic siloxane is attacked by a surface silanol group (*cf.*, Fig. 1), resulting in ring opening. The linear siloxane produced is bonded to the former surface silanol, while a new silanol group is formed at the free end of the siloxane. Further reaction with a second surface silanol group to build a bridge over a section of the surface, *i.e.*, to regenerate a cyclorosiloxane, would be the most desirable outcome (Fig. 1a). However, we expect the probability of this reaction to be relatively low, particularly on a strongly hydroxylated surface (as is that of leached glass), and with a siloxane containing sterically hindering groups such as phenyl. The only alternative would seem to be attack of terminal silanol groups on other siloxane molecules (cyclic and/or linear). At the high temperature used for persilylation, this type of reaction will occur very rapidly, and result in continued opening and closing of rings of different sizes, and in lengthening and shortening of linear chains; the average size of the rings and chains will rapidly approach the equilibrium size typical for the given temperature, or the chemical nature of the chosen cyclorosiloxane, respectively.

We believe the modest thermal stability of the system (insoluble, brown deposits formed) to be explained best by assuming unknown side reactions to occur during the silanol/siloxane reactions. Accordingly, end capping the linear siloxanes is expected to hinder the side reactions (Fig. 1b). However, the end-capping agent has to be sufficiently sterically hindered so as not to compete with the cyclorosiloxane

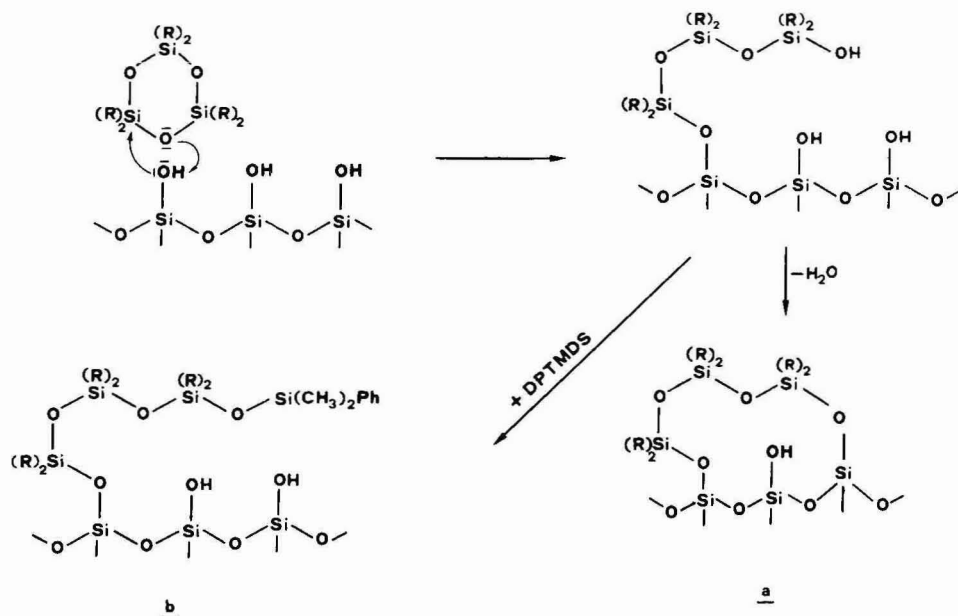


Fig. 1. Tentative mechanism for the reaction of a cyclic siloxane with a hydroxylated silica surface. (a) Double condensation (recyclization) on the silica surface; (b) Monofunctional reaction with the silica surface, followed by end capping with DPTMDS.

for reaction with the surface silanols. For instance, the common monofunctional silylating agent hexamethyldisilazane produces a primarily trimethylsilylated silica surface with little increase in surface energy.

In fact, persilylation with a mixture of bis(cyanopropyl)hexamethylcyclotetrasiloxane and diphenyltetramethyldisilazane (DPTMDS) could be carried out at 370°C for 8 h without any evidence of pyrolysis. The added monofunctional agent clearly increased the thermostability of the reacting system while not hindering the increase in surface energy.

A successful persilylation based on thermal degradation of polysiloxane phases has been described by Schomburg *et al.*³ It is known that, at temperatures above 300°C , linear polysiloxanes release cyclic ethers of various ring sizes^{4,5}. We believe, therefore, that persilylation with cyclic siloxanes, and with the degradation products of linear polysiloxanes, are based on the same mechanisms. Thus, there should be no disadvantage in replacing an individually synthesized, non-commercially available, cyclosiloxane² by a common stationary phase of corresponding structure.

The procedure we describe here is based on the use of a mixture of the traditional stationary phase XF-1150 (polysiloxane with 50% each of cyanoethyl and methyl groups) and DPTMDS. The deactivated silica surface obtained can successfully be coated with stationary phases of medium polarity.

EXPERIMENTAL

Leaching

Glass (Duran) and fused-silica capillaries (20 m \times 0.3 mm) were used. The Duran capillaries were filled with 20% hydrochloric acid to 92% of their volume. After sealing under vacuum, leaching was carried out at 180°C for 12 h¹. The fused-silica capillaries were rinsed with 3% hydrochloric acid, immediately sealed and kept at 220°C for 7 h⁶. All capillaries were then rinsed with twice their volume of 1% hydrochloric acid, and dried with both ends connected to a vacuum. The drying conditions were 280°C for 2 h for Duran, and 240°C for 1 h for fused-silica, capillaries.

Persilylation

The silylating mixture consisted of two volume of XF-1150 (Alltech/Socolabo, Pully-Lausanne, Switzerland) and one volume of DPTMDS (Fluka, Buchs, Switzerland). One volume of this mixture was diluted in four volumes of methylene chloride. The solution was sucked into the capillaries so as to fill 15% of their length. The plug was moved with nitrogen at a rate of 4 cm/s. When the solution left the capillary (without a buffer column), the carrier connection was immediately switched to the exit end, and the bulk of solvent was evaporated by a stream of nitrogen at a pressure of 0.5 bar for 10 min. Complete evaporation of methylene chloride was assured by keeping the capillaries for 10 min in a gas chromatograph at 80°C under 0.2 bar of hydrogen. Both ends were washed with methylene chloride, then connected to a vacuum for 15 min and flame-sealed under vacuum. The capillaries were kept at 360 \pm 5°C for 7 h, the fused-silica capillaries at 330 \pm 5°C for 12 h (the oven thermometer should be carefully calibrated). After cooling and opening, the capillaries were rinsed with toluene, methanol and diethyl ether, and dried under a stream of nitrogen.

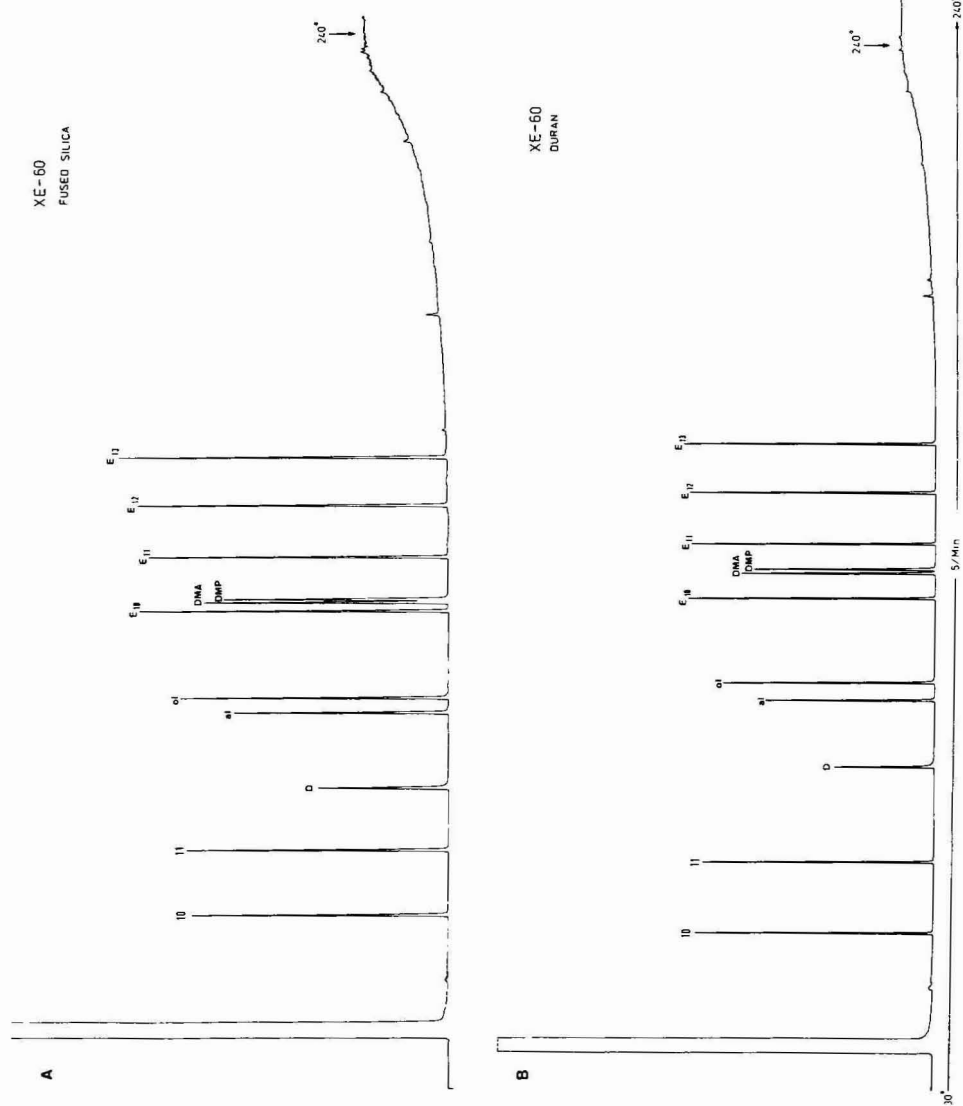
Coating and immobilization

The coating solution contained 0.4% XE-60 and 1% of its weight of dicumyl peroxide (Elfa, Zürich, Switzerland) in pentane-methylene chloride (1:1, v/v). Static coating was carried out according to ref. 1. At the inlet end, 1.5 m were left uncoated as a retention gap⁷. Both ends of the coated columns were connected to a vacuum and flame-sealed. The columns were then heated to 160°C and the temperature was programmed at a rate of 0.5°C/min to 200°C. After opening, the immobilized columns were kept at 200°C for 6 h and at 240°C for 4 h under a flow of hydrogen, and were then tested.

RESULTS AND DISCUSSION

Typical test chromatograms for XE-60 coatings on Duran glass and fused silica are shown in Fig. 2.

Whereas the separation efficiency and inertness of the two types of column are comparable, the thermal stability of XE-60 on Duran is better than on fused silica (less baseline drift with Duran column heated beyond 230°C). We attribute this difference to the larger density of surface silanols on Duran available for condensation with residual terminal silanols of the polysiloxane phase, which stabilizes the coating.



NOTES

Fig. 2. Chromatograms obtained on identical coatings (XE-60) on identically persilylated surfaces: A, fused silica (18 m × 0.32 mm); B, Duran glass (20 m × 0.32 mm). Hydrogen flow-rate: 0.5 m/s. Temperature: 30–240°C, at an 5°C/min. Peaks: 10 = *n*-decane; 11 = *n*-undecane; D = 2,3-butanediol; al = nonanal; ol = octanol; E₁₀ = methyldecanoate; E₁₁ = methylundecanoate; DMA = 2,6-dimethylaniline; DMP = 2,6-dimethylphenol; E₁₂ = methylidodecanoate; E₁₃ = methyltridecanoate. Note the smaller baseline drift and the increased polarity with Duran, probably due to residual surface silanols; there is virtually no difference in inertness.

We are aware of the very tentative character of our hypotheses concerning the functioning of a mono/bifunctional silylating agent. However, these ideas have provided a fruitful working model which is supported by various experimental evidence. Instead of reacting with the free ends of bonded polysiloxane sections, the end-capping agent will also compete with the siloxane for the surface silanols. However, we do not consider this competition to be serious, since XE-60 does not spread on a purely DPTMDS-persilylated surface of Duran or fused silica. Furthermore, our attempt to promote the competitiveness of the polysiloxane by increasing its relative concentration with respect to DPTMDS was unsuccessful. Lowering the proportion of the disilazane below the ratio indicated in Experimental resulted in a less thermally stable system, as shown by the partial pyrolysis which produced brown deposits. Similarly, the surface energy could not be increased by increasing the extent of phenyl substitution of the disilazanes⁸.

Coating a polar phase on Duran requires less optimization than on fused silica. Whereas the deionization and dehydration of Duran occurred under the same conditions as described for the preparation of apolar columns¹, the treatment of fused silica differed from that applied for apolar coatings. Increasing the amount of dehydration beyond that indicated caused the method to fail, probably because small amounts of water are necessary for the production and the reaction of degradation products of the polysiloxane.

As a radical generator for the immobilization of XE-60, we prefer dicumyl peroxide because of its greater efficiency compared to an azo compound. As expected, the immobilization improved the thermal stability of the coating. We were unable to detect any evidence for an influence of the peroxide on the functional groups of the phase, as recently presumed⁹.

REFERENCES

- 1 K. Grob, G. Grob, W. Blum and W. Walther, *J. Chromatogr.*, 244 (1982) 197.
- 2 K. Markides, L. G. Blomberg, J. Buijten and T. Wännmann, *J. Chromatogr.*, 254 (1983) 53.
- 3 G. Schomburg, H. Husmann and H. Borwitzky, *Chromatographia*, 12 (1979) 651.
- 4 M. Blazco, G. Garzó and T. Szekely, *Chromatographia*, 5 (1972) 485.
- 5 S. Hoffmann, L. G. Blomberg, J. Buijten, K. Markides and T. Wännmann, *J. Chromatogr.*, 302 (1984) 95 and references cited therein.
- 6 M. Galli, personal communication, 1985.
- 7 K. Grob, Jr., *J. Chromatogr.*, 237 (1982) 15.
- 8 K. Grob and G. Grob, *J. High Resolut. Chromatogr. Chromatogr. Commun.*, 4 (1980) 197.
- 9 B. E. Richter, J. C. Kuei, J. I. Shelton, L. W. Castle, J. S. Bradshaw and M. L. Lee, *J. Chromatogr.*, 279 (1983) 21.

Note

A microscopic investigation of the surface of carbon–silica adsorbents

II. Relationships between the type of information obtainable about the surface and the microscopic techniques used for its examination

ELZBIETA TRACZ* and ROMAN LEBODA

Central Laboratory, Maria Curie-Skłodowska University, Sq.MCS 3, 20–031 Lublin (Poland)

(Received June 13th, 1985)

In a previous paper¹ the replica technique was used for examination of the surface of complex carbon–silica adsorbents (Carbosils). The aim of the present study was to find the most appropriate technique of sample preparation for transmission electron microscopy (TEM) and scanning electron microscopy (SEM). Two opposite Everhart-Thornley detectors were used for examination of the surface in SEM.

EXPERIMENTAL

The characteristics of the examined adsorbents are given in Table I. The preparation of the Carbosils was described previously¹.

Samples for TEM were prepared using the carbon replica, carbon–platinum replica or direct carbon deposit technique. The replica technique depends on the evaporation of carbon or carbon and platinum onto the surface of the adsorbent, followed by treatment with a solution of silica in hydrofluoric acid. Because the

TABLE I
CONDITIONS FOR MODIFICATION OF SILICA GEL AND SURFACE PROPERTIES OF THE ADSORBENTS INVESTIGATED

S = Specific surface area; *L* = average layer thickness of deposited carbon; *C* = amount of carbon (the loss of mass of carbosils during heat treatment in the air).

Adsorbent	Modifier	Time of pyrolysis (h)	<i>S</i> (m ² /g)	<i>C</i> (%, w/w)	<i>L</i> (Å)
Initial silica gel	Unmodified	—	150.7	—	—
Carbosil A1	Dichloromethane	1	112.2	0.8	0.29
Carbosil A2	Pentanol	3	151.2	1.2	0.44
Carbosil A3	Dichloromethane	1	138.2	1.76	0.65
	Pentanol	3			
Carbosil A4	Pentanol	3	109.5	2.21	0.81
	Dichloromethane	1			

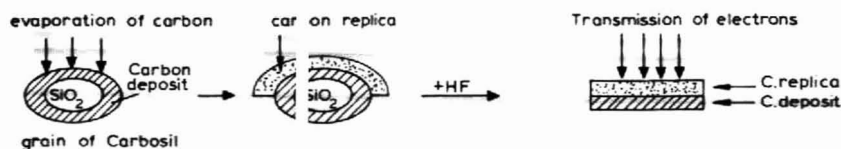


Fig. 1. Sample for TEM consisting of carbon replica and carbon deposit.

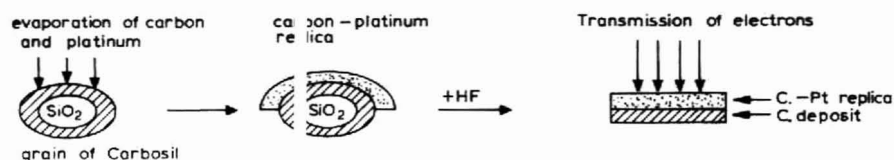


Fig. 2. Sample for TEM consisting of carbon-platinum replica and carbon deposit.

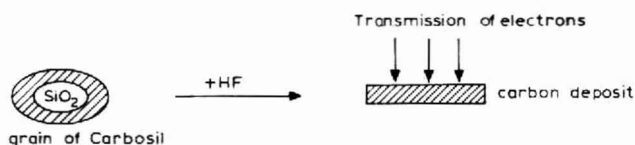


Fig. 3. Sample for TEM consisting of carbon deposit.

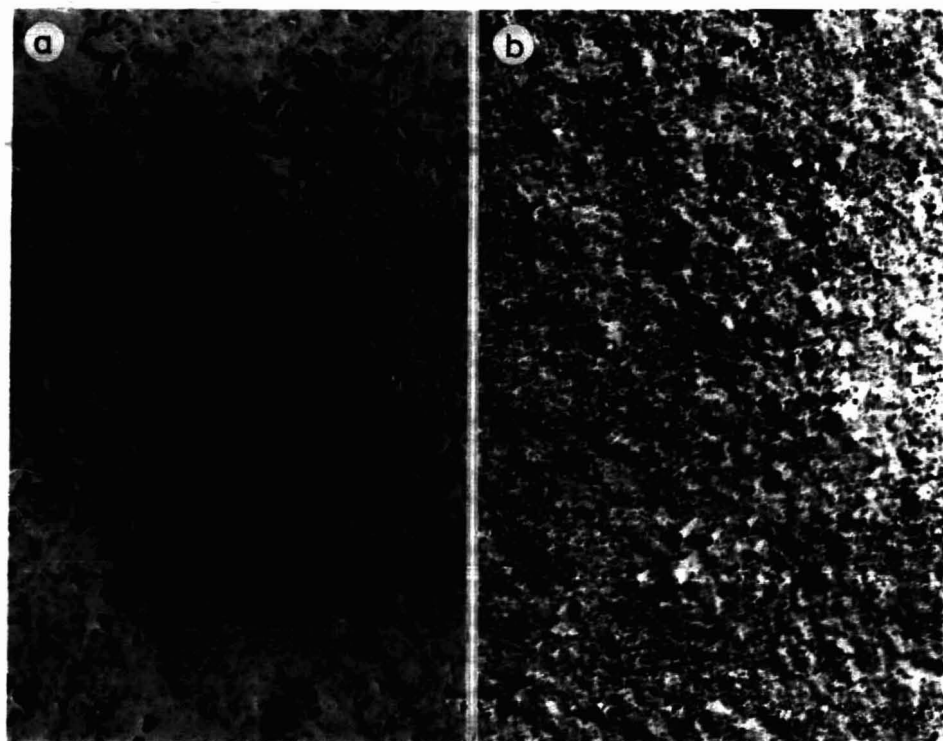


Fig. 4. Surface of initial silica gel examined by TEM, magnification $\times 5000$. Methods of preparation: a, carbon replica; b, carbon-platinum replica.

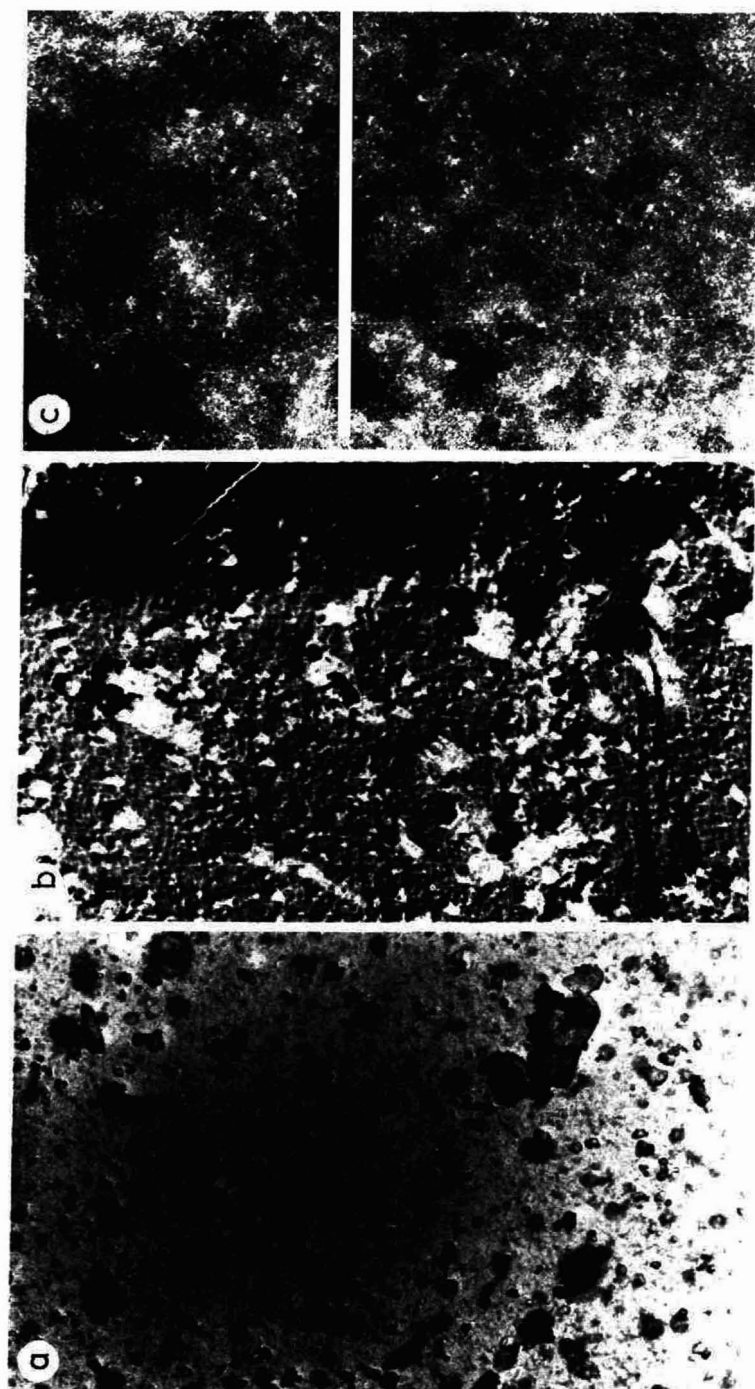


Fig. 5. Surface of Carbosil A1 (silica + dichloromethane). Details as in Fig. 4 except for part c which shows the film obtained by direct deposition of carbon.

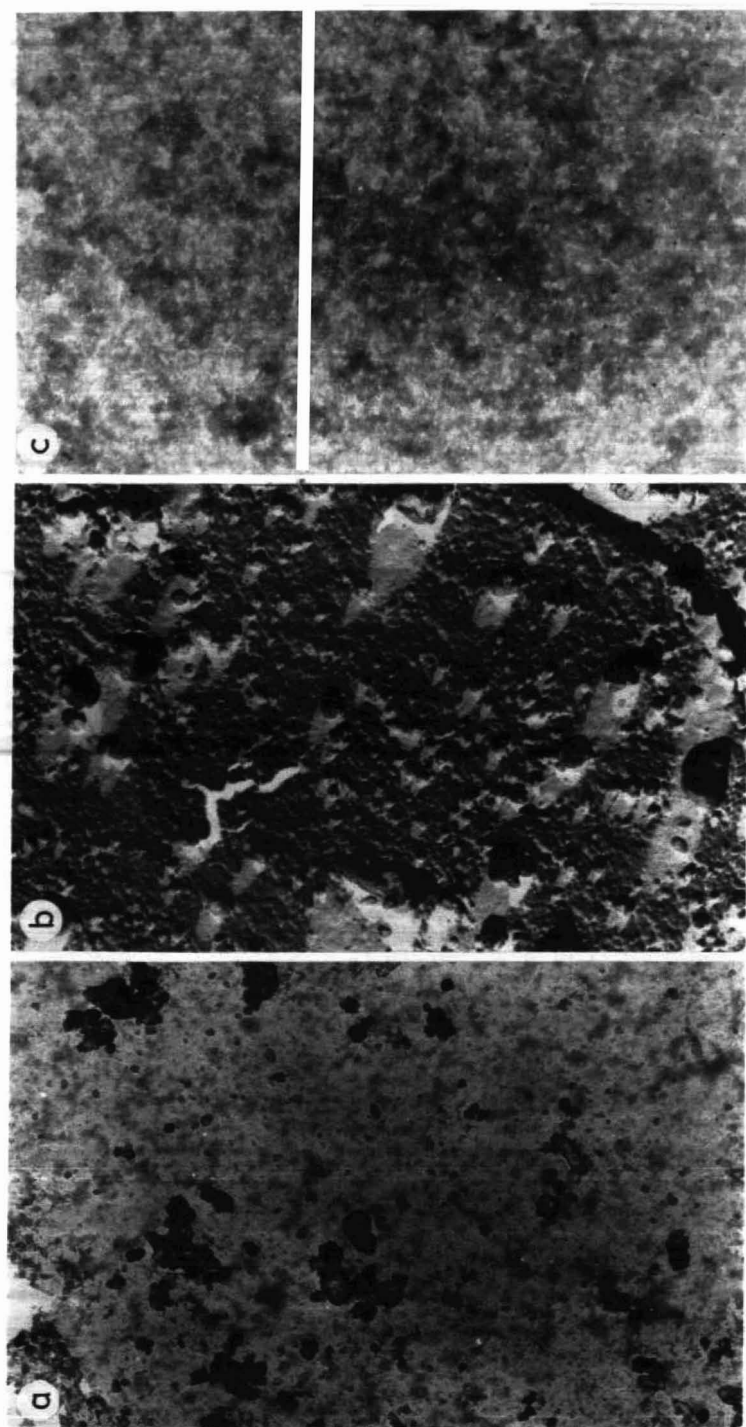


Fig. 6. Surface of Carbosil A2 (silica + pentanol). Details as in Fig. 5.

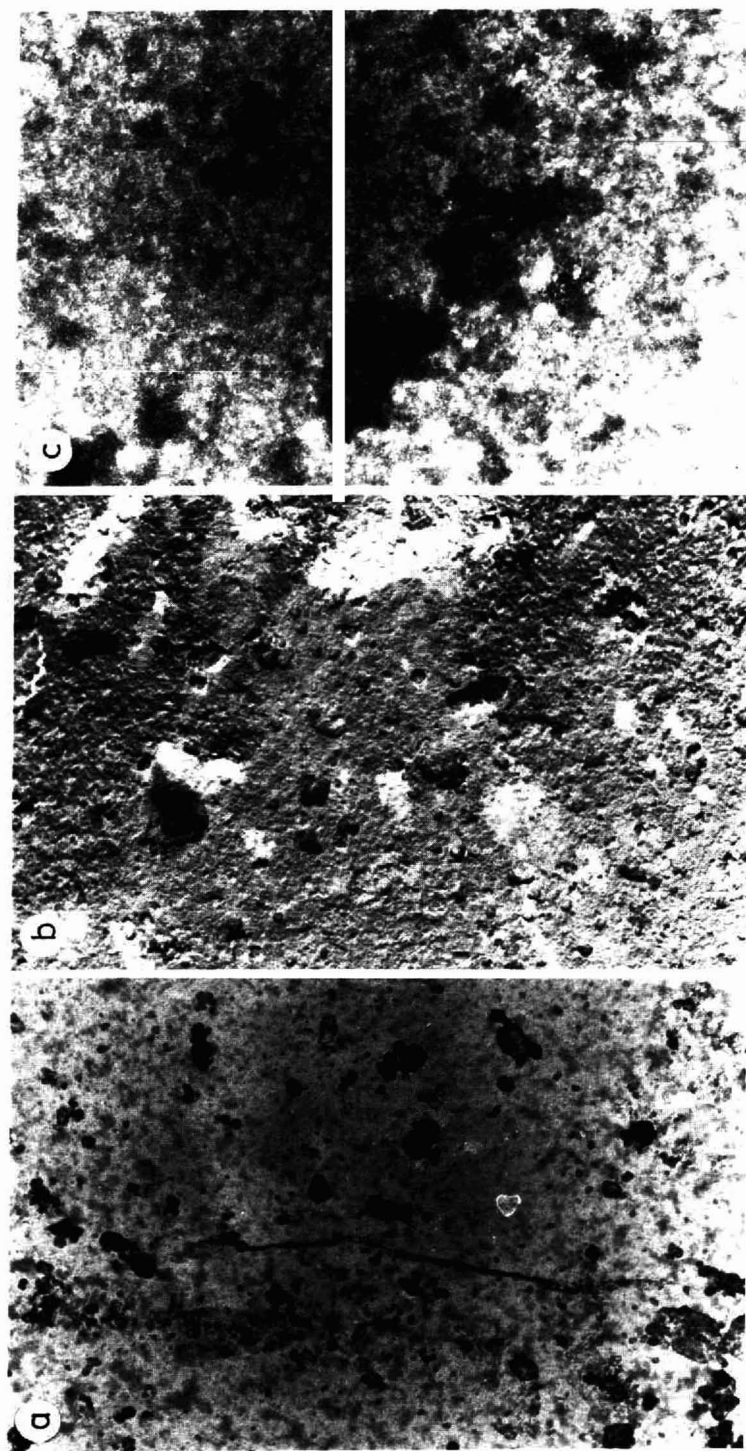


Fig. 7. Surface of Carbosil A3 (silica + dichloromethane + pentanol). Details as in Fig. 5.

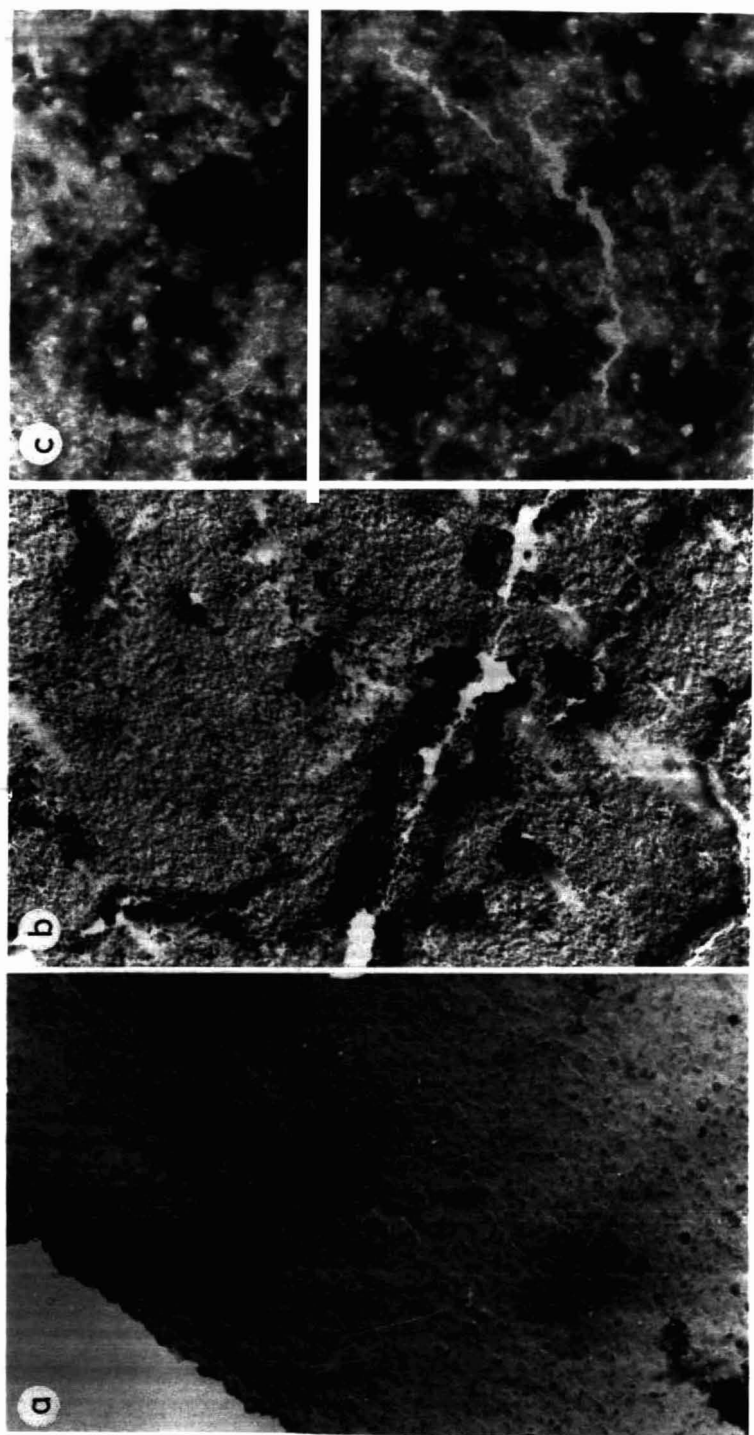


Fig. 8. Surface of Carbosil A4 (silica + pentanol + dichloromethane). Details as in Fig. 5.



Fig. 9.

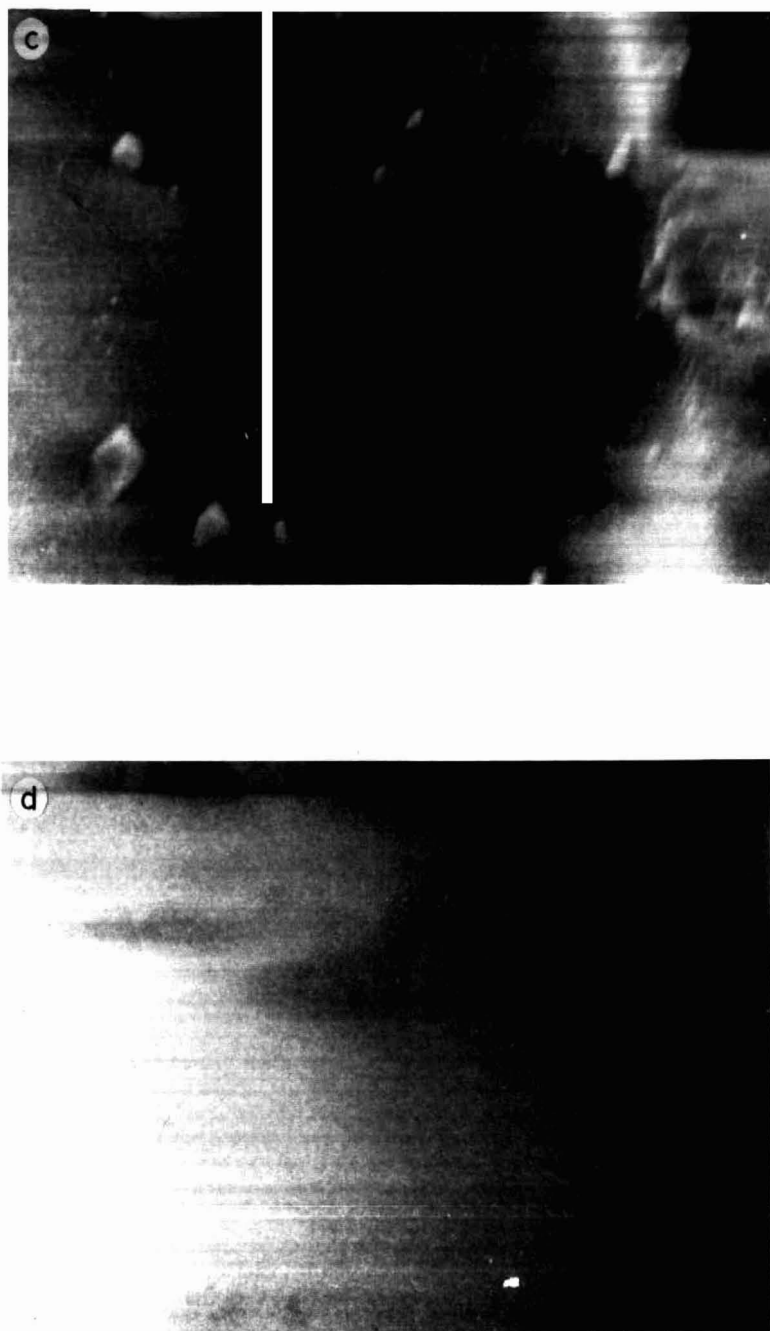


Fig. 9. Surface of the initial silica gel observed by SEM, magnification $\times 1000$. A two detector system with opposite Everhart-Thornley detectors was employed. BSE = Backscattered electrons; SE = secondary electrons. a, $A + B$, BSE image with material contrast; b, $A - B$, BSE image with imaging artifacts; c, $A + B$, SE image with material contrast; d, $A - B$, SE image with topographic contrast.

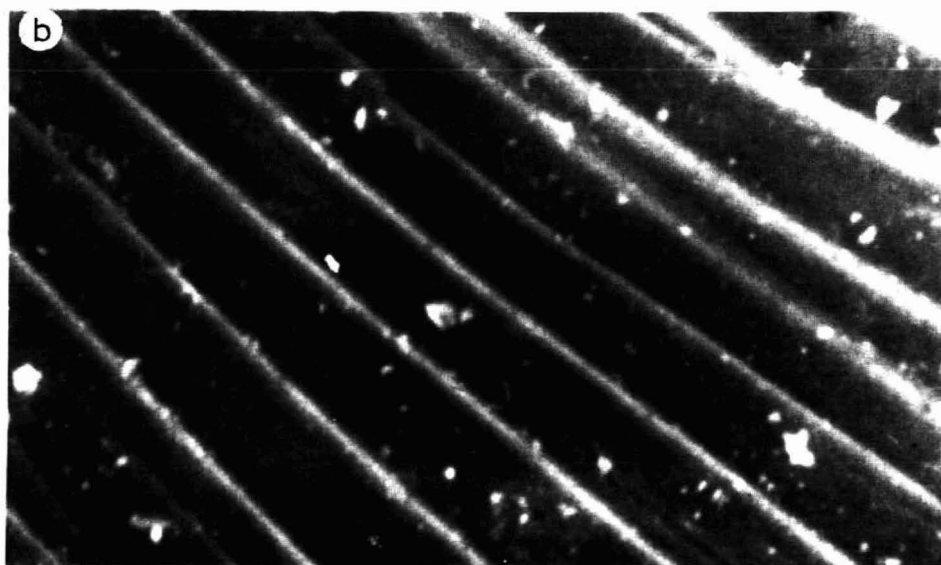
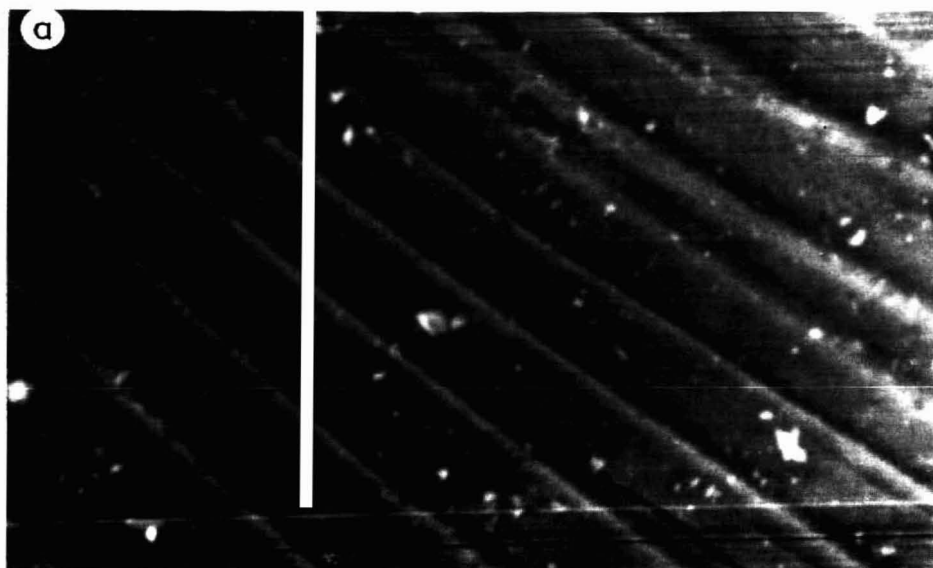


Fig. 10.

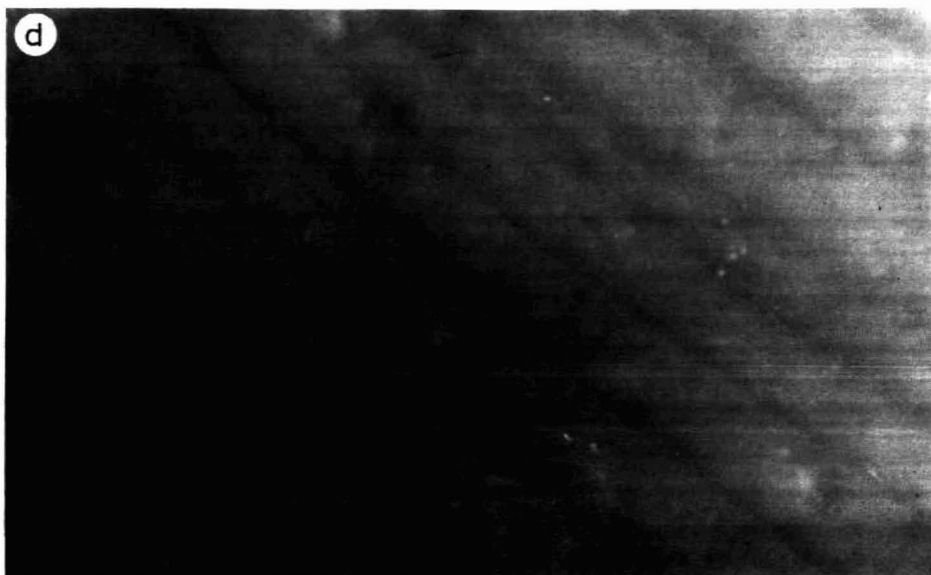
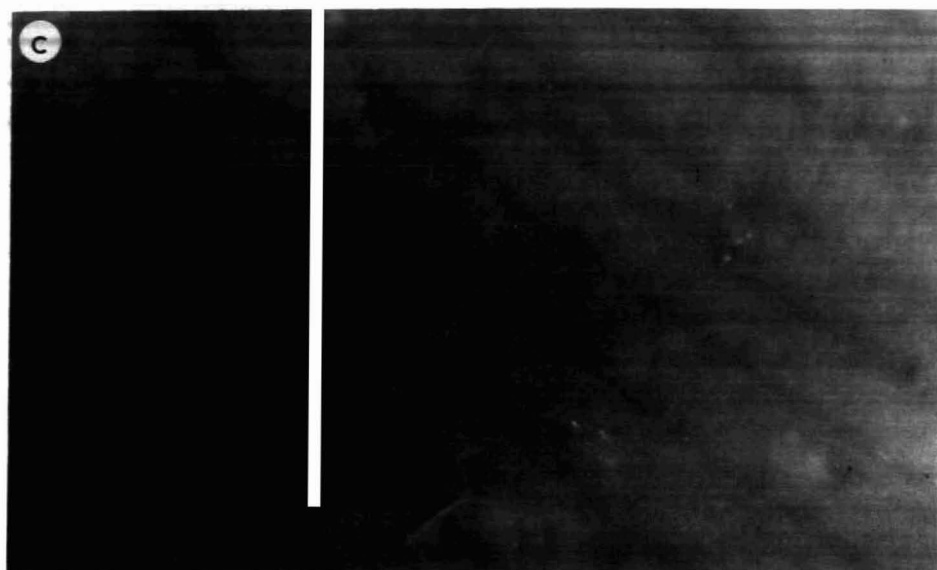


Fig. 10. Surface of Carbosil observed by SEM. Details as in Fig. 9.

carbon-silica adsorbent consists of silica and a deposited layer of carbon by dissolving silica in hydrofluoric acid the following samples were examined by TEM: carbon replica together with a carbon deposit (Fig. 1), carbon-platinum replica together with a carbon deposit (Fig. 2) and a carbon deposit alone (Fig. 3). The TEM micrographs were obtained using a TESLA BS 613 apparatus, magnification $\times 5000$.

For SEM, the initial silica gel and one of the Carbosils were chosen. Uncovered samples and those covered by a conductive layer of gold layer were examined. The micrographs were obtained by a SEM apparatus Type MR 1000 equipped in a two-detector system with two opposite Everhart-Thornley detectors², magnification $\times 1000$. Parts a of Figs. 4-8 show the surfaces of samples prepared by the carbon replica technique, parts b show the surfaces of samples prepared by the carbon-platinum replica technique and parts c show the film of carbon deposited directly on the silica gel by pyrolysis. The pictures are formed by the electrons transmitted through the layer of the evaporated carbon and carbon deposit (a), or the evaporated carbon-platinum and carbon deposit (b) and directly through the carbon deposit (c). It is seen that the pictures of the surface of each adsorbent are different and depend on the method of preparation. The micrographs in Figs. 4-8a are not very informative because the contrast is poor. In Figs. 4-8b the details of the surface are more visible. A comparison of the pictures for the initial silica gel (Figs. 4b) with those for adsorbents A1-A4 (Figs. 5-8b) indicates that during pyrolysis topographic changes take place. By use of the carbon-platinum replica technique it is possible to observe these topographic changes, but it is not possible to detect the carbon deposit. The morphology of carbon deposit can be examined using the electron diffraction technique³.

The aim of the SEM examination was to determine how the method of prep-



Fig. 11. Surface of the initial silica gel covered by a gold layer, as observed by SEM; magnification $\times 1000$.

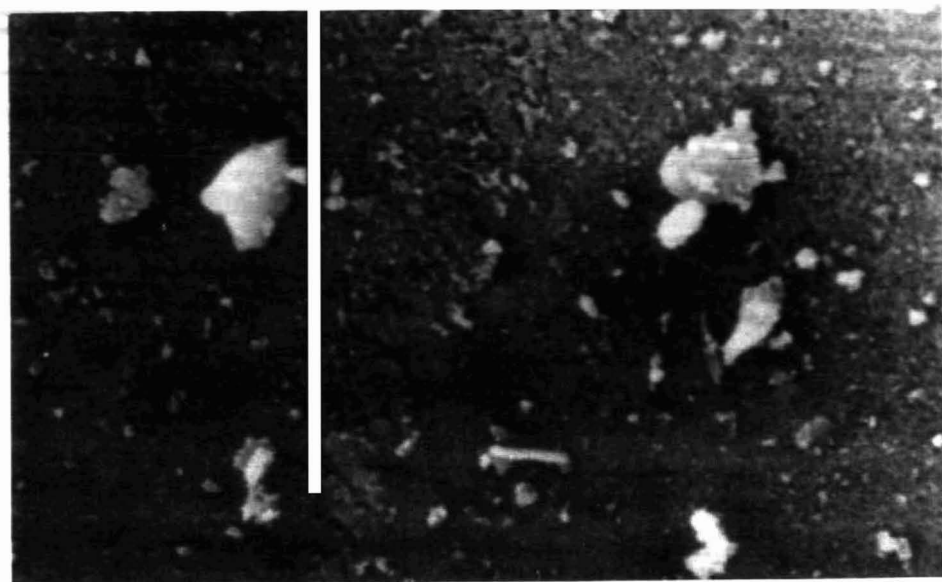


Fig. 12. Surface of Carbosil covered by a gold layer, as observed by SEM; magnification $\times 1000$.

aration of the samples and the system of detection influence the information obtained from the surface of the adsorbent. Figs. 9 and 10 show the SEM pictures observed for the same place on the sample obtained by use of different detection modes. Fig. 9 depicts the surface of silica gel without a gold layer. The typical charge effect for uncovered inorganic materials was observed. Topographic details could not be detected, the contrast and the resolution being poor because the brightness of the edges was strong. Fig. 10 depicts the surface of Carbosil, where the silica gel is covered by a layer of carbon which eliminates the charge effect. The lack of this effect is proof that a carbon deposit is present on the silica surface.

Figs. 11 and 12 present the same silica gel and Carbosil but covered by a gold layer. Although this layer eliminates the charge effect, it is still impossible to distinguish carbon from silica gel.

CONCLUSIONS

(1) By using different techniques of sample preparation for TEM, different features of the sample surface can be observed.

(2) The carbon-platinum replica technique of sample preparation is the most appropriate for TEM examination of the surface of Carbosils.

(3) The direct deposition of carbon is suitable for morphological examination, *e.g.*, by electron diffraction.

(4) By elimination of the charge effect it can be concluded that carbon is present on the surface of the silica gel, but distinction between carbon and silica by SEM is not possible. This is because the coefficients of the backscattered electrons for carbon and for silica are similar.

One of the most characteristic chromatographic parameters is the specific sur-

face area, which according to Guillemin⁴ should not be neglected. The pore diameter is directly related to the specific surface area. By use of the replica technique, which gives an impression of the surface, a relationship between the microscopic picture and the pore diameter can also be found.

Carbosil A2 had the highest value of the surface area (Fig. 6b) and Carbosil A4 the lowest one (Fig. 8b). The value of the pore structure (Fig. 6b and Fig. 8b) seems to be opposite to the value of the surface of these two adsorbents. The Carbosils had increasing amounts of carbon (% w/w, see Table I) on their surfaces (Figs. 5–8c). Fig. 5c shows the film of carbon deposit on Carbosil A1 (0.8% w/w) which seems to be homogeneous, while Fig. 8c shows the corresponding film for Carbosil A4 where the process of carbon agglomeration takes place (2.21% w/w).

Further investigations will be undertaken in order to determine to what extent the different methods of preparation of the carbon-silica adsorbents influence the morphology of the carbon deposit and its crystalline structure.

ACKNOWLEDGEMENT

We are grateful to Professor L. Reimer, Muenster University, for discussions and the SEM measurements in his laboratory.

REFERENCES

- 1 E. Tracz, J. Skubiszewska and R. Leboda, *J. Chromatogr.*, 287 (1984) 136–147.
- 2 L. Reimer, *Quantitative Electron Microscopy, Proc. 25th Scottish Universities Summer School in Physics, Glasgow, 1983*, pp. 217–250.
- 3 E. Tracz, E. Mizera and R. Leboda, to be published.
- 4 C. L. Guillemin, *J. Chromatogr.*, 158 (1978) 21–32.

CHROM. 17 952

Note

Comparative gas chromatographic studies of bonded and physically coated PEG 20M and its derivative phases with reference to some high-boiling isomeric solutes

S. B. BENDRE, A. N. KADAM and B. B. GHATGE*

National Chemical Laboratory, Pune 411 008 (India)

(First received March 18th, 1985; revised manuscript received May 30th, 1985)

Aue and co-workers^{1,2} first reported the abnormal behaviour of polyethylene glycol (PEG) stationary phases which remain chemically bonded with siliceous supports. Rapid mass transfer in the chemically bonded phases occurs as the film thickness is small³. They are sufficiently thermally stable and efficient⁴. Six to ten-fold reductions in retention times with enhancement of resolution have been observed on bonded phases compared with the corresponding coated phases. Their advantages over physically coated stationary phases have also been reported⁴. Even though the characteristics of PEG have been studied in detail¹, its possible utility over a wide temperature range needs further investigation. This paper describes the utility of chemically bonded PEG 20M and its derivatives as stationary phases for gas chromatography (GC). The retention behaviour of some high-boiling isomeric solutes, such as naphthols, naphthylamines and dihydroxybenzenes, has been studied.

EXPERIMENTAL

Materials

The following stationary phases based on PEG 20M (Varian Aerograph, Cat. No. 82-11:5) were used: PEG 20M diterephthalate (CTPA), PEG 20M disalicylate (CS) and PEG 20M dioleate (CoA), synthesized by methods described in the literature^{5–7}.

Chemically bonded stationary phases based on PEG-20M were prepared by Aue *et al.*'s procedure¹. Packed columns for bonded and conventional coated phases were prepared using stainless-steel tubes (2 m × 3 mm I.D.).

The solid support used was Celite (80–120 mesh) (BDH, Poole, UK). The column parameters are given in Table I.

Solutes

Anisidines, toluidines, nitrotoluenes, naphthylamines, naphthols, catechol, hydroquinone and resorcinol were used. Their purities were tested by measuring their melting points and were greater than 95%.

TABLE I
COLUMN PARAMETERS

No.	Stationary phase	Coating (%)	Total filling (g)	No.	Stationary phase	Amount bonded (%)	Total filling (%)
I	PEG 20M	1	10	I'	PEG 20M	0.1	10
II	CTPA	3	10	II'	CTPA	0.27	10
III	Cs	3	10	III'	Cs	0.28	10
IV	CoA	3	10	IV'	CoA	0.28	10

Apparatus

For GC studies, an AMIL-NCL dual-column gas chromatograph equipped with a thermal conductivity detector and a data processing system was used.

Procedure

The following operating parameters were used: column temperature, 130, 170 and 200°C; injector temperature, 170, 220 and 240°C, respectively; detector temperature, 180, 230 and 250°C, respectively; flow-rate of carrier gas (hydrogen), 100 ml/min; bridge current, 125 nA; and recorder operating speed, 600 mm/h.

RESULTS AND DISCUSSION

GC analysis on bonded stationary phases at 200°C showed a considerable reduction in retention time and efficient resolution compared with the results given by the corresponding coated stationary phases (Table II). Efficient resolution of *m*- and *p*-anisidines, -toluidines and -nitrotoluenes was achieved at 130°C. Usually non-polar stationary phases are recommended for analysis of high-boiling compounds such as naphthylamines, naphthols and dihydroxybenzenes. However, they are conveniently eluted and separated on all bonded phases. They cannot be eluted on the corresponding coated phases (1%) even at 200°C.

The order of bonding of PEG 20M and its derivative phases with the silanol (SiOH) groups of the support⁸ was expected to be PEG 20M > CS > CTPA > CoA. However, almost identical amounts of each derivative remained unextractable and assumed to be chemically bonded. Probably these molecules lie within the Van der Waals radius where Van der Waals forces⁹ interact to form partial chemical bonds such as hydrogen bonds, preventing their solvent extraction. The enhanced resolving power may be the result of sieving through gaps among the bristles in addition to donor-acceptor end groups.

CONCLUSION

The advantages of the bonded stationary phases are a substantial reduction in retention time and a lower operating temperature of about 70°C, a higher resolving power and sharp peaks as the absorption is negligible.

TABLE II
RESULTS OF ANALYSES ON COATED AND BONDED STATIONARY PHASES

The relative retention times (for *m*- and *p*-isomers relative to the corresponding *o*-isomers = 1) are given. Values in parentheses are absolute retention times (s). Column temperature, 200°C.

Sample	Coated phase			Bonded phase				
	I	II	III	IV	I'	II'	III'	IV'
<i>o</i> -Anisidine	1 (28.5)	1 (114.7)	1 (156.5)	1 (101.1)	1 (6.5)	1 8.0)	1 (9.6)	1 (13.0)
<i>m</i> -Anisidine	2.40	2.33	2.31	2.32	2.15	2.00	2.24	2.15
<i>p</i> -Anisidine	1.97	1.83	1.79	1.82	2.02	1.79	2.00	2.00
<i>o</i> -Toluidine	1 (17.5)	1 (68.1)	1 (94.0)	1 (61.0)	1 (4.4)	1 (5.0)	1 (5.6)	1 (7.5)
<i>m</i> -Toluidine	1.14	1.14	1.10	1.12	1.32	1.04	1.23	1.23
<i>p</i> -Toluidine	1.09	1.03	1.03	1.04	1.14	1.22	1.09	1.21
<i>o</i> -Nitrotoluene	1 (17.2)	1 (68.6)	1 (92.5)	1 (61.0)	1 (5.0)	1 (5.5)	1 (5.5)	1 (8.1)
<i>m</i> -Nitrotoluene	1.23	1.28	1.26	1.23	1.1	1.16	1.29	1.28
<i>p</i> -Nitrotoluene	1.41	1.43	1.42	1.41	1.4	1.44	1.73	1.49
α -Naphthylamine	—	—	—	—	1 (49.0)	1 (65.0)	1 (86.7)	1 (122.5)
β -Naphthylamine	—	—	—	—	2.18	2.05	2.16	2.15
α -Naphthol	—	—	—	—	1 (94.0)	1 (119.0)	1 (153.6)	1 (231.0)
β -Naphthol	—	—	—	—	1.04	1.13	1.24	1.08
Catechol	—	—	—	—	1 (54.0)	1 (62.0)	1 (84.5)	1 (129.5)
Hydroquinone	—	—	—	—	1.44	1.72	2.74	2.57
Resorcinol	—	—	—	—	1.81	3.45	3.63	3.03

REFERENCES

- 1 W. A. Aue, C. R. Hastings and S. Kapila, *J. Chromatogr.*, 77 (1973) 299.
- 2 W. A. Aue and D. R. Younker, *J. Chromatogr.*, 88 (1974) 7.
- 3 I. Sebastian and I. Halasz, *Angew. Chem., Int. Ed. Engl.*, 8 (1969) 453.
- 4 S. Mori, *J. Chromatogr.*, 135 (1977) 261.
- 5 B. Byare and G. Jordhan, *J. Gas Chromatogr.*, 2 (1964) 304.
- 6 K. Grob, *J. Gas Chromatogr.*, 3 (2) (1965) 52.
- 7 K. Assmann, G. Geppert, H. G. Struppe and O. Serfas, *Gas Chromatographie*, Akademie-Verlag, Berlin, 1968, p. 33.
- 8 I. Halasz and I. Sebastian, *J. Chromatogr. Sci.*, 12 (1974) 161.
- 9 A. V. Kiselev, N. V. Kovaleva and Yu. S. Nikitin, *J. Chromatogr.*, 58 (1971) 19.

CHROM. 17 989

Note

Determination of furosine by gas-liquid chromatography

W. BÜSER

Untersuchungsinstitut des Sanitätsdienstes der Bundeswehr I, Kopperpahler Allee 120, 2300 Kronshagen (F.R.G.)

and

H. F. ERBERSDOBLER*

Institut für Humanernährung und Lebensmittelkunde der Christian-Albrechts-Universität Kiel, Düsternbrook Weg 17–19, 2300 Kiel (F.R.G.)

(Received July 1st, 1985)

We have recently published¹ a method for the determination of lysinoalanine, a product of heat-damaged proteins, by gas-liquid chromatography (GLC). The question then arose as to whether this method would also be able to determine simultaneously furosine, another indicator of heat damage, lysinoalanine and the main nutritive amino acids. Furosine, ϵ -N-(2-furoylmethyl)-L-lysine, is formed at a constant rate from fructoselysine or lactuloselysine during hydrolysis with 7.75 M hydrochloric acid (Fig. 1). We first detected this helpful indicator of the main products of early Maillard reaction 20 years ago². Heyns *et al.*³ and Finot *et al.*⁴ investigated its structure and called it furosine. Meanwhile, furosine proved to be an ideal indicator

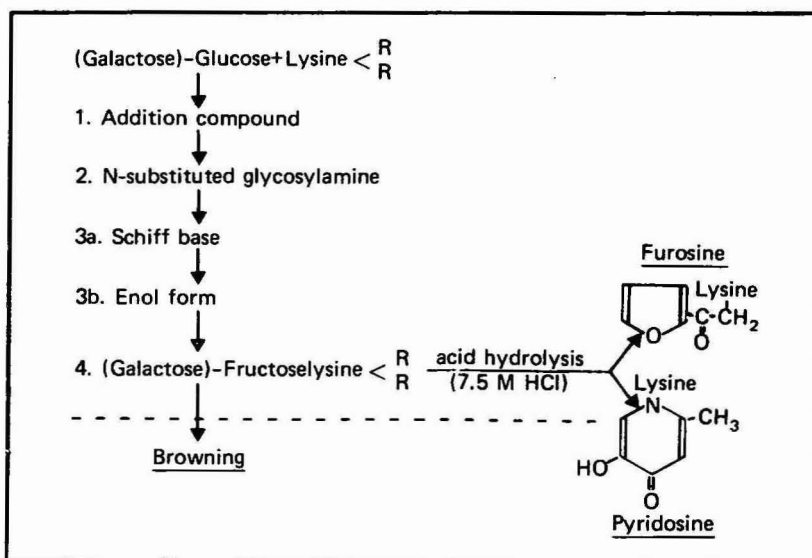


Fig. 1. Initial steps of the Maillard reaction with formation of furosine and pyridosine.

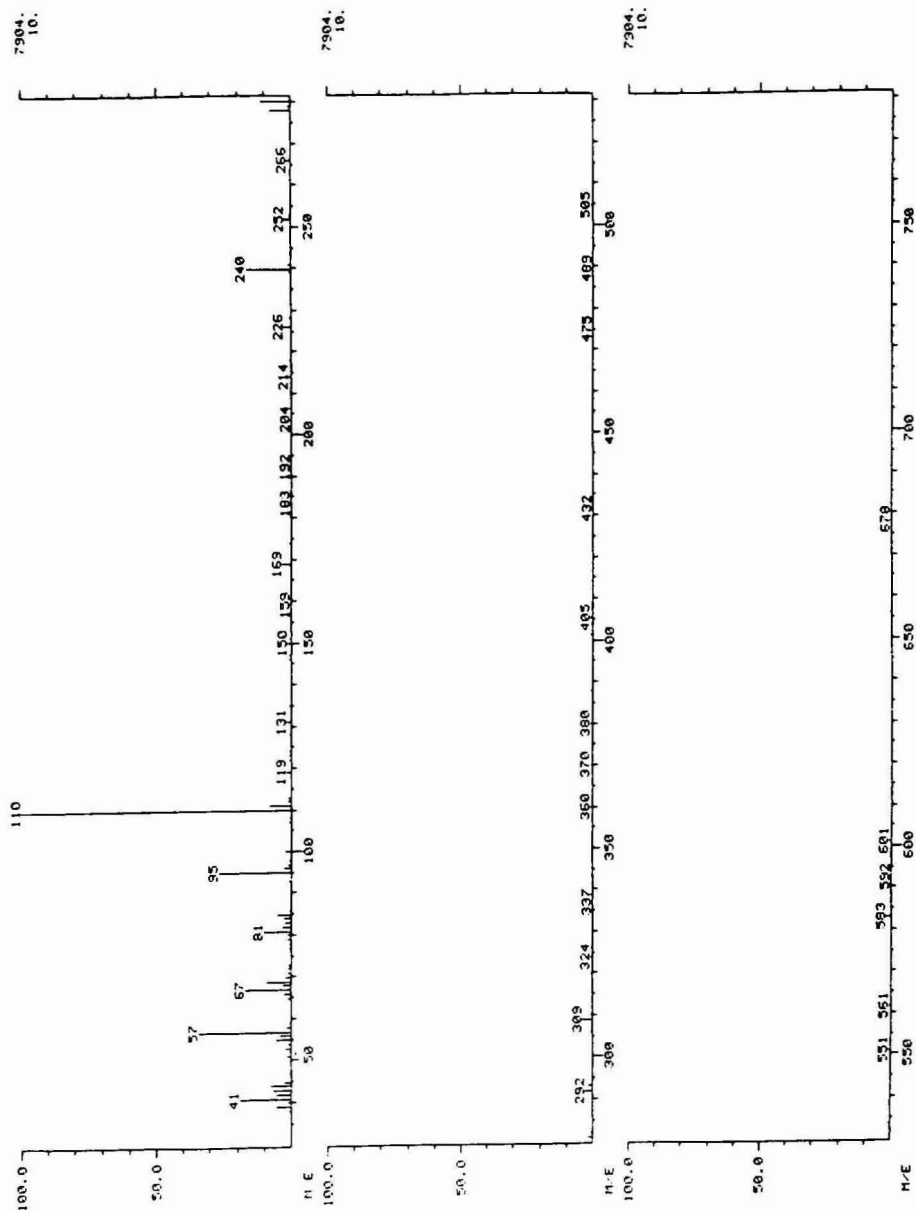


Fig. 2. Mass spectrum of the heptafluorobutyl isobutyl ester of furosine, measured with a 1020 MAT Finnegan quadrupole mass spectrometer operating at 70 eV, after GLC separation. The observed peaks at m/e 110 and 95 correspond to the 2-furoylmethyl moiety of furosine.

of the above mentioned amadori compounds which themselves are very unstable during the hydrolysis of heat-damaged proteins. Furosine determinations are applied in food science and nutrition, protein evaluation and quality control, *e.g.*, ref. 5, as well as in clinical research and in medical biochemistry for diabetic control and measuring the damage caused to proteins by elevated blood sugar concentrations, *e.g.*, ref. 6.

A method for the simultaneous determination of furosine and lysinoalanine by ion-exchange chromatography was published by us in 1979⁷. The determination of pyridosine, a second derivative formed upon acid hydrolysis of the fructoselysine moiety, proposed proved not to be easy in routine analyses of commercial food samples, but seems to be applicable in the GLC method described here. Furthermore, the method presented is suitable for those food laboratories which are not equipped with an amino acid analyser. To our knowledge, this is the first method to determine furosine and pyridosine by GLC.

EXPERIMENTAL

The material and methods were similar to those described previously¹. Furosine and the other amino acids were determined as their heptafluorobutyl isobutyl esters using a thermionic phosphorus–nitrogen detector¹ as described by MacKenzie and Tenaschuk⁸. As a pure standard for furosine and pyridosine is not available, we used a hydrolysate of pure ϵ -fructoselysine (prepared some years ago⁹) in order to detect the furosine and pyridosine peaks on the GLC chromatogram. Moreover, the identification of these peaks was confirmed by GLC–mass spectrometry (MS). The mass spectrum of the heptafluorobutyl isobutyl ester of furosine was comparable to that of the trifluoroacetyl methyl ester reported by Finot *et al.*⁴, as regards the main peaks, including the base peak corresponding to the 2-furoylmethyl moiety which is not derivatized. These peaks could also be found in the mass spectrum of furyl-2-methylketone. An example of the mass spectra is given in Fig. 2.

Furthermore, several hydrolysates from our routine analyses on an amino acid analyser, known to be rich in furosine, were used for comparison. A GLC chromatogram from such a food sample is shown in Fig. 3.

The compounds to be analysed and all the other amino acids for GLC analysis were prepared by esterification with isobutanol-3 *M* hydrochloric acid and acylation with heptafluorobutyric anhydride as described previously¹. The food samples corresponding to 200 mg of crude protein ($N \times 6.25$) were hydrolysed in Pyrex glass bottles with 25 ml of 7.75 *M* hydrochloric acid for 23 h at 110°C in an oven. Compared to the hydrolysis with 6 *M* hydrochloric acid (yield 20%), the higher concentration of acid gives a greater yield of furosine (constant in the range 32–36%)^{5,7,10}.

The chromatography was performed by using a Sigma 1 B gas chromatograph (Perkin-Elmer, Überlingen, F.R.G.) with a thermionic phosphorus–nitrogen detection (PND) as described previously¹. The mass spectrum of the heptafluorobutyl isobutyl ester of furosine was measured with a 1020 MAT quadrupole mass spectrometer (Finnegan, Bremen, F.R.G.) operating at 70 eV, after GLC separation on a 30-m fused-silica capillary column. The oven was programmed from 60 to 280°C at 20°C/min.

The calculation of the furosine content leads only to semiquantitative and

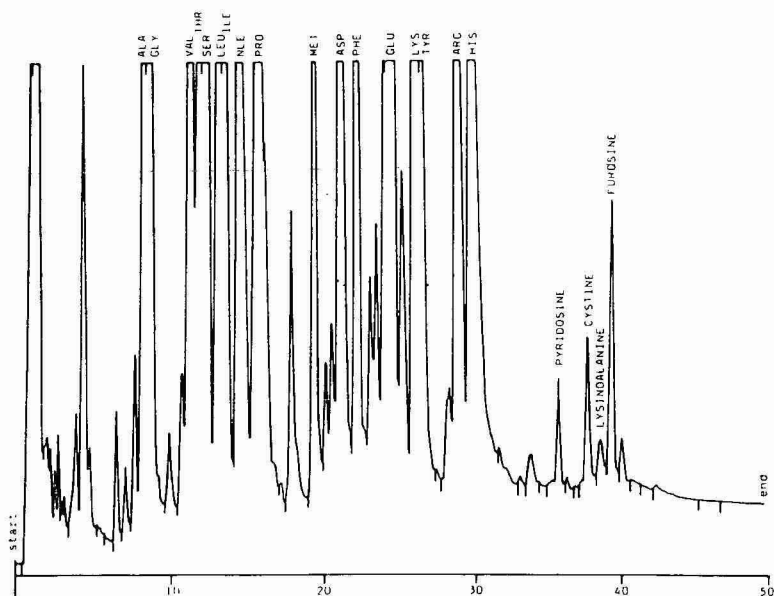


Fig. 3. Chromatogram of a hydrolysate from sterilized coffee cream showing the amino acid heptafluorobutyryl isobutyl esters. In order to obtain measurable values of the interesting substances, the concentration of hydrolysate (and of the most common amino acids) is greatly increased.

relative values since no furosine standard was available. The behaviour of the derivatives during chromatographic separation and the assumption that the response factors of the amino acids, using nitrogen-selective detection, depend on the nitrogen content of the molecule, formed the basis of the approximate calculation. Considering the nitrogen contents of the common amino acids and their response factors, a response factor of about 1.0 for furosine and pyridosine can be assumed. The furosine contents of food samples analysed by the GLC method were in good agreement with the amounts determined by ion-exchange chromatography (IEC) using the ninhydrin reaction for detection and another method of calculation.

RESULTS AND DISCUSSION

As Fig. 3 shows, the peak of furosine is fairly well separated from that of lysinoalanine. Difficulties are encountered only when there are very different amounts of furosine and lysinoalanine in a sample. Pyridosine is easily detectable and present in considerable amounts. Owing to the use of PND, purification of the samples was not necessary even in dark brown food material. One analysis requires approximately 50 min. The sensitivity of the determination is similar to that of normal IEC as is seen from Fig. 4. This figure shows a comparison of the furosine levels in ultra high temperature-(UHT)-treated milk samples analysed by IEC and by GLC. It should be mentioned that the detection of furosine in fresh commercial UHT-treated milks was not possible in earlier investigations¹¹ and can be performed only with the new and more sensitive generation of amino acid analysers.

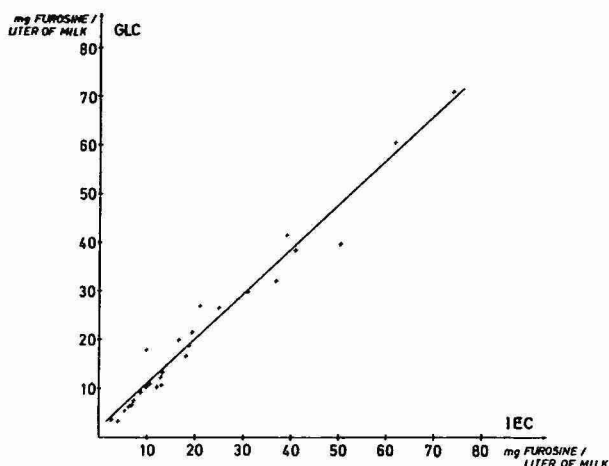


Fig. 4. Comparison of furosine determinations by IEC and the present GLC method. The results shown are given as mg furosine per litre of UHT-treated milk: $y = 0.92x + 1.89$; correlation coefficient, $R = 0.98$.

The advantage of the method presented here is that lysinoalanine, furosine and pyridosine can be analysed simultaneously, which is difficult to achieve by IEC. In particular, pyridosine is not easily detectable by an amino acid analyser equipped with highly resolving resins for rapid analyses. The fact that pyridosine is helpful in the evaluation of heat damage is demonstrated in Fig. 5. The ratio of furosine to pyridosine is not always constant in every kind of food, but there is a significant correlation in milk products.

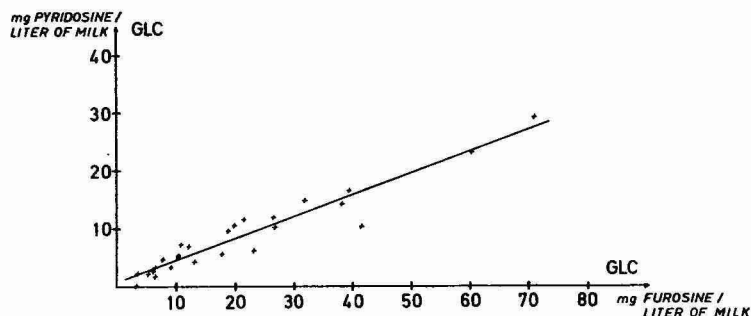


Fig. 5. Correlation between furosine and pyridosine determined by the present GLC method. The results are given as mg furosine and pyridosine per litre UHT-treated milk: $y = 0.38x + 0.73$; $R = 0.96$.

However, with the method presented here it seems to be possible for a laboratory equipped with a gas-liquid chromatograph and a thermionic phosphorus-nitrogen detector to analyse furosine and pyridosine in food samples and biological fluids.

ACKNOWLEDGEMENT

We thank Dr. P. Rösner, Kriminalpolizeiamt Kiel, for obtaining the mass spectra and for helpful comments.

REFERENCES

- 1 W. Büser and H. F. Erbersdobler, *J. Chromatogr.*, 303 (1984) 234.
- 2 H. Erbersdobler and H. Zucker, *Milchwissenschaft*, 21 (1966) 564.
- 3 K. Heyns, J. Heukeshoven and K.-H. Brose, *Angew. Chem.*, 80 (1968) 627.
- 4 P. A. Finot, J. Bricout, R. Viani and J. Mauron, *Experientia*, 24 (1968) 1097.
- 5 J. Steinig and A. Montag, *Z. Lebensm.-Unters.-Forsch.*, 174 (1982) 453.
- 6 E. Schleicher and H. O. Wieland, *J. Clin. Chem. Clin. Biochem.*, 19 (1981) 81.
- 7 H. F. Erbersdobler, B. Holstein and E. Lainer, *Z. Lebensm.-Unters.-Forsch.*, 168 (1979) 6.
- 8 S. L. MacKenzie and D. Tenaschuk, *J. Chromatogr.*, 171 (1979) 195.
- 9 H. F. Erbersdobler, A. Brandt, E. Scharrer and B. von Wangenheim, *Prog. Food Nutr. Sci.*, 5 (1981) 257.
- 10 P. A. Finot and J. Mauron, *Helv. Chim. Acta*, 55 (1972) 1153.
- 11 A. B. Möller, A. T. Andrews and G. C. Cheeseman, *J. Dairy Res.*, 44 (1977) 267.

Note

Determination of phenylurea herbicides by high-performance liquid chromatography with electrochemical detection

GIUSEPPE CHIAVARI* and CECILIA BERGAMINI

Istituto Chimico "G. Ciamician" Università di Bologna, Via Selmi, 2, 40100 Bologna (Italy)

(First received February 18th, 1985; revised manuscript received July 5th, 1985)

Substituted phenylureas have been extensively manufactured and used as selective herbicides in agriculture. The need to monitor industrial effluents and to determine traces of such compounds in crops, surface waters and soils has led to the development of new or modified analytical methods.

Chromatographic methods using gas and liquid chromatography have been used for the phenylurea herbicides. However, the polar nature of such compounds, their thermolability and low vapour pressure make difficult the direct analysis by gas chromatography (GC). It is therefore usually necessary to derivatize such compounds, which generally requires an anhydrous medium, consistent reaction times and controlled conditions for removal of excess of the reagent heptafluorobutyric anhydride (HFBA)^{1,2}. An indirect method of analysis has also been used, based on hydrolysis of the herbicide to its aniline, derivatization and selective GC with an electron capture detector. However, this procedure is not very specific.

The advent of high-performance liquid chromatography (HPLC) and the use of bonded phases in reversed-phase chromatography has permitted the development of sensitive analytical procedures for the direct determination of organic compounds in water without derivatization. The HPLC of phenylureas has been reported^{3,4} using UV detection at 254 nm. Electrochemical detection—the monitoring of changes in current associated with the reduction and/or oxidation of sample component—has proven to be a highly selective and extremely sensitive method for HPLC. Readily oxidizable species such as aromatic amines, phenols and carbonyl compounds can be detected at picomole levels^{5–8}. In the present study we have examined the application of this method to the phenylureas.

EXPERIMENTAL

Apparatus

The HPLC system consisted of an Hewlett-Packard 1010 chromatograph with a TW 1515 reciprocating pump (Orlita), a Rheodyne rotary injection valve with 20- μ l loop and a Erbasil C₁₈, 10- μ m column (250 \times 4.6 mm). The electrochemical detector was a Metrohm Model 656 equipped with a glassy carbon working electrode, a glassy carbon counter electrode and a silver–silver chloride electrode, 3 M potassium chloride, as a reference. The surfaces of the glassy carbon electrodes were renewed each

day by mechanical polishing using alumina powder (0.3 μm). A Metrohm 641 potentiostat was employed and the detector output was displayed on a Houston Omniscrite recorder or on a C-R1A Shimadzu data processor.

The eluent was water (triply distilled)–methanol (HPLC) (30:70, v/v) containing an electrolyte (1 g/l lithium perchlorate and 0.05 g/l sulphuric acid). All experiments were done at ambient temperature.

Materials

The herbicide standards were gifts from the Presidi Multizonali di Prevenzione of Bologna and Forlì.

The soil was sprayed with an aqueous solution containing 1 g/l of Dicuran (Ciba-Geigy) which contains 43.6% of active chlortoluron (see Table I). Samples were collected 24 h after this treatment. A 10-g amount of soil was stirred in 50 ml water for 2 h. The pH was then adjusted to 10.5 with 0.1 *M* sodium hydroxide. After centrifugation for 5 min at 1500 g, 20 μl of the supernatant were injected for HPLC.

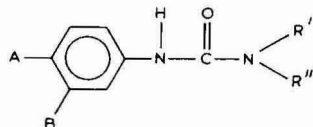
RESULTS AND DISCUSSION

Table I gives the names, structures and retention data for the twelve phenylureas studied. Fig. 1 shows a chromatogram of these compounds; a good separation is obtained for eight herbicides. Figs. 2–4 show the electrochemical responses of the phenylureas as a function of the applied potential. The responses are dependent on the anode conditions, but this does not affect the “relative” response; for a series of compounds. The use of sample concentrations higher than 10^{-5} *M* significantly re-

TABLE I

NAMES, STRUCTURES AND HPLC RETENTIONS (CAPACITY FACTORS, k') FOR PHENYLUREA HERBICIDES

Column: Erbasil C₁₈. Eluent: water–methanol (30:70, v/v) containing 1 g/l LiClO₄ and 0.05 g/l H₂SO₄.



Herbicide	Code	A	B	R'	R''	k'
Fenuron	Fe	H	H	CH ₃	CH ₃	0.86
Metoxyron	Mx	OCH ₃	Cl	CH ₃	CH ₃	1.21
Monuron	Mo	Cl	H	CH ₃	CH ₃	1.94
Fluometuron	Fm	H	CF ₃	CH ₃	CH ₃	2.02
Monolinuron	Ml	Cl	H	OCH ₃	CH ₃	2.59
Chlortoluron	Ct	CH ₃	Cl	CH ₃	CH ₃	3.10
Metobromuron	Mb	Br	H	OCH ₃	CH ₃	3.13
Isoproturon	Ip	(CH ₃) ₂ CH	H	CH ₃	CH ₃	3.36
Diuron	Di	Cl	Cl	CH ₃	CH ₃	4.38
Linuron	Li	Cl	Cl	OCH ₃	CH ₃	5.75
Neburon	Nb	Cl	Cl	C ₄ H ₉	CH ₃	12.65
Difluron*	Df	Cl	H	COC ₆ F ₂ H ₃	H	13.90

* N-*p*-chlorophenyl-N'-2,6-difluorobenzoylurea.

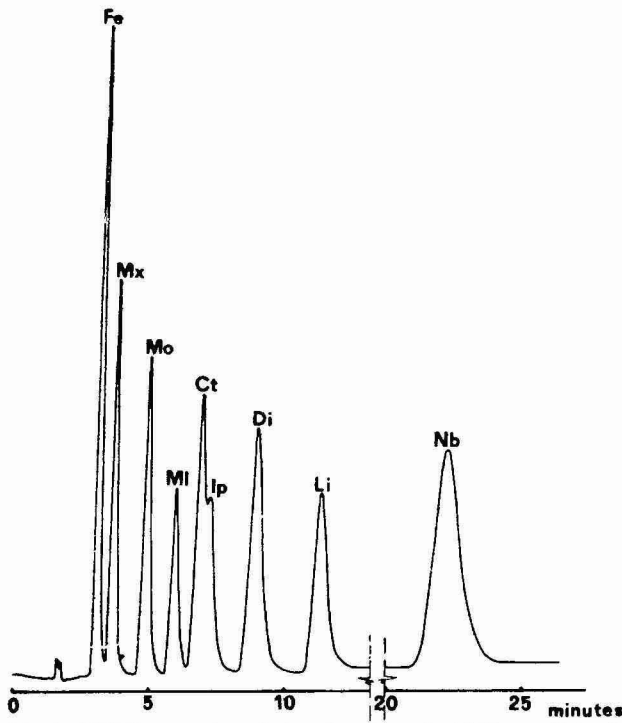


Fig. 1. HPLC separation of nine phenylurea herbicides on Erbasil C₁₈ with methanol–water (30:70) containing 1 g/l LiClO₄ and 0.05 g/l H₂SO₄ as eluent. Detector potential: 1.30 V.

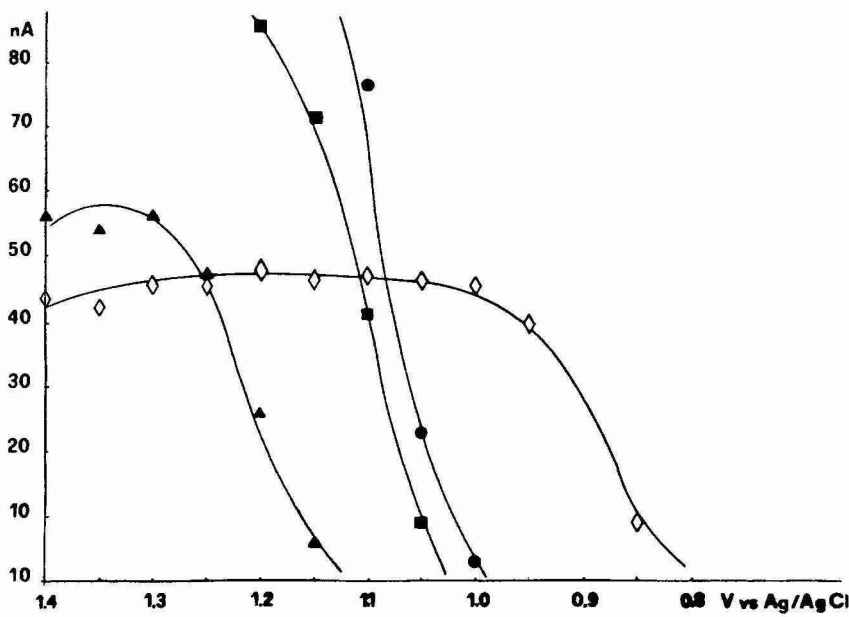


Fig. 2. Dependence of the electrochemical response (nA) on the applied potential (V, vs. Ag/AgCl) for 2 nmol each of fenuron (●—●), monuron (■—■), monolinuron (▲—▲) and metoxyron (◇—◇).

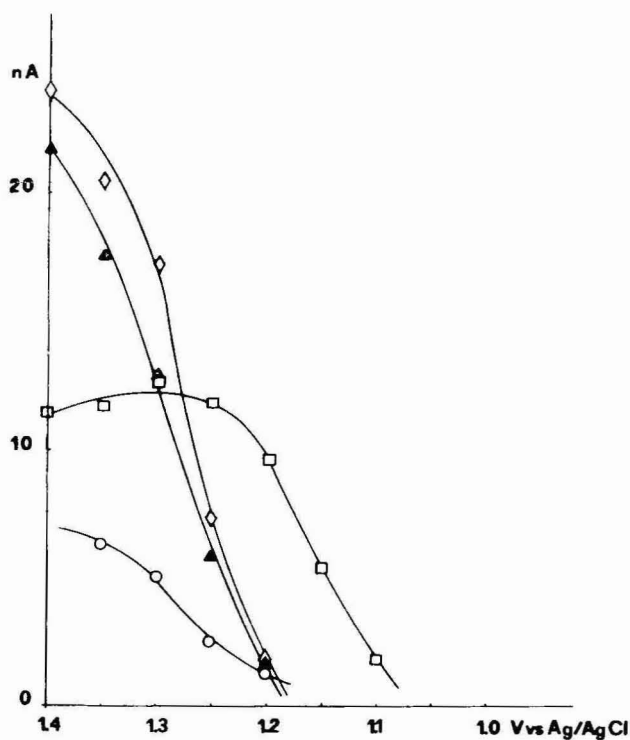


Fig. 3. Dependence of electrochemical response on applied potential as in Fig. 2 for difluron (○—○), fluometuron (▲—▲), neburon (□—□) and linuron (◇—◇).

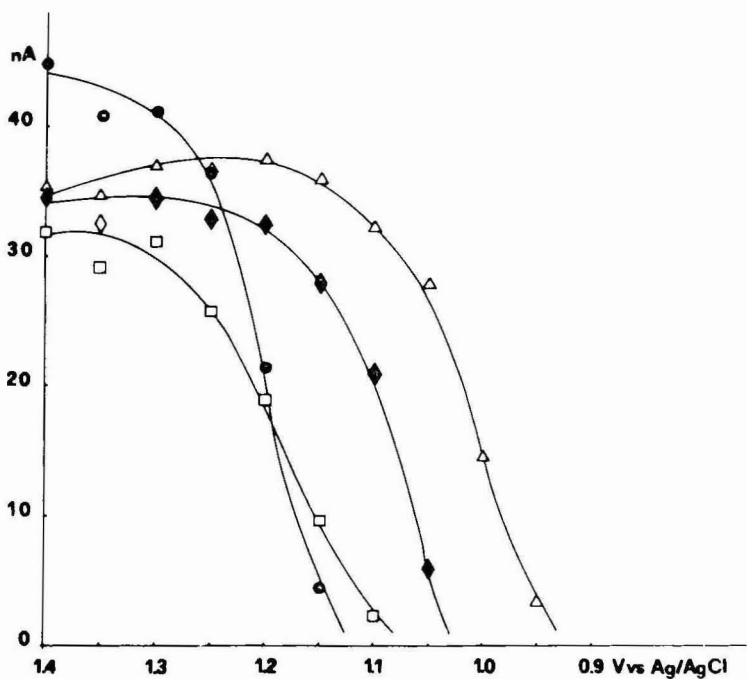


Fig. 4. Dependence of electrochemical response on applied potential as in Fig. 2 for metobromuron (●—●), isoproturon (△—△), chlortoluron (◆—◆) and diuron (□—□).

duces the electrode response after a few injections. In the case of more dilute solutions this problem can be neglected.

The curves for the individual herbicides are significantly different in response and shape. This fact can be usefully employed to vary the detection selectivity by simply changing the oxidation potential. Fig. 5 illustrates an application to a mixture of metabromuron and isoproturon; as reported in Table I, the separation of these two compounds is difficult because of the small difference in k' values and, in our case, still more problematic considering the concentration ratio (10:1). At an oxidation potential of +1.18 V, the two compounds, appear as a single peak with a shoulder on the tail; on lowering the potential, the response of metabromuron decreases and at +1.06 V only isoproturon is detectable. Similarly difficult separations such as monuron/fluometuron or chlortoluron/isoproturon can be solved by taking advantage of their different oxidation curves.

The detection limits for each compound are shown in Table II, based on a signal/noise ratio of ≥ 2 . Changes in $2k'$ or the detector potential will affect these values. In particular, the applied oxidation voltage affects the sensitivity; however, at higher potentials the background noise is increased.

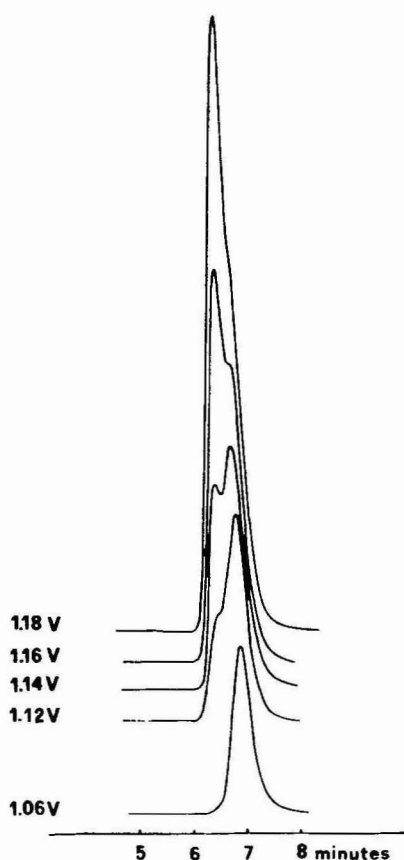


Fig. 5. Chromatogram of the pair metabromuron-isoproturon at various oxidation potentials.

TABLE II
LIMITS OF DETECTION

Based on the quantity required to give a response that is twice the noise level.

<i>Compound (code)</i>	<i>Limit (pmol)</i>	<i>Applied potential (V)</i>
Fe	7	1.25
Mx	6	1.25
Mo	5	1.25
Fm	18	1.25
Ml	6	1.25
Ct	6	1.25
Mb	6	1.25
Ip	6	1.25
Di	6	1.25
Li	8	1.25
Nb	30	1.35
Df	18	1.35

A plot of peak height vs. the amount of sample injected for metobromuron and linuron was linear between 5 and 200 pmol.

Studies are in progress to apply this method to the analysis of phenylureas in environmental samples and to determine whether its selectivity can circumvent the need for time-consuming clean-up procedures in order to remove interfering substances. A preliminary result is shown in Fig. 6; the chromatogram is of a soil sample treated as described in Experimental. The concentration of chlortoluron determined corresponds to a 10^{-5} M solution (21 mg per kg soil).

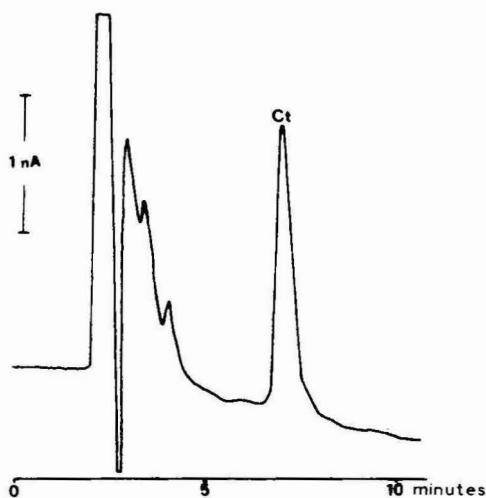


Fig. 6. Chromatogram of chlortoluron-treated soil extract: eluent as in Fig. 1. Detector potential: +11.18 V. Sensitivity: 5 nA f.s.

ACKNOWLEDGEMENT

The support of this work by C.N.R. Grant 83317/03 is gratefully acknowledged.

REFERENCES

- 1 A. de Kok, Y. J. Vos, van Garderen, T. de Jong, M. van Opstal, R. W. Frei, R. B. Geerdink and U. A. Th. Brinkman, *J. Chromatogr.*, 288 (1984) 71.
- 2 D. J. Caverly and R. C. Denney, *Analyst (London)*, 103 (1978) 368.
- 3 U. A. Th. Brinkman, A. de Kok and R. B. Geerdink, *J. Chromatogr.*, 283 (1984) 113.
- 4 A. de Kok, R. B. Geerdink and U. A. Th. Brinkman, *J. Chromatogr.*, 252 (1982) 101.
- 5 E. M. Lores, D. W. Bristol and R. F. Moseman, *J. Chromatogr. Sci.*, 16 (1978) 358.
- 6 V. Concialini, G. Chiavari and P. Vitali, *J. Chromatogr.*, 258 (1983) 244.
- 7 G. Chiavari, V. Concialini and P. Vitali, *J. Chromatogr.*, 249 (1982) 385.
- 8 G. Chiavari and C. Bergamini, *J. Chromatogr.*, 318 (1985) 427.

CHROM. 18 042

Note

Direct determination of acrylamide in tissue culture solution by liquid chromatography using column switching

NANCY L. FRESHOUR*, PATRICK W. LANGVARDT, STEPHEN W. FRANTZ and MARK D. DRYZGA

Health and Environmental Sciences, The Dow Chemical Company, 1803 Building, Midland, MI 48640 (U.S.A.)

(Received June 24th, 1985)

An analytical procedure for the determination of trace levels of acrylamide monomer (propenamide; AAm) in tissue culture solution was required for the development and use of a flow-through *in vitro* skin penetration technique. Applying this technique, a test compound or mixture is placed on a preparation of excised rat skin and penetration of the compound of interest is measured in the tissue culture solution flowing beneath the skin¹.

Although there were examples for the determination of acrylamide in complex biological and/or aqueous matrices^{2–4}, these methods all require time-consuming sample clean-up, and no specific method existed for this particular determination. A simplified technique was desired due to the expected sample load, however, the many interferences in the tissue culture solution matrix precluded direct quantitation of acrylamide by conventional analytical techniques⁵. By utilizing the different separating characteristics of two distinct liquid chromatographic (LC) columns, column switching⁶ provided the selectivity necessary for the direct determination of acrylamide in tissue culture solution at low ppb* concentrations.

This paper describes the instrumentation incorporated in the LC system used for the analysis, and includes validation data for the method.

MATERIALS AND METHODS

Materials

Chemicals used were acrylamide (99 + %, electrophoresis grade, Gold Label; Aldrich, Milwaukee, WI, U.S.A.); concentrated sulfuric acid (J. T. Baker, Phillipsburg, NJ, U.S.A.) and glass-distilled, deionized water. The tissue culture solution was minimum essential medium–D-valine (MEM D-VAL; Gibco Labs., Grand Island, NY, U.S.A.). It was buffered at a concentration of 25 mM 4-(2-hydroxyethyl)-1-piperazine-ethanesulfonic acid (HEPES, 99%; Sigma, St. Louis, MO, U.S.A.) and treated with an antimicrobial–antimycotic solution used at 1% strength (500 units penicillin, 500 µg streptomycin and 1.25 µg fungizone per 500 ml tissue

* Throughout the article the American billion (10⁹) is meant.

culture solution). The penicillin, streptomycin and fungizone were obtained from Sigma.

Standard preparation

A stock solution was prepared by dissolving a known weight of acrylamide in distilled, deionized water for a concentration of approximately 5000 $\mu\text{g/ml}$. This stock solution was diluted in water to concentrations in the range of 1.0 $\mu\text{g/ml}$ to 0.001 $\mu\text{g/ml}$ for a series of standards for analysis.

Sample preparation

No sample preparation was necessary; samples were injected directly into the LC system. Some samples were stored frozen and thawed to room temperature prior to analysis.

Preparation of fortified samples

Fortified tissue culture solution samples were prepared by adding an aliquot (usually 20–100 μl) of the appropriate acrylamide standard solution to a 2-ml or 5-ml sample of tissue culture solution. After spiking, the solution was shaken manually to ensure proper mixing.

Instrumentation and chromatography

Fig. 1 contains a schematic diagram of the LC system. A Varian Model 8050 LC Autosampler (Varian Assoc., Palo Alto, CA, U.S.A.) was used to inject samples into the system. Initial sample separation was done on column I, a 10- μm C₁₈ Radial-Pak column with a RCSS C₁₈ Guard-Pak (in a RCM-100 radial compression module). This column was preceded by a 2.54 \times 0.39 cm I.D. guard column packed with Bondapak C₁₈/Corasil 37–50 μm (all from Waters Assoc., Milford, MA, U.S.A.). A six-port valve (Rheodyne Model 7000 ARV switching valve with Model 7001 pneumatic actuator; Rheodyne, Cotati, CA, U.S.A.), in-line between the two analytical columns, was used to transfer automatically a selected fraction (spanning the retention time of acrylamide) from column I onto column II, a 11.0 \times 1.3 cm I.D. Aminex 50W-X4 30–35 μm column (Bio-Rad Labs., Richmond, CA, U.S.A.). Normally the valve was switched to "position B" 90 s after injection and then back to "position A" at 230 s (Fig. 1).

The flow of 0.001 *N* sulfuric acid (aqueous; filtered and degassed) mobile phase was maintained through column I at 3.0 ml/min (1000 p.s.i.) and at 1.5 ml/min through column II (<500 p.s.i.) by a pair of LDC ConstaMetric III pumps (LDC/Milton Roy, Riviera Beach, FL, U.S.A.). When the sample fraction was transferred between columns (valve position B) the flow through column I was temporarily 1.5 ml/min. A pre-column, 2.54 \times 0.39 cm I.D. Corasil Type II 37–50 μm (Waters Assoc.), was in-line between the pump delivering 3.0 ml/min and the sample injector.

A Kratos Spectroflow 773 ultraviolet detector (Kratos Analytical Instruments, Ramsey, NJ, U.S.A.) set at 210 nm, 0.005 A.U.F.S. and the time constant equal to 0.45, was used to monitor the effluent from column II. A Spectrum Model 1021A electronic filter (Spectrum Scientific, Newark, DE, U.S.A.) was placed between the detector and recorder to reduce high frequency noise (settings: output gain, 1; cut-off frequency, 0.01 Hz). A Varian A-25 recorder (Varian Assoc.) set at 2 mVfs as well

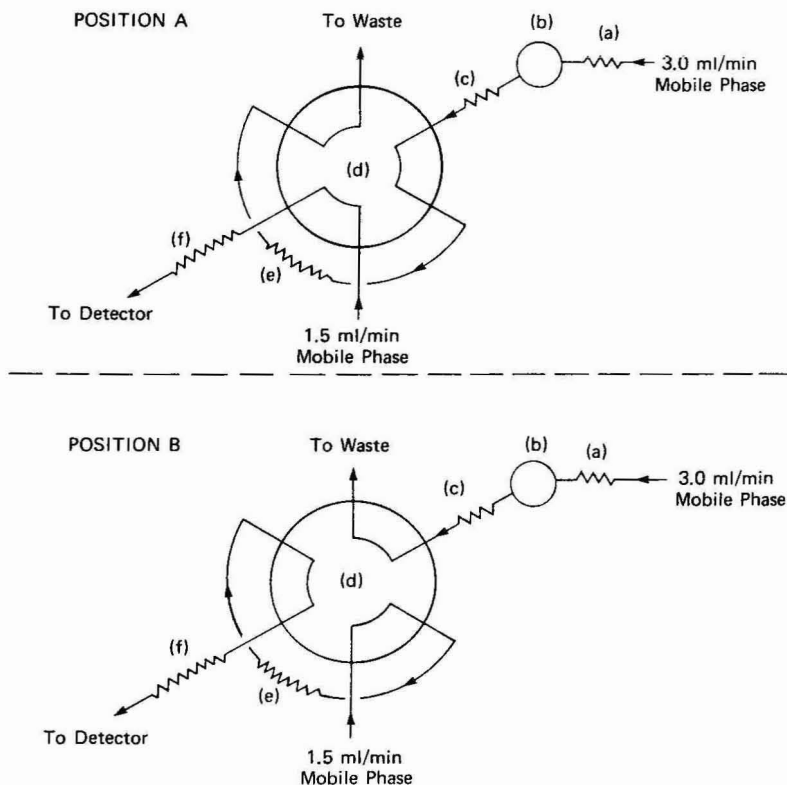


Fig. 1. Schematic of the LC system. Columns and valves: a = pre-column; b = autosampler injection valve; c = guard column; d = column-switching valve; e = column I, $10\ \mu\text{m}$ C_{18} Radial-Pak; f = column II, Aminex 50W-X4.

as a Hewlett-Packard 3354 laboratory automation system (Hewlett-Packard, Palo Alto, CA, U.S.A.) were used for data collection. (The laboratory automation system was also used to trigger the valve switching between analytical columns.) External standards were used to quantitate acrylamide concentrations in samples by peak height measurements.

RESULTS

Chromatography

The chromatographic profiles of blank tissue culture solution samples in contact with rat skin differed from those not in contact with rat skin and varied with time over the course of a 24-h skin penetration experiment. However, no significant interference was observed at the retention time of acrylamide using the column-switching technique.

Sensitivity

The limit of detection for acrylamide standards was $0.005\ \mu\text{g/ml}$. No response

was recorded for a 0.001- $\mu\text{g}/\text{ml}$ standard. The limit of quantitation for acrylamide spikes (in tissue culture solution) was 0.010 $\mu\text{g}/\text{ml}$. The acrylamide peak elutes on the tail of another peak precluding accurate quantitation below that concentration. (See Fig.2 for example chromatograms.)

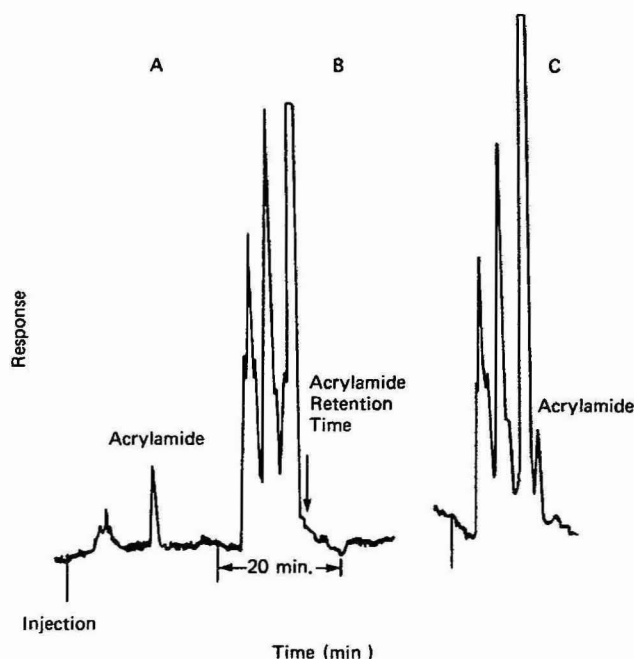


Fig. 2. Example chromatograms: (A) 0.010 $\mu\text{g}/\text{ml}$ acrylamide in water standard, (B) Blank pooled tissue culture solution in contact with rat skin, (C) 0.010 $\mu\text{g}/\text{ml}$ acrylamide spike in pooled tissue culture solution in contact with rat skin.

Linearity, recovery and reproducibility

The response for acrylamide was found to be linear for both samples and standards over the desired concentration range of 1.0 $\mu\text{g}/\text{ml}$ to 0.005 $\mu\text{g}/\text{ml}$ for this study. The mean recovery (\pm standard deviation) of acrylamide from spiked tissue culture solution samples based on five analyses at each of four concentration levels from 1.0 $\mu\text{g}/\text{ml}$ to 0.01 $\mu\text{g}/\text{ml}$ was $96.7 \pm 1.2\%$. The coefficient of variation ranged from 0.09% at a concentration of 0.998 $\mu\text{g}/\text{ml}$ to 2.3% at 0.01 $\mu\text{g}/\text{ml}$. Table I summarizes the AAm recovery data based on peak height measurements.

Stability

Long-term stability of samples was not evaluated for this study. However, fortified samples stored at approximately 1°C for one week or stored frozen for a few days then thawed prior to analysis showed no signs of acrylamide degradation.

TABLE I
ACRYLAMIDE RECOVERY DETERMINATIONS BY PEAK HEIGHT MEASUREMENTS

Acrylamide concentration (µg/ml)									
0.010									
0.050									
0.100									
0.998									
Peak height* of standard (cm)	Peak height* of spike (cm)	Peak height* of standard (cm)	Peak height* of spike (cm)	Peak height** of standard	Peak height** of spike	Peak height** of standard	Peak height** of spike	Peak height** of standard	Peak height** of spike
3.50	3.35	16.44	15.90	5382.91	5017.02	52 362.4	51 180.1		
3.38	3.34	16.30	15.80	5272.30	5142.74	52 857.1	51 264.4		
3.35	3.33	16.30	15.95	5269.57	5076.42	52 482.6	51 219.0		
3.32	3.31	16.52	15.90	5470.45	5106.62	52 824.6	51 177.3		
	3.24		15.90		5055.31		51 137.5		
Mean	3.29	16.39	15.89	5348.8	5079.6	52 631.7	51 195.7		
S.D.	0.08	0.11	0.05	96.8	48.0	246.8	48.0		
C.V. (%)	2.3	0.66	0.34	1.8	0.95	0.47	0.09		
Recovery (%)***		97.6	96.9		95.0		97.3		

* Measured manually.
** Determined using the laboratory automation system.
*** (Mean peak height of spike) – (mean peak height of standard) × 100 = recovery (%).

DISCUSSION

It was found that with constant use, the guard column needed to be changed periodically in order to prevent large, broad peaks from interfering with the analysis. These peaks were assumed to result from the breakthrough of slowly eluting substances that build up on the guard column.

The valve switching times needed to be reestablished each time the guard column was changed, but this could be done in about 1 h. Usually the switching times did not vary more than 30 s with the interval remaining virtually the same.

Peak area measurements were used in early method development. However, peak height measurements were shown to be more accurate for the low level determinations. This was probably due to the fact that the acrylamide peak in fortified tissue culture solution samples elutes on the tail of another peak (unlike standards in water) resulting in less accurate peak integration. A computer program facilitated automated peak height determinations via the laboratory automation system.

CONCLUSIONS

An LC procedure using column switching has been developed and validated for the direct determination of acrylamide in tissue culture solution. This novel analytical approach has provided selective removal of interferences to enable sensitive detection of acrylamide at a relatively non-selective wavelength with no sample preparation necessary. This method will facilitate the evaluation of the skin penetration characteristics of acrylamide monomer and could likely find applications to other complex aqueous matrices.

ACKNOWLEDGEMENT

The authors wish to thank Roy A. Campbell for his technical assistance with the laboratory automation system during the development of this procedure.

REFERENCES

- 1 J. M. Holland, J. Y. Kao and M. J. Whitaker, *Toxicol. Appl. Pharmacol.*, 72 (1984) 272–280.
- 2 P. W. Langvardt, C. L. Putzig, J. D. Young and W. H. Braun, *Abstract No. 323 presented at the Eighteenth Annual Meeting of the Society of Toxicology, New Orleans, LA, March 1979.*
- 3 L. Brown, M. M. Rhead and K. C. C. Bancroft, *Analyst (London)*, 107 (1982) 749–754.
- 4 C. F. Poole, W.-F. Sye, A. Zlatkis and P. S. Spencer, *J. Chromatogr.*, 217 (1981) 239–245.
- 5 N. E. Skelly and E. R. Husser, *Anal. Chem.*, 50 (1978) 1959–1962.
- 6 L. R. Snyder and J. J. Kirkland, *Introduction to Modern Liquid Chromatography*, Wiley-Interscience, New York, 2nd ed., 1979, Ch. 16.

CHROM. 18 019

Note

Séparation et dosage des différents constituants de la troxérutine par chromatographie liquide haute performance en phase inverse

Application au contrôle pharmaceutique

M. D. LE HOANG, E. POSTAIRE*, P. PROGNON et D. PRADEAU

Laboratoires de Contrôle de Qualité, Pharmacie Centrale des Hopitaux de Paris, 7 rue du Fer à Moulin, 75005 Paris (France)

et

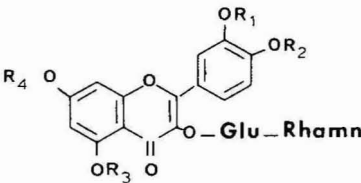
A. BLONDIN et J. SAUZIERE

Laboratoires NEGMA, 584 rue de Fourny, 78530 Buc (France)

(Reçu le 24 juin 1985)

La troxérutine est un dérivé des flavonoides destinée à réduire la fragilité et la perméabilité capillaire. Elle a été utilisée dans le traitement des hémorroïdes¹ et des désordres veineux des membres inférieurs². On note également quelques utilisations dans le cas de rétinopathies chez les diabétiques³ et de syndrome de Raynaud⁴.

La troxérutine commerciale n'est pas un composé chimiquement pur, il s'agit d'un mélange contenant 3 molécules: le trihydroxyéthylrutoside (tri-HER), composé majoritaire; le dihydroxyéthylrutoside (di-HER); le tétrahydroxyéthylrutoside (tétra-HER). Les structures chimiques sont reportées sur la Fig. 1.



	R ₁	R ₂	R ₃	R ₄
rutoside	H	H	H	H
di-HER	H	CH ₂ CH ₂ OH	H	CH ₂ CH ₂ OH
tri-HER	CH ₂ CH ₂ OH	CH ₂ CH ₂ OH	H	CH ₂ CH ₂ OH
tétra-HER	CH ₂ CH ₂ OH	CH ₂ CH ₂ OH	CH ₂ CH ₂ OH	CH ₂ CH ₂ OH

Fig. 1. Structure chimique des différents composés de la troxérutine.

En fait le dérivé le plus actif, le trihydroxyéthylrutoside est obtenu par action de la chlorhydrine du glycol sur la rutine, ce qui a pour conséquence l'obtention d'un dérivé hydrosoluble par l'introduction de groupements hydroxyéthyles⁵.

Le contrôle de la réaction étant délicat, on aboutit toujours à un mélange de trois dérivés substitués (di-, tri- et tétra-HER) contenant en majorité le dérivé tri-substitué.

Les polarités très proches de ces dérivés rendent impossible la purification totale du dérivé tri-HER.

C'est pourquoi, nous proposons ici une méthode de dosage de la troxérutine dans les matières premières destinées à la fabrication de différentes formes pharmaceutiques par chromatographie liquide avec appariement d'ions.

En effet, si la littérature est riche en travaux concernant la séparation par chromatographie liquide des flavonoides d'origine végétale⁶⁻⁸, peu d'auteurs se sont intéressés à l'analyse des flavonoides glycosylés⁹⁻¹², en particulier la rutine^{14,15}, et encore moins de travaux concernent les dérivés hydroxyéthyl rutosides¹⁶⁻²⁰.

Courbat *et al.*^{5,17} ont étudié leur séparation par chromatographie sur papier et leur identification par spectroscopie dans l'ultra-violet; Tan *et al.*¹⁸ ont proposé une méthode de dosage spectrofluorimétrique du dérivé tri-HER dans l'urine. Ainsi, à notre connaissance, aucune technique simple de chromatographie liquide haute performance n'avait été appliquée à la séparation des trois dérivés hydroxyéthyles du rutoside.

MATÉRIEL ET MÉTHODE

Appareillage

Le chromatographe Hewlett-Packard 1090 équipé d'un détecteur spectrophotométrique à réseau de diodes, réglé à 254 nm, longueur d'onde correspondant au maximum d'absorption de ces composés, et d'un injecteur à boucle (5 μ l) Rhéodyne 7010.

Les chromatogrammes sont enregistrés par un intégrateur Hewlett-Packard 3390 A.

Le spectromètre de masse est un Nermag 10 C, la température de la source est de 150°C.

Colonnes

Les colonnes suivantes ont été utilisées: colonne μ Bondapak C₁₈ 10 μ m (Waters Assoc.) 300 \times 4.1 mm; colonnes μ Porasil Si 10 μ m (Waters Assoc.) 300 \times 4.1 mm; colonne Hamilton PRP-1 10 μ m (Touzart et Matignon) 150 \times 4.1 mm.

La phase stationnaire est une résine à base de copolymère styrène-divinylbenzène de grande stabilité chimique permettant l'utilisation des solvants organiques courants ainsi que des éluants particulièrement acides (pH = 1) ou basiques (pH = 13).

Réactifs

Méthanol, éthanol pour analyse (Carlo Erba); acide acétique pour analyse (UCB); acide orthophosphorique R. P. Normapur (Prolabo); acétonitrile pour chromatographie (Merck); hydroxyde de tétrabutylammonium 40% (Sigma); dérivés di-, tri- et tétrahydroxyéthyles des rutosides (Laboratoire Negma).

Phase mobile: les solvants pour élution utilisés sont filtrés sur filtre millipore 0.45 μm et dégazés par l'hélium.

RÉSULTATS

Identification des composés par spectrométrie de masse

Avant toute étude chromatographique et afin de s'assurer de façon certaine de l'identité des trois composés chimiquement très proches: di-, tri- et tétra-hydroxyéthylrutoside. Une étude par spectrométrie de masse de la troxérutine et des di- et tétra-HER a été réalisée. La technique employée est une méthode de désorption-ionisation chimique (DCI-MS) classique pour les composés de ce type et permettant l'introduction directe de l'échantillon¹⁹. Les substances ont été étudiées en ionisation négative (NH_3/I) permettant ainsi une très faible fragmentation et une détermination facile des structures. Le couplage avec la chromatographie en phase gazeuse est ici exclu en raison de la très faible volatilité des composés, et de leur polarité. Enfin, la silylation des fonctions phénoliques aboutit à des composés de masse moléculaire trop élevée pour permettre une chromatographie en phase gazeuse.

Spectre de masse de la troxérutine (brute). La Fig. 2 reporte le spectre de masse de la troxérutine obtenu par la technique DCI/ NH_3 I.

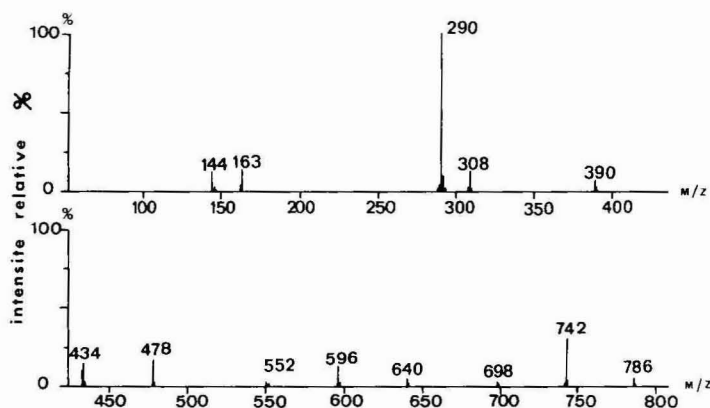


Fig. 2. Spectre de masse de la troxérutine (DCI/ NH_3 I).

La troxérutine correspondant à un mélange de di-, tri- et tétra-HER, on retrouve dans le spectre les ions parents correspondants à ces trois molécules en mélange ($m/z = 786$, $m/z = 742$ et $m/z = 698$). Chaque ion parent va perdre successivement un radical neutre rhamnosyl ($m/z = 146$) puis glucosyl ($m/z = 162$) pour donner apparition à des ions fragments tétra-, tri- et dihydroxyéthylglucosylquercétine.

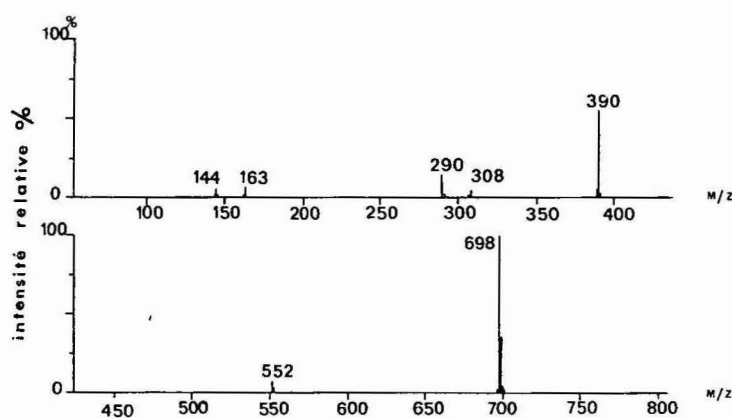
Le Tableau I rassemble les fragments spécifiques de chaque composé, le Tableau II comprend tous les fragments communs à ces trois molécules.

Spectre de masse des di- et tétra-hydroxyéthylrutine. Les Figs. 3 et 4 reportent les spectres de masse des dérivés di- et tétra-HER obtenus purs, les principaux ions fragments retrouvés confirment la fragmentation de la troxérutine vue précédemment.

TABLEAU I

MASSES DES MOLÉCULES OU FRAGMENTS SPÉCIFIQUES DES DI-, TRI- ET TÉTRA-HER

	<i>m/z</i>		
	<i>Tétra</i>	<i>Tri</i>	<i>Di</i>
Hydroxyéthylrutine	786	742	698
Hydroxyéthylglucosyl- quercétine	640	596	552
Hydroxyéthylquercétine	478	439	390

Fig. 3. Spectre de masse de la di-HER (DCI/NH₃ I).

En raison de la faible intensité des différents fragments spécifiques correspondants aux dérivés di- et tétra-HER, l'analyse directe de la troxérutine par spectrométrie de masse ne donne pas une précision acceptable, c'est pourquoi une analyse par chromatographie liquide a été envisagée.

Séparation par chromatographie liquide

La Fig. 5 montre une séparation satisfaisante sur colonne PRP1 des 3 dérivés tétra-, tri- et di-HER dont les temps de rétention sont respectivement 3,5, 5,4 et 6,7 min.

TABLEAU II

MASSE DES FRAGMENTS COMMUNS AUX TROIS MOLÉCULES

<i>m/z</i>	
Rutinosyl	308
Rutinosyl-H ₂ O	290
Glucosyl	162
Rhamnosyl	146

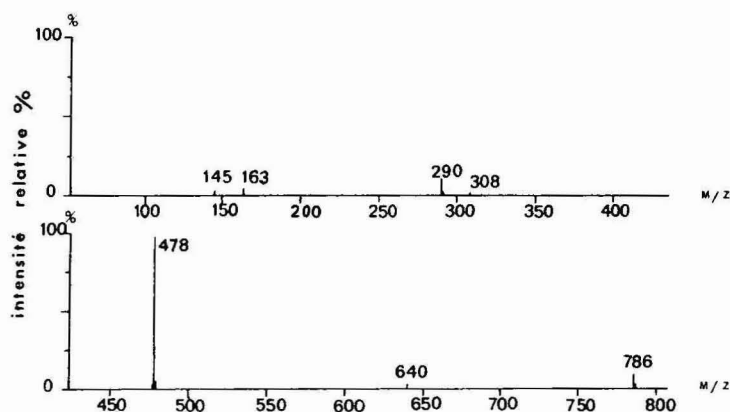


Fig. 4. Spectre de masse de la tétra-HER (DCI/NH₃ I) di-HER (3).

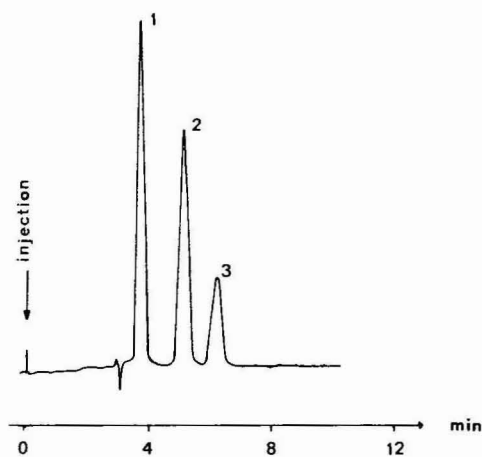


Fig. 5. Séparation des dérivés tétra- (1), tri- (2) et di-HER (3).

Conditions: colonne PRP 1: 150 × 4,1 mm (10 μ m); phase mobile: acétonitrile-solution aqueuse d'hydroxyde de tétrabutylammonium 0,005 *M* (1:4) (pH ajusté à 9 par une solution à 20% de H₃PO₄); débit: 1 ml/min; détection à 254 nm.

Le but de l'étude est la détermination simultanée de tétra-, di- et tri-HER. La teneur en dérivé di-, tri- et tétra-HER est calculée par étalonnage avec une gamme constituée par des quantités croissantes-dérives di-, tri- et tétra-HER. Les caractéristiques de la méthode ont été étudiées pour les trois dérivés.

Les limites de sensibilité de la tétra- et de la di-HER sont respectivement de 12 et 14 ng (pour un volume injecté de 5 μ l) ce qui correspond à 2,4 μ g/ml (0,003 μ M/ml) et 2,8 μ g/ml (0,004 μ M/ml). En raison de la forte proportion de tri-HER (environ 90%) il n'est pas nécessaire de déterminer de limite de sensibilité.

Les limites de détection suivantes (exprimées en pourcentage par rapport à l'aire du pic de la tri-HER) ont été trouvées: tétra-HER: 2%, di-HER: 3%.

La linéarité de la méthode est satisfaisante. Le coefficient de corrélation est de 0,998 pour des concentrations de 0–30 μg de tétra-HER par ml, celui de la di-HER est de 0,999 pour des concentrations de 0–36 $\mu\text{g}/\text{ml}$. La linéarité de la méthode pour la tri-HER a été étudiée de 0–3 mg/ml, le coefficient de corrélation est de 0,998.

La répétabilité de la méthode déterminée à partir de 10 injections du même échantillon donne des coefficients de variation de 5% pour la tétra-HER, 2,5% pour la tri-HER et 9% pour la di-HER.

DISCUSSION

La polarité de ces trois molécules ne diffère que par la présence d'un groupement hydroxyéthyle en plus ou en moins par rapport à la tri-HER. Nous nous sommes donc orientés vers une chromatographie d'adsorption sur une phase stationnaire de silice. Le caractère particulièrement polaire de ces composés laissait présager une meilleure séparation sur silice non greffée.

Essai de séparation sur silice non greffée

Après optimisation des différents paramètres chromatographiques, nous n'avons pu obtenir que des résultats très médiocres qui figurent dans le Tableau III.

TABLEAU III

RÉSULTATS DE LA CHROMATOGRAPHIE DE TROXÉRUTINE SUR SILICE AVEC COMME PHASE MOBILE UN MÉLANGE ISOCRATIQUE: ÉTHANOL-HEPTANE-CHLOROFORME-ACIDE ACÉTIQUE (55:40:5:0,4)

	Temps de rétention (min)	Résolution (R_s)	Facteur de capacité (k')
Tétra-HER	6,82		1,91
Tri-HER	5,09	0,9	1,14
di-HER	3,67	0,7	0,57

Ne pouvant réaliser une séparation satisfaisante sur ce type de phase stationnaire, nous nous sommes orientés vers une silice greffée en C_{18} .

Essais de séparation sur silice greffée en C_{18}

La séparation du dérivé tétra-HER des deux autres composés ne posant pas de problème, les essais de séparation des dérivés tri- et di-HER ont essentiellement retenu notre attention. La paramètre chromatographique que nous avons suivi est donc le facteur de résolution de ces deux molécules (R_s), dont l'étude figure dans le Tableau IV.

Nous n'avons pas pu retenir cette phase stationnaire en raison de la mauvaise résolution entre la di- et la tri-HER.

Essais de séparation sur copolymère styrène-divinylbenzène (PRP-1)

Ce type de phase stationnaire a la particularité essentielle de permettre l'emploi de phases mobiles de pH compris entre 1 et 13.

TABLEAU IV

ÉTUDE DE LA RÉOLUTION DI- ET TRI-HER SUR SILICE GREFFÉE EN C₁₈

	Phase mobile (1 ml/min)		
	A	B	C
Méthanol	30	30	33
Eau	70	70	67
Contre-ion	—	—	Perchlorate de tétrabutylammonium (0,005 M)
pH apparent	6,5	3,1 (HCl)	7,46 (NH ₄ OH)
di-HER t_R (min)	5,56	6,23	14,15
R_s	0,78	0,27	0,17
tri-HER t_R (min)	6,86	6,94	14,48

Les résultats obtenus ont été optimisés en réalisant une paire d'ions avec l'hydroxyde de tétrabutyl ammonium à pH 9, comme cela apparaît dans le Tableau V.

L'acétonitrile en raison de son caractère plus éluant que le méthanol a donc été retenu, puisqu'il permet une nette amélioration des facteurs de capacité et de la résolution. Le choix de l'hydroxyde de tétrabutylammonium à pH 9 a été guidé par le caractère acide faible de ces molécules lié à la présence des groupements hydroxyles phénoliques ionisés à pH alcalin et donc susceptibles de former une paire d'ions avec un sel d'ammonium quaternaire. Bien que les colonnes PRP1 supportent un pH de 13 et que le p*K* théorique des phénols soit voisin de 9, cette valeur de pH de phase mobile a été choisie pour ne pas détériorer la cellule de détection du spectrophotomètre. C'est donc la phase mobile D qui a été retenue.

TABLEAU V

OPTIMISATION DE LA PHASE MOBILE SUR COPOLYMÈRE STYRÈNE-DIVINYLBENZÈNE

	Phase mobile			
	A	B	C	D
Méthanol (%)	55	50	—	—
Acétonitrile (%)	—	—	15	20
Eau (%)	45	50	85	80
Contre-ion	—	hydroxyde de: tétrabutylammonium (0,005 M)	—	Hydroxyde de tétrabutylammonium (0,005 M)
pH apparent	6,5	9 (H ₃ PO ₄)	6,5	9 (H ₃ PO ₄)
tétra-HER t_R (min)	2,60	7,62	7,84	3,52
k'	0,63	0,41	2,61	0,51
tétra-, tri- R_s	2,4	1,85	4,52	3,15
tri-HER t_R (min)	4,20	11,63	16,12	5,36
k'	1,64	1,15	6,42	1,30
di-, tri- R_s	0,38	0,83	0,84	2,15
di-HER t_R (min)	4,55	12,94	17,93	6,96
k'	4,86	1,39	7,26	1,99

APPLICATION

A titre d'exemple nous indiquons dans le Tableau VI quelques teneurs en dérivés di-, tri- et tétrahydroxyéthyles dans différents lots de matière première.

TABLEAU VI

TENEURS EN DÉRIVÉS DI-, TRI- ET TÉTRA-HER DANS 2 MATIÈRES PREMIÈRES

	<i>di-HER</i> (%)	<i>tri-HER</i> (%)	<i>tetra-HER</i> (%)
Matière No. 1	5,1	92,3	2,6
Matière No. 2	7,8	89,9	2,3

CONCLUSION

L'identification et le dosage des trois principaux constituants de la troxérutine par chromatographie liquide haute performance en phase inverse permet le contrôle de qualité de ce principe actif entrant dans la formulation d'un grand nombre de médicaments utilisés dans le traitement de maladies du tissu conjonctif vasculaire. Le composé trihydroxyéthylrutine étant le composé le plus actif, il apparaît important d'en déterminer la teneur réelle.

BIBLIOGRAPHIE

- 1 C. S. Sinnatamby, *Clin. Trials J.*, 10 (1973) 45.
- 2 S. Allen, *Practitioner*, 205 (1970) 221.
- 3 M. Tschopp, *Diabetologia*, 102 (1970) 475.
- 4 A. H. Sorensen et H. Hansen, *Brit. Med. J.*, 3 (1969) 352.
- 5 P. Courbat, J. Faure, R. Guerne et G. Uhlmann, *Helv. Chim. Acta*, 49 (1966) 1203.
- 6 W. Acourt, *J. Chromatogr.*, 130 (1977) 287.
- 7 D. Strack et J. Krause, *J. Chromatogr.*, 156 (1978) 359.
- 8 J. M. Hardin et C. A. Stutte, *Anal. Biochem.*, 102 (1980) 171.
- 9 R. Galensa et K. Herrmann, *J. Chromatogr.*, 189 (1980) 217.
- 10 J. P. Bianchini et E. M. Gaydou, *J. Chromatogr.*, 190 (1980) 233.
- 11 K. Van de Castele, H. Geiger et C. F. van Sumere, *J. Chromatogr.*, 240 (1982) 81.
- 12 R. V. Tamma, G. C. Miller et R. Everett, *J. Chromatogr.*, 322 (1985) 236.
- 13 H. Becker, G. Wilking et K. Hostettmann, *J. Chromatogr.*, 136 (1977) 174.
- 14 L. W. Wulf et C. W. Nagel, *J. Chromatogr.*, 116 (1976) 271.
- 15 D. Daigle et E. J. Conkerton, *J. Chromatogr.*, 240 (1982) 202.
- 16 P. Dittrich, J. Ostrowski, E. Beubler, E. Schraven et N. Kukovetz, *Arzneim. Forsch.*, 35 (1985) 765.
- 17 P. Courbat, G. Uhlmann et R. Guerne, *Helv. Chim. Acta*, 49 (1966) 1420.
- 18 H. Tan, P. J. Mowry, W. A. Ritschel et C. Nel, *J. Pharm. Sci.*, 67 (1978) 1142.
- 19 W. Kuhn et H. Rembold, *Biomed. Mass Spectrom.*, 7 (1980) 269.
- 20 W. Kuhn, K. Zech, R. Lupp, G. Jung, W. Voelter et F. Matzkies, *J. Chromatogr.*, 272 (1983) 333.

CHROM. 18 001

Note

Reversed-phase high-performance liquid chromatography of natural and synthetic sauvagines

LUISA RUSCONI* and PIER CARLO MONTECUCCHI

Farmitalia Carlo Erba, Chemical Research & Development, Via dei Gracchi 35, 20146 Milan (Italy)

(Received July 5th, 1985)

Sauvagine (SAU) is a peptide isolated from the skin of the South American frog *Phyllomedusa sauvagei*^{1,2}, and occurs also in skin extracts from other *Phyllomedusa* species³. It consists of a straight chain of 40 amino acid residues with distinct hydrophobic characteristics, the sequence of which is shown in Fig. 1. In addition to displaying activity towards the cardiovascular system and the gastrointestinal tract, SAU stimulates the release of adrenocorticotrophic hormone (ACTH) from the pituitary gland⁵ both *in vivo* and *in vitro*. The peptide shows considerable similarities in biological activities with the corticotropin-releasing factor (CRF) isolated from the sheep hypothalamus⁶ and other homologous hypophysiotropic factors isolated from rat⁷, bovine⁸ and caprine⁹ hypothalami, and also with urotensin I (U_I), detected in the urophysis of two different species of bony fishes^{10,11}. These peptides are also closely related in structure, showing a sequence identity of at least 50% (see Fig. 1).

Natural SAU is known to occur in two forms with different electrophoretic mobilities, SAU I and SAU II, but displaying the same biological spectrum. The presence of one additional carboxyl group in SAU II (identified as [Glu²³]SAU I) was demonstrated by an automatic version of the Edman degradation and confirmed by the pseudo-titration curves of the two forms of sauvagine in isoelectric focusing–electrophoresis¹². Moreover, similarly to homologous ovine CRF⁶ and to other methionine-containing peptides, *e.g.*, substance P¹³, and tryptophyllin-13¹⁴, SAU is likely to be obtained partially in the methionine sulfoxide form by virtue of the purification procedure. [MetO¹⁷]SAU was found not to be significantly different from SAU in biological potency¹².

The conventional synthesis of the (18–40) fragment¹⁵, as well as the solid-

BOVINE CRF	SQEPPI SLDLTFHLLREVLEMTKADQLAQQAHNNRKL D I A	— ¹⁶
CAPRINE/OVINE CRF	SQEPPI SLDLTFHLLREVLEMTKADQLAQQAH S NRKLL D I A	— ¹⁶
HUMAN/RAT CRF	SEEPPI SLDLTFHLLREVLEMTKADQLAQQAH S NRKLL M E I I	— ¹⁷
SUCKER U _I	NDDPPI SLDLTFHLLRNMIEMARIENEREQAGLNRYLDEV	— ¹⁸
CARP U _I	NDDPPI SLDLTFHLLRNMIEMARNENOREQAGLNRYLDEV	— ¹⁹
SAUVAGINE	ZGPPISLDL SLELLRKMIEIEKOEKEKQQAANNR L L D T I	— ²⁰

Fig. 1. Primary structures of native peptides with corticotropin-releasing activity. The one-letter system of abbreviations for the amino acids has been used⁴. In particular, Z denotes pyrrolidonecarboxylic acid and the symbol ■ represents the amino group blocking the carboxyl end of the amino acid chain.

phase syntheses of the (17–40) fragment¹⁶ and of the complete amino acid sequence¹⁷, have recently been described. The product corresponding to the tetraconapeptide is now commercially available from different chemical companies. Nevertheless, no chromatographic comparison between the natural compound and the synthetic ones, and no complete characterization of extractive SAU by high-performance liquid chromatography (HPLC), has been reported. In this paper we describe the use of reversed-phase high-performance liquid chromatography (RP-HPLC) for the identification and resolution of the different forms of natural SAU, and for the analysis of two synthetic SAU samples.

EXPERIMENTAL

RP-HPLC was performed on a Hewlett-Packard 1084B apparatus, equipped with an HP 1040 diode-array detector controlled through an HP 85 computer.

One synthetic sample of SAU (referred to as sample 1) was obtained from Sigma (St. Louis, MO, U.S.A.): the other one (referred to as sample 2) was a kind gift from Dr. W. Vale (Salk Institute, La Jolla, CA, U.S.A.).

The natural compound was isolated as previously reported from the methanol extracts of skin from *Phyllomedusa sauvagei*^{1,2}. A semipurified pool (referred to as pool 1) was collected after gel filtration on Sephadex G-50 superfine (Pharmacia, Uppsala, Sweden). A part was employed for the HPLC characterization, whereas another amount was further purified on a DEAE-Sephacel (Pharmacia) column. Two other pools were collected, containing SAU I (pool 2) and SAU II (pool 3), respectively, and they were also analyzed by HPLC. All reagents were of analytical grade.

Quantitative amino acid analyses were carried out using a Kontron Chromakon 500 amino acid analyzer. Samples for amino acid analysis were hydrolyzed at 110°C for 48 h in 6 M hydrochloric acid under nitrogen atmosphere. The samples for chromatography were freshly dissolved in water (*ca.* 1 mg/ml) and analyzed on a μ -Bondapak C₁₈ column (300 \times 3.9 mm I.D.; Waters Assoc., Milford, MA, U.S.A.) using the following eluent systems: (I) A = 0.05% trifluoroacetic acid, B = acetonitrile; (II) A = 0.01 M sodium acetate, B = acetonitrile; (III) A = 0.02 M ammonium acetate, B = acetonitrile, always with gradient elution from 30 to 55% B in 25 min. All separations were performed at room temperature (*ca.* 25°C) and at a flow-rate of 1 ml/min. The detection wavelength was fixed at 220 nm.

RESULTS AND DISCUSSION

Pool 1 gave the elution pattern shown in Fig. 2 when analyzed on a μ Bondapak C₁₈ column with eluent system I. Two major, well resolved peaks (A and C) were present in the chromatogram, each being accompanied by a smaller peak at slightly higher retention time (peaks B and D). The retention time of peak C was coincident with that of synthetic peptides 1 and 2 (see Table I). This coincidence was confirmed when mixtures of an aliquot from pool 1 with samples 1 and 2 were analyzed under the same conditions; therefore peak C was attributed to native SAU I.

Peak A in Fig. 2 accounted for a product occurring in approximately equal amount to SAU I in pool 1. It could be identified as [MetO¹⁷]SAU I by comparison with a synthetic standard, obtained through mild oxidation (0.18% hydrogen per-

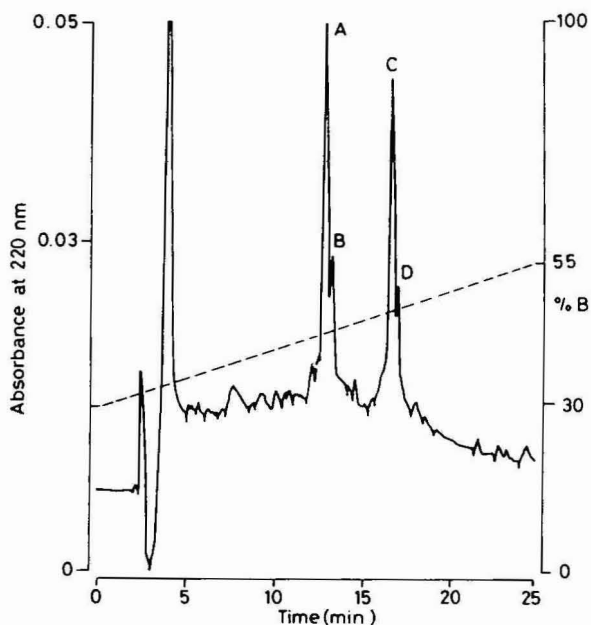


Fig. 2. RP-HPLC profile of extractive SAU from pool 1. Conditions: column, μ Bondapak C_{18} ; eluent A, 0.05% trifluoroacetic acid, eluent B, acetonitrile; gradient, as shown by the dotted line; flow-rate, 1 ml/min; sample load, 60 μ g. For peaks A–D, see Table I.

oxide in 0.05 *M* acetic acid, 15 min at room temperature, peptide concentration *ca.* 0.5 mg/ml) of sample 1. The elution profile of pool 1 coinjected with synthetic [MetO¹⁷]SAU I is shown in Fig. 3a. A comparable amount of native SAU was also oxidized by the above method: from the elution pattern in Fig. 3b, it is seen that after this treatment only two products were detected, with the same retention times as peaks A and B in Fig. 2. The first peak could definitely be attributed to [MetO¹⁷]SAU I, while the second one could only correspond to an oxidized de-

TABLE I

RP-HPLC BEHAVIOUR OF TWO SYNTHETIC SAU SAMPLES, OF NATURAL SAU I AND II AND THEIR RESPECTIVE METHIONINE SULPHOXIDE FORMS

Systems: (I) A = 0.05% trifluoroacetic acid; B = acetonitrile; (II) A = 0.01 *M* sodium acetate; B = acetonitrile; (III) A = 0.02 *M* ammonium acetate; B = acetonitrile. Samples were always eluted with a gradient from 30 to 55% B in 25 min.

Peak	Product	Retention time (min)		
		System I	System II	System III
A	[MetO ¹⁷]SAU I	12.7	10.9	12.1
B	[MetO ¹⁷]SAU II	13.1	8.8	10.1
C	SAU I	16.4	14.5	15.3
	Sample 1	16.4	14.5	15.3
	Sample 2	16.4	14.5	15.3
D	SAU II	16.7	12.5	13.5

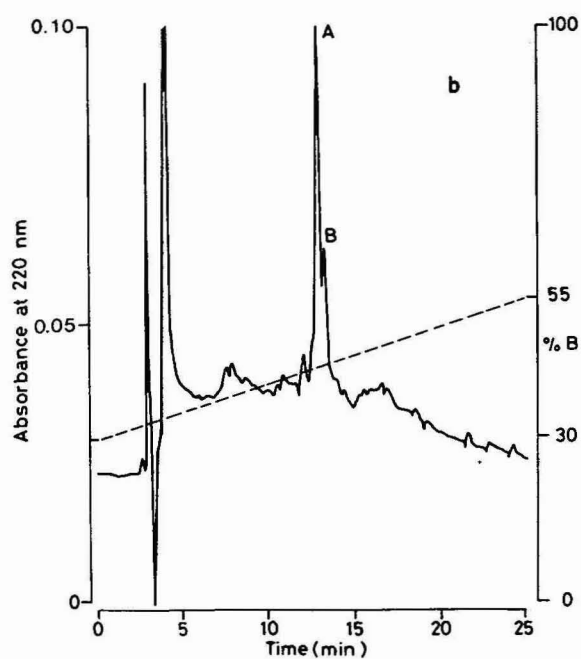
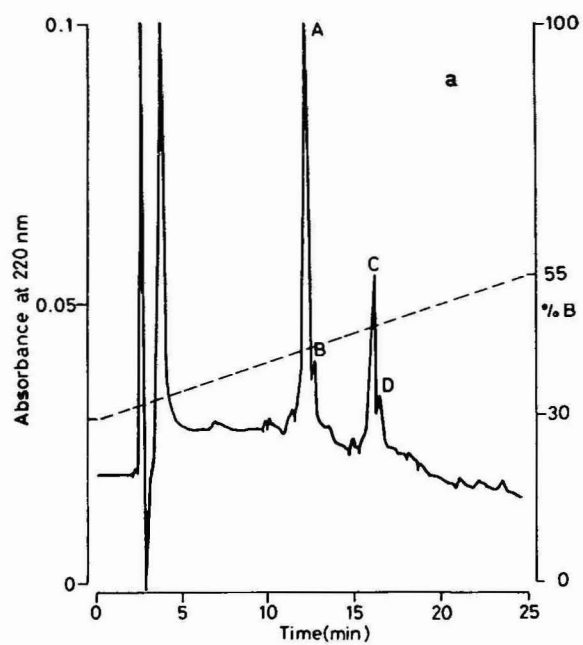


Fig. 3. RP-HPLC profiles of synthetic [MetO¹⁷]SAU I (15 µg) and extractive SAU from pool 1 (60 µg) (a) and of pool 1 (30 µg) after oxidation with peracetic acid (b). Conditions as in Fig. 2.

rivative of the product giving peak D in Fig. 2. As a consequence, peaks B and D were supposed to be [MetO¹⁷]SAU II and SAU II, respectively. In order to confirm this, pool 1 was further purified on a DEAE-Sephacel column under suitable conditions in order to separate SAU I and SAU II¹. Moreover, since the amino acid analysis of peak C in Fig. 2 did not fully correspond to that expected for SAU I, a further purification step was also necessary to get satisfactorily pure peptides. The two SAU-containing pools from DEAE-Sephacel chromatography were analyzed by the same method as for pool 1, both of them yielding two peaks with the expected retention times. Therefore, the products detected as peaks B and D in Fig. 2 could be ascribed to native [MetO¹⁷]SAU II and SAU II, respectively.

The chromatographic system so far employed (system I) was found to provide very good resolution between SAU I, II and their respective methionine sulfoxide forms. The method also allowed quick and substantial recovery of the peptides after lyophilization (more than 80%, based on reinjection).

The retention times observed with this method were quite high for SAU I and II, in agreement with their high content of hydrophobic amino acids. The relatively apolar character of the two peptides is further increased by the low pH of the buffer: both of them are fully protonated, that is, quite hydrophobic, due to their acidic isoelectric points. On the contrary, the oxidized forms were less strongly retained, because of the presence of the very polar sulfoxide function in the molecules.

To improve the resolution between SAU I and II, the system was modified by the introduction of 0.01 M sodium acetate as aqueous buffer (system II). Gradient elution with acetonitrile as organic modifier was performed on pool 1, and the results

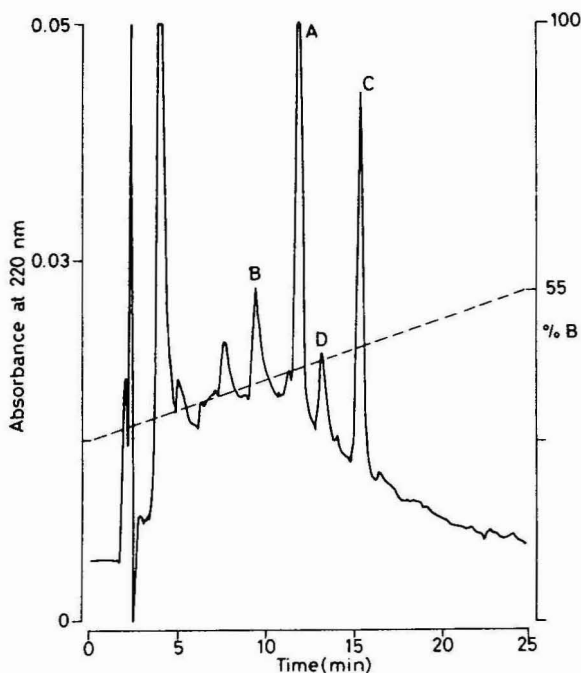


Fig. 4. RP-HPLC profile of extractive SAU from pool 1. Eluent A, 0.01 M sodium acetate. Other conditions as in Fig. 2.

are shown in Fig. 4. Four peaks were present in the chromatogram, and readily identified by comparison with the synthetic standards and the pure native peptides obtained in advance (see above). [MetO¹⁷]SAU II was eluted first, followed by [MetO¹⁷]SAU I, then the two non-oxidized peptides in the same order, that is, reversed with respect to that obtained in first chromatographic system. This reversal is due to the pH of the mobile phase (about 6.6, *cf.*, about 2.4 for the buffer used in system I), which causes dissociation of the carboxyl functions: as a consequence, SAU II and [MetO¹⁷]SAU II, which contain one additional ionized group, are eluted more rapidly than their respective [Gln²³] analogues. The method employing system II provides full resolution of the four SAU forms. A satisfactory separation was still observed (see Table I) when sodium acetate in the buffer was replaced by the corresponding ammonium salt (system III), to allow for recovery of the products after lyophilization. Moreover, the peptides obtained by preparative HPLC with pool 1 according to this method were already sufficiently pure, thus eliminating the need for the last purification step by ion-exchange chromatography.

CONCLUSION

We have reported the characterization of the two sauvagine forms by use of reversed-phase high-performance liquid chromatography. Their retention times were compared with those of two synthetic samples under different experimental conditions. The demonstration of the identity of natural SAU I and synthetic SAU, here reported for the first time, is particularly helpful for a more complete pharmacological investigation of the rôle of this molecule in mammalian tissues.

REFERENCES

- 1 P. C. Montecucchi, A. Anastasi, R. de Castiglione and V. Erspamer, *Int. J. Pept. Protein Res.*, 16 (1980) 191.
- 2 P. C. Montecucchi, A. Henschen and V. Erspamer, *Hoppe-Seyler's Z. Physiol. Chem.*, 360 (1979) 1178.
- 3 V. Erspamer, G. Falconieri Erspamer, G. Improta, L. Negri and R. de Castiglione, *Arch. Pharm. (Weinheim, Ger.)*, 312 (1980) 265.
- 4 Nomenclature and Symbolism for Amino Acids and Peptides, *Int. J. Pept. Protein Res.*, 24 (1984) 9.
- 5 V. Erspamer and P. Melchiorri, in E. E. Müller and R. M. MacLeod (Editors), *Neuroendocrine Perspectives*, Vol. 2, Elsevier, Amsterdam, 1983, p. 37.
- 6 W. Vale, J. Spiess, C. Rivier and J. Rivier, *Science (Washington, D.C.)*, 213 (1981) 1394.
- 7 J. Rivier, J. Spiess and W. Vale, *Proc. Natl. Acad. Sci. U.S.A.*, 80 (1983) 4851.
- 8 F. Esch, N. Ling, P. Böhlen, A. Baird, R. Benoit and R. Guillemin, *Biochem. Biophys. Res. Commun.*, 122 (1984) 899.
- 9 N. Ling, F. Esch, P. Böhlen, A. Baird and R. Guillemin, *Biochem. Biophys. Res. Commun.*, 122 (1984) 1218.
- 10 K. Lederis, A. Letter, D. Mc Master, G. Moore and D. Schlesinger, *Science (Washington, D.C.)*, 218 (1982) 162.
- 11 T. Ichikawa, D. Mc Master, K. Lederis and H. Kobayashi, *Peptides*, 3 (1982) 859.
- 12 P. C. Montecucchi, R. de Castiglione and V. Erspamer, in G. Rosselin, F. Fromageot and S. Bonfils (Editors), *Hormone Receptors in Digestion and Nutrition*, Elsevier/North-Holland Biomedical Press, Amsterdam, 1979, p. 101.
- 13 E. Floor and S. E. Leeman, *Anal. Biochem.*, 101 (1980) 498.
- 14 L. Rusconi, G. Perseo, L. Franzoi and P. C. Montecucchi, *J. Chromatogr.*, in press.
- 15 G. Wendlberger, *II Weygand-Scoffone Meeting on Perspectives of Peptides Research in Chemical and Pharmaceutical Industry, Galzignano, April 26, 1985*.
- 16 F. Santangelo, P. C. Montecucchi, L. Gozzini and A. Henschen, *Int. J. Pept. Protein Res.*, 22 (1983) 348.
- 17 J. Rivier, J. Spiess, C. Rivier, R. Galyean, W. Vale and K. Lederis, in K. Bláha and P. Maloň (Editors), *Peptides 1982*, Walter de Gruyter, 1983, p. 597.

CHROM. 17 981

Note

Analytical and preparative reversed-phase liquid chromatography of secoiridoid glycosides

DANIEL SCHAUFELBERGER and KURT HOSTETTMANN*

Institut de Pharmacognosie et Phytochimie, École de Pharmacie de l'Université de Lausanne, rue Vuillermet 2, CH-1005 Lausanne (Switzerland)

(Received June 25th, 1985)

Secoiridoid glycosides are typical constituents of Gentianaceae, such as *Gentiana* and *Swertia*. They have a bitter taste and show antimicrobial properties after enzymatic hydrolysis^{1,2}. Swertiamarin (1), gentiopicroin (2) and sweroside (3) are widespread, whereas their esters with hydroxybenzoic or diphenylcarbonic acids, which are among the most bitter natural products known^{3,4}, are less common. Previously⁵, we reported on the desorption/chemical ionization mass spectrometry (D/CI MS) of the underivatized glycosides, a useful method for structural analysis of these rather unstable compounds.

Analytical high-performance liquid chromatography (HPLC) has been proposed for the separation and quantitation of secoiridoid glycosides in medicinal plant extracts^{6–8}. The use of this technique together with the recently developed photodiode array detector^{9,10} represents an important advance in HPLC. Any separated compound can be characterized by its complete UV–VIS spectrum.

Preparative isolation techniques are, at the same time, important since bioassays or structural elucidations need a certain quantity of a pure compound. Preparative liquid chromatography has been carried out on silica gel in order to isolate secoiridoid glycosides from *Lomatogonium carinthiacum*¹¹ and *Centaurium spicatum*¹², using dichloromethane–methanol (82.5:17.5) and ethylacetate–methanol (95:5) as mobile phases respectively. However, very complex mixtures would not have been separated under these conditions. Sakamoto *et al.*¹³ isolated the glycosides 1–3 from *Swertia* species by semi-preparative reversed-phase (RP) HPLC with acetonitrile–water (20:80). This system is not suitable for a larger preparative scale, due to its expense and the toxicity of the organic solvent.

In the present paper we show the advantages of a new method for the isolation of secoiridoid glycosides. Preparative separations are carried out on a reversed phase (RP-8) with methanol–water as eluent, using a system which is generally described as medium-pressure liquid chromatography (MPLC)^{14,15}.

EXPERIMENTAL

Plant material and extracts

Gentiana lactea PHIL. and *Coutoubea spicata* AUBL. were collected in Chile

and in Panama, respectively. The dried plant material (aerial parts) was extracted with solvents of increasing polarities: light petroleum (b.p. 80–95°C), chloroform and methanol. The secoiridoid fractions were obtained by column chromatography of the crude methanolic extracts on Polyamide SC 6 (Macherey Nagel, Düren, F.R.G.) with 50% (*G. lactea*) or 20% aqueous methanol (*C. spicata*).

HPLC

HPLC was carried out on a Hypersil column RP-8, 5 μm (10 cm \times 4.6 mm I.D., Hewlett-Packard), with isocratic elution with 20% and 30% aqueous methanol (8 min after injection). The mobile phase was delivered at a flow-rate of 1.5 ml/min by a SP 8700/SP 8750 pump (Spectra Physics, San José, U.S.A.). The chromatogram at 254 nm and the UV/VIS spectra were recorded with a photodiode array detector HP 1040 A, coupled with a HP-85 personal computer (Hewlett-Packard). Details of the post-column derivatization are given in ref. 16.

Preparative liquid chromatography

Medium-pressure system. Separations were carried out with an MPLC liquid chromatograph B-680 and an UV detector B-638 (Büchi Laboratoriumstechnik, Flawil, Switzerland). A 46 cm \times 25 mm I.D. glass column, connected to a 11.5 cm \times 10 mm I.D. precolumn (Büchi), was packed with LiChroprep RP-8, 15–25 μm (E. Merck, Darmstadt, F.R.G.). The mobile phase, 20 and 30% aqueous methanol (90 min after sample introduction), was delivered at a flow-rate of 18 ml/min and under a maximum pressure of 36 bar. Samples were dissolved in 3–5 ml of mobile phase and introduced into the precolumn. The secoiridoid-containing fractions were collected and lyophilized.

Low-pressure system. Prepared Lobar® columns of LiChroprep RP-8, 40–63 μm (31 cm \times 25 mm I.D.), were purchased from E. Merck. The mobile phase of 20 and 30% aqueous methanol (100 min after sample introduction) was delivered by a Duramat pump (Chemie und Filter, Heidelberg, F.R.G.) at 9 ml/min and a maximum pressure of 4 bar.

RESULTS AND DISCUSSION

Fig. 1 shows the RP-HPLC separation of a secoiridoid fraction from *Gentiana lactea*. Compounds 1–4 could be separated in less than 15 min and their corresponding UV spectra recorded on-line by a photodiode array detector (LC-UV). Gentiopicroin (2) and the only secoiridoid ester detected, desacetylcentapicroin (4), are clearly distinguished from the glycosides 1, 3 and also from each other by their characteristic spectra. This example illustrates how the use of a photodiode array detector can improve the peak identification and also afford structural information about the separated compounds.

The HPLC separation of the secoiridoid fraction was repeated and an aqueous solution of 0.3 M potassium hydroxide added by means of a post-column derivatization system. The modified UV spectrum of compound 4 was recorded and compared with the spectrum obtained in pure eluent (Fig. 2). The bathochromic shift of the absorption maximum from 300 to 333 nm indicated a free phenolic group, which was deprotonated by the strong base. This technique of LC-UV and post-column

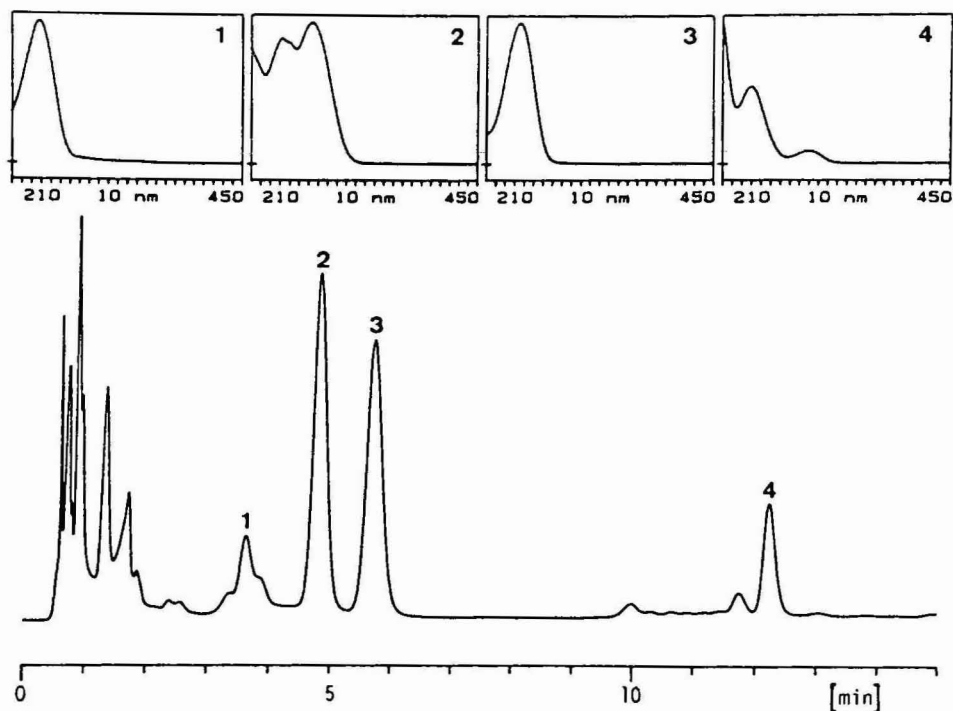


Fig. 1. RP-HPLC separation with photodiode array detection of secoiridoid glycosides from *Gentiana lactea*. Peaks: 1 = swertiamarin; 2 = gentiopicrin; 3 = sweroside; 4 = desacetylcentapicrin. Column: Hypersil RP-8, 5 μ m (10 cm \times 4.6 mm I.D.). Eluent: 20 and 30 % aqueous methanol; flow-rate 1.5 ml/min. Detection: 254 nm, spectra from 210 to 450 nm.

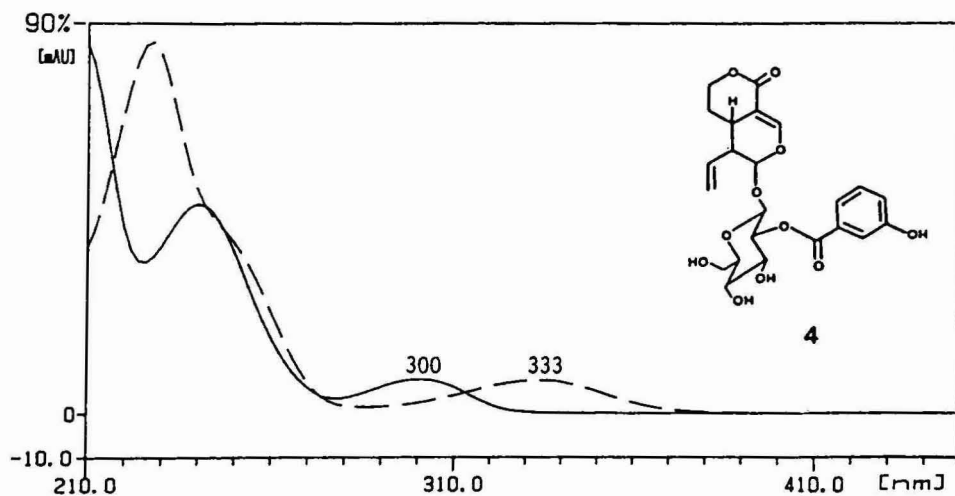


Fig. 2. HPLC of secoiridoid glycosides: UV spectra of desacetylcentapicrin 4 recorded on-line in pure eluent (aqueous methanol, —) and with potassium hydroxide (----) added by a post-column derivatization system.

derivatization has recently been discussed for polyphenolic compounds from gentians¹⁶. A systematic application to secoiridoid glycosides is currently underway.

The HPLC conditions were directly transposed to preparative liquid chromatography. Separations were carried out on reversed-phase material (RP-8, 15–25 μm) with 20 and 30% aqueous methanol at a maximum pressure of 40 bar. The system of MPLC used is described in Experimental. A crude secoiridoid fraction (1.5 g) from *G. lactea* was directly separated by MPLC on the reversed phase. The chromatogram is shown in Fig. 3. The resolution of this preparative separation is surprisingly high and can be compared with that of analytical HPLC (Fig. 1). The four bitter principles, 1 (8 mg), 2 (43 mg), 3 (37 mg) and 4 (14 mg), were isolated in pure form and in one separation step of less than 3 h. The same fraction was submitted to preparative liquid chromatography using the low-pressure system Lobar® (E. Merck). No baseline separation of the two major compounds, 2 and 3, could be obtained, although relatively small amounts of the secoiridoid fraction (300 mg) had been introduced.

As a further application of MPLC, the bitter principles of a tropical Gentianaceae, *Coutoubea spicata*, were separated under the same conditions as described in Fig. 3. The major bitter constituent, swertiamarin 1 (161 mg), and gentiopicroin 2 (4 mg) could be isolated within 1 h from 500 mg of a crude secoiridoid fraction.

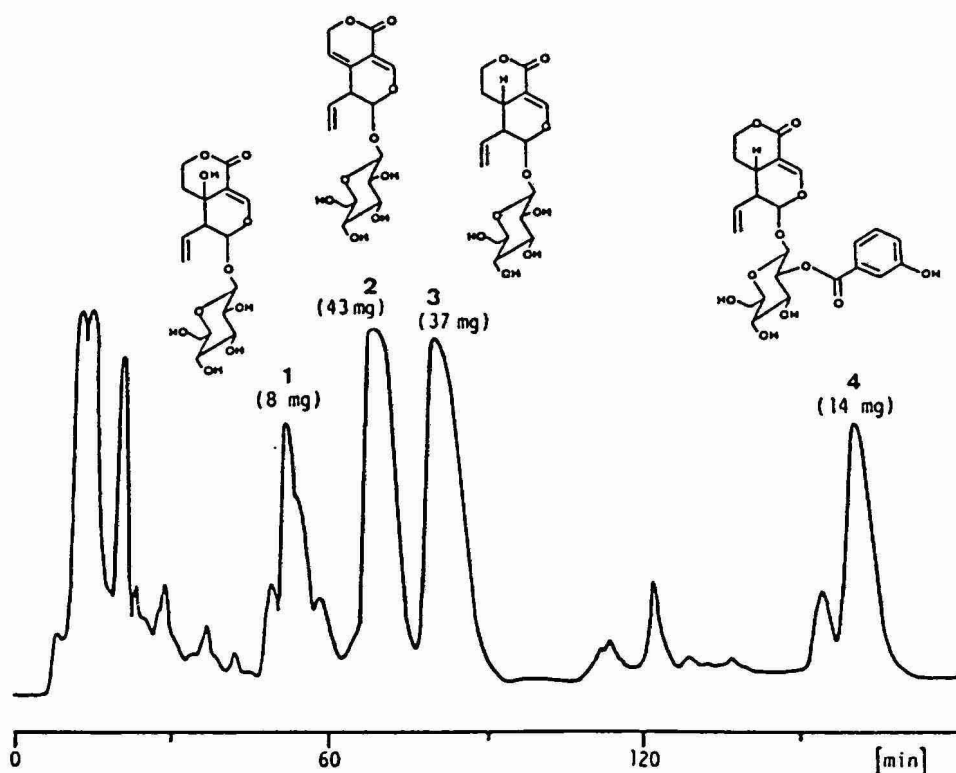


Fig. 3. Preparative MPLC of secoiridoid glycosides from *Gentiana lactea*. Column: LiChroprep RP-8, 15–25 μm (46 cm \times 25 mm I.D.). Eluent: 20 and 30% aqueous methanol; flow-rate 18 ml/min. Detection: 254 nm. Sample: 1500 mg of secoiridoid fraction.

CONCLUSION

High-performance liquid chromatography, coupled with a photodiode array detector (LC-UV), is of great interest for phytochemical investigations. Constituents, including secoiridoid glycosides, can be detected and characterized in complex mixtures such as plant extracts. If the same packing material is used for preparative liquid chromatography and HPLC, the separation conditions can easily be selected by LC-UV. A prepurification of crude extracts is recommended and simplifies the regeneration of the reversed-phase material. Interfering polyphenolics, e.g., flavonoids, can be removed by chromatography over polyamide.

The medium-pressure system of preparative liquid chromatography described has the advantage that mobile phases containing large proportions of water can be used with reversed-phase packing materials of small particle size. Crude and complex samples of more than 1 g can be separated in this system within 1–3 h and remarkable resolution can be obtained.

Medium-pressure liquid chromatography (MPLC) on a reversed phase is consequently a very promising technique for the isolation of secoiridoid glycosides and related natural compounds.

ACKNOWLEDGEMENTS

Financial support has been provided by the Swiss National Science Foundation. We are most grateful to Dr. J. Nunez-Alacron, Valdivia, Chile and to Professor M. Gupta, Universidad de Panama, Panama, for the collection of plant material.

REFERENCES

- 1 K. Ishiguro, M. Yamaki and S. Takagi, *Yakugaku Zasshi*, 102 (1982) 755.
- 2 W. G. Van der Sluis, J. M. Van der Nat and R. P. Labadie, *J. Chromatogr.*, 259 (1983) 522.
- 3 H. Wagner and K. Vasirian, *Dtsch. Apoth.-Ztg.*, 114 (1974) 1245.
- 4 W. G. Van der Sluis and R. P. Labadie, *Planta Med.*, 41 (1981) 150.
- 5 D. Schaufelberger, B. Domon and K. Hostettmann, *Planta Med.*, 50 (1984) 398.
- 6 O. Sticher and B. Meier, *Pharm. Acta Helv.*, 53 (1978) 40.
- 7 Y. Takino, M. Koshioka, M. Kawaguchi, T. Miyahara, H. Tanizawa, Y. Ishii, M. Higashino and T. Hayashi, *Planta Med.*, 38 (1980) 344.
- 8 V. Quercia, G. Battaglino, N. Pierini and L. Turchetto, *J. Chromatogr.*, 193 (1980) 163.
- 9 S. A. George and A. Maute, *Chromatographia*, 15 (1982) 419.
- 10 H. Elgass, A. Maute, R. Martin and S. George, *Int. Lab.*, 13 (1983) 72.
- 11 D. Schaufelberger and K. Hostettmann, *Phytochemistry*, 23 (1984) 787.
- 12 W. G. Van der Sluis and R. P. Labadie, *Planta Med.*, 41 (1981) 221.
- 13 I. Sakamoto, K. Morimoto, O. Tanaka and H. Inouye, *Chem. Pharm. Bull.*, 31 (1983) 25.
- 14 T. Leutert and E. Von Arx, *J. Chromatogr.*, 292 (1984) 333.
- 15 W. Dobler, *GIT Fachz. Lab.*, 27 (1983) 1078.
- 16 K. Hostettmann, B. Domon, D. Schaufelberger and M. Hostettmann, *J. Chromatogr.*, 283 (1984) 137.

CHROM. 18 006

Note

Analytical isoelectric focusing of native and modified haemoglobins after treatment with 4-hydroxymercuribenzoate

T. I. PŘISTOUPIL*, M. KRAMLOVÁ, H. FOŘTOVÁ and V. FRIČOVÁ

Institute of Haematology and Blood Transfusion, Prague (Czechoslovakia)

(Received June 25th, 1985)

Analytical isoelectric focusing (IEF) has been very useful for the characterization of stroma-free haemoglobin solutions (SFHs) investigated as oxygen-trans-
porting cell-free blood substitutes^{1–3}. Some of the most interesting pyridoxalated and
glutaraldehyde-treated SFH variants represent a highly polydisperse system of modi-
fied haemoglobin molecules. However, the *pI* values of the individual subfractions
are very similar mainly between about 6.6–7.2, so that the IEF patterns are very
diffuse and provide little information to enable an effective analytical monitoring of
SFH batches. For this purpose a more discrete fractionation of modified SFH or of
its dissociated subunits would be of great assistance.

The sodium salt of 4-hydroxymercuribenzoic acid (4-HMB) has been widely
used for determinations of SH groups⁴ and for dissociation of haemoglobin tetramers
into their subunits⁵. An erroneous designation of 4-HMB as *p*-chloromercuriben-
zoate (PCMB) was generally used in earlier literature.

The present paper describes our experiments on the fractionation of haemo-
globin subunits after treatment of SFH with 4-HMB. The possible application of
4-HMB-treated dry human oxyhaemoglobin as a coloured multicomponent *pI*
marker for the range *pI* 5–8 was also tested.

EXPERIMENTAL

Native human and bovine haemolyzates of washed erythrocytes were prepared
and freed from stroma by centrifugation and membrane filtration as is usual⁶. Sam-
ples were stored dry below 0°C after lyophilization with sucrose^{1,7}. The modification
of haemoglobins with pyridoxal-5-phosphate, glutaraldehyde, borohydride and in
some experiments also with serum albumin (PHIR-PGA) was performed according
to refs. 8–10. The reaction with 4-HMB was carried out according to ref. 5. An IEF
flat-bed apparatus Multiphor (LKB, Bromma, Sweden) equipped with 0.5-mm thin
layers of IEF agarose and Pharmalyte 5–8 (Pharmacia, Uppsala, Sweden)¹¹ was used.
To avoid the formation of air bubbles during filling the 0.5-mm wide space with hot
agarose, the following procedure was adopted: the glass plates were positioned hori-
zontally from the beginning, instead of at an angle of 30° as is usually recommended;
the warm agarose solution was poured slowly from a beaker into one corner of the
glass plates, instead of using a syringe to apply the solution at the centre. IEF patterns
were stained with Coomassie Blue 250.

RESULTS AND DISCUSSION

Fig. 1 shows the marked differences between the IEF patterns of native human SFH, its modified variant PHIR-PGA⁸ and of both 4-HMB-treated samples. During destaining in diluted acetic acid plus ethanol¹¹, two zones at *pI* about 6.5 and 6.8 showed a yellowish fluorescence when observed under direct sunshine against a dark background. A third fluorescent zone at *pI* 5.8 appeared after treatment of PHIR-PGA with 4-HMB. The very diffuse pattern of undissociated PHIR-PGA changed after treatment with 4-HMB into a series of 15–20 relatively distinct zones along a gradient of pH 5.5–7.7. Nevertheless, the diffuse background of the IEF pattern indicates a certain fine polydispersity even after dissociation of modified haemoglobin. Some subunits derived from PHIR-PGA showed lower *pI* values than those prepared from native haemoglobin. This is evidently due to the modification of basic, mostly amino, groups of the haemoglobin molecules by glutaraldehyde and pyridoxal-5-phosphate and to the presence of small amounts of albumin.

Glutaraldehyde and pyridoxal-5-phosphate are known to react also with the reactive SH group of β -93 cysteine during modification of SFH. This reaction, as

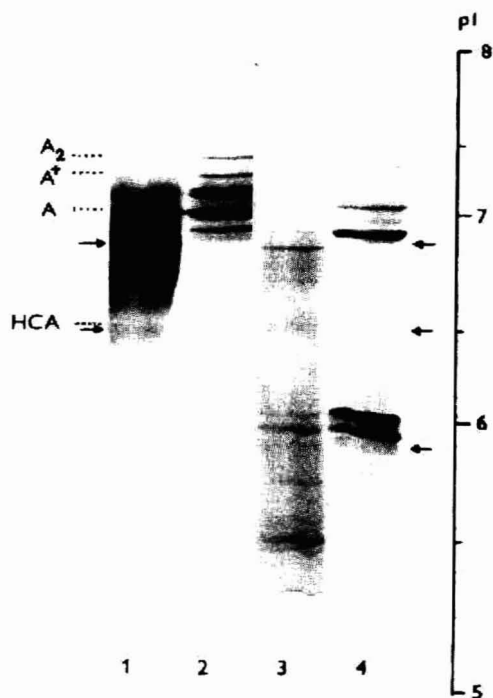


Fig. 1. Isoelectric focusing of human haemoglobin samples and their subunits after treatment with 4-hydroxymercuribenzoate. Samples: 1 = human stroma-free haemoglobin (SFH) modified with pyridoxal-5-phosphate, glutaraldehyde, borohydride and serum albumin⁶; 2 = native human SFH; 3 = sample 1 treated with 4-hydroxymercuribenzoate (4-HMB); 4 = sample 2 treated with 4-HMB. A, A⁺, A₂ = Positions of typical haemoglobin subfractions; HCA = human carbonanhydrase. The arrows indicate fluorescent zones. A 0.5-mm thin layer of IEF agarose, Pharmalyte 5–8, was stained with Coomassie Blue 250.

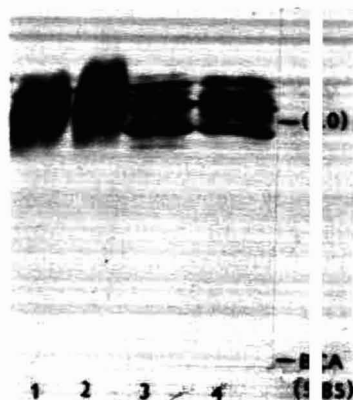


Fig. 2. Isoelectric focusing of bovine haemoglobin samples: 1 = bovine haemoglobin modified with pyridoxal-5-phosphate and glutaraldehyde followed by treatment with 4-HMB; 2 = sample 1 before 4-HMB treatment; 3 = bovine haemoglobin treated with 4-HMB; 4 = native bovine haemoglobin. BCA = Bovine carbonanhydrase. IEF conditions as in Fig. 1.

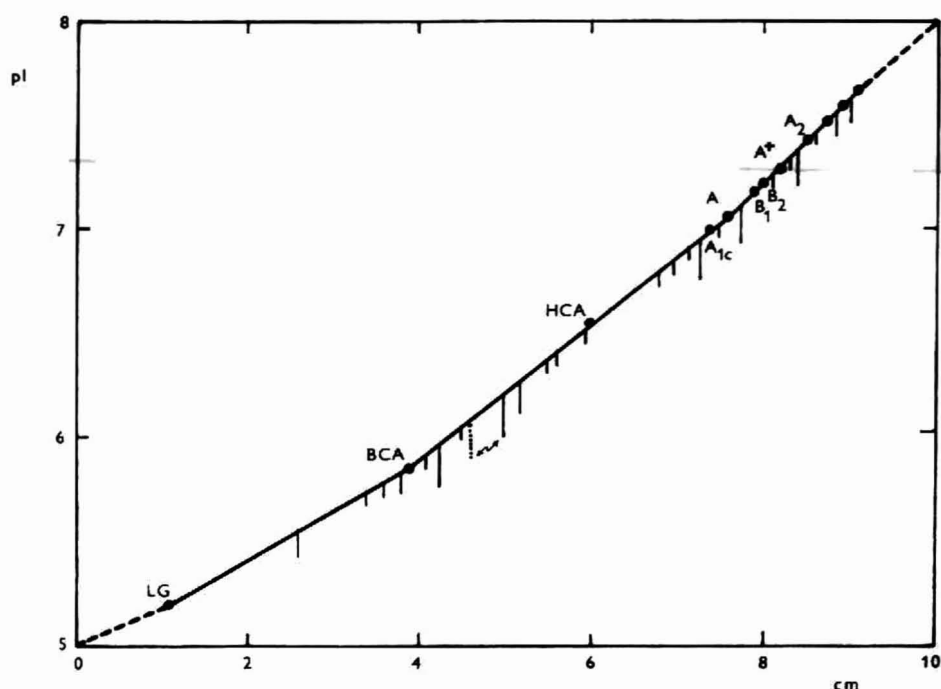


Fig. 3. Calibration curve for estimation of pI values from isoelectric focusing patterns. Full circles: LG = β -lactoglobulin; BCA = bovine carbonanhydrase; HCA = human carbonanhydrase; A_{1c} , A, B_1 , B_2 , A^* , A_2 and three unidentified dots are characteristic human haemoglobin subfractions. Perpendicular lines indicate the positions of zones of 4-HMB-treated native human haemoglobin. The length of the lines is roughly proportional to the intensity of the zones. For details see text.

well as that with amino groups, is not complete under the given conditions, since about 10–20% of the haemoglobin molecules in PHIR-PGA still behave as native ones. The unreacted part of β -93 cysteine and the less reactive α -104 cysteine and β -112 cysteine¹² react after longer treatment with 4-HMB. This leads to the dissociation of haemoglobin (Hb) subfractions, *e.g.*, HbA, HbA₂, etc., into their corresponding subunits and modified subunits, respectively. These subunits can be fractionated into more distinct zones by IEF. A given pattern may then serve as a characteristic fingerprint for a given variant of modified human SFH and as an indicator of the reproducibility of batches. A detailed identification of the separated subunits was not the aim of the present study.

In contrast to human SFH variants, only small changes were observed in IEF patterns of bovine SFH after treatment with 4-HMB (Fig. 2). This is due to the fact that SH groups are absent in the α -chains of bovine haemoglobin and only one (β -92 cysteine) is present in each β -chain¹². No differences were found between 4-HMB-treated and untreated samples of bovine SFH modified with glutaraldehyde and pyridoxal-5-phosphate.

Fig. 3 shows a typical pH gradient along the IEF pattern based on the relative positions of zones of native proteins with known *pI* values. The positions of human haemoglobin subunits after treatment of SFH with 4-HMB are indicated by perpendicular lines. This multicomponent system usually contains 20–24 distinct subfractions which can serve as *pI* markers covering the range *pI* 5.5–7.7. This colour kit is relatively easy to prepare from a stock of dry oxyhaemoglobin^{1,7} whenever needed. The positions of some zones around *pI* 6 are sensitive to the amount of sample applied. This is possibly due to some interaction of the subfraction with the components of the ampholyte. Further investigation of this effect is in progress. A combination of human haemoglobins and of their dissociation products after treatment with 4-HMB seems to be useful means for calibration of IEF in the range *pI* 5–8.

REFERENCES

- 1 T. I. Přistoupil, M. Kramlová, H. Fořtová, V. Fričová and L. Kadlecová, *J. Chromatogr.*, 288 (1984) 469.
- 2 M. Kramlová, T. I. Přistoupil, S. Ulrych, V. Fričová, J. Kraml and G. Hübner, *J. Chromatogr.*, 193 (1980) 515.
- 3 T. I. Přistoupil, M. Kramlová, S. Ulrych, V. Fričová and J. Kraml, *J. Chromatogr.*, 219 (1981) 128.
- 4 P. D. Boyer, *J. Am. Chem. Soc.*, 76 (1954) 4331.
- 5 M. A. Rosemeyer and E. R. Huehns, *J. Mol. Biol.*, 25 (1967) 253.
- 6 T. I. Přistoupil and S. Ulrych, *Czech. Pat.*, PV 674-71, 15400, A61 k27/10 (1973).
- 7 T. I. Přistoupil, M. Kramlová, H. Fořtová and S. Ulrych, *Haematologia*, 18 (1985) 45.
- 8 V. Fričová, T. I. Přistoupil, E. Paluska, M. Kramlová and S. Ulrych, *Czech. Pat. Appl.*, PV 9965-83 (1983).
- 9 M. Feola, H. Gonzales, P. C. Canizaro, D. Bingham and P. Periman, *Surg. Gynecol. Obstetr.*, 157 (1983) 399.
- 10 H. Fořtová, M. Kramlová and T. I. Přistoupil, in preparation.
- 11 *Agarose IEF, Pharmacia Instruction Manual No. 52-1536-001*, Pharmacia, Uppsala, 1980.
- 12 M. O. Dayhoff, L. T. Hunt, W. C. Barker, R. M. Schwartz and B. C. Orcutt, *Protein Sequence Dictionary 1978, Atlas of Protein Sequence and Structure*, Vol. 5, Suppl. 1, 2 and 3, National Biomedical Research Foundation, Washington, DC, p. 437.

CHROM. 18 008

Note

Gas chromatographic and mass spectrometric identification of sulphur gases in kraft digestion plants

JUHANI KANGAS

Kuopio Regional Institute of Occupational Health, Box 93, 70701 Kuopio (Finland)

(First received May 20th, 1985; revised manuscript received June 21st, 1985)

Little information has recently been published on gaseous emissions from the kraft digestion process in work areas. The sulphur gases from kraft digestion plants most often determined are hydrogen sulphide, methanethiol, dimethyl sulphide and dimethyl disulphide^{1,2}. Small amounts of 1-methylethanethiol and thiophene have also been analyzed in condensates³. The formation of 1-methylethanethiol and isopropyl sulphide occurs when eucalyptus chips are been used as a raw material in kraft digestion⁴. The main source of the sulphur gas emissions in digester plants are leaks in condensers, pumps and pipe seals¹.

In previous studies, identification of the sulphur compounds was by use of gas chromatography (GC)^{1,2}. The purpose of this study was to identify non-condensable sulphur compounds emitted in kraft digestion by use of gas chromatography–mass spectrometry (GC–MS).

MATERIALS AND METHODS

Samples were collected at a kraft pulp mill which used pine chips as raw material and a continuous digestion method. Non-condensable gases from the digester were collected after the turpentine condenser. Gases were allowed to pass from the gas line into a 10-l plastic bag. The direct analysis of samples with a mass spectrometer was not successful because nitrogen and oxygen interfered the mass spectrum of hydrogen sulphide and the concentrations of the sulphur gases were too low.

Sample gases were therefore concentrated using a cryogenic enrichment. The cold-traps were immersed in liquid nitrogen and the non-condensable gases collected were evacuated from the primary sampler bag through the trap using MSA pumps at a speed of 0.1 l/min. Sulphur gases condensed in the cold-trap and oxygen and nitrogen were thus excluded. After immersion of the cold-trap into a warm (30°C) water-bath, the expanded sulphur gases were collected in a 1-l plastic bag. High boiling sulphur compounds were extracted from the remainder in the cold-trap with 30 ml diethyl ether.

The samples were analyzed using a Hewlett-Packard 5790A gas chromatograph connected to a Jeol JMSD-300 mass spectrometer. A 25-m silica capillary column containing OV-101 was used. The gas samples were injected with a 0.5-ml gas-tight syringe. The injection-port temperature was 40°C and the oven temperature

was 0°C. Helium was used as a carrier gas at a flow-rate of 1 ml/min. For the analysis of liquid samples the injection-port temperature was 80°C, the oven temperature 60°C and the injection volume was 2 μ l. The mass spectrometer was used to detect the total ion current for the effluents from the column.

RESULTS

Chromatography of the sample evaporated from the cold-trap into the plastic bags yielded three main compounds, and of the sample extracted from the cold-trap

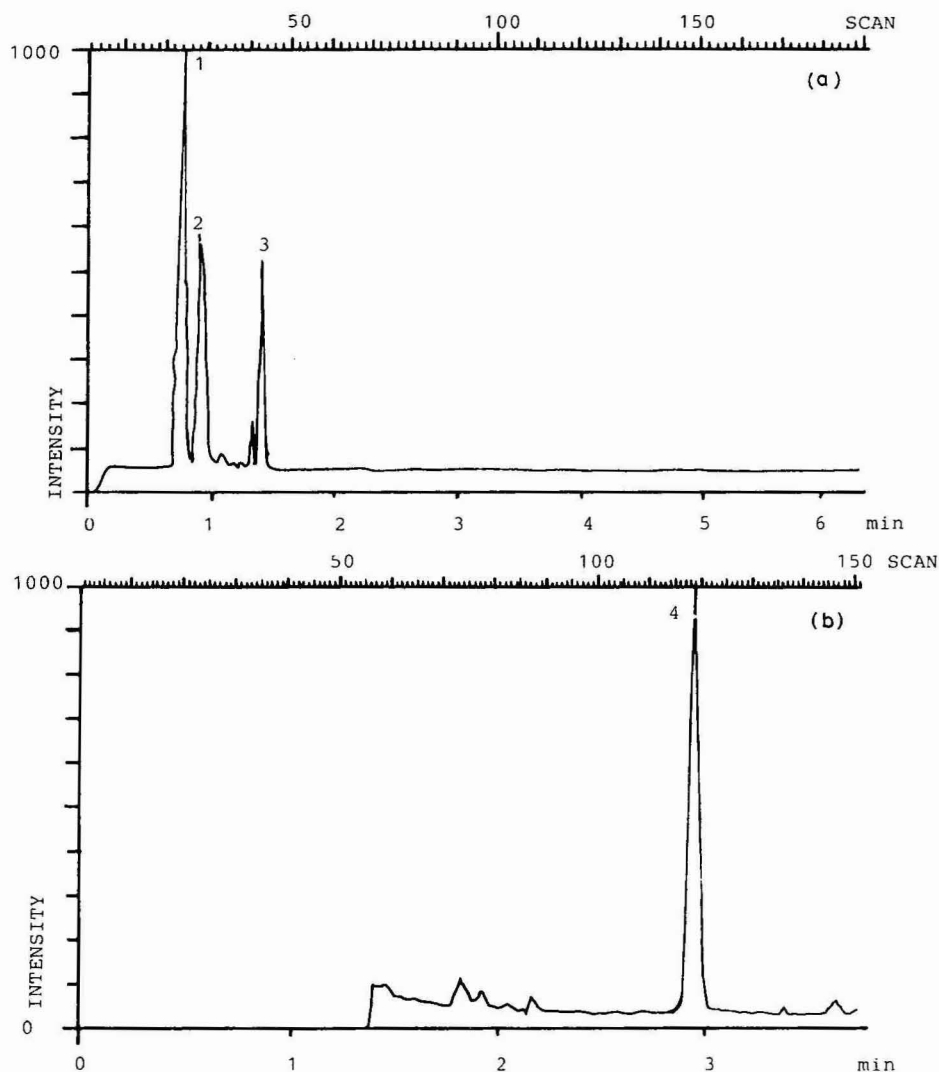


Fig. 1. Gas chromatogram of compounds evaporated from the cold-trap (a) and extracted with diethyl ether (b), recorded as the total ion current. Peaks: 1 = hydrogen sulphide; 2 = methanethiol; 3 = dimethyl sulphide; 4 = dimethyl disulphide.

with diethyl ether, one major compound. The gas chromatograms of both fractions recorded as the total ion current are presented in Fig. 1a and b.

Each compound eluted from the gas chromatograph was fed into the mass spectrometer. From the mass spectrum, hydrogen sulphide, methanethiol, dimethyl sulphide and dimethyl disulphide were identified by comparison with the prominent ions in the mass spectra of standard gases.

DISCUSSION

The sulphur gases emitted upon continuous sulphate cooking of pulp comprise: hydrogen sulphide, methanethiol, dimethyl sulphide and dimethyl disulphide. In this study the raw material used for digestion was pine chips. Under these conditions no other sulphur compounds were found among the non-condensable gases after the turpentine condenser. During the monitoring of industrial hygiene in a kraft pulp mill employing a continuous cooking system, only these four sulphur gases need be analyzed and among them hydrogen sulphide and methanethiol are of chief interest.

For successful mass spectrometric analysis of light sulphur compounds, the removal of oxygen and nitrogen is essential, because they may mask hydrogen sulphide.

REFERENCES

- 1 J. Kangas, P. Jäppinen and H. Savolainen, *Am. Ind. Hyg. Assoc. J.*, 45 (1984) 787.
- 2 J. M. Leach and L. T. K. Chung, *Tappi*, 65 (1982) 95.
- 3 B. R. Blackwell, W. B. MacKay, F. E. Murray and W. K. Oldham, *Tappi*, 62 (1979) 33.
- 4 P. O. Bethge and L. Ehrenborg, *Sven. Papperstid.*, 70 (1967) 347.
- 5 S. O. Farwell, S. J. Gluck, W. L. Barnesberger, T. M. Schulte and D. F. Adams, *Anal. Chem.*, 51 (1979) 609.

Note

Simple method for concentrating volatiles in water for gas chromatographic analysis by vacuum distillation

R. P. KOZLOSKI

The Connecticut Agricultural Experiment Station, P.O. Box 1106, New Haven, CT 06504 (U.S.A.)

(First received February 25th, 1985; revised manuscript received July 23rd, 1985)

In order to obtain mass spectrograms of the less concentrated contaminants in drinking water, a gas chromatographic–mass spectrometric (GC–MS) technique, capable of concentrating volatiles from large volumes of water, is required¹. Likewise there is a similar need if extremely low levels of trace contaminants are to be analyzed by the purge-and-trap technique using more conventional detectors.

The purge-and-trap techniques that are capable of handling liter-size water samples are either inefficient, involve the expense of constructing specialized equipment, or require long purge times or heating the water which can cause chemical changes to occur^{1–6}. The vacuum distillation apparatus described here is easily constructed and readily coupled to commercial purge-and-trap systems. The distillate of a 1-l water sample is condensed in a liquid nitrogen trap over a period of about 13 min. The purgeable components in the distillate are then transferred to a gas chromatograph by conventional gas purging. The losses of volatiles due to the formation of mists in the cryogenic trap is largely avoided by the formation of a closed system when an ice plug forms in the trap shortly after distillation begins.

EXPERIMENTAL

Purging system

A schematic diagram of the purging system is shown in Fig. 1. The purging vessel was a 1-l Pyrex 24/40 short-necked round-bottom boiling flask (1) with a 2 × 3/8 in. magnetic stirring bar (Cole-Parmer, Chicago, IL, U.S.A.) with hemispherical ends. The contents of the flask were stirred with a Thermolyne stirrer hot plate, Model SPA 1025B (2). A 20/40 JA-2790 adaptor (3) (SGA, Bloomfield, NJ, U.S.A.) connected the flask to the system. Only a small amount of silicone vacuum grease was used on the upper portion of the adaptor to reduce any possible adsorption of the volatiles. All tubing connections in the system were made with 1/4 in. I.D. polyethylene tubing (1/16 in. wall), which was softened with a heat gun for ease in making the connections. A 15-cm length of 0.7 cm O.D. glass tubing (4) connected the adaptor to the U-tube trap (5). The lower portion of the U-tube trap was 18.5 cm high and had arms of 1 cm O.D. glass tubing spaced 2.5 cm apart (center to center). The upper section of the U-tube trap was of 10 cm lengths of 0.7-cm tubing bent at right angles to the plane of the U-tube (shown on opposite sides and in the plane of the

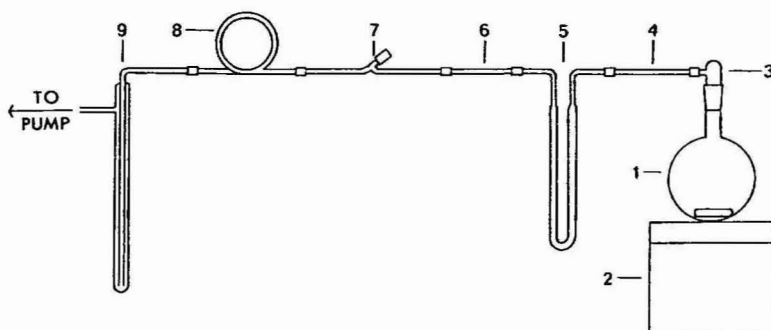


Fig. 1. Vacuum purging system. 1 = Purging flask and magnetic stirring bar; 2 = magnetic stirrer; 3 = adaptor; 4 = glass tube; 5 = U-tube trap containing glass beads; 6 = capillary tubing (optional); 7 = polytetrafluoroethylene stopcock; 8 = polyethylene tubing; 9 = vacuum trap.

U-tube in Fig. 1 to avoid overlap in the diagram). This provided a compact system and greater convenience in connecting the U-tube trap to the purge-and-trap sampler. The trap was filled with 5 g of 3-mm glass beads. The air in the system was evacuated through a 5-cm length of 0.49 mm I.D. capillary tubing (6) (cut from a 10- μ l microsyringe) connected to the trap. A Rotaflo polytetrafluoroethylene stopcock, Corning No. 7500-3 (Corning Glass Works, Corning, NY, U.S.A.) (7) isolated the capillary tube from the high vacuum portion of the system. A 10-cm diameter loop of polyethylene tubing (8) shaped by heating in a steam bath connected the stopcock to the liquid nitrogen vacuum trap (9) and provided flexibility to the system. The vacuum source for the system was a two stage mechanical vacuum pump.

Connection to purge-and-trap sampler

After concentrating the volatiles, the U-tube trap was connected to a Hewlett-Packard 7675A purge-and-trap sampler with 1/4 to 1/16 in. stainless-steel Swagelok reducing unions. The U-tube was joined to the reducing unions with 1/4 in. I.D. polyethylene tubing. The connections to the purge tube and purge return tube of the purge-and-trap sampler were of 15-gauge polytetrafluoroethylene tubing obtained from Penntube Plastics (Clifton Heights, PA, U.S.A.).

Purging technique

Before evacuating the system the U-tube trap was immersed in liquid nitrogen to a depth of 1 cm above the glass beads for a minimum of 2 min. The Dewar flask was filled with liquid nitrogen to within 6 cm of the top. The stopcock was slowly opened until gurgling from the vacuum pump was heard, at which time stirring at full speed was begun. With the stopcock open to the air, the flow-rate corresponded to about 350 ml/min. After 1 min the stopcock was slowly opened further. The Dewar flask was raised for 1 to 2 s each minute to the top of the U-tube. This helped to initiate a continuous distillation of water into the U-tube. If condensate was already moving down the lower portion of the tube the raising of the Dewar flask was delayed until the condensate reached the level of the liquid nitrogen. Once continuous distillation of the water began, the level of the liquid nitrogen was kept about 1 cm above the frozen section of the tube by raising the Dewar flask. The distillation was stopped

when the frozen condensate reached a mark 13 cm from the bottom of the tube. The average amount of water collected in the experiments was 4.41 ± 0.24 g S.D. ($n = 15$).

The U-tube is best removed from the system by cutting the polyethylene connections lengthwise with a razor blade so that the cuts form a shallow "V". The liquid nitrogen vacuum trap should be kept under vacuum when cooled to prevent possible hazardous liquid air accumulation.

Since the purge-and-trap sampler inlet and outlet were vented to the atmosphere when in the prepurge mode, the U-tube was connected to the sampler immediately, without concern for pressure build-up as the tube warmed. After bringing the tube to 25°C by placing it upright in a beaker of water, the concentrate was purged for 10 min with a helium flow-rate of 20 ml/min.

Gas chromatography

The purge-and-trap sampler was coupled to a Hewlett-Packard 5840A gas chromatograph equipped with a flame ionization detector. An 8 ft. \times 1/8 in. O.D. stainless-steel column packed with 1% SP-1000 on 60–80 mesh Carbowax B (Supelco, Bellefonte, PA, U.S.A.) was used for the analyses. The helium flow-rate was 30 ml/min. The temperature programming was started at 45°C with a 3-min hold followed by an 8°C/min heating rate to 200°C. Purge and column flow-rates were regulated with a mass flow controller.

Measurement of recoveries

To obtain the GC response factors of the volatiles selected for the determination of recovery efficiencies, a 5- μ l portion of the volatiles dissolved in methanol was transferred to a 10-ml purge-and-trap sampler tube. Heating was found to be unnecessary for the transfer of the compounds used in the recovery tests. Less volatile compounds can be transferred by placing aluminium foil behind the tube to act as a heat shield and heating the tube with a heat gun. Care must be taken to begin the purge before heating or a portion of the compounds may escape out the purge vents. Standards were analyzed after each vacuum distillation to compensate for time-dependent variations when calculating the recoveries.

While slowly momentarily stirring, the 1-l water samples were spiked directly in the flask with a 5- μ l injection of a methanolic solution of the volatiles.

RESULTS AND DISCUSSION

Not all stirring bars or magnetic stirrers were found to be able to achieve the high stirring speed used in this technique. Flat-ended stirring bars appeared to have much less rotational stability than those with rounded ends. This may be due to the flat-ended stirring bars slightly higher positioning in the flask and the resulting weaker interaction with the stirring plate magnet. Differences in stirring bar stability were also noted among the brands of magnetic stirrers. Some makes were unable to keep the stirring bar centered at high speed or their highest speed was insufficient to form a vortex 2.4 cm wide at the bottom of the flask. The speed of the stirrer under the stirring load used was 1280 rpm, which is significantly greater than the nominal speed listed by the manufacturer. A preliminary experiment with a lower-speed stirrer,

TABLE I
RECOVERIES AND PURGE RATIOS OF SELECTED COMPOUNDS

Compound	Recovery (%) \pm S.D. (n = 4)		Purge ratio
	With capillary	Without capillary	
Hexane	83 \pm 3	87 \pm 7	0.12
Carbon tetrachloride	85 \pm 1	85 \pm 3	0.14
Chloroform	82 \pm 2	83 \pm 2	0.32
Dichloromethane	81 \pm 3	82 \pm 3	0.42
Benzene	81 \pm 2	81 \pm 3	0.25
1,2-Dichloroethane	68 \pm 1	67 \pm 2	0.66
Diethyl ether	63 \pm 3	62 \pm 3	0.68
Methyl isobutyl ketone	12.3 \pm 0.3	12.2 \pm 0.6	0.96
Methyl acetate	11.8 \pm 0.6	11.2 \pm 0.6	0.94
Tetrahydrofuran	3.7 \pm 0.2	3.6 \pm 0.1	0.97

which formed a vortex reaching to within 3.5 cm from the bottom, gave an 11% lower average recovery of the volatiles than when the faster stirrer was used.

Differences in the weight and volume of flasks of even the same brand were found to have an effect on the stirring. The rotational stability of the stirring bars was greater in the lighter flasks. On the assumption that this greater stability was due to better interaction between the stirring bar and stirrer magnet because of thinner glass, the height of the stirrer magnet was increased by adjusting the set screw positioning the magnet. This resulted in a considerable increase in the rotational stability of stir bars used in the heavier flasks.

The volume of the flask used in the experiments was such that when it was filled to 1 l, the diameter of the surface of the water was 8.4 cm. The diameter of the water surface should be as wide as possible, since this will make a strong vortex easier to form. If necessary a smaller volume of water may have to be used in order to obtain a strong vortex.

A phenomenon is observed during the vacuum distillation that can mistakenly lead one to believe a leak is present in the system. After the initial condensation of water in the U-tube there is a period when no material appears to be distilling over. Normal distillation is eventually resumed when water begins to condense on the inside surface of the tube and then falls into the liquid nitrogen zone. This effect is believed to be the result of dissolved gases escaping from the water in the flask after the initial transfer of water seals off the flask from the vacuum pump. These residual gases which impede the transfer of water vapor finally become trapped in condensing moisture and normal distillation resumes.

Hexane, carbon tetrachloride, chloroform, dichloromethane, benzene, 1,2-dichloroethane, diethyl ether, methyl isobutyl ketone, methyl acetate and tetrahydrofuran were used to determine the recovery efficiencies achieved by vacuum distillation (Table I). The recovery tests were conducted at 25°C with the volatiles at a concentration of 40 ppb* by weight. Tests with and without the capillary tube were performed in quadruplicate. The purpose of the capillary tube in the system was to

* Throughout the article the American billion (10^9) is meant.

decrease the initial flow of gases through the U-tube and thus increase the trapping efficiency of the more volatile components. The results in Table I show that there are insufficient differences in the data sets to indicate a statistically significant difference in recoveries between the two techniques.

To determine if the recovery efficiencies of volatiles could be estimated, purge ratios⁷ were used. Purge ratios were calculated from GC data obtained by repeated purges of a water sample using a Hewlett-Packard purge-and-trap sampler. A 10-ml water sample was spiked with 5 μ l of the methanolic standard. The sample was purged for 5 min at 25°C with a stream of helium at a flow-rate of 20 ml/min. The purge ratios, which are a measure of the ease of purging a volatile component, were calculated by dividing the GC response of a purge by the response of the preceding purge. Since a low purge ratio indicates that a compound is easily purged from water, it should indicate a high recovery rate.

The data in Table I show that readily purged compounds with a purge ratio between 0.12 and 0.42 had a narrow recovery range of 81 to 87%. The less readily purged 1,2-dichloroethane and diethyl ether had purge ratios of 0.66 and 0.68, respectively, and were recovered in the 62-67% range. The difficult to purge compounds with purge ratios between 0.94 and 0.97 had recoveries from 4 to 12%.

Overall this vacuum distillation technique has been found to be an effective method of concentrating purgeable water contaminants for analysis.

REFERENCES

- 1 F. C. Kopfler, R. G. Melton, R. D. Lingg and W. E. Coleman, in L. H. Keith (Editor), *Identification and Analysis of Organic Pollutants in Water*, Ann Arbor Publ., Ann Arbor, MI, 1976, Ch. 6, p. 87.
- 2 A. Zlatkis, H. A. Lichtenstein and A. Tishbee, *Chromatographia*, 6 (1973) 67.
- 3 J. P. Mieure and M. W. Dietrich, *J. Chromatogr. Sci.*, 11 (1973) 559.
- 4 B. J. Dowty, D. R. Carlisle and J. L. Laseter, *Environ. Sci. Technol.*, 9 (1975) 762.
- 5 K. Grob, *J. Chromatogr.*, 84 (1973) 255.
- 6 J. Novák, J. Žlutický, V. Kubelka and J. Mostecký, *J. Chromatogr.*, 76 (1973) 45.
- 7 R. P. Kozloski and B. L. Sawhney, *Bull. Environm. Contam. Toxicol.*, 29 (1982) 1.

CHROM. 18 068

Note

Separation of phenylthiocarbamyl amino acids by high-performance liquid chromatography on Spherisorb octadecylsilane columns

CHAO-YUH YANG* and FELIX I. SEPULVEDA

Baylor College of Medicine and Department of Medicine, The Methodist Hospital, 6565 Fannin Street, Houston, TX 77030 (U.S.A.)

(Received July 10th, 1985)

The role of the reagent phenylisothiocyanate (PITC) for amino terminal degradation, discovered by Edman in 1956, has become increasingly important. All current liquid, solid, and gas phase protein sequencers are designed on the principal of Edman degradation chemistry¹. Many investigators have improved the analysis of phenylthiohydantoin (PTH) amino acids through the use of reversed-phase high-performance liquid chromatography (RP-HPLC) as a means for identification and quantification^{2–5}.

The application of PITC for precolumn derivatization of amino acids and the quantification of phenylthiocarbamyl (PTC) derivatives by RP-HPLC have been published⁶. A commercial system, PICO-TAG, is available from Waters Assoc. Most precolumn modification methods for amino acid analysis are very sensitive because of fluorescent amino acid derivatives^{7–10} or color chromophores of the reagent¹¹; however, these applications have been limited by either a lack of proline reaction from the *o*-phthalaldehyde method or an excess of reagent that interferes with the separation processes utilizing dansyl chloride¹⁰ and dimethylaminoazobenzene-4-sulfonylchloride¹¹, respectively. The application of PITC for amino acid analysis is rapid, sensitive, and simple to quantify, overcoming these disadvantages.

Our improvements of this method facilitate the separation of PTC-amino acid derivatives for analysis of smaller amounts of material in shorter periods of time. In this report we describe the separation of 22 PTC-amino acids by HPLC on Spherisorb ODS column in low picomole concentration.

EXPERIMENTAL

Chemicals

PITC, triethylamine (TEA), a standard mixture of amino acids, and a kit of individual amino acid standards were purchased from Pierce. Acetonitrile was an HPLC-grade product from Burdick and Jackson Labs. Water was deionized, then purified with the Milli-Q water system. Two peptides used for amino acid analysis were oxidized insulin A-chain and glucagon. Both peptides were obtained from Sigma.

Coupling of amino acids with PITC

PITC-amino acid derivatives were prepared according to the Waters PICO-TAG procedure with some improvement. The procedure involved two steps: (1) hydrolysis of the sample and (2) derivatization. Before sealing the samples in a vacuum for hydrolysis at 110°C for 24 h, the dry samples in small tubes (6 × 50 mm) were placed in the reaction vial with 200 μ l of 6 M HCl. The hydrolyzed samples were dried and redried by adding 20 μ l of ethanolic solution (ethanol–water–TEA, 1:1:1) to ensure that a trace amount of ammonia was left. For derivatization, the samples were coupled with 20 μ l of PITC solution (ethanol–water–TEA–PITC, 7:1:2:1) for 10 min, dried again in a Speedvac (Savant Instruments), and reconstituted in sample diluent for analysis. The sample diluent was a 0.5 M sodium phosphate buffer, pH 7.4, and 5% acetonitrile.

The 22 PTC-amino acid standard was prepared by adding 1 nmol of each of the individual amino acids (carboxymethylcysteine, Trp, Gln, S-sulfocysteine (Cys-SO₃H), hydroxyproline, and Asn) to 1 nmol of the Pierce amino acid mixture (Asp, Glu, Ser, Gly, His, Thr, Ala, Arg, Pro, Tyr, Val, Met, Cys, Ile, Leu, Phe, Lys) which was hydrolyzed and derivatized simultaneously with samples using the PICO-TAG procedure described above.

RP-HPLC separation of PITC-amino acids

A Hewlett-Packard HP 1090 liquid chromatograph and a Spherisorb ODS II (3 μ m, 150 × 4.6 mm I.D.; Custom LC, Houston, TX, U.S.A.) were used for the separation. The PITC derivatives were identified using an HP 1040A HPLC detection system at 254 nm. The chromatographic conditions were: column temperature 47°C; flow-rate 0.8 ml/min; buffer A: 0.03 M sodium acetate, 0.05% TEA, and 6% acetonitrile (pH 6.4); buffer B: 40% water in acetonitrile; mobile phase isocratic at 0% B for 1.5 min; first linear gradient from 0 to 12% B in 10 min; second linear gradient from 12% to 48% in 10 min, and final change to 95% B in 0.1 min; maintenance at 95% B isocratic flow for 5 min; return of the system to 0% B in 5 min.

RESULTS AND DISCUSSION

The separation of 50 pmol of the 22 PTC-amino acids on Spherisorb ODS (150 × 4.6 mm) is shown in Fig. 1. All amino acid derivatives, including ammonia and an unknown peak, were well separated under those conditions in 22 min. To achieve a better resolution between PTC-Cys-SO₃H and PTC-Asp, an isocratic elution of buffer A was used for 1.5 min.

The characteristics of PTC-amino acids separated on an ODS column with sodium acetate buffer system are similar to those of dimethylaminoazobenzenethiohydantoin (DABTH) amino acids and PTH-amino acids. This means that (1) the retention times of acidic and basic amino acid derivatives can be influenced by altering the pH of the sodium acetate buffer, (2) the position of the His and Arg derivatives can be altered by changing the salt concentration^{12–16}, and (3) the retention times of His and Arg derivatives gradually change during the lifetime of the column^{5,12,17–19}.

An elevated column temperature improves the resolution of the PTC-amino acids and reduces the pressure drop over the column. The retention time of PTC-Arg can be decreased by increasing the salt concentration of buffer A. Hence, the position

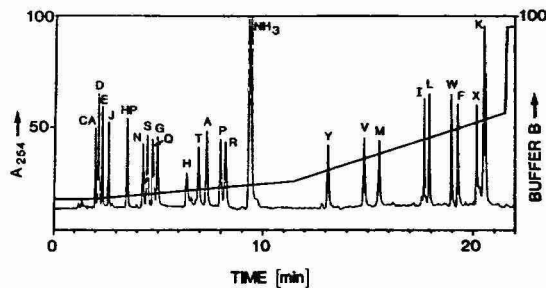


Fig. 1. HPLC chromatogram of a standard mixture of 22 PTC-amino acids (50 pmol each) on a column packed with Spherisorb ODS, 3 μ m column. Chromatographic conditions are described in the Experimental section. The solvent gradient is indicated in the figure. CA = Cysteic acid; D = aspartic acid; E = glutamic acid; J = carboxymethcysteine; HP = hydroxyproline; N = asparagine; S = serine; Q = glutamine; G = glycine; H = histidine; T = threonine; A = alanine; P = proline; NH₃ = ammonia; Y = tyrosine; V = valine; M = methionine; I = isoleucine; L = leucine; W = tryptophan; F = phenylalanine; X = unknown peak; K = lysine.

of the PTC-Arg on the chromatogram can be changed as desired in order to achieve a better separation. Using the Spherisorb ODS column and the conditions described in the Experimental section, the PTC-Arg can be changed from its position behind PTC-Pro to a position between PTC-His and PTC-Thr by changing the sodium ace-

TABLE I
AMINO ACID ANALYSIS OF GLUCAGON AND INSULIN A-CHAIN OXIDIZED FORM BY RP-HPLC OF PTC-AMINO ACIDS

A = Number of residues found; B = number of residues expected based upon the known sequences.

Amino acid	Glucagon		Insulin A-chain	
	A	B	A	B
Cys-SO ₃ H	—	—	4.12	4
Asp	4.10	4	1.88	2
Glu	3.00	3	4.22	4
Ser	3.82	4	1.99	2
Gly	1.08	1	1.09	1
His	0.82	1	—	—
Thr	2.92	3	—	—
Ala	1.18	1	1.00	1
Pro	—	—	—	—
Arg	2.10	2	—	—
Tyr	1.92	2	1.94	2
Val	1.10	1	1.74	2
Met	1.10	1	—	—
Ile	—	—	0.76	1
Leu	1.86	2	2.26	2
Phe	1.89	2	—	—
Lys	1.11	1	—	—
Trp	n.d.*	1	—	—
Total	28.00	29	21.00	21

* n.d. = Not determined.

tate concentration from 0.03 to 0.153 M, while the order of the other PTC-amino acids remains the same.

Amino acid analysis of an oxidized insulin A-chain and glucagon, obtained with the system as described in the Experimental section, is listed in Table I. Those data appear to be reliable at the 30-pmol level. According to the stable baseline shown in Fig. 1 (using 50 pmol of each amino acid), quantification of samples with less than 10 pmol of material is feasible.

The advantages of the present system for amino acid analysis are the following: (1) high resolution to separate all 22 PTC-amino acids; (2) possibility to analyze the samples containing carboxymethylcysteine and cysteic acid; (3) ability to shorten the analysis time as compared with the original method⁶; (4) possibility to analyze sample at the low picomole level; (5) ability to substantially save solvent consumption due to the slower flow rate (0.8 ml/min).

Over the past few years, RP-HPLC techniques have been improved in instrumental design, detection sensitivity, packing material for columns, and solvents. In order to increase detection sensitivity and to save solvent consumption and time, the use of microbore column has increased. Commercial columns are available from a number of different companies. Since the mobile phase flow-rate is proportional to the product of the linear velocity and the column cross-sectional area, solvent consumption can be reduced proportionally to the square of the column radius²⁰. Thus the microbore column reduces solvent consumption and increases mass sensitivity. The application of microbore columns for PTC-amino acid analysis would enable the analysis of amino acids at the femtomole level.

ACKNOWLEDGEMENTS

We thank Tseming Yang and Billy Touchstone for excellent technical assistance, Mrs. Susan Kelly for the artwork, and Mrs. Marjorie Sampel for preparation of this manuscript. This work was supported by a Specialized Center of Research on Atherosclerosis (HL27341).

REFERENCES

- 1 P. Edman, *Acta Chem. Scand.*, 10 (1956) 761.
- 2 L. E. Henderson, T. D. Copeland and S. Ososzlán, *Anal. Biochem.*, 102 (1980) 1-7.
- 3 G. E. Tarr, *Anal. Biochem.*, 111 (1981) 27-32.
- 4 J. Simmons and D. H. Schlesinger, *Anal. Biochem.*, 104 (1980) 254-258.
- 5 N. D. Johnson, M. W. Hunkapiller and L. E. Hood, *Anal. Biochem.*, 100 (1979) 335-338.
- 6 R. L. Heinrikson and S. C. Meredith, *Anal. Biochem.*, 136 (1984) 65-74.
- 7 W. Voelter and K. Zech, *J. Chromatogr.*, 112 (1975) 643-649.
- 8 K. V. J. Swedas, J. L. Galaev, I. L. Borislow and I. V. Berezin, *Anal. Biochem.*, 101 (1980) 188.
- 9 J. C. Hodgkin, *J. Liq. Chromatogr.*, 2 (1979) 1047.
- 10 T. Yamabe, N. Takai and H. Nakamura, *J. Chromatogr.*, 104 (1975) 359-365.
- 11 J. Y. Chang, R. Knecht and D. G. Braun, *Biochem. J.*, 199 (1981) 547-555.
- 12 C. Y. Yang and S. J. Wakil, *Anal. Biochem.*, 137 (1984) 54-57.
- 13 J. T. Chang, *Biochem. J.*, 199 (1981) 557-564.
- 14 K. Sugden, G. B. Cox and C. R. Loscombe, *J. Chromatogr.*, 149 (1978) 377-390.
- 15 E. Lundanes and T. Greibrokk, *J. Chromatogr.*, 149 (1978) 241-254.
- 16 W. D. Annan, *J. Chromatogr.*, 173 (1979) 194-197.
- 17 L. Scottrup-Jensen, T. E. Petersen and S. Magnusson, *Anal. Biochem.*, 107 (1980) 456-460.
- 18 S. J. Dimari, J. P. Robinson and J. H. Hash, *J. Chromatogr.*, 213 (1981) 91-97.
- 19 F. Lottspeich, *Hoppe-Seyler's Z. Physiol. Chem.*, 361 (1980) 1829-1834.
- 20 R. P. W. Scott (Editor), *Small Bore Liquid Chromatography Columns*, Wiley, New York, 1984.

CHROM. 18 010

Note

High-performance liquid chromatographic analysis of Aspartame

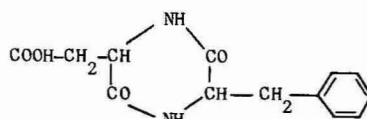
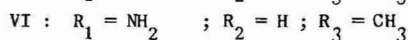
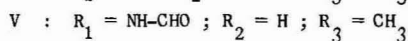
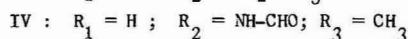
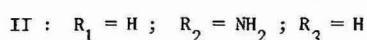
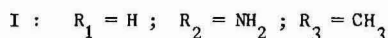
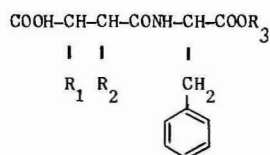
G. VERZELLA and A. MANGIA*

Pierrel S.p.A., Chemical Research and Development, Via Comelico 39, 20135 Milano (Italy)

(First received June 7th, 1985; revised manuscript received June 24th, 1985)

Aspartame¹ (L- α -aspartyl-L-phenylalanine methyl ester, I) is a sweetener discovered 20 years ago, but which has been marketed only since 1981 in the U.S.A. after final approval² by the Food and Drugs Administration. It has been used as a table-top sweetener mainly in European countries, and as a food additive and a sugar substitute in carbonated soft drinks in the U.S.A.

Its stability is strongly dependent on the pH in aqueous solution³ and on temperature⁴ during drying and storage; the products of degradation are the dipeptide L- α -aspartyl-L-phenylalanine (II) and chiefly 5-benzyl-3,6-dioxo-2-piperazine-acetic acid (III), hereafter diketopiperazine, which are non-toxic⁵ but devoid of sweetness¹.



III

The official method⁶ of analysis of Aspartame requires a titration with lithium methoxide, but chromatographic methods, using an amino acid analyzer^{7,8} or liquid chromatograph⁸⁻¹², are also available. We now report a method designed to obtain a very short analysis time and to separate Aspartame at a higher retention time with respect to the above degradation products, and intermediates in its synthesis.

EXPERIMENTAL

Materials and reagents

Reference standards of Aspartame (I), the dipeptide (II), diketopiperazine (III),

N-formyl- α -aspartame (IV), N-formyl- β -Aspartame (V), β -Aspartame (L- β -aspartyl-L-phenylalanine methyl ester, VI), were prepared in Pierrel's Chemical Synthesis Laboratories. Their purity was tested by high-performance liquid chromatography (HPLC), IR, ^1H NMR and C,H,N analysis and found to be not less than 99% on a dry basis. Aspartame samples were from Pierrel. Potassium dihydrogen phosphate and 85% phosphoric acid were reagent grade from E. Merck (Darmstadt, F.R.G.), while acetonitrile was HPLC grade from the same supplier.

HPLC

An Hewlett-Packard Model 1090 A chromatograph equipped with a Model 1040 variable-wavelength UV detector (diode array) operating at 215 nm and a Model 3390 A recording integrator was employed. The column (120 \times 4 mm) was packed with 5- μm Hypersil MOS (Hewlett-Packard, Cernusco sul Naviglio, Italy).

The mobile phase was prepared as follows. Potassium dihydrogen phosphate (1.36 g) was dissolved in distilled water (800 ml) and a 5% (w/v) solution of phosphoric acid was used to adjust the pH to 2.5. Finally the mixture was brought to volume (1 l) and filtered through a 0.45- μm membrane. This solution (770 parts) was diluted in acetonitrile (230 parts) and degassed in an ultrasonic bath by applying a moderate vacuum.

The temperature of the column was maintained at 25°C and the flow-rate of the mobile phase was 2 ml/min.

Sample and standard preparations

Aspartame (ca. 50 mg) was weighed in a volumetric flask (100 ml) and dissolved in acetonitrile (25 ml) and a 0.01 M phosphate buffer, pH 4.5. Solutions of compounds II–VI at concentrations 1/50 of that of Aspartame were prepared similarly. Aliquots (10 μl) of these solutions were injected into the chromatograph. Quantitation was performed by use of an appropriate external standard in similar concentration, in triplicate experiments.

RESULTS AND DISCUSSION

As Aspartame had been produced by Pierrel since 1981, we needed a procedure not only for the quantitation of Aspartame in the final product, but also for the identification of the impurities present. Apart from the amino acid analyzer^{7,8}, HPLC is usually more sensitive to small quantities of impurities. An excellent method for the separation of impurities in Aspartame bulk products was presented by Signoretti *et al.*¹⁰, requiring about 14–16 min.

In our synthesis¹³ of Aspartame there is the need to separate α - from β -Aspartame, derived respectively from the hydrolysis of N-formyl- α - or β -Aspartame, which result from the coupling between L-phenylalanine methyl ester and N-formyl-aspartic anhydride. In fact this acylation step affords a mixture of the α - and β -isomers. In the final product, mainly during the later steps of the synthesis and in the recovery of the dried products, dipeptide (II) and diketopiperazine (III) have to be monitored accurately, as stated before. Finally a very short analysis time is the key rapid monitoring of the process.

Fig. 1 shows the separation of an artificial mixture of Aspartame and related

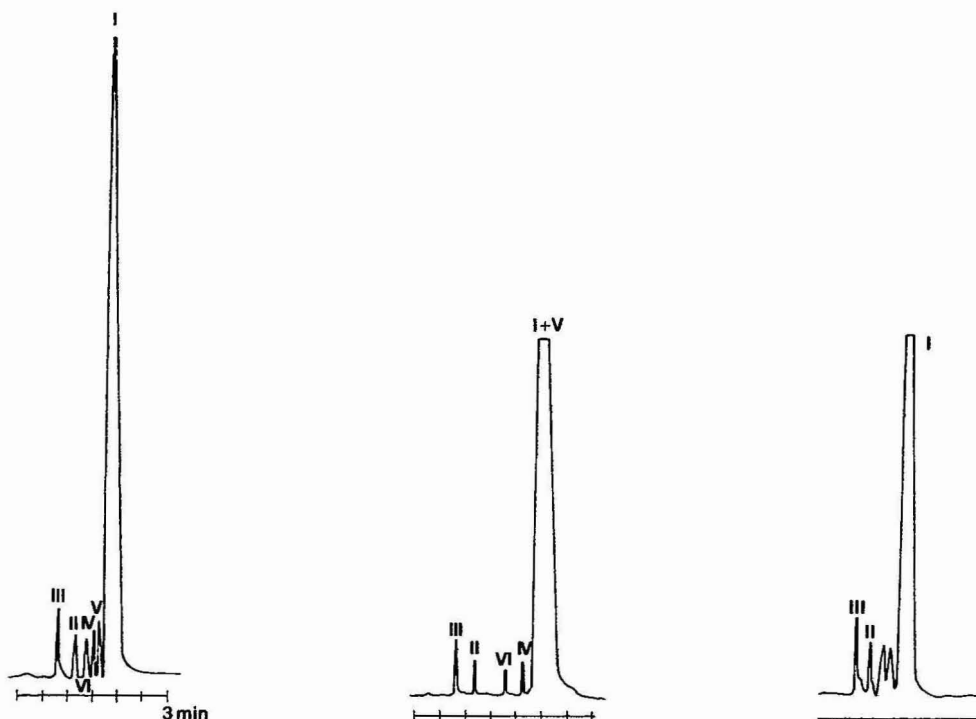


Fig. 1. Chromatogram of an artificial mixture of aspartame and related products.

Fig. 2. Chromatogram obtained by lowering the acetonitrile content in the mobile phase to 18%.

Fig. 3. Chromatogram obtained by increasing the acetonitrile content in the mobile phase to 25%. Compounds IV-VI are eluted in the two unlabelled peaks.

impurities II-VI, each at 1% of the level of I. The resolution of the six-component mixture is achieved in less than 2.5 min. The quantity of acetonitrile is the critical parameter in the separation of the substances: small changes in its concentration, lower or higher than the value of 23%, make the separation impossible. Lowering the acetonitrile concentration to 18% (fig. 2) results in better resolution of some products but causes compound V to overlap Aspartame; increasing its content to 25% (Fig. 3) does not allow a complete resolution, as compounds V and VI have the same retention time. Another important parameter is the pH. Fig. 4 shows a chromatogram of an artificial mixture in which Aspartame is approximately at the same concentration as those of the other products: it is seen that the retention times are completely different to those presented in Fig. 1; Aspartame is less retained than its isomer (VI) and intermediate (V). Thus it is practically impossible to determine compounds V and VI in a trace analysis (Fig. 5).

Table I collects the data corresponding to the calibration curve for Aspartame in Fig. 6, obtained under the same conditions as Fig. 1. The correlation coefficient¹⁴, $r = 0.9998$, is excellent in the range 0.4-0.6 mg/ml Aspartame, and the coefficient of variation is lower than 1% at each concentration tested. Table II shows data pertaining to the quantitation of compounds II-VI at a concentration relative to that

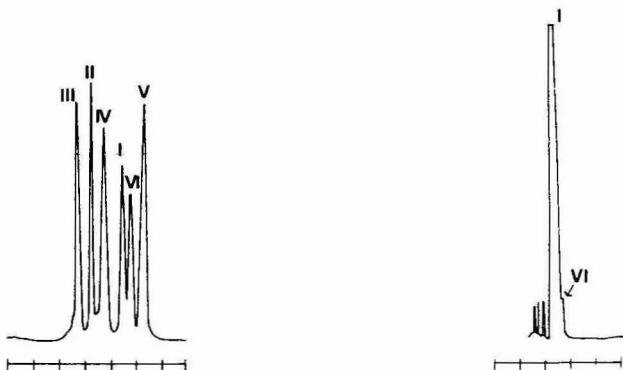


Fig. 4. Separation obtained at pH 4.5 of an artificial mixture of components I-VI each at 1% concentration.

Fig. 5. Chromatogram obtained under the same conditions as in Fig. 4, but with β -Aspartame (VI) at 1% of the concentration of Aspartame (I).

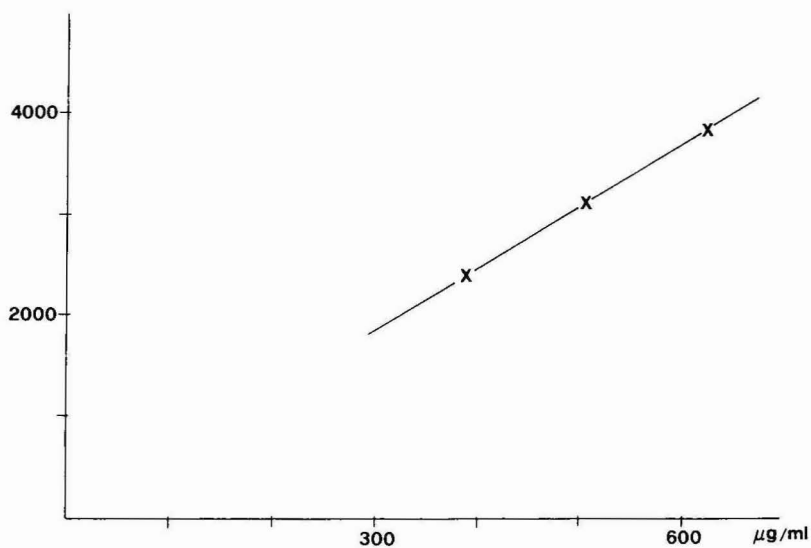


Fig. 6. Calibration curve of Aspartame (I) showing area counts vs. concentration ($\mu\text{g/ml}$).

of Aspartame of about 0.4% for diketopiperazine(III), the dipeptide II and β -Aspartame (VI) and 0.2% each for N-formyl- α - and β -Aspartame (IV) and (V), the last two compounds normally being absent in Aspartame batches.

The HPLC method described may be applied using different commercial columns and liquid chromatographs; Fig. 7 shows the chromatogram of the same artificial mixture as in Fig. 1 with the same mobile phase and chromatographic conditions, but using a 5- μm reversed-phase C_8 column of different size (25×0.4 cm; Brownlee Labs., Italab, Florence) and a Perkin-Elmer Model 3B chromatograph with

TABLE I
VALIDATION OF ASPARTAME ANALYSIS

Experiment	Aspartame concentration (mg/ml)		
	0.387	0.505	0.625
1	2413.9*	3095.0	3896.3
2	2371.0	3132.0	3895.2
3	2390.0	3130.0	3871.0
4	2415.0	3078.0	3811.0
5	2409.0	3085.0	3849.0
Average	2399.2	3104.0	3864.4
Standard deviation	18.5	25.4	35.9
Coefficient of variation (%)	0.77	0.81	0.92

* Area counts.

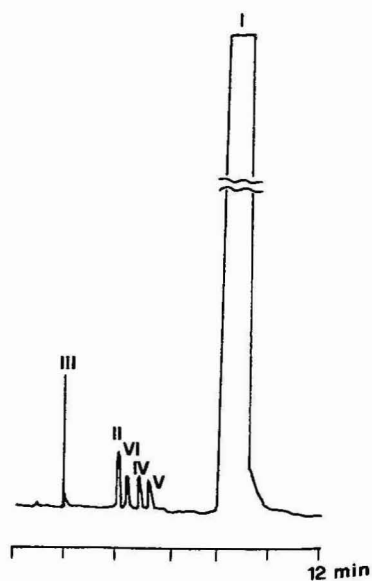


Fig. 7. Chromatogram of the same artificial mixture as in Fig. 1 but obtained on a Perkin-Elmer 3B chromatograph.

LC 75 detection and integrator Σ 10. The separation of impurities is excellent, but the analysis time is about four times that obtained with the previous columns; however, it is still less than needed by other methods.

Further work is in progress to find other methods for separating intermediates of the chemical synthesis.

TABLE II

STATISTICAL ANALYSIS OF THE IMPURITIES II-VI IN ASPARTAME

	<i>Diketopiperazine (III)</i>	<i>Dipeptide (II)</i>	<i>β-Aspartame (VI)</i>	<i>Formyl-α-Aspartame (IV)</i>	<i>Formyl-β-Aspartame (V)</i>
Concentration ($\mu\text{g/ml}$)	2.01	2.07	1.98	0.84	1.04
1	24.92*	15.51	9.99	4.78	4.63
2	22.5	14.65	10.40	5.15	4.91
3	23.56	14.47	9.94	5.69	5.34
4	24.23	16.45	9.14	4.98	4.89
5	22.10	15.02	10.56	5.33	4.64
Average	23.462	15.22	10.006	5.186	4.882
Standard deviation	1.17	0.79	0.56	0.35	0.288
Coefficient of variation (%)	4.98	5.2	5.6	6.7	5.9

* Area counts.

ACKNOWLEDGEMENTS

We thank Dr. Roberto Gaita (Hewlett-Packard) for kind permission to use the HPLC instruments and accessories.

REFERENCES

- 1 R. H. Mazur, J. M. Schlatter and A. H. Goldkamp, *J. Amer. Chem. Soc.*, 91 (1969) 2684.
- 2 *Fed. Reg.*, 46, 38285, Washington, DC, July 24th, 1981.
- 3 M. Prudel and D. Davidkova, *Nahrung*, 25 (1981) 193.
- 4 H. H. El-Shattaway, G. E. Peck and D. O. Kildsig, *Drug Develop. Ind. Pharm.*, 7 (1981) 605.
- 5 *Aspartame, Toxicological Evaluation of Certain Food additives*, World Health Organization, Food Additives Series, No. 15, Joint FAO-WHO Expert Committee on Food Additives, 1980, p. 18.
- 6 *Code of Federal Regulations*, Title 21, 172.804, 463, Washington, DC, 1979.
- 7 Z. Vesely, E. Davidkova and M. Prudel, *Nahrung*, 24 (1980) 525.
- 8 J. Scherz, J. C. Monti and R. Jost, *Z. Lebensm.-Unters.-Forsch.*, 177 (1983) 124.
- 9 L. Fox, G. D. Anthony and E. P. K. Lau, *J. Assoc. Anal. Chem.*, 59 (1976) 1948.
- 10 E. Ciranni Signoretti, A. Dell'Utri and A. De Salvo, *Boll. Chim. Farm.*, 122 (1983) 289.
- 11 C. J. Argoudelis, *J. Chromatogr.*, 303 (1984) 256.
- 12 R. Cross and B. Cunico, *LC, Liq. Chromatogr. HPLC Mag.*, 2 (1984) 678.
- 13 V. Giobbio, G. Ornato, L. Buracchi and A. Mangia, *U.S. Pat.*, 4,434,097 (1984).
- 14 G. W. Snedecor and W. G. Cochran, *Statistical Methods*, Iowa State University Press, Ames, IA, 1967.

CHROM. 18 060

Note

High-performance liquid chromatography system for the separation of ergot alkaloids with applicability to the analysis of illicit lysergide (LSD)

R. GILL* and J. A. KEY

Central Research Establishment, Home Office Forensic Science Service, Aldermaston, Reading, Berkshire RG7 4PN (U.K.)

(Received July 22nd, 1985)

The alkaloids isolated from ergot, along with their structurally related synthetic and semi-synthetic analogues, include several substances with important pharmacological activity. Forensic science laboratories require reliable methods to discriminate between these ergot alkaloids. Of particular importance are the substances which may arise in cases of illegal abortion (*e.g.* ergometrine) and cases of drug abuse involving the hallucinogenic compound lysergide (lysergic acid diethylamide, LSD).

Most ergot alkaloids are thermally unstable and/or photo-labile and consequently high-performance liquid chromatography (HPLC) is generally the technique of choice to separate mixtures of these compounds^{1–13}. Both normal-phase^{1–7} and reversed-phase^{6–13} systems have been used. Although isocratic conditions have been adopted in most situations, gradient elution has also been used for separating complex mixtures^{3,4,8,12}.

The high potency of LSD means that illicit preparations contain very small amounts of the drug. Typically, each small tablet ("microdot") or paper square ("blotter") may contain less than 100 µg of the drug and consequently sensitive methods are required for the analysis of such preparations. HPLC systems for the analysis of LSD have been reported in the literature using silica^{14–16}, octadecyl-silica (ODS-silica)^{17–21} and octyl-silica²² columns. However, reversed-phase systems have been shown to provide better discrimination for the identification of LSD¹⁹. Although UV detection has been used for the analysis of LSD in illicit preparations, fluorescence detection offers enhanced sensitivity and selectivity.

U.K. Forensic Science Laboratories have recently standardised on the HPLC packing materials used for routine work, namely one silica and one ODS-silica. This decision has arisen from the realisation that packing materials of the same type from different manufacturers can have markedly different properties. By sharing common materials the exchange of HPLC methods is facilitated while the stock of columns required in each laboratory is greatly reduced. We are currently engaged in the development of eluent systems to use with the recommended materials for the separation of specific drug groups. Retention data on the materials have already been published for amphetamines²³, barbiturates^{24,25}, local anaesthetics²⁶ and narcotic analgesics²³. The present note gives retention data for the chromatography of ergot

alkaloids on ODS-Hypersil and is based on original work from this laboratory¹⁹ which used an alternative material. The applicability of the system to the analysis of LSD in illicit preparations is demonstrated.

EXPERIMENTAL

Materials

Methanol (HPLC grade) was obtained from Rathburn (Walkerburn, U.K.) while all other chemicals were AnalaR grade from BDH (Poole, U.K.). All ergot alkaloids were from the drug collection of the Central Research Establishment, Home Office Forensic Science Service.

Chromatography

Chromatography was performed with an Applied Chromatography Systems pump (Model 351), a Rheodyne 7120 injection valve (fitted with a 20- μ l loop) and a Kratos UV detector (Model 773) fitted with an 8- μ l flow-cell or a Perkin-Elmer fluorescence detector (Model LC1000). The UV detector was operated at 220 nm while the fluorescence detector was operated at 312 nm excitation and 400 nm emission.

The stainless-steel analytical columns (10 or 16 cm \times 5 mm I.D.) were packed with 5- μ m ODS-Hypersil (Shandon Southern Products, Runcorn, U.K.) by a slurry procedure, dispersing the packing material in isopropanol and using hexane as the pressurising solvent.

A phosphate buffer was prepared by dissolving sodium dihydrogen phosphate dihydrate (3.43 g; 0.022 moles) and disodium hydrogen phosphate (3.97 g; 0.028 moles) in glass-distilled water (1000 ml). The eluent was prepared by mixing this buffer (400 ml) with methanol (600 ml). The pH of this 60% methanolic eluent was measured to be 8.1. A short column (5 cm \times 4.5 mm I.D.) packed with coarse silica (*ca* 40 μ m) was included between the pump and the injection valve to protect the column from the alkaline eluent. In addition the analytical column was never left in contact with static eluent and was washed out with methanol-water (60:40) at the end of each working day. An eluent flow-rate of 2 ml/min was used in all experiments.

Ergot alkaloids were injected onto the column dissolved in methanol. Retention data are expressed as capacity ratios (k') which are defined by $k' = (t_R - t_0)/t_0$ where t_R and t_0 are the retention times of the analyte and a non-retained compound, respectively. The injection of sodium nitrate (0.8 mg/ml in eluent) was used to determine t_0 .

Extraction of illicit LSD preparations

The procedure of McDonald *et al.*²¹ has been used involving the addition of methanol-water (50:50) to the "microdot" or "blotter" with ultrasonic vibration for 20 min. After centrifugation the extract was injected directly onto the column.

RESULTS AND DISCUSSION

The eluent finally selected for the separation of the ergot alkaloids on ODS-Hypersil was 60% methanol buffered at pH 8.1. This represents only a small change from the 65% methanol eluent used by Twitchett *et al.*¹⁹. Table I lists the k' values

TABLE I

HPLC RETENTION DATA FOR ERGOT ALKALOIDS (ARRANGED IN ORDER OF INCREASING RETENTION)

<i>Compound</i>	<i>k'</i>	<i>Compound</i>	<i>k'</i>
Isolysergide	0	Methysergide	2.33
Lysergic acid	0	Ergosine	7.08
Lysergamide	0.33	Ergotamine	9.58
Ergometrine	0.50	Ergocornine	10.17
Isolysergic acid	0.83	Dihydroergotamine	11.42
Lumi-LSD	0.83	Ergocryptine	15.17
Lysergol	0.83	Dihydroergocryptine	15.90
Methylergometrine	0.83	Ergocristine	17.30
2-Oxo-LSD	0.92	Ergosinine	17.70
Lysergide (LSD)	1.83	Dihydroergocristine	18.25
Lysergic acid		Bromocriptine	44.33
methylpropylamide (LAMPA)	1.98		

for 22 compounds measured on a 10-cm column and presented in order of elution. It can be seen that the k' values range from 0 to 44.3 with LSD eluting with $k' = 1.83$. Table II presents the same data but arranged in alphabetical order to facilitate the rapid retrieval of information on a specific compound. The good peak shapes which can be achieved on the present system are demonstrated in Fig. 1 for the separation of nine compounds in under 10 min.

The principal consideration in the recommendation of the present system for forensic examination is the separation of LSD from all the other ergot alkaloids examined. Thus, the unique retention time of LSD amongst the other common ergot alkaloids provides a useful parameter in the overall strategy for the identification of this drug. Initial experiments showed that although the ergot alkaloids can be chromatographed using acidic eluents, alkaline conditions (pH 8.1) were essential to maintain complete discrimination for LSD. Methysergide co-eluted with LSD at pH values

TABLE II

HPLC RETENTION DATA FOR ERGOT ALKALOIDS (ARRANGED IN ALPHABETICAL ORDER)

<i>Compound</i>	<i>k'</i>	<i>Compound</i>	<i>k'</i>
Bromocriptine	44.33	Isolysergic acid	0.83
Dihydroergocristine	18.25	Isolysergide	0
Dihydroergocryptine	15.90	Lumi-LSD	0.83
Dihydroergotamine	11.42	Lysergamide	0.33
Ergocornine	10.17	Lysergic acid	0
Ergocristine	17.30	Lysergic acid	
Ergocryptine	15.17	methylpropylamide (LAMPA)	1.98
Ergometrine	0.50	Lysergide (LSD)	1.83
Ergosine	7.08	Lysergol	0.83
Ergosinine	17.70	Methylergometrine	0.83
Ergotamine	9.58	Methysergide	2.33
		2-Oxo-LSD	0.92

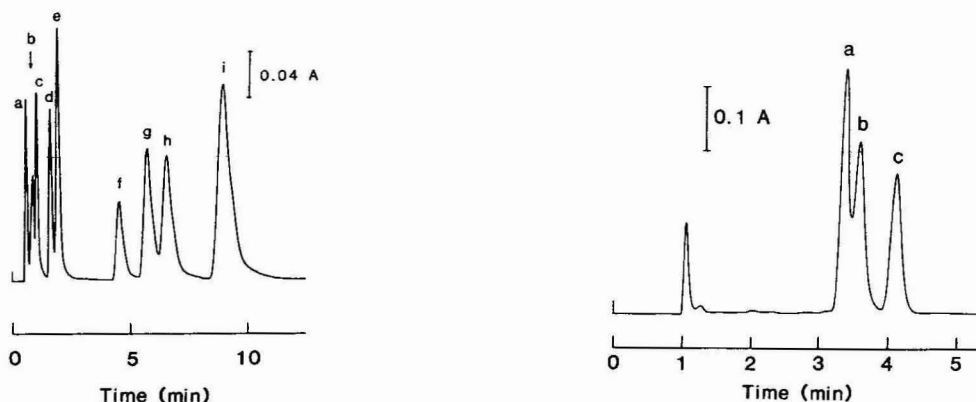


Fig. 1. Chromatography of ergot alkaloids on ODS-silica. Column: ODS-Hypersil, $5\ \mu\text{m}$ ($10\ \text{cm} \times 5\ \text{mm}$ I.D.). Eluent: 60% methanol containing phosphate buffer (pH 8.1). Flow-rate: 2 ml/min. Detection: UV absorbance at 220 nm. Peaks: a = lysergic acid; b = lysergamide; c = isolysergic acid; d = lysergide (LSD); e = methysergide; f = ergosine; g = ergotamine; h = dihydroergotamine; i = ergocryptine.

Fig. 2. Separation of LSD from LAMPA and methysergide. Column: ODS-Hypersil, $5\ \mu\text{m}$ ($16\ \text{cm} \times 5\ \text{mm}$ I.D.). Other conditions as in Fig. 1. Peaks: a = lysergide (LSD); b = lysergic acid methylpropylamide (LAMPA); c = methysergide.

of less than 7. Despite the fact that alkaline eluents can be corrosive towards ODS-silica columns, the adoption of a few simple precautions (see Experimental section), in line with our previous experience²⁷, can ensure that the columns have a long useful life.

The compounds which elute closest to LSD are lysergic acid methylpropylamide (LAMPA) and methysergide. Fig. 2 shows the resolution between these com-

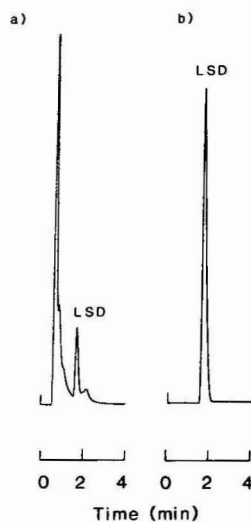


Fig. 3. Analysis of an illicit LSD preparation with (a) UV detection at 220 nm or (b) fluorescence detection with excitation at 312 nm and emission at 400 nm. Other conditions as in Fig. 1.

pounds which was achieved with the present system when using a 16-cm column. Clearly, this separation could be further increased by the use of an even longer column. LSD and LAMPA are isomers, differing only by the nature of the amide substituents, and consequently are generally considered difficult to separate. A previous separation by reversed-phase HPLC has been demonstrated²⁰ while capillary gas chromatography has also been used^{28,29}.

The applicability of the present HPLC system to the analysis of illicit LSD preparations has been tested and Fig. 3 shows typical chromatograms arising, in this case, from an aqueous methanolic extract of a "microdot". Fig. 3a shows UV detection at 220 nm while Fig. 3b shows fluorescence detection at 312 nm excitation and 400 nm emission. The selectivity of fluorescence detection is clearly demonstrated, being the detection method of choice for the routine analysis of LSD.

REFERENCES

- 1 R. A. Heacock, K. R. Langille, J. D. MacNeil and R. W. Frei, *J. Chromatogr.*, 77 (1973) 425.
- 2 G. Szepesi, M. Gazdag and L. Terdy, *J. Chromatogr.*, 191 (1980) 101.
- 3 M. Wurst, M. Flieger and Z. Řeháček, *J. Chromatogr.*, 150 (1978) 477.
- 4 M. Wurst, M. Flieger and Z. Řeháček, *J. Chromatogr.*, 174 (1979) 401.
- 5 M. Flieger, M. Wurst, J. Stuchlík and Z. Řeháček, *J. Chromatogr.*, 207 (1981) 139.
- 6 L. Szepesi, I. Fehér, G. Szepesi and M. Gazdag, *J. Chromatogr.*, 149 (1978) 271.
- 7 C. Eckers, D. E. Games, D. N. B. Mallen and B. P. Swann, *Biomed. Mass Spectrom.*, 9 (1982) 162.
- 8 F. Erni, R. W. Frei and W. Lindner, *J. Chromatogr.*, 125 (1976) 265.
- 9 J. Dolinar, *Chromatographia*, 10 (1977) 364.
- 10 V. Hartmann, M. Rodiger, W. Ableidinger and H. Bethke, *J. Pharm. Sci.*, 67 (1978) 98.
- 11 A. Yoshida, S. Yamazaki and T. Sakai, *J. Chromatogr.*, 170 (1979) 399.
- 12 J. C. Young, *J. Environ. Sci. Health*, B16 (1981) 83.
- 13 B. Herényi and S. Görög, *J. Chromatogr.*, 238 (1982) 250.
- 14 J. D. Wittwer and J. H. Kluckhohn, *J. Chromatogr. Sci.*, 11 (1973) 1.
- 15 I. Jane, *J. Chromatogr.*, 111 (1975) 227.
- 16 J. Christie, M. W. White and J. M. Wiles, *J. Chromatogr.*, 120 (1976) 496.
- 17 I. Jane and B. B. Wheals, *J. Chromatogr.*, 84 (1973) 181.
- 18 I. Lurie, *J. Assoc. Off. Anal. Chem.*, 60 (1977) 1035.
- 19 P. J. Twitchett, S. M. Fletcher, A. T. Sullivan and A. C. Moffat, *J. Chromatogr.*, 150 (1978) 73.
- 20 G. Megges, *Arch. Kriminol.*, 164 (1979) 25.
- 21 P. MacDonald, C. F. Martin, D. J. Woods, P. B. Baker and T. A. Gough, *J. Forensic Sci.*, 29 (1984) 120.
- 22 K. Harzer, *J. Chromatogr.*, 249 (1982) 205.
- 23 B. Law, R. Gill and A. C. Moffat, *J. Chromatogr.*, 301 (1984) 165.
- 24 R. Gill, A. H. Stead and A. C. Moffat, *J. Chromatogr.*, 204 (1981) 275.
- 25 R. Gill, A. A. T. Lopes and A. C. Moffat, *J. Chromatogr.*, 226 (1981) 117.
- 26 R. Gill, R. W. Abbott and A. C. Moffat, *J. Chromatogr.*, 301 (1984) 155.
- 27 R. Gill and A. C. Moffat, *J. Chromatogr.*, 233 (1982) 438.
- 28 H. S. Nichols, W. H. Anderson and D. T. Stafford, *J. High Resolut. Chromatogr. Chromatogr. Commun.*, 6 (1983) 101.
- 29 D. T. Stafford, H. S. Nichols and W. H. Anderson, *J. Forensic Sci.*, 29 (1984) 291.

CHROM. 18 063

Note

Plantes médicinales africaines

XIX. Dosage de la vitexine par chromatographie liquide haute performance dans un extrait brut de *Combretum micranthum* G. Don

E. BASSENE et A. LAURANCE

Laboratoires de Pharmacognosie et de Chimie des Substances Naturelles, Faculté de Médecine et de Pharmacie, Dakar (Sénégal)

D. OLSCHWANG

Laboratoire de Chimie Physique et Analytique, Faculté des Sciences, Dakar (Sénégal)

et

J. L. POUSSET*

Laboratoires de Pharmacognosie et de Chimie des Substances Naturelles, Faculté de Médecine et de Pharmacie, Dakar (Sénégal)

(Reçu le 14 mai 1985; manuscrit modifié reçu le 22 juillet 1985)

Le *Combretum micranthum* (kinkéliba) est une des espèces les plus populaires de la pharmacopée sénégalaise¹.

De très nombreuses spécialités pharmaceutiques utilisées comme cholagogue ou cholérétique contiennent des extraits de *Combretum*, ce qui a été justifié par plusieurs de nos travaux antérieurs^{2,3}.

Étant donné, en outre, la présence d'hétérosides flavoniques majoritaires, comme la vitexine et l'isovitexine⁴, en équilibre par le réarrangement bien connu de Wesely-Moser⁵, il nous a semblé intéressant d'identifier et de doser la vitexine —soit la C-glucosyl-8 apigenine— dans un extrait brut de kinkéliba, et de déterminer la teneur des feuilles de cette plante en vitexine. Le dosage par chromatographie liquide haute performance est actuellement la méthode la plus fiable et la plus rapide pour l'identification et le dosage de ce type de composés^{6,7}.

MATÉRIEL ET MÉTHODES

Chromatographe liquide à haute performance Waters Assoc., Modèle 6000, équipé d'un détecteur d'absorption à 254 nm (Modèle 440) et d'un injecteur UGK. La sensibilité utilisée est 0,1.

La colonne (30 cm × 3,9 mm) est préemplie avec du μ Bondapak C₁₈ de 10 μ m. Les solvants utilisés sont filtrés sur membrane Millipore de 0,45 μ m et dégazés sous vide.

Matériel végétal: feuilles récoltées dans la région de Thiès (Sénégal).

Extraction: 10 g de feuilles séchées à l'abri de la lumière solaire sont finement broyées, dégraissées à l'éther de pétrole, puis extraites par deux fois 500 ml d'eau

bouillante. Après concentration jusqu'à 200 ml et filtration, la solution est évaporée à sec, sous pression réduite, et le résidu repris par 20 ml de méthanol bouillant. Une deuxième filtration permet l'élimination d'un précipité, lavé, et l'ensemble des filtrats rejoints et évaporés à sec conduisent à un résidu de 1,81 g, soit un rendement de 18% en masse.

Témoins: vitexine et isovitexine isolées et identifiées selon une méthode déjà décrite⁸.

Identification des flavonosides de l'extrait: injection simultanée de témoin authentique.

Dosage de la vitexine: une gamme étalon est effectuée par dix injections de 2 μ l de vitexine témoin à des quantités comprises entre 0,1 et 1 μ g.

RÉSULTATS ET DISCUSSION

N'ayant pas la possibilité de travailler en gradient de solvant, les meilleurs résultats ont été obtenus avec le mélange eau-méthanol-acide acétique (65:30:5), et avec un débit de 2 ml/min à la pression de 2000 p.s.i. Les résultats sont représentés sur la Fig. 1, où les pics 1 et 2 correspondent respectivement à la vitexine et à l'isovitexine (temps de rétention 2 min 24 s et 3 min 24 s).

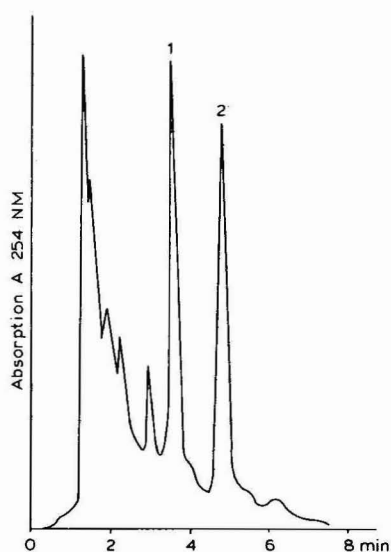


Fig. 1. Chromatogramme d'un extrait brut de *Combretum micranthum* G. Don.

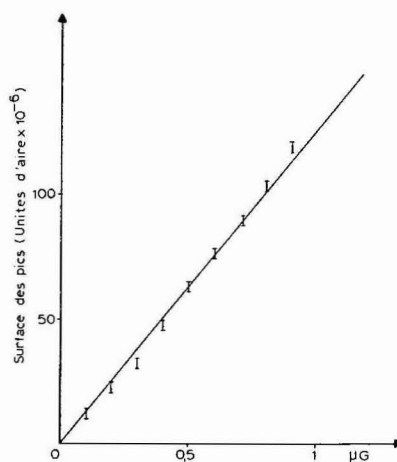


Fig. 2. Graphique d'étalonnage de la vitexine (intervalle de confiance $\pm 1,5 \cdot 10^{-6}$ pour $p < 0,05$).

La courbe étalon, indiquée sur la Fig. 2, montre une relation linéaire entre la quantité de vitexine injectée et l'intensité de l'absorption à 254 nm.

Des essais de reproductibilité ont été effectués en injectant dix fois la même quantité de vitexine (0,3 μ g). Pour une probabilité $p < 0,05$, l'intervalle de confiance est de $\pm 1,5 \cdot 10^{-6}$ unités d'aire.

La droite de régression correspondant à la gamme étalon a un coefficient de corrélation de 0,999 (établie à l'ordinateur).

L'extraction de la vitexine à partir d'un même échantillon de feuille a été répétée cinq fois. Le coefficient de variation pour le dosage est dans ces conditions inférieure à 9%.

45 μg de l'extrait brut correspondent à 0,56 μg de vitexine, soit une teneur de 1,24 g%. Compte tenu du rendement de l'extraction, la teneur en vitexine des feuilles de *Combretum micranthum* utilisées pour ce dosage est de 0,22%.

CONCLUSION

Ces résultats montrent que la chromatographie liquide haute performance est une méthode simple et fiable pour le dosage de la vitexine dans un extrait de kinkéliba: cette technique peut être parfaitement adaptée à un contrôle systématique d'une spécialité pharmaceutique.

BIBLIOGRAPHIE

- 1 J. Kerharo et J. G. Adam, *La Pharmacopée Sénégalaise Traditionnelle*, Vigot Frères, Paris, 1974, p. 346.
- 2 E. Bassene, D. Olschwang et J. L. Pousset, *Dakar Médical*, 26 (1981) 219.
- 3 E. Bassene, D. Olschwang et J. L. Pousset, *J. Afr. Med. Plants*, soumis pour publication.
- 4 K. Jentzsch, P. Spiengel et L. Fuchus, *Planta Medica*, 10 (1962) 1.
- 5 S. K. Mukerjee et T. R. Seshadri, *Chem. Ind. (London)*, (1955) 271.
- 6 D. J. Daigle et E. J. Conkerton, *J. Chromatogr.*, 240 (1982) 202.
- 7 I. McMurrough, *J. Chromatogr.*, 218 (1981) 683.
- 8 E. Bassene, *Étude de la composition chimique du Combretum micranthum G. Don*, Thèse de doctorat des Sciences pharmaceutiques, Dakar, 1985, p. 24.

CHROM. 18 044

Note

Semi-preparative isolation of crepenynic acid, a potential inhibitor of essential fatty acid metabolism

GLENN L. FORD

Food Research Laboratory, CSIRO, Division of Food Research, P.O. Box 52, North Ryde, N.S.W. 2113 (Australia)

(Received July 18th, 1985)

Crepenynic (octadec-*cis*-9-en-12-ynoic) acid has been identified as a major component (25%) of the fatty acids of the oil from seeds of *Ixiolaena brevicompta* F. Muell. (Compositae)¹. The mature seeded plant is considered responsible for causing muscular degeneration and extensive mortalities in sheep on the riverine flood plains of western New South Wales and Queensland².

A number of eighteen and twenty carbon acetylenic fatty acids have been found to interfere with complex lipid metabolism in animals. These effects include inhibition of essential fatty acid synthesis^{3,4} and selective inhibition of cyclooxygenase and lipoxygenase enzyme pathways⁵⁻⁷. Previous studies^{5,8} have given no indication that crepenynic acid could be sufficiently toxic to cause deaths in sheep although our recent studies⁹ suggest that crepenynic acid is indeed the toxic component in *I. brevicompta* seed oil.

The application of high-performance liquid chromatography (HPLC) to the preparation of individual fatty acids (or esters) in quantity for metabolic studies has received little attention. HPLC has been used for the isolation of fatty acid methyl esters using a dedicated preparative instrument¹⁰, but the capital expenditure required for such machines would be unwarranted where limited amounts of material are required.

This report describes a simple reversed-phase HPLC technique for the isolation of the methyl ester of crepenynic acid in gram quantities necessary for small-scale feeding trials with laboratory animals. The technique involves the use of conventional analytical HPLC equipment and a micro-particulate semi-preparative column and could be applied to the isolation of other unsaturated fatty acid esters from complex mixtures.

EXPERIMENTAL

Preparation of crude methyl esters

The mature seeds of *I. brevicompta* (5 kg) were crushed to a fine flour in a Reitz mill (0.3-mm screen), soaked and extracted three times with 10 dm³ hexane. Transmethylation of the oil was carried out by scaling-up an analytical method¹¹, in which the oil was reacted with a 1 M solution of sodium propoxide in propanol

at room temperature for 1 h, followed by acidification with 1 *M* hydrochloric acid and extraction using the procedure of Bligh and Dyer¹². Column chromatography on Florisil¹³ was used to clean up the methyl ester fraction. The fatty acid composition of the methyl esters was obtained by gas-liquid chromatography (GLC) with a Carlo Erba HRGC 5160 gas chromatograph, using a bonded-phase BP20 fused-silica column (SGE, Australia).

Preliminary enrichment of methyl esters

Removal of pigments with activated charcoal was carried out to reduce the risk of column deterioration and blockage. The orange-coloured fatty acid methyl ester mixture (234 g) was dissolved in hexane and clarified by passage through a column (500 × 55 mm I.D.) containing two layers of Florisil (2 × 100 g) separated by a mixed bed of activated carbon and Florisil (50:50) (100 g).

The methyl ester mixture was further fractionated by urea inclusion to remove long-chain saturated esters which may be strongly retained on a reversed-phase HPLC column. The clarified methyl esters (230 g) were boiled with a mixture of methanol (2 dm³) and urea (250 g).

The urea adduct which formed at room temperature was filtered off and the filtrate, monitored by GLC was found to be enriched in the desired unsaturated esters. A further treatment with 50 g urea produced a filtrate which was greatly enriched in unsaturated esters and was devoid of saturates. The remaining filtrate was acidified with 1 dm³ 1 *M* hydrochloric acid, extracted twice with 1 dm³ hexane, dried over anhydrous sodium sulphate and filtered through a 0.45- μ m filter. The final filtrate after evaporation yielded 160 g of an enriched unsaturated methyl ester fraction for HPLC separation.

HPLC solvents

Methanol (analytical grade) and water were passed through a 0.45- μ m filter before use.

HPLC apparatus

A Waters Model 590 pump, Altex Model 500 injector, Dupont Model 845 refractometer and Linear Instruments Model 282 chart recorder were used. A semi-preparative column, Regis 250 × 10 mm I.D., packed with 10- μ m particles coated with ODS phase was selected.

The methyl ester mixture (100 mg/cm³ or 400 mg/cm³ in methanol) was injected onto the column, using a 1-cm³ injection loop. When the 100 mg/cm³ mixture was used the mobile phase was 100% methanol. However, with the larger injection the mobile phase was altered to methanol-water (95:5) to maintain adequate resolution. The flow-rate in both cases was 2.5 cm³/min.

Identification of fatty acid methyl esters

Fatty acid methyl esters from HPLC runs were identified by comparison of GLC retention times with authentic standards. Methyl crepenynate standard was available from *I. brevicompta* seed oil¹.

RESULTS AND DISCUSSION

Figs. 1 and 2 show HPLC chromatograms of the fatty acid methyl ester mixtures before and after urea enrichment, respectively. The fatty acid composition of the components eluted by HPLC (Figs. 1 and 2) was determined by collection and GLC analysis.

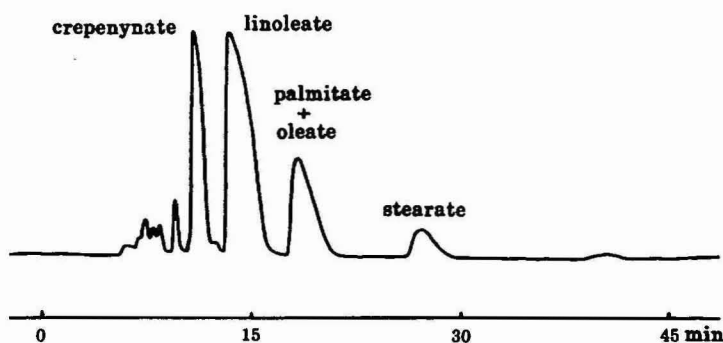


Fig. 1. HPLC trace of methyl esters prepared from the oil extract from *I. brevicompta* seed; 100 mg injection with a flow-rate of 2.5 cm³/min methanol.

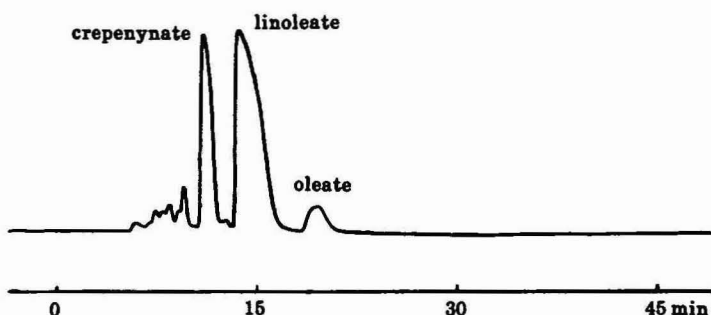


Fig. 2. HPLC trace of methyl esters following enrichment of unsaturated esters using urea inclusion; 100 mg injection with a flow-rate of 2.5 cm³/min methanol.

The original fatty acid composition of the oil extract (5%) from this batch of mature seeds of *I. brevicompta* was palmitic (8%), stearic (5%), oleic (8%), linoleic (53%) and crepenynic (22%) acids (Fig. 1). Urea inclusion was used to remove most of the saturates and some of the mono-unsaturated fatty ester components leaving a fraction which was comprised of oleic (6%), linoleic (67%) and crepenynic (27%) acids (Fig. 2).

HPLC separation of the enriched fraction, using sample loads up to 400 mg (methanol-water, 95:5, and flow-rate of 2.5 cm³/min) could be completed in less than 50 min with near-baseline separation between methyl crepenynate and methyl linoleate. The cycle time to re-injection could be further reduced to 30 min by flushing the column with methanol at 6 cm³/min for 5 min immediately after the elution of methyl crepenynate (20 min), followed by re-equilibration with methanol-water

(95:5) at 5 cm³/min for 5 min. At this stage, the flow-rate was reduced to 2.5 cm³/min and the sample injection and HPLC separation repeated as described above.

Using repetitive injection, a total of 15 g of methyl crepenynate (98% pure by GLC) was conveniently isolated for use in animal feeding trials. Subsequently, similar amounts of methyl linoleate and linolenate were isolated by this procedure from safflower oil and linseed oil respectively¹⁴. The technique could be applied to the isolation of a wide variety of unsaturated esters, and could be readily scaled-up for preparative isolations.

REFERENCES

- 1 G. L. Ford, F. B. Whitfield and K. H. Walker, *Lipids*, 18 (1983) 103.
- 2 K. H. Walker, D. R. Walker, D. R. Thompson and J. T. Seamen, *Aust. Vet. J.*, 56 (1980) 64.
- 3 L. D. Tobias and J. D. Hamilton, *Lipids*, 14 (1978) 181.
- 4 R. Wood, *Lipids*, 17 (1982) 763.
- 5 D. T. Downing, J. A. Barve, F. D. Gunstone, F. R. Jacobsberg and M. Lie Ken Jie, *Biochim. Biophys. Acta*, 280 (1972) 343.
- 6 T. E. Wilhelm, S. K. Sanlarappa, M. Van Rollins and H. Sprecher, *Prostaglandins*, 21 (1981) 323.
- 7 F. F. Sun, J. C. McGuire, D. R. Morton, J. E. Pike, H. Sprecher and W. H. Kunau, *Prostaglandins*, 21 (1984) 333.
- 8 K. Bernhard and E. Kaempf, *Helv. Chim. Acta*, 52 (1969) 1742.
- 9 K. H. Walker and G. L. Ford, in A. A. Seawright, M. P. Hegarty, R. F. Keeler and L. F. James (Editors), *Plant Toxicology, Proc. 2nd Australia-U.S.A. Poisonous Plants Symp., Brisbane, May 14-18, 1984*, Queensland Poisonous Plants Committee, Brisbane, 1985, in press.
- 10 E. Bascetta, F. D. Gunstone and C. M. Scrimgeour, *Lipids*, 19 (1984) 801.
- 11 R. L. Glass and S. W. Cristopherson, *Chem. Phys. Lipids*, 3 (1969) 405.
- 12 E. G. Bligh and W. J. Dyer, *Can. J. Biochem. Physiol.*, 37 (1981) 911.
- 13 K. K. Carroll, *J. Lipid Res.*, 2 (1961) 135.
- 14 G. L. Ford, unpublished results.

CHROM. 18 027

Note

Rapid and convenient separation of pentachlorophenol from human fat using silica Sep-PakTM cartridges

G. A. S. ANSARI* and PAMELA Y. HENDRIX

Chemical Pathology Laboratory and Division of Biochemistry, The University of Texas Medical Branch, Galveston, TX 77550 (U.S.A.)

(Received July 2nd, 1985)

Pentachlorophenol (PCP) is widely used as an insecticide, fungicide, herbicide, and wood preservative. Due to its extensive usage, PCP has been found to be a ubiquitous environmental contaminant. Humans can be exposed to PCP mainly through inhaling contaminated air or consuming contaminated food and water, however it can also be absorbed through the skin. Since compounds such as hexachlorobenzene and γ -hexachlorocyclohexane can also be metabolized to PCP¹ this could further contribute to the magnitude of human exposure. Presently, it is not known to what extent these possible sources contribute to the total PCP body burden.

Previous investigators have shown a slow elimination of PCP from body tissue and significant levels have particularly been found in human adipose tissue. PCP residues were measured in human adipose tissue taken at autopsy in the United States (range 12–52 ppb*)², Canada (range 0–277 ppb)³, and Japan (range 10–570 ppb)⁴. In fat samples analyzed^{2–4}, only 75–80% of the PCP was recovered and the procedures used were time consuming and cumbersome. In the present study, a simple and reproducible method was developed using a Sep-PakTM silica cartridge as a clean-up step for the analysis of PCP in adipose tissue. The recovery of PCP from human adipose tissue was 92–97%.

EXPERIMENTAL

Materials

All solvents were pesticide grade (Burdick and Jackson, Muskegan, MI, U.S.A.), [¹⁴C]pentachlorophenol (PCP) (1.83 mCi/mmol) with a radiochemical purity of 91%, as determined by thin-layer chromatography, was provided by Dow Chemical, Midland, MI, U.S.A. Non-radioactive PCP (99+ % purity, gold label) was purchased from Aldrich, Milwaukee, WI, U.S.A. Bio-beads SX2, 200–400 mesh was obtained from Bio-Rad Labs. (Richmond, CA, U.S.A.). C₁₈ and Silica Sep-PakTM cartridges were obtained from Waters Assoc., Milford, MA, U.S.A. Human fat samples obtained at autopsy were excised from the anterior abdominal wall and frozen at –80°C until analyzed.

* Throughout the article the American billion (10⁹) is meant.

Gel permeation chromatography (GPC)

One gram of human fat was supplemented with ^{14}C -PCP (50 ppb, $3.4 \cdot 10^{-4}$ μCi), dissolved in 1 ml of cyclohexane and applied to a Bio-beads SX2 column (27 cm \times 20 mm I.D.), pre-equilibrated with cyclohexane. The column was eluted with cyclohexane at a flow-rate of 4 ml/min. Fractions of 1 ml were collected and analyzed for fat and radioactivity as described later.

Sep-Pak chromatography

Fat (300–500 mg) containing ^{14}C -PCP (31 ppb, $2.1 \cdot 10^{-4}$ μCi) was dissolved in 1 ml of acetonitrile and applied to a C_{18} Sep-Pak cartridge. The sample was eluted with acetonitrile.

Silica Sep-Pak. Fat (300–500 mg) containing ^{14}C -PCP (100 ppb, $6.9 \cdot 10^{-4}$ μCi) was dissolved in 900 μl hexane and applied to a silica Sep-Pak cartridge. The column was eluted with various amounts of hexane and chloroform as shown in Figs. 2 and 3. The column was further eluted with tetrahydrofuran to determine the effect on fat recovery.

Fat and ^{14}C -PCP recoveries

Effluent from Sep-Pak cartridges was collected in 2-ml fractions and evaporated to dryness under vacuum at room temperature on a Searle vortex evaporator (Buchler Instruments, Fort Lee, NJ, U.S.A.). Vials were weighed to determine fat recovery and the residue was dissolved in hexane. An aliquot was removed, dissolved in Scintiverse (Fisher Scientific, Fair Lawn, NJ, U.S.A.) and radioactivity was measured on a Packard Mark III 6880 liquid scintillation counter (Searle Analytics, Des Plaines, IL, U.S.A.). Counting efficiency was determined by external standardization.

RESULTS AND DISCUSSION

Using SX-2 column chromatography the recovery of ^{14}C -PCP was 86.5% (Table I). The representative profile of fat and ^{14}C -PCP recovery is shown in Fig. 1. Using silica gel Sep-Pak columns and eluting with hexane (10 ml) followed by chloroform (17 ml) gave a recovery of 92.3% ^{14}C -PCP in 8 ml of chloroform and had fat contamination $< 1\%$. When an intermediate elution step (hexane–chloroform, 1:1, 5 ml) was added, the recovery of ^{14}C -PCP was increased to $\approx 97\%$. With this

TABLE I

RECOVERY OF ^{14}C -PCP FROM FAT BY CHROMATOGRAPHY

Mean of three determinations.

Column	Fat recovery (%)	^{14}C -PCP recovery (%)	Fat contamination of ^{14}C -PCP (%)
SX-2 bead	81 ± 3.8	86.5 ± 7.4	0.5 ± 0.1
Silica Sep-Pak*	100 ± 12.7	92.3 ± 10.3	0.8 ± 0.3
Silica Sep-Pak**	99.5 ± 4.2	96.8 ± 2.1	4.0 ± 0.5

* Column eluted with 10 ml hexane, 17 ml chloroform (Fig. 2).

** Column eluted with 10 ml hexane, 5 ml hexane–chloroform, 1:1 (v/v), 15 ml chloroform (Fig. 3).

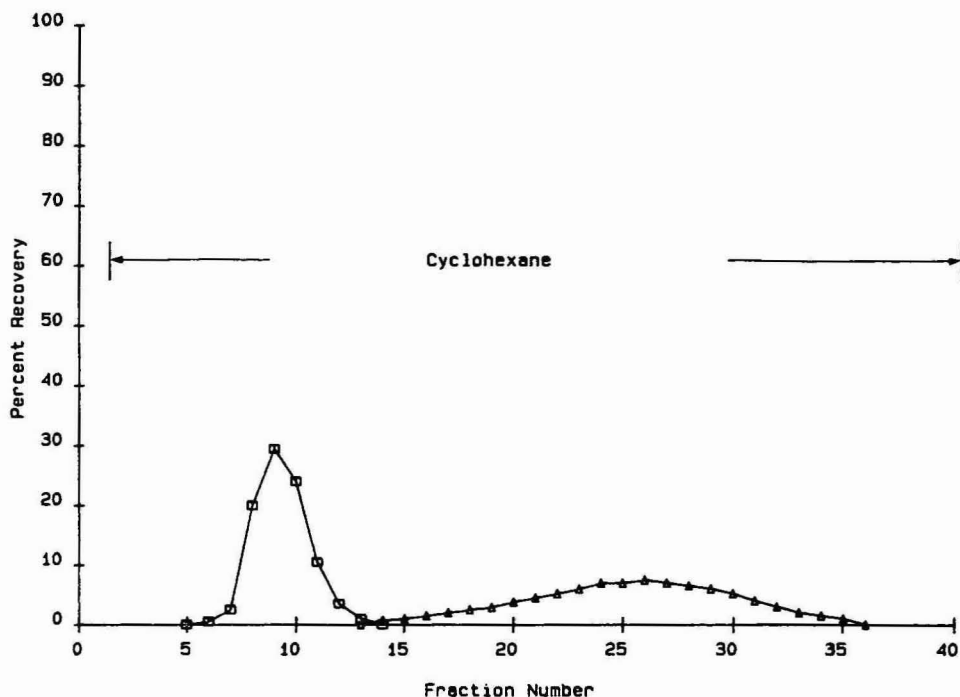


Fig. 1. Elution profile of human fat (□) and ^{14}C -PCP (△) using SX-2 column chromatography.

increase, fat contamination also increased to $\approx 4\%$ (representative profiles are shown in Figs. 2 and 3).

In some experiments when ≈ 500 mg fat was used a small amount of radioactivity ($< 1\%$) was eluted in the hexane fraction. After elution with chloroform a small amount of fat ($< 2\%$) was recovered when the column was further eluted with tetrahydrofuran (4 ml).

Attempts were made to utilize the Sep-Pak C_{18} cartridge. Using a Sep-Pak C_{18} column and acetonitrile or methanol-water (9:1, v/v) fat and ^{14}C -PCP eluted together in 5 ml volume and therefore the C_{18} cartridge cannot be used for enrichment of PCP from fat.

The PCP enriched fraction obtained from silica gel Sep-Pak column chromatography can be analyzed either by capillary gas chromatography⁵⁻⁶ or by high-performance liquid chromatography⁷⁻¹⁰.

In summary, a procedure was developed by which PCP can be recovered from fat samples in high yields. This procedure is less cumbersome and less time consuming than procedures used earlier²⁻⁴. Recently, *in vitro*¹¹ and *in vivo*¹² studies have shown that PCP may exist in human fat as a fatty acid ester. The present method does not account for PCP-ester in the recovery. The effect of prior hydrolysis of fat followed by silica Sep-Pak separation has not been attempted.

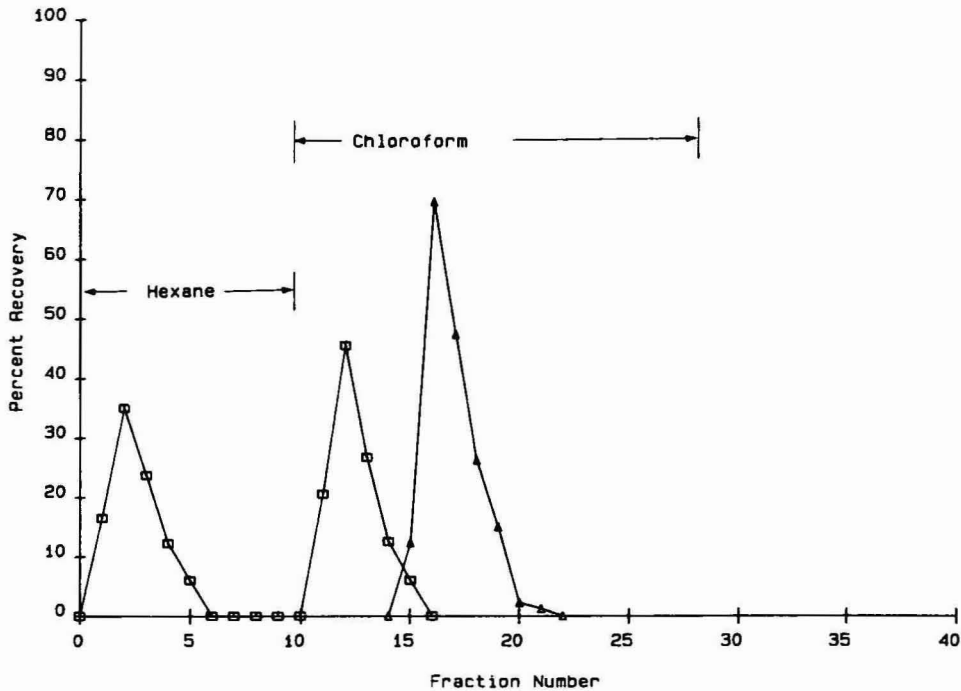


Fig. 2. Elution profile of human fat (□) and ¹⁴C-PCP (Δ) using silica Sep-Pak column chromatography. Column eluted with hexane followed by chloroform.

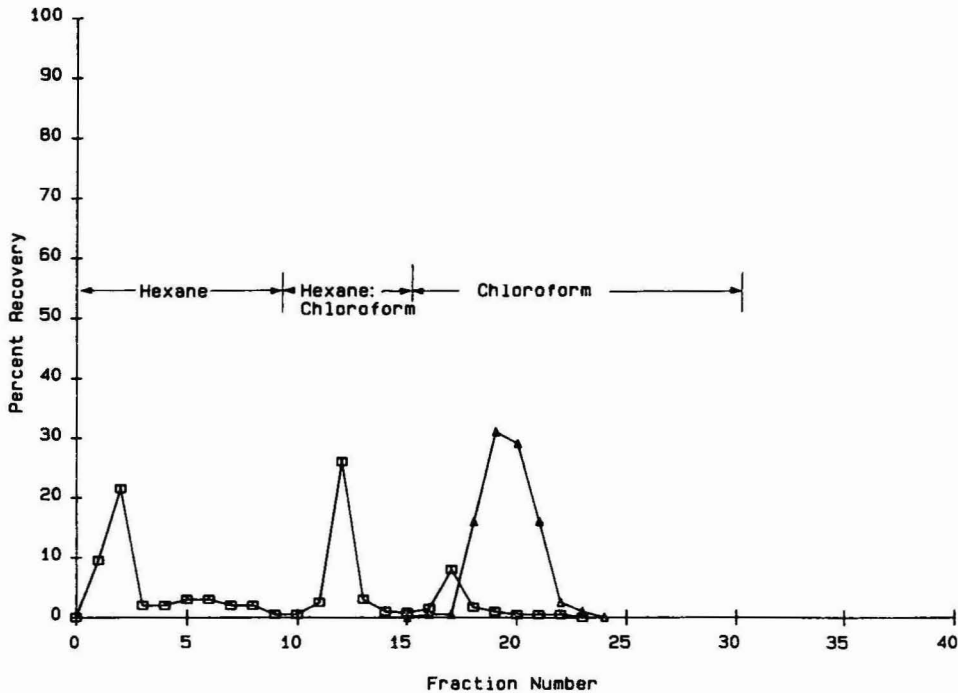


Fig. 3. Elution profile of human fat (□) and ¹⁴C-PCP (Δ) using silica Sep-Pak column chromatography. Column eluted sequentially with hexane, hexane-chloroform (1:1, v/v) and chloroform.

ACKNOWLEDGEMENTS

The authors wish to thank Avis Morgan and Sandy Campanello for secretarial assistance. This work was supported by grant AM 27135 from the NIH.

REFERENCES

- 1 R. Engst, R. M. Macholz and M. Kujawa, *Bull. Environm. Contam. Toxicol.*, 16 (1976) 248.
- 2 T. M. Shafik, *Bull. Environm. Contam. Toxicol.*, 10 (1973) 57.
- 3 D. T. Williams, G. LaBel and E. Junkins, *J. Toxicol. Environm. Hlth.*, 13 (1984) 19.
- 4 T. Ohe, *Bull. Environm. Contam. Toxicol.*, 22 (1979) 287.
- 5 D. A. Kalman, *J. Chromatogr. Sci.*, 22 (1984) 452.
- 6 I. O. O. Korhonen, *J. Chromatogr.*, 303 (1984) 197.
- 7 N. G. Buckman, J. O. Hill, R. J. Magee and M. J. McCormick, *J. Chromatogr.*, 284 (1984) 441.
- 8 K. D. McMurtrey, A. E. Holcomb, A. U. Ekwenchi and N. C. Fawcett, *J. Liq. Chromatogr.*, 7 (1984) 953.
- 9 J. Nair, K. M. Munir and S. V. Bhide, *J. Liq. Chromatogr.*, 6 (1983) 2829.
- 10 H. A. McLeod and G. Laver, *J. Chromatogr.*, 244 (1982) 385.
- 11 E. G. Leighty and A. F. Fentiman, Jr., *Bull. Environm. Contam. Toxicol.*, 28 (1982) 329.
- 12 G. A. S. Ansari, S. G. Britt and E. S. Reynolds, *Bull. Environm. Contam. Toxicol.*, 34 (1985) 661.

CHROM. 18 003

Note

A rapid method for the separation and quantification of simple phenolic acids in plant material using high-performance liquid chromatography

MICHAEL F. WILSON

Agricultural Science Service, Tolworth Laboratory, Ministry of Agriculture, Fisheries and Food, Hook Rise South, Tolworth, Surbiton, Surrey KT6 7NF (U.K.)

(First received May 3rd, 1985; revised manuscript received July 4th, 1985)

In the past few years there has been a proliferation of methods for the determination of phenolic acids and other phenolic compounds in plant material and plant products^{1–8}. Interest has centred around the effects of this group of compounds on the flavour of foods^{9–14} and beverages^{15–17} and on their possible significance for the diet selection of certain agricultural pests^{18–21}.

Phenolic acids can be adequately separated using reversed-phase high-performance liquid chromatography (RP-HPLC) providing that the aqueous solvent is of sufficiently low pH to suppress any ionisation of phenolic hydroxyl or carboxyl groups^{3,7–8}. Most workers have adopted the use of 25–30 cm C₁₈ (5- or 10- μ m packing)^{1,2,5–8} columns with aqueous phases containing either acetic or formic acid although a novel technique employs a polystyrene-divinyl benzene column²². Separations of the complex mixtures of phenolics arising from plant products have been achieved with gradient run times of approximately 1 h.

This paper describes an analogous method based on the use of a 10-cm C₁₈ (3- μ m packing) column eluted with a gradient of 5% (v/v) aqueous formic acid and 75% (v/v) aqueous methanol. Separations of the phenolic acids commonly found in plant products can be achieved in under 25 min. Because the column is of conventional internal dimensions (4 mm I.D.), not small- or micro-bore but uses 3- μ m packing, it provides a useful compromise between micro-bore columns which require modifications to sample injection and detection systems and conventional columns. The separations achieved are comparable with those obtained with larger columns but with a considerable saving of solvent usage and analysis time.

The method described in this paper has been used to look at the phenolic content of two varieties of orchard pear bud. Pear buds are susceptible to severe damage by bullfinches²³ and in an attempt to reduce this, a multi-disciplinary project has been set up to study the chemistry and biology of diet selection in this species in situations where it is a pest. The variety "Conference" is particularly susceptible to disbudding by bullfinches whilst "Doyenné du Comice" is less favoured. Previous work has shown that gross nutritional factors such as protein or carbohydrate levels cannot adequately explain the preferences of the birds²⁴ thus this method was developed to look at the levels of potentially organoleptic phenolic acids in pear buds.

EXPERIMENTAL

Apparatus

The chromatograph consisted of two Waters Model 6000 A pumps, a Waters Model 710 B Wisp autosampler, a Waters Model 481 variable-wavelength UV detector set at 280 nm (detector sensitivity 0.10 a.u.f.s.), a Waters Model 730 data module printer/plotter and a Waters Model 721 system controller (Millepore-Waters, Harrow, U.K.). The column was maintained at 35°C using a Jones Chromatography 30-cm column block heater. (Anachem, Luton, U.K.). Separations were achieved on a Rainin Short-one 10 × 0.4 cm, 3- μ m C₁₈ packed reversed-phase column supplied by Anachem.

Elution

The two solvents employed were: (A) 5% (v/v) aqueous formic acid and (B) 75% (v/v) aqueous methanol. Both solvents were filtered through 0.45- μ m membrane filters, degassed under reduced pressure and stored under helium throughout their use. Elution was carried out at 1.0 ml/min using the complex gradient described in Table I.

TABLE I

GRADIENT CONDITIONS USED TO ELUTE SIMPLE PHENOLIC ACIDS FROM A RAININ SHORT-ONE 3 μ m C₁₈ REVERSED-PHASE COLUMN

Solvent A: 5% (v/v) aqueous formic acid; solvent B: 75% (v/v) aqueous methanol. Flow-rate 1 ml/min throughout.

Time (min)	A (%)	B (%)	Curve*
0	97	3	
0.5	97	3	6
5	92	8	6
10	61	39	4
16	43	57	6
18	0	100	6
22	0	100	6
25	97	3	6

* Curve shape as designated by Millepore-Waters system controller, 6-linear gradient, 4-convex gradient.

Standards

The compounds named in the results were obtained from a variety of commercial sources, with the exception of isochlorogenic acid which was kindly donated by Prof. J. B. Harborne (Reading University, U.K.). All standards were 0.1 mg/ml in 5% (v/v) aqueous formic acid excepting isochlorogenic acid which was used as a qualitative standard only. In order to identify peaks in the standard mixture (Fig. 1), compounds were first chromatographed individually or in mixtures of two or three where identification would not be confusing. The tentative identification of compounds in the plant material extracts was achieved by co-chromatography with the appropriate standards.

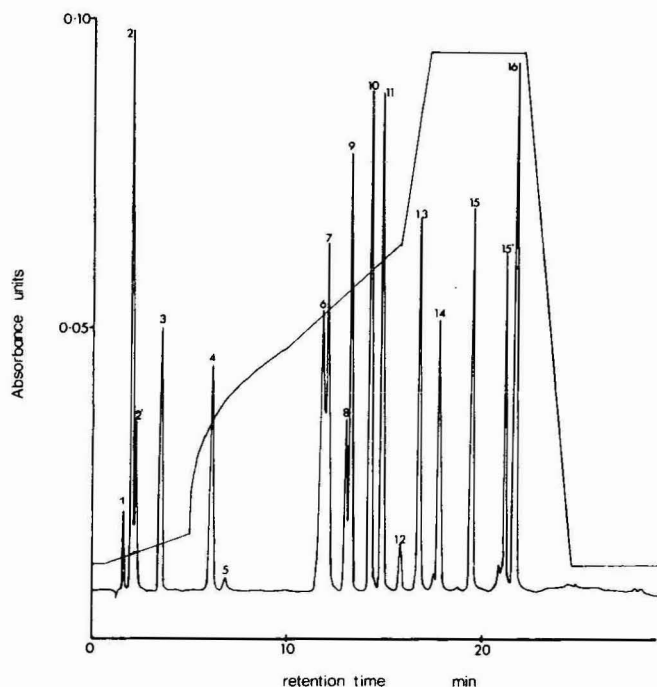


Fig. 1. Separation of 17 phenolic acid standards (0.1 mg/ml) on a Rainin short-one 3 μ m C₁₈ reversed-phase column. The gradient is as depicted and described in the text. The compounds are: 1, arbutin (retention time 1.65 min); 2, gallic acid (2.05 min); 2', hydroquinone (2.15 min); 3, protocatechuic acid (3.59 min); 4, *p*-hydroxybenzoic acid (6.25 min); 5, gentisic acid (6.97 min); 6, vanillic acid (11.94 min); 7, caffeic acid (12.21 min); 8, homovanillic acid (13.16 min); 9, chlorogenic acid (13.40 min); 10, syringic acid (14.49 min); 11, *p*-coumaric acid (15.05 min); 12, benzoic acid (16.03 min); 13, ferulic acid (16.96 min); 14, synapic acid (18.03 min); 15 + 15', isochlorogenic acid (19.44 min and 21.23 min); 16, cinnamic acid (22.06 min).

Plant extractions

Plant material collected from an orchard site in south-east England was lyophilised immediately on return to the laboratory and stored desiccated at 4°C until required for analysis. Prior to analysis the outer scale-like tissue (not consumed by the bird) was removed from the developing flower initial and the latter finely macerated. A portion of the chopped initial (50 mg) was extracted in ethanol-methanol (1:1) (5 ml) at 80°C for 1 h. After cooling the alcoholic solvent was removed by evaporation under a stream of nitrogen. A volume of 5 ml 5% (v/v) aqueous formic acid was added and the resultant solution extracted into 4 × 5 ml diethyl ether. The bulked ether extracts were evaporated under nitrogen and the residue redissolved in 5% (v/v) aqueous formic acid (3 ml) prior to HPLC analysis. All samples were stored under nitrogen in sealed amber vials to prevent excessive phenolic oxidation.

RESULTS AND DISCUSSION

Fig. 1 shows the separation of 17 phenolic components commonly found in plant material. This separation was achieved in less than 25 min and represents a

TABLE II

THE RELATIVE LEVELS OF THE SIX PRINCIPAL PHENOLIC COMPONENTS OF PEAR FRUIT BUD FLOWER INITIALS AS DETERMINED BY RP-HPLC

All results are quoted in arbitrary peak area units as determined at 280 nm. The retention times are quoted in parenthesis.

	<i>Doyenne du Comice</i>	<i>Conference</i>
1,4-Dihydroxybenzene (2.15 min)	3.21	2.15
X (9.77 min)	0.84	0.59
Chlorogenic acid (13.41 min)	3.28	3.14
X (13.94 min)	1.31	0.19
Syringic acid (14.41 min)	1.20	0.84
Isochlorogenic acid (19.46 min)	8.58	6.03

considerable saving of both time and solvents, etc., when compared with similar methods employing conventional columns. It should be noted that the "pure" isochlorogenic acid gives rise to two peaks (15 and 15') which as this compound is the di-caffoyl ester of quinic acid presumably represent two isomeric forms. There appears to be no practical reason why this rapid separation technique could not be employed to study other plant phenolics such as flavonoids, etc.

The method described in this paper was applied to the analysis of pear flower initials in the bud collected in mid-January 1985, the period when maximum bird damage is likely to occur^{24,25}. Table II shows the levels of the major phenolic acids in the two varieties studied and a chromatogram for one variety, "Doyenné du Comice" is shown in Fig. 2. The chromatogram demonstrates that the bud flower initials contain three principal components, hydroquinone (1,4-dihydroxybenzene), chlorogenic acid and isochlorogenic acid. It appears likely that the hydroquinone detected is the breakdown product of arbutin (the glucoside of hydroquinone) produced during extraction, particularly as arbutin, chlorogenic acid and isochlorogenic acids have long been recognised as the major phenolic constituents of pear leaves and bark²⁶. Fig. 2 also shows the presence of three additional components, one which co-chromatographs with syringic acid, and two, as yet are unidentified peaks (X).

The bullfinch shows a marked preference for buds of "Conference" pears whilst avoiding those of "Doyenné du Comice". Although physical factors such as shape, size and texture may have a role in these preferences²⁷, it would appear that there is also a chemical basis for diet selection and knowledge of the compounds involved will assist in the development of suitable pest management techniques. There seems to be little or no difference between varieties in terms of their gross nutritional value or in the levels of high-molecular-weight polyphenolic materials (tannins). It is interesting to note, however, that the preferred variety, "Conference" has the lower levels of the phenolics determined in this study particularly isochlorogenic acid and the unidentified peak at 13.94 min. No attempt has been made to quantify fully the data primarily because of the lack of standards for isochlorogenic acid and the two unknowns. Work is in hand to see if these chemicals affect dietary selection of birds in the laboratory.

Although there are a great number of phenolic substances known to occur in plant material⁷, this method offers the analyst a rapid and economical technique for

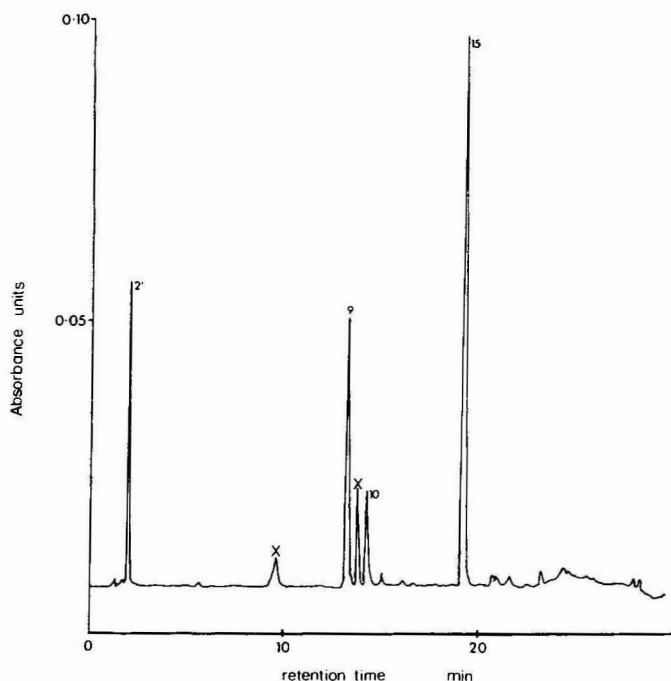


Fig. 2. Separation of the diethyl ether soluble phenolic acids from fruit bud flower initials of "Doyenné du Comice". The gradient is as described in the text and the numbering system is the same as that used in Fig. 1 (X = unidentified components).

the quantification of such substances. Naturally, the final identification of any component within a particular plant tissue must be based not solely on a chromatographic separation but on what might reasonably be expected in a specific plant and on other confirmatory analytical techniques.

ACKNOWLEDGEMENTS

I would like to thank Miss C. A. Blunden for her assistance in this work and Prof J. B. Harborne for his kind gift of isochlorogenic acid.

REFERENCES

- 1 J. B. Murphy and C. A. Stutte, *Anal. Biochem.*, 86 (1978) 220-228.
- 2 J. M. Hardin and C. A. Stutte, *Anal. Biochem.*, 102 (1980) 171-175.
- 3 E. Bartscher, H. Binder, R. Concini and O. Bobleter, *J. Chromatogr.*, 252 (1982) 167-176.
- 4 C. A. Stutte and J. M. Hardin, *J. Chromatogr.*, 248 (1982) 446-450.
- 5 F. Villeneuve, G. Abravanel, M. Moutounet and G. Alibert, *J. Chromatogr.*, 234 (1982) 131-140.
- 6 J. M. Anderson and W. B. Pederson, *J. Chromatogr.*, 259 (1983) 131-139.
- 7 K. Vande Castele, H. Geiger and C. F. Van Sumere, *J. Chromatogr.*, 258 (1983) 111-124.
- 8 K. Vande Castele, H. Geiger, R. De Loose and C. F. Van Sumere, *J. Chromatogr.*, 259 (1983) 291-300.
- 9 C. M. Cater, S. Gheysuddin and K. F. Mattil, *Cereal Chem.*, 49 (1972) 508-514.

- 10 W. M. Walter, A. E. Purcell and G. K. McCollum, *J. Agric. Food Chem.*, 27 (1979) 938–941.
- 11 H. Kozłowska, D. A. Rotkiewicz, R. Zadernowski and F. W. Sosulski, *J. Am. Oil Chem. Soc.*, 60 (1983) 1119–1123.
- 12 R. Zadernowski and H. Kozłowska, *Lebensm.-Wiss.-Technol.*, 16 (1983) 110–114.
- 13 A. Malmberg and O. Theander, *Swedish J. Agric. Res.*, 14 (1984) 119–125.
- 14 A. Seo and C. V. Morr, *J. Agric. Food Chem.*, 32 (1984) 530–533.
- 15 A. G. H. Lea, *J. Chromatogr.*, 238 (1982) 253–257.
- 16 C. G. Barroso, R. C. Torrijos and J. A. Perez-Bustamante, *Chromatographia*, 17 (1983) 249–252.
- 17 M. H. Salagoity-Augguste and A. Bertrand, *J. Sci. Food Agric.*, 35 (1985) 1241–1247.
- 18 D. S. Kirkham, *J. Gen. Microbiol.*, 17 (1957) 120–134.
- 19 B. K. Hwang, *Phytopath. Z.*, 108 (1983) 1–11.
- 20 M. F. Wilson and C. A. Blunden, *J. Sci. Food Agric.*, 34 (1983) 973–978.
- 21 P. W. Greig-Smith and M. F. Wilson, *Oikos*, 44 (1985) 47–54.
- 22 J. G. Buta, *J. Chromatogr.*, 295 (1984) 506–509.
- 23 I. Newton, *J. Appl. Ecol.*, 1 (1964) 265–279.
- 24 M. F. Wilson, J. H. Blackford and C. A. Blunden, *J. Sci. Food Agric.*, 34 (1983) 794–802.
- 25 P. W. Greig-Smith and G. M. Wilson, *J. Appl. Ecol.*, 21 (1984) 401–422.
- 26 A. H. Williams, J. B. Pridham (Editor), *Phenolics in Plants in Health and Disease*, Pergamon, Oxford, 1960, pp. 3–7.
- 27 D. D. B. Summers and L. W. Huson, *Crop Protection*, 3 (1984) 335–341.

CHROM. 18 002

Note

Reversed-phase high-performance liquid chromatography of methyl isocyanate

C. D. RAGHUVeerAN* and M. P. KAUSHIK

Defence Research and Development Establishment, Tansen Road, Gwalior-474002, Madhya Pradesh (India)

(Received June 3rd, 1985)

Methyl isocyanate (MIC) is a toxic chemical intermediate like the other industrially used organic isocyanates. It has a high vapour pressure and due care should be exercised while working with this compound. High-performance liquid chromatographic (HPLC) methods are available for the determination of toluene diisocyanate (TDI), hexamethylene isocyanate (HMI), etc., but we believe that so far no HPLC procedure has been described for MIC. The above methods depend on the conversion of the isocyanates into more stable, UV-absorbing^{1,2} or fluorescing³ urea derivatives by use of suitable primary or secondary amines.

We report here a reversed-phase HPLC procedure for the determination of MIC by reaction with a readily available aromatic amine to form a urea derivative absorbing at 254 nm. The method is sensitive to nanogram quantities of MIC.

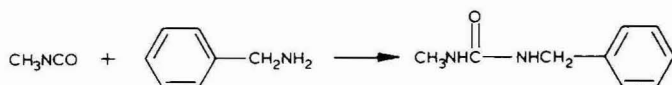
EXPERIMENTAL

Equipment

The liquid chromatograph used was assembled from the following components: an SP-8750 ternary solvent delivery system (Spectra-Physics, U.S.A.) equipped with a Rheodyne Model 7125 injector and a 10- μ l loop; a PRP-1 column (Hamilton, Bonaduz, Switzerland) packed with styrene-divinylbenzene (10 μ m, 150 \times 4.1 mm); an SF-773 variable-wavelength detector (Kratos Analytical, U.S.A.) operated at 254 nm; a C-R1B Chromatopac data processor (Shimadzu, Japan). The chromatograph was operated in isocratic mode.

Chemicals

MIC was prepared in our laboratory by refluxing acetyl chloride with sodium azide in the presence of a phase-transfer catalyst⁴. It was distilled, collected in a chilled receiver and characterized by spectroscopic techniques. Benzylamine (Riedel), distilled with zinc dust, was used for derivatizing MIC into N-benzyl-N'-methylurea (BMU) according to the reaction:



The structure and purity of BMU synthesized as above were established by elemental and spectroscopic (IR, ^1H NMR and electron impact mass spectrometry) analysis. This substance served as a reference for the identification of MIC. Quantitation was, however, achieved by forming BMU *in situ* in aqueous methanol containing benzylamine.

The solvents used for the mobile phase were methanol (guaranteed reagent; E. Merck, India) and water, distilled in an all-glass triple distillation apparatus. The two solvents were mixed in the proportion 90:10 together with 0.0025% perchloric acid, and filtered over a Millipore filtration system.

Procedure for BMU in situ

About 0.2 ml of MIC were accurately weighed and dissolved in a solution of benzylamine in the eluent used for LC*. The molar concentration of the amine was always in excess of that of MIC to ensure an adequate concentration for the formation of BMU. The ratio of the concentrations of MIC to benzylamine was 1:1.5. This solution served as a stock solution.

The precautions taken while preparing this stock solution were as follows: (i) MIC was weighed in a leak-proof container (a 10-ml graduated stoppered test-tube, with a quickfit stopper kept in place by a thin film of silicone grease; (ii) MIC weighed as above was kept chilled in an ice-bath till dissolution in the amine solution; (iii) the benzylamine solution was also chilled before mixing with MIC. This procedure was adopted so as to minimize the loss of MIC during the *in situ* reaction and to maximize the trapping of the substance in the bulk of the solution.

Working standards in the range 0.01–0.1 μg (10–100 ng) were made by serial dilution in methanol. A 10- μl volume of each standard was injected into the column.

RESULTS AND DISCUSSION

The *in situ* generation of BMU has been devised with a view to using a solution of benzylamine as a trapping fluid for MIC in the atmosphere. Other isocyanates are usually trapped in toluene containing an amine. The solvent is removed by evaporation and the residue is reconstituted in the eluents to be employed for reversed-phase HPLC⁵. In the procedure described here, the amine solution containing BMU can be injected into the column after suitable dilution in the mobile phase. Thus losses during the sample work-up can be minimized.

BMU is eluted at 1.75 min under the chromatographic conditions described. Fig. 1 shows a chromatogram of the synthesized BMU. In the *in situ* process (Fig. 2), the corresponding chromatogram contains a peak for the unreacted benzylamine (peak 1) which is eluted before BMU. The amine peak is sharp due to the presence of perchloric acid in the mobile phase. Fig. 3 shows a chromatogram of a benzylamine solution intended for trapping MIC and suitably diluted before the injection.

A calibration for MIC was performed according to the procedure described in the Experimental. An aliquot of the stock solution of BMU equivalent to 100 mg of MIC was diluted in methanol so as to give a concentration equivalent to 10 mg/ml of MIC. The calibration curve was plotted on the basis that 2.8 parts by weight of

* MIC is highly volatile. Measuring out accurate volumes of it was rendered difficult due to high ambient temperatures.

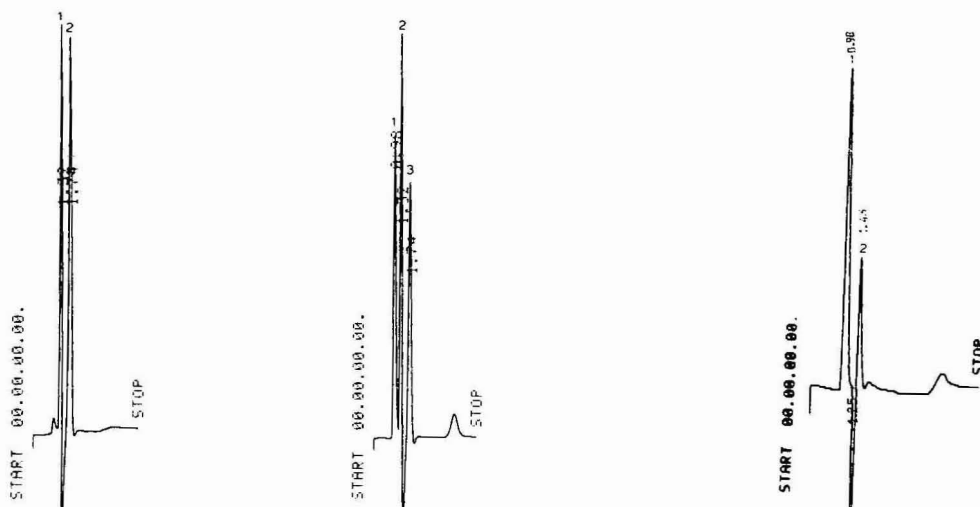


Fig. 1. Chromatogram of synthesized BMU. Conditions column, PRP-1; eluent, methanol-water (90:10) containing 0.0025% perchloric acid; flow-rate, 1 ml/min; sample size, 10 μ l; detection, UV, 254 nm, 0.01 a.u.f.s., C-R1B attenuation 2. Peaks: 1 = unknown (from methanol); 2 = BMU.

Fig. 2. Detection of MIC as BMU *in situ*. Conditions as in Fig. 1. Peaks: 1 = benzylamine; 2 = unknown (from methanol); 3 = MIC (60 ng).

Fig. 3. Benzylamine injected as a blank. Conditions as in Fig. 1. Peaks: 1 = benzylamine (diluted); 2 = unknown (from methanol).

BMU are equal to 1 part by weight of MIC. The working standards were made from this solution by dilution in methanol. A plot of the concentration of MIC (0.01–0.1 μ g) versus peak height is linear (Fig. 4). Such a calibration plot can be useful for monitoring MIC in the atmosphere.

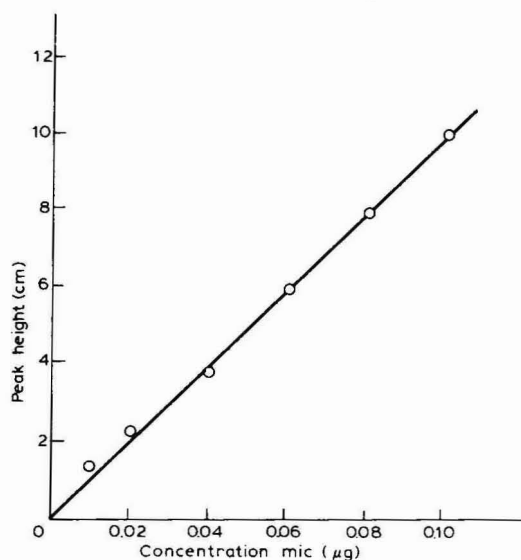


Fig. 4. Calibration plot for MIC.

The choice of the solvent for the amine reagent was based on experiments with water, methanol, acetonitrile and methanol-water (90:10) (with and without perchloric acid). Standards of BMU of identical concentration were injected in each of these solvents and the peak heights compared. Only water-methanol (80:20), acetonitrile and methanol-water (90:10) containing perchloric acid, *i.e.*, the mobile phase, gave linear calibration plots. The data are presented in Table I from which it is evident that the mobile phase is the best medium for preparing the amine reagent.

TABLE I
CHOICE OF SOLVENT FOR BENZYLAMINE

Concentration of MIC: 10 ng; sensitivity setting: 0.01 a.u.f.s.; recorder setting (C-R1B): attenuation 2.

<i>Solvent</i>	<i>Peak height of MIC (cm)</i>
(1) Water-methanol (80:20)	5.5
(2) Acetonitrile	6.8
(3) Methanol-water (90:10) containing 0.0025% perchloric acid	7.5

CONCLUSION

A reversed-phase HPLC procedure has been developed which makes use of a commonly available reagent, *viz.*, benzylamine, for derivatizing MIC into a urea derivative detected at 254 nm. The method is linear in the range 0.01–0.1 μg (10–100 ng) MIC. For trapping MIC from sources like air and water, the benzylamine solution can be prepared in the mobile phase. Work is in progress to utilize the technique for air monitoring.

ACKNOWLEDGEMENT

We thank Dr. P. K. Ramachandran, Director, Defence Research & Development Establishment, Gwalior for active encouragement and guidance.

REFERENCES

- 1 D. A. Bagon and C. J. Purnell, *J. Chromatogr.*, 190 (1980) 175–182.
- 2 S.-N. Chang and W. R. Burg, *J. Chromatogr.*, 246 (1982) 113–120.
- 3 L. H. Kermes, R. L. Sandridge and J. Keller, *Anal. Chem.*, 53 (1981) 1122–1125.
- 4 A. Brandstrom, B. Lamm and I. Palmertz, *Acta Chem. Scand., Ser. B*, 28 (1974) 699.
- 5 D. A. Bagon, C. A. Warwick and R. H. Brown, *Am. Ind. Hyg. Assoc. J.*, 45 (1984) 39–43.

CHROM. 17 950

Note

High-performance liquid chromatographic determination of melamine extracted from cups made of melamine resin

TAKIKO INOUE, HAJIMU ISHIWATA*, KUNITOSHI YOSHIHIRA and AKIO TANIMURA

National Institute of Hygienic Sciences, 1-18-1, Kamiyoga, Setagaya-ku, Tokyo 158 (Japan)

(First received May 1st, 1985; revised manuscript received June 3rd, 1985)

Melamine (2,4,6-triamino-*s*-triazine) is an important material in the manufacture of thermosetting plastics used in housewares. Kitchenware and tableware made of melamine resin are widely used in homes, school and office cafeterias and restaurants, but the migration of melamine from these wares has not been well studied.

This paper describes a sensitive high-performance liquid chromatographic procedure for the determination of melamine based on the methods reported by Beilstein *et al.*¹ and the National Toxicology Program² and the application of the proposed method to migration solutions obtained from cups made of melamine resin.

EXPERIMENTAL

Apparatus

A Yanaco (Tokyo, Japan) Model L-2000 high-performance liquid chromatograph equipped with a Model 215 spectrometer set at 235 nm (range at 0.08) was used. A Yanapak (Tokyo, Japan) ODS-A column (250 × 4.6 mm I.D.) was employed. A Shimadzu (Kyoto, Japan) UV-240 spectrophotometer was utilised.

Materials and chemicals

Cups of volume 255 ml, made of melamine resin were used.

All chemicals and reagents were of Japanese Industrial Standards special grade. Melamine (Wako, Kyoto, Japan) was 99.0% pure.

Mobile phase. A 0.1 M phosphate buffer (pH 3.0) containing monopotassium phosphate and phosphoric acid was prepared. To determine the optimum pH, 0.1 M phosphate buffers of pH 8.0, 7.0, 6.0 and 5.0 containing disodium phosphate and monopotassium phosphate were prepared and buffers of pH 4.0 and 2.0 were prepared in the same manner as the buffer of pH 3.0. The flow-rate was set at 0.78 ml/min.

Sample preparation

A 220-ml portion of a food-simulating solvent, water or 4% (v/v) acetic acid, which had been preliminary warmed to 60°C, was poured into melamine resin cups so that the solvent surface was 5 mm below the rim. The cups were covered with watch-glasses, then stood at 60°C for 30 min. The migration solution (200 ml) was

evaporated to dryness using a rotary evaporator at 65–70°C, the residue was dissolved in 2 ml of water and volumes of 10 μ l of this solution were injected into the chromatograph.

Recovery study

A volume of 200 ml of the food-simulating solvents and 20 μ g of melamine were placed in a round-bottomed flask, the mixture was allowed to stand at 60°C for 30 min and was then treated in the same manner as the migration solution.

RESULTS AND DISCUSSION

The pH of the mobile phase strongly affected both the retention time (Fig. 1a) and the absorbance of melamine (Fig. 1b). The retention time of melamine decreased with decrease in pH. The wavelength of maximum absorption (λ_{max}) of melamine (235 nm) was not shifted by changes in pH, but the intensity of the absorption increased when the pH was lowered. The peak height of melamine increased with increasing acidic conditions, especially at pH 2.0 and 3.0. However, use of a mobile phase of pH 2.0 was not suitable because the retention time of melamine at pH 2.0 was close to the water peak and a pH of 2.0 represented the limit that could be tolerated by the column. Neither the retention time nor the peak height of melamine was affected when the concentration of buffers of pH 3.0 was varied from 0.05 to 0.5 M. Citric acid, which had been used to adjust the pH of the buffer to 3.0², was not suitable for obtaining a linear baseline with the proposed sensitivity.

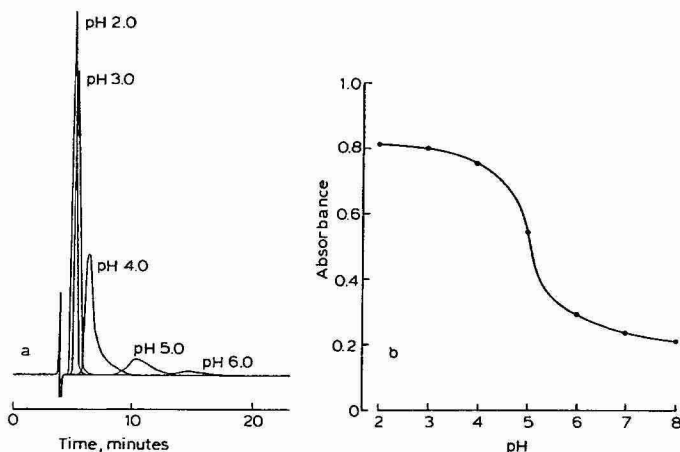


Fig. 1. Effect of pH on (a) retention time in HPLC and (b) absorbance in spectrophotometry. The concentration of melamine was 10 μ g/ml in each buffer. Determination was carried out at 235 nm.

On the basis of these results, subsequent experiments were carried out using 0.1 M phosphate buffer of pH 3.0.

The recoveries of melamine from food-simulating solvents were more than 98.8% (Table I). Results of the determination of melamine in the migration solution are presented in Table II. The concentration of melamine in the migration solution

TABLE I
RESULTS OF RECOVERY STUDY

20 μ g of melamine were added to 200 ml of the solvent. Results are averages of four determinations.

<i>Solvent</i>	<i>Recovery \pm S.D. (%)</i>
Water	99.2 \pm 0.9
4% acetic acid	98.8 \pm 1.0

TABLE II
RESULTS OF ANALYSIS OF MELAMINE IN MIGRATION SOLUTION

Results are averages of four determinations.

<i>Solvent</i>	<i>Melamine (ng/ml \pm S.D.)</i>
Water	19.0 \pm 2.7
4% acetic acid	23.6 \pm 5.2

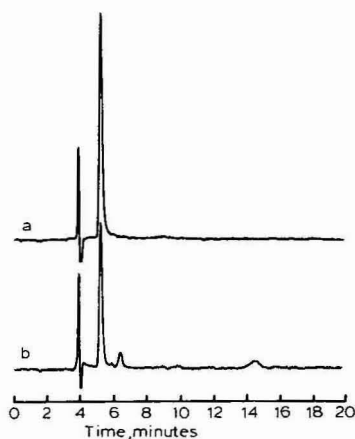


Fig. 2. Chromatograms of standard solution of (a) melamine and (b) migration solution in 4% acetic acid. Melamine standard solution corresponded to 50 ng/ml of migration solution.

was about 20 ng/ml. Higher standard deviations of the amount migrated than those given by the recovery tests may be caused by the differences in the surface roughness and the content of residual melamine in the individual cups. Formaldehyde, which could be present in the migration solution, did not interfere with the determination of melamine at a level of 4000 ng. A typical chromatogram is shown in Fig. 2.

The limit of determination of melamine by the proposed method was 2.5 ng/ml in the migration solution (signal-to-noise ratio = 5).

REFERENCES

- 1 P. Beilstein, A. M. Cook and R. Hutter, *J. Agr. Food Chem.*, 29 (1981) 1132.
- 2 National Toxicology Program, *Carcinogenesis Bioassay of Melamine in F344/N Rats and B6C3F₁ Mice*, U.S. Department of Health and Human Services, MD, 1983, p. 154.

CHROM. 17 984

Note

Gradient separation of fatty acids (C₁₄–C₃₀) by reversed-phase high-performance liquid chromatography

TOMÁŠ ŘEZANKA* and MILOSLAV PODOJIL

Department of Biogenesis of Natural Substances, Institute of Microbiology, Czechoslovak Academy of Sciences, CS-142 20 Prague 4 (Czechoslovakia)

(First received March 23rd, 1985; revised manuscript received June 25th, 1985)

Gas chromatography (GC) is routinely employed in the analysis of fatty acid mixtures. During the past ten years high-performance liquid chromatography (HPLC) has become increasingly important for analysis, quantitation and preparative separation of fatty acids¹. Fatty acids can be separated as their phenacyl and naphthacyl esters, or as esters with 9-diazomethylantracene that strongly absorbing in the UV region at 254 nm^{2–4}, and as methyl esters that can be detected via their refraction indexes^{5,6} or by UV absorption (203–214 nm)⁷. Most frequently, the stationary phase RP-18 was used^{2,3,5–7}; phases RP-8⁸, RP-9⁹ and RP-30¹⁰ were used only occasionally under stricter elution conditions (acetonitrile, aqueous phosphoric acid). The stationary phase RP-18 was employed for the separation of those methyl esters of fatty acids with up to 22 carbon atoms^{2,7}, with the exception of highly unsaturated very long-chain fatty acids (e.g. C_{24:4} up to C_{30:5})¹¹. Owing to their relatively high polarity the retention times of these acids do not exceed 60 min. Fatty acids with up to 32 carbon atoms were rather separated as *m*-methoxyphenacyl esters¹², whose high polarity facilitated the use of phase RP-18.

When the analyses of fatty acids by HPLC and GC are to be correlated it is most useful to prepare methyl esters. These, however, have a lower polarity (especially those of saturated acids and acids with a higher number of carbon atoms) than e.g. *m*-methoxyphenacyl esters, and therefore they do not separate on the reversed-phase RP-18. For this reason we used the more polar phase RP-1 as the stationary phase in this work.

EXPERIMENTAL

Fatty acid (even-numbered saturated C₁₄ to C₃₀ and monoenic C₁₆–C₂₀ and C₂₄) were purchased from Fluka (Switzerland) and Sigma (U.S.A.). The other fatty acids (see Table I) were isolated from the green freshwater alga *C. kessleri*¹³.

HPLC was carried out with the SP 8000 apparatus (Spectra Physics, U.S.A.) on a 50 cm × 6 mm I.D. column (Separon SI C1, Laboratory Instruments, Czechoslovakia). The mobile phase linear gradient (2 ml/min) ran from a mixture of methanol–water (50:50) into methanol (30 min) and further methanol (60 min); detection was by a UV detector at 210 nm. The column efficiency was 8700–10 000

TABLE I

CAPACITY RATIOS (k') OF METHYL ESTERS OF FATTY ACIDS BY MEANS OF REVERSED-PHASE HPLC ON STATIONARY PHASE RP-1

Number	Methyl ester	Apparent k'	Number	Methyl ester	Apparent k'
1	14:0	0.808	16	20:0	8.616
2	15:0	1.358	17	20:1	7.208
3	15:1	0.566	18	21:0	9.783
4	16:0	2.941	19	22:0	11.200
5	16:1	1.183	20	23:0	12.500
6	16:2	0.566	21	24:0	13.858
7	16:3	0.358	22	24:1	12.591
8	17:0	4.275	23	25:0	15.083
9	17:0*	3.466	24	26:0	16.033
10	17:1	2.733	25	26:1	15.323
11	18:0	5.666	26	28:0	17.483
12	18:1	4.158	27	28:1	17.111
13	18:2	2.791	28	29:0	18.103
14	18:3	2.016	29	30:0	20.410
15	19:1	7.058	30	30:1	20.013

* 2-Methylhexadecanoic acid.

plates, $V_0 = 4$ ml, and t_R of methyl stearate was 800 sec. Acids present in the natural mixture were identified by gas chromatography on both capillary and packed columns, combined with mass spectrometry using the Hewlett-Packard 5992 B apparatus¹³. The methyl esters of fatty acids were prepared by means of boron trifluoride-methanol¹⁴. The purity and supplementary identification of the individual peaks from HPLC were verified by GC using the Varian Aerograph 2740 apparatus (Varian, U.S.A.), and a column (180 cm \times 2 mm I.D.) packed with 3% XE-60 on Chromosorb AM DMCS 80/100 (Lachema, Czechoslovakia). The carrier gas was nitrogen (flow-rate 25 ml/min), the injector temperature 240°C, the column temperature 180°C, and the detector temperature 250°C.

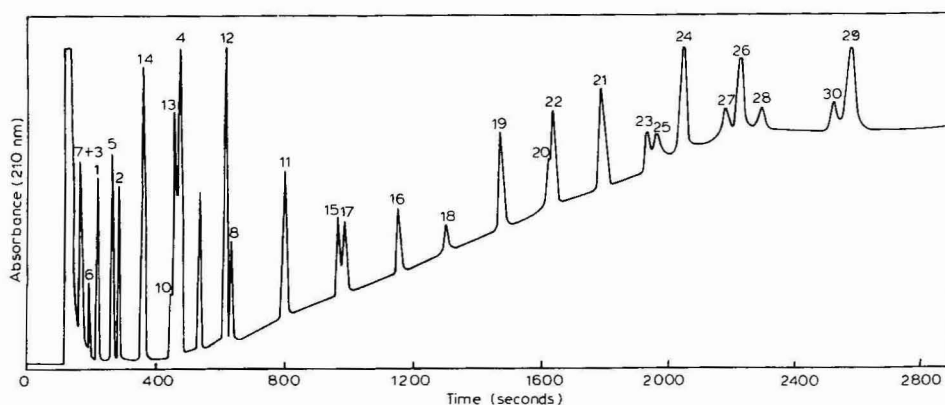


Fig. 1. Chromatogram of a 10- μ l sample containing 0.1 mg/ μ l fatty acid methyl esters (commercial standards and natural mixture from *C. kessleri*). The detector was set at 0.08 a.u.f.s. and at 210 nm. For peak numbers see Table I.

RESULTS AND DISCUSSION

The use of reversed-phase HPLC on Separon SI C1 made it possible to separate saturated and mono unsaturated methyl esters of fatty acids ranging from C₁₄ to C₃₀ within less than 1 h (Fig. 1). It is thus possible to identify fatty acids by means of HPLC as well as GC.

The disadvantage of decreased sensitivity while detecting methyl esters of fatty acids by UV spectra is counterbalanced by their easy identification.

From our experimental data it follows that the influence of the double bond decreases as the number of carbons in the chain of a given methyl ester increases, *i.e.* the quotient of the capacity ratios for saturated and mono unsaturated methyl esters approaches one.

ACKNOWLEDGEMENT

The authors thank Dr. J. Zima for HPLC analyses.

REFERENCES

- 1 M. S. P. Lie Ken Jie, *Advan. Chromatogr.*, 18 (1980) 1.
- 2 J. P. Roggero and S. V. Coen, *J. Liquid Chromatogr.*, 4 (1981) 1817.
- 3 S. A. Barker, J. A. Monti, S. T. Christian, F. Benington and R. D. Morin, *Anal. Biochem.*, 07 (1980) 116.
- 4 M. J. Cooper and M. W. Anders, *Anal. Chem.*, 46 (1974) 1849.
- 5 T. S. Pei, R. S. Henly and S. Ramachandra, *Lipids*, 10 (1975) 152.
- 6 C. R. Scholfield, *Anal. Chem.*, 47 (1975) 1417.
- 7 M. Özçimder and W. E. Hammers, *J. Chromatogr.*, 187 (1980) 307.
- 8 M. I. Avelidano, M. Van Rollins and L. A. Horrocks, *J. Lipid Res.*, 24 (1983) 83.
- 9 H. D. Durst, M. Milano, E. J. Kikta, Jr., S. A. Connelly and E. Grushka, *Anal. Chem.*, 47 (1975) 1797.
- 10 K. Takayma, H. C. Jordi and F. Benson, *J. Liquid Chromatogr.*, 3 (1980) 61.
- 11 W. McLean Grogan, *Lipids*, 19 (1984) 341.
- 12 N. E. Bussell, A. Gross and R. A. Miller, *J. Liquid Chromatogr.*, 2 (1979) 1337.
- 13 T. Řezanka, J. Vokoun, J. Slaviček and M. Podojil, *J. Chromatogr.*, 268 (1983) 71.
- 14 L. D. Metcalfe and A. A. Schmitz, *Anal. Chem.*, 33 (1961) 363.

CHROM. 17 986

Note

Reversed-phase high-performance liquid chromatographic separation of closely related furocoumarins

C. A. J. ERDELMEIER, B. MEIER and O. STICHER*

Pharmazeutisches Institut, Eidgenössische Technische Hochschule Zürich, CH-8092 Zürich (Switzerland)

(Received July 1st, 1985)

Furocoumarins are known to exhibit several biological effects, most prominent of which are their photosensitizing and the mutagenic activities^{1–4}. Many plant species contain furocoumarins, and these potently active and toxic substances necessitate efficient analytical methods for their qualitative and quantitative determination.

In the last few years, high-performance liquid chromatography (HPLC) has been used increasingly for furocoumarin separations and determinations. It was shown to be a rapid and sensitive method for the detection of phototoxic psoralens in Citrus essential oils^{5–9}. Such oils are commonly used in the fragrance and flavour industry. The application of HPLC to the determination of the strong photosensitizer bergapten in perfumes and suntan cosmetics has also been reported^{10,11}. Of special interest is the HPLC determination of 8-methoxypsoralen plasma levels in conjunction with photochemotherapy in the treatment of psoriasis^{12–14}. Furthermore, HPLC has proven useful for the investigation of plants containing furocoumarins^{14–19}; these very complex mixtures require efficient separation methods. Two recent publications have dealt with the separation of a large number of natural and synthetic coumarins^{20,21}. Van de Castele *et al.*²⁰ separated 43 coumarins including 6 furocoumarins using a combination of isocratic and linear gradient systems on a RP-18 column. Thompson and Brown²¹ studied the behaviour of 67 coumarins (including 19 furocoumarins) on normal phase silica and on RP-18 columns and found that the two types of columns can complement each other.

In this paper a reversed-phase separation system for closely related furocoumarins is presented. These compounds (Fig. 1) occur in several Umbelliferae genera²², e.g., *Heracleum*, *Angelica* and *Peucedanum*, and show very similar chromatographic behaviours. For improvement of the peak identification, the HPLC system was equipped with a photodiode array detector²³ which has already been shown to be helpful in the HPLC of flavonoids^{24,25}, xanthenes²⁴ and iridoids²⁵.

MATERIALS AND METHODS

All solvents were of HPLC quality, purchased from Fluka (Buchs, Switzerland). HPLC separations were carried out with a Waters gradient system consisting of two M 6000 A pumps, a Model 720 system controller and a WISP 710 B autosampler. For UV detection a 1040 A high speed spectrophotometric detector (Hew-

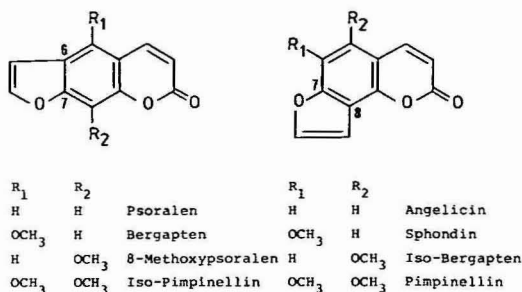


Fig. 1. Structures of investigated furocoumarins.

lett-Packard, Waldbronn, F.R.G.) was used at 310 nm. The gradient separations were carried out using a Knauer Spherisorb ODS II (3 μ m) cartridge column (100 \times 4 mm I.D.). Solvent A was tetrahydrofuran–water (3.5:96.5) and solvent B was methanol. The gradient profile was as follows: 0–20 min, 25% B in A (isocratic); 20–40 min, 25–45% B in A (linear gradient). The flow-rate was 1.0 ml/min.

Bergapten, isobergapten, pimpinellin, isopimpinellin and sphondin were isolated from *Heracleum sphondylium* roots using centrifugally accelerated thin-layer chromatography (TLC). Angelicin and psoralen were synthesized²⁶ and isolated from the reaction mixture by centrifugally accelerated TLC. 8-Methoxypsoralen was obtained from Fluka. The reference sample concentration for HPLC was about 0.1 mg/ml in methanol and the injection volume 10 μ l.

The dried plant material was extracted with chloroform. For analyses, the crude extracts were dissolved in methanol at a concentration of 10 mg/ml and pre-purified over Bond-Elut C₁₈ cartridges (Analytichem Intern., Harbor City, CA, U.S.A.). *Heracleum sphondylium* roots were obtained from Dixia (St. Gallen, Switzerland) and *Heracleum mantegazzianum* leaves were collected in Germany.

RESULTS AND DISCUSSION

An efficient separation of the eight furocoumarins could be achieved with the described HPLC system (Fig. 2). From the obtained results it is supposed that the use of a small (3 μ m) spherical octadecylsilane packing material represents a significant improvement for HPLC separations of such compounds of low polarity. The peak shape and symmetry observed is improved in comparison with those found on the 10- μ m irregular ODS material. As the compounds lie in a narrow polarity range the analysis time must be kept relatively long. At higher solvent strengths the resolution between the first three peaks becomes unsatisfactory. The mobile phase flow-rate cannot be increased since the column pressure is 4000 p.s.i. with the solvent system used. The first three components eluted were difficult to separate. A sufficient mobile phase selectivity was obtained by addition of tetrahydrofuran: higher or lower amounts of tetrahydrofuran than that added impaired the separation of the former group of furocoumarins.

In spite of the retention time variation, a certain peak identification is nevertheless possible by use of the photodiode array detector due to the characteristic UV spectra of each of the components. The gradient system has proven suitable for the

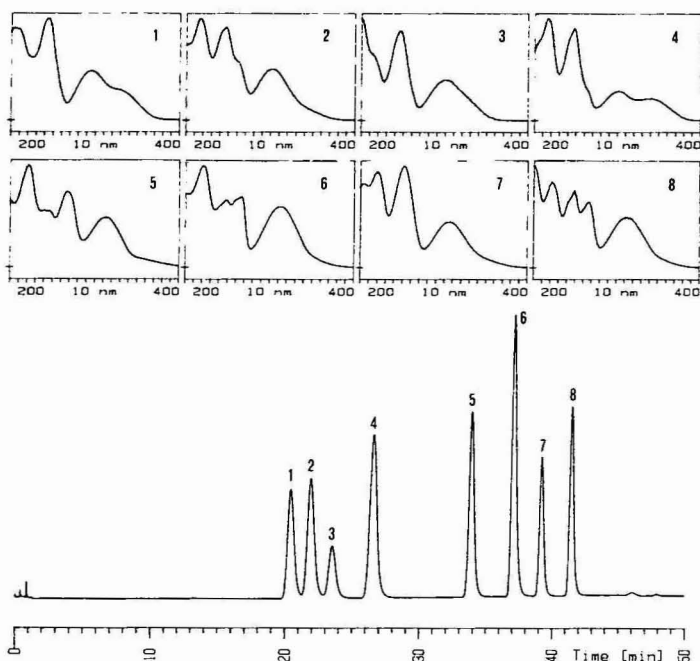


Fig. 2. Gradient HPLC separation of furocoumarin references with on-line UV detection. Column: Knauer Spherisorb ODS II cartridge, 3 μ m, 100 \times 4 mm I.D. For gradient profile see text. Peaks: 1 = psoralen; 2 = 8-methoxypsoralen; 3 = angelicin; 4 = sphondin; 5 = isopimpinellin; 6 = bergapten; 7 = pimpinellin; 8 = isobergapten.

analysis of plant extracts (Figs. 3 and 4). From the chromatograms it is seen that *Heracleum sphondylium* roots contain predominantly the compounds 4–8 (Fig. 3), while in *Heracleum mantegazzianum* leaves the first eluting compounds 1–3 and 6 (Fig. 4) represent the main furocoumarins. The photodiode array detector allows an unambiguous identification of even low amounts of coumarins in the extracts. UV spectra over the range 200–400 nm can be compared with reference spectra (attenuation > 8 m.a.u.).

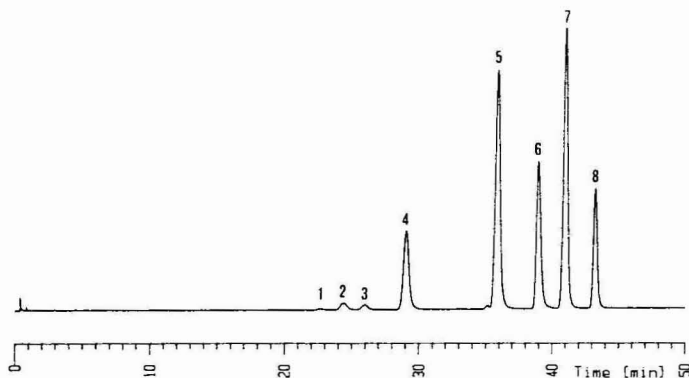


Fig. 3. Gradient HPLC separation of *Heracleum sphondylium* root furocoumarins. For conditions see Fig. 2 and text. All peaks were identified by on-line UV detection between 200 and 400 nm.

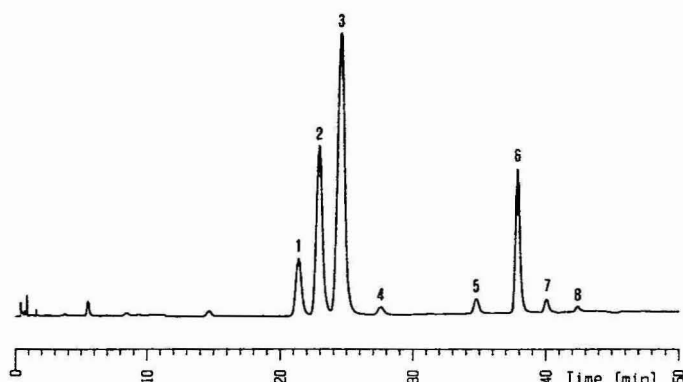


Fig. 4. Gradient HPLC separation of *Heracleum mantegazzianum* leaf furocoumarins. For conditions see Fig. 2 and text. All peaks were identified by on-line UV detection between 200 and 400 nm.

As these furocoumarins are widespread in some plant families, they could serve as chemotaxonomic markers. This is of importance, *e.g.*, for the Umbelliferae family, since many of the species are botanically not easy to define or to distinguish. The presented HPLC gradient system may be appropriate for such a chemotaxonomic investigation as the two plant examples given indicate. The clean-up procedure for the crude extracts is very easy and efficient, and the automated HPLC system allows continuous analyses. The amount of plant material required for an analysis is about several hundred milligrams, depending on the furocoumarin content of the plant. Further work will be done to examine the furocoumarin contents of various plants and pharmaceutical preparations, together with the phototoxic and photomutagenic activities.

REFERENCES

- 1 B. R. Scott, M. A. Pathak and G. R. Mohn, *Mutat. Res.*, 39 (1976) 29.
- 2 B. Bridges and G. Strauss, *Nature (London)*, 283 (1980) 523.
- 3 E. L. Grant, R. C. von Borstel and M. J. Ashwood-Smith, *Environ. Mutagenesis*, 1 (1979) 55.
- 4 O. Schimmer, *Planta Med.*, 47 (1983) 79.
- 5 P. J. Porcaro and P. Shubiak, *J. Assoc. Off. Anal. Chem.*, 57 (1974) 145.
- 6 C. K. Shu, J. P. Walradt and W. I. Taylor, *J. Chromatogr.*, 106 (1975) 271.
- 7 H. W. Latz and D. A. Ernes, *J. Chromatogr.*, 166 (1978) 189.
- 8 J. F. Fisher and L. A. Trama, *J. Agric. Food Chem.*, 27 (1979) 1334.
- 9 R. Glandian and F. V  rillon, *Gilson HPLC application sheet*, Gilson International, Middleton, WI, 12/81/as 02, 1981.
- 10 A. Bettero and C. A. Benassi, *Farmaco Ed. Prat.*, 36 (1980) 140.
- 11 A. Bettero and C. A. Benassi, *J. Chromatogr.*, 280 (1983) 167.
- 12 C. V. Puglisi, J. A. F. de Silva and J. C. Meyer, *Anal. Lett.*, 10 (1977) 39.
- 13 B. Ljunggren, D. M. Carter, J. Albert and T. Reid, *J. Invest. Dermatol.*, 74 (1980) 59.
- 14 J. G. Montbaliu, M. T. Rosseel and M. G. Bogaert, *J. Pharm. Sci.*, 70 (1981) 965.
- 15 F. R. Stermitz and R. D. Thomas, *J. Chromatogr.*, 77 (1973) 431.
- 16 H. E. Nordby and S. Nagy, *J. Chromatogr.*, 207 (1981) 21.
- 17 G. Innocenti, A. Bettero and G. Caporale, *Farmaco Ed. Sci.*, 37 (1982) 475.
- 18 G. W. Ivie, R. C. Beier and D. L. Holt, *J. Agric. Food Chem.*, 30 (1982) 413.
- 19 R. G. Enriquez, M. L. Romero, L. I. Escobar, P. Joseph-Natan and W. F. Reynolds, *J. Chromatogr.*, 287 (1984) 209.

- 20 K. vande Castele, H. Geiger and Ch. F. van Sumere, *J. Chromatogr.*, 258 (1983) 111.
- 21 H. J. Thompson and S. A. Brown, *J. Chromatogr.*, 314 (1984) 323.
- 22 R. D. H. Murray, J. Méndez and S. A. Brown, *The Natural Coumarins, Occurrence, Chemistry and Biochemistry*, Wiley, Chichester, 1982, p. 107.
- 23 S. A. George and A. Maute, *Chromatographia*, 15 (1982) 419.
- 24 K. Hostettmann, B. Domon, D. Schaufelberger and M. Hostettmann, *J. Chromatogr.*, 283 (1984) 137.
- 25 A. Lenherr, B. Meier and O. Sticher, *Planta Med.*, 50 (1984) 403.
- 26 J. Reisch and I. Mester, *Chem. Ber.*, 112 (1979) 1491.

CHROM. 17 953

Note

Shelf-life of unused high-performance liquid chromatographic columns

N. G. S. GOPAL* and G. SHARMA

ISOMED, Bhabha Atomic Research Centre, Bombay 400 085 (India)

(Received June 7th, 1985)

Manufacturers of prepacked high-performance liquid chromatographic (HPLC) columns claim that columns are prepared on a large scale with stringent controls that ensure uniformity and reproducible selectivity. They emphasize that all columns have a finite lifetime before their efficiency and selectivity diminish to unacceptable levels. When one considers lifetime, two aspects have to be considered: first the shelf-life of a column that is stored for later use and second the lifetime of a column in use.

Precautions are taken to protect a column during its use *e.g.*, the mobile phase must have a pH range compatible with the column and the mobile phase and sample solution must be free from particulate matter.

Overseas users often need to order more than one column at a time for economy and to safeguard the continuity of the work, as there is considerable batch-to-batch variation, as can be seen from the characteristics of two silica (10 μ m) columns from one manufacturer given in Table I.

In order to establish the effect of column storage, we examined five different types of columns (A-E), all of 25 cm \times 4.6 mm I.D. The stationary phase, mobile phase and flow-rate (according to the manufacturer's certificate), the non-retained solute employed for the determination of t_0 and the value of t_0 were as follows: (A) silica, 10 μ m; heptane; 0.67 ml/min; hexane; 4.28 min; (B) octadecylsilane, 10 μ m; methanol-water (7:3); 1 ml/min; KNO₃; 2.52 min; (C) strong anion exchanger, 10 μ m; 0.05 M phosphate, pH 3.35; 0.67 ml/min; 0.01 M KH₂PO₄, 4.67 min; (D) strong cation exchanger, 10 μ m; 0.02 M phosphate, pH 3.5; 0.67 ml/min; KNO₃; 3.78 min;

TABLE I

CHARACTERISTICS OF TWO COLUMNS SUPPLIED BY ONE MANUFACTURER

t_0 = Retention time of unretained sample; t_R = retention time; N = plates per column.

Column	t_0 (min)	Carbon tetrachloride		Benzene		Naphthalene	
		t_R (min)	N	t_R (min)	N	t_R (min)	N
1	4.25	4.68	6160	6.00	7520	7.32	7300
2	4.69	5.72	10 670	7.65	10 890	10.20	10 840

TABLE II

COMPARISON OF COLUMN CHARACTERISTICS REPORTED IN THE CERTIFICATE AND THOSE DETERMINED IN OUR LABORATORY

The dates and figures given in parentheses pertain to our work.

Column	Date of testing	Test mixture*	Column characteristics			
			t_R (min)	N	k'	R
A	29.8.79 (11.1.85)	CCl ₄	4.68 (4.97)	6160 (3109)	0.10 (0.14)	5.11 (3.76)
		Benzene	6.00 (6.32)	7520 (4579)	0.41 (0.45)	4.20 (4.93)
		Naphthalene	7.32 (5.30)	7300 (5646)	0.72 (0.91)	
B	11.2.80 (20.12.84)	Benzene	4.24 (4.00)	5990 (1883)	0.56 (0.59)	5.45 (2.55)
		Naphthalene	5.83 (5.00)	5110 (2443)	1.14 (0.97)	
		Biphenyl	7.17 (5.80)	4710 (2430)	1.64 (1.25)	3.41 (1.67)
C	4.6.80 (14.6.84)	CMP	5.82 (5.78)	3730 (2738)	0.39 (0.24)	2.96 (2.48)
		AMP	7.19 (6.95)	3170 (2898)	0.72 (0.48)	3.28 (2.14)
		UMP	8.97 (8.06)	4410 (3064)	1.14 (0.73)	6.68 (5.47)
		GMP	13.68 (12.44)	4410 (3660)	2.27 (1.66)	
D	1.2.79 (12.6.84)	Uracil	5.84 (5.29)	6800 (1843)	0.36 (0.40)	4.35 (4.10)
		Guanine	7.60 (8.12)	4630 (2283)	0.77 (1.15)	3.52 (5.20)
		Cytosine	9.54 (13.22)	4640 (2878)	1.22 (2.50)	
E	15.7.82 (19.12.84)	Benzyl alcohol	— (3.80)	13 799 (2885)	1.02 (0.64)	—

* CMP = cytidine-, AMP = adenosine-, UMP = uridine- and GMP = guanosine-5'-monophosphate (disodium salt).

and (E) trimethylsilane, 6 μ m; methanol-water (1:1); 1.3 ml/min; KNO₃; 2.32 min.

Using test mixtures similar to those mentioned in the manufacturer's certificate, the following column characteristics were determined¹: retention time (t_R); number of theoretical plates (N) per unit column length; capacity factor (k'); and resolution (R). The results in Table II show that stored, unused columns (silica, reversed-phase, ion-exchange) undergo considerable decrease in efficiency and selectivity.

Manufacturers of HPLC columns should, therefore, advise customers about the shelflife of their columns and supply them only from stocks of recent manufacture.

REFERENCE

- 1 N. G. S. Gopal awnd G. Sharma, *J. Liq. Chromatogr.*, 5 (1982) 869-879.

CHROM. 18 000

Note

Separation of organic quaternary salts by reversed-phase thin-layer chromatography

S. MUNAVALLI*, F.-L. HSU, S. F. HATEM* and E. J. POZIOMEK

Research Directorate, Chemical Research and Development Center, Aberdeen Proving Ground, MD 21010-5423 (U.S.A.)

(Received June 18th, 1985)

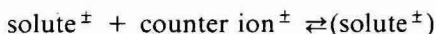
During the past five years, reversed-phase thin-layer chromatography (RP-TLC) has received considerable attention in the separation of a wide variety of compounds^{1–4}. Its popularity is mainly due to the fact that the results obtained with RP-TLC substantially correlate with high-performance liquid chromatography (HPLC)^{5,6}. RP-TLC is particularly suited for the separation and analysis of polar compounds which do not migrate on ordinary TLC plates. Also the resolution achieved by RP-TLC is far superior to that obtained on regular silica gel plates. The ease of manipulation of the solvent systems, the commercial availability of the bonded plates and the use of aqueous media have further enhanced the usefulness of RP-TLC. The preparation and properties of commercially bonded phases have been well documented^{7,8}. Silanes are used to modify the hydroxy groups of the stationary phase. These modifications endow the layers with a very high degree of hydrophobic character, retention, capacity, selectivity and stability. The selectivity of RP-TLC layers has been shown to increase with the corresponding increase in the water content of the solvent system⁹. However, the use of increasing amounts of water itself causes problems¹⁰.

One of the advantages of RP-HPLC is the simplicity involved in the selection of a suitable solvent system to give satisfactory resolution. The conditions for optimizing solvent systems of RP-HPLC¹¹, have been found to be applicable to RP-TLC¹². The polarity of the sample to be separated increases, with increasing water content of the solvent system⁹. Contrary to conventional TLC, the compounds migrate in order of decreasing polarity on the RP-TLC plates; the most polar moving the farthest and least polar migrating the least¹³.

The addition of various ion-pairing salts to the mobile phase has been reported to considerably enhance the resolution capability of the RP-TLC by influencing the surface characteristics and properties of the silanized groups^{14,15}. Although the mechanism by which this is brought about is not yet completely understood, it may either be due to an ion-exchange reaction or liquid–liquid partition of the neutralized

* Undergraduate Summer Research Participant from Johns Hopkins University, Baltimore, MD 21211, U.S.A.

ion pair on the silanized layers. The formation of a zwitter ion of the type has been suggested¹⁰:



Ion-pairing salts such as sodium chloride, ammonium chloride, ammonium acetate, at a concentration of 0.5 *M* permit the use of up to 50% of water in the solvent without disrupting the bonding properties of the layers and without affecting the separation. The separation of organic quaternary salts by conventional TLC is beset with many problems. It imposes certain limitations on the choice and use of aqueous solvent systems. Most often, adequate resolution on ordinary TLC plates cannot be achieved by using conventional solvent systems. Because of the almost unlimited wettability of the RP-TLC plates [recently Woelm has introduced RPTLC plates with 250 micron thickness of the coating that can withstand the use of 100% water (Catalog number 92101)], RP-TLC is particularly suited for use in reversed-phase ion chromatography.

In connection with our work on the synthesis of 4,4'-bipyridyl derivatives¹⁶, we encountered complex mixtures containing variously quaternized 4,4'-bipyridyl quaternary salts. These salts carried 1 to 6 positive charges. The separation of these salts by conventional TLC proved fruitless. This led us to explore the use of RP-TLC to separate organic quaternary salts.

EXPERIMENTAL

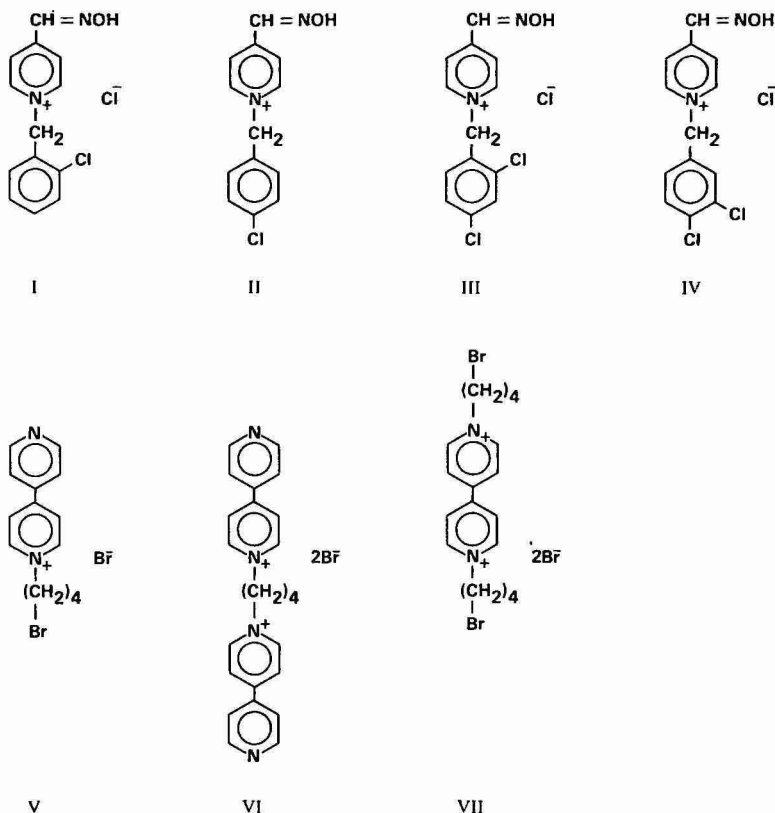
Watman MKC₁₈F chemically bonded reversed-phase 7.5 × 2.5 cm (lot number 000230) and 20 × 10 cm RP-TLC plates were used. Individual solutions were prepared at 2–4 μg/μl in distilled water. The standardized mixtures were prepared from the individual solutions. Initial spots were applied 2 cm away from the bottom edge of the plates. Development was carried out at room temperature in circular glass jars containing 2–3 ml of the respective solvent. The solvent was introduced into the developing chamber with no paper lining and allowed to saturate the chamber before the introduction of the RP-TLC plates. The development required 20–30 min in the case of small plates and 2–3 h in the case of longer plates. The plates were air dried and spots were detected under ultraviolet light (254 nm).

Chemicals

N-(2-Chlorobenzyl)- (I), N-(4-chlorobenzyl)- (II), N-(2,4-dichlorobenzyl)- (III), N-(3,4-chlorobenzyl)-4-aldoxime pyridinium chloride (IV) were prepared by refluxing an alcoholic solution of 4-pyridinealdoxime and the respective benzylchloride and filtering the solid on cooling and/or on evaporating the solvent under reduced pressure. The remaining three compounds, 4,4'-(4-bromobutyl)-bipyridinium- (V); 1,4-(bis-4,4'-bipyridinium) butane- (VI) and 4,4'-(bis-4-bromobutyl)-bipyridiniumbromide (VII) were prepared by refluxing a solution of 1,4-dibromobutane and 4,4'-bipyridyl in N-methylpyrrolidone.

RESULTS AND DISCUSSION

Prior to attempting the separation of the quaternary salts, optimum conditions



were determined for the satisfactory separation of the Analtech Test Dye 30-03. In this quest, we explored some 40 odd solvent systems. Best resolution was obtained using a solvent consisting of methanol-0.45 *M* ammonium acetate (7:3). We also examined the effect of salt concentration on the resolution of the quaternary salts. In general, we observed that increasing the salt concentration reduced trailing and gave better resolution and that salt concentrations greater than 0.5 *M* had no pronounced effect on the resolution. The use of ammonium hydroxide and sodium phosphate caused excessive trailing.

Fig. 1 shows the separation of mono- and di-substituted *N*-benzylpyridinium salts. When these conditions were applied for the separation of the multiply charged 4,4'-bipyridinium quaternary salts, poor resolution was observed. Excessive trailing was also seen. Attempts to improve the separation by substituting solvents within the selectivity groups were not successful. However, the combination of hydrochloric acid and acetic acid with ethanol and methanol resulted in satisfactory separation. Acetic acid did cause some trailing. Fig. 2 shows the separation of variously quaternized 4,4'-bipyridinium derivatives on longer RP-TLC plates.

The addition of ammonium hydroxide and ammonium chloride in place of hydrogen chloride and acetic acid gave poor separation. Better resolution of the spots was achieved with solvent A (Fig. 2). Attempts to separate these multiply-charged quaternary salts by SDS gel electrophoresis were not successful.

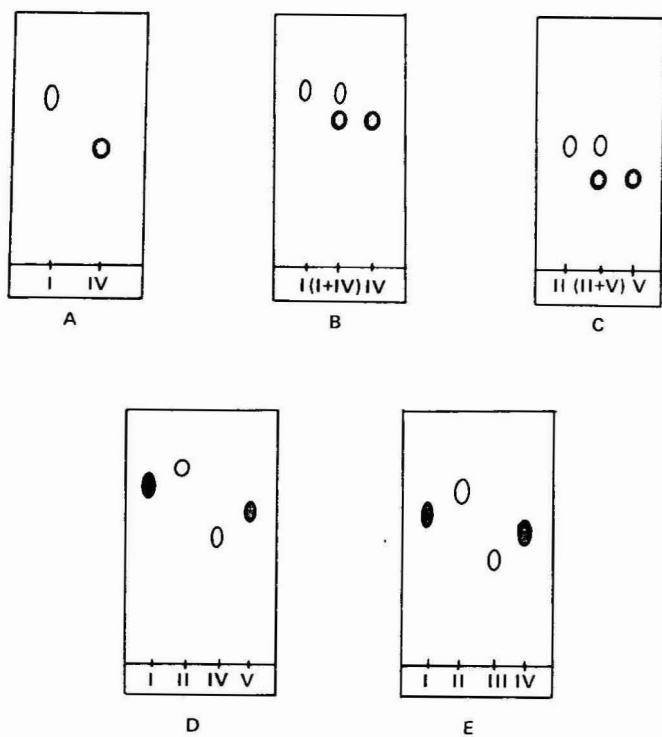


Fig. 1. Separation of N-benzylpyridinium-4-aldoxime salts. (A) I and IV; solvent, methanol-0.5 *M* ammonium acetate (7:3). (B) I, IV and I-IV mixture; solvent, methanol-0.38 *M* ammonium acetate (7:3). (C) II, V and II-V mixture; solvent, methanol-0.2 *M* sodium chloride (7:3). (D) I, II, III and IV; solvent, methanol-0.45 *M* ammonium acetate (6:4). (E) I, II, III and IV; solvent, dimethyl sulfoxide-0.2 *M* sodium chloride (3:2).

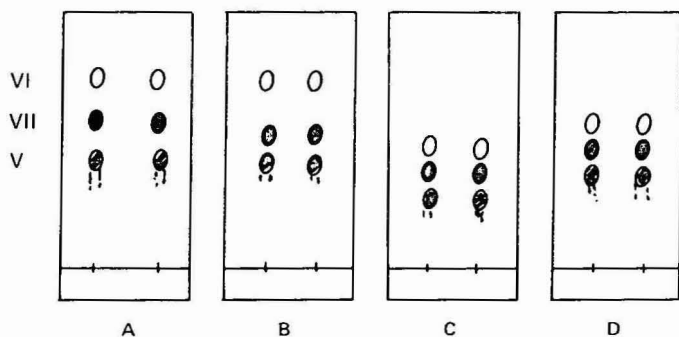


Fig. 2. Separation of variously quaternized 4,4'-bipyridyl derivatives on longer plates (20 × 10 cm), with (A) methanol-water-concentrated hydrochloric acid (7.5:2.45:0.05); (B) ethanol-water-concentrated hydrochloric acid (7.5:2.45:0.05); (C) methanol-water-glacial acetic acid (7.5:2.45:0.05); (D) ethanol-water-glacial acetic acid (7.5:2.45:0.05).

REFERENCES

- 1 M. Faupel and E. von Arx, *J. Chromatogr.*, 211 (1981) 262.
- 2 W. Meier and J. F. Conscience, *Anal. Chem.*, 105 (1980) 334.
- 3 H. R. Pfaendler, J. Costel and R. B. Woodward, *J. Am. Chem. Soc.*, 102 (1980) 2039.
- 4 J. Sherma, R. Krywicki and T. E. Regan, *Am. Lab.*, 1 (1981) 117.
- 5 R. K. Gilpin and W. R. Sisco, *J. Chromatogr.*, 124 (1976) 257.
- 6 E. von Arx and M. Faupel, *J. Chromatogr.*, 154 (1978) 68.
- 7 E. Grushka and E. J. Kikta, Jr., *Anal. Chem.*, 50 (1978) 1048A.
- 8 M. C. Hennion, C. Picard and M. Caude, *J. Chromatogr.*, 166 (1978) 21.
- 9 U. A. Th. Brinkman and G. de Vries, *J. Chromatogr.*, 192 (1980) 331.
- 10 A. M. Siouffi, T. Wawrzynowicz, F. Bressolle and G. Guiochon, *J. Chromatogr.*, 186 (1979) 563.
- 11 R. Lehrer, *Am. Lab.*, 10 (1981) 113.
- 12 J. Sherma and S. Charvat, *Am. Lab.*, 2 (1983) 140.
- 13 I. Halasz, *Anal. Chem.*, 52 (1980) 1393A.
- 14 H. H. W. Thijssen, *J. Chromatogr.*, 133 (1977) 355.
- 15 H. E. Hauck and W. Jost, *Am. Lab.*, 8 (1983) 72.
- 16 S. Munavalli and E. J. Poziomek, unpublished results.

CHROM. 18 036

Letter to the Editor

Effect of copper(II) sulphate impregnation of Chromarods on the sensitivity of the Iatroscan detection system to lipids

(Received July 15th, 1985)

Sir,

A recently published paper¹, indicates that the sensitivity of the Iatroscan TLC/FID to certain lipid classes can be considerably enhanced by impregnation of the Chromarods with copper(II) sulphate. As we routinely carry out lipid class analysis, we have investigated this claim in our own laboratory. Although the signal enhancements we obtained (*i.e.* *ca.* 37% for triglyceride, 30% for diglyceride, 4% for monoglyceride) were not as great as those obtained by Kaimal and Shantha, we can confirm that enhancement did occur. However we also found that the benefits obtained by copper sulphate impregnation were outweighed by the disadvantages, *i.e.*

(1) Following the proposed cleaning regime for the rods, signal enhancement decreases with successive re-impregnation, until after only 3 or 4 cycles a slight attenuation of the signal (when compared with new un-impregnated rods) becomes noticeable particularly with monoglycerides.

(2) The effect of repeated cleaning/impregnation cycles is to shorten considerably the life of the chromarods, because solvent elution times increase significantly, and perhaps partly as a consequence of this, separations become poorer. This renders the rods virtually unusable after *ca.* 10 cleaning-impregnation cycles (unimpregnated rods we find to last for about 100 runs).

It may be that the authors have ways of restoring the rods not described in the paper, but in our view the method, as published, offers no real advantages.

Cadbury Schweppes PLC,
The Lord Zuckerman Research Centre,
The University,
Whiteknights,
PO Box 234,
Reading RG6 2LA (U.K.)

A. S. RITCHIE

¹ T. N. Kaimal and N. C. Shantha, *J. Chromatogr.*, 288 (1984) 177.

Author Index

- Albert, K.
—, Nieder, M., Bayer, E. and Spraul, M.
Continuous-flow nuclear magnetic resonance 17
- Ansari, G. A. S.
— and Hendrix, P. Y.
Rapid and convenient separation of pentachlorophenol from human fat using silica Sep-Pak™ cartridges 435
- Baker, J. O.
—, Tucker, M. P. and Himmel, M. E.
Noble, diatomic and aliphatic gas analysis by aqueous high-performance liquid chromatography 93
- Bassene, E.
—, Laurance, A., Olschwang, D. and Pousset, J. L.
Plantes médicinales africaines. XIX. Dosage de la vitexine par chromatographie liquide haute performance dans un extrait brut de *Combretum micranthum* G. Don 428
- Bayer, E., see Albert, K. 17
- Beecher, G. R., see Khachik, F. 237
- Bendre, S. B.
—, Kadam, A. N. and Ghatge, B. B.
Comparative gas chromatographic studies of bonded and physically coated PEG 20M and its derivative phases with reference to some high-boiling isomeric solutes 359
- Bergamini, C., see Chiavari, G. 369
- Bertrand, O.
—, Cochet, S., Kroviarski, Y., Truskolaski, A. and Boivin, P.
Protein precipitation induced by a textile dye. Precipitation of human plasminogen in the presence of Procion Red HE3B 111
- Biggs, W. R., see Fetzer, J. C. 81
- Blondin, A., see Le Hoang, M. D. 382
- Blum, W.
— and Grob, K.
Preparation of glass and fused-silica capillary columns coated with immobilized XE-60 341
- Bohov, P., see Krupčík, J. 33
- Boivin, P., see Bertrand, O. 111
- Büser, W.
— and Erbersdobler, H. F.
Determination of furosine by gas-liquid chromatography 363
- Čellár, P., see Matisová, E. 177
- Charlton, J. P.
A combined recycling affinity column-filtration technique 247
- Chiavari, G.
— and Bergamini, C.
Determination of phenylurea herbicides by high-performance liquid chromatography with electrochemical detection 369
- Cho, S. H., see Smith, L. A. 291
- Clinch, R. M., see Colenutt, B. A. 25
- Cochet, S., see Bertrand, O. 111
- Colenutt, B. A.
— and Clinch, R. M.
Chromatographic properties of oxidised OV-17 stationary phase 25
- Dalene, M., see Skarping, G. 191
- Drevin, I., see Johansson, B.-L. 255
- Dryzga, M. D., see Freshour, N. L. 376
- Erbersdobler, H. F., see Büser, W. 363
- Erdelmeier, C. A. J.
—, Meier, B. and Sticher, O.
Reversed-phase high-performance liquid chromatographic separation of closely related furocoumarins 456
- Faigle, J. W., see Francotte, E. 321
- Fetzer, J. C.
— and Biggs, W. R.
Liquid chromatographic retention behavior of large, fused polycyclic aromatics. Normal bonded phases 81
- Ford, G. L.
Semi-preparative isolation of crepenynic acid, a potential inhibitor of essential fatty acid metabolism 431
- Fořtová, H., see Přistoupil, T. I. 401
- Francotte, E.
—, Stierlin, H. and Faigle, J. W.
Isolation and stereospecific determination of the enantiomers of oxindazac by direct liquid chromatographic resolution on triacetylcellulose 321
- Frantz, S. W., see Freshour, N. L. 376
- Freshour, N. L.
—, Langvardt, P. W., Frantz, S. W. and Dryzga, M. D.
Direct determination of acrylamide in tissue culture solution by liquid chromatography using column switching 376
- Fričová, V., see Přistoupil, T. I. 401

- Funazo, K.
 —, Tanaka, M., Morita, K., Kamino, M., Shono, T. and Wu, H.-L.
 Pentafluorobenzyl *p*-toluenesulphonate as a new derivatizing reagent for gas chromatographic determination of anions 215
- Fürst, P., see Stehle, P. 271
- Ghatge, B. B., see Bendre, S. B. 359
- Gill, R.
 — and Key, J. A.
 High-performance liquid chromatography system for the separation of ergot alkaloids with applicability to the analysis of illicit lysergide (LSD) 423
- Goliáš, J.
 — and Novák, J.
 Äthenmessung durch eine gaschromatographische Anreicherungstechnik mit Flammenionisationsdetektion 43
- Gopal, N. G. S.
 — and Sharma, G.
 Shelf-life of unused high-performance liquid chromatographic columns 461
- Goto, M.
 —, Irino, K. and Ishii, D.
 Multichannel spectrophotometric detector for fused-silica capillary tube isotachophoresis 167
 —, see Ito, Y. 161
- Grob, K., see Blum, W. 341
- Haddad, P. R., see Jackson, P. E. 125
 —, Jackson, P. E. and Heckenberg, A. L.
 Performance characteristics of some commercially available low-capacity anion-exchange columns suitable for non-suppressed ion chromatography 139
- Halkiewicz, J., see Ośmiałowski, K. 53
- Hara, S., see Yamaguchi, M. 227
- Hatem, S. F., see Munavalli, S. 463
- Heckenberg, A. L., see Haddad, P. R. 139
- Hendrix, P. Y., see Ansari, G. A. S. 435
- Hilgers, H., see Schmitz, F. P. 69
- Himmel, M. E., see Baker, J. O. 93
- Hjertén, S.
 — and Zhu, M.-D.
 Adaptation of the equipment for high-performance electrophoresis to isoelectric focusing 265
- Hoang, M. D. Le, see Le Hoang, M. D. 382
- Hoogmartens, J., see Kibwage, I. O. 309
- Hostettmann, K., see Schaufelberger, D. 396
- Hsu, F.-L., see Munavalli, S. 463
- Inoue, T.
 —, Ishiwata, H., Yoshihira, K. and Tanimura, A.
 High-performance liquid chromatographic determination of melamine extracted from cups made of melamine resin 450
- Irino, K., see Goto, M. 167
- Ishii, D., see Goto, M. 167
 —, see Ito, Y. 161
- Ishiwata, H., see Inoue, T. 450
- Ishiwatari, R., see Takada, H. 281
- Ito, Y.
 —, Takeuchi, T., Ishii, D. and Goto, M.
 Direct coupling of micro high-performance liquid chromatography with fast atom bombardment mass spectrometry 161
- Jackson, P. E., see Haddad, P. R. 139
 — and Haddad, P. R.
 The occurrence and origin of system peaks in non-suppressed ion chromatography of inorganic anions with indirect ultraviolet absorption detection 125
- Janssen, G., see Kibwage, I. O. 309
- Johansson, B.-L.
 — and Drevin, I.
 Three independent methods for quantitative determination of octyl covalently coupled to Sepharose CL-4B 255
- Kadam, A. N., see Bendre, S. B. 359
- Kaliszan, R., see Ośmiałowski, K. 53
- Kamino, M., see Funazo, K. 215
- Kangas, J.
 Gas chromatographic and mass spectrometric identification of sulphur gases in kraft digestion plants 405
- Kaushik, M. P., see Raghuveeran, C. D. 446
- Key, J. A., see Gill, R. 423
- Khachik, F.
 — and Beecher, G. R.
 Decapreno- β -carotene as an internal standard for the quantification of the hydrocarbon carotenoids by high-performance liquid chromatography 237
- Kibwage, I. O.
 —, Janssen, G., Roets, E., Hoogmartens, J. and Vanderhaeghe, H.
 Isolation of erythromycins and related substances from fermentation residues of *Streptomyces erythreus* by high-performance liquid chromatography on silica gel 309
- Klesper, E., see Schmitz, F. P. 69
- Kočan, A., see Matisová, E. 177
- Kozloski, R. P.
 Simple method for concentrating volatiles in water for gas chromatographic analysis by vacuum distillation 408
- Kramlová, M., see Přistoupil, T. I. 401
- Kroviarski, Y., see Bertrand, O. 111
- Krupčík, J.
 — and Bohov, P.
 Use of equivalent chain lengths for the characterization of fatty acid methyl esters separated by linear temperature-programmed gas chromatography 33
 —, see Matisová, E. 177

- Langvardt, P. W., see Freshour, N. L. 376
Laurance, A., see Bassene, E. 428
Leboda, R., see Tracz, E. 346
Le Hoang, M. D.
—, Postaire, E., Prognon, P., Pradeau, D., Blondin, A. and Sauziere, J.
Séparation et dosage des différents constituants de la troxérutine par chromatographie liquide haute performance en phase inverse. Application au contrôle pharmaceutique 382
Lorenschat, B., see Schmitz, F. P. 69
Mangia, A., see Verzella, G. 417
Mathiasson, L., see Skarping, G. 191
Matisová, E.
—, Krupčík, J., Čellár, P. and Kočan, A.
Quantitative analysis of hydrocarbons in gasolines by capillary gas-liquid chromatography. II. Isothermal and temperature-programmed analyses 177
Matsunaga, R., see Yamaguchi, M. 227
Meier, B., see Erdelmeier, C. A. J. 456
Montecucchi, P. C., see Rusconi, L. 390
Morgan, E. D., see Scalia, S. 301
Morita, K., see Funazo, K. 215
Munavalli, S.
—, Hsu, F.-L., Hatem, S. F. and Poziomek, E. J.
Separation of organic quaternary salts by reversed-phase thin-layer chromatography 463
Nakamura, M., see Yamaguchi, M. 227
Nieder, M., see Albert, K. 17
Norman, H. A., see Smith, L. A. 291
Novák, J., see Goliáš, J. 43
Ohkura, Y., see Yamaguchi, M. 227
Olschwang, D., see Bassene, E. 428
Ośmiałowski, K.
—, Halkiewicz, J., Radecki, A. and Kaliszan, R.
Quantum chemical parameters in correlation analysis of gas-liquid chromatographic retention indices of amines 53
Podojil, M., see Řezanka, T. 453
Poppe, H., see Van Vliet, H. P. M. 149
Postaire, E., see Le Hoang, M. D. 382
Pousset, J. L., see Bassene, E. 428
Poziomek, E. J., see Munavalli, S. 463
Pradeau, D., see Le Hoang, M. D. 382
Přistoupil, T. I.
—, Kramlová, M., Fořtová, H. and Fričová, V.
Analytical isoelectric focusing of native and modified haemoglobins after treatment with 4-hydroxymercuribenzoate 401
Prognon, P., see Le Hoang, M. D. 382
Przyjazny, A.
Evaluation of the suitability of selected porous polymers for preconcentration of organosulphur compounds from water 61
Radecki, A., see Ośmiałowski, K. 53
Raghuvveeran, C. D.
— and Kaushik, M. P.
Reversed-phase high-performance liquid chromatography of methyl isocyanate 446
Rapsomatiotis, A., see Voss, R. H. 205
Renman, L., see Skarping, G. 191
Řezanka, T.
— and Podojil, M.
Gradient separation of fatty acids (C₁₄–C₃₀) by reversed-phase high-performance liquid chromatography 453
Ritchie, A. S.
Effect of copper(II) sulphate impregnation of Chromarods on the sensitivity of the Iatrascan detection system to lipids 468
Roets, E., see Kibwage, I. O. 309
Rusconi, L.
— and Montecucchi, P. C.
Reversed-phase high-performance liquid chromatography of natural and synthetic sauvages 390
Sakabe, Y., see Terada, H. 333
Sangö, C., see Skarping, G. 191
Sauziere, J., see Le Hoang, M. D. 382
Scalia, S.
— and Morgan, E. D.
Simultaneous determination of free and conjugated ecdysteroids by liquid chromatography 301
Schaufelberger, D.
— and Hostettmann, K.
Analytical and preparative reversed-phase liquid chromatography of secoiridoid glycosides 396
Schmitz, F. P.
—, Hilgers, H., Lorenschat, B. and Klesper, E.
Separation of oligomers with UV-absorbing side groups by supercritical fluid chromatography using eluent gradients 69
Sepulveda, F. I., see Yang, C.-Y. 413
Sharma, G., see Gopal, N. G. S. 461
Shono, T., see Funazo, K. 215
Skarping, G.
—, Renman, L., Sangö, C., Mathiasson, L. and Dalene, M.
Capillary gas chromatographic method for the determination of complex mixture of isocyanates and amines 191
Smith, L. A.
—, Norman, H. A., Cho, S. H. and Thompson, Jr., G. A.
Isolation and quantitative analysis of phosphatidylglycerol and glycolipid molecular species using reversed-phase high-performance liquid chromatography with flame ionization detection 291
Spraul, M., see Albert, K. 17

- Stehle, P.
 — and Fürst, P.
 Isotachophoretic control of peptide synthesis and purification. A novel approach using ultraviolet detection at 206 nm 271
- Sticher, O., see Erdelmeier, C. A. J. 456
- Stierlin, H., see Francotte, E. 321
- Takada, H.
 — and Ishiwatari, R.
 Quantitation of long-chain alkylbenzenes in environmental samples by silica gel column chromatography and high-resolution gas chromatography 281
- Takeuchi, T., see Ito, Y. 161
- Tanaka, M., see Funazo, K. 215
- Tanimura, A., see Inoue, T. 450
- Terada, H.
 — and Sakabe, Y.
 Studies on the analysis of food additives by high-performance liquid chromatography. V. Simultaneous determination of preservatives and saccharin in foods by ion-pair chromatography 333
- Thompson, Jr., G. A., see Smith, L. A. 291
- Tracz, E.
 — and Leboda, R.
 A microscopic investigation of the surface of carbon-silica adsorbents. II. Relationships between the type of information obtainable about the surface and the microscopic techniques used for its examination 346
- Truskolaski, A., see Bertrand, O. 111
- Tucker, M. P., see Baker, J. O. 93
- Vanderhaeghe, H., see Kibwage, I. O. 309
- Van Vliet, H. P. M.
 — and Poppe, H.
 The performance of some cell designs for laser-induced fluorescence detection in open-tubular liquid chromatography 149
- Verzella, G.
 — and Mangia, A.
 High-performance liquid chromatographic analysis of Aspartame 417
- Vliet, H. P. M. van, see Van Vliet, H. P. M. 149
- Voss, R. H.
 — and Rapsomatiotis, A.
 An improved solvent-extraction based procedure for the gas chromatographic analysis of resin and fatty acids in pulp mill effluents 205
- Wells, G.
 Theory of anion contributions to non-linear electron-capture detector response 1
- Wilson, M. F.
 A rapid method for the separation and quantification of simple phenolic acids in plant material using high-performance liquid chromatography 440
- Wu, H.-L., see Funazo, K. 215
- Yamaguchi, M.
 —, Hara, S., Matsunaga, R., Nakamura, M. and Ohkura, Y.
 3-Bromomethyl-6,7-dimethoxy-1-methyl-2(1H)-quinoxalinone as a new fluorescence derivatization reagent for carboxylic acids in high-performance liquid chromatography 227
- Yang, C.-Y.
 — and Sepulveda, F. I.
 Separation of phenylthiocarbamyl amino acids by high-performance liquid chromatography of Spherisorb octadecylsilane columns 413
- Yoshihira, K., see Inoue, T. 450
- Zhu, M.-D., see Hjertén, S. 265

Erratum

J. Chromatogr., 329 (1985) 43–56

Page 43, the fifth line of the Introduction section should read “acids^{8–10} and chloropropyl esters of *n*- and isoalkanoic acids¹¹. More recently, the”.

INSTRUMENTUNE-UP

A Computer Program for Improving the Performance of Common Laboratory Instruments

**Authors: S.N. Deming and
S.L. Morgan**

- based on the sequential simplex method of optimization
- adjust as many as ten continuous variables simultaneously
- available for the Apple II series and IBM-PC
- clear, fully descriptive manual with tutorial
- full source code listings
- easy to use
- US \$ 150.00

AVAILABLE FROM

Elsevier Scientific Software (JIC)
52 Vanderbilt Avenue
New York, NY 10017 USA
Phone: (212) 370 5520
Telex: 420643

or
Elsevier Scientific Software
P.O. Box 330
1000 AH Amsterdam
THE NETHERLANDS
Phone: (020) 5803 911
Telex: 18582

*Write to us for further
information on our other
programs.*

No shipping
charge if
paid in
advance



AAS



Apple is a registered trademark
of Apple Computer, Inc.
IBM-PC is a registered trademark of IBM.

BALANCE

A Program to Compare the Means of Two Series of Measurements

Authors: D.L. Massart et al.

- requires no profound knowledge of statistics
- guides user with playful ease to the correct statistical test
- incorporates:
 - paired t-test (parametric)
 - Wilcoxon test (non-parametric)
 - Student's t- and Cochran's tests (parametric)
 - Mann-Whitney's U-test (non-parametric)
 - tests for small and large numbers of measurements
 - one/two tailed (sided) tests
- full source code listings
- clear, fully descriptive manual with worked examples
- US \$ 150.00

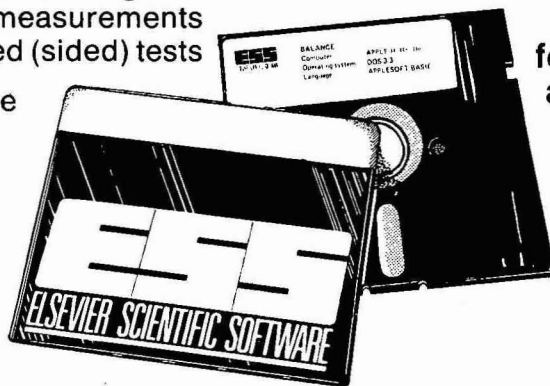
AVAILABLE FROM

Elsevier Scientific Software (JIC)
52 Vanderbilt Avenue
New York, NY 10017 USA
Phone: (212) 370 5520
Telex: 420643

or
Elsevier Scientific Software
P.O. Box 330
1000 AH Amsterdam
THE NETHERLANDS
Phone: (020) 5803 911
Telex: 18582

Write to us for further information on our other programs.

No shipping charge if paid in advance



**for: IBM-PC
and
Apple II
series**

ESS
ELSEVIER SCIENTIFIC SOFTWARE

Apple is a registered trademark
of Apple Computer, Inc.
IBM-PC is a registered trademark of IBM.

applied catalysis

NOW IN ITS
SIXTH YEAR!

An international journal devoted to
catalytic science and its applications

EDITOR-IN-CHIEF

B. Delmon
Louvain-la Neuve, Belgium

REGIONAL EDITORS

L. Guzzi
Institute of Isotopes,
Hungarian Academy of Sciences,
P.O. Box 77, 1525 Budapest, Hungary

J.F. Roth
Air Products and Chemicals Inc.,
P.O. Box 538,
Allentown, PA 18105, U.S.A.

D.L. Trimm
School of Chemical Engineering and
Industrial Chemistry,
University of New South Wales,
P.O. Box 1,
Kensington, N.S.W. 2033, Australia

J.C. Vedrine
Institut de Recherches sur la Catalyse,
Centre National de la Recherche
Scientifique,
2, Avenue Albert Einstein,
69626 Villeurbanne, France

D.A. Whan
Catalysts Group, Research Department,
Agricultural Division,
Imperial Chemical Industries plc.,
P.O. Box 1,
Billingham, Cleveland, U.K.

EDITOR: NEWS BRIEF

J.R.H. Ross
Department of Chemical Technology,
Twente University of Technology,
P.O. Box 217,
7500 AE Enschede, The Netherlands

The scope includes

- * catalytic phenomena occurring in industrial processes or in processes in the stage of industrial development and in conditions similar to those of industrial processes. Both heterogeneous and homogeneous catalysis are included, together with aspects of industrial enzymatic catalysis;
- * scientific aspects of preparation, activation, ageing, poisoning, rejuvenation, regeneration and start-up transient effects;
- * methods of catalyst characterization when they are both scientific and of potential interest for industrial catalysts;
- * aspects of chemical engineering relevant to the science of catalysis;
- * new catalytic reactions of potential practical interest, and new catalytic routes.

The journal features:

- * rapid publication of full length research papers, short communications, review articles and letters to the Editors;
- * A News Brief section, provided by correspondents, which contains information gathered from patents, technical journals etc., on new catalytic reactions, catalysts and processes, new methods of catalyst preparation and on new scientific facts related to the Science of catalysis;
- * Book reviews, reports on recent events and developments, and a calendar of forthcoming events of topical interest.

Contributions should be sent to the appropriate editor as follows:

Western Europe: Dr. D.A. Whan or Prof. J.C. Vedrine

Australia and Asia: Prof. D.L. Trimm

North and South America: Dr. J.F. Roth

Eastern Europe and Africa: Prof. L. Guzzi

Contributions to News Brief should be sent to Prof. J.R.H. Ross

**Write now for a
Free Sample Copy**

Applied Catalysis is abstracted/indexed in: Chemical Abstracts, Current Contents: Physical, Chemical and Earth Sciences, Current Contents: Engineering, Technology and Applied Sciences, Engineering Index, Metals Abstracts.

1985 - Vols. 13-17 (12 issues): US \$ 438 / Dfl. 1185.00, including postage.

1986 - Vols. 18-25 + cumulative index vols. 1-20 (8 volumes, 17 issues): US \$ 708.25 /
Dfl. 1912.00, including postage.



ELSEVIER SCIENCE PUBLISHERS

P.O. Box 211, 1000 AE Amsterdam, The Netherlands

7329

journal of controlled release

Official journal of the Controlled Release Society



Editors

JAN FEIJEN, Department of
Chemical Technology, Twente
University of Technology,
P.O. Box 217, 7500 AE Enschede,
The Netherlands

JORGE HELLER, Director, Polymer
Sciences Department, SRI Interna-
tional, Menlo Park, CA 94025,
U.S.A.

A new international journal dealing with the science and technology of the controlled release of active agents. The term 'controlled release' is used in its broadest sense to include control over rate of release using - either singly or in combination - diffusion, chemical reactions, dissolution, osmosis or mechanical devices, as well as control over the site of action of the active agent using pro-drugs or carriers such as water-soluble polymers, microcapsules or liposomes.

The journal is intended to serve a wide range of specialists and to bring together high quality papers dealing with various aspects of controlled release of therapeutic agents for human and animal use, as well as those dealing with insect and other pest management, fertilizers, weed control and marine antifouling applications.

1985: Volume 2 (4 issues)

Subscription price: US \$ 82.25 /

Dfl. 222.00 including postage

A free specimen copy is available from

ELSEVIER



P.O. Box 211
1000 AE Amsterdam
The Netherlands

52 Vanderbilt Ave.,
New York, NY 10017
USA

ANATECH'86

An International Symposium on Applications of Analytical Chemical Techniques to Industrial Process Control

Noordwijkerhout, The Netherlands

22 - 24 April, 1986

Organised under the sponsorship of

- Royal Netherlands Chemical Society (KNCV)
section for Analytical Chemistry
- Federation of European Chemical Societies (FECS)

SCOPE

The importance of analytical techniques for the control of industrial processes is steadily increasing.

The development of process analysers has taken place to a great extent outside the analytical laboratory. This has led to a distinct gap between experts in the field of process analysis and analytical chemists. Bridging this gulf is one of the main objectives of this symposium which is aimed at an interdisciplinary audience of industrial and academic analytical scientists and those involved in process control and process analysis.

The scientific programme will consist of invited plenary lectures, keynote lectures and submitted research papers dealing with

- ★ State of the art of analytical techniques already successfully applied in process analysis
- ★ Sampling procedures and sampling strategy
- ★ Selection of analytical procedures and instruments with regard to optimum process control
- ★ New analytical techniques of possible interest for process control.

An exhibition of instruments within the scope of the symposium will be held.

Those wishing to present a paper or who would like to receive full details, please write to:

Professor Dr. W.E. van der Linden
Laboratory for Chemical Analysis
Dept. of Chemical Technology
Twente University of Technology
P.O. Box 217
NL - 7500 AE Enschede, The Netherlands
Telephone: (53) 892436



★ **Books on Chemical Structure Analysis**

Quantitative Approaches to Drug Design

Proceedings of the Fourth European Symposium on Chemical Structure-Biological Activity: Quantitative Approaches, Bath, U.K., September 6-9, 1982.

edited by JOHN C. DEARDEN, School of Pharmacy, Liverpool Polytechnic, Liverpool, U.K.
(Pharmacochemistry Library, Volume 6)

For medicinal chemists in the pharmaceutical industry and in academia, as well as for pesticide chemists and biologists, here is a comprehensive, timely up-to-date of the quantitative approaches to drug design that covers all aspects of QSAR - including a number of novel approaches. Reflecting the latest thinking and advances in this rapidly expanding field of research, the book contains the full texts of the plenary and communicated papers, plus detailed abstracts of the poster presentations. Among the topics dealt with are: parameters and modelling in QSAR; enzymes and receptors; molecular graphics and conformational studies; pharmacokinetics and rate effects; series design; and QSAR in practice.

1983 x + 296 pages
US \$ 59.25 / Dfl. 160.00

ISBN 0-444-42200-5

Computer Applications in Chemistry

Proceedings of the Sixth International Conference on Computers in Chemical Research and Education (ICCCRE), held in Washington, DC, July 11-16, 1982.

edited by STEPHEN R. HELLER and RUDOLPH POTENZONE Jr.,
U.S. Environmental Protection Agency, Washington, DC, U.S.A. (Analytical Chemistry Symposia Series, Volume 15)

A highly comprehensive overview of the application of computers in chemistry, this proceedings volume includes up-to-date details on a number of areas of growing interest, e.g. QSAR, pattern recognition, molecular graphics, and spectral analysis for structural elucidation. The book also provides an introduction to macromolecular graphics - illustrated by some excellent colour photographs. With its wide-ranging coverage, plus its particularly thorough computer index, it will be an invaluable reference for the researcher and will also provide the senior level/graduate student with an excellent background to many areas of non-numeric applications of computers in chemistry.

1983 xii + 398 pages
US \$ 77.75 / Dfl. 210.00

ISBN 0-444-42210-2

Structural Analysis of Organic Compounds by Combined Application of Spectroscopic Methods

by J.T. CLERC, E. PRETSCH and J. SEIBL
(Studies in Analytical Chemistry, Volume 1)

In this concise, logically structured reference work, the authors demonstrate how the combined application of spectroscopic methods can substantially increase their overall effectiveness. Covering a wide variety of chemical structures and spectroscopic capabilities, the book presents numerous examples of different methods of approach and reasoning, supplemented by comments on previously neglected analytical aspects.

1981 288 pages
US \$ 59.25 / Dfl. 160.00

ISBN 0-444-99748-2

Write now for detailed information on these titles.

Elsevier

P.O. Box 330
1000 AE Amsterdam
The Netherlands

P.O. Box 1663
Grand Central Station
New York, NY 10163, USA

7273A

PUBLICATION SCHEDULE FOR 1986

Journal of Chromatography (incorporating *Chromatographic Reviews*) and *Journal of Chromatography, Biomedical Applications*

MONTH	O 1985	N 1985	D 1985	J 1986	The publication schedule for further issues will be published later
Journal of Chromatography	346 347/1	347/2 347/3 348/1	348/2 349/1 349/2 350/1 350/2	351/1	
Chromatographic Reviews					
Bibliography Section					
Biomedical Applications				374/1 374/2	

INFORMATION FOR AUTHORS

(Detailed *Instructions to Authors* were published in Vol. 329, No. 3, pp. 449-452. A free reprint can be obtained by application to the publisher.)

Types of Contributions. The following types of papers are published in the *Journal of Chromatography* and the section on *Biomedical Applications*: Regular research papers (Full-length papers), Short communications and Notes. Short communications are preliminary announcements of important new developments and will, whenever possible, be published with maximum speed. Notes are usually descriptions of short investigations and reflect the same quality of research as Full-length papers, but should preferably not exceed four printed pages. For review articles, see page 2 of cover under Submission of Papers.

Submission. Every paper must be accompanied by a letter from the senior author, stating that he is submitting the paper for publication in the *Journal of Chromatography*. Please do not send a letter signed by the director of the institute or the professor unless he is one of the authors.

Manuscripts. Manuscripts should be typed in double spacing on consecutively numbered pages of uniform size. The manuscript should be preceded by a sheet of manuscript paper carrying the title of the paper and the name and full postal address of the person to whom the proofs are to be sent. Authors of papers in French or German are requested to supply an English translation of the title of the paper. As a rule, papers should be divided into sections, headed by a caption (*e.g.*, Summary, Introduction, Experimental, Results, Discussion, etc.). All illustrations, photographs, tables, etc., should be on separate sheets.

Introduction. Every paper must have a concise introduction mentioning what has been done before on the topic described, and stating clearly what is new in the paper now submitted.

Summary. Full-length papers and Review articles should have a summary of 50-100 words which clearly and briefly indicates what is new, different and significant. In the case of French or German articles an additional summary in English, headed by an English translation of the title, should also be provided. (Short communications and Notes are published without a summary.)

Illustrations. The figures should be submitted in a form suitable for reproduction, drawn in Indian ink on drawing or tracing paper. Each illustration should have a legend, all the legends being typed (with double spacing) together on a *separate sheet*. If structures are given in the text, the original drawings should be supplied. Coloured illustrations are reproduced at the author's expense, the cost being determined by the number of pages and by the number of colours needed. The written permission of the author and publisher must be obtained for the use of any figure already published. Its source must be indicated in the legend.

References. References should be numbered in the order in which they are cited in the text, and listed in numerical sequence on a separate sheet at the end of the article. Please check a recent issue for the layout of the reference list. Abbreviations for the titles of journals should follow the system used by *Chemical Abstracts*. Articles not yet published should be given as "in press", "submitted for publication", "in preparation" or "personal communication".

Dispatch. Before sending the manuscript to the Editor please check that the envelope contains three copies of the paper complete with references, legends and figures. One of the sets of figures must be the originals suitable for direct reproduction. Please also ensure that permission to publish has been obtained from your institute.

Proofs. One set of proofs will be sent to the author to be carefully checked for printer's errors. Corrections must be restricted to instances in which the proof is at variance with the manuscript. "Extra corrections" will be inserted at the author's expense.

Reprints. Fifty reprints of Full-length papers, Short communications and Notes will be supplied free of charge. Additional reprints can be ordered by the authors. An order form containing price quotations will be sent to the authors together with the proofs of their article.

Advertisements. Advertisement rates are available from the publisher on request. The Editors of the journal accept no responsibility for the contents of the advertisements.

FIRST ANNOUNCEMENT

International Symposium on Coal Characterisation for Conversion Processes Rolduc, The Netherlands, 28th April - 1st May 1986

Scope

The past decade has been characterized by a renewed interest in coal as an energy source and as a basic material for the chemical industry. This has induced a revival in coal research activities both from a fundamental and an applied point of view. Due to changing economics, however, the large scale introduction of new coal conversion processes has been postponed and, as a consequence, more time is available for research to gain fundamental insights into coal structure and to obtain a better understanding of its impact on conversion processes. In view of this, the initiative has been taken to organize the international "Rolduc Symposia on Coal Science". These are intended to fill the need for small-scale working symposia on specific subjects and with a limited number of participants (about 150), as a supplement to the large-scale Coal Science Conferences. The opportunity for in-depth discussions and maximum profit from exchange of knowledge and ideas can thereby be assured.

The first symposium of the series will be devoted to "Coal Characterisation for Conversion Processes". Its aim is to build a bridge between the techniques and methods nowadays available for coal characterisation and the need for relevant parameters to operate and design coal conversion processes.

Scientific Program

The scientific program will cover Coal Characterisation in relation to Gasification, Combustion, Pyrolysis, and Liquefaction. A full symposium day will be devoted to each of the four processes and each day's session will commence with a plenary lecture by an invited expert:

Gasification: **K.H. van Heek**
(Bergbau-Forschung GmbH, Germany)

Combustion: **P.A. Roberts**
(Int. Flame Research Foundation, The Netherlands)

Pyrolysis: **R. Cyprès**
(Free University Brussels, Belgium)

Liquefaction: **C. Snape**
(British Gas, U.K.)

Poster sessions and discussions on selected topics will be organized. There are no parallel sessions. The congress language will be English.

Proceedings

The participants will receive a hard-bound edition of the proceedings. This will be a reprint of a special issue of the journal *Fuel Processing Technology*, published by Elsevier.

Fee

A special symposium package, including registration, accommodation for four nights, all meals, and a copy of the proceedings will be available at approximately Dfl. 1050 per participant (about US \$ 350).

Further Information

Further information can be obtained from
F. Kapteijn,
Secretary First International Rolduc Symposium on Coal Science,
Institute for Chemical Technology of the University of Amsterdam,
Nieuwe Achtergracht 166,
1018 WV Amsterdam,
The Netherlands.
Telephone 31 - (0) 20-522 3490/2265.
Telex FACWN 16460.

